# First Annual High-Speed Research Workshop

*Compiled by*
Allen H. Whitehead, Jr.
*Langley Research Center*
*Hampton, Virginia*

Date for general release    April 30, 1994
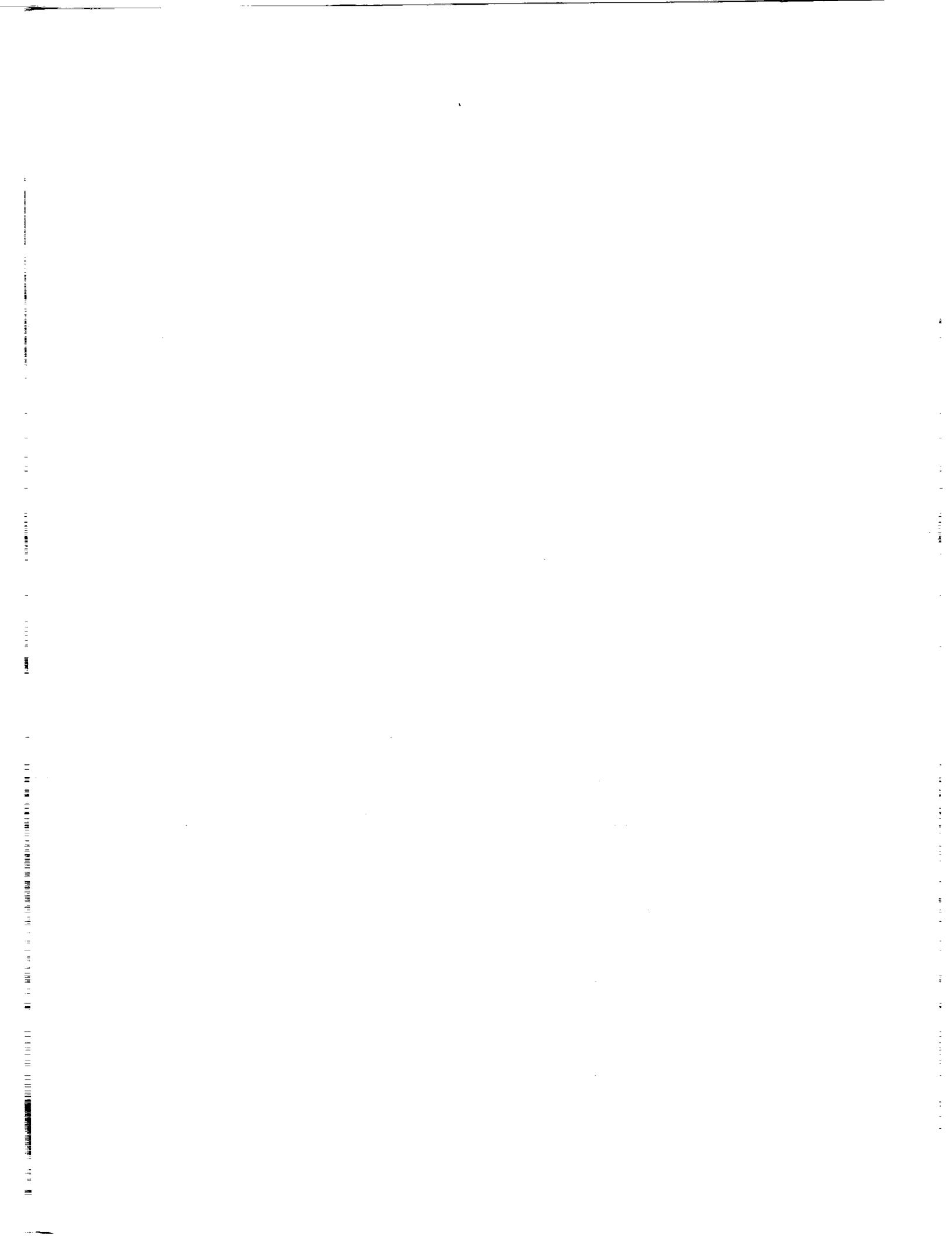
# FOREWORD

The First Annual High-Speed Research (HSR) Workshop was hosted by NASA Langley Research Center and was held May 14-16, 1991, in Williamsburg, Virginia. The purpose of the workshop was to provide a national forum for the government, industry and university participants in the program to present and discuss important technology issues related to the development of a commercially viable, environmentally compatible U.S. High-Speed Civil Transport. The workshop sessions and this publication are organized around the major task elements in NASA's Phase I - High-Speed Research Program which basically addresses the environmental issues of atmospheric emissions, community noise and sonic boom.

The opening Plenary Session provided program overviews and summaries by senior management from NASA and industry. The remaining twelve technical sessions were organized to preview the content of each program element, to discuss planned activities and to highlight recent accomplishments.

Attendance at the workshop was by invitation only and included only industry, academic and government participants who were actively involved in the High-Speed Research Program. The technology presented at the meeting is considered commercially sensitive, and as such, the conference results and this publication are protected by the NASA designation LIMITED DISTRIBUTION.

THIS PAGE INTENTIONALLY BLANK

# TABLE OF CONTENTS

## Part I*

*Published under separate cover.*

**PRECEDING PAGE BLANK NOT FILMED**

# Part II*

*Published under separate cover.

iv

## SESSION VII. -- Emission Reduction (continued)

# Part III

## SESSION VIII. -- Aeroacoustic Analysis and Community Noise

## SESSION IX. -- Sonic Boom (Human Response and Atmospheric Effects)

# Part IV*

*Published under separate cover.*

# Session VIII. Aeroacoustic Analysis and Community Noise

**THIS PAGE INTENTIONALLY BLANK**

# Session VIII. Aeroacoustic Analysis and Community Noise

Aeroacoustics Analysis and Community Noise Overview
*Robert A. Golub, NASA Langley Research Center; and Paul T. Soderman, NASA Ames Research Center*

THIS PAGE INTENTIONALLY BLANK

# AEROACOUSTICS ANALYSIS
# AND
# COMMUNITY NOISE
# OVERVIEW

*3/- O2*
*/2031*

## CHAIRMAN

Robert A. Golub
ANOPP Manager
Aeroacoustics Branch
Acoustics Division
NASA LaRC

## CO-CHAIRMAN

Paul T. Soderman
Fixed Wing Aerodynamics Branch
Full-Scale Aserdynamics Research Division
NASA ARC

# FIRST ANNUAL
# HIGH SPEED RESEARCH WORKSHOP
# WILLIAMSBURG, VA
## MAY 15, 1991

# AEROACOUSTIC ANALYSIS AND COMMUNITY NOISE SESSION AGENDA

This is an agenda figure which lists session title, date, and time. It spells out the workshop objectives and lists the session chairman and co-chairman. It presents a detailed agenda of the presentation times, titles, and authors.

## AEROACOUSTIC ANALYSIS AND COMMUNITY NOISE SESSION AGENDA

MAY 15 th, 1991      1:00 TO 4:30 P.M.

**OBJECTIVES**

A). REPORT AND DISCUSS TECHNICAL PROGRESS

B). EVALUATE AND RECOMMEND PROGRAM PLAN CHANGES

|  |  |
|---|---|
| **Robert A. Golub**<br>Chairman | **Paul Soderman**<br>Co-Chairman |

| Time | Title / Author |
|---|---|
| 1:00 P.M. | Element Overview<br>Robert A. Golub |
| 1:15 | Generation of a New Jet Shock Noise Model and Computer Code for ANOPP<br>N. N. Reddy |
| 1:45 | Boeing Perspective of Community Noise Technology Needs<br>Gene Nihart |
| 2:15 | Current Status of HSR System Noise<br>Allan Mortlock |
| 2:45 | ANOPP / VMS HSCT Ground Contour Study<br>Lou Glabb / John Rawls |
| 3:15 | High-Performance-Jet-Engine Flight Test Data Base for HSR<br>Jeff Kelly |
| 3:45 | Status and Plans for the ANOPP HSR Prediction System<br>Sandra Nolan |
| 4:15 | Summary Discussion<br>Robert A. Golub |

The goals of the High Speed Research Program are focused on three major environmental issues: atmospheric effects, airport conmmunity noise, and sonic boom.  These issues are basic concerns that require better understanding before further HSRP endeavors can be addressed.

Economically viable solutions will be sought for these issues including:

- Valid ozone effect predictions

- Reduction of engine emissions, and the technical basis for acceptability criteria

- Reduction of noise, and compliance with Federal Air Regulation, Part 36, Stage III

- Sonic boom reduction or efficient subsonic overland cruise, and the technical basis for boom acceptability criteria.

This vu-graph expands upon the general research to be performed for community noise compliance.

# COMMUNITY NOISE RESEARCH

**"Public acceptance of the HSCT will depend upon its ability to meet noise levels standards, currently assumed to be the FAR 36, Stage III levels now applied to newly designed subsonic transports. Reasearch is required to assure reliable prediction of HSCT airport community noise and evaluation of new noise reduction technologies.  The research must also examine the feasibility of still further HSCT noise reduction which may be required in the future."**

# COMMUNITY NOISE REDUCTION ELEMENTS

The noise heard on the ground as an aircraft flies overhead is not only a function of the propulsion system, but also dependent on the aircraft flight path and atmospheric propagation characteristics. In particular, a wing with good takeoff lift performance will help reduce observed noise by quickly carrying the offending engines to high altitudes.

Using noise source models developed in the propulsion noise research, with particular emphasis on takeoff conditions, the Community Noise research will include the following elements:

- Update of atmospheric propagation models.

- Investigation of innovative flight operations to minimize perceived noise, particularly utilization of high lift aerodynamics.

- Prediction of noise footprints (i.e., the ground area subjected to threshold or greater noise levels of interest such as FAR 36, Stage III) for assessment of overall acoustic performance.

## COMMUNITY NOISE REDUCTION   HIGH-SPEED RESEARCH PROGRAM

## ELEMENTS

### HIGH-LIFT AERODYNAMICS



### FLIGHT OPERATIONS

Advanced High Lift

Current Technology

Altitude

Runway

Downrange

### ATMOSPHERIC PROPAGATION



### REDUCTIONS IN NOISE FOOTPRINTS

HSCT 5.1 mi²     Airport     Concorde 74.8 mi²
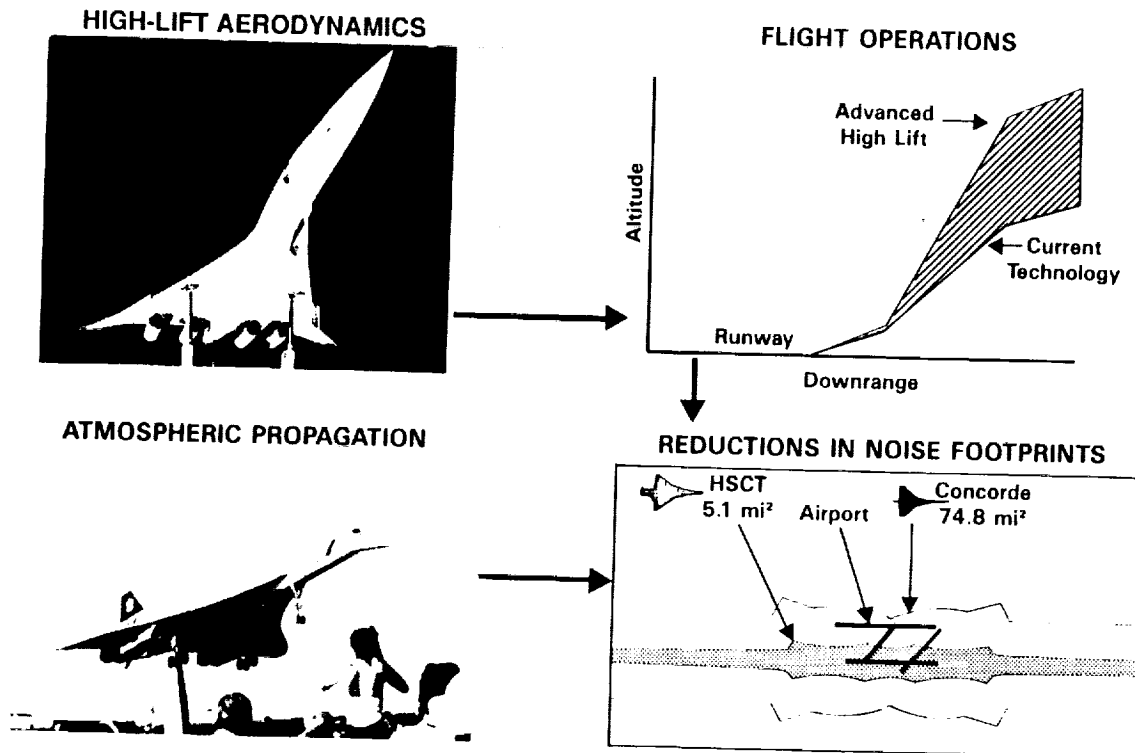
This figure illustrates two of the HSR Community Noise Issues.

The first issues is that of how the HSCT aircraft will be certified. The FAA issued on May 30, 1990 a Notice of Proposed Rulemaking that would require future supersonic transports to meet noise limits consistent with those required for future subsonic aircraft. It leaves open the possibility of providing sufficient flexibility in flight and measurement conditions to allow for optimization of aircraft environmental and economic characteristics and the use of computer controlled aerodynamic and thrust management systems. This allowed flexibility must be, of course, consistent with the required safety.

Based on experiences with the Concorde aircraft and from initial predictions of thrust necessary to achieve economic supersonic flight, it appears that noise from the propulsion plants will have to be reduced by about 20 dB. It appears possible to achieve about 12 to 15 dB reduction from new engine technology including the use of suppressor/ejectors. This still leaves about 5 dB which may have to be eliminated through the use of high-lift technology and advanced operating procedures.

One key element will be the development of system noise prediction capability to allow trade studies to be performed to allow optimal utilization of current and emerging aircraft and engine technologies.

# HSR COMMUNITY NOISE ISSUE

NOISE CERTIFICATION
???
NPRM

COMMUNITY
NOISE

APPROACH

SIDELINE

TAKEOFF
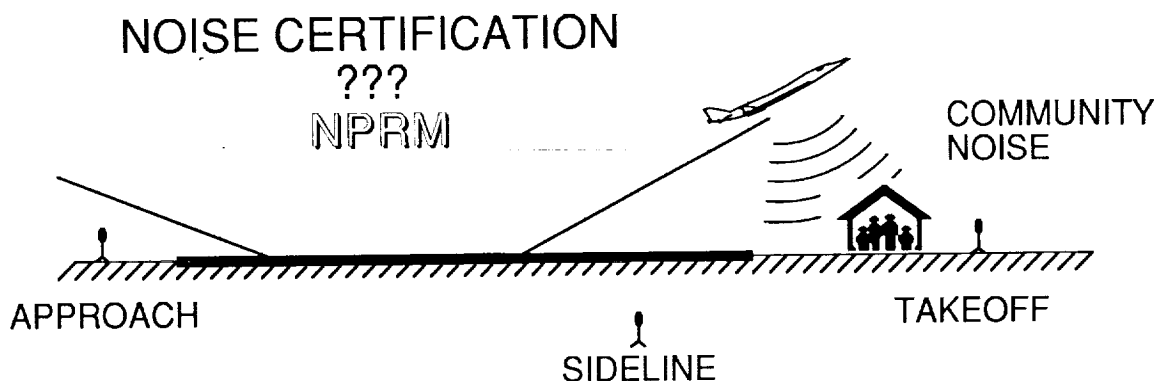
## 20 dB NOISE REDUCTION NEEDED

SOURCE NOISE REDUCTION                      15 dB POSSIBLE

ADVANCED OPERATING PROCEDURES }
HIGH LIFT TECHNOLOGY                      }          5 dB   ???

1069

## COMMUNITY NOISE REDUCTION APPROACH

Major advances have occurred recently in the capability to predict the complex vortical flows associated with highly swept wings operating at high angles of attack. The resulting high-lift aerodynamic techniques will be coupled with noise predictions for the advanced engine concepts being evaluated in the HSRP. Community noise computer codes will be modified to incorporate new modules that reflect advances such as active and passive jet noise suppression, and various nozzle geometries and exit velocity profiles.

Component and model-scale tests will be conducted to provide input to the predictive techniques and to help verify the accuracy of the completed analyses. These experiments will address the far-field community noise and the engine/airframe performance integration, as well as the high-lift devices that augment basic wing performance. Tradeoffs of operational procedures will then be conducted to develop new low-noise/high-lift systems for HSCT aircraft.

Concept verification in the HSRP will include a suitable combination of analysis and experiment.

## *COMMUNITY NOISE REDUCTION*   HIGH-SPEED RESEARCH PROGRAM

### APPROACH

| FY 1990 | FY 1991 | FY 1992 | FY 1993 | FY 1994 | FY 1995 |
|---------|---------|---------|---------|---------|---------|

**PREDICTIVE METHODOLOGY**
- SUPERSONIC AIRCRAFT NOISE          - ENROUTE NOISE COUPLING
- NONLINEAR WING THEORY

**SUPPORTING EXPERIMENTS**
- HIGH-LIFT SYSTEMS
- LOW NOISE/HIGH-LIFT SYSTEMS

**CONCEPT VERIFICATION**
- ENGINE/AIRFRAME INTEGRATION
- LOW NOISE/HIGHLY SWEPT WINGS

1070
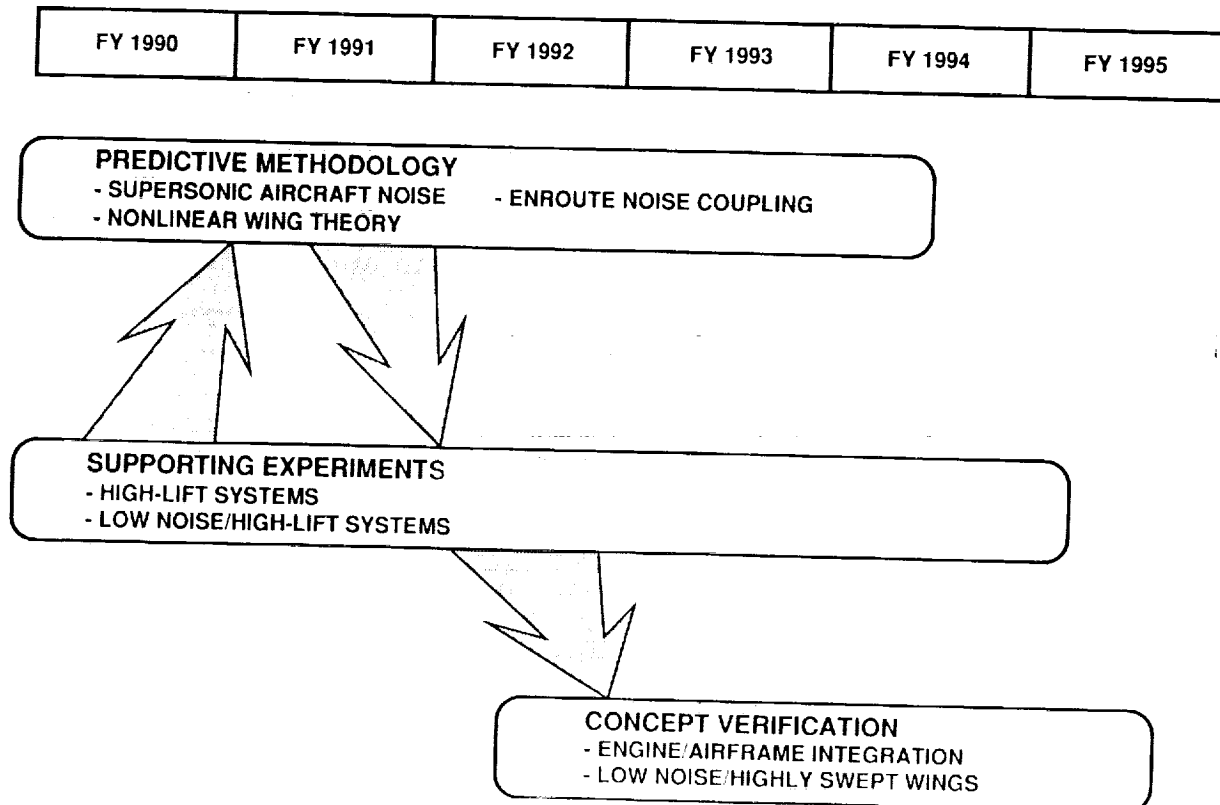
# PROGRAM SCHEDULE/MILESTONES

The schedule and milestones for the Aeroacoustic Analysis and Experiments (AA&E) technology area were originally laid out to provide by the 1995 time frame a sufficiently robust "jet noise" prediction capability to permit environmental and economic system trade-off studies using the potential benefits from concepts such as high-lift, laminar flow, jet exhaust suppression, etc. While the emphasis and ,hence, milestones of the schedule may change as new research/development modifies the relative importance of noise source contribution to community noise, the end goal has to remain firm. The challenge to meet this end lies in the ability to absorb into the on-going AA&E code development and prediction studies the unknown and unexpected elements which may arise. It is expected that this be accomplished in a manner that is consistent with the resources available to meet our established goals. However, one of our jobs - and one of the purposes of this workshop - is to identify any programmatic oversights or short-comings that may not be consistent with our assigned resources and to report to higher management viable alternatives towards meeting the the established goals.

## HIGH-SPEED RESEARCH PROGRAM (2 Level) — PROGRAM SCHEDULE/MILESTONES - LaRC



Schedule/milestones chart spanning years 1990–1995 (by quarter) with the following program elements:

- **537-01 ATMOSPHERIC EFFECTS**
  - 11 Analysis & Prediction Methods — 1st Model Assessment; Artic A/C Mission; 2nd Model Assessment; Antarctic A/C Mission; Model Validation
  - 22 System Studies — Contract Award; Standard Data Set; High-Lift Concepts; 3rd Model Assessment; Engine Concepts; Flt. Path Optimiz.; SLFC Sys. Eval.; Final Reports
- **537-02 EMISSIONS & SOURCE NOISE**
  - 22 Source Noise Anal. & Verif. Exps. — High Temp Effects; Low-Noise Nozzle; Flt. Effects Eval.; Low Noise & Prop. Integ. Eval.; Generic Nozzle Eval.; Coupled Source Noise Code; Passive/Active Control
- **537-03 COMM. NOISE & SONIC BOOM**
  - 20 Aeroacoustic Analysis & Experiments — Initial ANOPP Update; Airframe Noise Module; ANOPP Update; Jet Noise Module; Turbomachinery Module; Initial Jet Noise Update
  - 21 Sonic Boom Minim. & Acceptability — Method Validation; Refined Config.; Improved Design Method; Flight Tests; Interim Criteria; Program Decision; Opt. Studies
  - 22 High-Lift Technology — Concepts Refined; Separation Criteria; Piloted Simulation Assessment; Verification Tests
  - 23 Supersonic Laminar Flow Control — Swept Cyl. Tests; Apply Trans. Codes; Scaling Effects; Ph. 1 Flt. Tests; Adv. Config. Studies; CDR LE Panel; CDR Ext. Panel; Concept Optimiz.; Ph. 3 Flt. Tests; Ship 2 Arrive DFRC; Quiet Tunnel Test; Suct. Reqmnts; Calibrate Trans. Codes; Ph. 2 Flt Tests

◇ PLANNED MILESTONE   ◇–◇ DELAYED MILESTONE   ◆ COMPLETED MILESTONE

THIS PAGE INTENTIONALLY BLANK

1072

# Session VIII. Aeroacoustic Analysis and Community Noise

New Broadband Shock Noise Model and Computer Code for ANOPP
*N. N. Reddy, Lockheed Aeronautical Systems Company*

**THIS PAGE INTENTIONALLY BLANK**

$S_2 - 7 /$
$/2032$

# NEW BROADBAND SHOCK NOISE MODEL
# AND COMPUTER CODE FOR ANOPP

N. N. Reddy

Lockheed Aeronautical Systems Company
Marietta, Georgia

Figure 1

## BROADBAND SHOCK NOISE PREDICTION

The basic mechanism for broadband shock noise in the supersonic jets is the interaction between the shock waves and the turbulence in the jet exhaust. This source is in addition to jet mixing noise.

Far-field noise prediction method for this source was developed by Harper-Bourne and Fisher in 1974 by using very limited data (ref. 1). This method was extended by Tanna using hot jet data of convergent nozzles and was adopted as an SAE recommended procedure for shock associated jet noise (ref. 2). During the same time, Stone of NASA-Lewis developed an empirical procedure using the test data (ref. 3). Both of these methods were incorporated in ANOPP (ref. 4). The SAE method is applicable for single stream convergent circular nozzles. The Stone's method was applicable for single/dual stream coaxial nozzles. The flight effects are incorporated as $[1-M_\infty\cos\theta]^{-4}$ (figures 1 and 2).

≡✈️*Lockheed*

# Broadband Shock Noise

- **Mechanism**
  - **Interaction Between Shock Waves and Turbulence**
  - **Addition to Turbulent Mixing Noise**

- **Prediction**

  - **ANOPP/SAE**
    - **Harper-Bourne and Fisher - 1974**
    - **SAE - 1976**
    - **Convergent Nozzles**
    - **Flight Effects - $[1-M_\infty \cos\theta]^{-4}$**

  - **ANOPP/Stone**
    - **Single/Duel Stream Coaxial Jets**
    - **Empirical Derivation**
    - **Not Sensitive to Jet Temperature**
    - **Flight Effects - $[1-M_\infty \cos\theta]^{-4}$**

1076

Figure 2

Self Explanatory

*Lockheed*

# Broadband Shock Noise Prediction Code

| ANOPP - Shock Noise |
| --- |

| SAE<br>- Harper - Bourne<br>  Tanna<br>  Convergent - Circular<br>    Single Stream<br>    Nozzles | Stone - NASA Lewis<br>Data Correlation<br>Convergent<br>  Single/Duel Stream<br>  Coaxial Nozles |
| --- | --- |
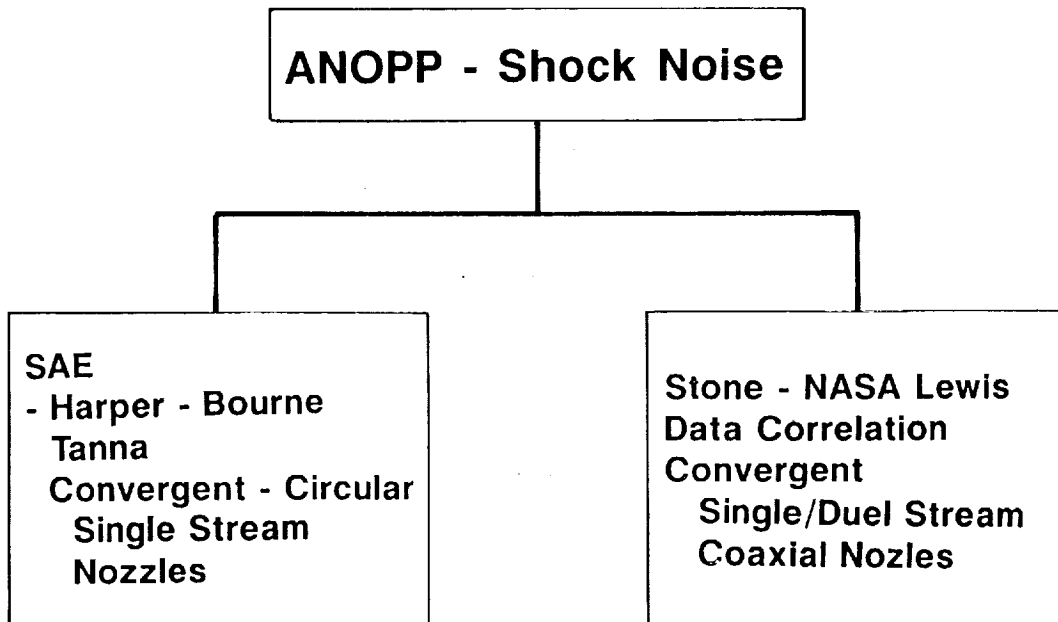
Figure 3

ANOPP VALIDATION FOR SHOCK NOISE

The existing ANOPP predictions for shock noise are evaluated using NASA's ambient temperature static C-D nozzle data (ref. 5). The typical results are shown in Figure 3. Both SAE method and Stone's method underpredict the peak noise levels. The spectral characteristics appears to be different. To improve the accuracy, development of new prediction code for broadband shock noise was initiated.

≡Lockheed     **Validation of ANOPP**

## NASA's Data

**Nozzle Exit Diameter = 0.04989m;**

$M_d$ = 1.50;  $M_j$ = 1.80

Figure 4
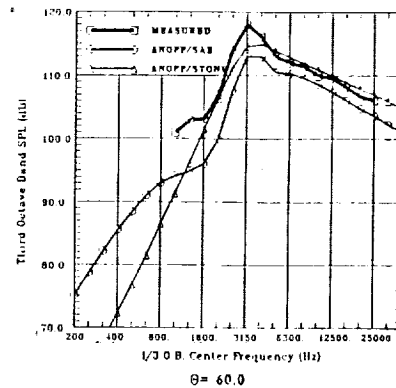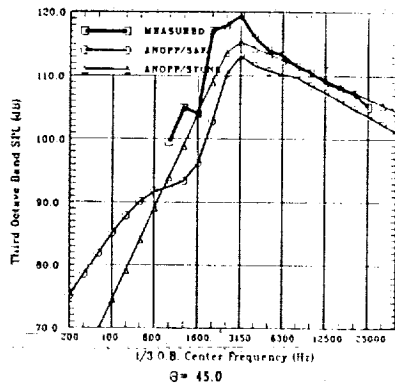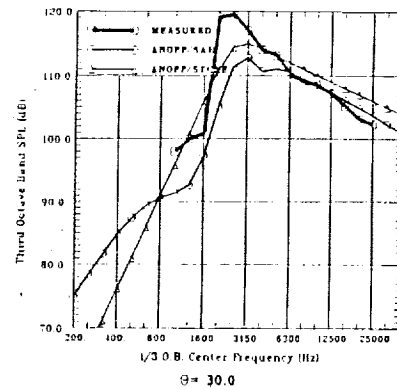
## NEW BROADBAND SHOCK NOISE PREDICTION CODE

Recently C. K. W. Tam has developed a stochastic model theory to predict near- and far-field noise for supersonic jets (ref.6). This theoretical formulation is based on the proposition that broadband shock noise is generated by the interaction of the downstream propagating large scale turbulence structures and shockcell system. This method is applicable for moderately imperfectly expanded circular single stream jets. The jet temperature effects are included. The important input parameters to predict the shock noise levels are shown in Figure 4.

A computer code for ANOPP is being developed using this prediction method. Initially, the prediction code is applicable for circular nozzles with static (without flight effects) conditions.

# ≡Σ)Lockheed
# Broadband Shock Noise

- **New Prediction Model**

  - **Background - Tam's Theory-1989-90 [JSV(1990) 140(1) 55-71]**
    - **Interaction Between Large Turbulence Structure and Shock Cells**

  - **Method - Convergent and C-D Nozzles**
    - **Moderately Imperfectly Expanded Jets (Over and Under Expanded)**
    - **Jet Temperature Effects Included**

  - **Variables - $M_d$, Design Jet Mach Number**
    - **$M_j$ , Jet Mach Number**
    - **$D_n$ , Nozzle Exit Diameter**
    - **$D_j$, Fully Expanded Jet Diameter**
    - **$T_t$, Jet Stagnation Temperature**
    - **$T_\infty$, Ambient Temperature**

Figure 5

NEWS BROADBAND SHOCK NOISE CODE - VALIDATION

The new prediction code is validated against two sets of static test data: (1) NASA-Langley data obtained by Norum and Seiner (ref. 5), and (2) Lockheed/USAF data (ref. 7).

≡⁊*Lockheed*

# Broadband Shock Noise

## Validations

- **NASA Data (Norum & Seiner - NASA TM84521, 1982)**
  - Ambient Temperature Jets
  - Convergent Nozzle
  - C-D Nozzle ($M_d = 1.5$)
    * Overexpanded ($M_j < M_d$)
    * Underexpanded ($M_j > M_d$)
  - C-D Nozzle ($M_d = 2.0$)
    * Overexpanded
    * Underexpanded

- **Lockheed Data (AFAPL-TR-76-65, 1976)**
  - Ambient and Heated Jets
  - Convergent Nozzle

1080

Figure 6

## EFFECT OF TABS (SCREECH SUPPRESSIONS)

The test data in reference 5 are presented for jet, ambient temperature static conditions for three nozzles. The three nozzles used were, convergent nozzle, Mach 1.5 C-D nozzle and Mach 2.0 CD nozzle. The test data were obtained with and without using any tabs at the nozzle exit (screech suppressors). In order to compare the prediction with the measured data, the effect of tabs on the broadband shock noise was evaluated by comparing the spectra with and without spectra as shown in Figure 6. It is clear from this figure that the tabs reduce the peak broadband noise in addition to eliminating the screech tones. Therefore, the data without tabs were used in validating the prediction code. It should be noted that the data for 45° angle shows that there is about 5db difference throughout the frequency range. This difference at 45° angle appears to be consistent for most of the data points.



Effect of Tab (Screech Suppressor)

$M_d = 1.0$ , $M_j = 1.221$ $(\beta = 0.70)$

Figure 7

Self Explanatory

**Lockheed**
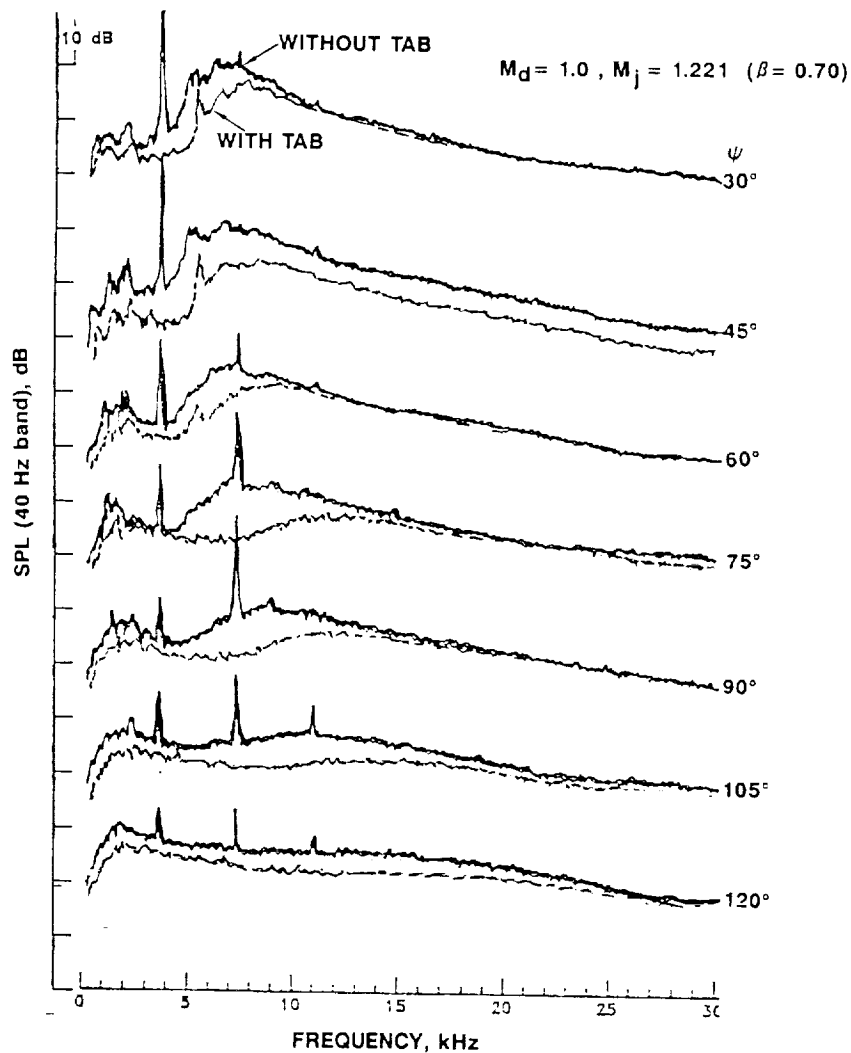
# Broadband Shock Noise

## Validation

### NASA Convergent Nozzle Data

## VALIDATION - NASA CONVERGENT NOZZLE DATA

The predicted results are compared with the measured data for convergent nozzles in the following two figures (8 and 9). The angles indicated in these figures are the angles from forward axis. Figure 8 is for jet Mach number of 1.221 and Figure 9 is for jet Mach number of 1.672. It is clear from these figures that there is a good agreement between prediction and measurement at all angles.

# Compaison of TAM's Prediction with NASA's Measured Data

$M_d = 1.0$; $M_j = 1.221$ ($\beta = 0.70$), $Dn = 0.03982\,m$

# Comparison of TAM's Prediction with NASA's Measured Data



$M_d = 1.0$; $M_j = 1.672$ ($\beta = 1.34$), $Dn = 0.03982$ m

10 dB

MEASUREMENT

PREDICTION

SPL (40 Hz band), dB

$\psi$
30°

45°

60°

75°

90°

105°

120°

FREQUENCY, kHz

0    5    10    15    20    25    3(

1084
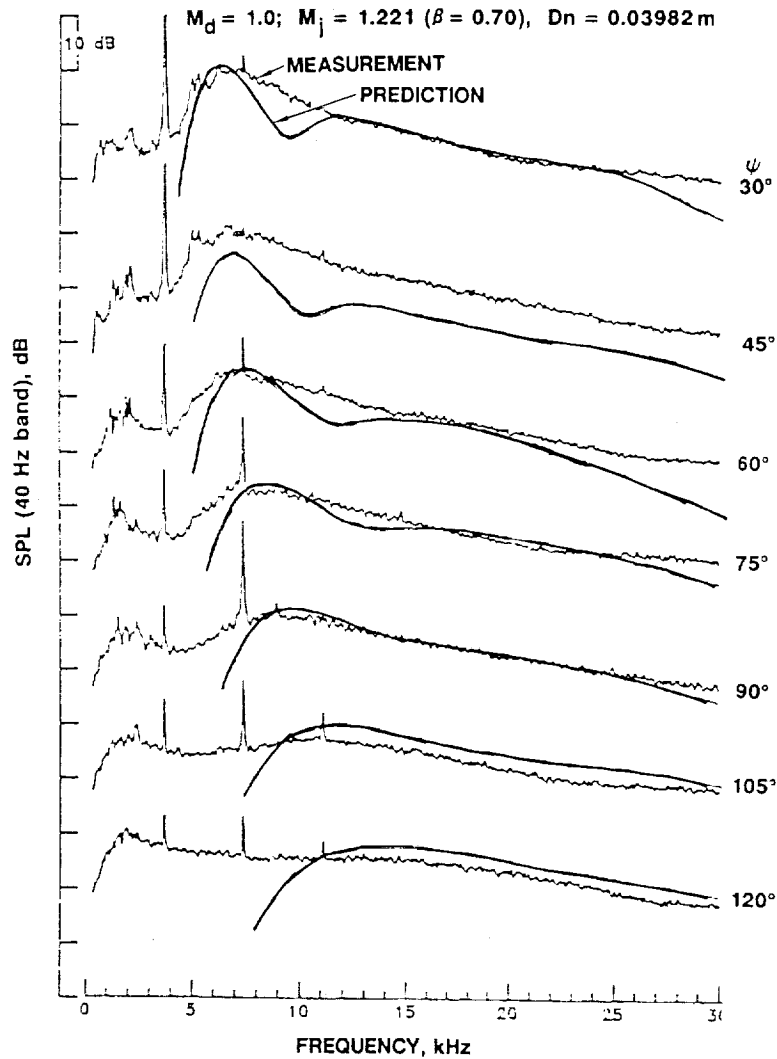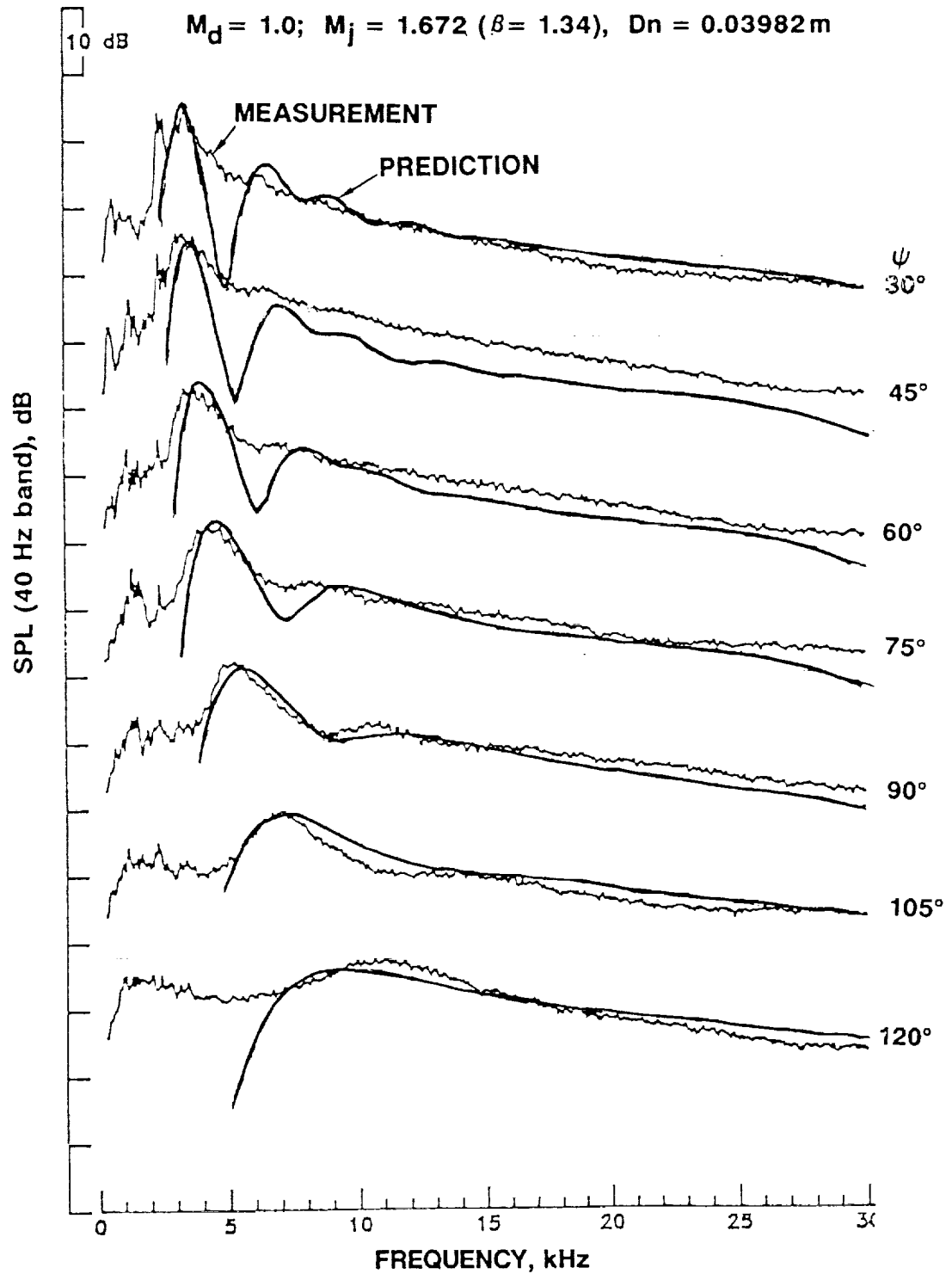
VALIDATION - NASA MACH 1.5 CD NOZZLE DATA

The following two figures illustrate the comparison of prediction with the measured data for convergent divergent nozzle with design Mach number of 1.5. The test data used in these comparisons is obtained from the nozzles without tabs. Figure 20 is for Mach 1.5 nozzle with overexpanded jet (MJ=1.28). Figure 11 is the comparison of prediction with measurement for Mach 1.5 nozzle with underexpanded jet (MJ=1.99).

## Comparison of TAM's Prediction with NASA's Measured Data



$M_d = 1.5$; $M_j = 1.28$ ($\beta = 0.80$), Dn = 0.04267m
CD NOZZLE OVER EXPANDED

MEASUREMENT
PREDICTION

$\psi$
30°
45°
60°
75°
90°
105°
120°

SPL (40 Hz band), dB

FREQUENCY, kHz

# Comparison of TAM's Prediction with NASA's Measured Data

$M_d = 1.5$;  $M_j = 1.990$ ($\beta = 1.72$), $D_n = 0.04267\,m$

CD NOZZLE UNDER EXPANDED
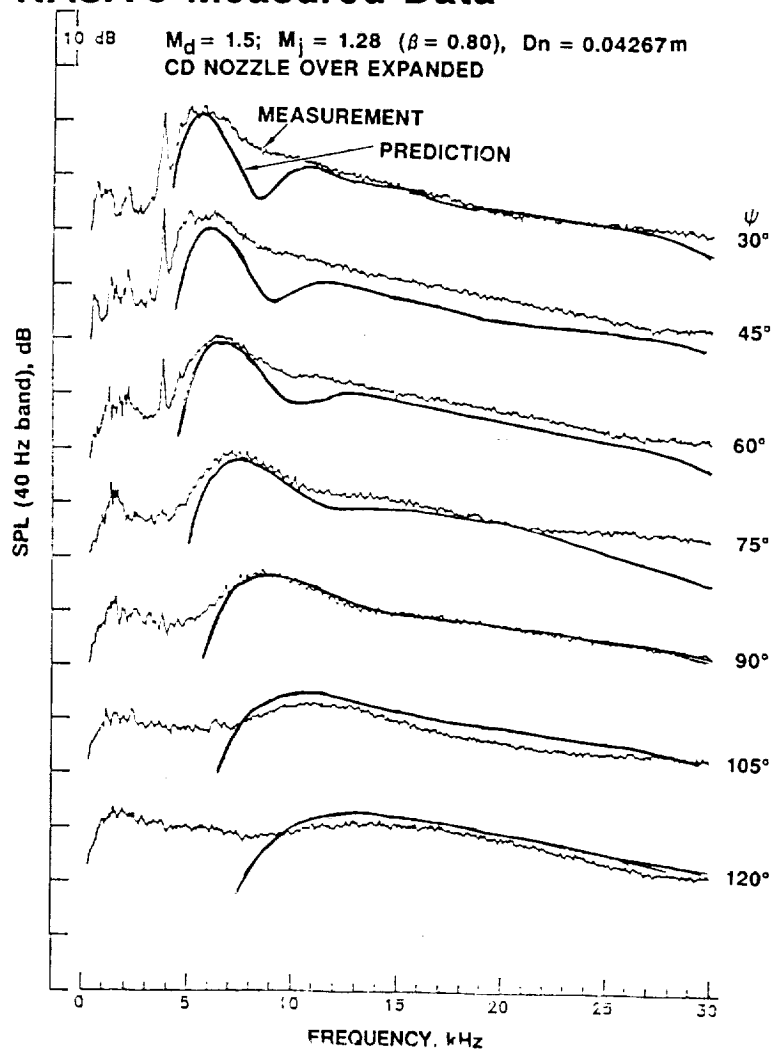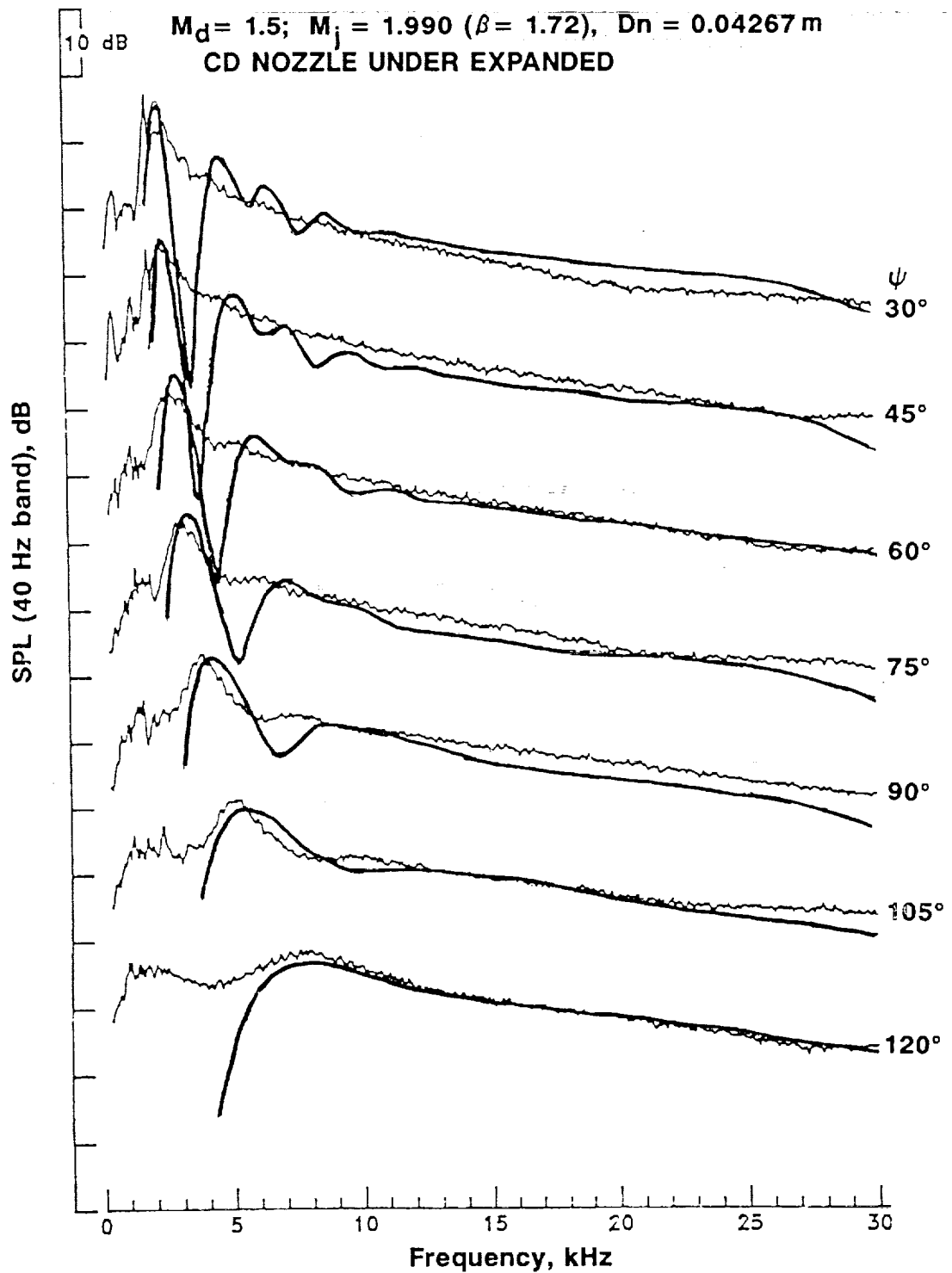
Figure 12

Self Explanatory

**Lockheed**

# Broadband Shock Noise

## Validation

### NASA CD Nozzle Data

## VALIDATION - NASA MACH 2.0 CD NOZZLE

The following two figures (13 and 14) illustrate the comparison of prediction with the measured data for convergent divergent nozzle with design Mach number of 2.0. There is a good agreement between the prediction and data.

# Comparison of TAM's Prediction with NASA's Measured Data

$M_d = 2.0$;  $M_j = 1.487$ ($\beta = 1.10$),  $D_n = 0.4989\,m$
CD NOZZLE OVER EXPANDED

10 dB

$\psi$

30°

45°

60°

75°

90°

105°

120°

SPL (40 Hz band), dB

FREQUENCY, kHz

1088
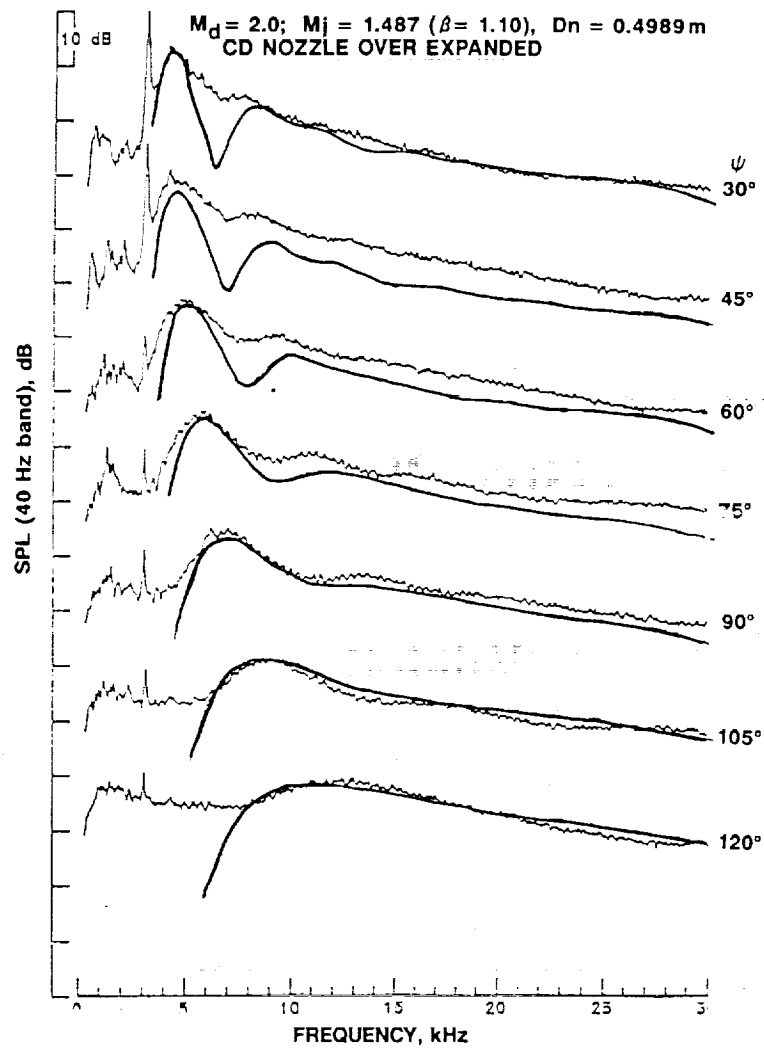
# Comparison of TAM's Prediction with NASA's Measured Data

$$M_d = 2.0, \quad M_j = 2.24 \; (\beta = 2.00) \quad Dn = 0.04989 \, m$$

### CD NOZZLE UNDER EXPANDED
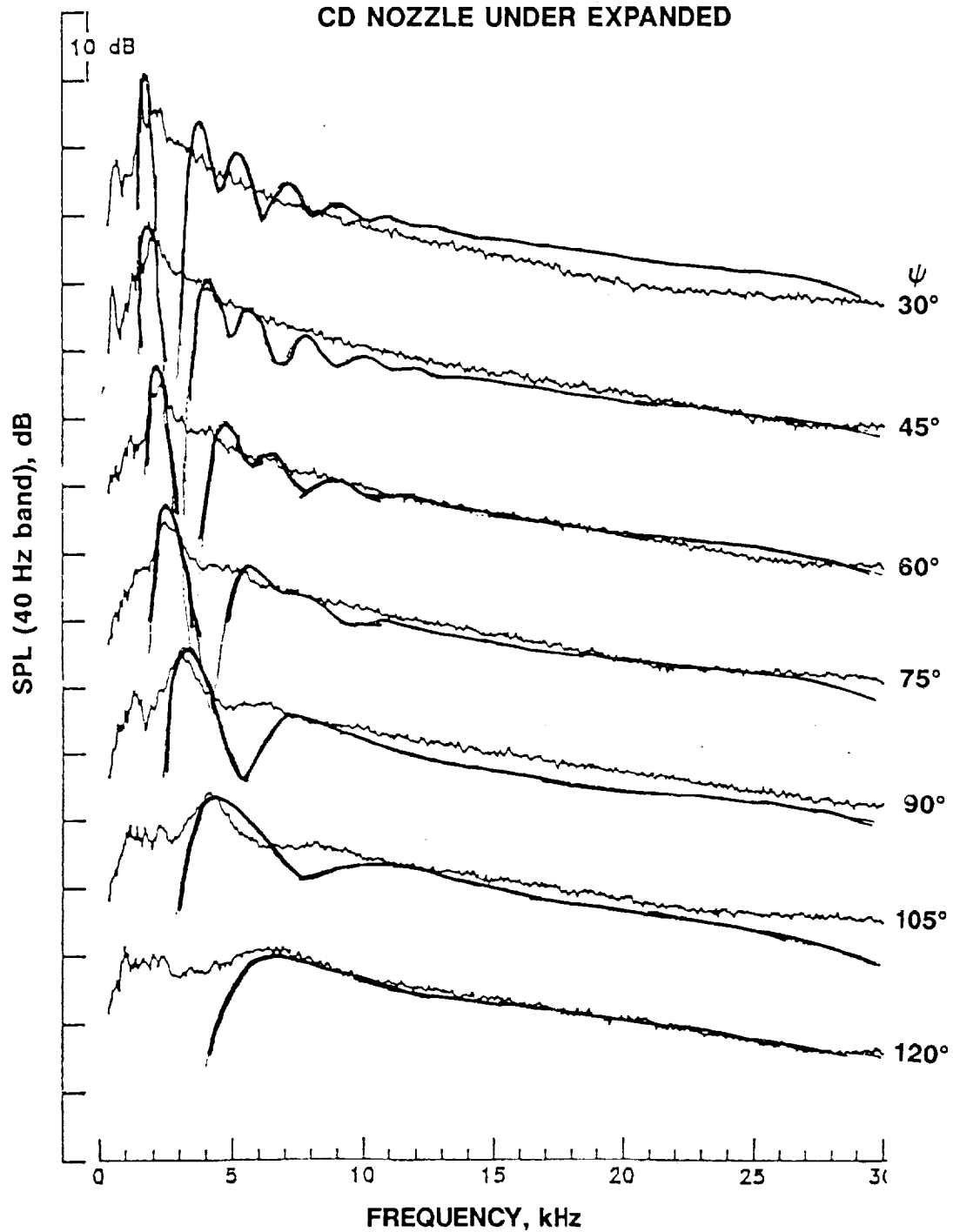
Figure 15

Self Explanatory

**≡☆Lockheed**

# Broadband Shock Noise

## Validation

### Lockheed Data

Figure 16

## VALIDATION - LOCKHEED DATA

The following figures (16a-16f) compare the predictions with Lockheed's test data. These data were obtained for convergent nozzles with ambient temperature jet and heated jet. Figures 16a and 16b are for ambient temperature jets (jet stagnation temperature = ambient temperature). Figures 16c and 16d are for isothermal jets (jet temperature=ambient temperature). Figures 16e and 16f are for hot jets (jet temperature is higher than ambient temperature). The tests were conducted with tabs (screech suppressors) at the nozzle exit. The general spectral characteristics of prediction agrees with the measured data. The peak levels of the measured data, however, are less than the prediction. These differences in the peak levels are attributed to the presence of the tabs as illustrated in figure 6.

**≡⅋Lockheed** **Comparison of TAM's Prediction with Lockheed's Data**

$M_d = 1.0$   $M_j = 1.49$;   $Dn = 0.0508\,m$   $\psi = 45°$   $\dfrac{T_t}{T_\infty} = 1.0$
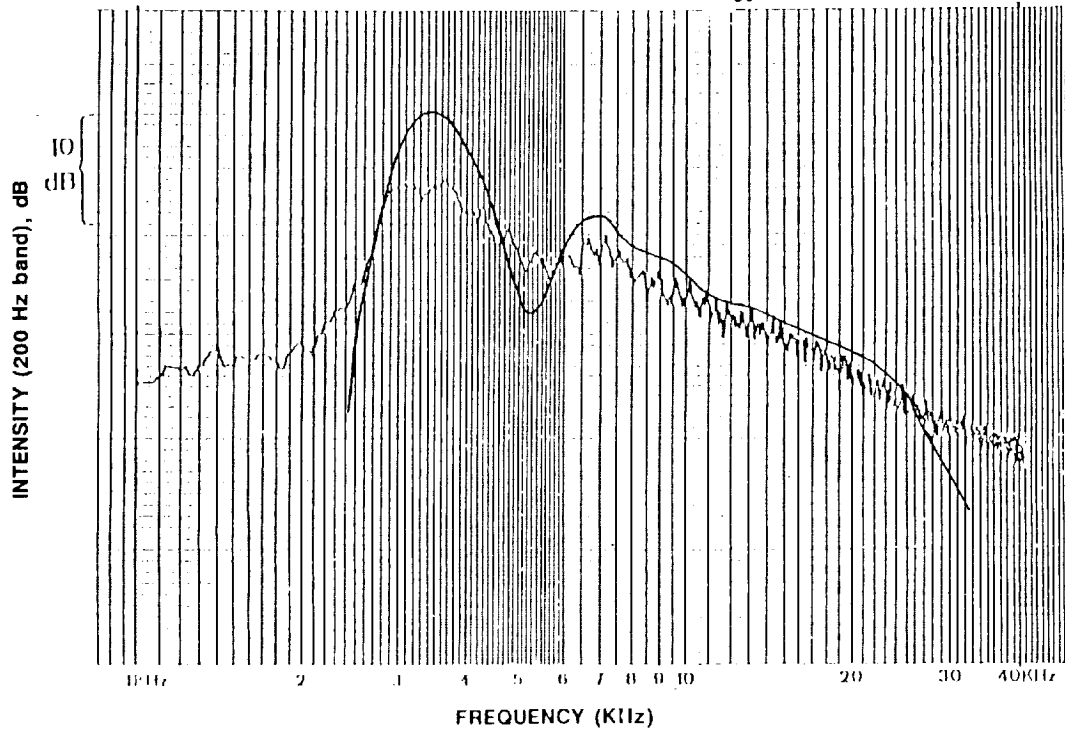


FREQUENCY (KHz)

**Comparison of TAM's Prediction with Lockheed's Data**

$M_d = 1.0$  $M_j = 1.49$;  $Dn = 0.0508m$  $\psi = 90°$  $\dfrac{T_t}{T_\infty} = 1.0$



INTENSITY (200 Hz band), dB

10 dB

FREQUENCY (KHz)

1KHz  2  3  4  5  6  7  8  9  10  20  30  40KHz

1092
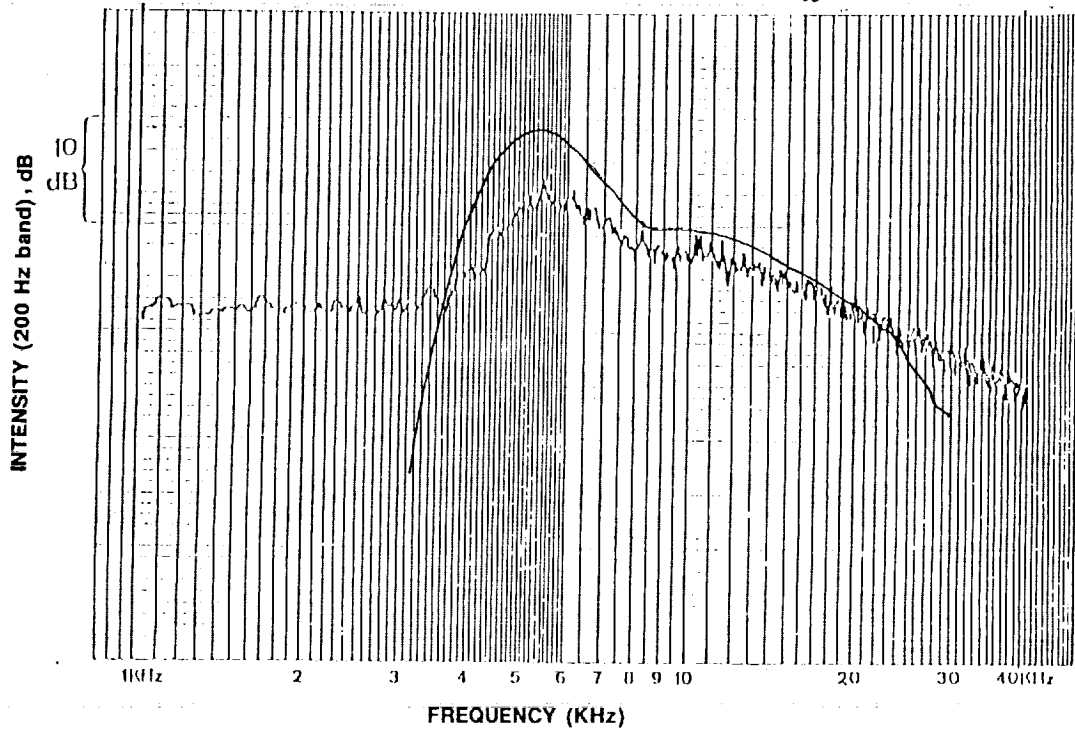
**≡⋦ꟾLockheed** **Comparison of TAM's Prediction with Lockheed's Data**

$M_d = 1.0$; $M_j = 1.372$; $Dn = 0.0508m$ $\psi = 45°$ $\frac{T_t}{T_\infty} = 1.367$, $\frac{T_J}{T_\infty} = 1.0$

INTENSITY (200 Hz band), dB

10 dB

1KHz    2    3    4    5    6    7    8    9    10    20    30    40KHz

FREQUENCY (KHz)
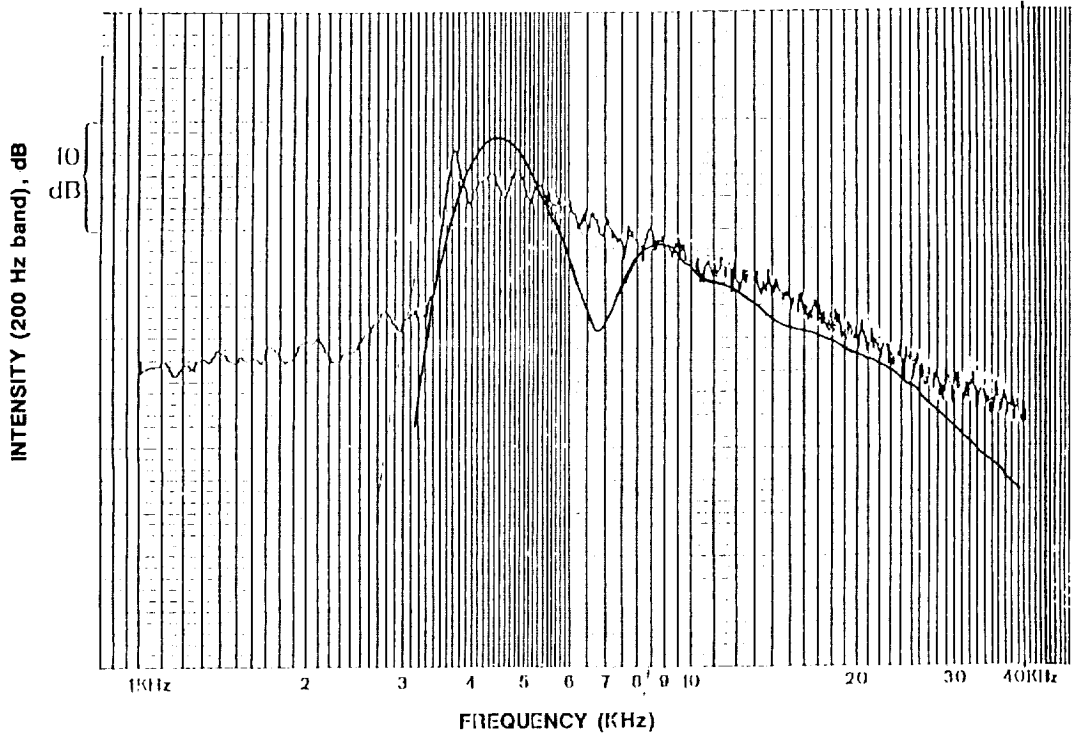
**Lockheed** Comparison of TAM's Prediction with Lockheed's Data

$M_d = 1.0$; $M_j = 1.49$; $\psi = 90°$ $Dn = 0.0508\,m$ $\dfrac{T_t}{T_\infty} = 1.367,$ $\dfrac{T_j}{T_\infty} = 1.0$

INTENSITY (200 Hz FILTER), dB

10 dB

1KHz 2 3 4 5 6 7 8 9 10 20 30 40KHz

FREQUENCY (KHz)

1094
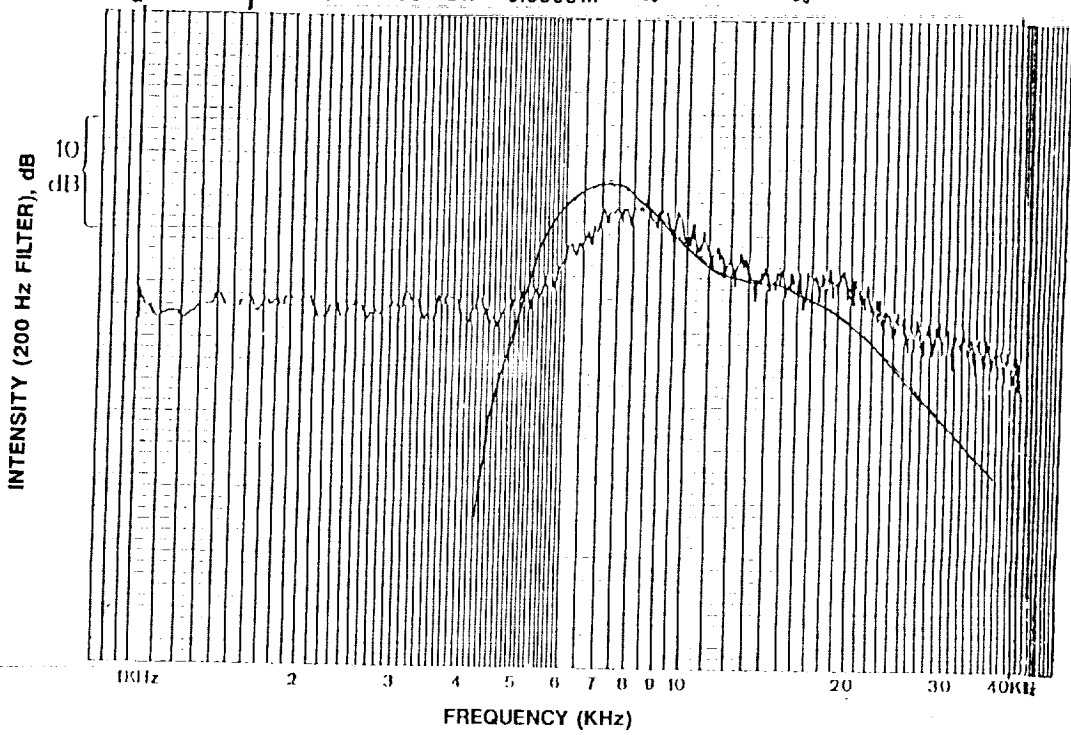
**Lockheed** Comparison of TAM's Prediction with Lockheed's Data

$M_d = 1.0$; $M_j = 1.49$; $\psi = 45°$  Dn = 0.0508m      $\dfrac{T_t}{T_\infty} = 2.524$
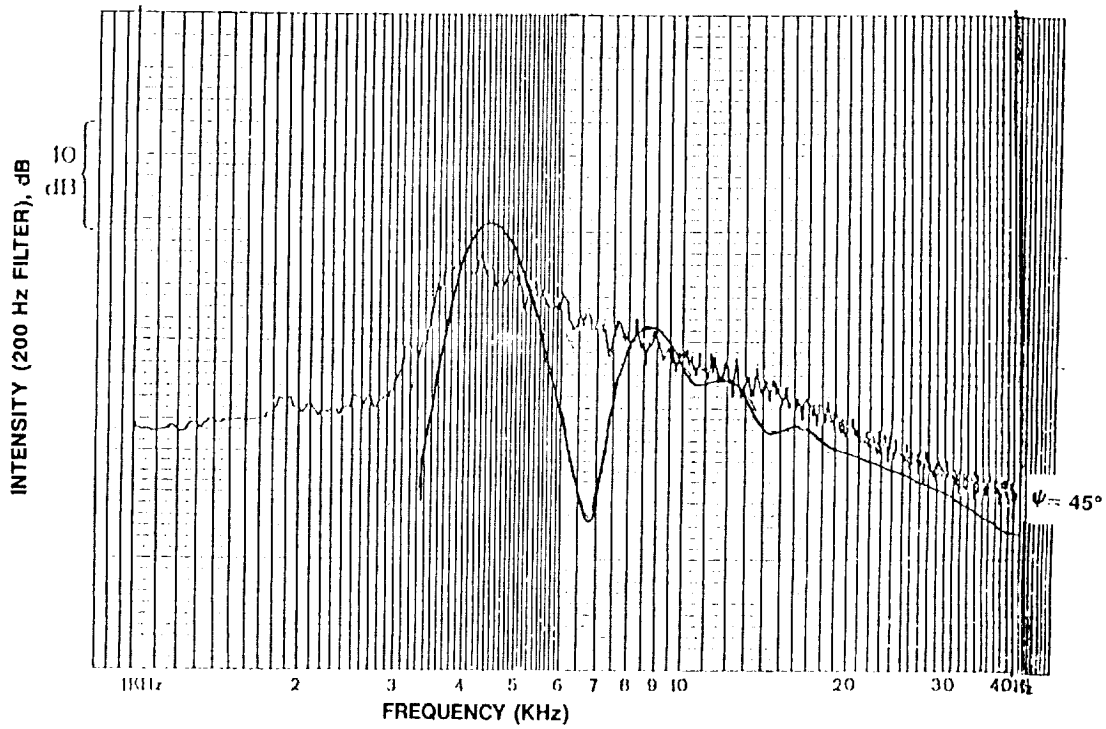
# ≡≥∤Lockheed   Comparison of TAM's Prediction with Lockheed's Data

$M_d = 1.0$;   $M_j = 1.48$;   $\Psi = 90°$   $Dn = 0.0508\,m$   $\dfrac{T_t}{T_\infty} = 2.524$

INTENSITY (200 Hz FILTER), dB

10 dB

1 Hz   2   3   4   5   6   7   8   9   10   20   30   40 kHz

FREQUENCY (KHz)

Figure 17

Self Explanatory

**Lockheed**
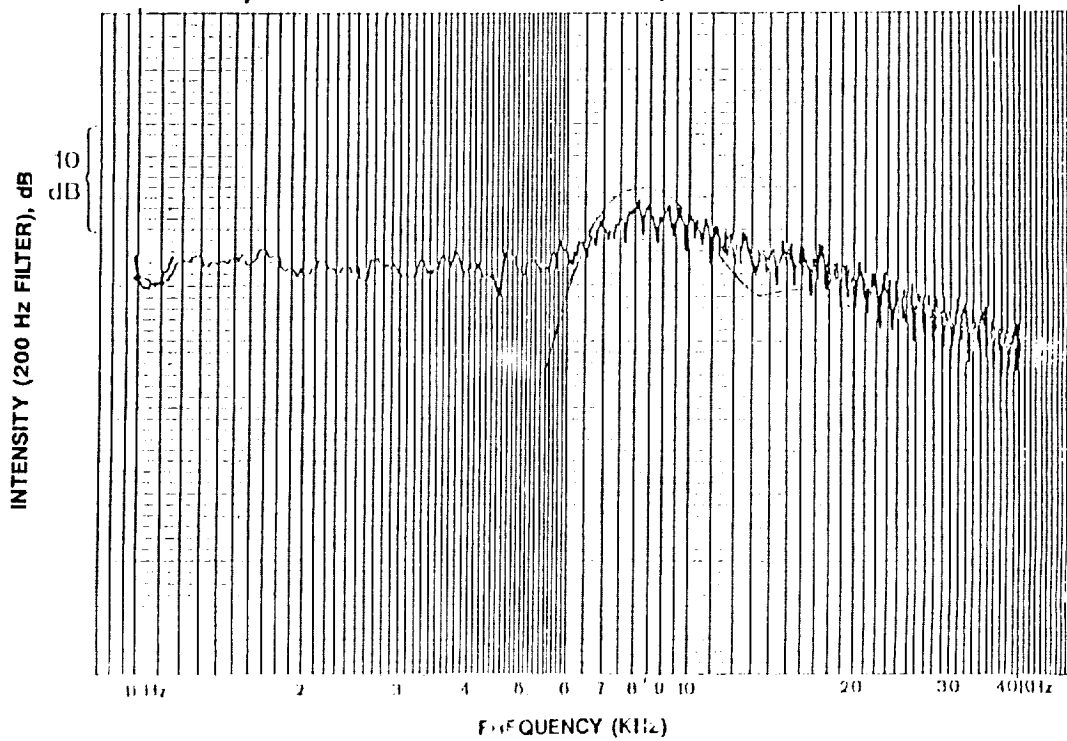
# Comparison of
# New Model With Existing Models

- ANOPP/SAE
- ANOPP/Stone

Figure 18

# COMPARISON OF NEW MODEL WITH EXISTING ANOPP

The new spectral results from the new shock noise prediction code are compared with the results from the existing ANOPP codes (SAE and Stone) in the following figures 18a and 18b. These comparisons are for circular nozzles ambient temperature jet and static condition. Figure 18a is for convergent nozzle and figure 18b is for Mach 1.5 CD nozzle.

≡b/Lockheed

## Comparison of TAM's Prediction with ANOPP
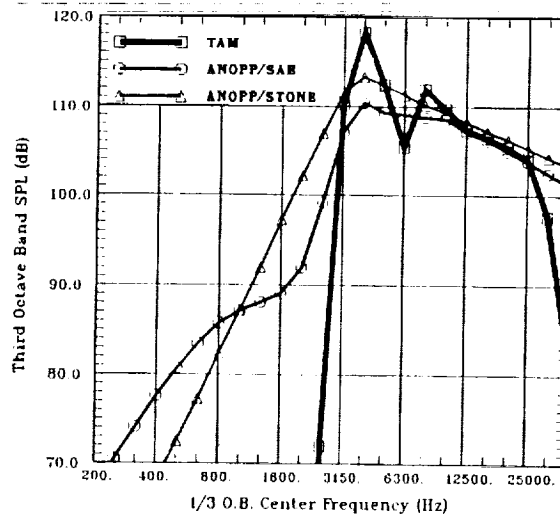


Nozzle Exit Diameter=0.03982 m;   Md= 1.00;   Mj= 1.49
Θ= 30.0

# Comparison of TAM's Prediction with ANOPP
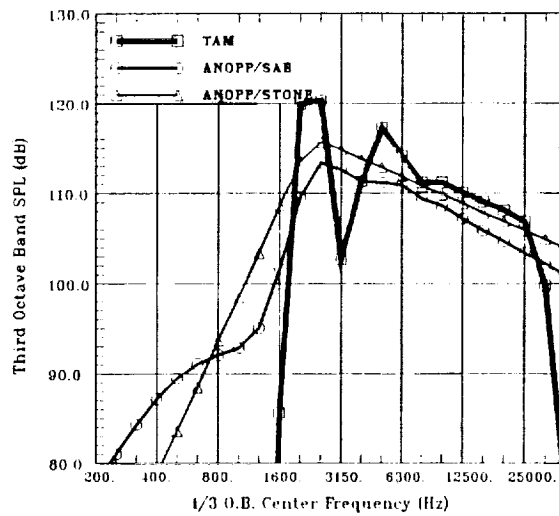


Nozzle Exit Diameter=0.04267 m;   Md= 1.50;   Mj= 1.99
θ= 30.0

Figure 19

CONCLUDING REMARKS - FURTHER DEVELOPMENTS

The new prediction code is based on theoretical background using small scale experimental data. This procedure is applicable for convergent, convergent divergent circular nozzles for moderately imperfectly expanded jets. The temperature effects are included, however, the flight effects are not included. This prediction code is validated against two independent sets of model data. The correlation between prediction and measurement are excellent.

This prediction method must be extended to account for flight effects and to noncircular nozzles. The code must be validated against a larger data base including flight test data. The flight effects on shock noise appears to be an important issue to be resolved. This required a good data base.

≡⟩Lockheed

# Broadband Shock Noise

## Further Developments

- Flight Effects

- Noncircular Nozzles

- Validations
  - Hot Jet Data
  - Flight Test Data

- Require More Data

1100

## REFERENCES

1. Harper-Bourne, M. and Fisher, M. J.: The Noise from Shock Waves in Supersonic Jets. AGARD-CP-131, March 1974.

2. Gas Turbine Jet Exhaust Noise Prediction. ARP 876, Appendix C, Soc. Automot. Eng., March 1978.

3. Stone, James R. and Montegani, Francis J.: An Improved Prediction Method for the Noise Generated in Flight by Circular Jets. NASA TM-81470, 1980.

4. Zorumski, William E.: Aircraft Noise Prediction Program - Theoretical Manual, NASA Technical Memorandum 83199, Part 2, February 1982.

5. Norum, T. D. and Seiner, J. M.: Measurements of Mean Static Pressure and Far-Field Acoustics of Shock-Containing Supersonic Jets.

6. Tam, C. K. W.: Broadband Shock-Associated Noise of Moderately Imperfectly Expanded Supersonic Jets, Journal of Sound and Vibration

7. The Generation and Radiation of Supersonic Jet Noise, Volume IV Shock Associated Noise Data. Technical Report AFAPL-TR-76-65, June 1976.

**THIS PAGE INTENTIONALLY BLANK**

1102

# Session VIII. Aeroacoustic Analysis and Community Noise

*Cmif*

Community Noise Technology Needs - Boeings Perspective
*Gene L. Nihart, Boeing Commercial Airplane Group*

THIS PAGE INTENTIONALLY BLANK

# COMMUNITY NOISE TECHNOLOGY NEEDS
## BOEINGS PERSPECTIVE

*S3 - 71*

*12033*

G. L. Nihart

Boeing Commercial Airplane Group

Seattle, Washington

High Speed Research
First Annual Workshop
May 14-16, 1991

# COMMUNITY NOISE TECHNOLOGY NEEDS
## BOEING PERSPECTIVE

1106

Airport community acceptance of HSCT noise levels will depend on the relative noise levels to airplanes flying at the time of introduction. The 85 dBA noise contours for the range of large subsonic airplanes that are expected to be in service in the early 21st century are shown as a shaded area. A certifiable HSCT noise contour, as shown, would be somewhat wider along the runway but about the same in the residential areas downrange. An HSCT noise rule should insure this noise capability.

# COMMUNITY NOISE

## 85 dBA FOOTPRINTS

HSCT

Range of Large Subsonic Airplanes

<--- 1 Mile --->
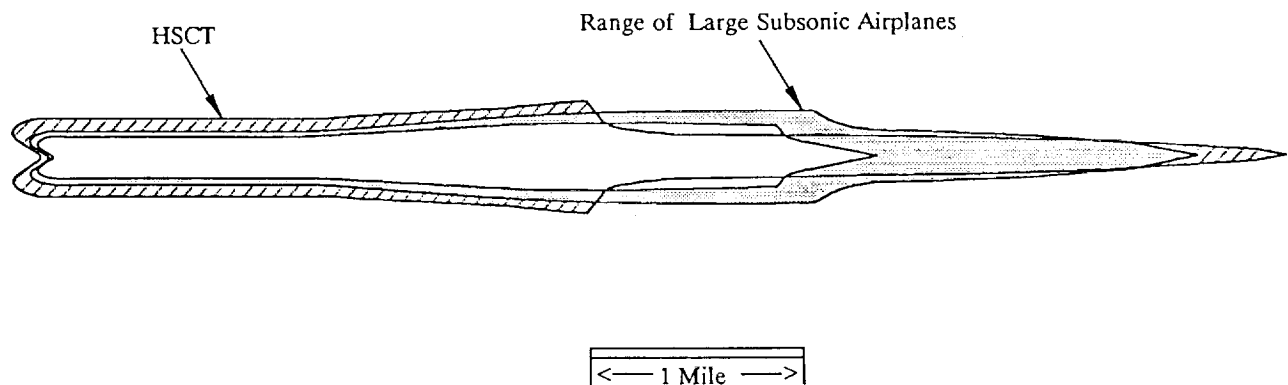
FIGURE 1

# COMMUNITY NOISE SOURCES

Jet noise is the primary noise source at the sideline measuring point but at the downrange and approach measuring points burner noise is also important In addition turbine and air-frame noise are important sources during approach. Prediction accuracy for all of the sources and for noise reduction features, such as the jet exhaust noise suppression nozzle, will have a major impact on design features such as engine sizing.
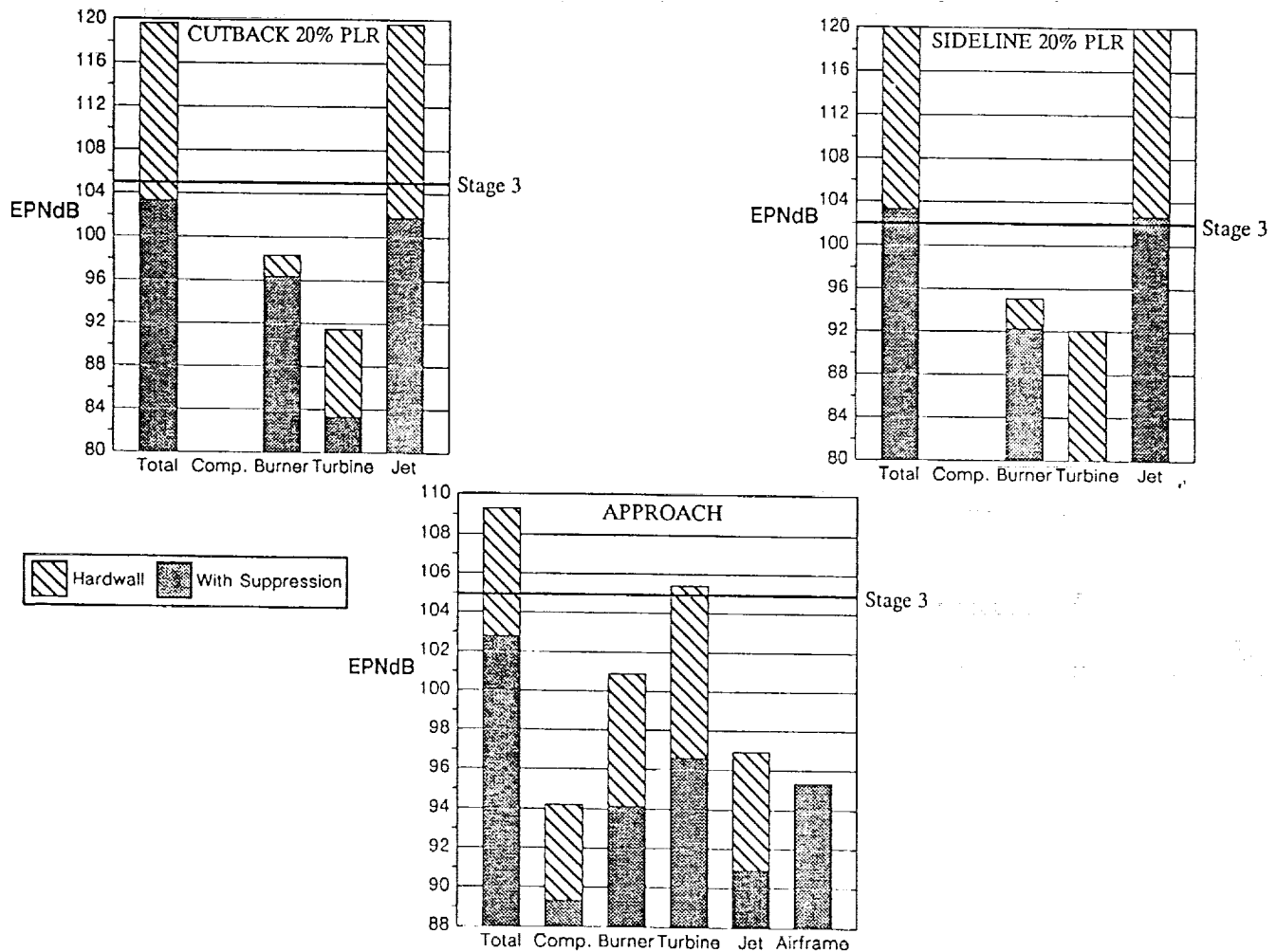


Figure 2  Noise Components Turbine Bypass Turbojet Engine

# JET NOISE PREDICTION TECHNOLOGY

CURRENT PROCEDURES ARE :

* EMPIRICAL

* PREDICT UNSUPPRESSED JET ; ie, R–C

* PREDICT SPECIFIC SUPPRESSION CONFIGURATIONS

IDEAL PROCEDURE :

* ANALYTICAL PROCEDURE THAT PREDICTS ABSOLUTE LEVELS

* FLEXIBLE SUCH THAT SUPPRESSION DEVICES CAN BE SCREENED

* USES PREDICTABLE FLOW PARAMETERS OR RESULTS OF CFD
  MODELING

FIGURE 3

# NFM NOZZLE PREDICTION VERSUS DATA

The basic low bypass ratio jet noise prediction program at Boeing is empirical
and is for a round convergent (RC) nozzle. This program was used to predict
externally generated noise based on the fully mixed stream and the internal noise
from one of the primary nozzles using the aspirated flow as the free stream. The
predicted noise levels are then added. Shock cell noise predicted for the primary
nozzle is reduced by 7 dB to account for the convergent–divergent (CD)
expansion of the primary nozzle.
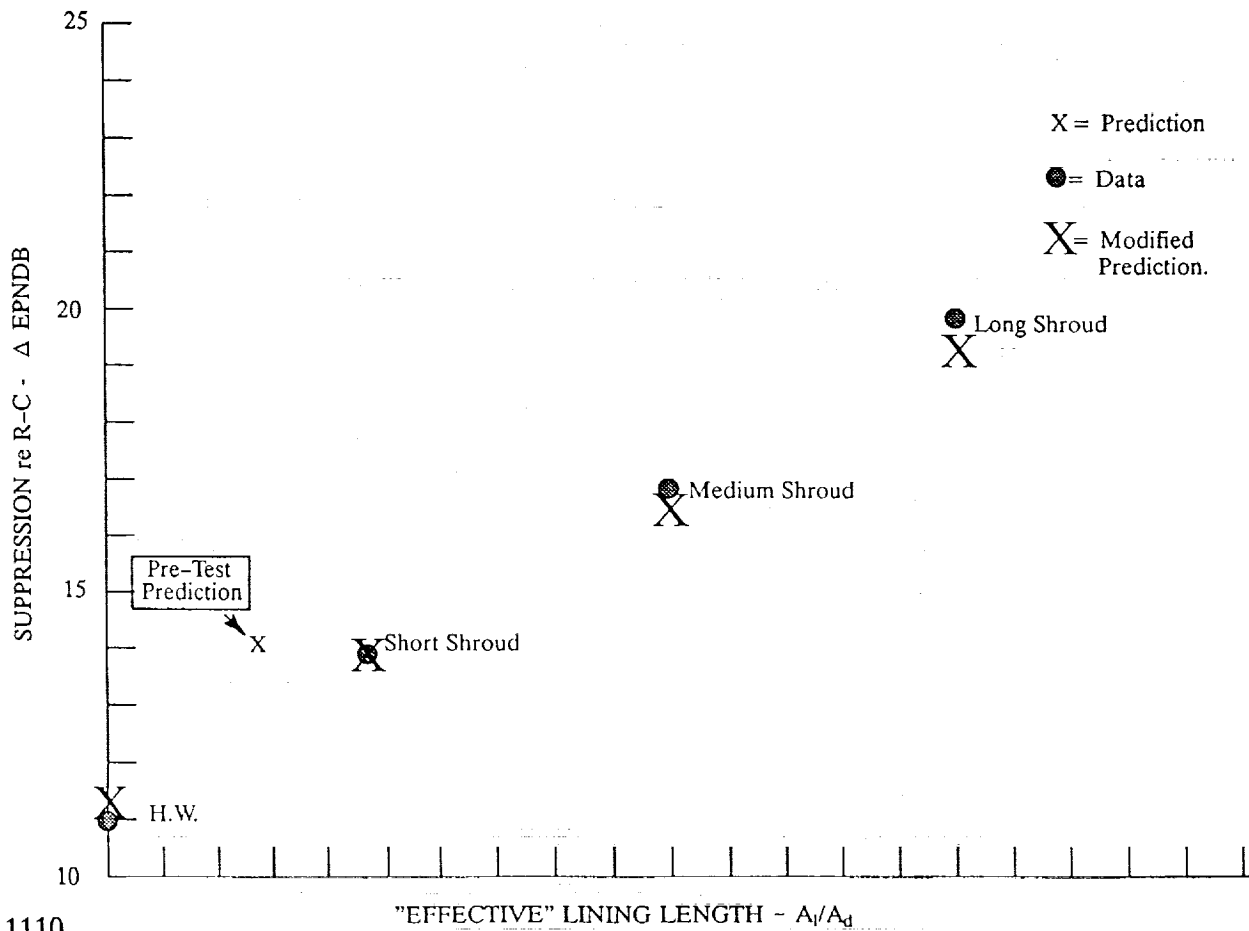


FIGURE 4. NFM NOZZLE PREDICTION VS DATA

## JET NOISE PREDICTION PROCEDURE DEVELOPMENT

A computer prediction program is being developed at Boeing incorporating the recent nozzle test data modeling externally generated mixing noise, internally generated mixing noise and internal shock cell noise components. A status comparison to test data in the forward and aft arc are shown.


# H S C T   JET  NOISE


## SEMI-EMPIRICAL COMPONENT MODELLING
## TO GUIDE NOZZLE / AIRPLANE DEVELOPMENT


Forward Radiated
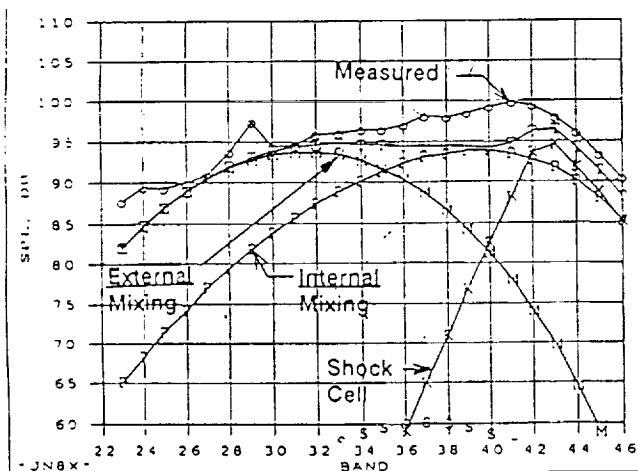
Aft Radiated
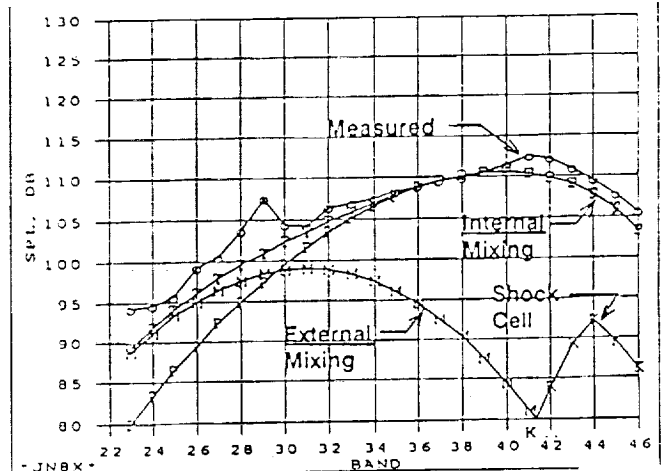


1111

FIGURE 5

Techniques are being studied to cross–correlate internal fluctuating jet velocities with far field sound pressure. If this is successful, noise source locations and their frequency characteristics can be determined inside the ejector. This would be useful in improving the mixer nozzle and ejector lining designs.

*BOEING*

# APPLICATION OF CROSS CORRELATION TECHNIQUES

Present Opportunities for Better Under-
standing of Internal Noise Sources

Nozzle

$p(\vec{x}, t)$

Probe

$\varrho(\vec{y}, t)$

$v_x(\vec{y}, t)$

Signal Processing:
  Sampling, Recording, Fil-
tering,      Differentiating,
Multiplying,  Cross–Corre-
lating

1112

FIGURE 6

In order to determine the number of samples (proportional to processing time) needed to obtain useful cross–correlation functions, a digitally simulated random test signal was buried in a noise signal and delayed. Resulting cross–correlations between the second derivative of the original test signal and the test and noise signal combination, are shown where the signal to noise ratio is about 10. The reducion in the variance in the correlation with increasing number of samples is evident. Frequency characteristics are obtained by fourier transforming the cross correlation.

# SIMULATED CROSS–CORRELATION

## Results – Time Domain – Noise > Signal



FIGURE 7

1113
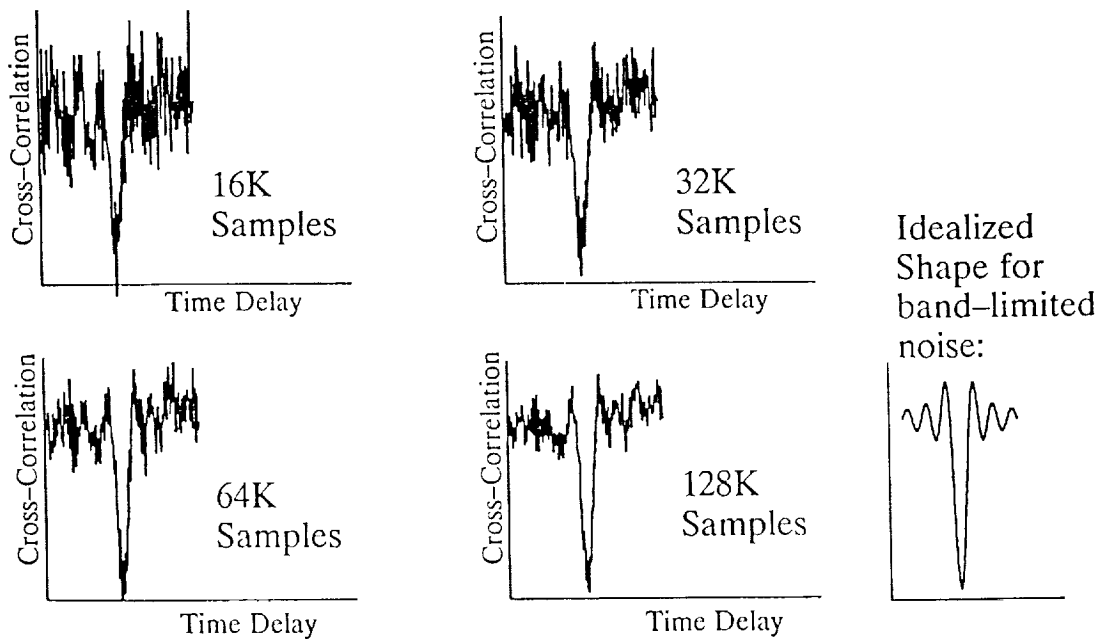
# CFD AND NOZZLE DESIGN

Computational Fluid Dynamics (CFD) has the potential of being a very useful tool in nozzle design. Currently CFD is used to evaluate new designs, prior to fabrication, in order to find potential flow problems. Data gathered during wind tunnel testing is used to validate CFD modeling increasing confidence in the CFD results.

Comparison of Coarse and Fine Grid Pressure Contours

Flow Conditions:   PR1=3.5, TR1=1.01, PR2=1.16, TR2=1.01, $M_\infty$=0.24



$P/\gamma P_\infty$

| 0.8200 |
| 0.8050 |
| 0.7900 |
| 0.7750 |
| 0.7600 |
| 0.7450 |
| 0.7300 |
| 0.7150 |
| 0.7000 |
| 0.6850 |
| 0.6700 |
| 0.6550 |
| 0.6400 |
| 0.6250 |
| 0.6100 |
| 0.5950 |
| 0.5800 |
| 0.5650 |
| 0.5500 |
| 0.5350 |
| 0.5200 |

Refined Grid Region

Coarse Grid

FIGURE 8
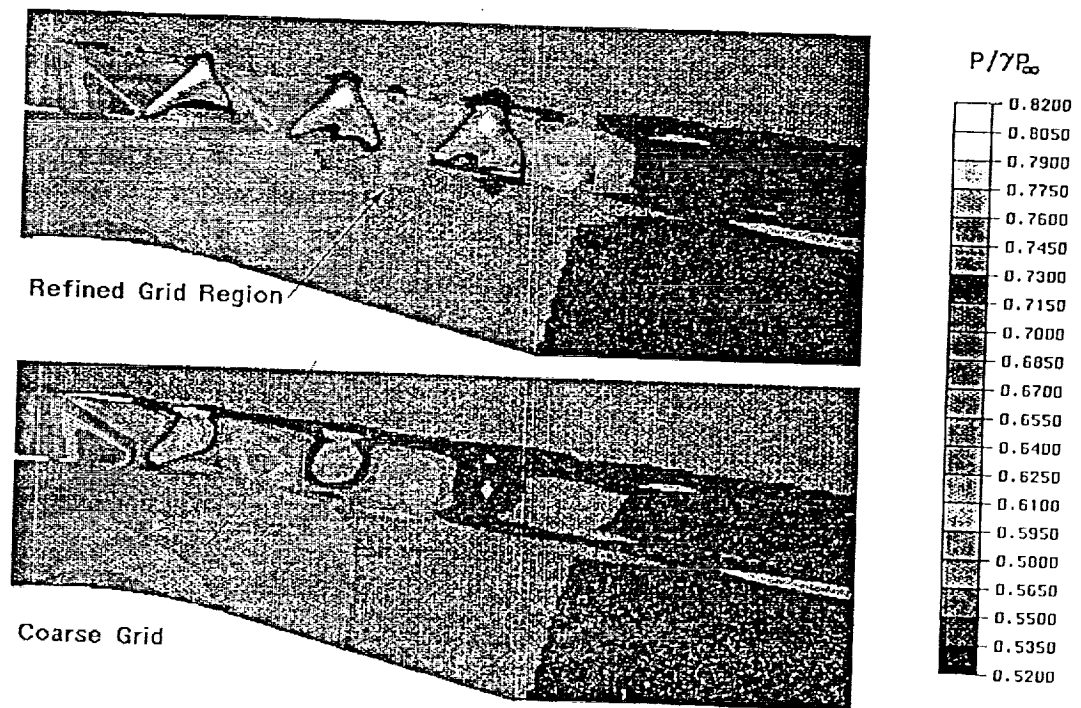
# OTHER PREDICTION TECHNOLOGY NEEDS

SIDELINE SHIELDING AND GROUND REFLECTION / ATTENUATION

* CURRENT METHODS ARE BASED ON HBPR ENGINES AND SUBSONIC AIRPLANE CONFIGURATIONS

INSTALLATION EFFECTS

* EFFECT ON SUPPRESSION SYSTEM

* NOISE REFLECTION, ETC.

OTHER NOISE SOURCES

* TURBOMACHINERY

* BURNER NOISE (LOW EMISSION BURNERS)

* AIRFRAME NOISE

FIGURE 9

Current sideline shielding prediction programs were developed using sideline noise measurements of 747 and 767 airplanes with the same engines. The shielding is then for high bypass ratio engines mounted off of the leading edge of the wing and with many configuration differences from current HSCT designs. There is currently little capability to accuratly predict shielding sensitivities to configuration layout changes.

# Size Comparison
## HSCT Versus 747-400

747-400

HSCT

211 ft 5 in

132 ft

231 ft 10 in

311 ft

CO-318R1
G-8-1
P1642.29 H

FIGURE 10
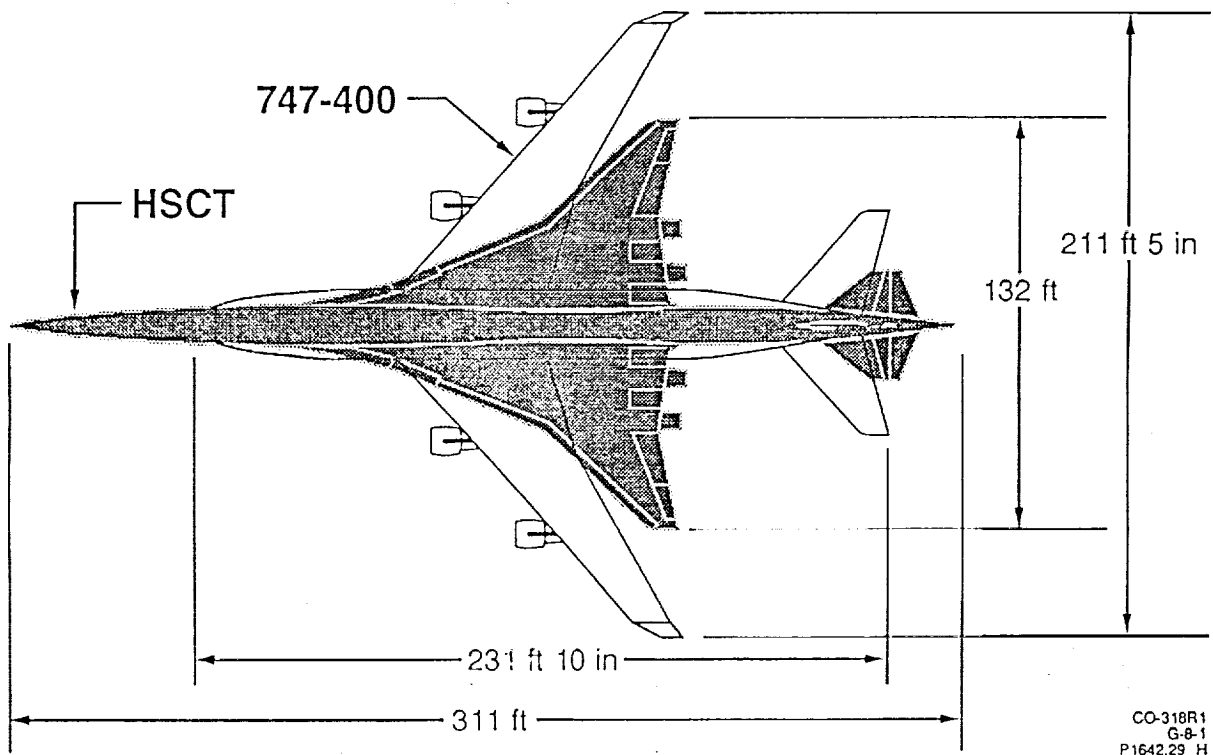
# DESIGN MARGIN IMPORTANCE

A design margin on the order of 80% confidence will be required to launch an HSCT production program. The current status is less than 50% with a one sigma variation of 5. To reach 80% confidence will require improvements in the airplane, such as an improvements in the jet suppression nozzle, but will also require improved prediction capability to reduce the variation.

## JET NOISE SUPPRESSION AND PREDICTION ACCURACY EFFECT ON CONFIDENCE LEVEL
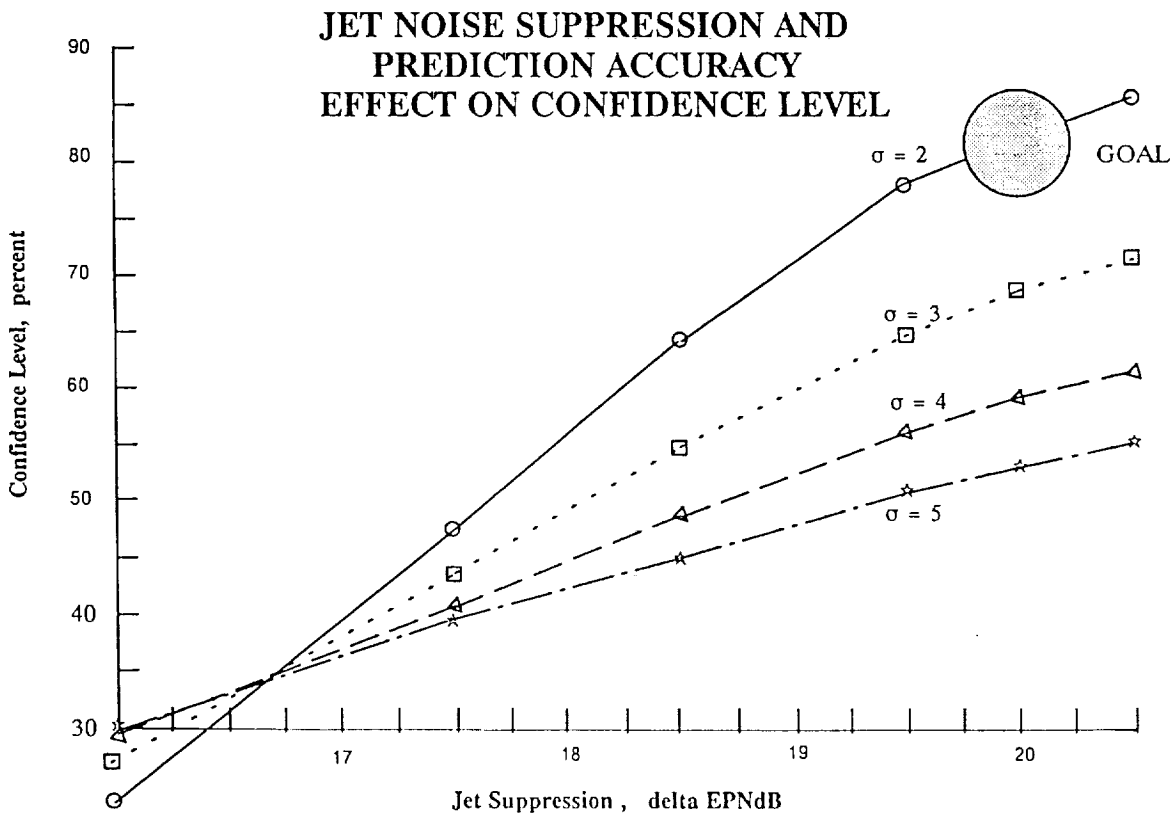


FIGURE 11

# PREDICTION UNCERTAINTY SOURCES

Prediction uncertainty includes the uncertainty of each of the contributing noise sources (A–D). The total accumulated measurement variation includes (E) the single test variability (data scatter) but also (F) any true error (bias). To improve the total prediction to demonstration uncertainty (G) each noise source prediction procedure should be evaluated for accuracy and improved if possible. Improvements in prediction of propagation, installation effects, shielding, ground reflection and airplane performance will also be required.

## PREDICTION UNCERTAINTY

FIGURE 12
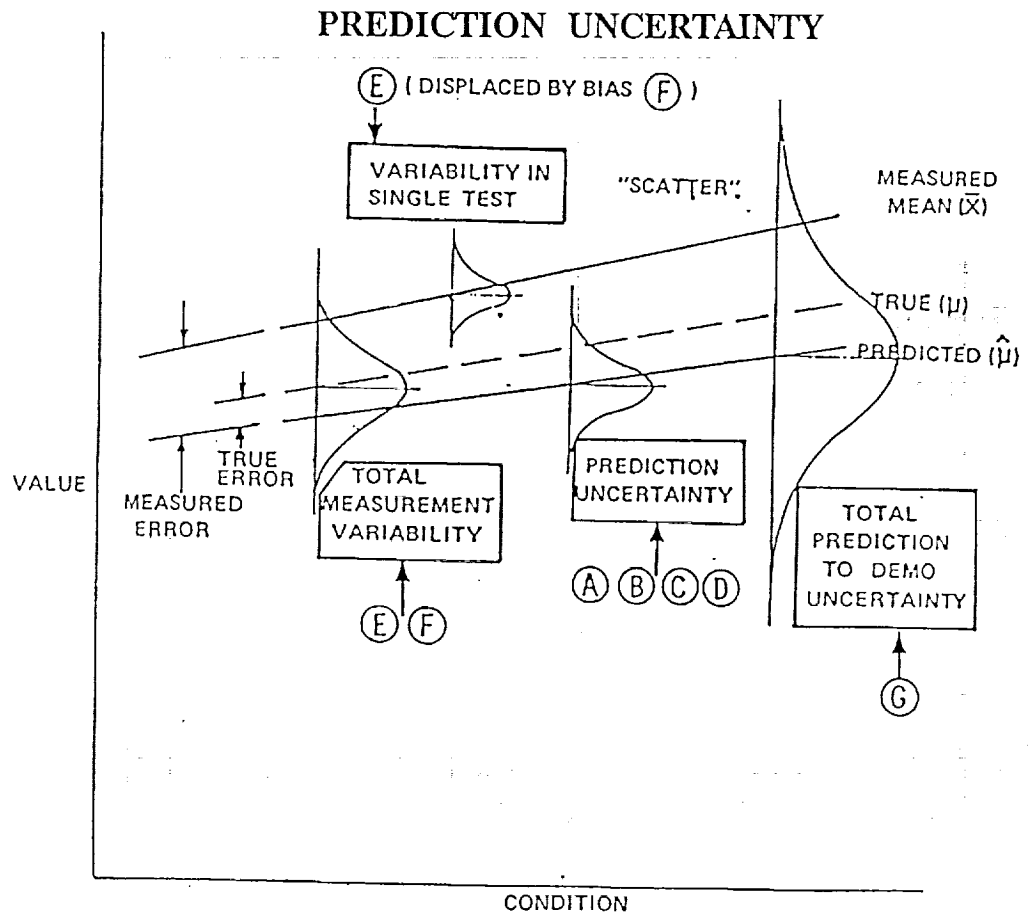
# CONCLUSIONS

∗ JET NOISE PREDICTIONS ARE PRIMARILY EMPIRICAL AND PREDICT TESTED NOZZLE
CONFIGURATIONS.

∗ FLEXIBLE AND MORE ANALYTICAL PREDICTION PROCEDURES ARE NEEDED THAT
ACCURATELY PREDICT ABSOLUTE LEVELS.

∗ ALSO, IMPROVEMENTS ARE NEEDED IN PREDICTION PROCEDURES FOR THE OTHER
NOISE SOURCES TOGETHER WITH IMPROVEMENTS IN INSTALLATION EFFECTS, SIDELINE
SHIELDING AND GROUND REFLECTION PREDICTIONS.

THIS PAGE INTENTIONALLY BLANK

1120

# Session VIII. Aeroacoustic Analysis and Community Noise

HSCT Climb to Cruise Noise Assessment
*Alan K. Mortlock, Douglas Aircraft Company*

**THIS PAGE INTENTIONALLY BLANK**

# SESSION #8
# AERO ACOUSTIC ANALYSIS
## AND
# COMMUNITY NOISE

*54-71*
*12034*

# HSCT
# CLIMB TO CRUISE NOISE ASSESSMENT

ALAN K. MORTLOCK

DOUGLAS AIRCRAFT COMPANY

3855 LAKEWOOD BLVD.

LONG BEACH,

CA 90846

FIRST ANNUAL HSRP WORKSHOP

WILLIAMSBURG, VIRGINIA

14-16 MAY 1991

# INTRODUCTION

*The widely accepted industry HSCT design goal for exterior noise is to achieve FAR Part 36 Stage 3 noise limits currently required for new subsonic aircraft. To date the HSRP has focussed research to achieve this Stage 3 noise goal.*

*However, noise certification is an entirely different situation compare to operating the aircraft at the world's international airports. Three takeoff operational phases must be carefully reviewed to ensure community noise acceptability after the year 2005.*

*The three phases of concern are: 1) airport noise abatement at communities close to the airport, 2) climb power opening-up procedures and 3) the climb to cruise phase affecting communities far from the airport shown in Figure 1 below:*
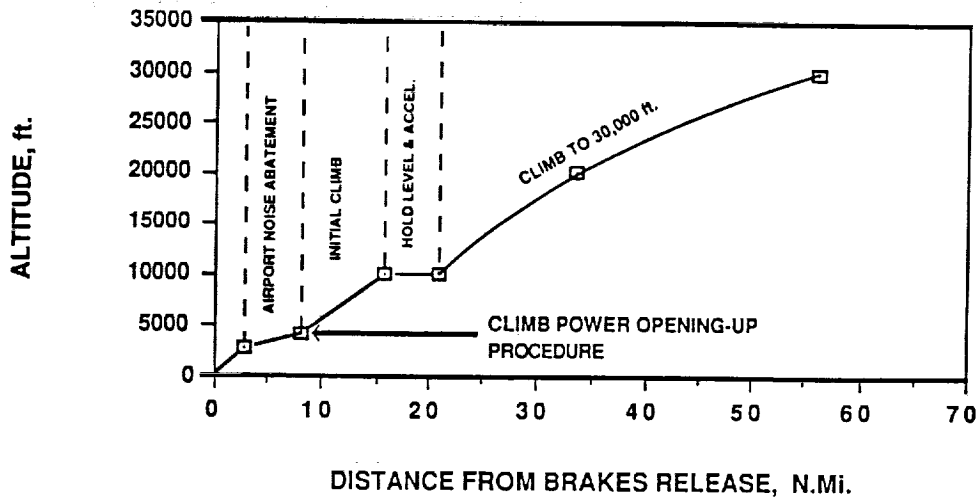


FIGURE. 1.- TYPICAL HSCT TAKEOFF PROFILE

# DEFINING A POTENTIAL CLIMB NOISE PROBLEM

*Now the stage has been set regarding takeoff operational procedure phases that could affect community noise reaction the issue of noise level and number of operations has to be addressed. The FAA have issued guidance on air route changes which gives insight into defining the climb to cruise problem.*

*Firstly, it has been determined that a 5dB increase in sound exposure level for a given minimum number of aircraft overflights will likely to cause significant complaints.*

*This determination has been based primarily on the operations of Stage 2 aircraft. If no Stage 2 aircraft operate at a given airport 5% of the Stage 3 operations are used to determine community noise acceptability. The minimum number of operations are reduced, regarding compliants, as the residential community moves from noisy urban to quiet suburb areas as shown in Table 1 below.*

**TABLE 1.**   Minimum Number of Daily Operations by Large Jet Airplanes (>75,000 lbs) on the Affected Route

| Aircraft Altitude (ft.,AGL) | Departures | | | | Arrivals | | | |
|---|---|---|---|---|---|---|---|---|
| | Residential Community (See table below) | | | | Residential Community (See table below) | | | |
| | Quiet Suburb | Normal Suburb | Urban | Noisy Urban | Quiet Suburb | Normal Suburb | Urban | Noisy Urban |
| 3000 | 2 | 7 | 22 | 68 | 65 | 205 | >500 | >500 |
| 5000 | 6 | 20 | 63 | 198 | 198 | >500 | >500 | >500 |
| 10000 | 34 | 109 | 343 | >500 | | | | |
| 15000 | 109 | 343 | >500 | >500 | | | | |

| Residential Community | Description |
|---|---|
| Quiet Suburb | Single family detached dwellings on large lots |
| Normal Suburb | Single family detached dwellings on 1/4 to 1/3 acre lots |
| Urban | Multi-family dwellings (apartment buildings, row housing, ect.) |
| Noisy Urban | Multi-family dwellings (high rise apartments) near busy roads or industrial areas |

# PAST UHB EXPERIENCE

In the early 1980's the aerospace industry assessed the ultra high bypass engine (UHB) powered aircraft for noise acceptability and economic viability. The UHB aircraft were compared to the existing subsonic fleet regarding climb to cruise and cruise noise. The subsonic fleet were categorized into three categories: 1) high by-pass ratio engine, 2) low by-pass ratio engine and 3) turboprop. The noise data for these categories were obtained from USA and European data bases and a summary of the data is shown in Figure 2 below. The range of noise levels in dBA show the low bypass ratio engine (Stage 2 equivalent) to be significantly higher than the high bypass ratio engine (Stage 3 equivalent). It should be noted that the Stage 2 fleet is likely to be retired after 2005 based on phase out regulations currently being discussed by the regulatory agencies.

H - HIGH BYPASS RATIO ENGINE
L - LOW BYPASS RATIO ENGINE
(1) TURBOPROP POWER SETTING UNCERTAIN
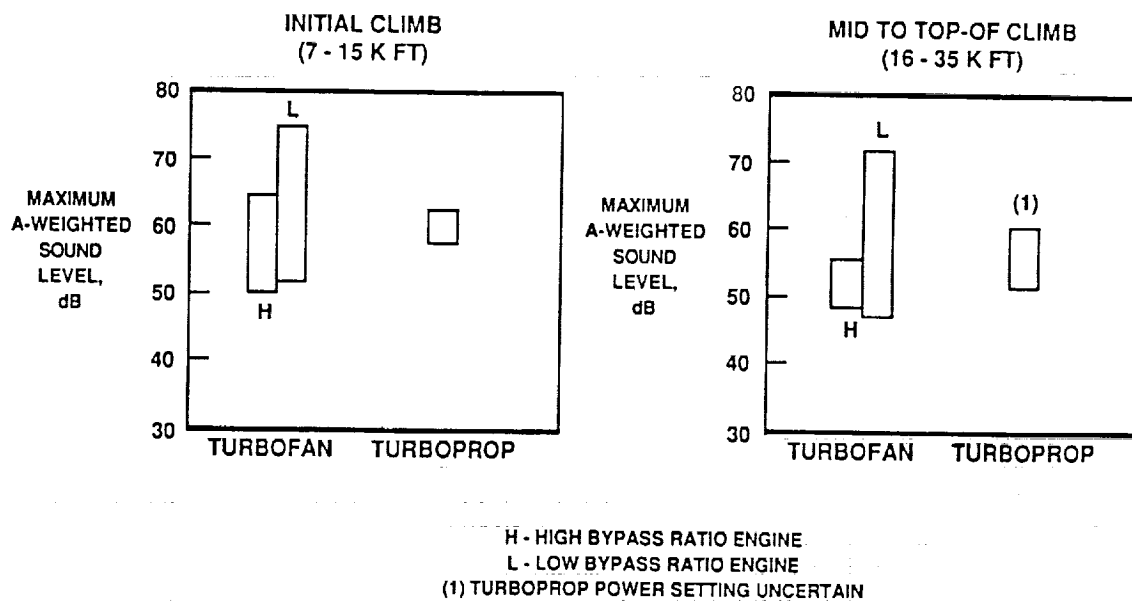
## FIGURE. 2.- SUBSONIC CLIMB NOISE DATA

1126

# CONCORDE MEASURED INITIAL CLIMB NOISE LEVELS

Since 1975 Concorde has been operating regularly from London (Heathrow), Paris (Charles De Gaulle), New York (JFK) and Washington (Dulles). There exists an abundance of noise measurements, particularly over the early years, of Concorde initial climb operations. USA Department of Trade and UK Civil Aviation Authority Reports show that Concorde operations are significantly higher than the current subsonic fleet as shown in Figure 3 (Reference 1). This shows that for 15 years the community at distances 20km and 30km from LHR have received noise from Concorde in excess of 20 PNdB above the 747 and Tristar fleet. As the number of Concorde operations at LHR have typically been 5-6 per day the number of complaints have been minimal in later years. However, if the number of operations increased significantly the picture on community noise acceptance could change dramatically.

Also it should not be assumed that other communities around international airports having 5-6 Concorde operations per day would accept the same situation. For comparison in dBA an exchange rate of approximately dBA = PNdB -11 should be used for these conditions.

At Washington (Dulles) airport the communities at 20 and 30 kilometers from the airport objected initially to Concorde noise during the power opening up operations, after the noise abatement phase, such that the procedure had to be adjusted to gradually increased power.
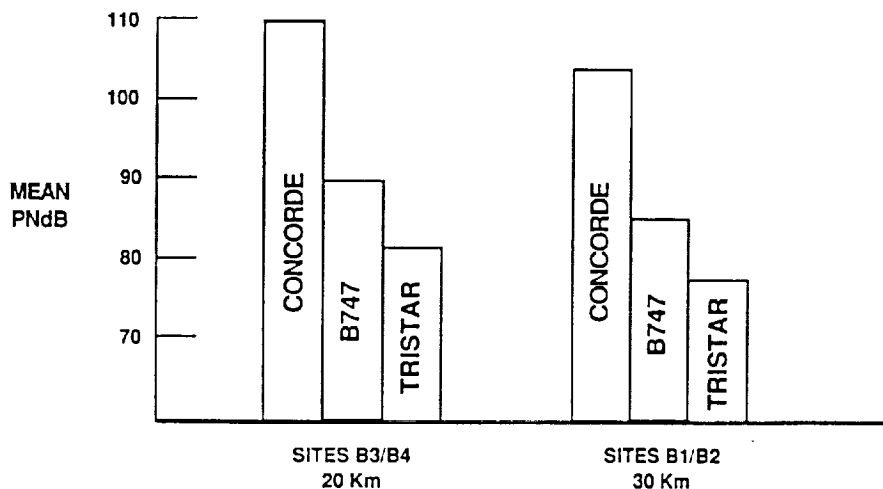


**FIGURE. 3.- LONDON (HEATHROW NOISE MEASUREMENTS)**

# CLIMB POWER OPENING-UP PROCEDURES

As mentioned before there has been some past problems with Concorde during the engine power opening-up phases on climb-out. It has been estimated that the HSCT increase in noise from 4% climb gradient power, used during airport noise abatement, to climb power is approximately 7dBA in the suppressed exhaust condition. This would increase to 27dBA if the noise suppression is removed. Therefore it may be necessary to produce a segmented power opening-up procedure at some airports to minimize community noise impact. This is illustrated below in Figure 4 by showing engine power requirements and aircraft profile.



DISTANCE FROM BRAKES RELEASE, N.Mi.
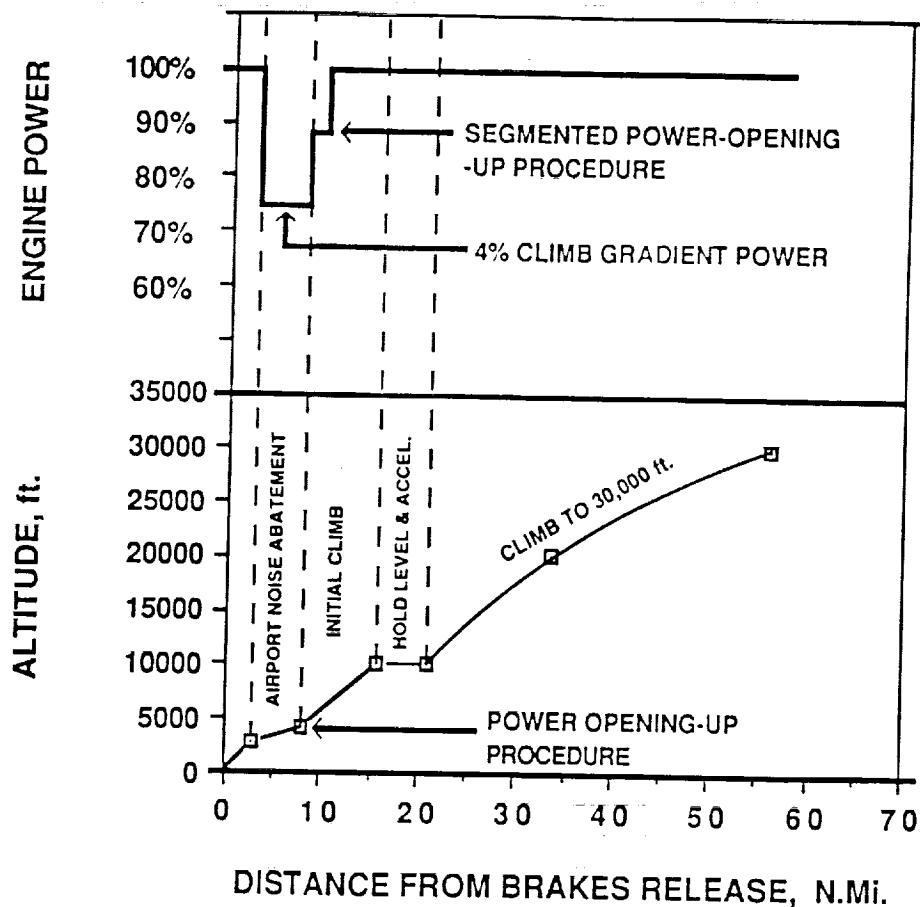
## FIGURE. 4.- INITIAL CLIMB-OUT PROCEDURE

# HSCT
# CLIMB TO CRUISE NOISE ASSESSMENT

To date DAC has attempted to evaluate the climb to cruise noise of two
HSCT engine cycles on a Mach 3.2 configuration.  Further assessments at
Mach 2.2 and 1.6 will be conducted under a new system study contract.  The
noise results for the P&W-TBE with a mixer/ejector nozzle in the
unsuppressed mode are presented below in Figure 5.  A typical takeoff
mission profile is shown. An acceleration phase at 10,000 ft is used to
achieve Mach 0.7 before a further climb is initiated to achieve Mach 0.98
at 30,000 ft.

Our existing jet noise prediction codes for mixing and shock noise is only
validated by measurements in a restricted operating envelope, typically up
to NPR = 3.5, Tj = 2,500K, M = 0.35.  Altitude = 10,000 ft.  As can be
seen in Figure 5, large extrapolations are necessary to conduct the HSCT
climb to cruise noise assessment.  Three standards of jet noise prediction
have been assessed:  1) mixing only, 2) mixing plus shock (no flight
effects) and mixing plus shock with convective amplification due to
forward speed effects.  As can be seen some extremely high noise levels
are predicted particularly if shock noise is estimated using current
codes.  From this point in the discussion only jet mixing noise will be
considered.
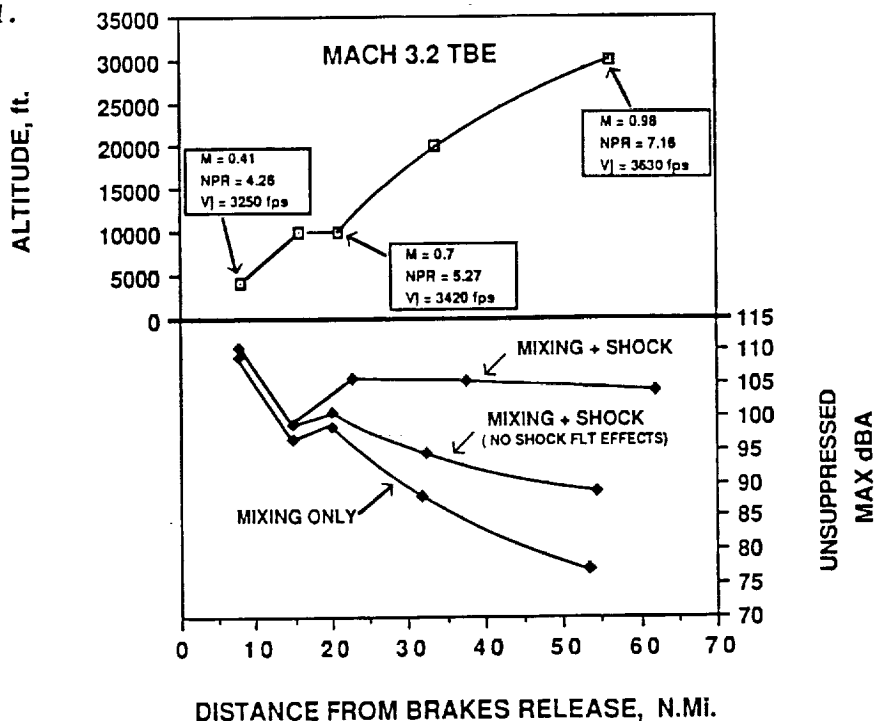


FIGURE. 5. - HSCT CLIMB TO CRUISE NOISE PREDICTIONS

1129

# HSCT
# COMMUNITY NOISE CONCERNS
# AFTER YEAR 2005

It is likely that the Stage 2 subsonic fleet will be virtually retired by 2005. This means that the communities will be virtually unaffected by the remaining Stage 3 aircraft at large distances from the airport. The introduction of HSCT operations are likely to impact the far out communities as the current prediction levels are well in excess of the current subsonic Stage 2 and Stage 3 fleet (see Figure 6). This indicates that noise suppression is likely to be required upto 30,000 ft. altitude.

The data presented below is based on peak single event dBA noise levels under the aircraft flight path. If only the Stage 3 subsonic fleet remains after 2005, having acceptable climb to cruise noise levels, it is clear that the introduction of HSCT operation will increase the noise exposure level at an alarming rate, well in excess of a 5dB increase, based on earlier discussions.
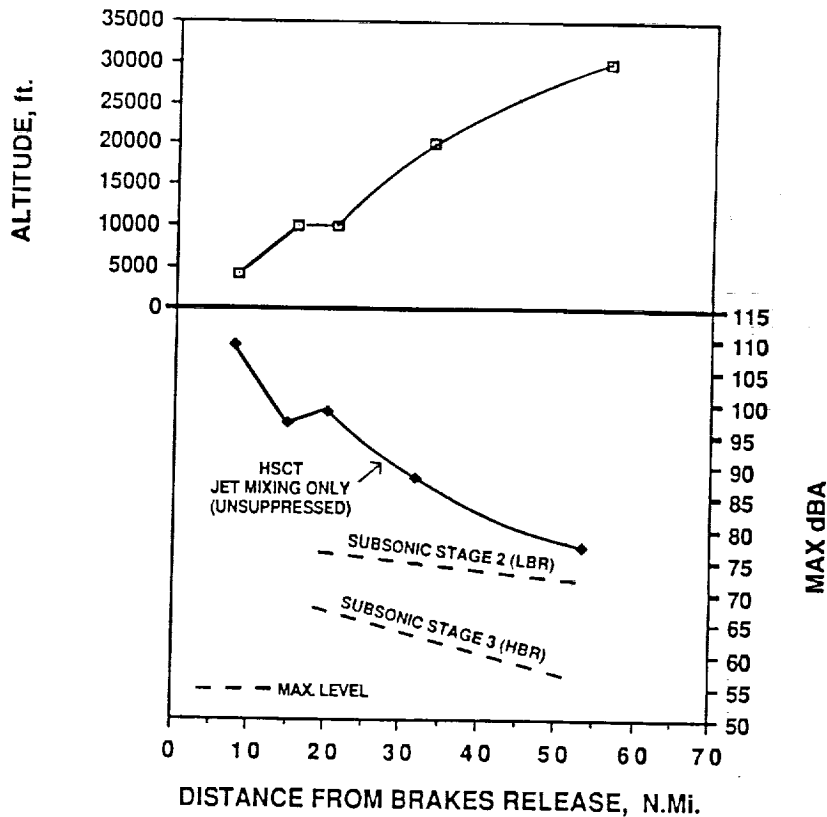


FIGURE. 6.- CLIMB NOISE HSCT VS SUBSONICS

1130

# JET NOISE PREDICTION CONCERNS

It is a concern at this time that the current HSCT noise prediction codes for climb to cruise noise are inadequate, particularly in predicting shock noise. The HSCT engine cycles have increased exhaust pressure ratios and total exhaust temperatures compared to those validated in the existing subsonic aircraft jet noise prediction codes. This also raises some doubt about the validity of the jet mixing noise estimates for HSCT.

Therefore there is an urgent action to evaluate the need for a flight test data base to extend the existing jet noise data base. The new flight data base should encompass the flight conditions and envelope shown Figure 7 below. The question of an existing suitable flight test vehicle needs to be reviewed and discussed with the acoustic specialists.
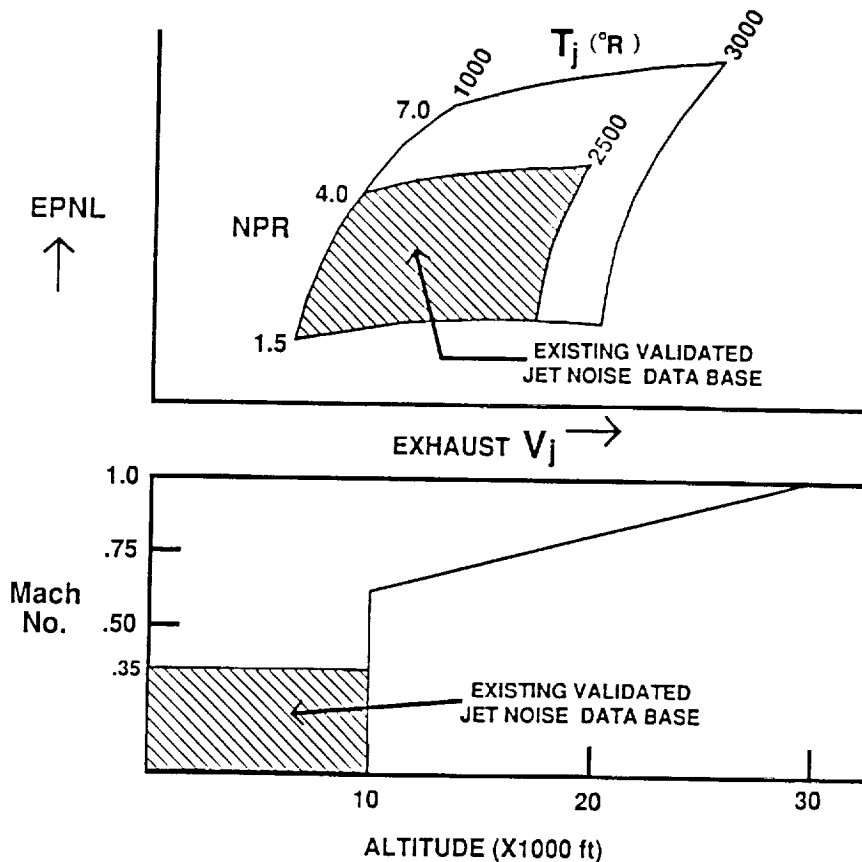


FIGURE .7.- REQUIRED HSCT TEST DATA ENVELOPE

# CONCLUSIONS

o   The existing Stage 2 subsonic fleet is likely to be phased out by the time the HSCT operates in significant numbers.

o   Current unsuppressed HSCT climb to cruise noise levels, considering jet mixing noise only, are higher than the maximum levels of existing Stage 2 subsonic aircraft.

o   The Stage 3 subsonic fleet noise exposure level will be significantly lower than the unsuppressed HSCT levels.  However, the Stage 3 fleet may not be the measure for community noise acceptance of the HSCT.

o   After the year 2005 it is likely that significant noise suppression upto 30,000 ft. altitude will be required for the HSCT engine cycle in order to operate from some international airports.

o   If jet shock noise becomes dominant during the climb to cruise phase the problem will significantly escalate.

o   The current noise prediction codes for HSCT climb to cruise noise are inadequate and not validated.

# *HSCT CLIMB TO CRUISE NOISE ASSESSMENT RECOMMENDATIONS*

o   *Extend in-flight jet noise data base to include HSCT climb to cruise noise conditions.*

o   *Evaluate suitable existing flight test research vehicle*

o   *Determine an acceptable increase in community noise exposure level after the Stage 2 subsonic fleet has been retired (after 2005?) i.e. re. Stage 3 subsonic fleet or background level.*

THIS PAGE INTENTIONALLY BLANK

# Session VIII. Aeroacoustic Analysis and Community Noise

ANOPP/VMS HSCT Ground Contour System
*John W. Rawls, Jr. and Louis J. Glaab, Lockheed Engineering and Sciences Company*

THIS PAGE INTENTIONALLY BLANK

1136

*S5-71*
*12035*

# ANOPP / VMS HSCT GROUND CONTOUR SYSTEM

John Rawls, Jr. & Lou Glaab
Lockheed Engineering and Sciences Company
Hampton, Virginia

First Annual High-Speed Research Workshop
May 15, 1991

# HIGH-SPEED RESEARCH PROGRAM

This viewgraph shows the integration of the Visual Motion Simulator with ANOPP. ANOPP is an acronym for the Aircraft NOise Prediction Program. It is a computer code consisting of dedicated noise prediction modules for jet, propeller and rotor powered aircraft along with flight support and noise propagation modules, all executed under the control of an executive system. The VMS is a ground based motion simulator with six degrees of freedom. The transport-type cockpit is equipped with conventional flight and engine-thrust controls and with flight instrument displays. Control forces on the wheel, column, and rudder pedals are provided by a hydraulic system coupled with an analog computer. The simulator provides variable-feel characteristics of stiffness, damping, coulomb friction, breakout forces, and inertia. The Visual Motion Simulator provides a wide range of realistic flight trajectories necessary for computing accurate ground contours. The NASA VMS will be discussed in detail later in this presentation. An equally important part of the system for both ANOPP and VMS is the engine performance. This will also be discussed in the presentation.



HIGH-SPEED RESEARCH PROGRAM

Pilot's controls and displays

Integrating flight simulation and aircraft noise prediction

Automated flight controls

Flight trajectory

Three axis motion

Visual motion simulator

Aircraft noise prediction program

Engine deck

Effective noise level contours (EPNdB)
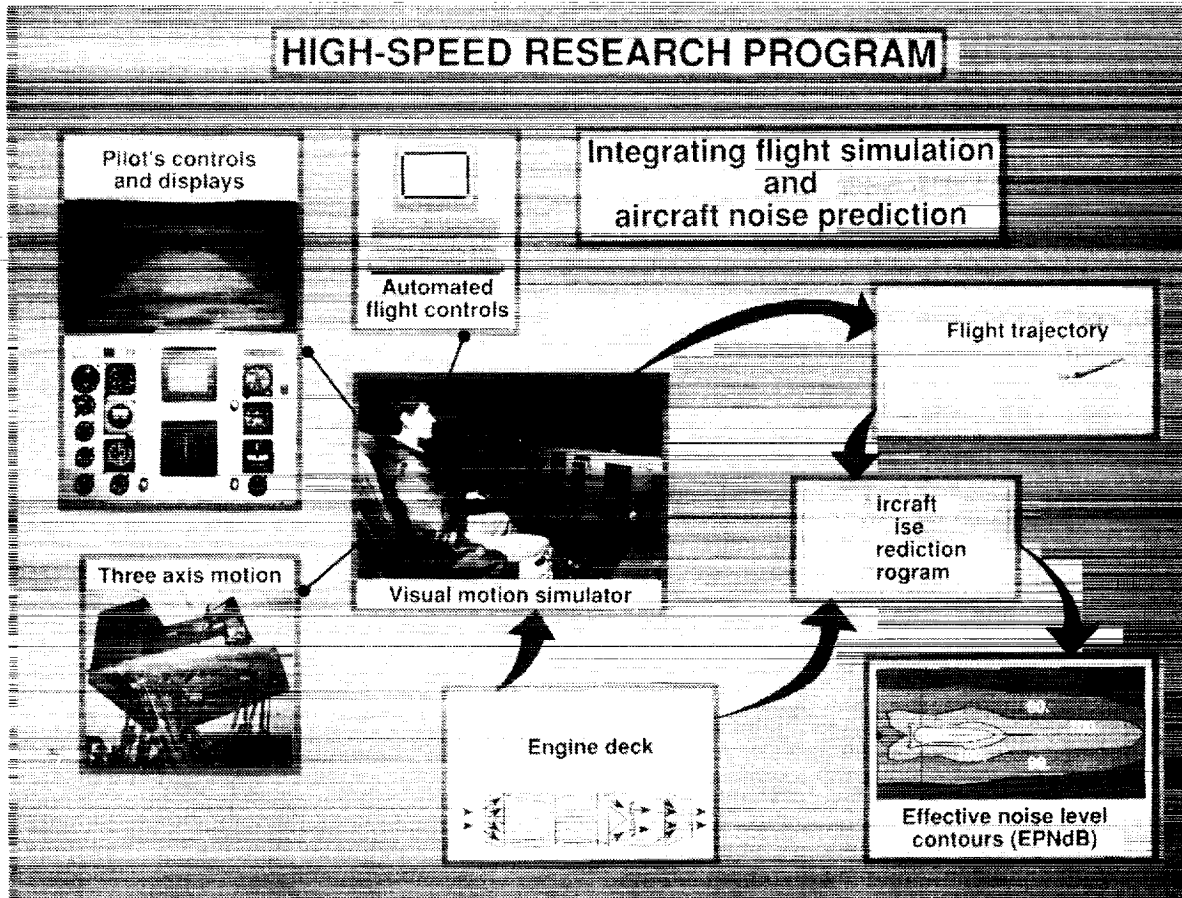
# HSR NOISE PREDICTION SYSTEM

This viewgraph shows a diagram of the functional path that is used by ANOPP to execute a prediction for airport community noise. It shows the types of prediction modules that are required to perform the prediction and the order in which they are executed. To produce the contours, the normal ANOPP output pass through a formatting program and then to a contour plotting program. A contour plotting program to accompany ANOPP is under development.

# HSR NOISE PREDICTION SYSTEM

```
                HSR                        ENGINE
              FLIGHT                       STATE
             DYNAMICS                      TABLES
              MODULE
                                              |
  ATMOSPHERIC      OPTION                  SOURCE        OBSERVER
    MODEL                                  NOISE         LOCATION
                                         PREDICTION
                                                            |
            AERODYNAMICS                               CALCULATE
              FLIGHT                                     NOISE
             SIMULATOR                                   METRIC
```

GROUND CONTOUR



1139
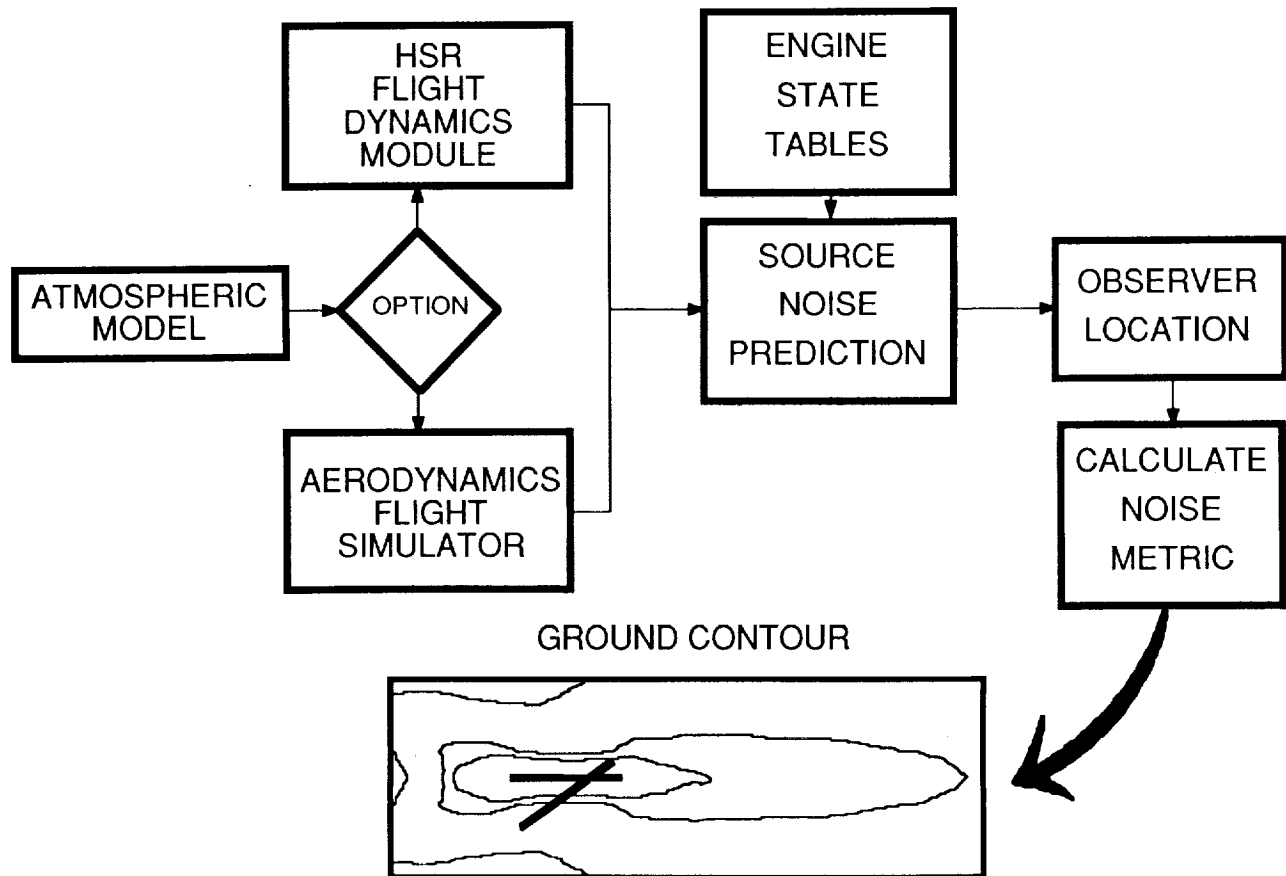
UPDATES TO HSR SYSTEM

The HSR Noise Prediction System started as the Conventional Take-Off and Landing (CTOL) System completed by NASA in 1982. This viewgraph shows updates that have been made for the HSR System.

# UPDATES TO HSR SYSTEM

- Incorporated two new Flight Dynamics Modules
    JTO    -    Jet Takeoff Module
    JLD    -    Jet Landing Module

- Added atmospheric absorption coefficients developed by Dr. Zuckerwar

- Updated Jim Stone jet noise prediction method to include modification made after the CTOL system was completed in 1982

- Developed a formatting module to produce an output file for plotting EPNL, Max. A-weighted, and/or Max. PNLT

- Coupled the HSR Noise Prediction System with the Visual Motion Simulator

- Coupled Engine State Tables produced by the Navy NASA Engine Program (NNEP) with ANOPP

1140

CURRENT WORK & FUTURE PLANS

This viewgraph is self explanatory.

# CURRENT WORK

- Developing a contour plot program to accompany the HSR Noise Prediction System

- Investigating the noise problem associated with climb-to-cruise

- Developing TEMPLATES to better explain the use of the HSR Noise Prediction System

# FUTURE PLANS

- Incorporate into the HSR Noise Prediction System two new jet noise modules based on the MGB and MS codes developed by GE

- Incorporate into the HSR Noise Prediction System a broadband shock noise module based on the theory of C. Tam

The Engine State Tables provide the acoustic input parameters to the noise modules as a function of the aircraft Mach number and the engine power setting. An engine state table is required at the inlet and the exit of the fan, combustor and the turbine. A single engine state table is require for a single flow nozzle such as a turbojet jet. An additional table is required for dual flow nozzles. Each engine state table has the same format so that the same computer code can be used to read the tables. As shown, the first entry into the table is the area (for example the jet exit area), the second is the fuel-to-air ratio, the third is the mass flow rate, the forth is the total temperature, the fifth is the total pressure and the last is the rotational speed. A takeoff noise prediction requires hundreds of input parameters since the aircraft Mach number continually changes. The takeoff profile can be further complicated by power changes due to cutback. The Engine State Tables are provided to ANOPP by the Vehicle Integration Branch in the Advanced Vehicle Division. Currently, the computer code used to generate the Engine State Tables is the Navy NASA Engine Program or NNEP.

# ENGINE STATE TABLES

## Provide acoustic input parameters to noise modules for a specified range of power settings and Mach numbers

**[Area, Fuel-to-Air Ratio, Mass Flow Rate, Total Pressure, Total Temperature, Rotational Speed]**

| | |
|---|---|
| **FAN** | **INLET** |
| | **EXIT** |
| **CORE** | **INLET** |
| | **EXIT** |
| **TURBINE** | **INLET** |
| | **EXIT** |
| **JET** | **PRIMARY** |
| | **SECONDARY** |
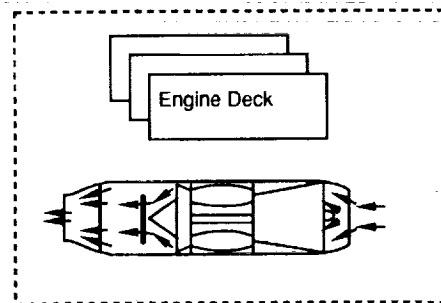


Engine Deck

**An engine deck consisting of 6 power settings, 5 Mach number, 4 noise sources, 6 parameters for inlet and exit conditions = 1440 entries**

**Engine State Table output directly from Navy NASA Engine Program (NNEP)**

USE OF ENGINE STATE TABLES IN ANOPP

The Engine State Tables are provided as an ASCII file in a format that can be incorporated directly into an ANOPP program. Shown on the left side of this viewgraph is a representation of an ANOPP program starting with the ANOPP $ statement and ending with the ENDCS $ statement. The engine state tables are input prior the four CALL PROCLIB(noise source) statements. ANOPP automatically computes the input parameters required at each point along the takeoff trajectory from the Engine State Tables. This is shown graphically on the left side of the viewgraph.

# USE OF ENGINE STATE TABLES IN ANOPP

**ANOPP $**

●
●
●

*INSERT ENGINE STATE TABLES VIA EDITOR*

.

CALL PROCLIB(THDNFAN) $
CALL PROCLIB(TGECOR) $
CALL PROCLIB(TGETUR) $
CALL PROCLIB(TSTNJET) $

●
●
●

ENDCS $

TYPICAL TAKEOFF NOISE PREDICTION
1/2 SECOND INTERVALS
150 SECONDS

FAN    CORE    TURBINE    JET

FLIGHT
TRAJECTORY

1143
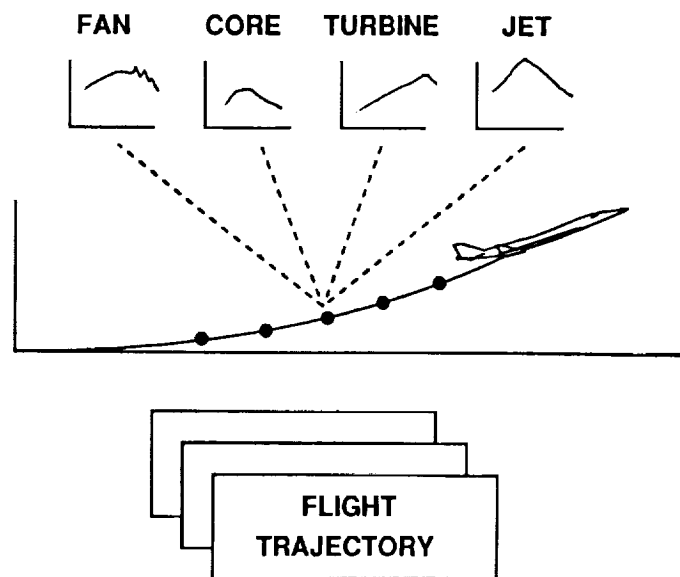
# HSR TAKE-OFF FLIGHT PROFILES

This viewgraph shows the details of the aircraft flight dynamics and the two certification positions involved in the execution of the high lift noise prediction take-off problem. It depicts two cases for take off, one a power setting of 100% and a normal lift configuration, and another which depicts the use of high lift to rotate and lift off earlier. The centerline FAR 36 measurement is far enough down range so that most modern turbine engines and aircraft do not have a problem meeting the requirements. The problem with more modern turbofan powered aircraft as is true for the HSCT is meeting the requirement of the FAR 36 sideline point. This point remains 1476 feet from the centerline of the flight path but is adjusted to the flight profile. Experience has show that the peak sideline noise level occurs when the aircraft reaches an altitude of 1000 feet. The FAA allows the passage through this altitude to be the sideline measurement point. As shown in the viewgraph, the sideline measurement point for the high lift case is closer to brake release than for the standard lift case. Any noise gain will have to be a result of the aircraft being able to climb out at a steeper angle so that the reduction in noise is proportional to 20 log r, where r is the distance between the measuring point and the aircraft. There will also be a similar noise benefit at the downrange centerline measuring point.

# HSR TAKE-OFF FLIGHT PROFILES

AST-205-1 BLENDED BODY

GE21/JII-B14A SCALED ENGINES

- - - - - HIGH LIFT CONFIGURATION   O

———— STANDARD LIFT CONFIGURATION   ●

BRAKE RELEASE

1000 FT

MOVES

SIDELINE MEASUREMENT POINT(FAR 36)

CENTERLINE CERTIFICATION POINT (FAR 36)
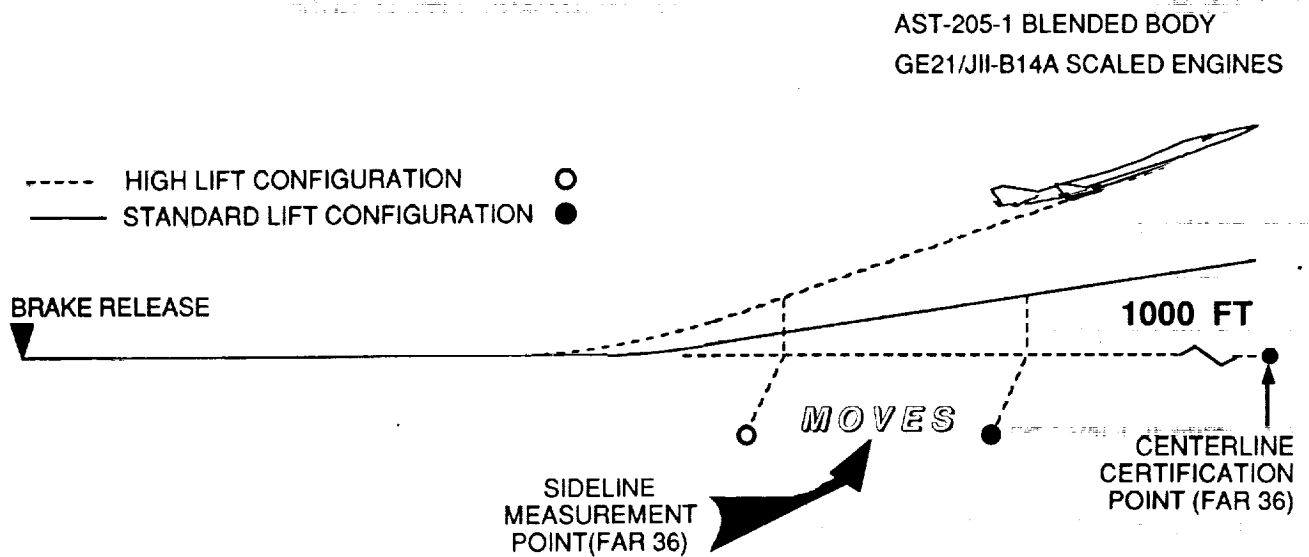
## FOR DISTANCE R, SPL ∝ 20 LOG R

## FOR JET VELOCITY V, SPL ∝ 65 LOG V

1144

ANOPP SYSTEM NOISE PREDICTION FOR HSCT
Effective Noise Level Contours (EPNdB)

This viewgraph shows predicted results using the HSR Noise Prediction System that demonstrates an alternative way to utilize the benefits of high lift . That is to use the high lift to reduce the jet thrust. The advantage of this technique, like a power cut back presently used with current turbofan aircraft, is that the reduction in noise is proportional to 65 log V, where V is the jet exhaust velocity. The two color contours explicitly demonstrate the differences in contour areas between a 100% thrust, standard lift configuration for take-off and the use of a 80% thrust, 60% increase in lift where the increased lift has been utilize by providing the reduced thrust. The values to the right of the contour show the reduction in the sideline and centerline EPNL values due to changes in thrust and lift. (It should be mentioned that increases in lift of these magnitudes would require significant technological advances. For this study increases in lift were assumed to result from increasing L/D with no increase in drag. A constant rotation of 3 degrees per second and a subsequent constant climb angle of 8 degrees was used in both cases.) The results show clearly that the greatest gain for reducing the sideline noise level comes from using the high lift to reduce jet thrust.

# ANOPP SYSTEM NOISE PREDICTION FOR HSCT
## Effective Noise Level Contours (EPNdB)

**100% THRUST, STANDARD LIFT CONFIGURATION**
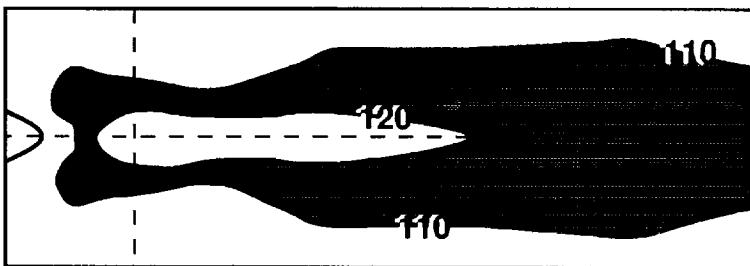


- Sideline 116.3
- Centerline 116.2

**80% THRUST, 30% LIFT INCREASE**
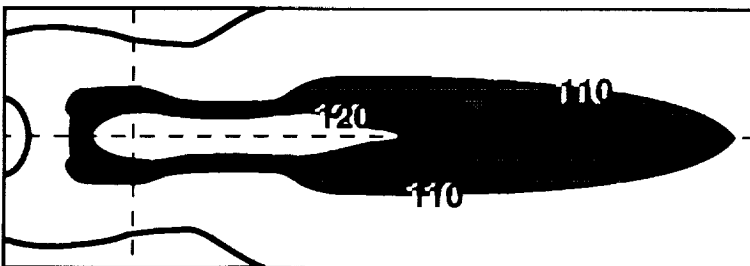


- Sideline 112.3
- Centerline 112.2

● , ● Noise certification points

# HSCT Piloted Simulation Background

The piloted simulation effort resulted from the projected inability of current HSCT concepts to meet proposed noise regulations.

Previous studies have shown reductions in airport-community noise resulting from:

- Increases in $C_L$
- Advanced takeoff and landing operating procedures
- Modifications to engine characteristics

1146

## HSCT Piloted Simulation Objectives

The objectives of the piloted simulation program are as indicated.

- Document noise reduction resulting from increase in $C_L$ and L/D and modifications to engine characteristics

- Develop and evaluate advanced takeoff and landing pilot operating procedures, which fully exploit noise reduction benefits without compromising safety

# HSCT Piloted Simulation Approach

The approach to noise prediction is shown on the accompanying chart. The research uses the Langley Visual Motion Simulator (VMS) which has three axis motion capability (three axis translation and three axis rotation). The pilot has a standard display panel and controls, and a computer graphics image of the runway and airport surroundings. The simulation provides automated flight control capability and allows different levels of stability augmentation systems to be considered. The pilot can perform take-off and landing procedures and the resulting flight trajectories (coupled with the engine characteristics) are input to the Aircraft Noise Prediction Program (ANOPP) which is then used to compute noise contours. An initial objective of this research effort was to develop the VMS/ANOPP interface. To permit rapid accomplishment of this objective, the AST-105 configuration (because of the available and comprehensive data base) was selected for initial study.
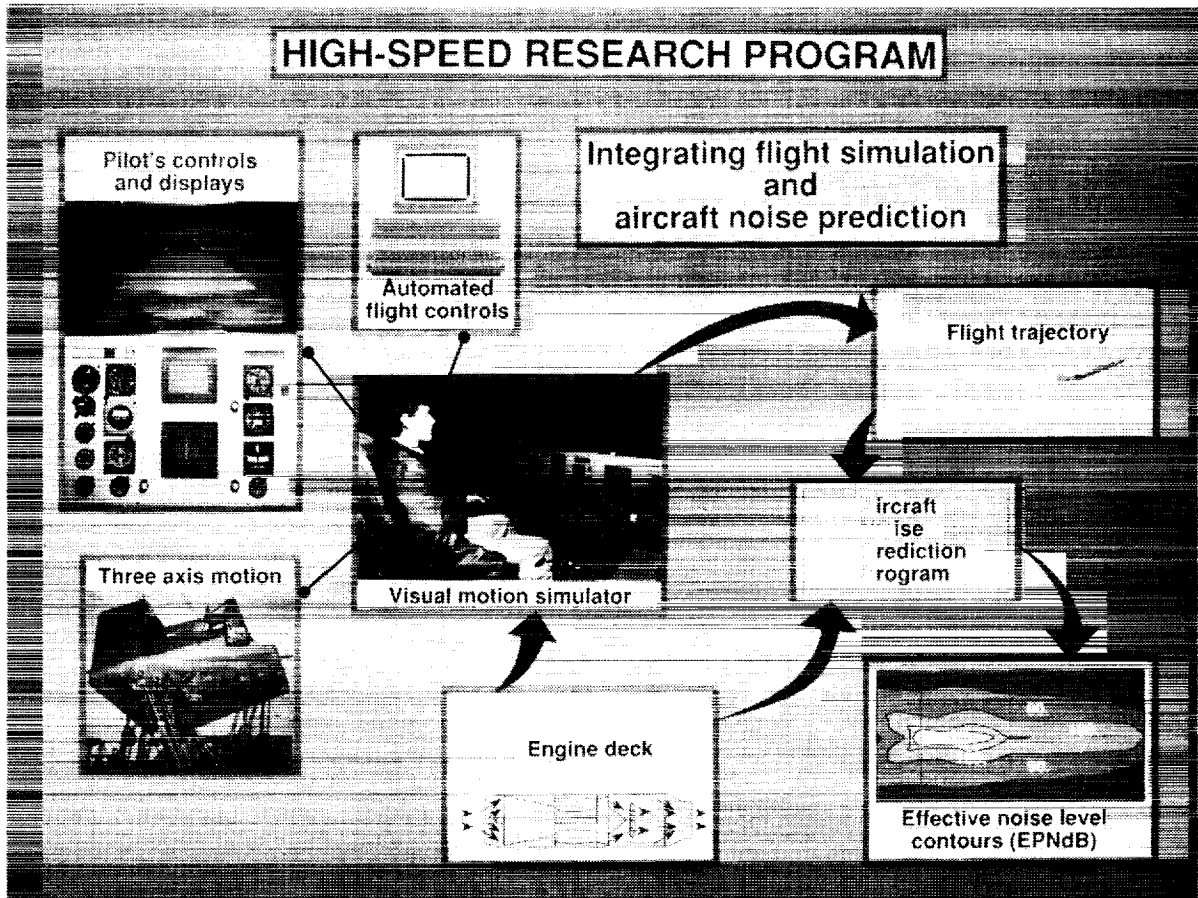
## Current Simulator Capabilities

The current simulator capabilities are as shown. A six degree of freedom Visual Motion Simulation (VMS) provides the aircraft motion ques. The atmosphere model for this simulation is capable of simulating numerous meteorological conditions including varying turbulence levels, wind direction and magnitudes as well as non standard conditions. The computer generated pilot visual scene provides the pilot with both front and peripheral views on a total of four simulated cockpit "windows". Various flight conditions can be simulated using this system, for example a flight at night with thunderstorm activity. The pilot is provided flight information from a suite of computer generated CRT displays, which include an Electronic Attitude Director Indicator (EADI), Horizontal Situation Indicator (HSI) and engine data information. Currently the pilot is provided with a sidestick controller, rudder pedals, engine throttles and wing spoilers. The engines can be controlled either manually via the four power levers or automatically using the auto-throttle option, which consists of an indicated airspeed hold system.

# CURRENT SIMULATOR CAPABILITIES

- 6 Degree of freedom motion simulation

- Variable atmosphere model

- Computer generated out the window visual scene

- Computer generated pilot information displays (EADI, HSI, and engine data)

- Sidestick controller, rudder pedals, engine throttles and wing spoiler controls

- Auto-throttle (indicated airspeed hold)

# HSCT Simulation Baseline Configuration

Due to the existence of a comprehensive data base the AST-105 configuration was selected as a simulation model. Although this configuration was developed in the late 1970's it is representative of current HSCT conceptual designs.
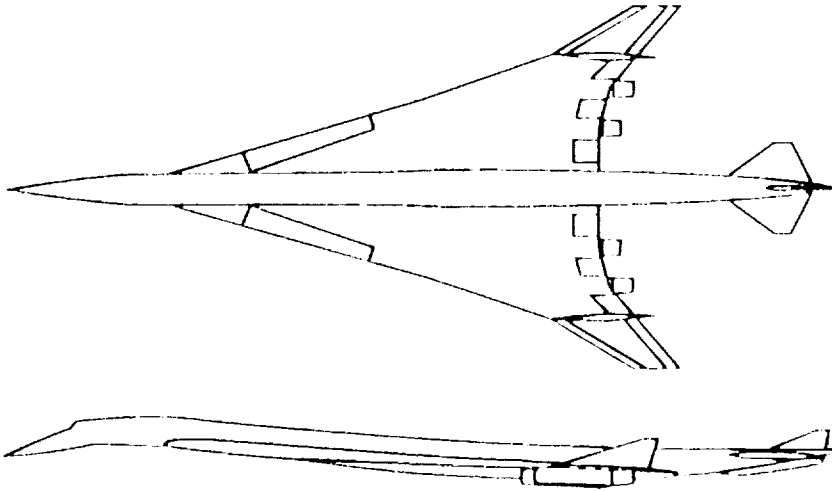
**Airframe AST-105-1 (1979)**

$W_{T.O.}$ (lbf) $= 686,000$

$W_{App.}$ (lbf) $= 392,250$

$S$ (ft$^2$) $= 8366$

$b$ (ft) $= 126.215$

$c$ (ft) $= 88.162$

$\Lambda_{L.E.}$ (deg) $= 74/70.3/60$

Range (n. mi.) $= 4500$

$M_{cruise} = 2.7$

$T/W = 0.254$

$L/D_{max} = 9.39$

**Engine (4) VSCE-516 (1979)**

Bypass ratio $= 1.3:1$

OPR $= 16:1$

Wa (lbm/sec) $= 608$

$V_f/V_p = 1.7:1$

1150

# Control Surface Layout

The configuration control surfaces used in this simulation are as shown. Wing controls on this configuration consist of leading-edge flaps, trailing-edge flaps and flaperons. Control surface 1 is a pure flap and has a range of rotation from 0 to 40 degrees. Control surface 3 is called the inboard flaperon and is biased to the same position as control surface 1, it also can rotate +/- 10 degrees from its biased flap position. Control surfaces 5 and 7 are also flaperons. They are biased to 5 degrees trailing edge down if the inboard flaps are deployed and can deflect +/- 35 degrees from this position. For purposes of this present low-speed simulation control surfaces 9, 11 and 13 are preset to 30, 30 and 45 degrees respectively while horizontal and vertical tail deflections are limited to +/- 20 degrees +/- 25 degrees respectively.

## CONTROL SURFACE LAYOUT
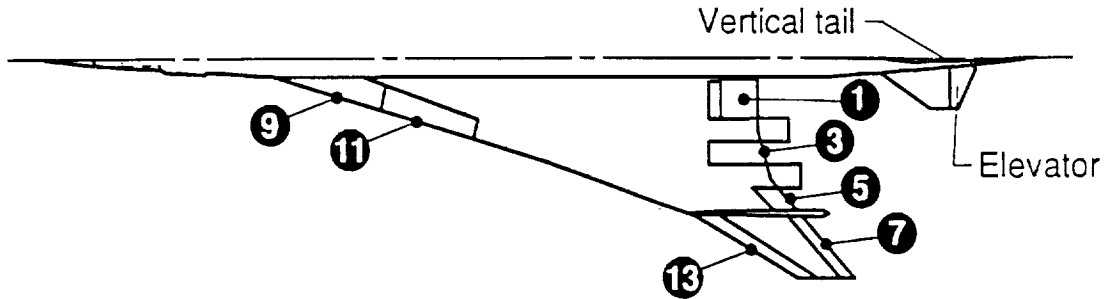


| Number | Area, $m^2$ ($ft^2$) each | $\delta$, deg |
|--------|---------------------------|---------------|
| 1 | 11.734 (126.3) | 0 - 40 |
| 3 | 8.101 (87.2) | 0 - 40 |
| 5 | 4.692 (50.5) | 5 |
| 7 | 7.665 (82.5) | 5 |
| 9 | 15.440 (166.2) | 30 |
| 11 | 16.397 (176.5) | 30 |
| 13 | 8.454 (91.0) | 45 |
| Elevator ± 20   Vertical tail ± 25 | | |

## Flight Control System

Three basic types of flight control systems are currently used in the simulation. These vary in complexity from a basic stick-to-surface command system to an attitude hold system and are described in the accompanying figure. Flight control system 1 is a basic non-augmented stick to surface system. Although this system would not be used on an actual aircraft it is useful to examine the non-augmented aircraft flying qualities. Flight control system 2 is a rate command system and incorporates some basic stability augmentation concepts, such as pitch rate and roll rate dampers. This system does provide a "flyable" study configuration but is not considered adequate. Flight control system 3 is representative of current technology and is more complex than either of the other two systems. It is a rate command and attitude hold type control system. This system incorporates various feedback loops and provides pitch and roll attitude hold, wing leveler, and aileron rudder interconnect. This is the default system used for the present research simulation.

# FLIGHT CONTROL SYSTEM

| Control System | Pilot Command Type | Descriptive Comments |
|---|---|---|
| 1 | Acceleration command | • Stick to surface servos |
| 2 | Rate command | • Hi-gain pitch rate damper<br>• Roll rate feedback |
| 3 | Rate command and attitude hold | • Pitch and roll attitude hold<br>• Wing leveler<br>• Aileron-rudder interconnect |

## Electronic Attitude Director Indicator
## (EADI)

The accompanying figure shows the Electronic-Attitude-Director Indicator (EADI). This instrument is located centrally in the instrument panel and has been found to provide the pilot with the majority of the necessary flight information. On the periphery of the EADI starting at the lower left hand corner moving upwards are indicated airspeed (IAS) in knots, Mach meter and radio altimeter. Roll bank angle is displayed across the top of the EADI. Proceeding down the right side on this instrument, pressure referenced altitude and glide slope error information are displayed; while on the bottom of the instrument, localizer information is displayed. Localizer error is referenced to the extended runway centerline, and glide slope error is referenced to a 3 degree glide slope. In the center of the instrument pitch angle bars are displayed along with the aircraft reference waterline. The triangular icon in the center on the EADI is the velocity vector which continuously displays were the aircraft is going. The pitch command bar is also displayed in the center of the EADI and, for this investigation is configured such that the aircraft will have a 4% climb gradient when the command bar is on top of the reference waterline bar.

# ELECTRONIC ATTITUDE DIRECTOR INDICATOR
# (EADI)



1153
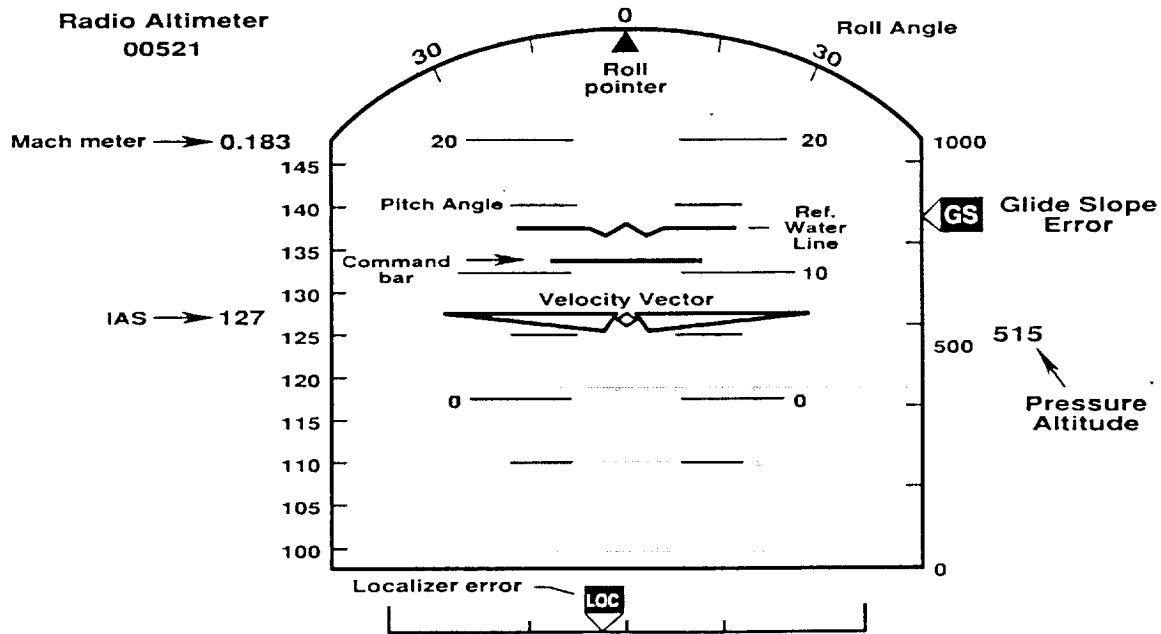
## VSCE-516  Characteristics

The AST-105 configuration is equipted with four Pratt-Whitney VSCE-516 engines. They are dual-stream duct-burning low-bypass ratio turbo-fan engines and make use of an inverted velocity profile for noise reduction. Engine characteristics used in the simulation are shown. These characteristics are input for both the piloted simulation and the Aircraft Noise Prediction Program (ANOPP). The piloted simulation requires net thrust data whereas ANOPP requires flow state variables.

## *ENGINE CHARACTERISTICS*

### VSCE-516
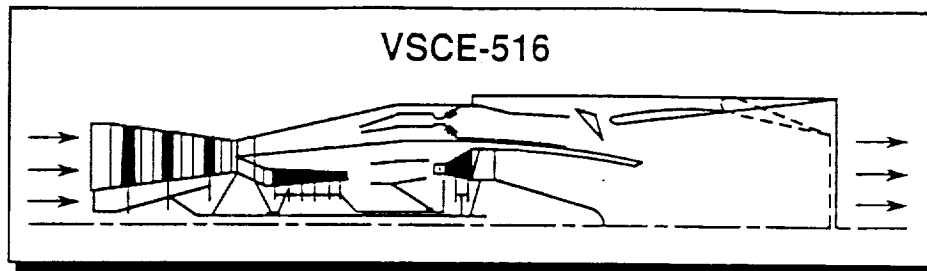
**Simulation Input:**
- Performance variables
* Net Thrust
  $$T \equiv F(T_{max}, PSET)$$
  $$T_{max} \equiv F(H, M)$$

**ANOPP Input:**
- Flow state variables
  (primary & secondary streams)
* Jet area $\equiv F(H, M, PSET)$
* Mass flowrate $\equiv F(H, M, PSET)$
* Total pressure $\equiv F(H, M, PSET)$
* Total temperature $\equiv F(H, M, PSET)$

**Note:** Noise prediction is for jet mixing effect only

1154

C-2 .

# Ground Noise Contours

Very recently acquired results from the present piloted simulation are shown. These ground noise contours are presented to illustrate that the Visual Motion Simulation/Aircraft Noise Prediction Program (VMS/ANOPP) interface is operational.

## GROUND NOISE CONTOURS
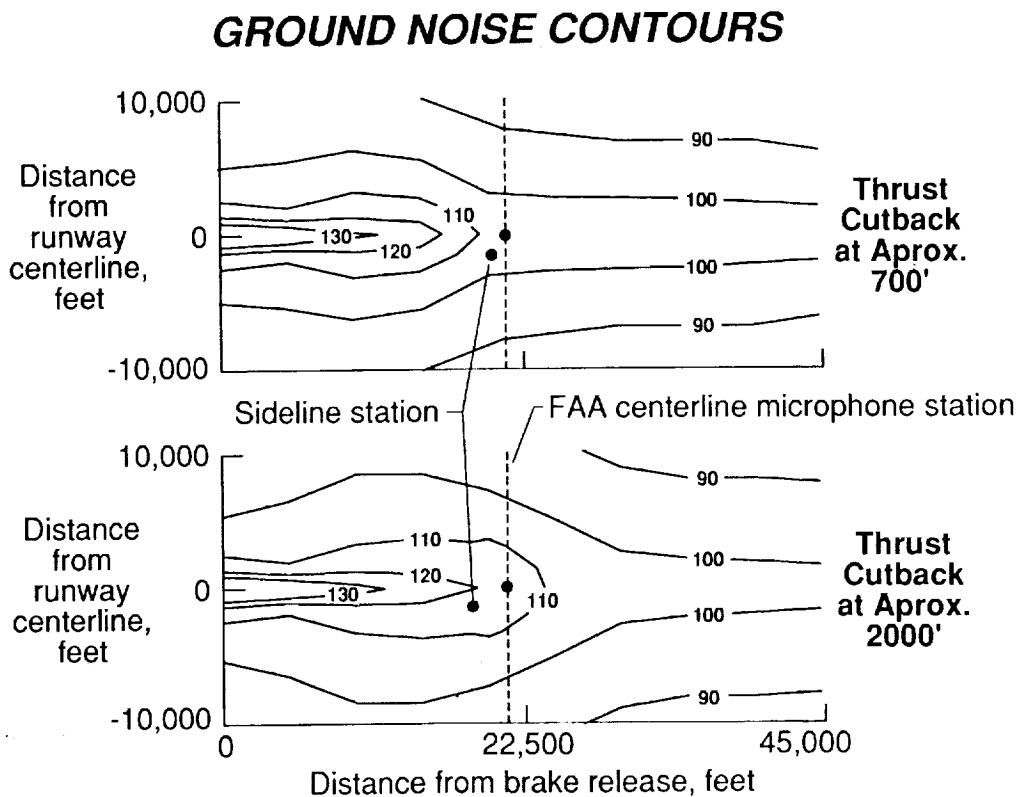
# HSCT Piloted Simulation Status

The status of the piloted simulation research is as indicated.

- AST-105 aerodynamic data base and VSCE-516 engine deck incorporated in Visual Motion Simulation

- VMS/ANOPP interface developed

- AST baseline noise characteristics evaluated

- Advanced engine and advanced operating procedures investigations in progress

1156

# HSCT Piloted Simulation Plans

Near term plans for the piloted simulation are as indicated. This study is intended to be a long term activity and will be updated to reflect current HSCT concepts as the experimental and computational data become available.

# *NEAR TERM PLANS*

- Complete community noise evaluation of (AST-105) configuration, assess impact of advanced engines, advanced piloting procedures

- Enhance high-lift aerodynamics and evaluate community noise
    - $C_L$ - Assume potential flow
    - $C_D$ - Asume 90-percent suction
    - $C_m$ - No pitchup, alternate trim concepts

- Evaluate community noise characteristics for NASA advanced baseline HSCT configuration

THIS PAGE INTENTIONALLY BLANK

# Session VIII. Aeroacoustic Analysis and Community Noise

High Performance Jet-Engine Flight Test Data Base for HSR
*Jeffrey Kelly, Lockheed Engineering and Sciences Company*

THIS PAGE INTENTIONALLY BLANK

1160

# HIGH PERFORMANCE JET-ENGINE FLIGHT TEST DATA BASE FOR HSR

$\overline{\jmath} 6 - 7 /$

$/ 2036$

Jeffrey Kelly

Lockheed Engineering and Sciences Company
Langley Program Office
Hampton, Virginia

First Annual High-Speed Research Workshop

May 14-16, 1991

The primary acoustic priority of the flight test data base for HSR is the validation of the NASA Aircraft Noise Predication Program (ANOPP) and other source noise codes. Also, the noise measurements are an important support function for the High Lift Program devoted to HSR. Another concern that will be addressed is a possible noise problem 7-20 miles from take-off during climbout. The attention arises from the higher speeds envisioned for the HSCT compared to conventional aircraft causing levels to increase because of Doppler amplification in conjunction with high source levels due to jet noise. An attempt may be made to measure airframe noise for the F-16XL test which would provide an assessment of this noise component for delta wing aircraft.

# GOALS FOR ACQUISITION OF AN ANOPP VALIDATION DATA BASE

I.  The primary acoustic goal is the acquisition of a data base to validate ANOPP and source noise codes

II. Support the High Lift Program

III. Look at the potential noise problem during climb-out (7 to 20 miles out)

IV. Consider the possibility of measuring airframe noise

## CRITERIA FOR SELECTING AIRCRAFT

The first acoustic concern in the selection of the aircraft for the flight test program is that they be equipped with turbojet or low-bypass turbofan engines with afterburner. This requirement guarantees that the dominant noise source will be jet noise. Also, it would be beneficial for the aircraft to have calibrated engines since this would reduce any errors in the engine state data input to ANOPP. Single engine vs. dual engine powered aircraft is another topic of consideration. A single engine aircraft will provide a more detailed description of the noise mechanisms (mixing, shocks, etc.). But since the HSCT will be multi-engined a dual engine aircraft would show the effects of jet shielding. The F-16XL, which is single engined, has a planform similar to that envisioned for the HSCT. It also will be equipped with high lift devices (slats, flaps) proposed for the HSCT. In addition, the F-16XL could provide an airframe-noise data base for delta-wing-configured aircraft. The F-18 satisfies the dual engined proviso.

# CRITERIA FOR SELECTING AIRCRAFT

I.    Similarity to the HSCT

    1.    Turbojet engine with afterburner

    2.    Planform

    3.    High lift capability

    4.    Calibrated engines

    5.    Single vs. dual engines

II.    Two planes considered

    1.    F-16XL

        a.    Delta wing with planform similar to the HSCT

        b.    Modified version will have high lift capability

        c.    Single engine

        d.    Could provide delta wing data base for airframe noise

    2.    F-18

        a.    Dualed engined; includes jet shielding effects

        b.    Would provide an independent data base for ANOPP

PROPOSED AIRCRAFT OPERATING CONDITIONS
AND RESULTING DATA SET

The flight test program can be divided into four segments. Of primary importance are level flyovers at constant velocity where ensembled averaged data is collected to validate ANOPP. This acoustic data can also be used to characterize jet noise. Measurements will also be performed on the aircraft in take-off and landing flight modes. This procedure will provide some insight into certification and community noise issues. The proposed speeds at particular altitudes that the HSCT is expected to experience during climbout must be emulated in the test phase and acoustic data collected. By doing this could yield some knowledge about the community noise concerns due to increased jet noise levels and Doppler amplification. Measurements carried out during a static test should be included in the data base. Use can be made of this data in ANOPP validation and characterization of noise source mechanisms.

# PROPOSED AIRCRAFT OPERATING CONDITIONS AND RESULTING DATA SET

| Operating condition | Data set |
|---|---|
| I. Level flyover at constant velocity | Ensemble averaged data; characterization of jet noise; ANOPP validation |
| II. Take-off and landing | Certification; community noise |
| III. Climb-out | Community noise; Doppler amplification |
| IV. Static test | ANOPP validation; source characterization (spectral content, directivity) |

1164

## ANOPP VALIDATION

For the ANOPP validation phase of the test program both the accuracy of the measured acoustic data and the measured input parameters to ANOPP are critical. Accurate tracking of the aircraft flight path is essential for input to ANOPP and ensemble averaging the measured data to enhance the confidence in the collected data. An instrumented, tethered balloon will be employed to collect the weather data to be input to ANOPP (temperature, pressure, humidity). The effect of ground impedance can be minimized by mounting the microphones in planar ground boards. Engine state data for the particular aircraft involved in the test should be provided before the test program is initiated. During the data analysis that will result from the data base, accurate tracking histories are required for ensemble averaging. Also, the narrow-band spectra must be converted to 1/3-octave band spectra to compare against ANOPP.


# ANOPP VALIDATION

I.  ANOPP input requirements
   1. Flight profile

   2. Atmosphere (temperature, pressure, humidity)

   3. Ground impedance

   4. Engine deck to characterize noise sources

II. Data collection requirements
   1. Ensembled averaged data

   2. 1/3-octave band spectra

   3. Accurate aircraft tracking data

   4. Measure ambient conditions (temperature, pressure, humidity)

For the level flyover segment of the flight test program, the purpose of which is to validate ANOPP, one altitude is selected, 1200 ft. Nine passes are proposed of the microphone array at the stipulated Mach numbers. Each case should be flown at least twice to check repeatability.

# FLIGHT TEST CONDITIONS FOR LEVEL FLYOVER - ANOPP VALIDATION

### Altitude = 1200 ft.

| Aircraft Mach number | Aircraft speed, ft./sec |
|---|---|
| .2 | 223 |
| .3 | 335 |
| .4 | 446 |
| .5 | 558 |
| .6 | 669 |
| .7 | 781 |
| .8 | 892 |
| .9 | 1004 |
| .95 | 1059 |

Fly each case twice to check repeatability

1166

# WEATHER MONITORING SUBSYSTEM

An instrumented, tethered balloon system will provide values for the ambient atmosphere for input to ANOPP (temperature, pressure, humidity). Prior to the flyovers, the atmosphere can be surveyed by the balloon system up to the flight altitude of 1200 feet, thus providing the ambient quantities as a function of altitude.

## WEATHER MONITORING SUBSYSTEM

WEATHER BALLOON

INSTRUMENTS & TRANSMITTER

ELECTRONIC WINCH

### MEASUREMENTS

- BAROMETER PRESSURE
- WET & DRY BULB TEMP.
- WIND SPEED
- WIND DIRECTION
- ETC.

### FEATURES

- .1 Hz UPDATE RATE
- REAL TIME DIGITAL OPERATION
- NUMERIC ERROR CHECKING
- FIELD TESTED
- LAYERED ATMOSPHERIC MODELING

BALLOON VAN

RECEIVER

MICROPROCESSOR

IEEE-488 INTERFACE

EXTERNAL CONTROL COMPUTER

TO PCM PROCESS CONTROL COMPUTER

PRINTER

1167
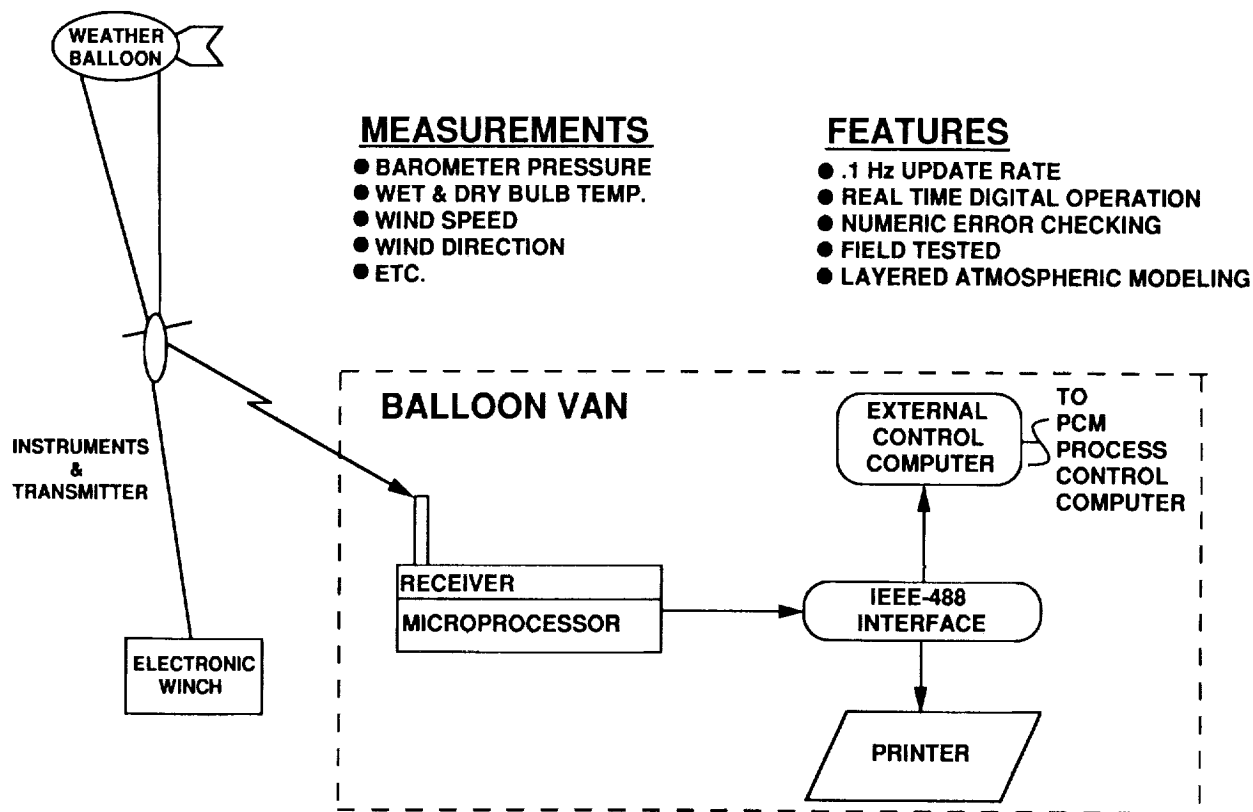
# ENGINE STATE DATA REQUIRED FOR ANOPP PREDICATION

   The evaluation of turbojet or turbofan engine noise source levels by ANOPP requires that the inlet and exit conditions for area, fuel-to-air ratio, mass flow rate, total pressure, total temperature and rotational speed be specified. This must be done for all four engine stages or components, i.e., fan, core, turbine and jet.

## ENGINE STATE DATA REQUIRED FOR ANOPP PREDICTION

**[Area, Fuel-to-Air Ratio, Mass Flow Rate, Total Pressure, Total Temperature, Rotational Speed]**

| | |
|---|---|
| **FAN** | **INLET** |
| | **EXIT** |
| **CORE** | **INLET** |
| | **EXIT** |
| **TURBINE** | **INLET** |
| | **EXIT** |
| **JET** | **PRIMARY** |
| | **SECONDARY** |

Engine Deck
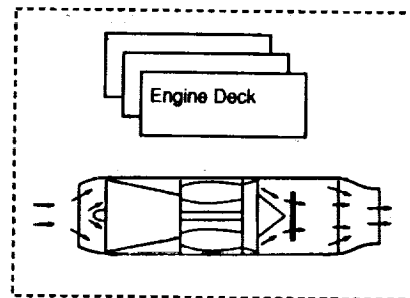
Use of ANOPP can be made in the prediction of noise levels that may impact community noise regulations concerning operation of the HSCT. To accomplish a prediction of a noise metric, ANOPP must be supplied with the ambient atmospheric quantities, flight trajectory and engine state tables.

# HSR NOISE PREDICTION SYSTEM

```
                                    ┌──────────────┐
                                    │    ENGINE    │
                                    │    STATE     │
                                    │    TABLES    │
                                    └──────┬───────┘
                                           │
                                           ▼
┌──────────────┐   ┌──────────────┐   ┌──────────────┐   ┌──────────────┐
│ ATMOSPHERIC  │──▶│    FLIGHT    │──▶│    SOURCE    │──▶│   OBSERVER   │
│    MODEL     │   │  TRAJECTORY  │   │    NOISE     │   │   LOCATION   │
└──────────────┘   └──────────────┘   │  PREDICTION  │   └──────┬───────┘
                                       └──────────────┘          │
                                                                 ▼
                                                          ┌──────────────┐
                                                          │  CALCULATE   │
                                                          │    NOISE     │
                                                          │    METRIC    │
                                                          └──────────────┘
```
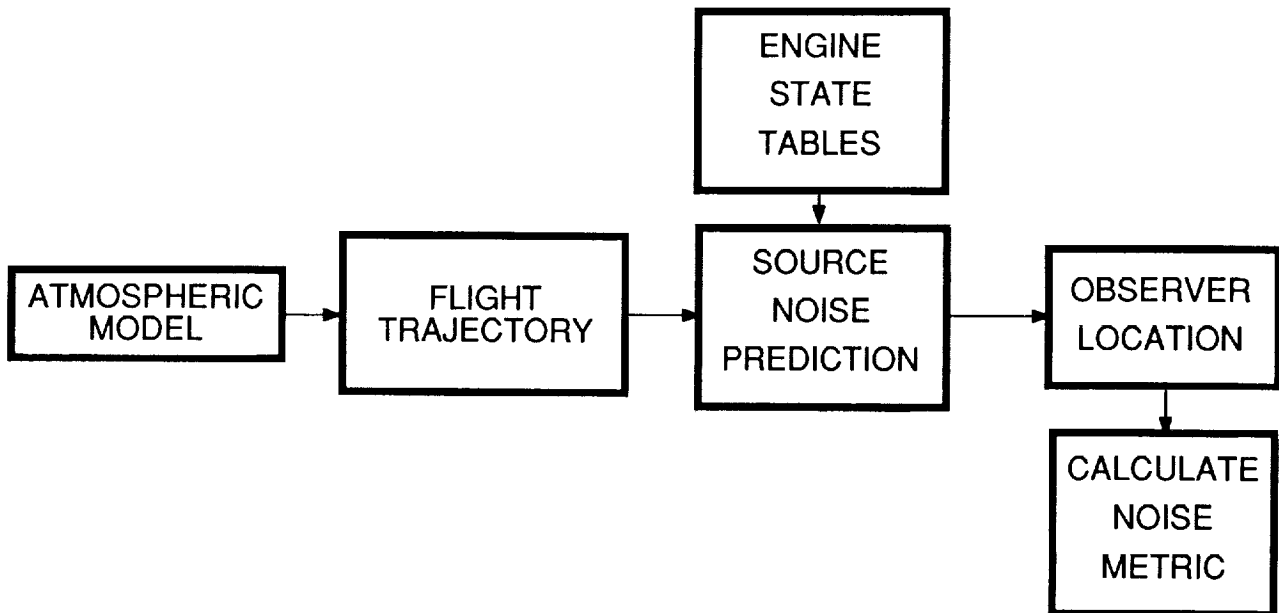
MICROPHONE CONFIGURATION

A linear array of nine microphones will be used to acquire the acoustic data. Spacing between the microphones is tentatively set at 200 feet. The analog-to-digital conversion unit is in the microphone housing. Thus, each channel will be recorded in a digital format. The sample rate of the A-D unit will be greater than 25 kHz so that the Nyquist frequency will be above 12.5 kHz.

# MICROPHONE CONFIGURATION

Linear array of at least 9 microphones will be employed

Microphones are digital, i.e, the A-D unit is in the microphone

Signals will be recorded in a digital format

Microphones will be deployed on planar ground boards to reduce the effect of ground impedance

Sample rate of the A-D unit will be greater than 25 kHz, thus Nyquist frequency will be above 12.5 kHz

1170

## MICROPHONE ARRAY SUBSYSTEM

The microphones will be mounted on planar ground boards to reduce reception of reflected signals. The usual procedures will be taken to avoid aliasing (sufficiently fast sample rate, low-pass filter). Calibration of the microphones is to be performed immediately prior to the flight test.

## MICROPHONE ARRAY SUBSYSTEM

.5" B & K 4146S
CONDENSER MIC.
W/PREAMP &
W/WINDSCREEN

**FEATURES**

- .01 Hz - 40 KHz FREQUENCY RESPONSE
- 160 dB MAX SPL
- FIELD RELIABLE

O-GRAPH
RECORDS

14 - TRACK TAPE

| HIGH GAIN AMPLIFIERS | BAND-PASS FILTER ARRAY | TAPE RECORDER |

10 Hz - 16 KHz
TYPICAL

46 dB DYNAMIC
RANGE TYPICAL
(RECORDING SPEED
DEPENDENT)

**MICROPHONE VAN**

PLANAR
GROUND
BOARD

**GROUND - PLANE MICROPHONE DEPLOYMENT
(4 SHOWN, 6 PER ROW PROPOSED)**

1171
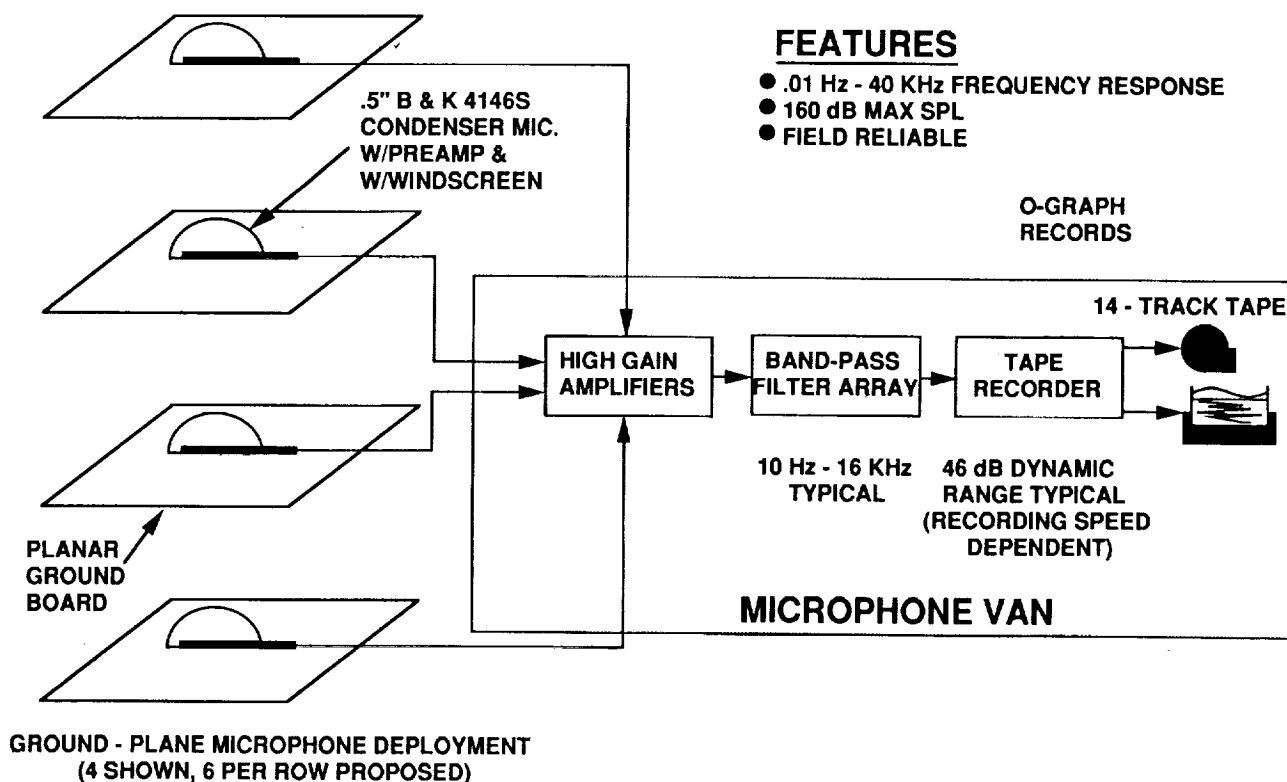
# FLIGHT ENSEMBLE AVERAGING

With the use of a laser/radar tracking system accurate position data can be determined and thus providing a means of correlating the position history of the aircraft with the microphone pressure time histories. For the level flyover situation, this allows ensemble averaging across the microphones that see the same emission angles.

# FLIGHT ENSEMBLE AVERAGING



1172
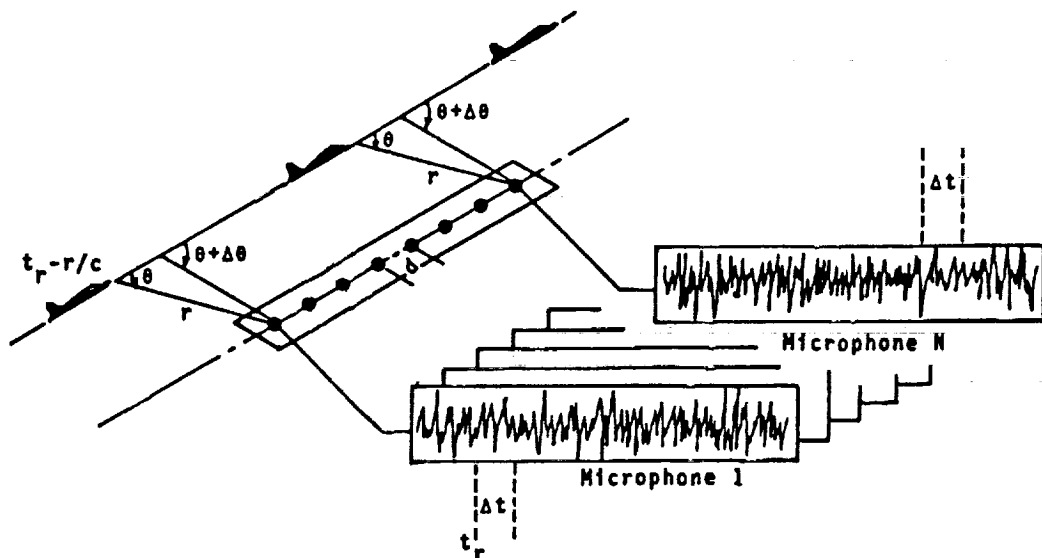
# DIGITAL SIGNAL ANALYSIS PARAMETERS

For digitally recorded signals the sample rate, $\Delta t$, is determined at the time of acquisition and is a set value of the A-D unit. But, the number of points, per block N, can be varied during the signal processing. The window duration is determined from the relation $T=N\Delta t$. From the reciprocal of this $(1/T)$, the bin width or frequency resolution is deduced, i.e., $\Delta f = 1/T$. The number of blocks, $n_d$, per segment for each channel defines the segment length, $T_{TOT} = n_d T$. The number of averages involved in the the FFT samples is given by $n_d x$ the number of microphones.

## DIGITAL SIGNAL ANALYSIS PARAMETERS
### Example for two different bin widths

|  | case 1 | case 2 |
|---|---|---|
| sample rate (sec) | .00004 | .00004 |
| number of points per block | 2048 | 16384 |
| window duration (sec) | .08192 | .65536 |
| frequency resolution (Hz) | 12.2 | 1.53 |
| number of blocks per segment | 5 | 1 |
| segment length (sec) | .4096 | .65536 |
| number of microphones | 9 | 9 |
| number of samples in ensemble average | 45 | 9 |

## ILLUSTRATION OF RECORD DETERMINATION
## FOR A BIN WIDTH OF 12.2 Hz

For smear angles, $\Delta\theta$, small enough, ensemble averaging can be implemented within each microphone measurement in addition to across the array. This increases the number of averages which reduces noise in the signal. But a trade-off is that decreasing the smear angle implies that the window duration, T, also decreases and leads to a loss in resolution.

## ILLUSTRATION OF RECORD DETERMINATION FOR A
## BIN WIDTH OF 12.2 HZ
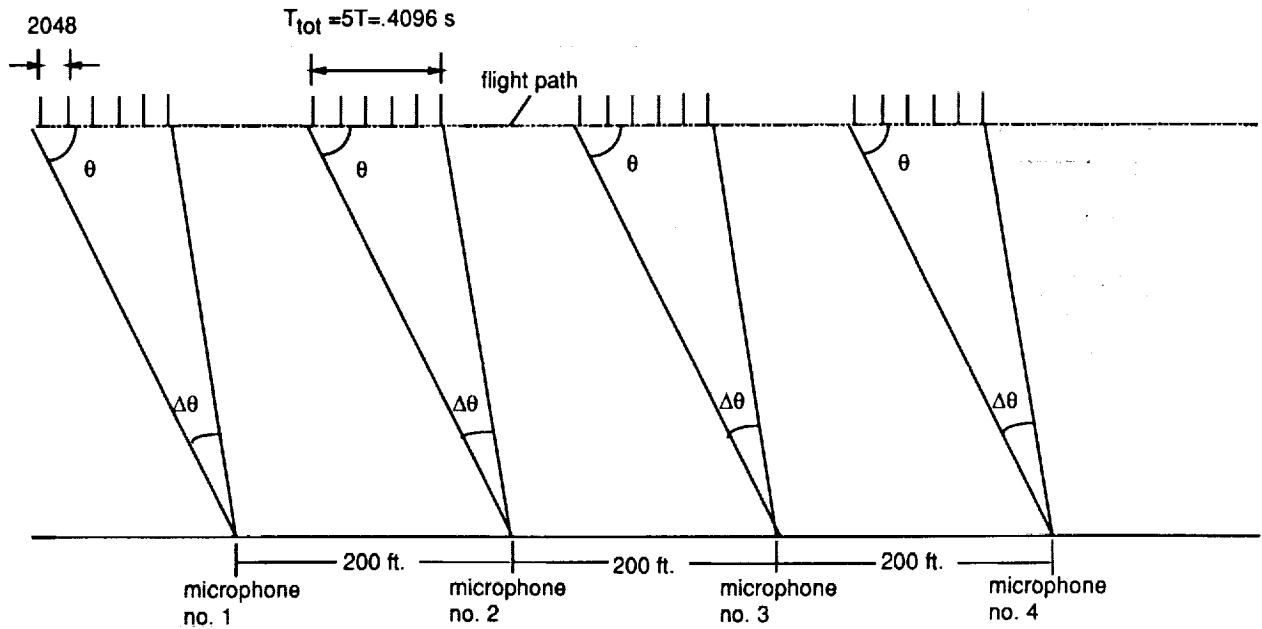
## TAKE OFF AND LANDING TEST CONDITIONS

For take-off and landing flight modes the passes are to be performed over the same linear microphone array as was used for the level flyovers. In addition, the three certification microphones on 1.2 meter poles are now included. Ensemble averaging presents a problem since each microphone sees a different time history. By executing multiple passes, ensemble averaging might be performed across these passes if repeatability presents no problem. Since jet noise is in general broadband ensemble averaging is not as important as in highly tonal spectra. An ILS equipped runway would provide the aircraft with the appropriate glide slope to obtain the required altitude above the certification microphone. During some of the take-off passes afterburner operation is to be included, since this is the worse case scenario for community noise. For the F-16XL on approach, if engine power can be reduced so that the level of jet noise is below the estimated value for airframe noise, acoustic data will be collected.

# TAKE-OFF AND LANDING TEST CONDITIONS

Include the three certification microphones on 1.2 meter poles

Desirable to vary approach and climb angle and their associated speeds within the performance limit of the aircraft

Advantageous to have an ILS equipped runway to guarantee the 397 ft. of altitude above the approach certification microphone

Afterburner operation should be included in some of the take-off flights

For the F-16XL an attempt may be made to measure airframe noise if power can be reduced enough without jeopardizing flight safety

LEVEL FLYOVER TEST CONDITION TO EMULATE CLIMB-OUT
ALTITUDES AND VELOCITIES

Level flyovers of the microphone array will be performed to emulate climb-out altitudes and speeds. These flyovers are to be executed at a Mach number of .95 from 2000 to 30000 ft. as shown in the figure. Due to Doppler amplification caused by the envisioned higher speeds of the HSCT and the higher source jet noise, noise annoyance could arise in previously unaffected areas.

# LEVEL FLYOVER TEST CONDITIONS TO EMULATE CLIMB-OUT ALTITUDES AND VELOCITIES

Higher speeds envisioned during climb-out for the HSCT compared to conventional aircraft could produce significantly higher levels due to Doppler amplification

Use the linear microphone array to collect the data

Compare measured values with ANOPP

Test to be performed at a fixed flight Mach number of .95 at the following altitudes

| Test case | Altitude (ft.) |
|-----------|----------------|
| 1 | 2000 |
| 2 | 5000 |
| 3 | 10000 |
| 4 | 15000 |
| 5 | 20000 |
| 6 | 25000 |
| 7 | 30000 |

1176

STATIC TEST

    A static test is to be performed in the vicinity of the microphone array. By executing a rosette, the aircraft will display a directivity pattern to the array in the horizontal plane. At each test orientation, the sound field will be stationary and this can yield a reference data base to characterize the noise mechanisms of the aircraft. The measured data can then be compared to ANOPP predictions which in this situation can isolate the performance of individual modules.

# STATIC TEST

runway

microphone array
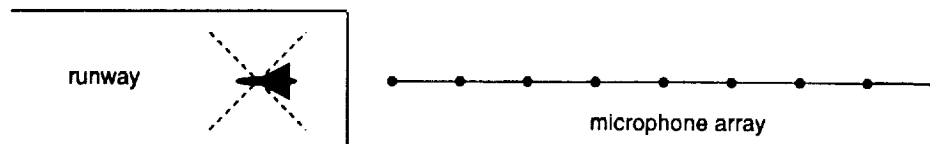
Aircraft executes a rosette, thus array will record the directivity of the noise sources in a horizontal plane

Sound field will be stationary: this will provide a reference data base to characterize the noise

Compare measured data with ANOPP: this would give a better idea of the performance of individual modules than flight data

**THIS PAGE INTENTIONALLY BLANK**

# Session VIII.  Aeroacoustic Analysis and Community Noise

Status and Plans for the ANOPP/HSR Prediction System
*Sandra K. Nolan, Lockheed Engineering and Sciences Company*

THIS PAGE INTENTIONALLY BLANK

57-71
12037

# STATUS AND PLANS FOR THE ANOPP / HSR PREDICTION SYSTEM

S. K. Nolan
Lockheed Engineering and Sciences Company
Hampton, Virginia

First Annual High-Speed Research Workshop
May 15, 1991

ANOPP is a comprehensive prediction system which has been developed and validated by NASA. Because ANOPP is a system prediction program, it allows industry to create trade-off studies with a variety of aircraft noise problems. The extensive validation of ANOPP allows the program results to be used as a benchmark for testing other prediction codes.

# AIRCRAFT NOISE PREDICTION PROGRAM ( ANOPP )

ANOPP is a system noise prediction program which the

government has been developing over many years to help

industry with trade off studies for a large variety of aircraft

noise problems.

1182

ANOPP is made up of two types of modules, control modules which comprise the ANOPP Executive System and dedicated prediction modules, each of which predicts a particular noise component. The dedicated modules make up the four prediction systems within ANOPP. The Conventional Takeoff and Landing System (CTOL) predicts conventional turbofan and turbojet aircraft noise. The Propeller Analysis System (PAS) predicts propeller noise. The Helicopter Noise Prediction System (ROTONET) predicts helicopter noise. The High-Speed Research System (HSR) predicts high speed aircraft noise. Each of the dedicated modules executes under the control of the ANOPP Executive System.

# AIRCRAFT NOISE PREDICTION PROGRAM (ANOPP) OVERVIEW

```
                    ┌─────────────────────────┐
                    │         ANOPP           │
                    └─────────────────────────┘
                                 │
  ┌──────────────────────────────────────────────────────────┐
  │          ┌─────────────────────────────────┐             │
  │          │       EXECUTIVE SYSTEM           │             │
  │          └─────────────────────────────────┘             │
  │                  CONTROL  MODULES                         │
  └──────────────────────────────────────────────────────────┘
                                 │
  ┌──────────────────────────────────────────────────────────┐
  │      ┌──────┐    ┌──────┐   ┌────────┐   ┌──────┐         │
  │      │ CTOL │    │ PAS  │   │ROTONET │   │ HSR  │         │
  │      └──────┘    └──────┘   └────────┘   └──────┘         │
  │                                                          │
  │    Conventional  Propeller   Helicopter     High         │
  │      Turbofan    Analysis      Noise        Speed        │
  │        and        System     Prediction    Aircraft      │
  │      Turbojet                  System                    │
  │      Aircraft                                            │
  │            DEDICATED PREDICTION MODULES                  │
  └──────────────────────────────────────────────────────────┘
```

1183

The ANOPP Executive System processes user supplied input in the form of control statements. Based on this input, the Executive System maintains the ANOPP data base, controls procedure and dedicated module execution, and directs the order in which the modules are executed. The Executive System provides a checkpoint and restart capability, which allows the user to create a break at any point in the execution and restart a prediction from that point with or without modifications. Extensive error checking and reporting of error messages is maintained by the Executive System.

# ANOPP EXECUTIVE CAPABILITIES

```
+-------------------------------------------------------------------+
|                   +-----------------------------+                 |
|                   |     EXECUTIVE SYSTEM        |                 |
|                   +-----------------------------+                 |
|                              |                                    |
|              +------------------------------------+               |
|              |   CONTROL STATEMENT PROCESSING     |               |
|              +------------------------------------+               |
|                              |                                    |
|      +-----------------------+------------------------+           |
|  +--------+          +-----------+         +-----------+          |
|  | DATA   |          | DEDICATED |         |CHECKPOINT/|          |
|  | BASE   |          | MODULE    |         | RESTART   |          |
|  |MANAGER |          | EXECUTION |         +-----------+          |
|  +--------+          +-----------+                                |
| +-----------+    +-------------+     +-----------+                |
| |PROCEDURE  |    |CONDITIONAL  |     |  ERROR    |                |
| |EXECUTION  |    |   FLOW      |     |CHECKING/  |                |
| +-----------+    +-------------+     |REPORTING  |                |
|                                      +-----------+                |
|                    CONTROL  MODULES                               |
+-------------------------------------------------------------------+
```

1184
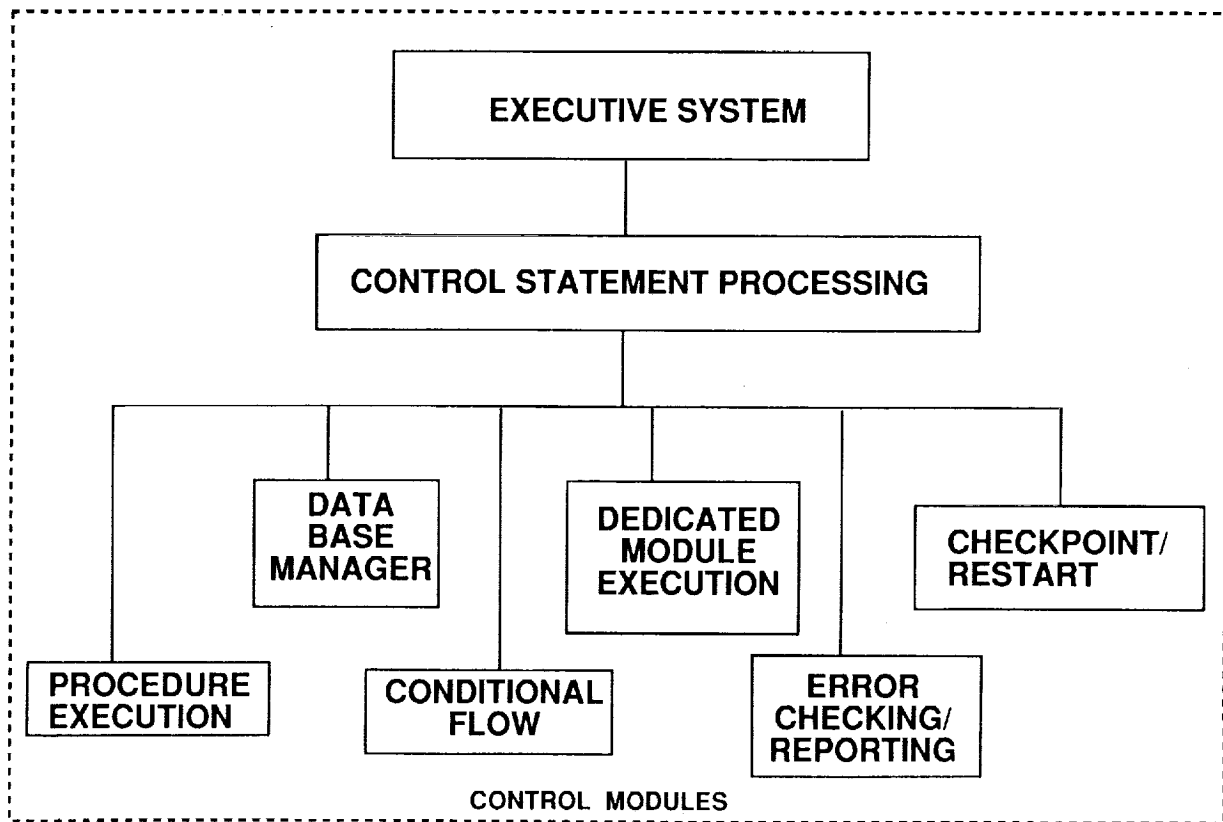
EVALUATION OF ANOPP EXECUTIVE SYSTEM

In the evaluation of ways to improve ANOPP, replacing the executive system with a smaller less flexible system or eliminating the executive system entirely and going to small stand-alone programs was considered. The evaluation concluded that the current capabilities and flexibility of the Executive System are required by ANOPP users. The ANOPP Executive System has many advantages. It contains its own database manager which makes the code portable to different computer systems. The system is flexible and easy to modify and customize, which allows users to easily create their own model from which to predict aircraft noise. The extensive error checking and reporting done by the Executive System aids the ANOPP support team in quickly responding to user questions and problems. Because most users of ANOPP would be unwilling to give up the capabilities of the current system, it was concluded that the perception of ANOPP being too large or complex, not the actual program size or capabilities, may cause any negative feelings toward ANOPP. One solution to change this perception is to increase the user friendliness of ANOPP.

# EVALUATION OF ANOPP EXECUTIVE SYSTEM

Advantages of ANOPP Executive System:

Portable

Flexible

Easy to Modify and Customize

Easy to Respond to User's Questions and Problems

ANOPP users require the capabilities and flexibility of the current ANOPP Executive System

Perception of ANOPP system, not the program, causes any negative attitude towards ANOPP.

Solution to problem is to increase user friendliness of ANOPP

When dealing with system noise predictions, regardless of the prediction system selected, the program will be large and complex due to the scope and complexity of aircraft noise problems. When first confronted with such a diverse system, some users perceive that ANOPP is difficult to learn, user unfriendly, too complex, and hard to understand. In order to change this perception and make ANOPP more user friendly, some enhancements to the HSR system are currently under development. These enhancements include an introductory User's Guide, to aid new users or users trying new capabilities of the system; an Interactive Input Program, which will prompt the user for input data and create an input deck in the format required by ANOPP; Templates, which will contain example user supplied input decks for a variety of noise prediction problems; a Glossary / Cross Reference which will contain definitions of ANOPP terms; and a Contour Package, which will allow the user to create ground contours.

# SOLUTIONS TO PERCEIVED PROBLEMS WITH ANOPP

| Perceived Problem: | Solution: |
|---|---|
| Difficult to learn | User's Guide<br>Hands-on Training<br>User Support |
| User Unfriendly | Interactive Input Program |
| Too Complex | Templates |
| Hard to Understand | Glossary/ Cross Reference |
| No Graphic Output | Contour Package |

The HSR User's Guide will provide new or infrequent users with a concise reference to explain the capabilities of the HSR system and how to initiate its use. It will contain an overview of ANOPP and the HSR system, a list of the types of noise prediction problems that HSR can solve, a list of available dedicated modules with an explanation of their function, and a flow chart of the HSR system which will indicate the order in which the dedicated modules can be used. The User's Guide will also contain information about computer systems for which an ANOPP version exists, information about system design with a general description of the different types of database items, and a description of available HSR templates that can be used as modifiable examples of user supplied input decks.

# HSR USER'S GUIDE

PURPOSE: To provide new users with a concise manual to explain the capabilities of the HSR system and how to initiate its use.


DESCRIPTION:

1. Overview of ANOPP and the HSR prediction system.

2. Types of problems that the HSR prediction system can execute.

3. Available dedicated modules with flow charts and general input and output requirements.

4. Available computer system versions of ANOPP.

5. Pertinent information about HSR system design.

6. Description of available HSR input templates.

In order to produce noise prediction data with HSR, the user must provide a file of input data in the specific format required by ANOPP.  The Interactive Input Program that is currently being developed will provide users with a menu driven method of creating this input file.  The program will display available options  and will insure a logical execution flow.  Default input values will be displayed and the user will be given the option to change any or all of the default values.  An HSR input file will be created and will contain comments to explain where to insert or modify additional data.  Optionally, the user can issue a command within the Input Program to execute HSR using the created input file.

# HSR INTERACTIVE INPUT PROGRAM

PURPOSE:      To provide an interactive, menu driven method
              of creating an input deck for HSR execution.


DESCRIPTION OF PROGRAM:

1.  Displays available options.

2.  Guides the user in creating an HSR input deck.

3.  Prompts the user for input data.

4.  Creates an input deck with comments on where
    to insert or modify data.

5.  Optionally executes ANOPP using the created HSR
    input deck.

1188

Example HSR input files for a wide range of noise prediction problems are being developed. These examples are called HSR Templates. The user will select and modify the Template closest to the problem that they are modeling. The input deck will be fully documented with a description of both the prediction problem and listed data. Templates will include but not be limited to noise predictions with takeoffs, landings, steady flyovers, stationary single or multiple noise sources, propagation from source to observers, and ground contours.

# HSR  TEMPLATES

PURPOSE: To provide examples of HSR input decks for specific noise prediction problems and to assist users in creating their own input decks by modifying the example templates.

DESCRIPTION:

1. Fully documented with an explanation of the template prediction problem and data.

2. Templates will be provided to include but not limited to the following types of noise predictions:

   Takeoffs
   Landings
   Steady flyovers
   Stationary single or multiple noise source
   Propagation
   Contours

A Glossary of ANOPP terms with a cross reference to where these terms are used in ANOPP is being designed. The ANOPP terms will come from both input and output data. The glossary will contain a global list of user parameter names with descriptions related to industry standard quantities and a cross references to the dedicated modules that require or produce them. It will also contain a global list of ANOPP database members with descriptions of the data that they contain and cross references to the dedicated modules that require or produce them. These cross references are important because the output from one or more dedicated modules is used as input data to other dedicated modules.

# ANOPP GLOSSARY / CROSS REFERENCE

PURPOSE: To provide users with a description of ANOPP input and output data.

DESCRIPTION:

1. Will contain a global list of user parameter with descriptions related to industry standard quantities and cross references to dedicated modules which require or produce them.

2. Will contain a global list of ANOPP data base unit members and tables with cross references to dedicated modules which require or produce them.

HSR CONTOUR CAPABILITY

The capability to produce ground contours from within an HSR
system procedure is under development. HSR currently contains a Contour
Module which creates a file containing contour data. This data can be used
to produce contours using an external graphics package such as DI3000.
The HSR Contour Package will be distributed with the ANOPP executable
tapes and will produce contours using the data from the Contour Module.
The additions of the Contour Module and Contour Package to HSR will
result in a single procedure that will execute an HSR prediction and produce
a ground contour.

# HSR CONTOUR CAPABILITY

PURPOSE:     To provide HSR users with the ability to produce
             contours within ANOPP procedures.


DESCRIPTION:

1.  Contouring package currently under development.

2.  Contour module to output contour data within an HSR
    execution is currently available.

3.  Contour package will be delivered to users on ANOPP
    update tapes.

4.  Contours will be produced using noise data from HSR
    predictions

5.  A single control structure will be used to run HSR
    predictions and /or produce contours

Enhancements to the ANOPP/HSR Prediction System are scheduled to be completed by Spring of 1992. The HSR Templates will be completed by the Summer of 1991. The HSR User's Guide will be completed by the Fall of 1991. The HSR Interactive Program and Contour Package will be completed by the Winter of 1992. The Glossary / Cross Reference will be completed by the Spring of 1992.

# SCHEDULE FOR COMPLETETION OF HSR ENHANCEMENTS

|  | Summer '91 | Fall '91 | Winter '92 | Spring '92 |
|---|---|---|---|---|
| User's Guide | ----------------------X | | | |
| Interactive Input Progam | -----------------------------------------X | | | |
| Templates | --------X | | | |
| Glossary/ Cross Reference | ----------------------------------------------------------X | | | |
| Contour Package | ---------------------------------------X | | | |

COMPUTER VERSIONS OF ANOPP

In addition to the efforts to make ANOPP more user friendly, work has been initiated to increase the types of computer systems on which ANOPP can be executed. ANOPP was originally designed to run on a Control Data Corporation (CDC) Cyber computer under the NOS operating system. In 1986 because of computer access limitations and requests from users in industry, ANOPP was converted to run on Digital Equipment Corporation (DEC) VAX computers under the VMS operating system. In 1987, an IBM-PC version of the ANOPP Propeller Analysis System (PAS) was completed.

In 1989, because of NASA Langley's decision to decrease CDC computer support and use CONVEX and CRAY, UNIX based computers , and because of requests from industry and other government agencies, the conversion to a a UNIX version of ANOPP was initiated. In 1990, the initial conversion of ANOPP to run on a CONVEX computer was completed. A generic UNIX version that will run on most UNIX based computers with only minor code changes is currently under development. This conversion will make ANOPP available on a greater variety of faster UNIX based computers and workstations.

When the UNIX conversion is completed later this year, we will announce a schedule to discontinue support and updates to the CDC version of ANOPP, which currently represents 35-40% of our maintenance effort and represents only 3 of the over 65 distributed copies of ANOPP which we support.

# COMPUTER VERSIONS OF ANOPP
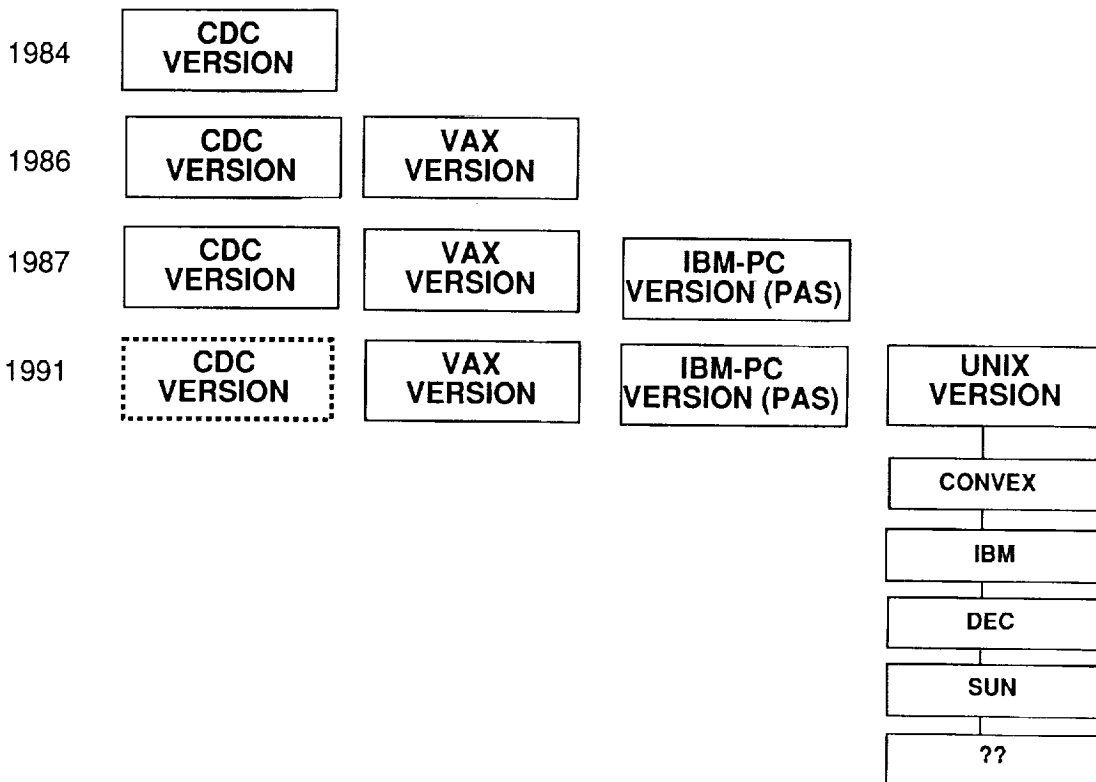
Multiple control methods are used to restrict access to ANOPP and
data related to ANOPP. These restrictions include limited access to ANOPP
source code, ANOPP executables, ANOPP database files, any NASA
supplied data under ANOPP maintenance and any user supplied data from
industry or other government agencies.

# GENERAL POLICY FOR SECURE HANDLING OF ANOPP CODE AND USER SUPPLIED INPUT DATA

Restricted access to :

1. ANOPP source code

2. ANOPP executable

3. ANOPP data base

4. NASA data

5. User supplied data

GENERAL POLICY FOR SECURE HANDLING OF ANOPP CODE
AND USER SUPPLIED DATA

Our protection methods include restricted access to computer systems
containing ANOPP code and data. A user must have an account and
password in order to access the computer. The source code and restricted
data are stored on a separate computer used only for ANOPP development.
Within that computer system, ANOPP is stored on a separate disk that
requires permission on a control list to access the disk and directories on
which the code or data is stored. Source code and restricted input data are
stored in a version control library where the user must be on a restricted list
to extract code or data from the library. Finally, all files can be protected
with an individual control list .

# GENERAL POLICY FOR SECURE HANDLING OF ANOPP CODE AND USER SUPPLIED INPUT DATA

Protection Methods:

Restricted access to computer systems containing
ANOPP code and data.

Password required for all computer access.

Source code and restricted access code stored on
computer used only for ANOPP development and noise
prediction runs.

Controlled access list for disk and directories on which
items are stored.

Source code and restricted input data stored in version
control library with restricted access list.

Individual files can be  protected with a controlled access list.

SUMMARY

An evaluation of ANOPP, the Executive System, and the HSR
Prediction System resulted in five action items to increase the user
friendliness of ANOPP / HSR. The conversion of ANOPP to a UNIX
version will make ANOPP available on a greater variety of faster computers
and workstations. Multiple control methods are used to insure restricted
access to ANOPP code and related data.

# SUMMARY

- Overview of ANOPP/HSR Prediction Program and
  Evaluation of the ANOPP Executive

- Action Items to Increase ANOPP User Friendliness

     HSR User's Guide
     Interactive Input Program
     HSR Templates
     Glossary / Cross Reference
     Contour package

- Conversion Of ANOPP to UNIX Version

- Secure Handling of ANOPP Code and User
  Supplied Input Data.

1196

# Session IX. Sonic Boom (Human Response and Atmospheric Effects)

THIS PAGE INTENTIONALLY BLANK

# Session IX. Sonic Boom (Human Response and Atmospheric Effects)

*ɡ̣ ṃ / ̓*

Atmospheric Effects on Sonic Boom--A Program Review
*Dr. Gerry L. McAninch, NASA Langley Research Center*

THIS PAGE INTENTIONALLY BLANK

$SB-91$
$12038$

# ATMOSPHERIC EFFECTS ON
## SONIC BOOM
## A PROGRAM REVIEW

**Gerry L. McAninch**
**Acoustics Division**
**NASA Langley Research Center**
**Hampton, Virginia**

**First Annual**
**HIGH-SPEED RESEARCH WORKSHOP**
**May 15, 1991**

PROGRAM GOALS

The program goals were determined after consideration of the weaknesses in our understanding of atmospheric effects on sonic boom waveforms left in the wake of the cancellation of the U. S. SST in the 70's, and the advancements in acoustics and atmospheric science since that time. For example, a considerable body of knowledge on molecular absorption had been built up in the acoustics community over the last 15 years and this had not been incorporated into the sonic boom theory. Further, it was felt that the understanding of atmospheric turbulence had also advanced considerably during that time period. Therefore, key elements of the current program are the development of an improved atmospheric absorption model, and an improved atmospheric turbulence model. The advances made in computer power over the last 15 years were also considered, and will be utilized to remove restrictions on the analytical model for turbulence effects on sonic boom waveforms. Although the majority of disturbing sonic booms will not occur at focuses or caustics, it was felt that this was an area that required further understanding, thus it to will be looked into.

Finally, in order to insure that the current effort, which is basically analytical in nature, retains a firm grasp on reality, a data base of sonic boom waveforms and associated weather data is being compiled, and a set of scale model experiments is being planned to guide the overall effort.

# PROGRAM GOALS

- Improved Atmospheric Absorption Model

- Improved Atmospheric Turbulence Model

- Improved Model For Turbulence Effects On Boom

- Understanding of Boom at Focuses and Caustics

- Readily Available, Easily Accessible Data Base for Model Validation

- Scale Model Experiments for Model Validation

1202

I am forced to break the work in progress into two mutually exclusive sets. Obviously the first breakdown that might occur to you is work that is done, and work that remains to be done, however, a different grouping is used here. Due to various constraints some of the people doing work under this program are not able to make presentations. Thus, if I do not very briefly recap their work, it will go unnoticed. This would provide a distorted view of the total program. Thus we may introduce the two groupings alluded to earlier. The "Hidden Agenda", and "Papers to be Presented". Since each of the later group will have their time to present their work I will concentrate on the former group. This group consists of Professor David Blackstock, of The University of Texas, who is working on some scale model experiments, and Mr. Dominic Maglieri, of Eagle Engineering, who is working on a data base of sonic boom waveforms.

# WORK IN PROGRESS

- **HIDDEN AGENDA**
  **Model experiments - D. Blackstock**
  **Data Base - D. Maglieri**

- **PAPERS TO BE PRESENTED**
  **Relaxation and Turbulence Effects - A. Pierce**

  **Turbulence Modeling and Turbulent Scattering Theory - K. Plotkin**

  **Rise Time Correlations of Sonic Boom Data - H. Bass**

Some things of interest to us for the sonic boom problem are neither analytically tractable nor easily investigated in full scale experiments. Examples include the field at a focus, or at a caustic, which evade analysis at the current time because of the breakdown in the essentially linear methods used, and the essential nonlinearity of the problem, and which are difficult to measure in a large scale experiment because of the limited spatial domain over which the relevant phenomena occur and the difficulty of predicting precisely where this domain exists. These phenomena are ideally suited to investigation in small scale experiments, and this is the task being undertaken by Professor Blackstock, who has proposed a scale model experiment to:

- Test the waveform freezing theory
- Obtain measurements at a focus
- Obtain measurements of diffraction into the shadow
- Obtain measurements of turbulence induced waveform distortion
- Determine the role of nonlinearity

At the current time Professor Blackstock is in the midst of designing the experiments.

# HIDDEN AGENDA - BLACKSTOCK

## University of Texas - Austin

## Scale Model Effects of Stratification and Turbulence

- ### Test of waveform freezing

- ### Measurement at focus

- ### Measurement of diffraction into shadow

- ### Measurement of turbulence induced distortion

- ### Determination of role of nonlinearity

### DESIGN OF EXPERIMENTS IN PROGRESS

For most things full scale experiments provide the best experience for developing physical insight, and provide the only acceptable means of theory validation. Therefore a readily available and easily accessible data base of existing sonic boom waveforms would be a valuable resource. Dominic Maglieri, of Eagle Engineering is in the process of putting together a data base of sonic boom waveforms obtained in the 1960's. This is a unique data set because it will provide actual digitized waveforms from which we may calculate not only rise times, but also Fourier transforms to obtain the frequency spectra of the waveform. This later is probably required to determine acceptability. In any case, the figures are as shown here, 39 flights, 53 sonic boom runs, and 330 sonic boom signatures on which to test our theories.

# HIDDEN AGENDA - MAGLIERI

## EAGLE ENGINEERING

**Develop data base of all XB-70 sonic boom waveforms with relevant meteorological data.**

**Total Number of:**
**Flights** 39
**Sonic Boom Runs** 53
**Sonic Boom Signatures** 330

This chart is reasonably self explanatory, and provides several things a data base may be used for. As mentioned earlier, it will provide test cases for the new theories being developed, in many cases the only test cases acceptable to some. Further, the data may be used to obtain physical insight, or an empirical approach to sonic boom prediction. Finally, the Fourier transform of the signal is required to determine the acceptability of sonic boom waveforms, and those waveforms residing in the data base have real atmospheric effects imposed upon them.

# UTILIZATION OF SONIC BOOM DATA BASE

- Provide reliable and acceptable test cases for model validation

- Provide physical insight for the development of theoretical models

- Provide basis for empirically based prediction methods

- Provide means for examining acceptability of sonic boom waveforms modified by turbulence etc.

1206

PAPERS FOLLOWING

The final group is here to defend themselves. I'll introduce them in turn. Thus I turn the podium over to Dr. Allen Pierce who will discuss his theory of molecular absorption, and recently initiated efforts to determine the effects of turbulence on the sonic boom waveform.

# PAPERS FOLLOWING
## A. PIERCE - ABSORPTION & TURBULENCE
## K. PLOTKIN - TURBULENCE & ABSORPTION
## H. BASS - TURBULENCE EFFECTS

THIS PAGE INTENTIONALLY BLANK

# Session IX. Sonic Boom (Human Response and Atmospheric Effects)

*omit*

Relaxation and Turbulence Effects on Sonic Boom Signatures
*Dr. Allan D. Pierce and Victor W. Sparrow, Pennsylvania State University*

THIS PAGE INTENTIONALLY BLANK

# RELAXATION AND TURBULENCE EFFECTS
# ON SONIC BOOM SIGNATURES

$5g-71$
$12039$

Allan D. Pierce and Victor W. Sparrow
Graduate Program in Acoustics
Pennsylvania State University
University Park, PA 16802

First Annual High-Speed Research Workshop
Williamsburg, Virginia
May 14–16, 1991

## OVERVIEW

The rudimentary theory of sonic booms predicts that the pressure signatures received at the ground begin with an abrupt shock, such that the overpressure is nearly abrupt. This discontinuity actually has some structure, and a finite time is required for the waveform to reach its peak value. This portion of the waveform is here termed the rise phase and it is with this portion that the present presentation is primarily concerned.

Any time characterizing the duration of the rise phase is loosely called the "rise time." Various definitions are used in the literature for this rise time; for the present discussion it can be taken as the time for the waveform to rise from 10% of its peak value to 90% of its peak value. The available data on sonic booms that appears in the open literature[1] suggests that typical values of shock overpressure lie in the range of 30 Pa to 200 Pa, typical values of shock duration lie in the range of 150 ms to 250 ms, and typical values of the rise time lie in the range of 1 ms to 5 ms.

The understanding of the rise phase of sonic booms is important because the perceived loudness of a shock depends primarily on the structure of the rise phase. A longer rise time typically implies a less loud shock. A primary question is just what physical mechanisms are most important for the determination of the detailed structure of the rise phase.

A prevalent viewpoint in current literature on sonic booms is that molecular relaxation is the dominant physical mechanism for establishing the finite rise times of sonic booms. That such should be the case was first proposed by Hodgson[2] in 1973. The other contender for being the dominant mechanism is distortion by atmospheric turbulence, and earlier theories as to how this mechanism affects the rise phase had been proposed by Pierce[3] and by Plotkin and George[4], but without any attention to the effects of molecular relation. A subsequent analysis by Ffowcs-Williams and Howe[5] suggested, however, that turbulence was too weak a mechanism to account for the observed magnitudes of the rise times, and these authors concluded their article with a statement to the effect that molecular relaxation appeared to be sufficient to explain the existing data. Bass and his colleagues[6] carried out some numerical simulations of long range weak shock propagation under the influence of molecular relaxation and confirmed that the general trends observed regarding the ranges of rise time and their dependences on peak overpressures could be more or less well explained in terms of a molecular relaxation mechanism. Tubb[7], and also Bass and other colleagues[8], carried out laboratory-scale experiments on the propagation of weak shocks through turbulence and did not observe that the presence of turbulence caused appreciable increased thickening of weak shocks (i.e., increased rise times).

Although there appears to be no doubt now that the molecular relaxation theory does indeed predict the correct order of magnitude of the rise time, the dismissal of turbulence as a dominant mechanism is not at all justified by the work cited above. The theoretical work of Ffowcs-Williams and Howe cannot be regarded as definitive and has recently been criticised in a review article by Plotkin[9]. The laboratory-scale experiments of Tubb[7] and of Bass et al.[8] are also criticised by Plotkin, on the basis that the type of turbulent distortion that affects sonic booms requires long propagation distances and that such cannot be easily be simulated in a laboratory environment.

Notwithstanding the reservations mentioned above concerning atmospheric turbulence, it is possible to begin with the assumption that molecular relaxation is indeed the overwhelmingly dominant mechanism as a working hypothesis and then to test it with a combination of experiment and theory. Until recently, an adequate test of such a hypothesis had not yet been carried out. The numerical predictions of rise times of sonic booms have been based on either relatively crude theories or on unwieldy and somewhat erratic results of lengthy computer runs.

To test the hypothesis that molecular relaxation satisfactorily explains the rise phase portion of sonic boom waveforms, one does not need to explicitly consider turbulence. If the test suggests that the

1212

hypothesis is grossly incorrect, then one does not necessarily conclude that turbulence is the correct explanation, but the stage is certainly set for giving turbulence further serious consideration.

For propagation of sonic booms and of other types of acoustic pulses in nonturbulent model atmospheres, there exists a basic overall theoretical model that has evolved as an outgrowth of geometrical acoustics. This theoretical model depicts the sound as propagating within ray tubes in a manner analogous to sound in a wave guide of slowly varying cross-section. The propagation along the ray tube is quasi-one-dimensional, and a wave equation for unidirectional wave propagation is used. A nonlinear term is added to this equation to account for nonlinear steepening and the formulation has been carried through to allow for spatially varying sound speed, ambient density, and ambient wind velocities. The model intrinsically neglects diffraction, so it cannot take into account what has previously been mentioned in the literature as possibly important mechanisms for turbulence-related distortion. The existing ray-tube type model is reviewed by Plotkin[9] and there exist computational codes based on this model. The two rudimentary codes are those of Hayes *et al.*[10] and Thomas.[11] Taylor[12] extended Hayes's model such that the resulting program was applicable for the analysis of booms that proceeded initially obliquely upwards and which were eventually refracted back to the ground by sound speed and wind speed gradients. His modification also yields waveforms that have come along paths that touched caustics. The model as it presently exists can predict an idealized N-waveform which often agrees with data in terms of peak amplitude and overall positive phase duration. It does not take dissipation or relaxation effects explicitly into account, so it does not predict detailed shock structure and rise times. It is possible, however, develop a simple method based on the physics of relaxation processes for incorporating molecular relaxation into the quasi-one-dimensional model of nonlinear propagation along ray tubes.

The theory, developed in recent work by Pierce and Kang[13] and described in detail in the recent doctoral thesis of Kang[14], for the incorporation of molecular relaxation into the overall ray-tube propagation model hypothesizes that molecular relaxation is important only in the rise phase of waveforms. Such is justified because the characteristic times, such as positive phase duration, associated with other portions of the waveform are invariably much longer than the characteristic relaxation times for molecular relaxation. During most of the time at which the waveform is being received, it is reasonable to assume that the air is in complete quasi-static thermodynamic equilibrium. Molecular relaxation is a nonequilibrium thermodynamic phenomenon and is important only when pressure is changing rapidly, with characteristic times of the order of a few milliseconds or less.

A second hypothesis, which is related to the first, but which requires some extensive analysis for its justification, is that the rise phase of the waveform is determined solely by the peak overpressure of the shock and the local properties of the atmosphere. Strictly speaking, one expects the waveform received at a local point to be the result of a gradual evolution that took place over the entire propagation path, so it depends in principle on the totality of the atmospheric properties along the path. However, the N-wave shape, or at least the positive phase portion, is often established fairly close to the source (i.e., the flight trajectory in the case of sonic boom generation) relative to the overall propagation distance. With increasing propagation distance, the peak overpressure decreases, but does so very slowly, and the positive phase duration increases, but also does so very slowly. There is a net loss of energy from the wave and the loss takes place almost entirely within the rise phases of the shocks. However, the manner in which the peak overpressure decreases and the positive phase duration increases is virtually independent of the energy loss mechanism. The rise phase structure of the waveform is basically a tug-of-war between nonlinear steepening and molecular relaxation. When the boom passes through a region where the molecular relaxation is weaker, the nonlinear steepening causes the waveform to sharpen up and causes the rise time to decrease until the mechanisms balance each other out. One can associate some characteristic adjustment time with this restoration of the balance between the two mechanisms. The second hypothesis rests on the assertion that this characteristic adjustment time is substantially less than any characteristic time it takes for the waveform to propagate over a path segment within which the relevant atmospheric properties (especially the absolute humidity) change appreciably.

That this second hypothesis has some credibility can be seen at once when one considers that a upper limit for the relaxation time is about 20 ms (corresponding to the relaxation time of $N_2$ in very dry

air)[15]. The waveform moves with roughly the sound speed, which is of the order of 340 m/s, so a hypothetical relaxation process would take place over a propagation distance of less than 10 m. If the atmospheric humidity does not vary appreciably over such a distance, then one might argue that any relaxation process that was initiated by waveform onset must have taken place at nearly constant atmospheric humidity and that the appropriate value to use is that value that prevails locally. However, this argument is a little simplistic because the characteristic adjustment time is not necessarily the same as the relaxation time. Kang[14] gives an estimate of this adjustment time based on rigorous physical principles and finds that the characteristic adjustment time is of the order of 100 ms, corresponding to a propagation distance of 34 m.

The two hypotheses mentioned above imply that a plane wave propagation model is sufficient to predict the rise phase of the waveform. Another implication is that one can always carry out the calculation in a reference frame where there is no wind, so the model need not consider ambient fluid velocity. This leads one to a relatively simple model of determining a frozen shock profile. The boundary conditions for the calculation of the rise phase then can be reduced to the idealizations that the acoustic portion of the pressure goes to zero far ahead of the shock, and that this pressure asymptotically approaches a constant value $P_{sh}$ far behind the shock.

For the simplified planar model of a step in overpressure propagating through a medium with internal relaxation, a relatively simple set of governing partial differential equations are available. The principal member of this set is here called the augmented Burgers's equation, and it modifies the linear wave equation by including the nonlinear, thermoviscous, and molecular relaxation terms. It was first derived by Pierce[15] in 1981. The remaining equations govern the time dependence of the relaxation of internal variables. These equations are solved by Kang[14] for atmospheric propagation in air consisting of oxygen, nitrogen, and water molecules, using the frozen profile hypothesis. The idea of using such a hypothesis goes back to Taylor[16] and Becker[17], but the application to the augmented Burgers's equation model with two relaxation processes included is relatively recent. Based on the frozen shock profile assumption, the augmented Burgers's equation and relaxation equation are reduced to a set of coupled nonlinear ordinary differential equations, and these can be solved by numerical integration, once appropriate boundary conditions are established.

The predictions of the theoretical model developed in this thesis are compared with actual waveforms of sonic booms, recorded by the US Air Force in the Mojave Desert in 1987, and it is found that molecular relaxation cannot sufficiently explain the finite rise time of sonic booms. In the majority of cases, the rise times of experimental data are larger than predictions by the factor of 2 to 5. A possible explanation for the discrepancy is that atmospheric turbulence may be the dominant mechanism underlying the thickening of weak shocks. Such a supposition is supported by the observations that there is a random scattering in the values of the experimental rise times and that, in a few cases, there is extremely good agreement of the predicted with the experimental waveforms. The data comparison suggests, moreover, that the model based on molecular relaxation provides a lower bound to rise time and an upper bound to loudness.

1214

# Sonic Boom - SR-71 Airplane

# Mach 2.6, Flight Altitude = 66,000 ft
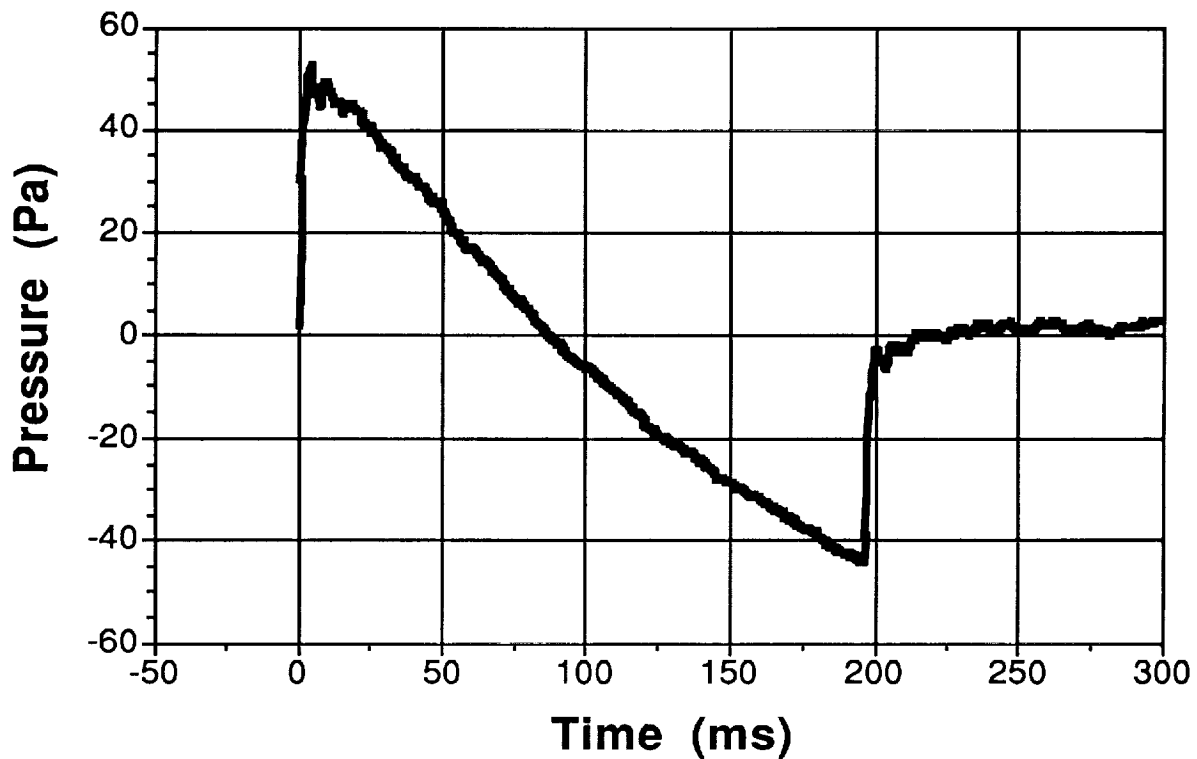


Acoustic Pressure versus Time

recorded on ground directly below aircraft flight track

# Sonic Booms - -

# basic result of idealized theory  - -

**Pressure**
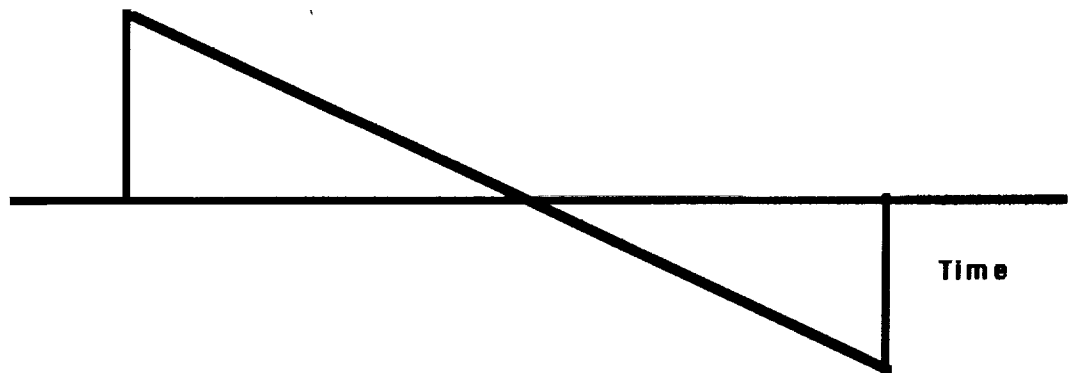


**Time**

## Waveform asymptotically approaches N-wave shape with increasing propagation distance from aircraft

For the Concorde:

Pressure jump approx 100 Pa

Time duration approx 100 ms

1216

Flight path
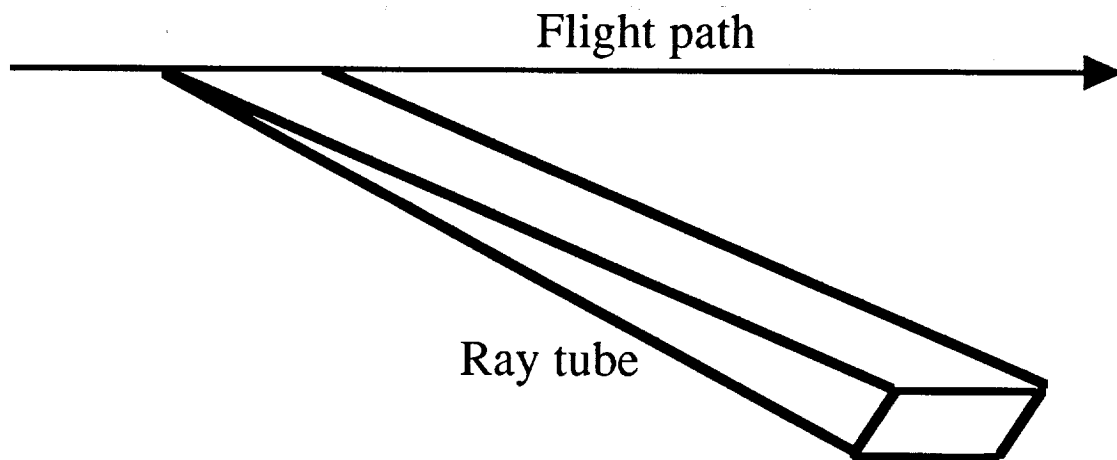
Ray tube

In first approximation:

boom propagates along ray tube

like sound in a waveguide

of slowly varying cross-section

Waveform near
flight track is
affected by
aircraft shape
and speed

*s*
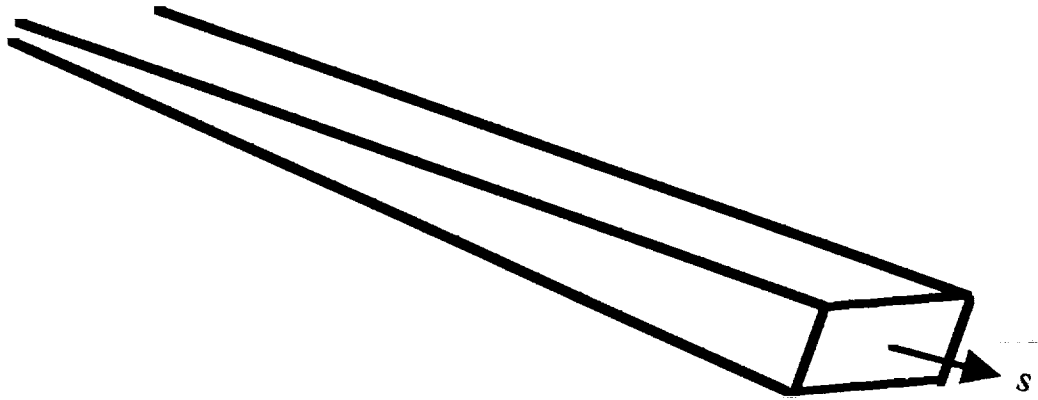
Waveform near ground is
strongly distorted by
propagation through
the atmosphere.

Variations caused by
details of aircraft design
are washed out.

# Sonic Booms - -

## prediction of idealized theory - -

## waveform at the ground for

## possible next generation of SST's
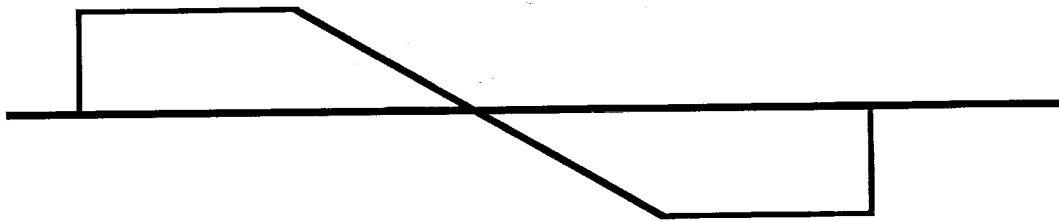
Asymptotic N-wave shape not yet realized - -

Smaller pressure jumps than nominally expected - -

Would this achievement reduce the annoyance?

1219

**Actual pressure jumps are not abrupt - -**
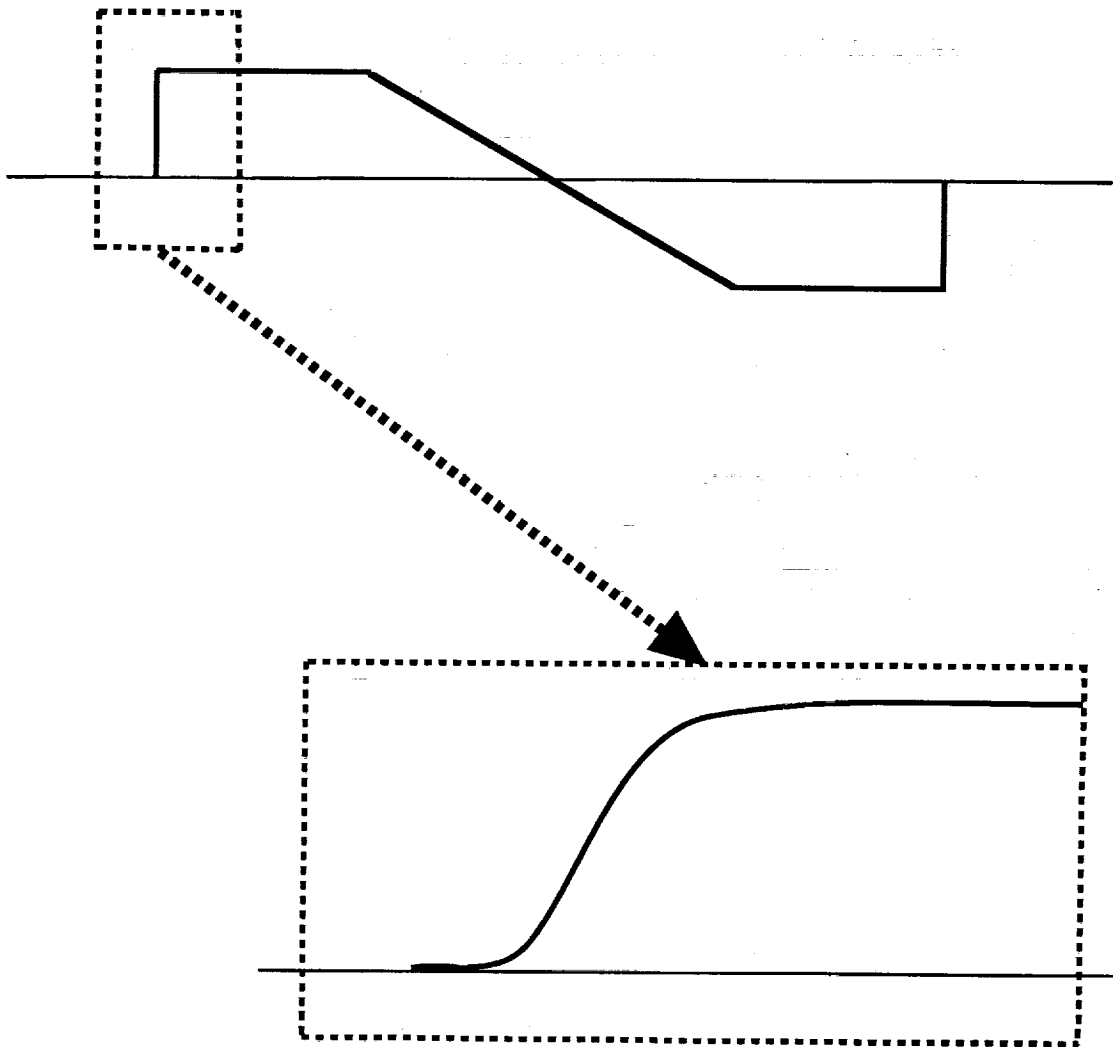
**Extent of the absence of abruptness  is important - -**

**the less abrupt the better.**

**Rise time is a descriptor of absence of abruptness.**

# Rise phase of a sonic boom - (leading shock in the N-wave)

Pressure (ms)

60

50

40

30

20

10

0

0  1  2  3  4  5  6

Time (ms)
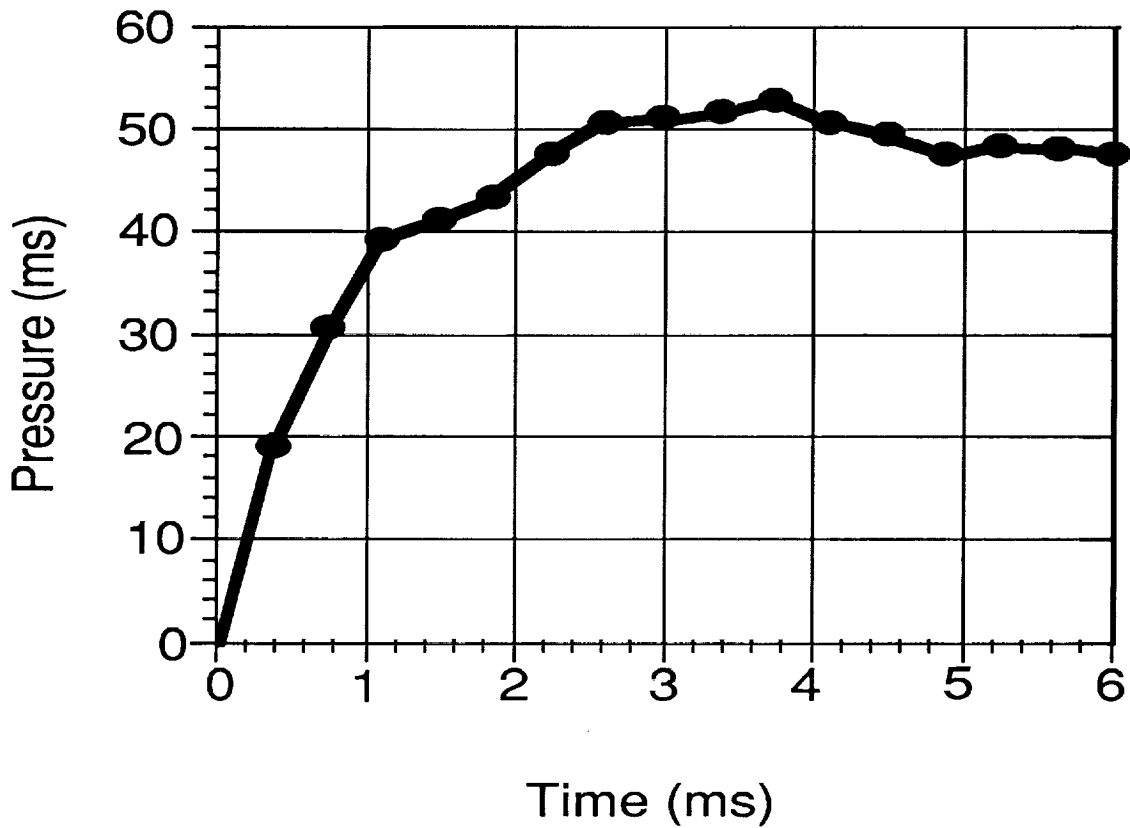
**SR-71 airplane at Mach 2.6;**    **Flight Altitude is 66,000 ft**

**Flying over the Mojave desert  on August 5, 1987, 9:00 a.m.**

# Hypotheses (to be checked)

Turbulence usually increases rise-time

Real gas effects establish minimum expected rise-times

For real gas effects, the profile portion around a shock is independent of

- rest of profile

- evolution along propagation path
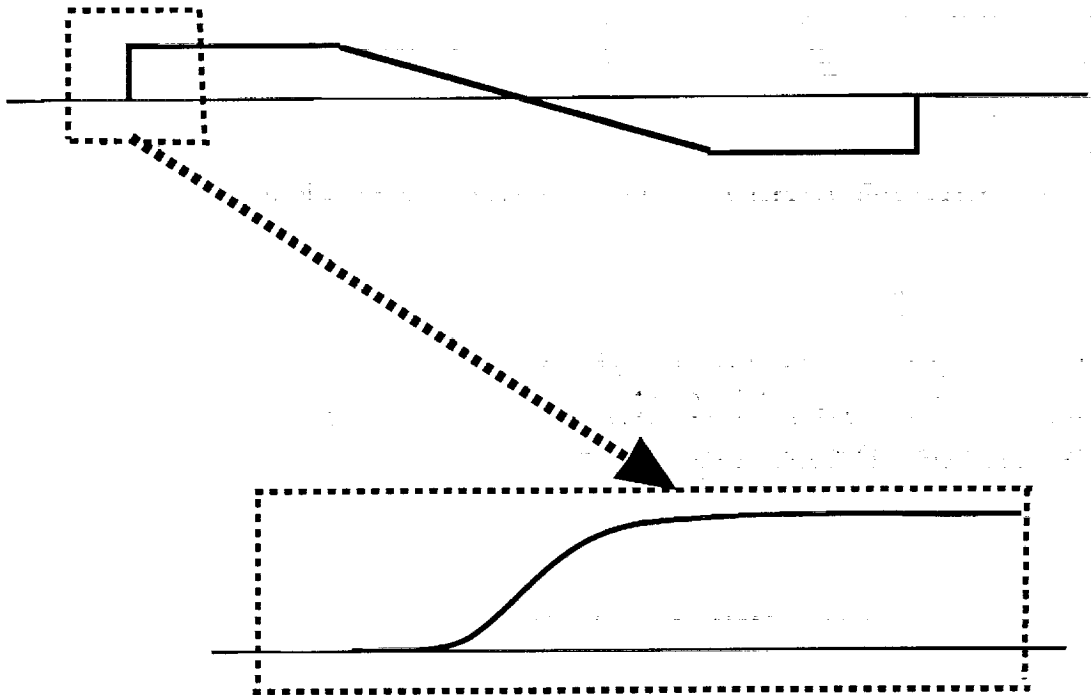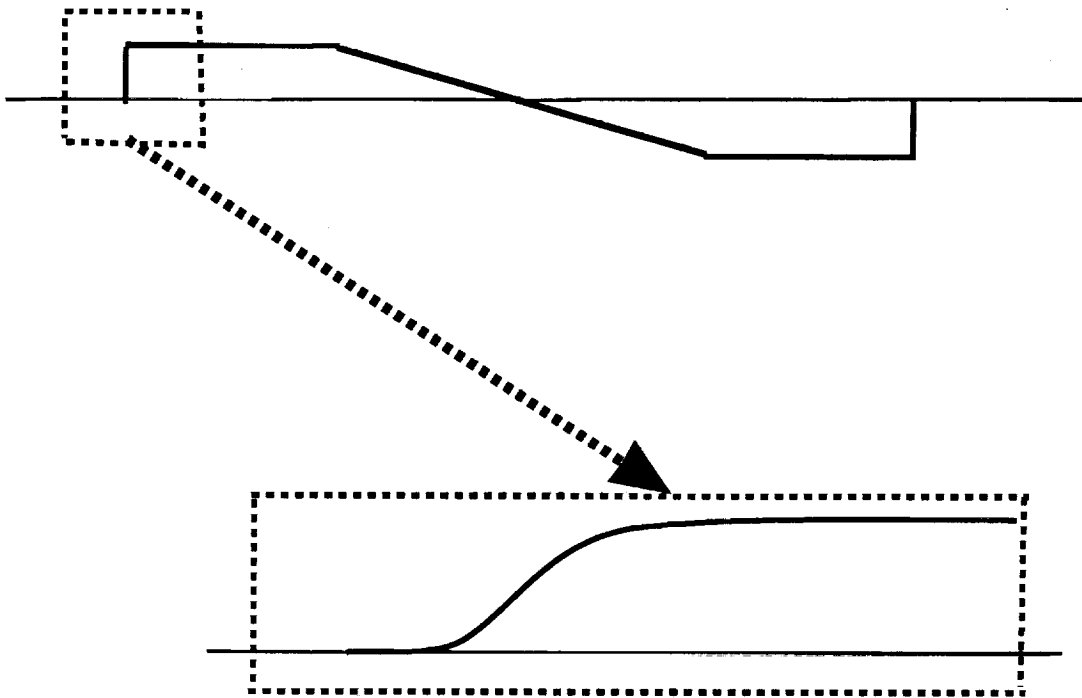
(A consequence - for real gas effects)

Detailed structure of a sonic-boom waveform
near the nominal time of arrival of a shock
is determined by only

    a.  The net pressure jump

    b.  The local properties of the
        atmosphere

# What is molecular relaxation?

N〜〜〜N
spring

## Nitrogen molecule

Vibrational
energy
levels

——————— First
excited
state
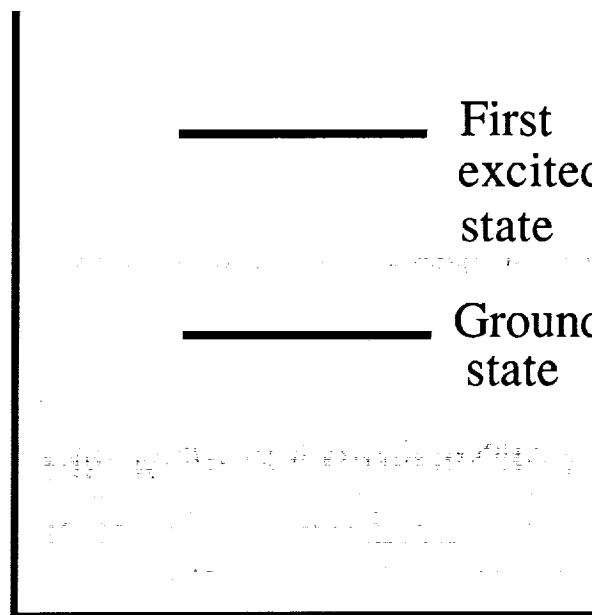
——————— Ground
state

$$\frac{\text{Number in excited state}}{\text{Number in ground state}} = \text{function of temperatu;e}$$

But this is so only for thermodynamic equilibrium.

## Assumptions accompanying molecular relaxation model

- Shocks are weak  (typical range:  300Pa max.)

- Molecular relaxation important only in rise phase for oxygen and nitrogen processes

- Rise phase determined solely by peak overpressure of shock and local properties of atmosphere

- Rise phase much shorter in duration than positive phase of the shock

---

The shock is modeled as a "frozen profile"

i.e. the shock appears to stand still with respect to $\xi$

- change of variables:  $\xi = x - V_{sh} t$

- $V_{sh}$ = speed of shock propagation.

# Molecular relaxation model

## Developed by Kang and Pierce, 1990

## Uses augmented Burger's equation (Pierce, 1981):

$$\frac{\partial p}{\partial t} + c\frac{\partial p}{\partial x} + NST + TVT + MRT = 0$$

Molecular relaxation term

Thermal viscosity term

Nonlinear steepening term

## Coupled with Relaxation equation:

$$p_v + \tau_v\frac{\partial p_v}{\partial t} = \tau_v\frac{\partial p}{\partial t}$$

$$v = O_2, N_2 \text{ process}$$

**Using the steady-state version of Burger's equation,**

The theoretical rise phase is determined using asymptotic and numerical solution methods:
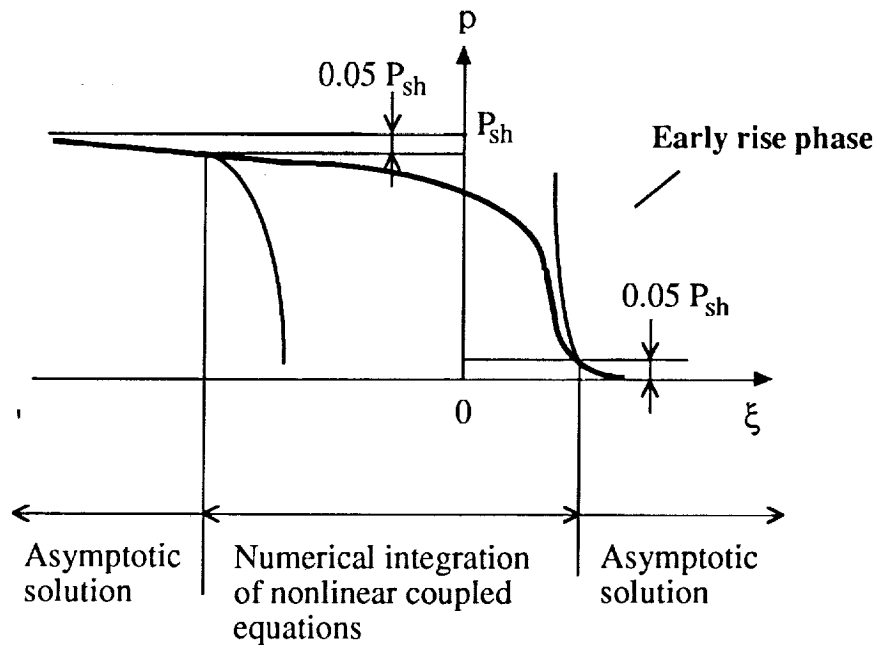


**Early rise phase: $O_2$ relaxation dominates**
**Later rise phase: $N_2$ relaxation dominates**

# Schematic of sonic boom recording setup
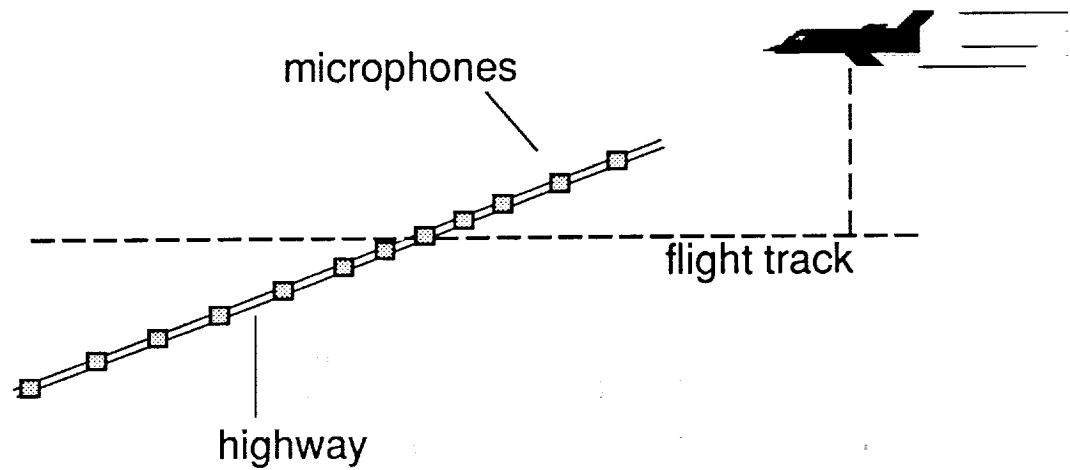


- Microphones in inverted mounts, approximately at ear height

- Flight track perpendicular to highway, and parallel to ground

1228

# Pressure vs time recordings of sonic booms:

### SR-71 aircraft, altitude 66,000 ftMSL
### Mach 2.6
### Recording from microphone four miles from flight track
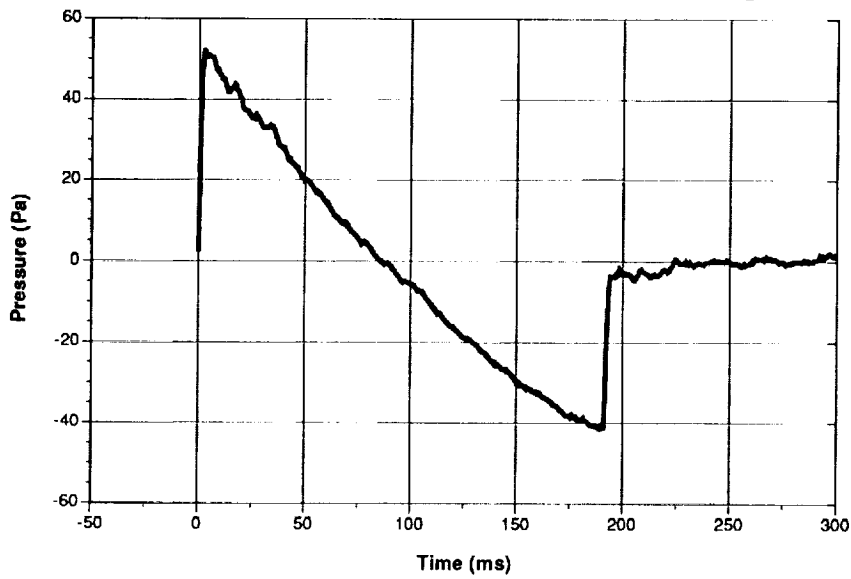


### F-16 aircraft, altitude 13,100 ftMSL
### Mach 1.16
### Recording from microphone sixteen miles from flight track



1229
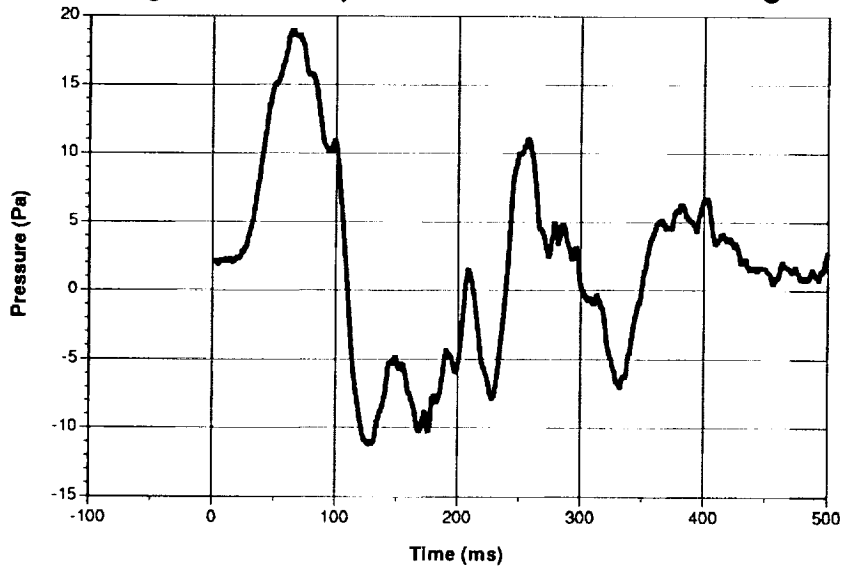
# Rise times of recorded sonic booms vs steady state shock overpressure
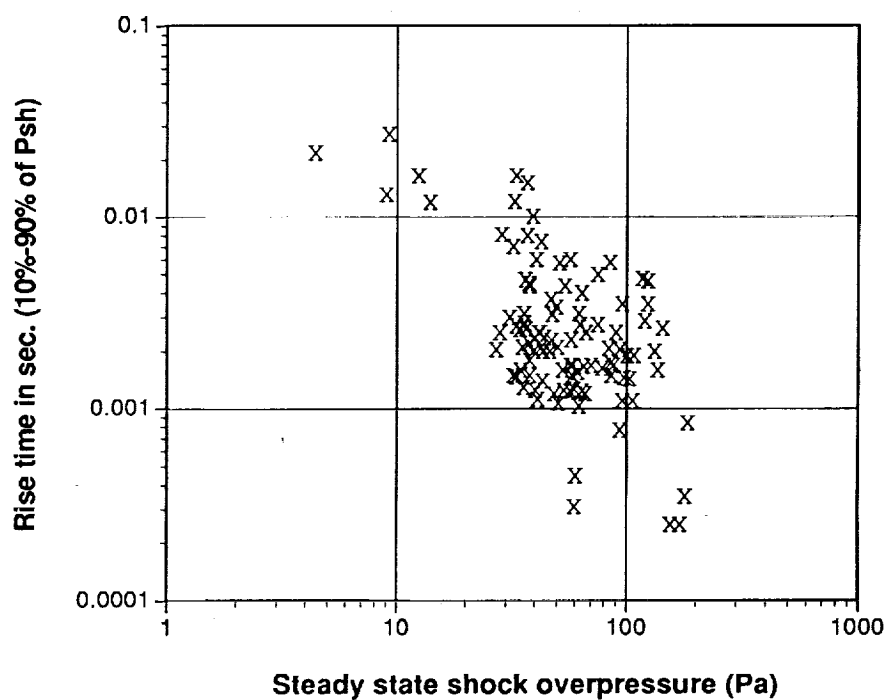


- Average rise time 2-3ms for steady state shock overpressure range of 30-100Pa

- Rise time inversely proportional to Psh

1230

# Rise times of sonic booms vs steady state shock overpressure, as compared to our molecular relaxation model
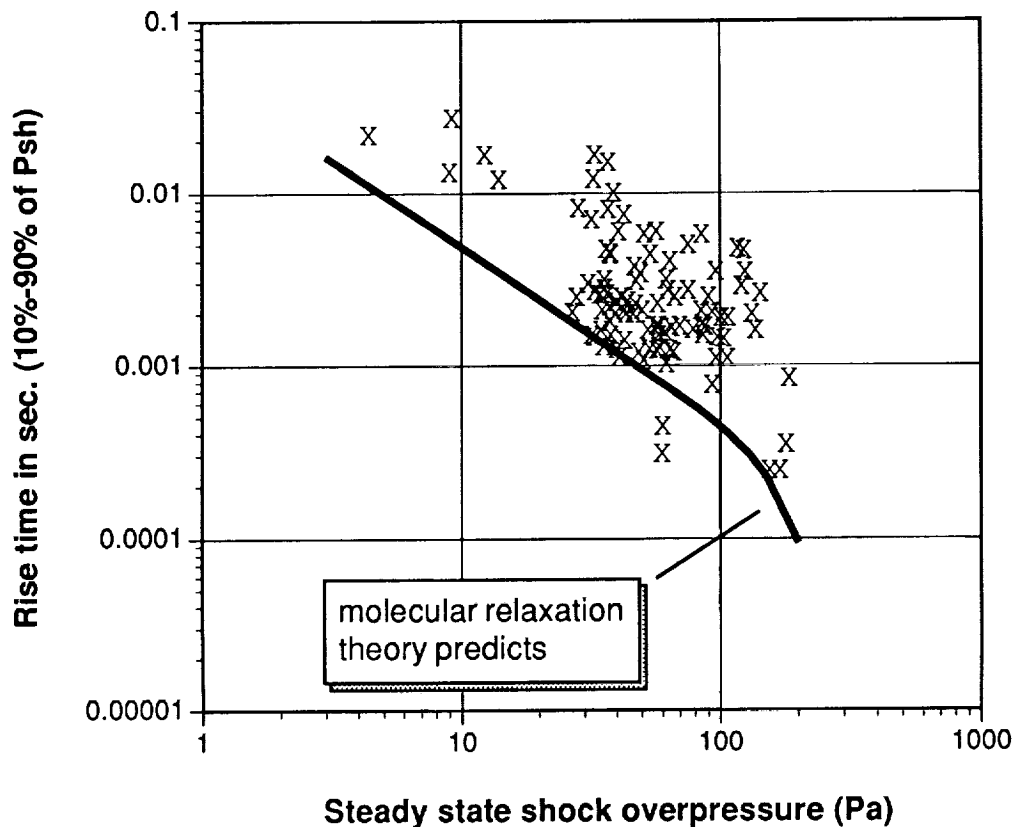


- **At time of experiment:** Temp = 30 - 38°C
  Relative humidity = 19 - 26%

- **This is a log-log plot**

# Experiment vs Theory Comparison:

- Experimental rise times are typically two to five times longer than theory would predict.

- Theoretical rise times appear to form a lower bound for experimental rise times.

- Approximately 10% of our experimental data agrees well with theory.

- In the majority of cases, molecular relaxation theory does not satisfactorily predict rise time.

## Humidity considerations:

- Humidity change affects relaxation theory results

- Weather data: humidity changes with altitude:
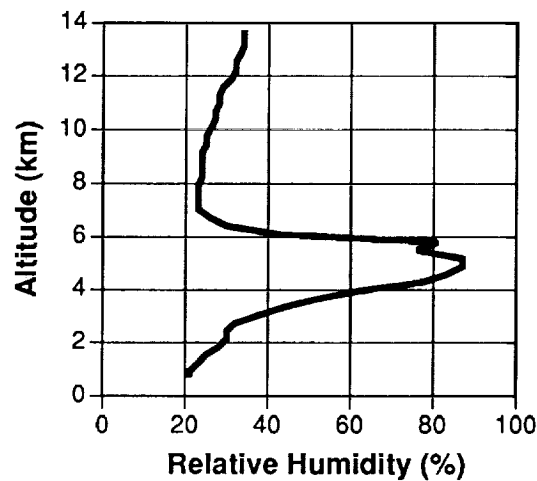


- humidity at its lowest near the ground

- If theoretical rise times calculated for <u>much lower</u> humidity than is actually present, the theory predicts a better match to experimental data

- Considering the higher-humidity regions also, instead of just the humidity at the ground (the current practice), would lead to a worse theoretical prediction.

- There is still discrepancy between theory & data

# Explanation of spiked
# and rounded waveforms

Turbulence ripples

wavefronts

Ray tubes
focus and
defocus
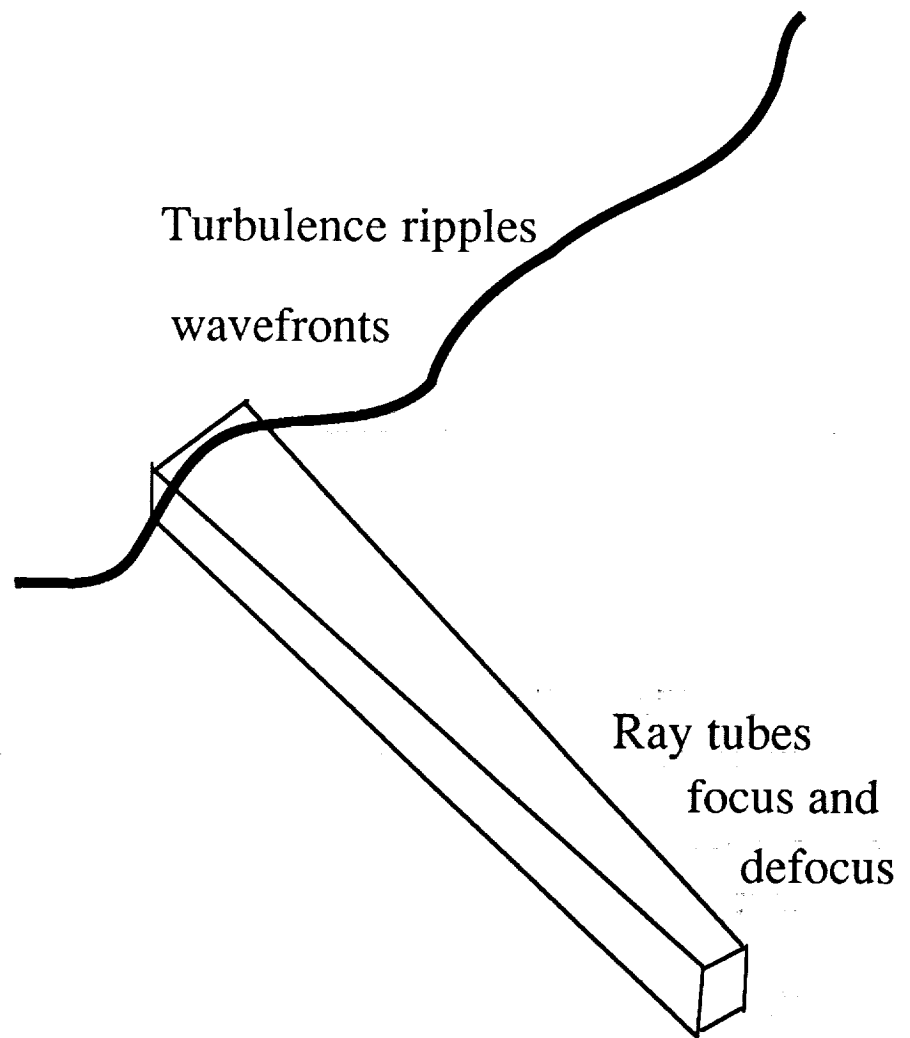
(verified by Davy and Blackstock (1971)

1234

p

# Normal waveform

s

p

# Magnified or focused waveform

s
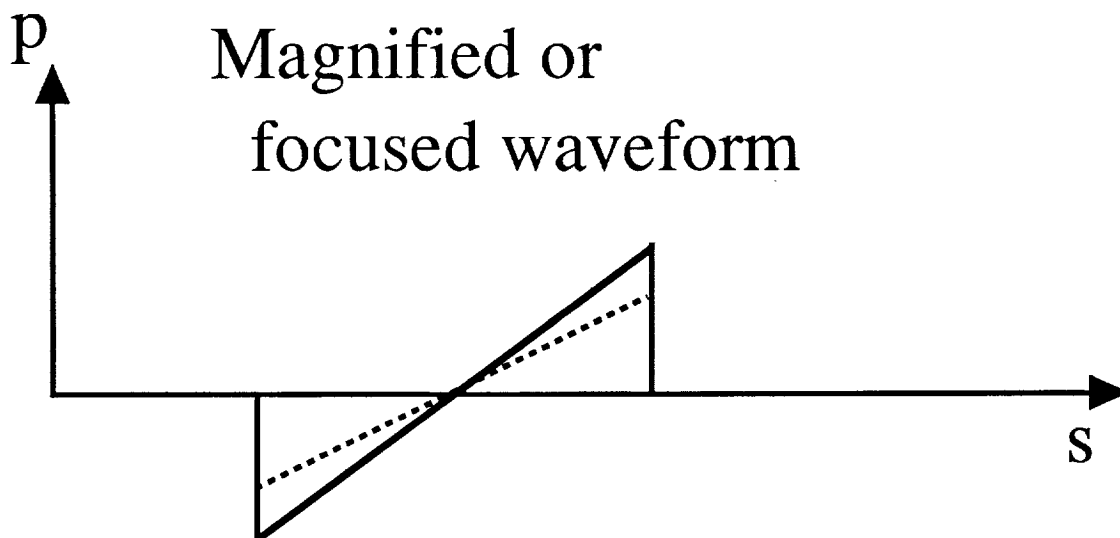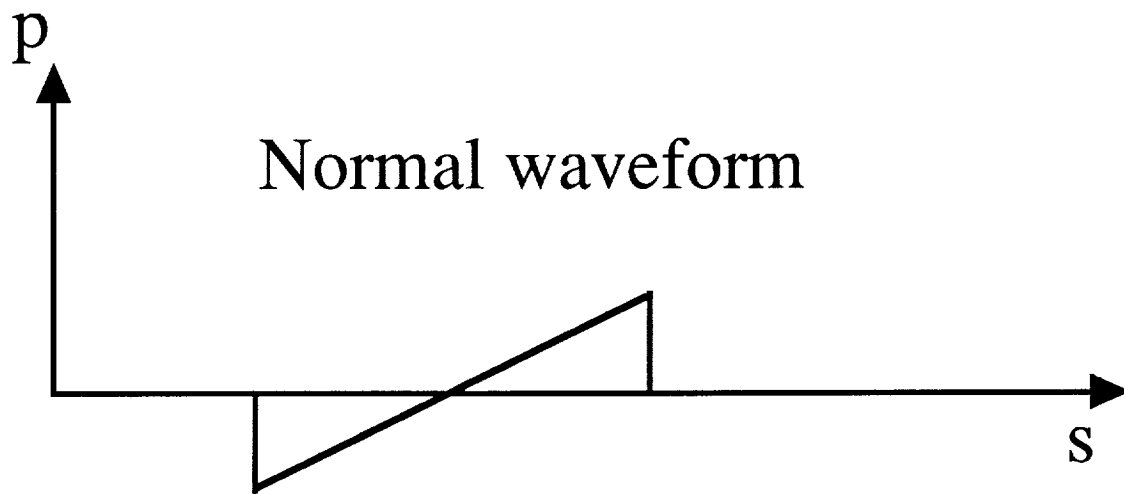
But not all parts of waveform are magnified

or demagnified equally.

Normal waveform

insensitive
to focusing
or defocusing

obeys
geometrical
acoustics

obeys
geometrical
acoustics

Spiked waveform

Rounded waveform
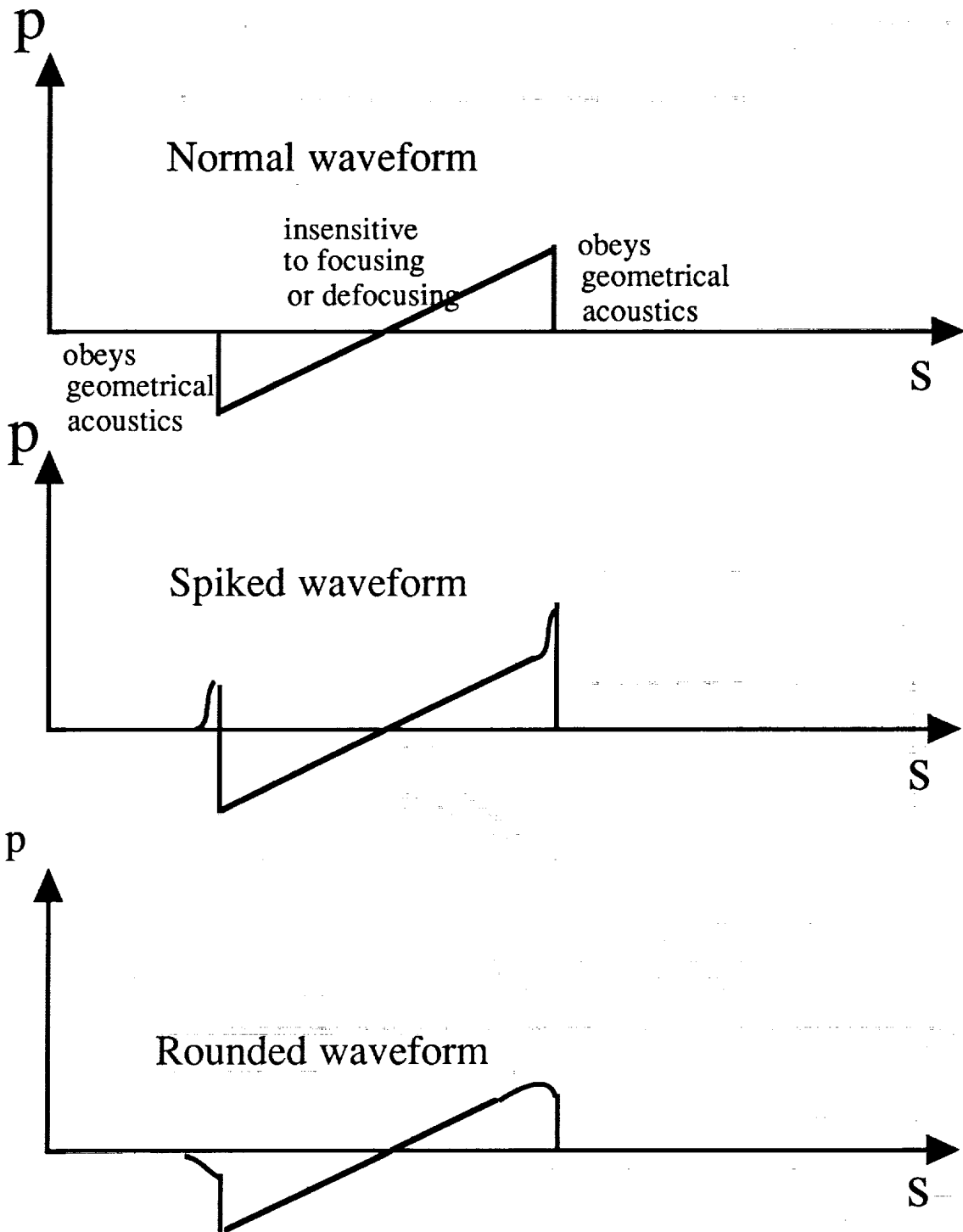
# Paradox:

Why should turbulence affect thickness of shocks?

**Rays twist and bend as they move through turbulence**

**but discontinuities stay abrupt**

1237
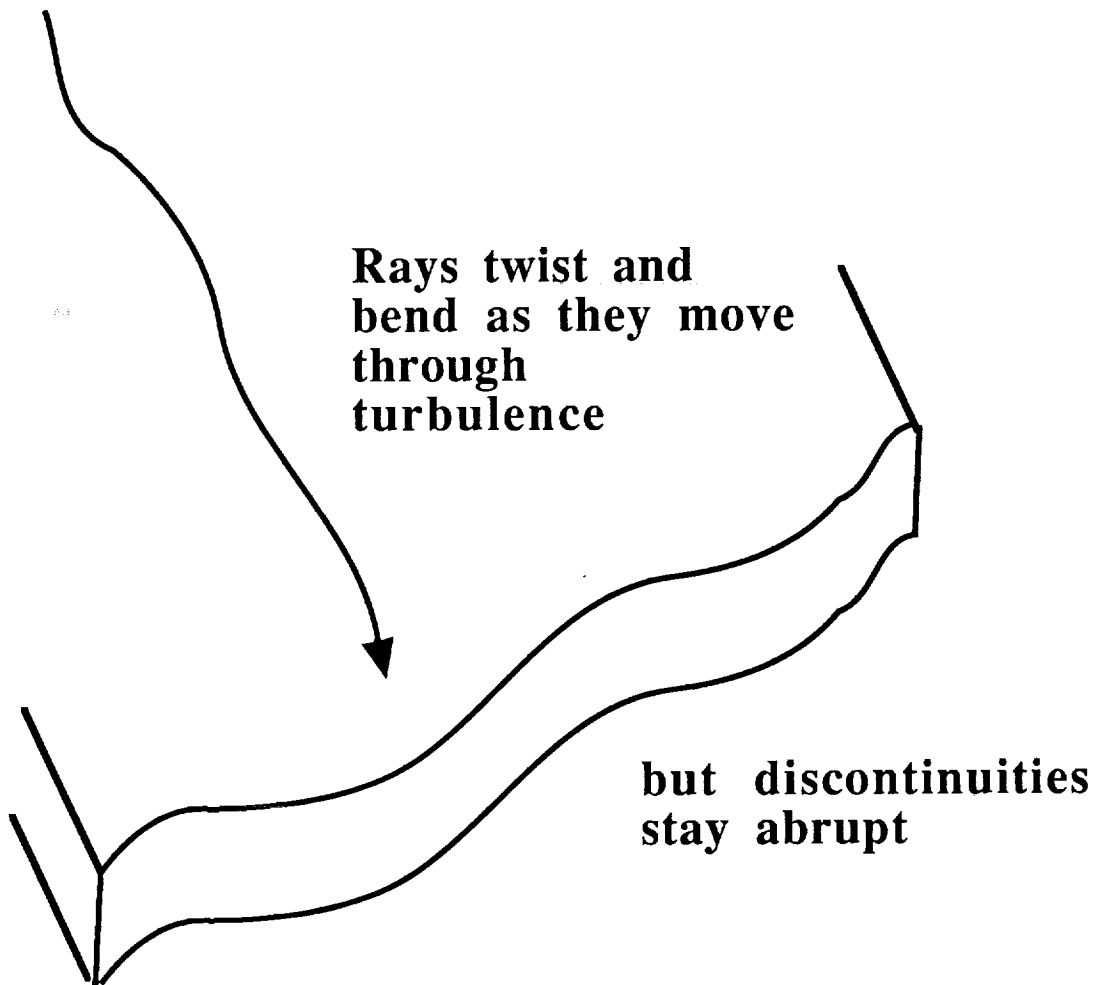
## Luneburg-Keller ``theorem"

(also Christoffel, Love, Hadamard, Courant,

Friedlander, Copson, Bremmer, possibly others)

# Once a shock,
## always a shock

# Old shocks never die;
## they just fade away
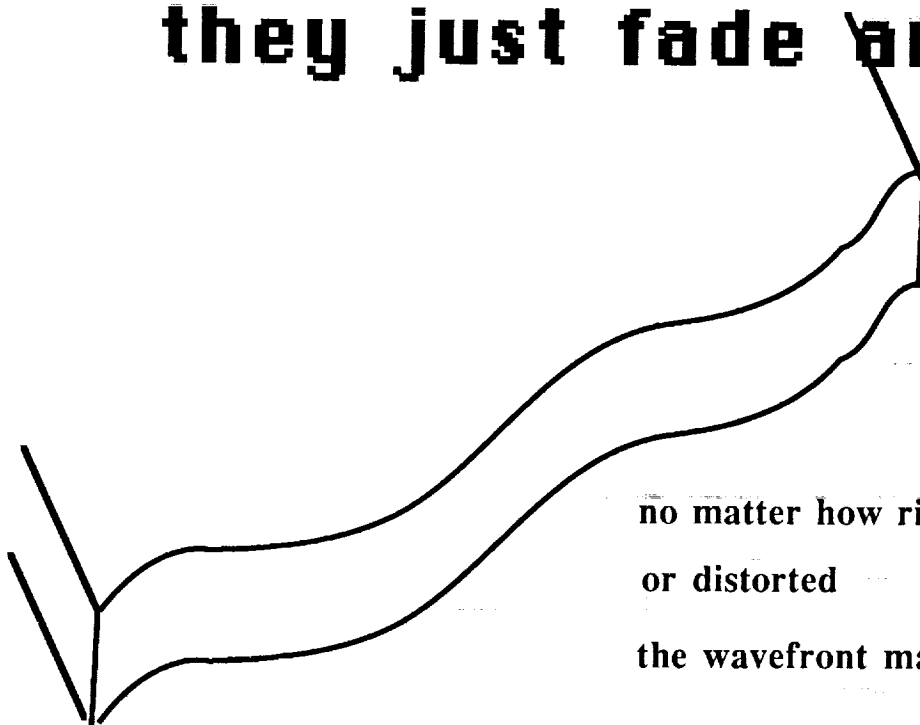
**no matter how rippled**

**or distorted**

**the wavefront may be**

p

microshocks

t
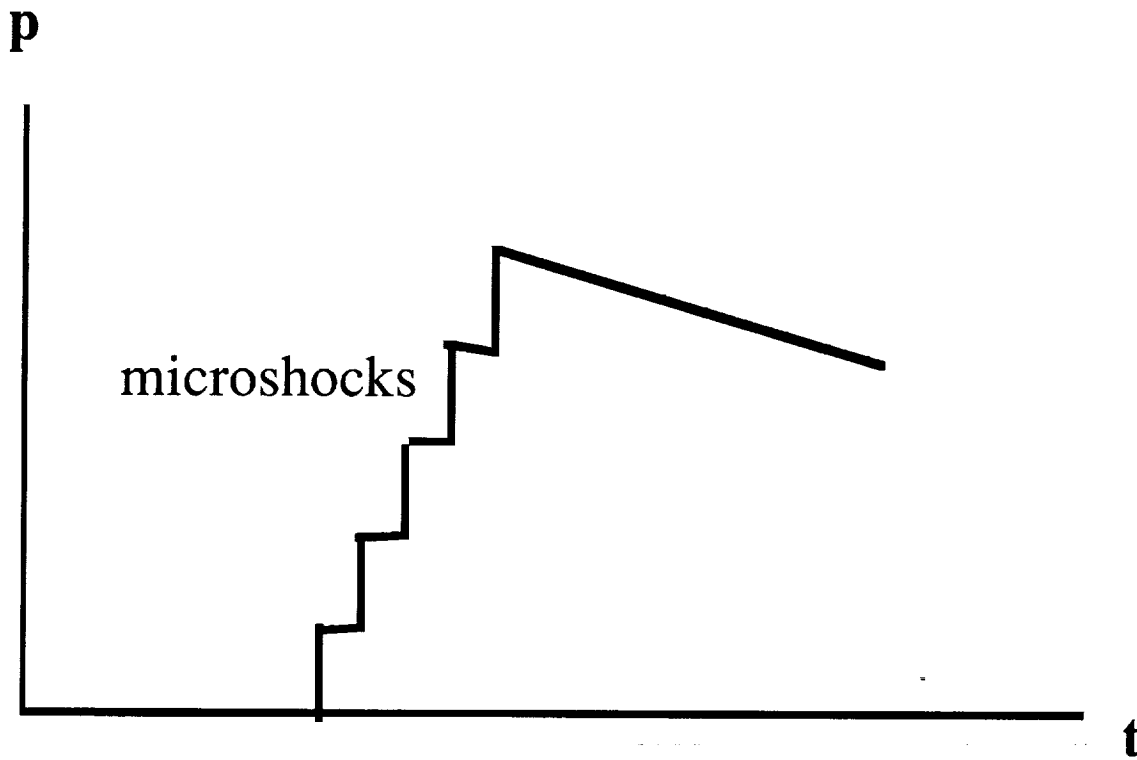
**Different rays arrive at closely spaced intervals.**

**Each ray carries its own microshock.**

**These build up to one big shock.**

# REFERENCES

1. D.J. Maglieri, Sonic boom ground pressure measurements for flights at altitude in excess of 70,000 feet and at Mach number up to 3.0, 2nd conference on sonic boom research, NASA SP-180, pp. 19–27 (May 1968).

2. J.P. Hodgson, Vibrational relaxation effects in weak shock waves in air and the structure of sonic bangs, *J. Fluid Mech.* 58(1), 187–196. (1973).

3. A.D. Pierce, Statistical theory of atmospheric turbulence on sonic boom rise times, *J. Acoust. Soc. Am.* 49(3), 906–924 (March 1971).

4. K.J. Plotkin and A.R. George, Propagation of weak shock waves through turbulence, *J. Fluid Mech.* 54(3), 449–467 (1972).

5. J.E. Ffowcs-Williams and M.S. Howe, On the possibility of turbulent thickening of weak shocks, *J. Fluid Mech.* 58(3), 461–480. (1973).

6. H.E. Bass, J. Ezell and R. Raspet, Effect of vibrational relaxation on rise times of shock waves in the atmosphere, *J. Acoust. Soc. Am.* 74(5), 1514–1517 (Nov. 1983).

7. P.E. Tubb, Measured effects of turbulence on the rise time of a weak shock, AIAA-75-543 (March 1975).

8. H.E. Bass, B.A. Layton, L.N. Bolen and R. Raspet, Propagation of medium strength shock waves through the atmosphere, *J. Acoust. Soc. Am.* 82(1), 306–310 (July 1987).

9. K.J. Plotkin, Review of sonic boom theory, AIAA 12th Aeroacoustics Conference, AIAA-89-1105, April 10–12, 1989, San Antonio, TX.

10. W.D. Hayes, R.C. Haefeli, H.E. Kulsrud, Sonic boom propagation in a stratified atmosphere, with computer program, NASA CR-1299, Aeronautical Research Associates of Princeton, Inc. (1969).

11. C.L. Thomas, Extrapolation of sonic boom pressure signatures by the waveform parameter method, NASA TN D-6832 (June 1972).

12. A.D. Taylor, The TRAPS sonic boom program, Air Resource Lab. NOAA Tech. Memo. ERL ARL-87.

13. A. D. Pierce and J. Kang, Molecular relaxation effects on sonic boom waveforms, in *Fontiers of Nonlinear Acoustics: Proceedings of 12th ISNA*, Elsevier Publishing, London (1990), pp. 165–170.

14. J. Kang, *Nonlinear Acoustic Propagation of Shock Waves through the Atmosphere with Molecular Relaxation*, Ph.D. Thesis, Department of Mechanical Engineering, The Pennsylvania State University, May 1991.

15. A.D. Pierce, *Acoustics: An introduction to its physical principles and applications* (McGraw-Hill, New York, 1981), pp. 371–408, 547–562, 566–603.

16. G.I. Taylor, The conditions necessary for discontinuous motion in gases, *Proc. Roy. Soc. London*, A84, 371–377 (July 1910).

17. R. Becker, Shock waves and detonation, *Zeit. Physik* 8, 321–362 (1922).

# Session IX. Sonic Boom (Human Response and Atmospheric Effects)

*omit*

The Effect of Turbulence and Molecular Relaxation on Sonic Boom Signatures
*Dr. Kenneth J. Plotkin, Wyle Laboratories*

THIS PAGE INTENTIONALLY BLANK

*510-71*
*12040*

# THE EFFECT OF TURBULENCE AND MOLECULAR RELAXATION ON SONIC BOOM SIGNATURES

## KENNETH J. PLOTKIN
## WYLE LABORATORIES

## NASA HIGH SPEED RESEARCH WORKSHOP
## 14–16 MAY 1991

# Typical Flight Test Measurements for
## Two Different Meteorological Conditions.
## From Hilton, Huckel, & Maglieri (1966).
## (a) Low wind velocity.          (b) Strong gusty wind.

These are typical sonic boom measurements. Under turbulent conditions, signatures are distorted. Rise times are longer and are variable. Differences between booms such as (a) and (b) have been clearly demonstrated to be associated with atmospheric turbulence.



(a)                                     (b)
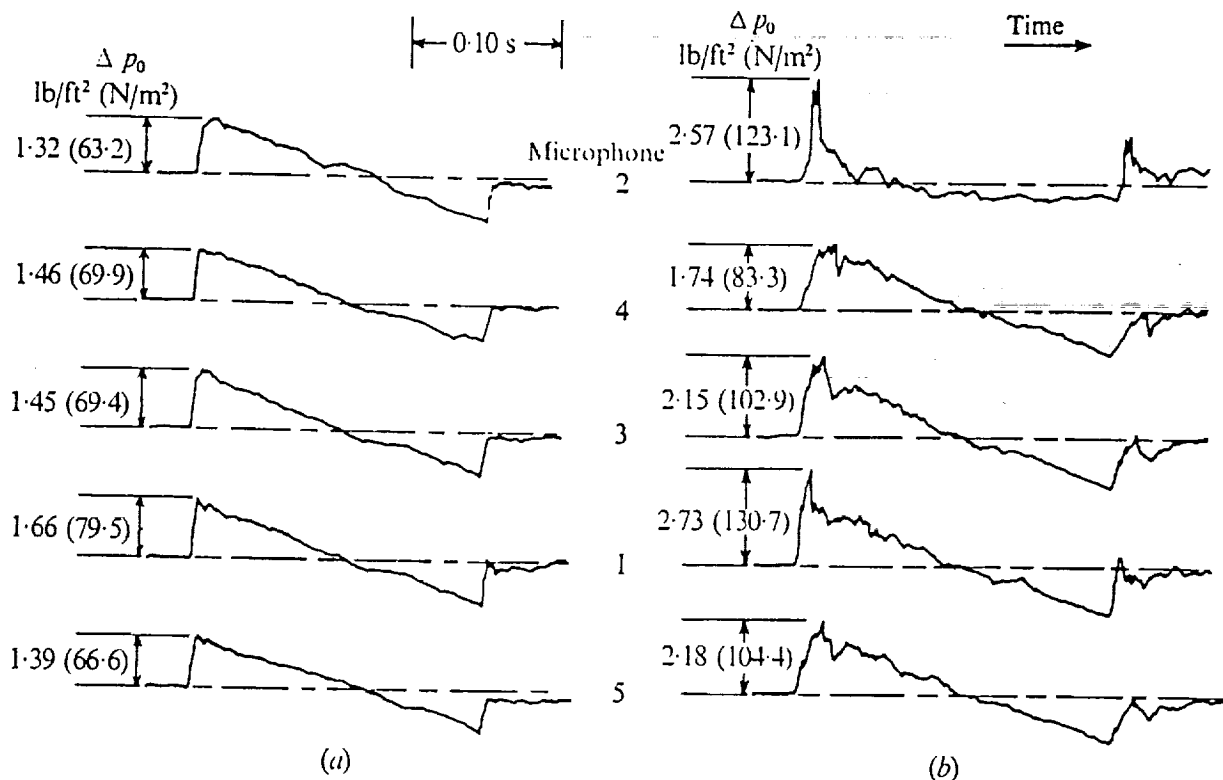
# Planetary Boundary Layer

The pertinent turbulence is in the mixed layer of the planetary boundary layer. Sonic boom flight tests in the 1960s with microphones on towers and balloons have clearly demonstrated that. Most atmospheric models (e.g., Monin-Obukhov scaling, Turner classes, etc.) deal with the surface layer and do not relate to the mixed layer. Over the past couple of decades, there have been substantial advances in measuring and modeling mixed layer turbulence.

**Free Atmosphere**

$z_i$ -------

**Inversion Layer**
**0.8 $z_i$ to 1.2 $z_i$**

**Planetary Boundary Layer**
**1 to 2 km daytime**
**200 to 300 meters nighttime**

**Mixed Layer**

**Mean Velocity Profile**

**Surface Layer**
**$\simeq$ 10% PBL**

**Laminar Sublayer**
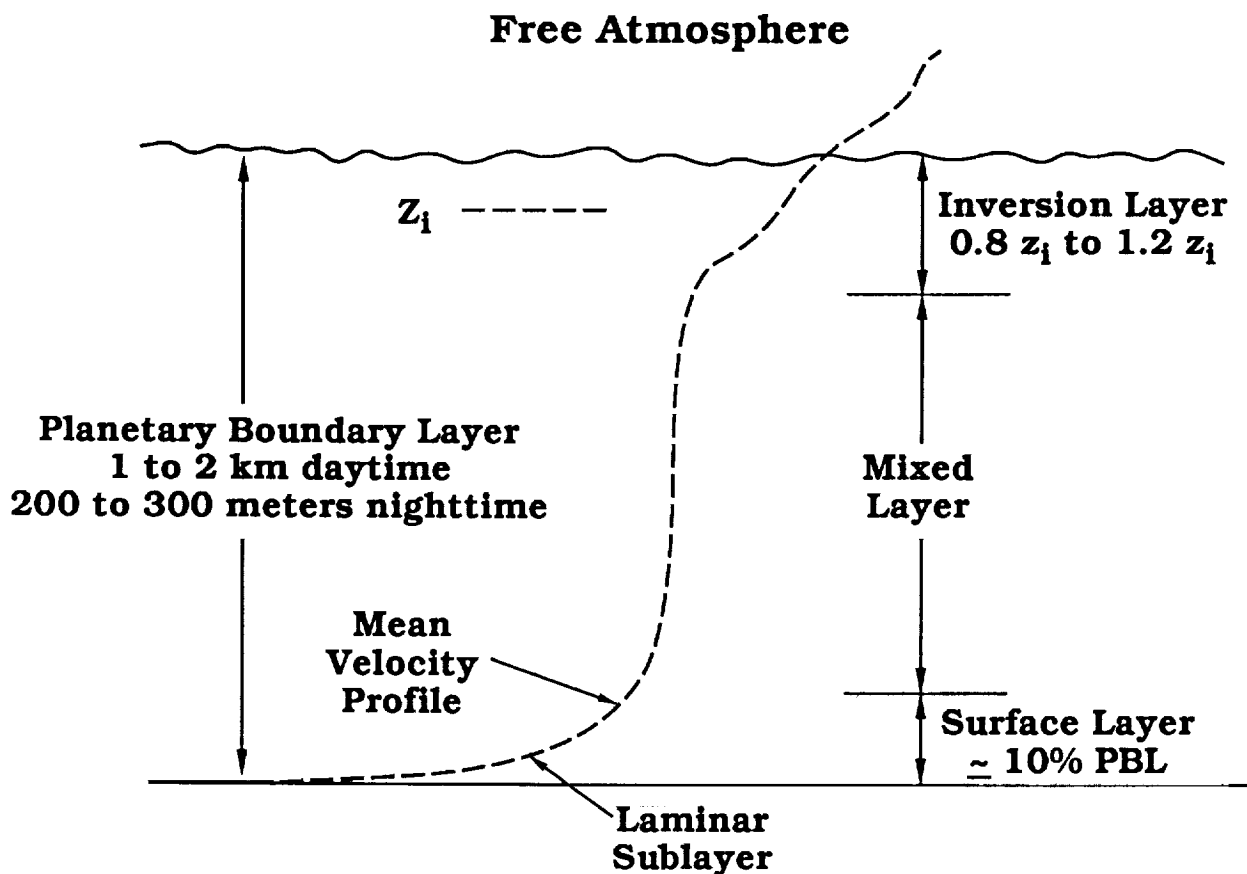
# Objectives

Our objectives are to assess the effect of turbulence and molecular absorption (which is now known to be a key factor in sonic boom shock structure) on shaped sonic booms. Today I will discuss the combination of physical mechanisms for idealized turbulence. In parallel, we are reviewing models for mixed layer turbulence, and these physical effects will eventually be generalized.

- **Identify Effects on Loudness of Shaped Booms.**

- **Combined Turbulence and Relaxation Effects.**

- **Realistic Turbulence Models – Including Variations of PBL Structure.**

- **ANSI S1.26-1978 Absorption.**

- **Current Status: Combine Physical Mechanisms For a Simple Shock in Homogeneous Turbulence.**

# Schematic Representation of Scattering

This is a schematic of turbulent scattering. When an incident wave interacts with a local inhomogeneity, a secondary scattered wave is emitted. These "first scattered" waves have long been considered to be the distortion on sonic booms. The energy in the first scattered waves is extracted from the shocks (scattering is strongest for high frequencies), causing the anomalous long rise times under turbulent conditions.

Classical analyses of scattering (as in the books by Chernov and Tatarskii) consider scattering of continuous harmonic waves, and scattering is considered to be associated with a 3-D scattering volume. Application of this formulation to sonic booms is very difficult due to the concentrated nature of a shock front.

Scattered waves

Inhomogeneity

Incident wave at time $t_0$

Transmitted wave at $t+\Delta t$
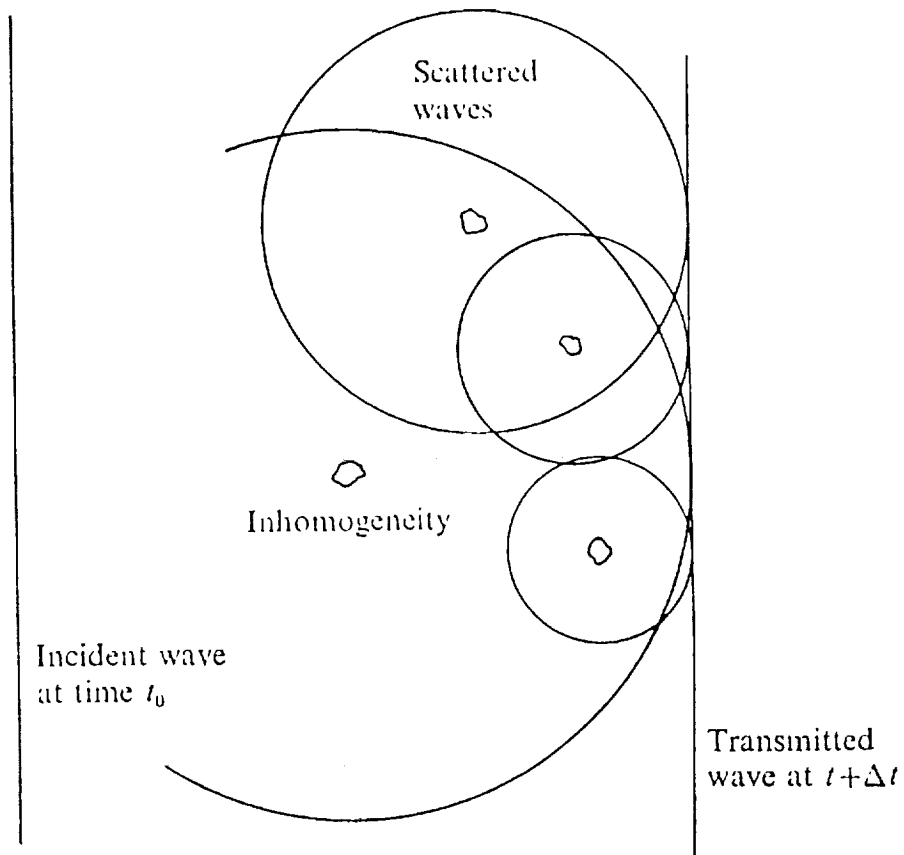
# Crow's Paraboloid of Dependence

Crow formulated scattering directly in the time domain, noting that the scattering volume reduces to a paraboloid which is equidistant between the receiver point (a distance  h  behind the shock) and the shock front.  This formulation loses frequency information (which may be important for loudness), but exhibits very important physical characteristics.  It also leads to a tractable solution.
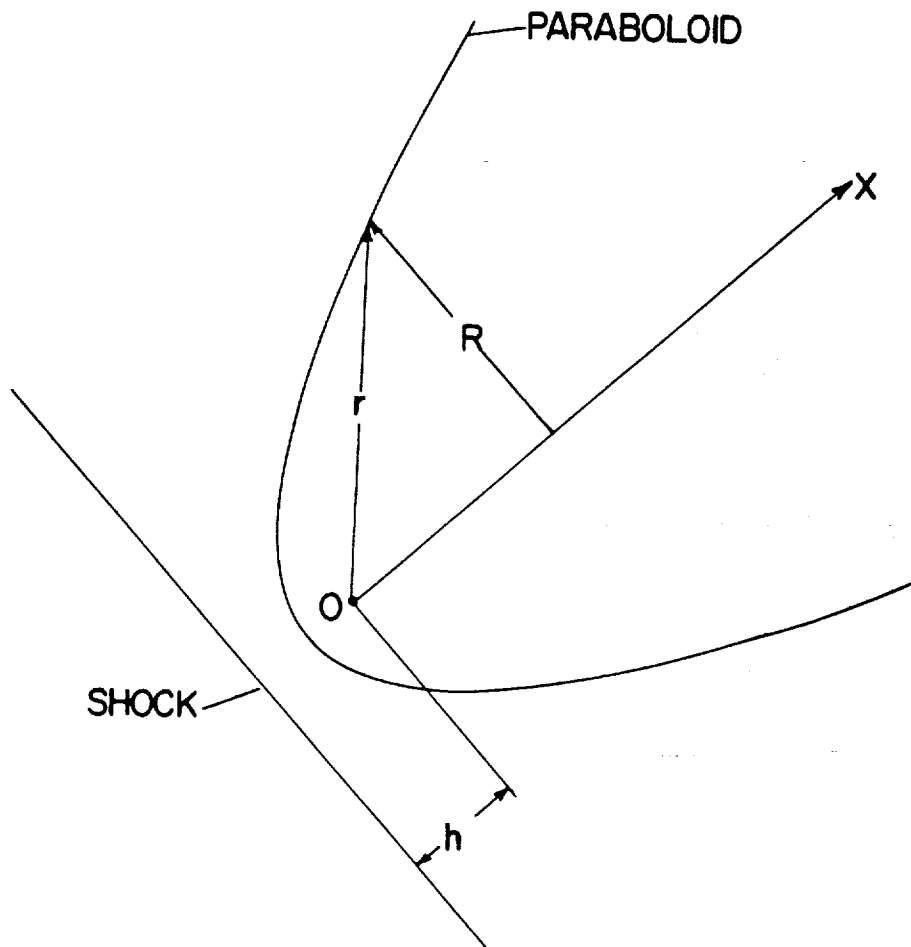
# Crow's Result

Crow's final result for mean square fluctuations (arrived at after a series of reasonable approximations) can be expressed as a simple integration of the turbulent dissipation function through the turbulent layer. This form corresponds to the paraboloid being within the Kolomogorov inertial subrange. Assuming the planetary boundary layer to be similar to a flat-plate wind tunnel boundary layer, Crow obtained a reasonable value for $h_c$. Kamali and Pierce have shown this to be in good agreement with flight test data, beyond the first few feet of the shock.

$$\left(\frac{p_1}{\Delta p}\right)^2 = \frac{1}{h^{7/6}} \int_0^\infty x^{5/6} A E^{2/3} (x) \, dx$$

$$= (h_c / h)^{7/6}$$

$$h_c \approx 0.7 \text{ ft}$$

- **Agrees With Flight Test Data.**

- **Singular at $h = 0$.**

- **No Spectral Information or Structural Details.**

- **Somewhat Sensitive to Turbulence Model.**

- **Assumed Kolmogorov Inertial Subrange.**

# Apply Crow Result to Thickened Shock

The singularity at $h = 0$ is due to a singularity in the scattering equations for very high frequencies. If we distribute his result over a finite shock structure, the singularity vanishes. This figure is for $T = h_c$. In most flight test data, $T$ is at least several times bigger, in which case the RMS envelopes are smaller. Note that away from the shock itself, the simple step function result merges with the distributed form.

For the rest of today's talk, it is sufficient to use Crow's step function result.

$$\langle p_1^2 \rangle^{1/2} \leq \int_{-\infty}^{h} \left(\frac{h - \tau}{h_c}\right)^{-7/12} \frac{d\,p_o}{d\,\tau}\, d\,\tau$$



THICKENED SHOCK

STEP-FUNCTION SHOCK
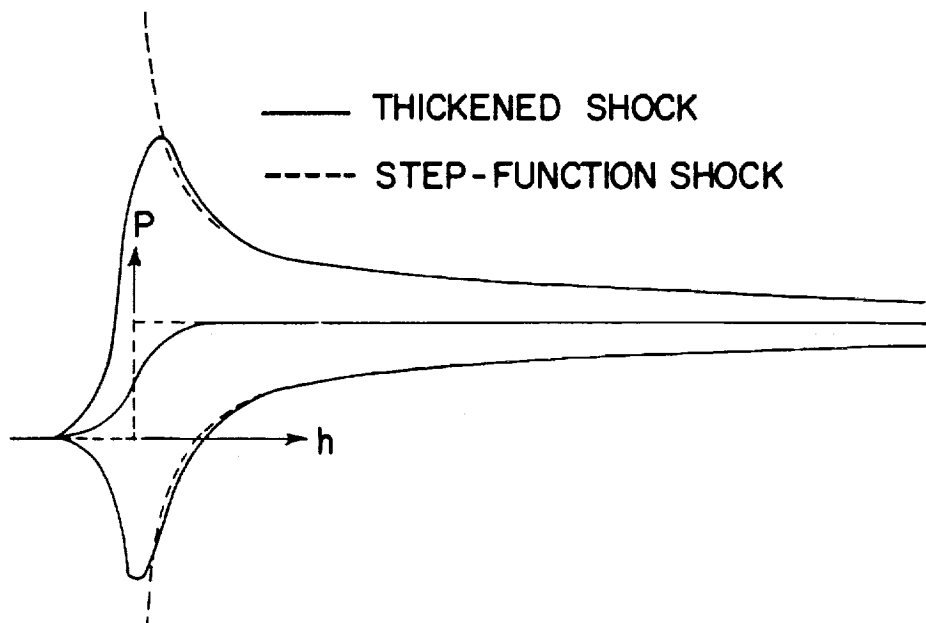
## Root–Mean–Square Perturbations for a Thickened Shock of Thickness $T = h_c$ and $(h_c/h)^{7/12}$.

# Extensions of Crow Model

Crow's model clearly captures the essence of shock wave scattering, and we would like to extend it. The first extension is to consider that the Kolmogorov subrange applies only up to some maximum eddy size. The second would be to allow a general turbulence model. Much of the simplification Crow obtained by assuming the Kolmogorov spectrum served to make some closed form integrals solvable in closed form. Today, we are not so shy about using numerical methods. It would also be nice to include loss processes, since we now know that molecular absorption can be important for the frequencies and distances involved.

We ultimately would like to recover the spectral characteristics of the scattered waves. The RMS envelopes by themselves may not tell an adequate story for loudness. Also, molecular relaxation is frequency dependent, and is difficult to estimate without spectra.

## 1. Paraboloid Larger than Eddy Size $L_o$

$$\left\langle \left| \frac{p_1}{\Delta p} \right|^2 \right\rangle = \frac{1}{h^{7/6}} \int_0^{L_o^2/8h} A \, E^{2/3} \, x^{5/6} \, dx$$

$$+ \frac{1}{h^{3/2}} \int_{L_o^2/8h}^{\infty} C \, x^{1/2} \, dx$$

## 2. General Turbulence Model and Attenuation

$$\left\langle \left| \frac{p_1}{\Delta p} \right|^2 \right\rangle = \frac{1}{h^{7/6}} \int_0^{\infty} G(x) \, e^{-\alpha x} \, dx$$

## 3. Include Spectral Characteristics

$$\left\langle \left| \frac{p_1}{\Delta p} \right|^2 \right\rangle = \frac{1}{h^{7/6}} \int_0^{\infty} G(x) \, \Phi(f) \, e^{-\alpha x} \, dx$$

# Spectral Content of Scattered Sound

Classical harmonic scattering analysis provides spectra of scattered waves as a function of scattering angle and turbulence characteristics. This is a result for high frequencies. This type of formula has been well verified by experiments.

This is written in terms of wave number, which is easily converted to frequency. I have also introduced the macroscale length, which is a convenient quantity directly related to the eddy size.

$$\langle |p_1|^2 \rangle \propto k^4 E\left(2\, k \sin \frac{\theta}{2}\right)$$

# For a Shock With Power Spectrum $1/k^2$ ,

$$\langle |p_1|^2 \rangle \propto \begin{cases} k^2 & ,\ k \le \dfrac{\pi}{5\, L_o\, \theta} \\[2ex] k^{-5/3}\, \theta^{-11/3} & ,\ k > \dfrac{\pi}{5\, L_o\, \theta} \end{cases}$$

$$\left(L_o \approx \frac{2}{5} L_o\right)$$

1252

# Scattering Angle From Paraboloid

It turns out that the scattering angle is very simply obtained from the shape of the paraboloid.
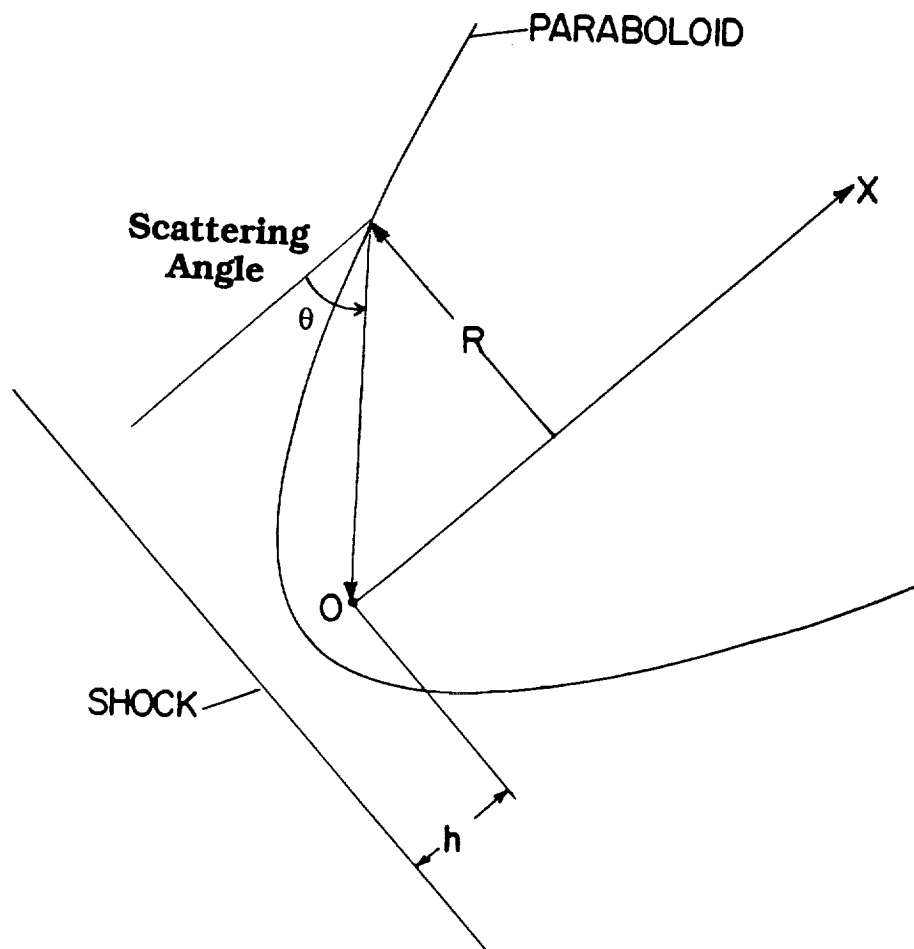


$$R \approx (2\,hx)^{1/2}$$

$$\theta = (2\,h/x)^{1/2}$$

The spectrum can then very simply be applied to the general model, with all expressed in terms of x, h and turbulence parameters. This form includes the frequency content of the incident shock as well as the scattering dependence.

$$\Phi(f) = \frac{6}{11\, f_o} \left\{ \begin{array}{ll} (f/f_o)^2 & f < f_o \\ (f/f_o)^{-5/3} & f > f_o \end{array} \right.$$

**where** $\quad f_o = \frac{a}{10\, L_o} \left(\frac{x}{2h}\right)^{1/2} \quad , \quad \int_0^\infty \Phi(f)\, df = 1$

**so that**

$$\left\langle \left|\frac{p_1}{\Delta p}\right|^2 \right\rangle = \frac{1}{h^{7/6}} \int_0^\infty G(x)\ \Phi(f)\ e^{-\alpha(f)x}\, dx$$

**Note that spectral contribution from distance x will have peak at $f_o$.**

# Peak Scattering Angles

This shows the peak frequency of the scattered sound as a function of h and x. Note that, while scattering is generally thought of as a high-frequency phenomenon, there is considerable scattered energy at low frequencies. This is consistent with the large-scale distortions seen in measured signatures.
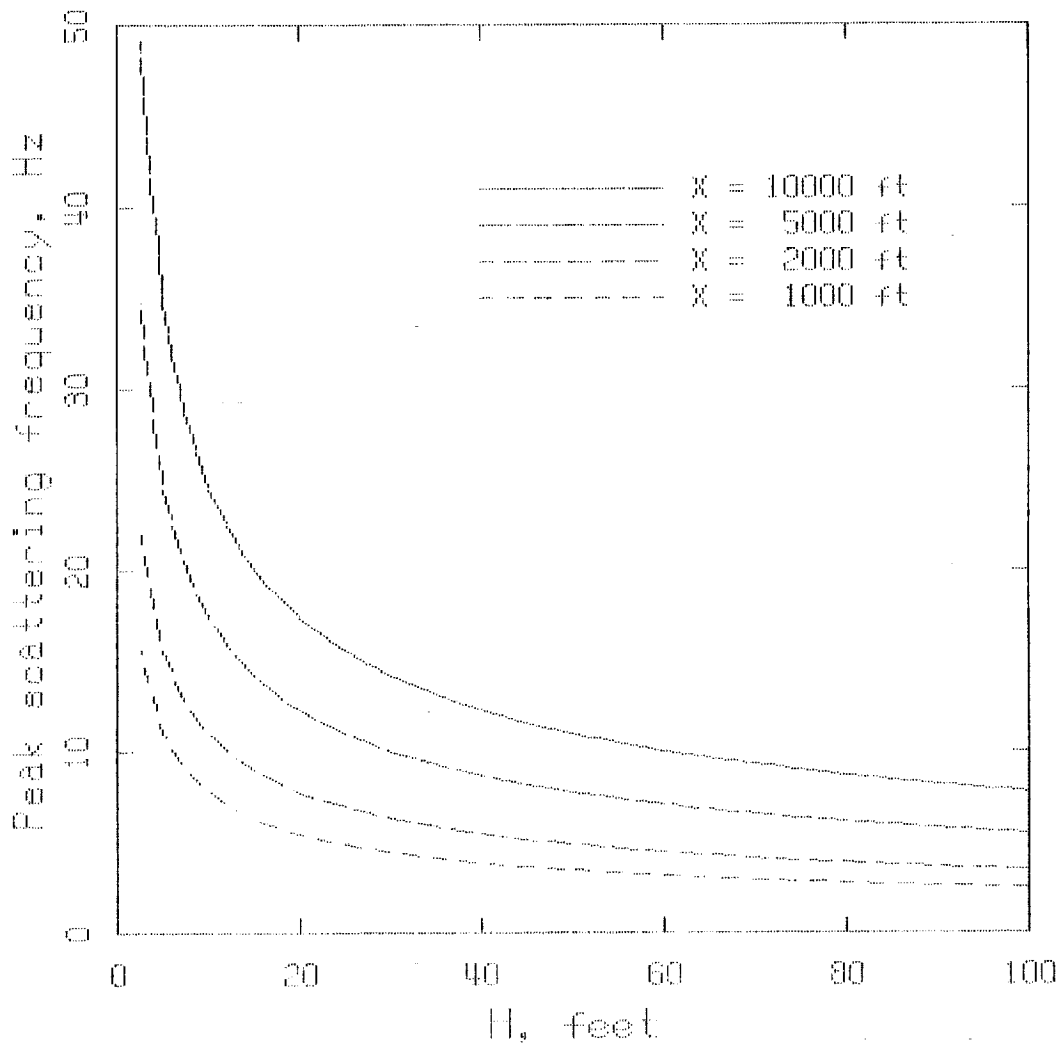
C-3.

# Attenuation by Multiple Scattering

One thought is that, since energy scattered from the shock can be treated as a dissipation mechanism (Plotkin/George theory for anomalous rise times), perhaps it can also attenuate scattered waves. This is the result of such a calculation. It is nice that there is an absolute cap on the perturbation envelopes. It is a little puzzling that the result is so insensitive to turbulence amplitude and to shock thickness. The fatal flaw with this model is that it does not say where the energy is dissipated to. Scattering can redirect sound, but it cannot destroy it. This is therefore a specious result.

$$\alpha = 2 \epsilon^2 L_0 k^2 \quad \text{(Plotkin/George rise time theory)}$$

## Take $\alpha$ at $f_0$ for each $h, x$

ROOT MEAN SQUARE PERTURBATIONS

WAVELENGTH = 200'

$$\frac{\Delta p}{p_\infty} = \frac{1}{2} \times 10^{-3}$$

$L_0 = 100'$

—— $\epsilon^2 = 10^{-3}$

---- $\epsilon^2 = 10^{-7}$
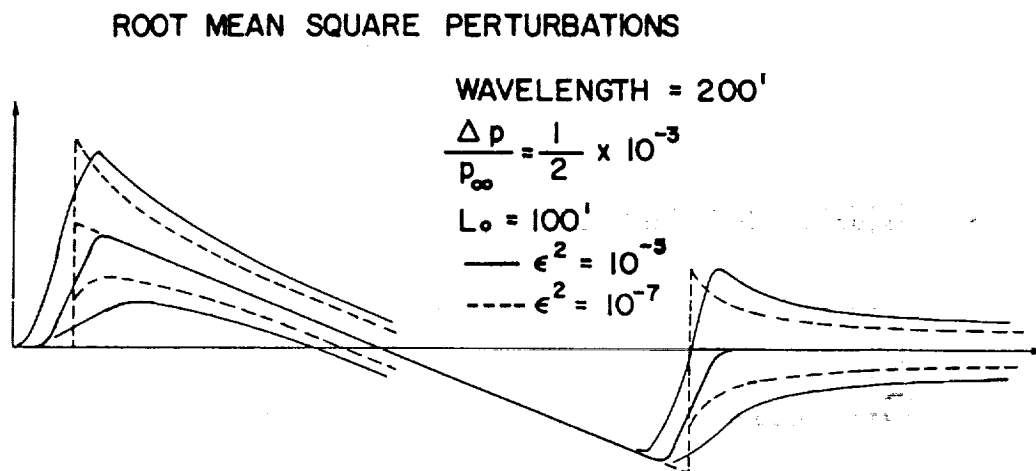
- **Relatively insensitive to turbulence.**

- **Question as to where the multiple scattered energy went.**

# Attenuation by Molecular Absorption

The same formulation can easily handle molecular absorption, which is a genuine dissipation mechanism. The main result I have to show today is a calculation of the scattered spectrum including absorption.

- **ANSI S1.26-1978.**

- **Varies strongly with humidity.**

- **Current results: spectra of fluctuations.**

    - **Spectra at various h**
    - **Effect of humidity**

This shows the spectrum at three distances from the shock, one for humidity. Except at higher frequencies, where absorption kicks in, these spectra have a flatter shape than the f² shape of the incident shock. This is consistent with the high-frequency nature of scattering. This has the potential for a distorted boom to have greater high-frequency content than a clean boom. The high-frequency energy scattered out of the shock is regenerated by nonlinear steepening, but (as will be discussed later) the scattered waves are less susceptible to nonlinear distortion.



1258
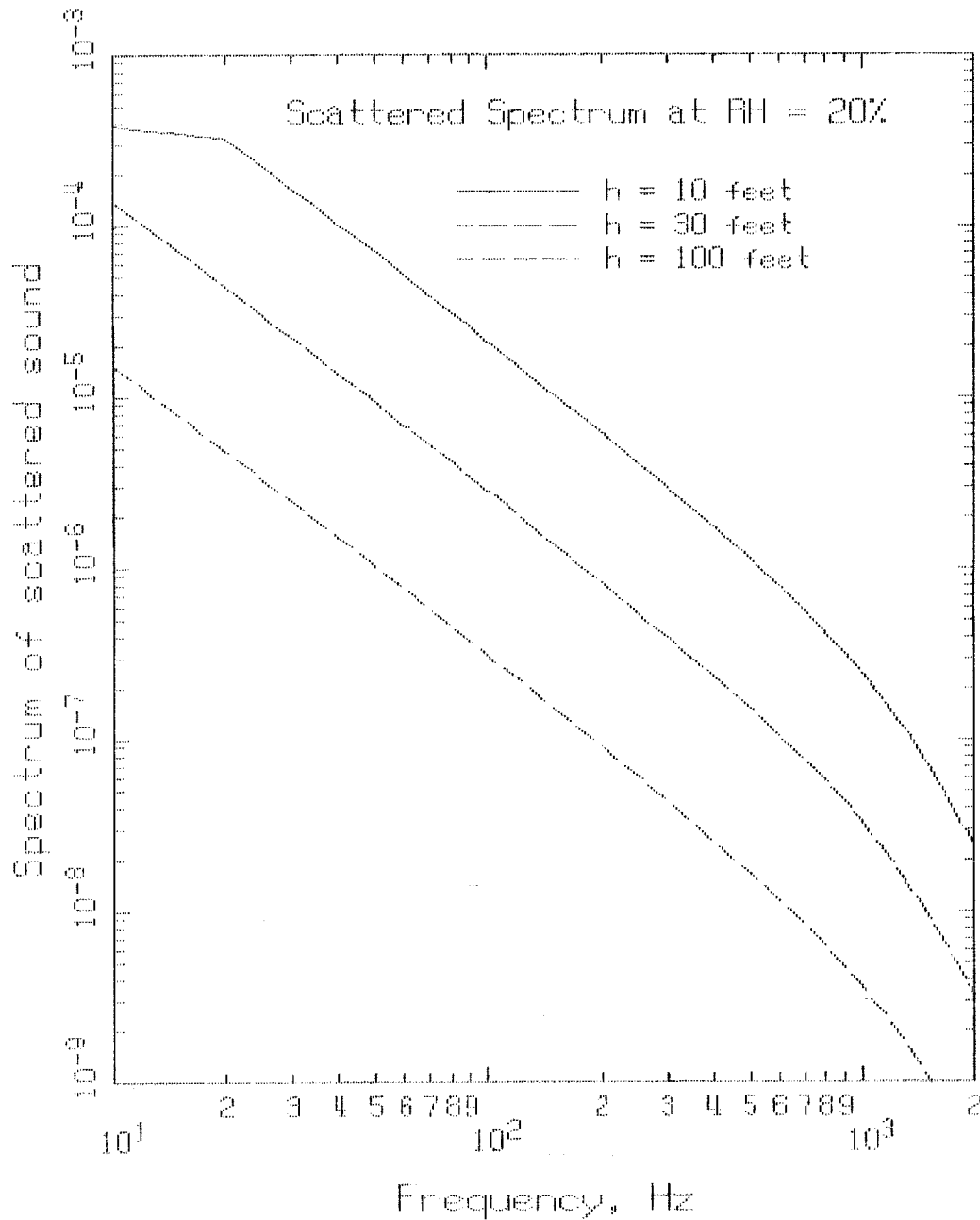
This shows the effect of humidity on the scattered spectrum. Absorption effects are important only at the higher frequency range of this figure, which corresponds to the range where absorption limits the frequency content of the shock itself. The potential "enhanced high frequency" content of a distorted boom involves frequencies which are lower than the frequencies associated with the basic relaxation-dominated shock structure.

1259
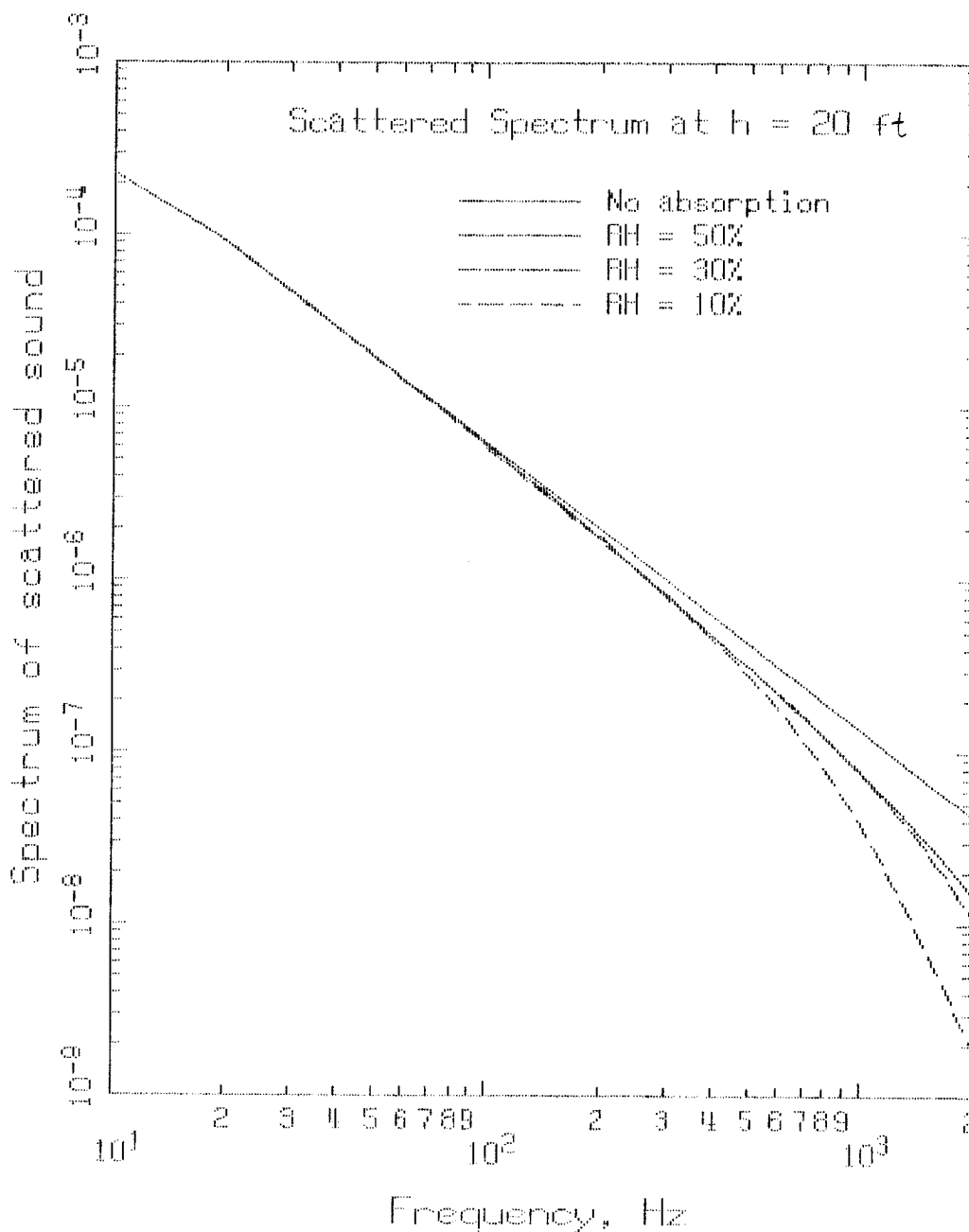
# Nonlinear Considerations

The nonlinear aspect of sonic boom must be considered. Unless the scattering angle is large enough for the scattered sound to fall behind the shock, it will not separate from the shock. This relation can be used *ad hoc* to justify leaving out very small scattering angles, which are singular, but is also a physical reality on what can be considered to be scattered.

## Nonlinear wave propagates at speed

$$a_\infty \left( 1 + \frac{\gamma + 1}{2\gamma} \frac{\delta p}{p} \right)$$

## Shock wave propagates at speed

$$a_\infty \left( 1 + \frac{\gamma + 1}{4\gamma} \frac{\Delta p}{p} \right)$$

## For scattered wave to fall behind shock, require

$$\cos(\theta) < 1 - \frac{\gamma + 1}{4\gamma} \frac{\Delta p}{p}$$

# Nonlinear Attenuation

The existence of the shock (regardless of structure and mechanism) is what causes energy to be lost. A far-field N-wave decays as distance to the 3/4, rather than 1/2, entirely due to this. A short pulse will decay faster than a long one. This leads to the thought that perturbations may be susceptible to nonlinear decay. However, since they are smaller in magnitude, that is not likely to be the case. Scattering may actually cause more energy to get through – simply by removing it from the coherent front which is moving energy into the shock. A more complete analysis, examining the change in spectral content, is required. A psychoacoustic understanding is also needed of the effects of medium-frequency perturbations following a shock.

- **Steepening causes energy to flow into shock, where it is lost.**

  - **Total energy loss is governed by Rankine-Hugoniot relations, independent of actual dissipation mechanism.**

  - **Detailed structure of shock depends on mechanism.**

- **Scattered waves will steepen.**

  - **Rate of steepening proportional to local pressure jump.**

  - **Perturbations steepen slower than original wave.**

# Conclusions

We are out to establish whether turbulent distortion has any effect (adverse or not) on sonic boom loudness. The material presented today is an indication of the approaches we are taking. The main new result is that scattering does not substantially enhance the highest frequencies (those associated with the shock), but does apparently enhance somewhat lower frequencies. Scattering does not appear to be a potential mechanism for increasing overall attenuation of sonic booms. As our analysis proceeds, we will be examining realistic atmospheric models and applying our analysis to minimized boom signatures.

- **Have estimated spectral content of scattered fluctuations.**

- **Medium frequencies are enhanced.**

- **Current model is being expanded to general turbulence.**

- **Seeking an understanding of interaction between various physical mechanisms.**

1262

# Session IX. Sonic Boom (Human Response and Atmospheric Effects)

*omit*

Statistical and Numerical Study of the Relation Between Weather and Sonic Boom Characteristics
*Lixin Yao, Dr. Henry E. Bass and Richard Raspet, The University of Mississippi; and Walton E. McBride, Planning Systems, Inc.*

THIS PAGE INTENTIONALLY BLANK

1264

# Statistical and Numerical Study of the Relation Between Weather and Sonic Boom Characteristics

*5/1 - 71*
*/2041*

Lixin Yao, Henry E. Bass and Richard Raspet

Physical Acoustics Research Group
The University of Mississippi
University, MS 38677

and

Walton E. McBride

Planning Systems, Inc., Christian Lane, Slidell, LA 70458

NASA measured sonic boom characteristics near Edwards Air Force Base from 11/66 to 1/67. 34 flights of F-104 were performed at an altitude of about 31, 000 feet and flying speed of Mach 1.3 . 42 microphones were placed on the ground directly under the fight track. Each microphone recorded boom shape, rise time, peak overpressure, total boom duration, positive duration and positive impulse.

# TEST CONDITIONS

## EDWARDS TEST (11/66 - 1/67)

F-104, 34 FLIGHTS

31, 000 FEET
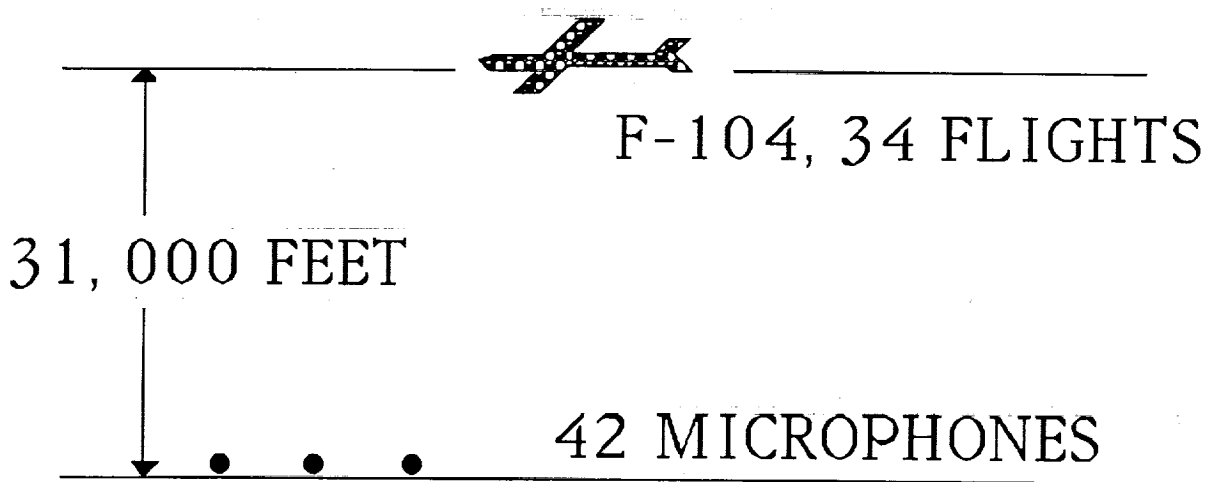
42 MICROPHONES

## EACH MICROPHONE RECORDS: SHAPE, RISE TIME, AND OTHER PARAMETERS.

## TEST CONDITIONS OF OKLAHOMA CITY AREA TEST

Another test was performed in the Oklahoma City area from 2/64 to 7/64. Four types of aircraft flew at various altitude. Only the data obtained with F-104 at approximately 31, 000 feet  have been analyzed in this study. There were 168 such flights. Three microphones were located on the ground, with one underneath, one at 5 miles lateral distance and the 3rd at 10 miles lateral distance. Same information of boom was recorded as in Edwards test.

# OKLAHOMA TEST (2/64-7/64)

F-104, 168 FLIGHTS

31, 000 FEET

1267
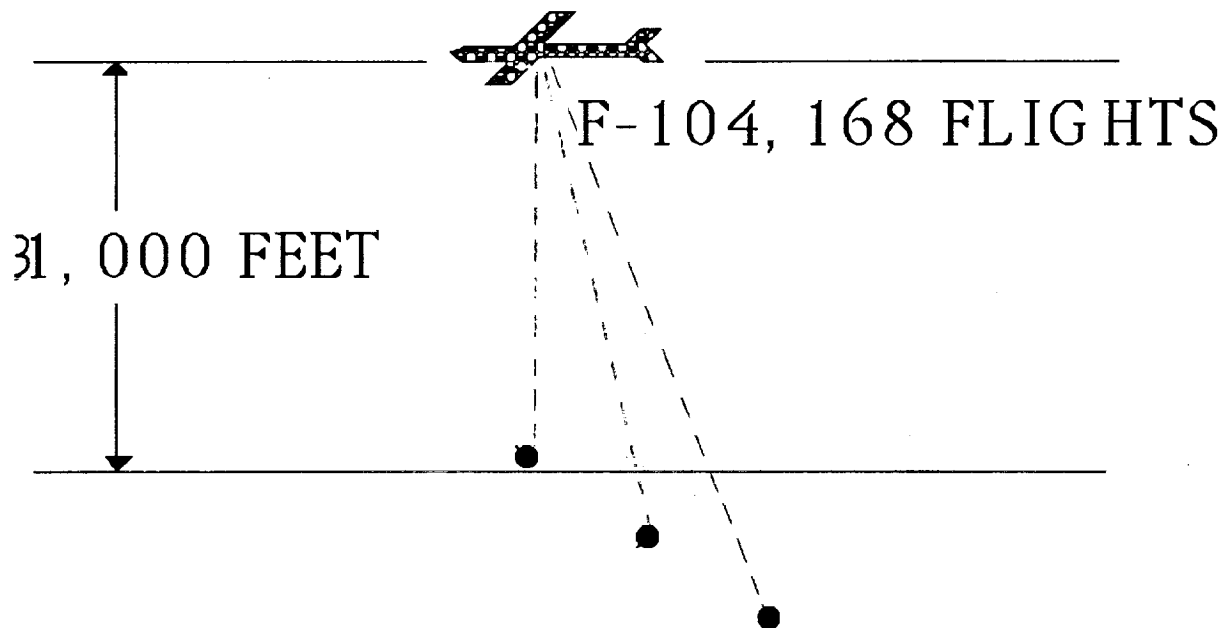
# DEFINITION OF TURNER CLASS

Weather conditions including wind speed, temperature and cloud cover at the time of operation along with time of the flights were also recorded. From this information, a meteorological parameter called Turner Class can be derived. Turner Class has seven integer values, from 1 to 7, with 1 representing dominant convective turbulence, 4 for strong mechanical turbulence and 7 for stable stratification. Values between are mixing states of these three extreme conditions. Under fixed wind speed, when downward radiation increases, Turner Class shifts toward 1, when upward radiation increases, it approaches 7. Under fixed radiation index, when wind speed increases, the Turner Class approaches 4. Turner Class was calculated to indicate the turbulence condition at each flight time.

## DEFINITIONS OF TURNER CLASSES

| Wind Speed (knots) | Net Radiation Index | | | | | | |
|---|---|---|---|---|---|---|---|
| | 4 | 3 | 2 | 1 | 0 | -1 | -2 |
| | DOWNWARD RADIATION INCREASES | | | | UPWARD RADIATION INCREASES | | |
| 0-1 | 1 | 1 | 2 | 3 | 4 | 6 | 7 |
| 2-3 | 1 | 2 | 2 | 3 | 4 | 6 | 7 |
| 4-5 | 1 | 2 | 3 | 4 | 4 | 5 | 5 |
| 6 | 2 | 2 | 3 | 4 | 4 | 5 | 6 |
| 7 | 2 | 2 | 3 | 4 | 4 | 4 | 5 |
| 8-9 | 2 | 3 | 3 | 4 | 4 | 4 | 5 |
| 10 | 3 | 3 | 4 | 4 | 4 | 4 | 5 |
| 11 | 3 | 3 | 4 | 4 | 4 | 4 | 4 |
| ≥12 | 3 | 4 | 4 | 4 | 4 | 4 | 4 |

# SONIC BOOM SIGNATURE PARAMETERS

Boom shapes were originally sorted into 10 types: N, NP, NR, P, PP, SP, SPR, PR, R and CO. They were grouped into three main categories in our statistical analysis, with N, NP to N-Wave Type, P, PP, SPR and PR to Peaked Type, and R and NR to Rounded Type. The 1st type is basically a N- wave. The 2nd type has an abrupt rise followed by an abrupt drop at the front shock. The 3rd type is much more rounded comparing with others. Rise times cover a wide range from 1 to 20 ms. They were also grouped into 4 major domains, with 1 covering from 1 to 5 ms, 2: 5 - 7 ms, 3: 7 - 9 ms and 4: 9 - 20 ms. The non-uniform grouping is based on the consideration that there should be a considerable occurrence for each domain. 7 wind speeds appeared in Edwards test: 0, 1, 2, 4, 5, 6, 7 and 16 knots. They were grouped too, with 11.5 (average value) representing 7 and 16, 5 for 4, 5 and 6, 1 for 0 and 2 knots.

Sonic Boom Signature Parameters
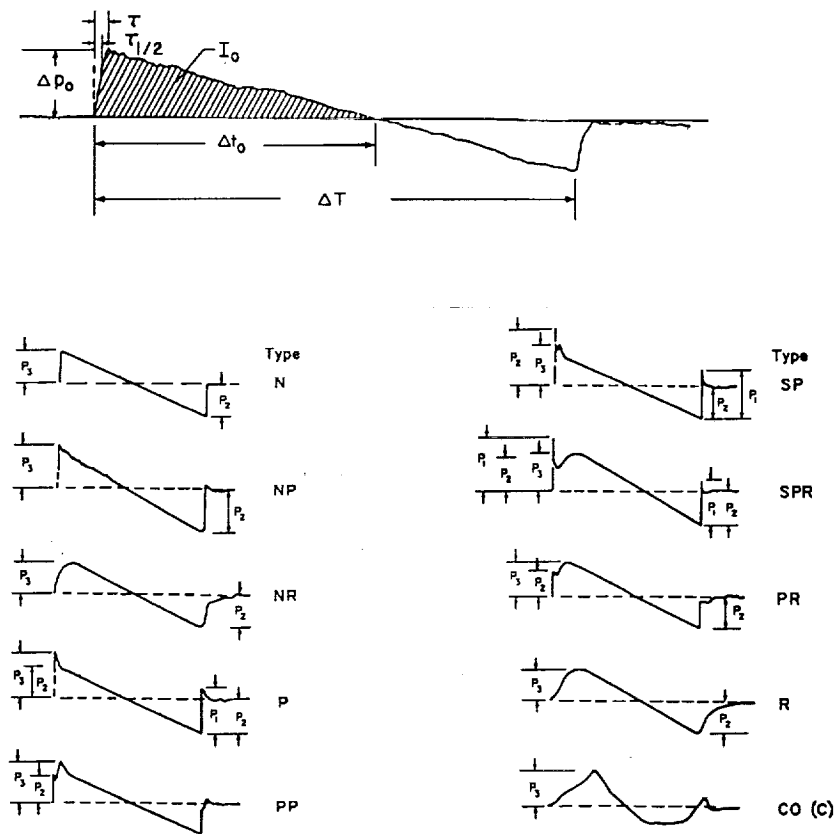




Fig    Diagrams of waveforms which represent the various categories of measured sonic-boom signatures.

# FREQUENCY TABLE OF TURNER CLASS AND RISE TIME

Each flight has a corresponding Turner Class. Each flight led to many shapes with varying rise times and other boom parameters. Thus, one certain Turner Class is associated with many rise times, which can be categorized into one of the 4 major domains and we can count how many rise times fall into each individual domain. In this way, a frequency table for Turner Class and rise time was generated. Only Edwards data were processed for this table. There were 1, 330 valid cases.

# FREQUENCY TABLE OF TURNER CLASS AND RISE TIME

| Turner Class | Rise Time | | | |
|---|---|---|---|---|
| | 1 | 2 | 3 | 4 |
| 4 | 97 | 99 | 97 | 192 |
| 5 | 119 | 65 | 52 | 117 |
| 6 | 149 | 92 | 87 | 125 |
| 3 | 19 | 9 | 6 | 5 |

## NORMALIZED FREQUENCY TABLE OF TURNER CLASS AND RISE TIME

Each row of the preceding table was normalized to give the following table. By doing this, we can see the distribution of rise times under each Turner Class. Note that for pure mechanical turbulence (Turner Class 4), there are more long rise times. When mechanical turbulence becomes less dominant (3) or damped (5, 6), there are more short rise times.

# NORMALIZED FREQUENCY TABLE OF TURNER CLASS AND RISE TIME

| Turner Class | Rise Time | | | |
|---|---|---|---|---|
| | 1 | 2 | 3 | 4 |
| 4 | 0.20 | 0.20 | 0.20 | 0.40 |
| 5 | 0.34 | 0.18 | 0.15 | 0.33 |
| 6 | 0.33 | 0.20 | 0.19 | 0.28 |
| 3 | 0.49 | 0.23 | 0.15 | 0.13 |

## NORMALIZED FREQUENCY TABLE OF TURNER CLASS AND WAVE SHAPE

A similar frequency table can be obtained for Turner Class and wave shapes, and row normalization can be done also. Only the normalized tables will be provided from now on. We see that weather conditions which result in strong mechanical turbulence give rise to the largest percentage of rounded wave shapes. When mechanical turbulence becomes less dominant (convective turbulence becomes more dominant, Turner Class 3,2,1) or damped (Turner Class 5, 6) this percentage decreases, while the N-wave type wave shape becomes more common until dominant. The table also shows that the peaked wave shapes are quite rare and occur most commonly for Turner Class 3 and 6. Turner Class 3 is mildly convective and Turner Class 6 is moderately stable. We speculate that the presence of peaked type wave forms is an indicator of large scale refractive structures in the atmosphere. The effects of these structures are overwhelmed by scattering from smaller scale mechanical turbulence as wind increases.

# NORMALIZED FREQUENCY TABLE OF TURNER CLASS AND WAVE SHAPE

| Turner Class | Wave Shapes | | |
| --- | --- | --- | --- |
| | N-wave | Peaked | Rounded |
| 4 | 0.26 | 0.04 | 0.70 |
| 5 | 0.34 | 0.06 | 0.60 |
| 6 | 0.21 | 0.12 | 0.66 |
| 3 | 0.46 | 0.13 | 0.41 |
| 2 | 0.80 | 0.00 | 0.20 |
| 1 | 0.86 | 0.00 | 0.14 |

## ROW-NORMALIZED FREQUENCY TABLE OF RISE TIME AND WAVE SHAPE

Mechanical turbulence tends to increase rise time and induce rounded boom shapes according to previous tables, indicating the relationship between the two boom characteristics. This can be shown with another normalized frequency table for shape and rise time, (based on Edwards data). It is clear from the table that rounded wave shapes are associated with longer rise times (domain 4), while the peaked and N-wave types are more likely to have a shorter rise time (domain 1).

# ROW-NORMALIZED FREQUENCY TABLE OF RISE TIME AND WAVE SHAPE

| Rise Time | Wave Shapes | | |
|-----------|--------|--------|---------|
|           | N-wave | Peaked | Rounded |
| 4 | 0.06 | 0.05 | 0.89 |
| 3 | 0.08 | 0.05 | 0.87 |
| 2 | 0.19 | 0.07 | 0.73 |
| 1 | 0.59 | 0.12 | 0.29 |

# NORMALIZED FREQUENCY TABLE OF WIND AND RISE TIME

Wind is an important factor in determining the Turner Class. We look specifically into the relationship between wind and rise time. A normalized table was obtained as following. The statistics shows that strong winds tend to associate with long rise times and weak winds are more likely associated with a short rise time. Similar statistics were examined for each Turner Class. There was no similar indication that strong wind has a trend to increase the rise time within a fixed Turner Class. The frequency tables for wind speed versus shape does not reveal any correlation.

# NORMALIZED FREQUENCY TABLE OF WIND AND RISE TIME

| Wind | Rise Time | | | |
|------|------|------|------|------|
| | 1 | 2 | 3 | 4 |
| 11.5 | 0.16 | 0.16 | 0.22 | 0.46 |
| 5.0 | 0.33 | 0.18 | 0.17 | 0.32 |
| 1.0 | 0.30 | 0.25 | 0.18 | 0.27 |

# INITIAL SHAPE OF SONIC BOOM

A physical model was established to investigate the propagation of a sonic boom through turbulence. We simulated the turbulent atmosphere with a distribution of spherical turbules randomly distributed in space (100 by 100 by 100 m, the turbules occupy 13% of the total volume of the space). An initial N-wave type boom shape is assumed, which is then Fourier transformed. The initial shape has a rise time of 0.2 ms. (defined as from onset of shock to the maximum peak overpressure) Each frequency component (spherical wave) is first order scattered by each turbule under Rytov approximation and the scattering waves from all of the turbules are summed to give the amplitude and phase of the pressure of this particular component at the receiver. An inverse Fourier transform is then applied to obtain the boom shape at the receiver.
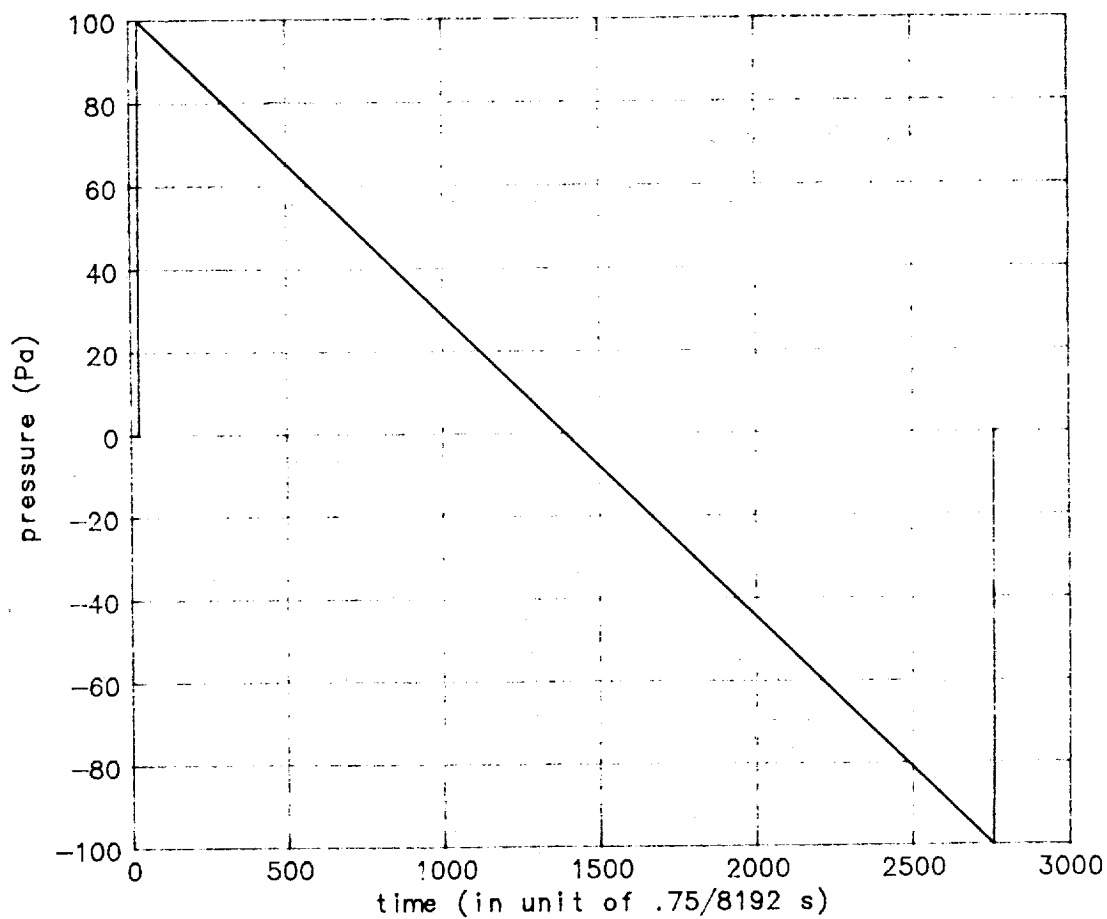
Fig            INITIAL SHAPE OF SONIC BOOM

# SHAPE FROM REALIZATION 8 FOR TURBULE SIZE OF 1 M

32,000 turbules with radius 1 m are randomly distributed in the 100 by 100 by 100 m space. The resulting shape at the receiver 100 away from the source is simply a N-wave type. This shape has rise time of 1.282 ms. We see that the turbulence represented by this configuration does not deform the original shape except that some small wiggles are added to the boom.
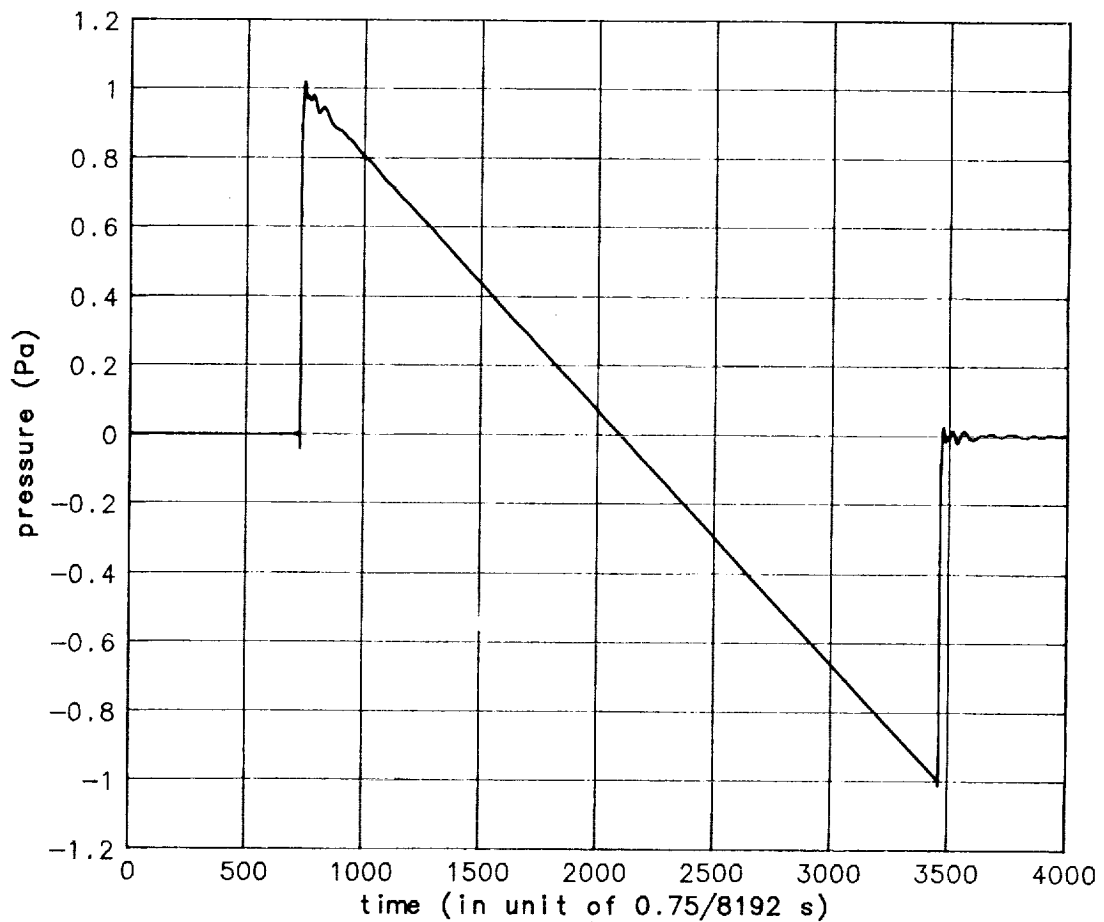


Fig    SHAPE FROM REALIZATION 8 FOR TURBULE SIZE OF 1 M

# SHAPE FROM REALIZATION 6 FOR TURBULE SIZE OF 10 M

32 turbules with radius 10 m are randomly distributed in the space. The final shape belongs to the PR type, with a rise time of 10.254 ms. Here the effect of turbulence is obvious, the shape becomes rounded and the rise time is much increased. The expected rise time due to molecular relaxation is on the order of 1-3 ms.
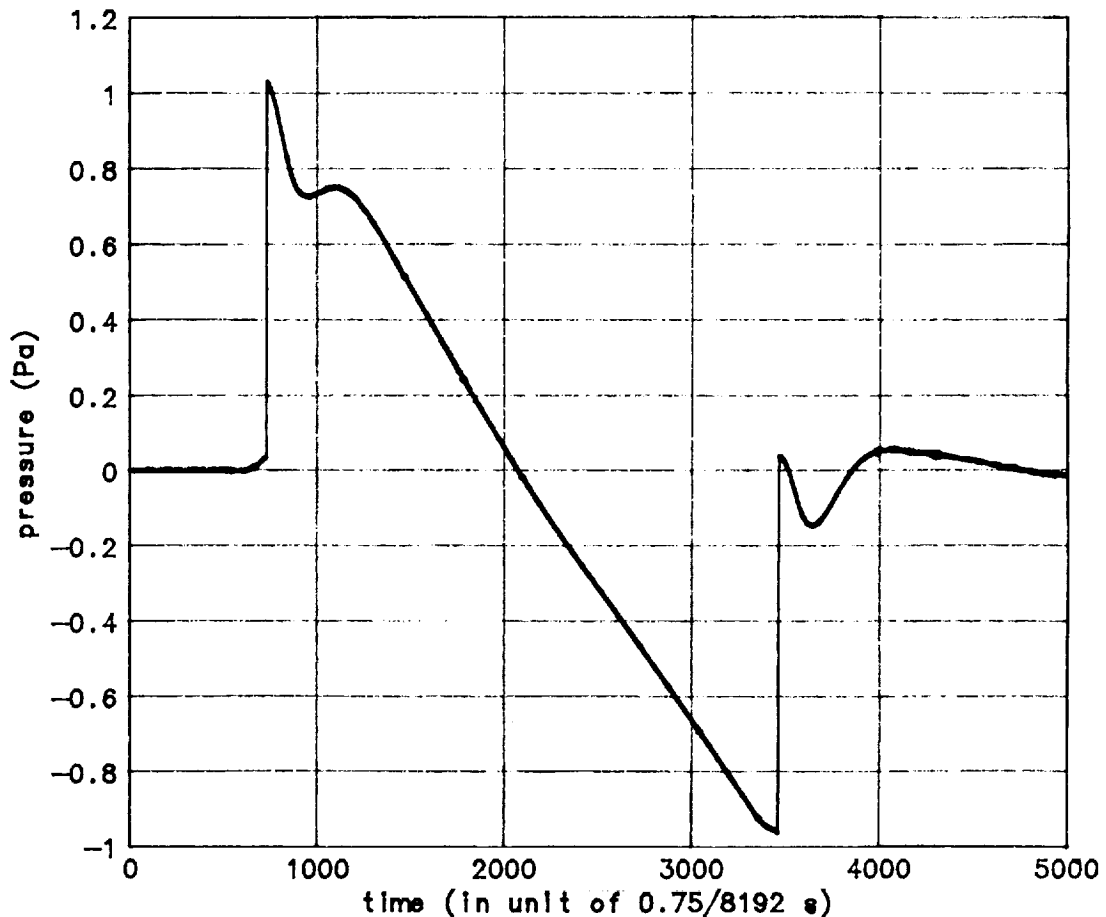


Fig    SHAPE FROM REALIZATION 6 FOR TURBULE SIZE OF 10 M

# SHAPE FROM REALIZATION 8 FOR TURBLUE SIZE OF 10 M

One more realization of 32 turbules generates the following R type boom shape. The rise time is 16.479 ms. The turbulence makes the shape very rounded and the rise time very long, up to the order of long rise times really observed in the previously described tests.
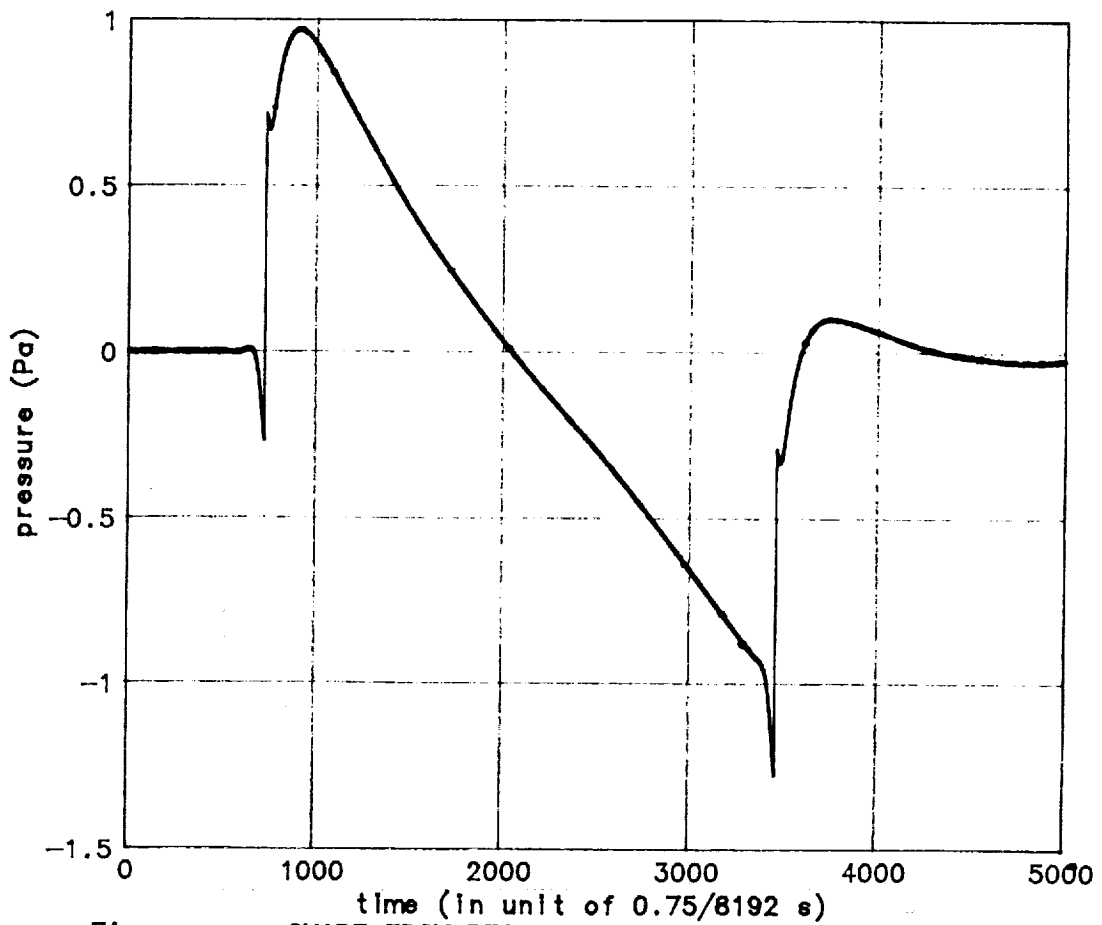


Fig        SHAPE FROM REALIZATION 8 FOR TURBULE SIZE OF 10 M

# SHAPE FROM REALIZATION 7 FOR TURBULE SIZE OF 10 M

Another realization of 32 turbules gives the following shape. The amazingly strong wiggles at both the front and the back shock are very impressive. The rise time of this shape is 4.578 ms. The details of front and back shock are shown by the two pictures following this one. The symmetry between the front shock and the back shock is consistent with the feature of the shapes observed.
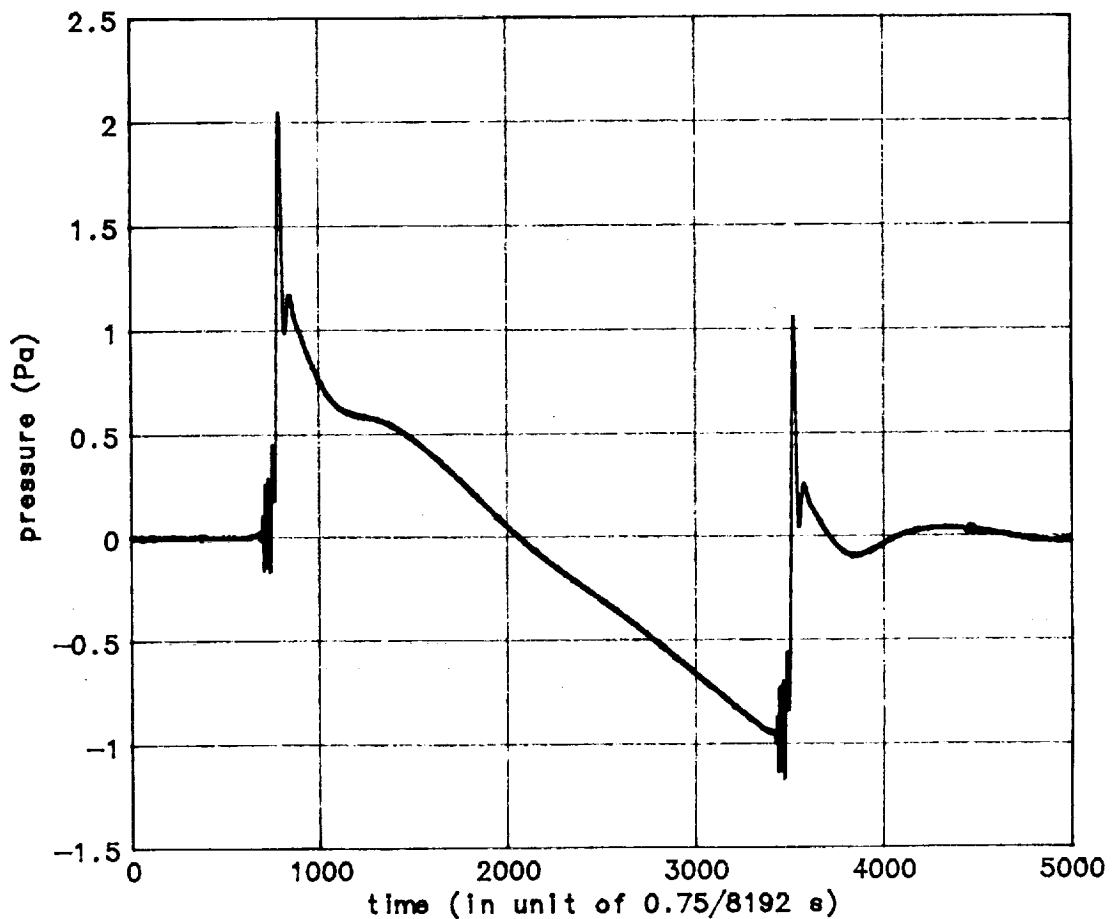


Fig          SHAPE FROM REALIZATION 7 FOR TURBULE SIZE OF 10 M
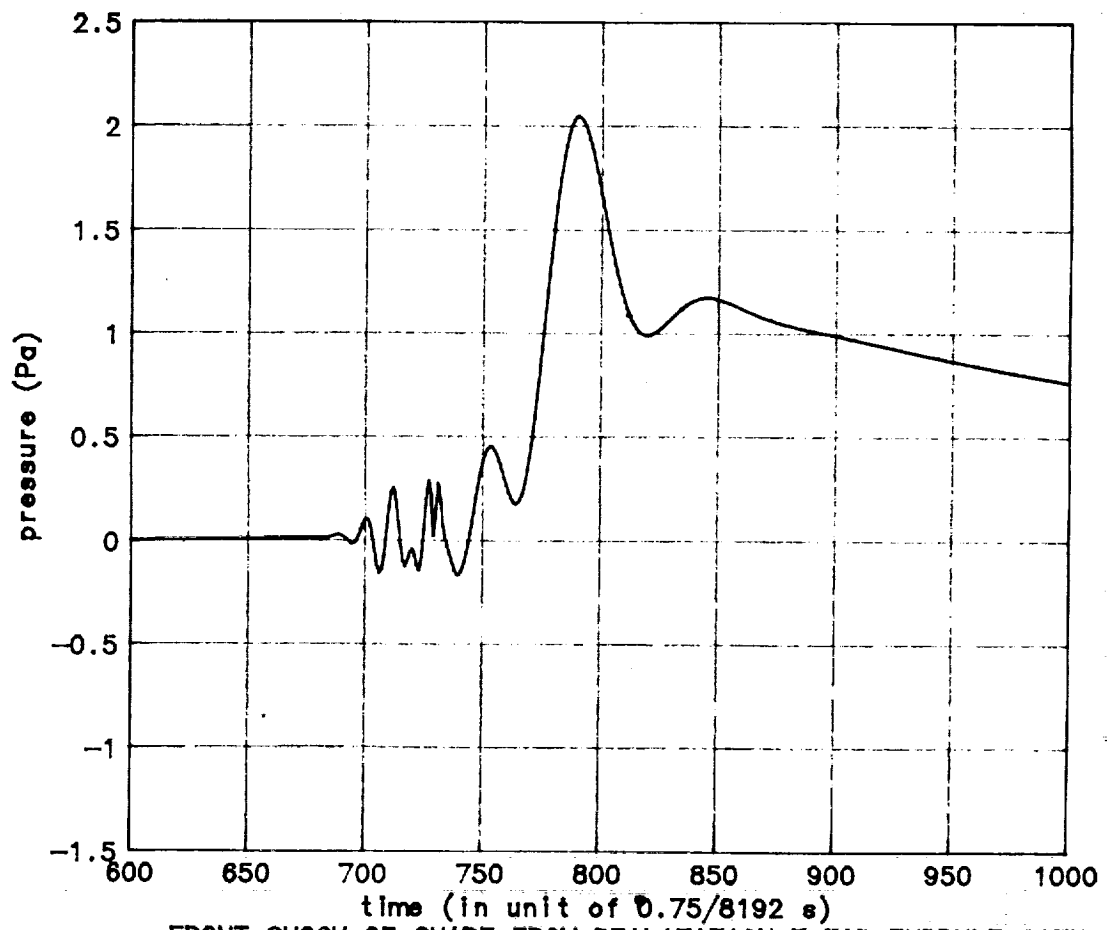
Fig　　　　FRONT SHOCK OF SHAPE FROM REALIZATION 7 FOR TURBULE SIZE OF 10 M
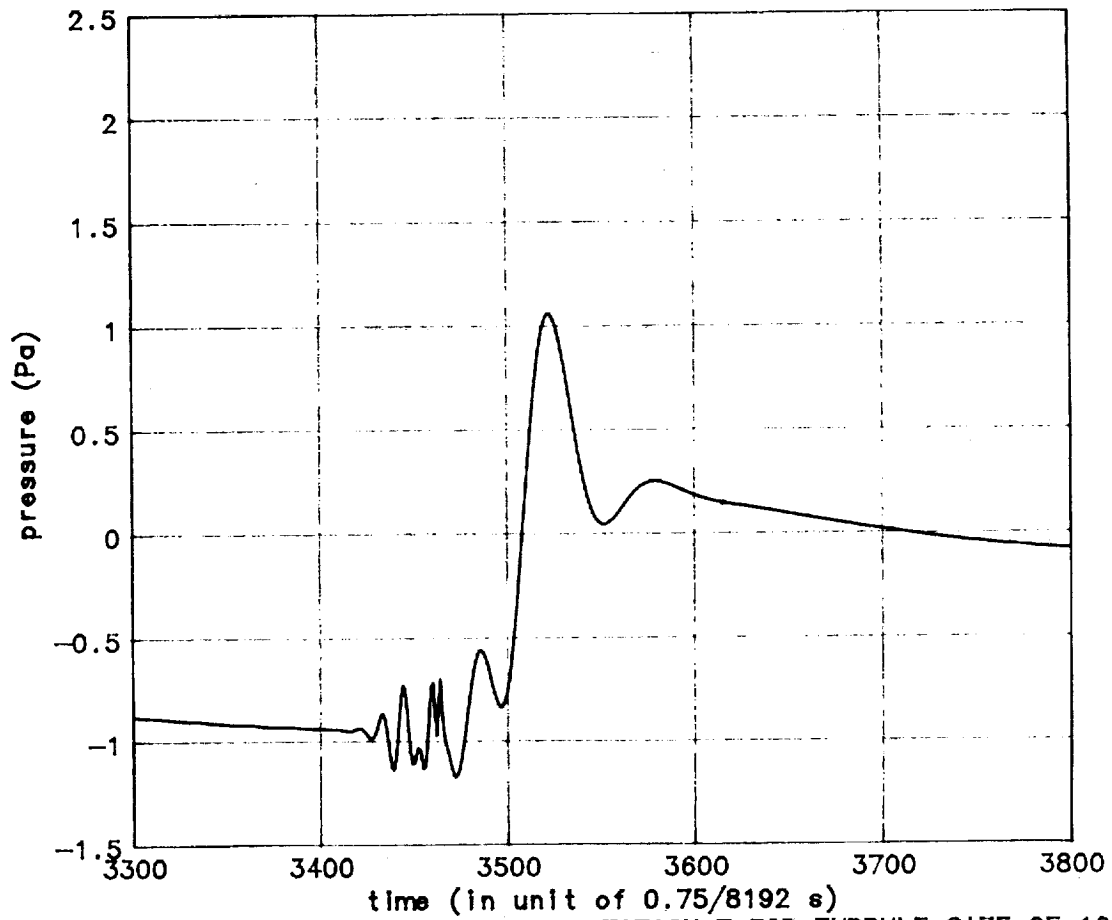
Fig      BACK SHOCK FROM REALIZATION 7 FOR TURBULE SIZE OF 10 M

# CONCLUSION

1. Turbulence and sonic boom propagation are related.

2. Strong mechanical turbulence is associated with long rise times and rounded boom shapes.

3. Presence of convective turbulence or stable stratification is associated with short rise times and N-wave type shapes.

4. Since rise time is both sensitive to wind and Turner Class, while boom shape is only correlated with Turner Class, rise time can be considered a more suitable indicator to judge the influence of turbulence (mechanical).

5. Numerical calculation based on a turbulence scattering model does predict the rounded wave shapes and long rise times, which is consistent with above statistical conclusion. We infer that pure mechanical turbulence has the proper turbule size which results in these rounded type shapes, while strong convective turbulence does not. Stable stratification certainly is not involved with turbulence and N-wave type shapes are expected to be observed at the receiver.

# REFERENCES

1. Domenic J. Maglieri, Vera Huckel, Herbert R. Henderson and Norman J. McLeod, "Variability in Sonic-Boom signatures Measured Along an 8000 -foot Linear Array," NASA TN D-5040 (1969).

2. Domenic J. Maglieri and Victor E. Sothcott, "Summary of Sonic Boom Rise Times Observed During FAA Community Response Studies Over a 6-Month Period in the Oklahoma City Area," NASA Contract Report 4277 (1990).

3. Hans A. Ponofsky and John A. Duton, Atmospheric Turbulence, Model and Method for Engineering Applications, (John wiley & Sons, New York, 1984).

4. Henry E, Bass, Jean Ezell and Richard Raspet, "Effect of Vibrational Relaxation on Rise Times of Shock Waves in the Atmosphere," J. Acoust. Soc. Am., 74, 1514-1517 (1983).

5. Jongmin Kong and Allan D. Pierce, "The Effect of Molecular Relaxation Processes in Air on Rise time of Sonic Booms," International Congress on Recent Developments in Air- and Structure- Borne Sound and Vibration, March 6-8, 1990, Auburn University, USA.

6. Walton E. McBride, Henry E. Bass and Richard Raspet, "Scattering of Sound by Atmospheric Turbulence," (to be published.)

THIS PAGE INTENTIONALLY BLANK

# Session IX. Sonic Boom (Human Response and Atmospheric Effects)

*Sm II*

Overview of NASA Human Response to Sonic Boom Program
*Dr. Kevin P. Shepherd, NASA Langley Research Center*

THIS PAGE INTENTIONALLY BLANK

1286

HSR SONIC BOOM
ACCEPTABILITY

$5/2 - 52$
$/2042$

# OVERVIEW OF NASA
# HUMAN RESPONSE TO SONIC BOOM
# PROGRAM

BY

KEVIN P. SHEPHERD
NASA LANGLEY RESEARCH CENTER

For some routes the ability to fly at supersonic speeds over land as well as over water would greatly enhance the time benefit to the passenger. It would also increase the productivity and and economic viability of the aircraft. There are no reliable guidelines which can be used to determine a sonic boom exposure which would be acceptable for over land supersonic flight. In addition to the peak pressure of the sonic boom, the detailed shape of the signature will also influence the perception, and therefore the community response, to sonic boom exposures.

Initially, the program aims to develop the capability to predict human response to individual sonic booms. This will enable a quantitative assessment of the benefit of "low boom" aircraft configurations and will also serve to guide the design of the aircraft and its operating conditions. This capability will form the foundation of studies to determine the relationship between sonic boom exposure and community response. Only then will it be possible to assess the feasibility of acceptable overland supersonic flight.

| HSR SONIC BOOM ACCEPTABILITY | PROGRAM OBJECTIVE |
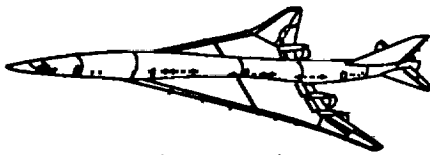
• Establish feasibility of acceptable overland supersonic flight

OR

• Economic viability assuming subsonic overland restriction

# PROGRAM APPROACH

The assessment of the feasibility of acceptable overland supersonic flight requires that consideration be given to the range of sonic booms that are achievable through aircraft design. The determination of an appropriate single-event sonic boom assessment method can be used to guide the design of "low boom" configurations and their operating conditions, since these influence the sonic boom that reaches the ground. Furthermore, it is necessary to quantify the effects of the atmosphere on the sonic boom signature passing through it.

**HSR SONIC BOOM ACCEPTABILITY** | **APPROACH**

• Define acceptable sonic boom exposure
• Assess feasibility through aircraft design and operation
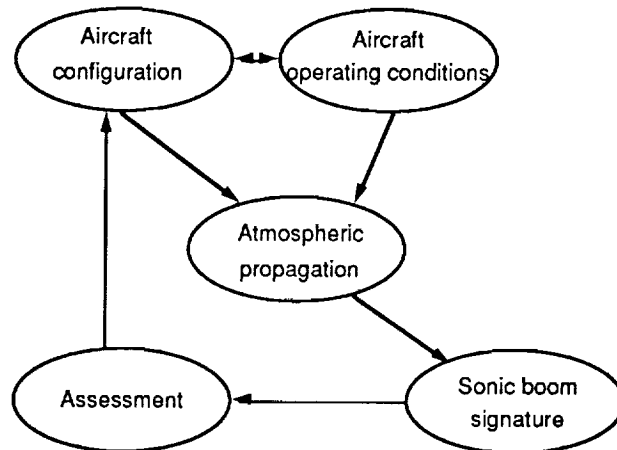
# ELEMENTS OF THE SONIC BOOM ACCEPTABILITY PROGRAM

The determination of a sonic boom exposure which would be acceptable to the general population requires, as a first step, a method to quantify human response to individual sonic booms. Laboratory studies are being conducted to determine human response to simulated sonic booms. The sonic booms include the classical N-wave as well as those shapes which might be produced by "low-boom" configurations. These studies are aimed at identifying a noise metric which can predict, with confidence, human response to arbitrary sonic boom shapes and amplitudes. These studies also include the simulation of sonic booms as they would be heard indoors, by incorporation of the acoustic transmission properties of residential structures. Human response to sonic booms within a structure is a function of both the transmitted acoustic signal and any perceivable vibration or secondary acoustic radiation due to rattling of windows, pictures, etc. Thus, analytical and experimental studies are being performed to assess the response of typical structures to excitation by sonic booms.

The response of people who experience sonic booms on a regular basis in their homes will be influenced by many factors such as the number of booms, the time of day that they occur, the activity that the person is engaged in, etc. An in-home sonic boom generation system will be installed in volunteers' homed for an extended period of time in order to examine some of these variables. It will also be possible to compare the residents' response to sonic booms with their response to more familiar sounds such as aircraft flyover noise.

The determination of the relationship between sonic boom exposure and community response will be derived from studies of populations which are routinely exposed to sonic booms. Studies of this type provide the information to answer public policy questions regarding acceptable levels of sonic boom exposure.

| HSR SONIC BOOM ACCEPTABILITY | PROGRAM ELEMENTS |
| --- | --- |

- LABORATORY RESPONSE STUDIES
  - Single event sonic boom metric (outdoor listening conditions)
  - Single event sonic boom metric (indoor listening conditions)
  - Quantify benefits of sonic boom shaping

- BUILDING RESPONSE STUDIES
  - Building response and acoustic transmission
  - Contribution of vibration & rattles to human response

- IN-HOME RESPONSE STUDIES
  - Sonic boom exposure metric
  - Comparison with familiar noise sources (aircraft noise, road traffic)

- COMMUNITY RESPONSE STUDIES
  - Sonic boom exposure criteria
  - Comparison with familiar noise sources

1290

# SONIC BOOM ACCEPTABILITY CRITERIA

The determination of sonic boom acceptability criteria initially requires the determination of a method to assess individual sonic booms. The sonic boom simulators shown on the left of the figure are designed to examine human response to sonic booms. The booth, located at the NASA Langley Research Center, is equipped with loudspeakers which generate simulated sonic booms. The signal provided to the speakers is computer-generated, to allow flexibility in the range of signals and to enable compensation for some of the inadequacies of the sound reproduction system. The simulator can simulate sonic booms having overpressures as high as 4 psf, with rise times as short as 1 msec. The sketch represents a house with external acoustic sources that is being built at the Georgia Institute of Technology, and is intended for studies of both human and structural response to sonic booms. In contrast to the NASA simulator, the simulation will examine additional factors such as perceivable building vibration and secondary acoustic radiation due to the rattling of picture frames, etc.

The in-home simulation system, shown in the center of the figure, is designed for deployment in homes for relatively long periods of time. This approach adds a degree of realism that is not present in the laboratory, and enables the number of sonic booms and the time at which they occur to be examined. The system generates sonic boom sounds, measures noise levels in the home, and records the resident's reaction to the sonic boom exposure. A prototype system is to be pilot tested in the near future.

An absolute determination of human response to sonic booms requires that a population be routinely exposed to real sonic booms over an extended period. Military operations will hopefully provide this opportunity.
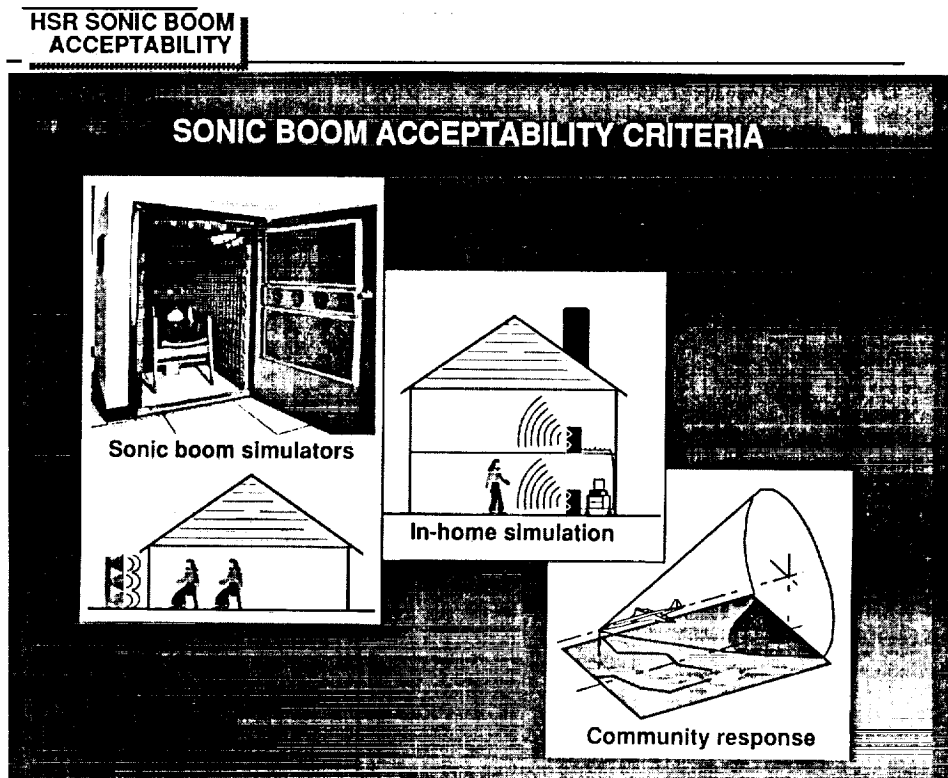


Sonic boom simulators

In-home simulation

Community response

THIS PAGE INTENTIONALLY BLANK

1292

# Session IX. Sonic Boom (Human Response and Atmospheric Effects)

*omit*

Sonic Boom Acceptability Studies

*Dr. Kevin P. Shepherd, NASA Langley Research Center; Brenda M. Sullivan, Lockheed Engineering and Sciences Company; and Dr. Jack E. Leatherwood and David A. McCurdy, NASA Langley Research Center*

THIS PAGE INTENTIONALLY BLANK

*5 13 - 71*
*12043*

# SONIC BOOM ACCEPTABILITY STUDIES

Kevin P. Shepherd, Brenda M. Sullivan*,
Jack D. Leatherwood and David A. McCurdy

Structural Acoustics Branch
NASA Langley Research Center

* Lockheed Engineering and Sciences Company

# OUTLINE

- Loudness model
    - predicted benefits through shaping

- Sonic boom simulator
    - description and results summary

- In-home simulation system
    - description and purpose

- Community response survey
    - status and plans

- Concluding remarks

# SONIC BOOM LOUDNESS PREDICTION MODEL

The determination of the magnitude of sonic boom exposure which would be acceptable to the general population requires, as a starting point, a method to assess and compare individual sonic booms. There is no consensus within the scientific and regulatory communities regarding an appropriate sonic boom assessment metric. Loudness, being a fundamental and well-understood attribute of human hearing was chosen as a means of comparing sonic booms of differing shapes and amplitudes.

The figure illustrates the basic steps which yield a calculated value of loudness. Based upon the aircraft configuration and its operating conditions, the sonic boom pressure signature which reaches the ground is calculated. This pressure-time history is transformed to the frequency domain and converted into a one-third octave band spectrum. The procedure is based largely on an approach described by Johnson and Robinson (ref. 1), and utilizes Stevens' Mark VII loudness method (ref. 2). The essence of the loudness method is to account for the frequency response and integration characteristics of the auditory system. The result of the calculation procedure is a numerical description (perceived level, dB) which represents the loudness of the sonic boom waveform.

## SONIC BOOM LOUDNESS PREDICTION MODEL
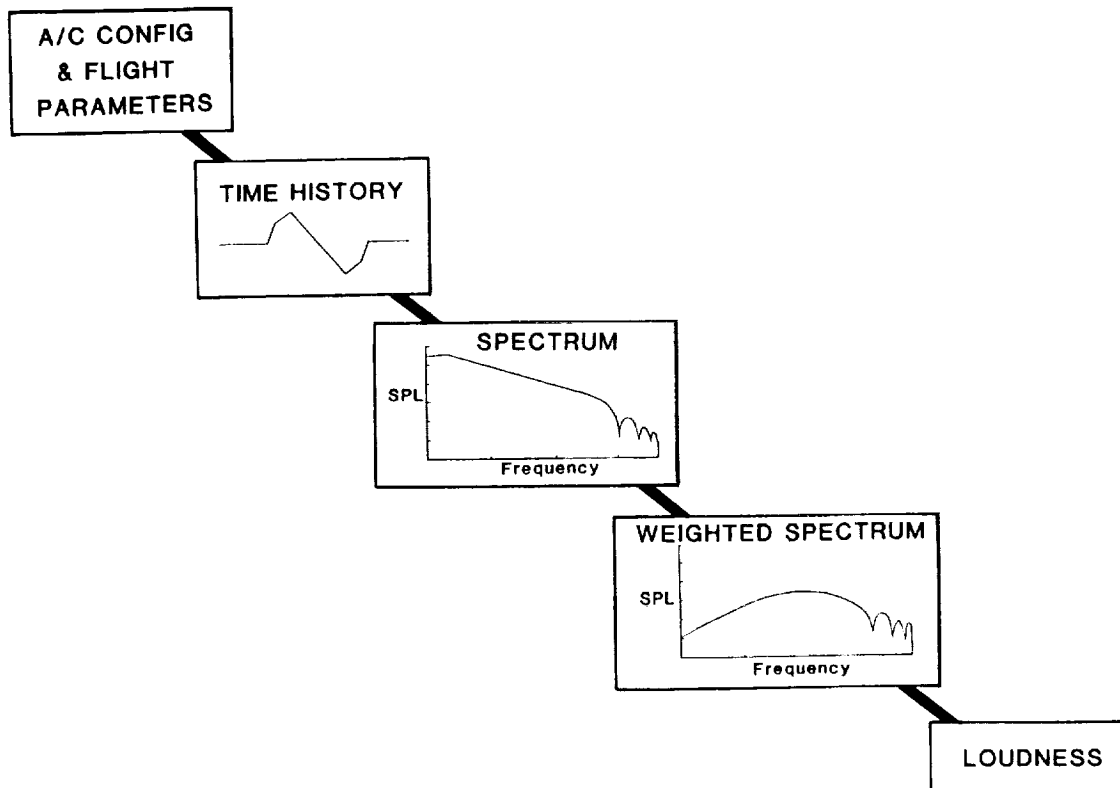
# LOUDNESS OF SHAPED SONIC BOOMS

The loudness calculation procedure was applied to a range of shapes of sonic boom signatures. The shapes are illustrated at the bottom of the figure and include the classical N-wave and a range of other symmetrical shapes. All have the same peak overpressure and initial rise time; the amplitude of the initial shock is varied over a range from 1 psf to 0.125 psf. Calculated loudness is seen to systematically decrease with decreasing values of the initial shock amplitude. Although the acoustic energy contained in each boom shape is approximately the same, the high frequency content is reduced when the initial shock amplitude is reduced. The observed decrease of loudness is a reflection of the greater sensitivity of the auditory system to high frequencies rather than low ones.

Measured noise reduction provided by typical residential structures was used to calculate indoor loudness levels for the same range of sonic booms. The results presented in the figure are normalized to the N-wave sonic boom loudness level, for conditions of windows open and closed. The same trends are observed for both indoor and outdoor listening conditions. This assessment of indoor levels obviously makes no attempt to include effects of building vibration or secondary acoustic radiation due to rattling objects.

## OUTDOOR/INDOOR LOUDNESS OF SHAPED BOOMS



1298
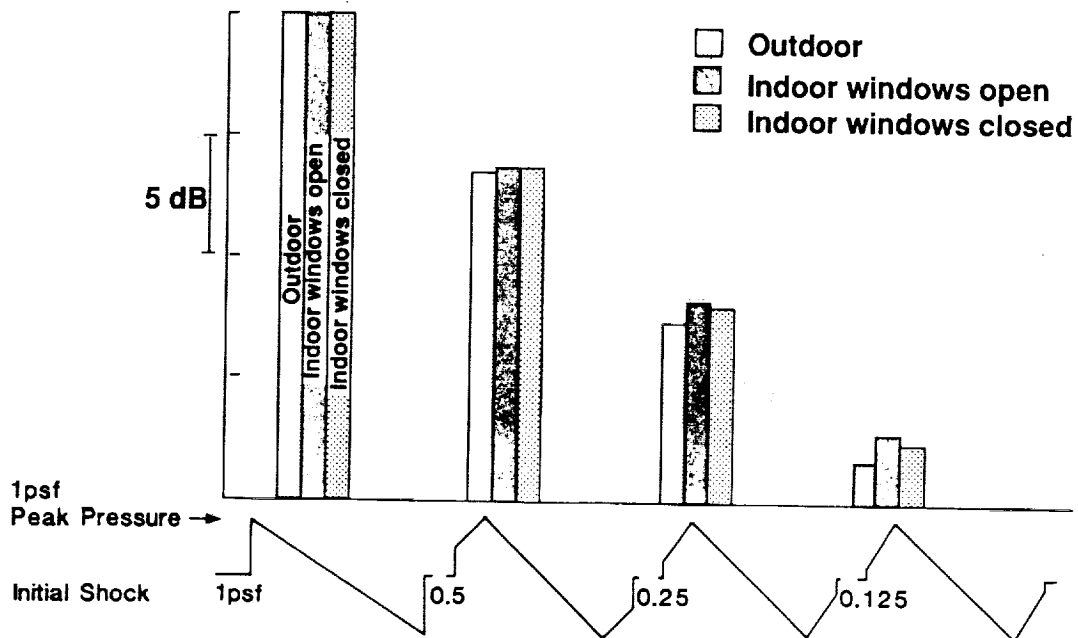
# SONIC BOOM SIMULATOR

A sonic boom simulator (ref. 3) has been constructed at the NASA Langley Research Center to enable loudness measurements to be made with test subjects using sonic booms of the types described above. The simulator is patterned on one previously used at the University of Toronto (ref. 4). The acoustic signals are computer-generated to enable compensation for inadequacies present in the sound reproduction system and distortion produced by the acoustical characteristics of the enclosure. The rigid, airtight, concrete enclosure is driven by eight loudspeakers. The system is capable of generating approximately 140 dB sound pressure level (4 psf) and has a low frequency limit of approximately 0.4 Hz.



**SONIC BOOM SIMULATOR**
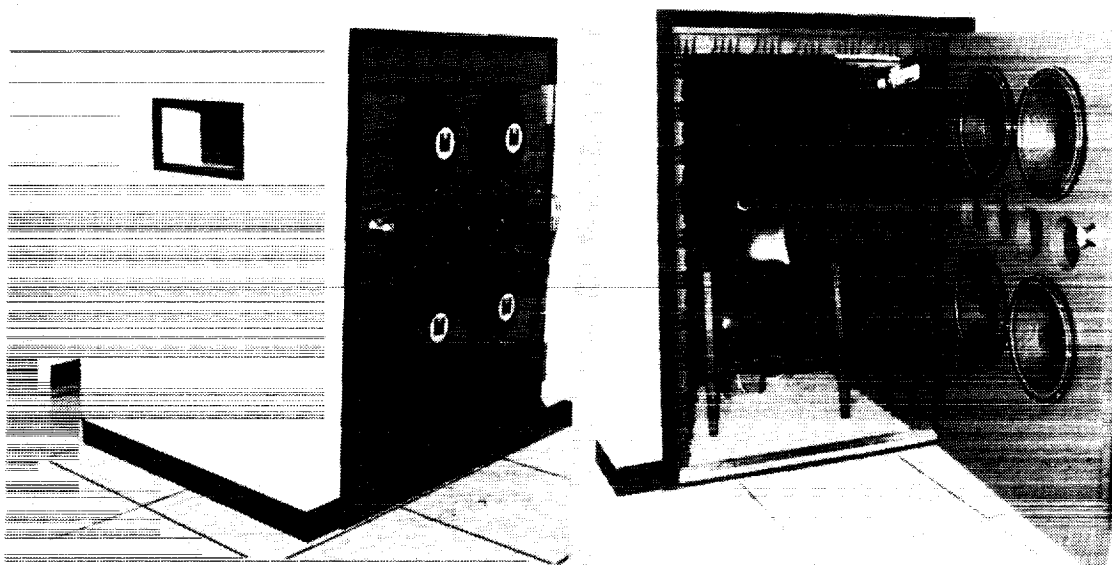
EQUALIZATION BY PRE-DISTORTION

The sonic boom simulator has an inherently poor frequency response. At low frequencies, the loudspeakers drive the enclosed volume of air very efficiently. At higher frequencies, efficiency is reduced and phase distortion is introduced by the loudspeaker crossover electronics and by acoustic resonances within the enclosure. To obtain an undistorted sonic boom in the simulator requires a broadband equalization filter with good frequency resolution and good low frequency response. To accomplish this a time domain method was used to design a broadband equalization filter. The time domain method used was the Widrow-Hoff least mean-square adaptive algorithm. Further details are given in reference 5.

The figure illustrates the results of the equalization process. On the left are shown the waveforms which are required. On the right are the waveforms as measured by a microphone in the simulator. The signals which were generated by the computer to achieve these waveforms are shown in the center.

# EQUALIZATION BY PRE-DISTORTION



**Desired**          **Pre-distorted**          **Obtained**

1300
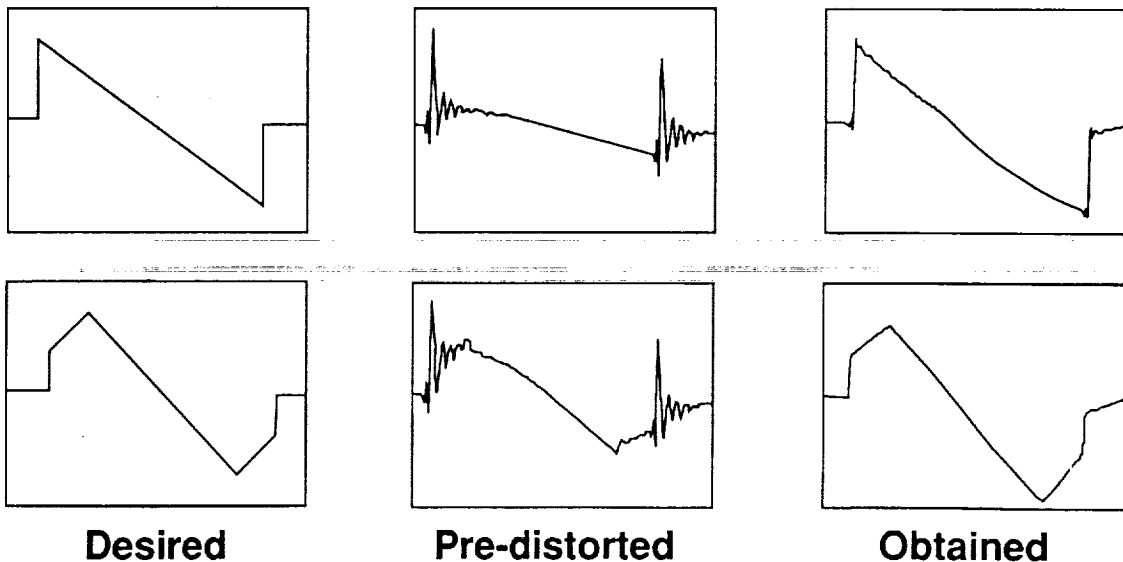
## SUMMARY OF SIMULATOR EXPERIMENTS

A summary of the tests conducted in the sonic boom simulator are described in the figure. The pilot study was aimed at examining testing procedures and to confirm that the simulator was fully operational and reliable. The test sounds consisted of mostly N-waves with a range of overpressures and rise times. Two shaped booms were also included. The psychometric method employed was the constant stimulus difference method (paired comparisons). The results in terms of the effects of rise time on judged loudness were in accord with earlier studies, and were predictable by the loudness calculation procedure. The second study concentrated on a large range of N-waves and a smaller number of shaped booms. All the characteristics of a N-wave were systematically varied. The method of category scaling was employed using both loudness and annoyance descriptors. The results confirmed the loudness model predictions and no differences were found between loudness and annoyance judgements. The most recent study examined a wide range of shaped booms. In contrast with the earlier studies a few non-symmetrical booms were also included. The loudness judgements for the symmetrical booms were in good agreement with the predictions of the loudness model.

**HSR SONIC BOOM ACCEPTABILITY**

# SONIC BOOM SIMULATOR

*SUMMARY OF EXPERIMENTS*

| | # subjects/ # booms | Test Sounds | Major findings |
|---|---|---|---|
| Pilot Study | 32 / 72 | Symmetric N-waves Rise time, pressure. | Effects of rise time & pressure predicted by loudness model. |
| Exploratory study of boom shaping | 72 / 150 | Symmetric N-waves & shaped booms. Duration, initial rise time and peak pressure. | Validated loudness model. Loudness = annoyance. Duration unimportant. |
| Quantification of boom shaping | 60 / 248 | Symmetric and asymmetric shaped booms. Initial and secondary rise times. Initial/peak pressure. | Validated loudness model. Secondary rise time unimportant. |

# SONIC BOOM SIGNATURES OF EQUAL LOUDNESS

The figure illustrates a range of sonic boom signatures which were judged to be equally loud by a group of 32 test subjects. For the N-waves it is evident that the rise time (RT) is related to loudness such that, for equal overpressure, the shorter the rise time the greater is the loudness. The shaped booms (MINA and MINB) have an initial rise time of two milliseconds and a relatively slow rise to the peak pressure. It is clear that the loudness of the shaped booms is dominated by the initial, sharp pressure rise.

## SIGNATURES JUDGED EQUALLY LOUD
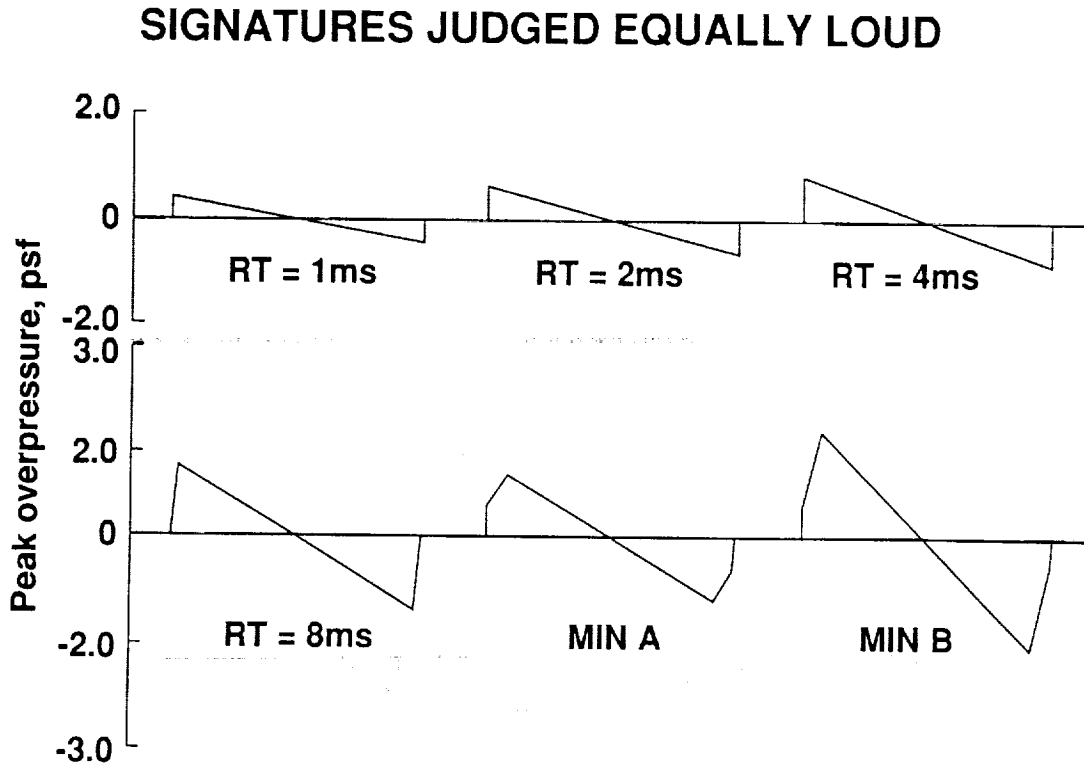
# SUBJECTIVE RESPONSE TO N-WAVES AND SHAPED BOOMS

Loudness category scale judgements were obtained for a wide range of N-waves and a limited range of shaped booms. The loudness judgements were converted to a scale having decibel-like properties and, in the left figure, are plotted against the peak overpressure of the signatures. The range of subjective loudness, for a particular peak overpressure, is vast. In the case of the N-waves this variation is largely attributable to the rise time of the signatures. For the shaped (ramp) signatures the peak overpressure of the signature is a poor predictor of the loudness since the loudness is largely governed by the strength of the initial shock.

The right hand figure shows the same subjective judgements plotted against predicted loudness based on the loudness model (perceived level). It is clear that the measured and predicted loudness values are in good agreement. The loudness model is able to largely account for the effects of rise time and the differences in boom shapes.



PREDICTION OF SUBJECTIVE RESPONSE
TO SONIC BOOMS
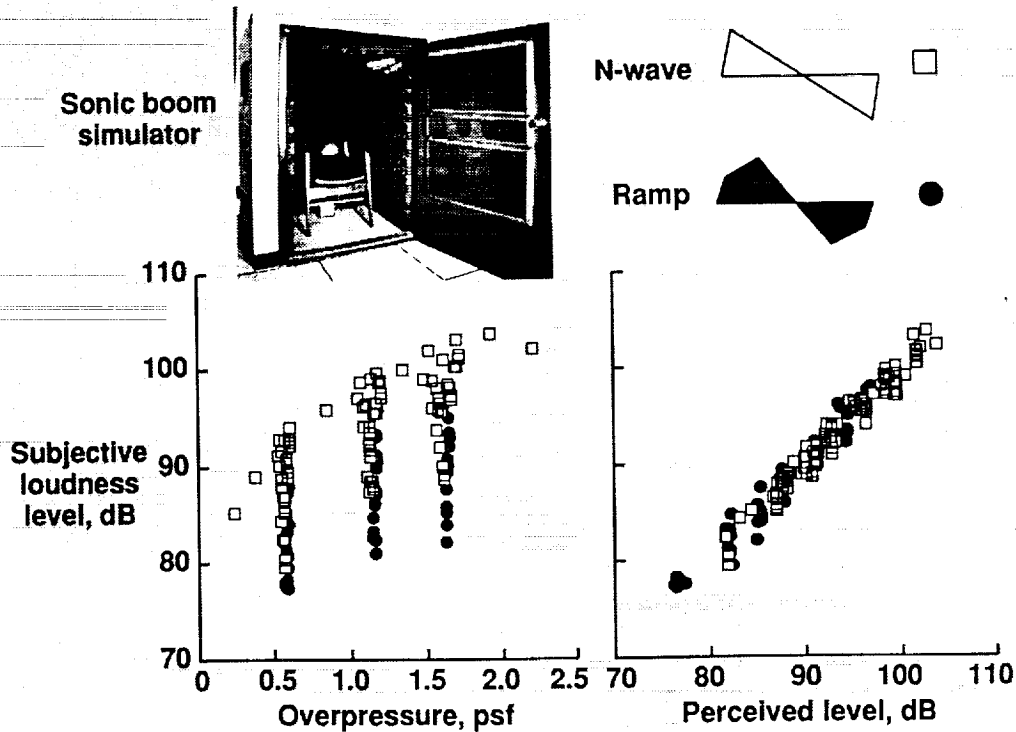
# EFFECTS OF RISE TIME AND DURATION

The data from the previous figure were examined to determine if the loudness prediction method was able to fully explain the effects of rise time and the duration of the signatures. The figures illustrate prediction error as a function of rise time and duration. The prediction error is a measure of residual variation which the loudness metric is unable to explain. The results for two metrics are shown; perceived level (PL) and A-weighted sound pressure level. A positive prediction error can be interpreted as meaning than the sound was judged to be louder than the calculated metric would indicate. For the case of rise time the residual effect not explained by PL is very small (+/- 0.5 dB). For A-weighted sound pressure level ($L_A$) the residual variation is significantly greater. The residual effect of duration is small for both metrics, particularly when one considers that the range of practical interest for a supersonic transport if from 200-400 msecs.



1304
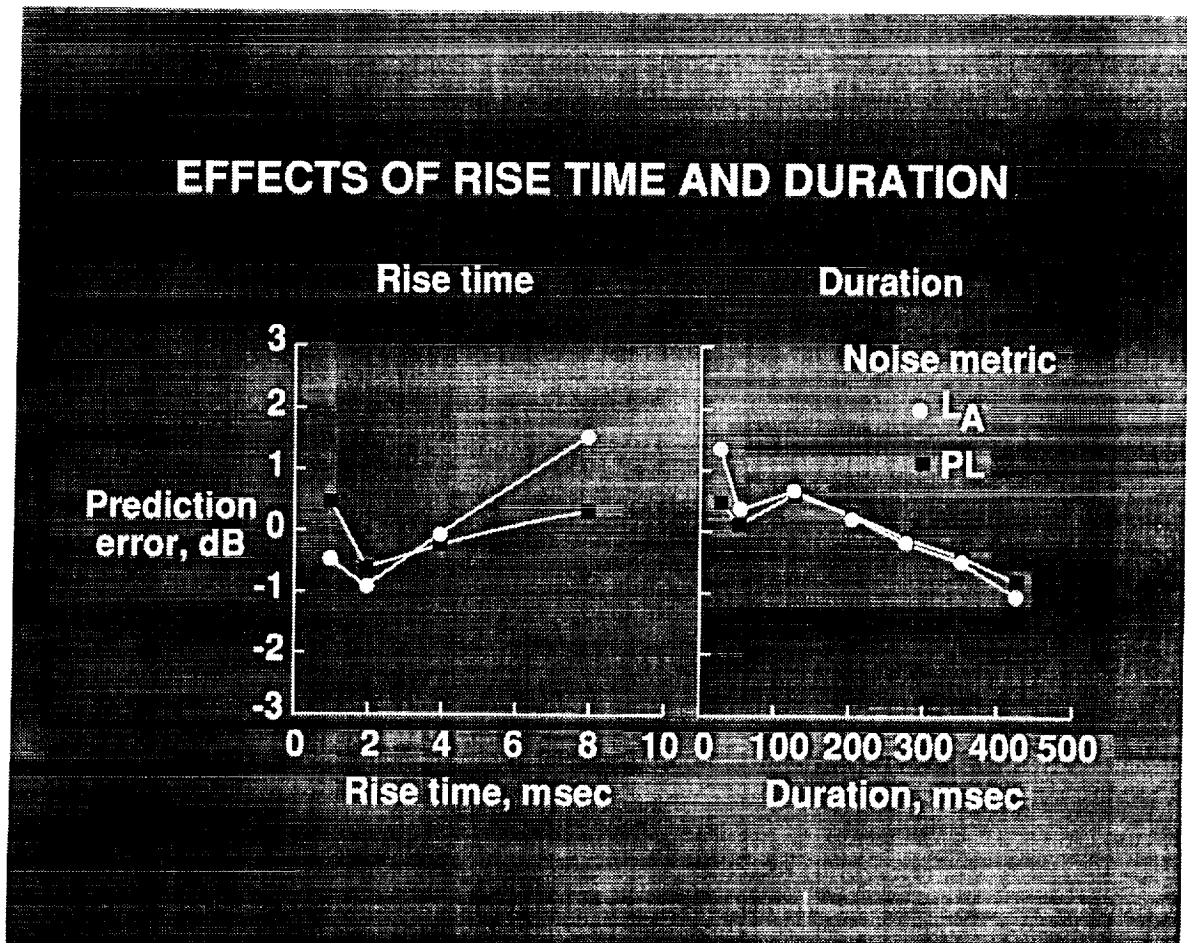
# BENEFIT OF BOOM SHAPING

   The most recent simulator test was aimed at investigating the loudness of a
large range of shaped booms. The signature in the figure is representative of the test
stimuli. With the exception of the total length (duration ) of the signature, all
parameters were systematically varied. For a given peak overpressure, the loudness
was highly dependent on the amplitude and the rise time of the front (and rear) shock.
The loudness was found to be independent of the secondary rise time (between
points B and A) which ranged from 20-50 msecs. The total duration of the booms was
held constant at 300 msecs.
   The figure presents the mean loudness ratings for a subset of the test stimuli.
The effects of rise time and initial shock amplitude are evident.
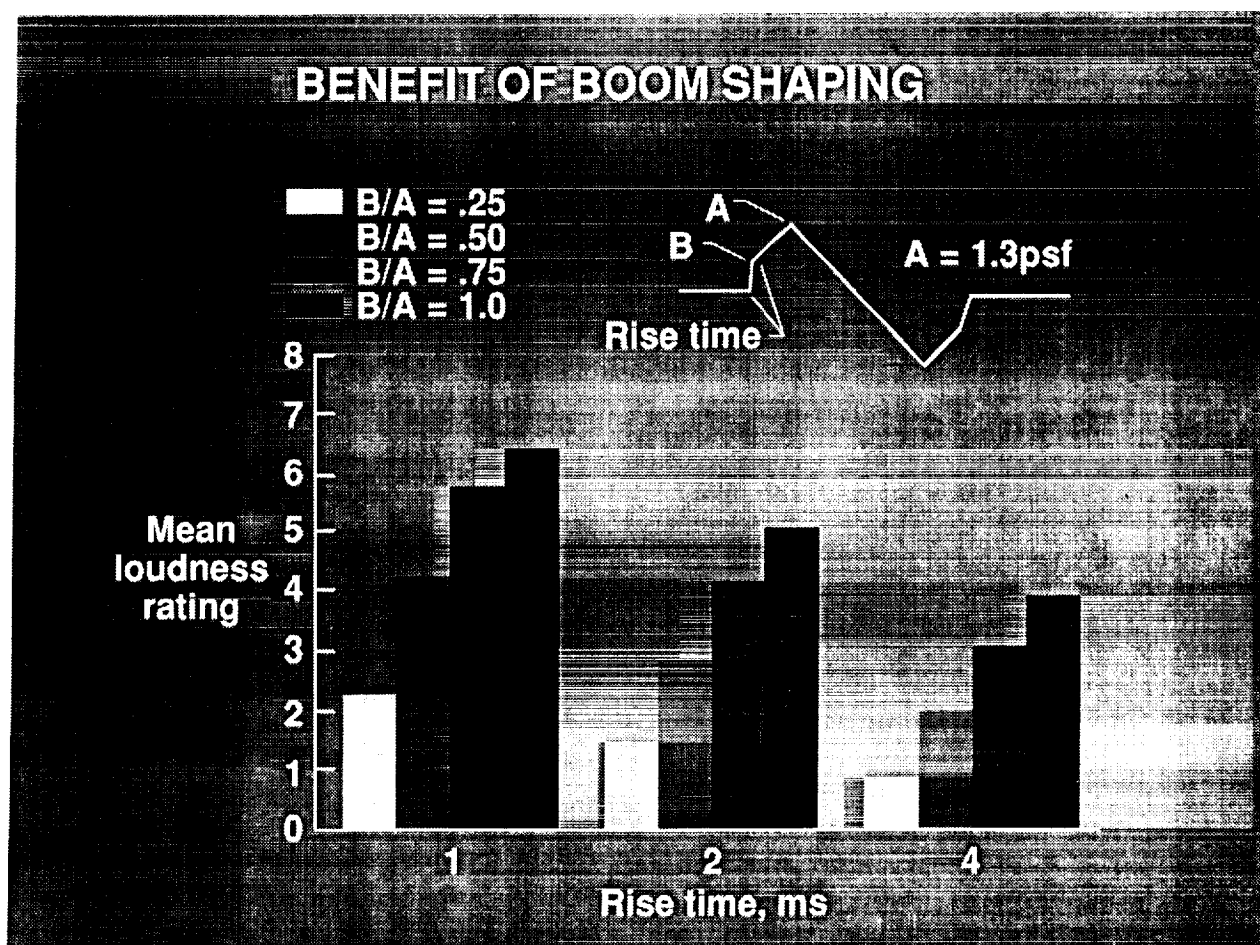
# PREDICTION OF SUBJECTIVE RESPONSE TO SHAPED BOOMS

The ability of the loudness model to predict the subjective response to a large range of shaped booms is illustrated in the figure. The mean loudness ratings are shown as a function of the predicted values expressed in units of perceived level, dB. It is evident that the variance of the mean ratings which is not predicted by the metric calculation procedure is approximately +/- 2dB. Ongoing analyses are addressing the source of this residual variation.



**PREDICTION OF SUBJECTIVE RESPONSE TO SHAPED SONIC BOOMS**
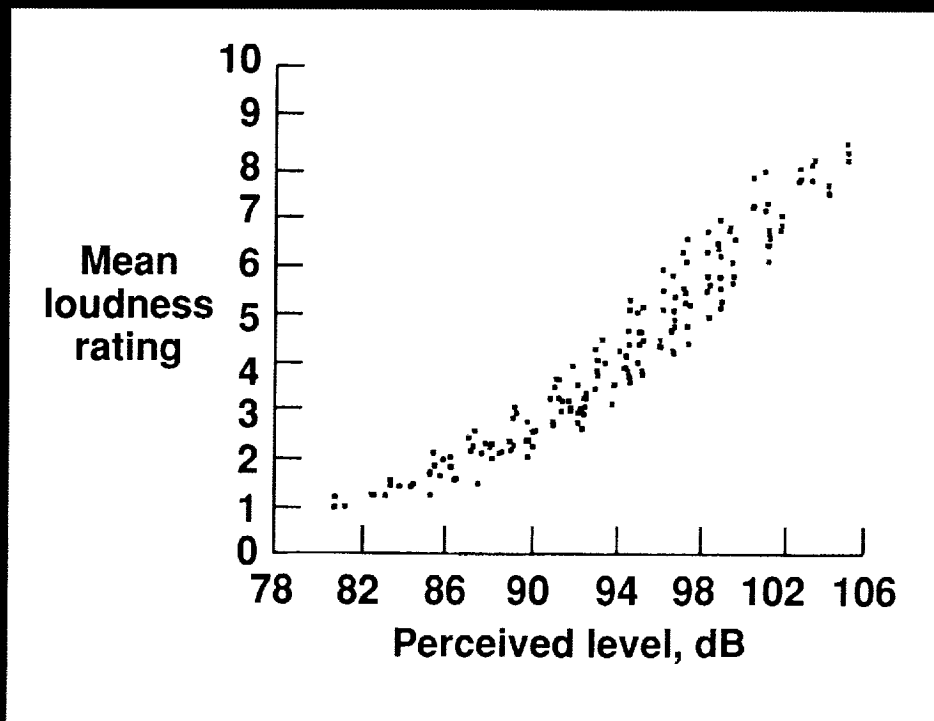
# IN-HOME NOISE MONITOR-CONTROL-RESPONSE SYSTEM

The preceding laboratory studies were aimed at investigating the characteristics of sonic booms which affect their perceived loudness. Such studies are not suitable for determining a sonic boom exposure that might be acceptable to the general population. To establish a relationship between acceptability and exposure requires that people be exposed to sonic booms on a regular basis as part of their everyday lives.

The figure shows, schematically, the components of a computer-based system which will be used to examine peoples' responses to sonic booms in their homes. A prototype system is currently operational and is to be pilot tested in the near future. The system has three major functions. The first is the generation of simulated sonic booms. This is accomplished by means of a pre-recorded compact disk containing a range of sonic booms. The sonic booms are generated at programmed times and amplitudes by the computer-controlled CD player. The second function of the system is noise monitoring. This is to ensure that the sonic boom generation hardware is working properly, and also to measure the levels of sonic booms and ambient noise. The third function of the system is to record the residents' reactions to their noise environment. The resident will be prompted at periodic intervals to answer a battery of questions regarding their response to the sonic booms, activities affected, etc. The test conductor at the Langley Research Center is able to communicate with the computer in the home in order to transfer data, to ensure that the system is functioning correctly and, if necessary, to re-program elements of the study. This approach should enable response to be related to the amplitude and frequency of the sonic booms.

## IN-HOME NOISE MONITOR-CONTROL-RESPONSE SYSTEM



1307
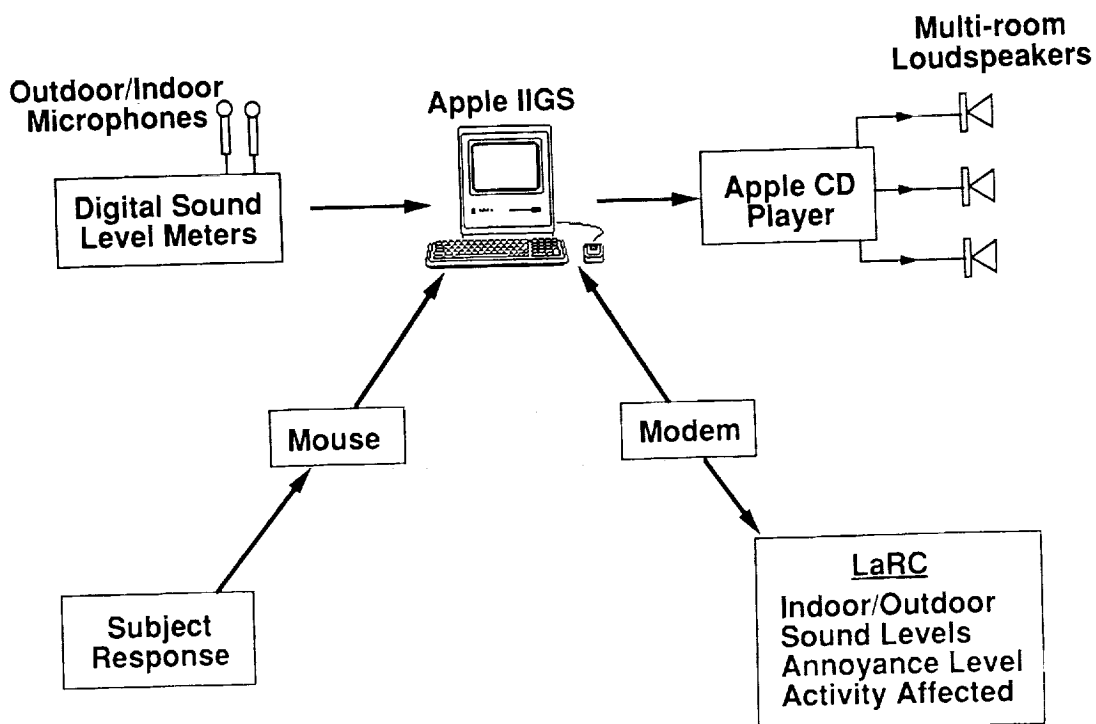
# COMMUNITY RESPONSE TO SONIC BOOMS

The laboratory studies and the in-home system enable human response to sonic booms to be studied under relatively well-controlled conditions. However, they can be criticized on two grounds. The first is that the sonic boom simulation is less than perfect, and the second, more important criticism, is that the residents' response in an experiment may be different from that which occurs in an environment of long-term sonic boom exposure. To address these issues requires that a situation of long-term exposure be identified. An opportunity was provided by routine supersonic SR-71 training flights which have occurred in the western part of the United States for a number of years.

Unfortunately, during the planning phase of a community response survey the SR-71 fleet permanently ceased their training flights, so the proposed study was abandoned. In expectation of identifying alternate sites, a preliminary study was conducted with the major aim of developing a sonic boom response questionnaire. This study took place six months after the cessation of flights, but the delay was not considered to be a critical issue for questionnaire development. During the course of the study a small number of people were interviewed. The findings, although of only a qualitative nature, were found to be in general accord with earlier sonic boom response surveys.

## PRELIMINARY SONIC BOOM SURVEY

**Surveyed areas**
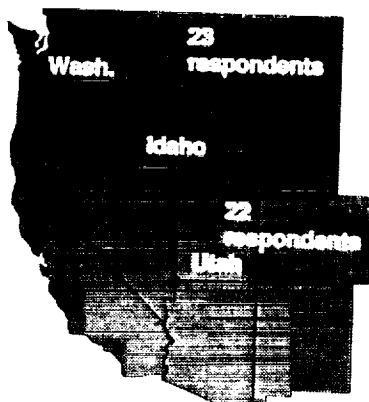


- **Objectives:**
  - Develop sonic boom response questionnaire
  - Provide preliminary data on extent of sonic boom annoyance

- **Sonic boom exposure:**
  - Long term SR-71, 0.5 to 1.0 psf, ~ 1 per week
  - Exposure ceased 6 months prior to study

- **Findings:**
  - Little to moderate annoyance
  - Startle reaction frequently noted
  - Vibration frequently noted, some damage attributed to sonic booms

1308

## USAF/NASA SONIC BOOM STUDY

A joint study between the Air Force and NASA is being conducted in the Nellis Range in Nevada. The study has two major components. The first is the development and validation of a sonic boom exposure model which can predict the amplitudes and locations of sonic booms on the ground which result from a variety of supersonic operations. To support this objective, a large number of sonic boom measurements will be made over a six month period and will be related to aircraft operational information. The second component of this joint study is to conduct a community response survey of people exposed to these supersonic operations. The feasibility of performing such a survey is currently under investigation.

# USAF/NASA SONIC BOOM STUDY

## Nellis Range:
- **Tactical Air Command supersonic operations**
- **>1000 sonic booms per year**
- **0 - 3 p.s.f.**
- **Impacted population ~ 5000**

## USAF:
- **Sonic boom exposure prediction model**
- **Model validation**
  - **Aircraft tracking**
  - **Sonic boom measurements (40 stations, 6 months)**

## NASA:
- **Community response survey**

**Nevada**

**Nellis Range**

**Las Vegas**

**CONCLUSIONS**
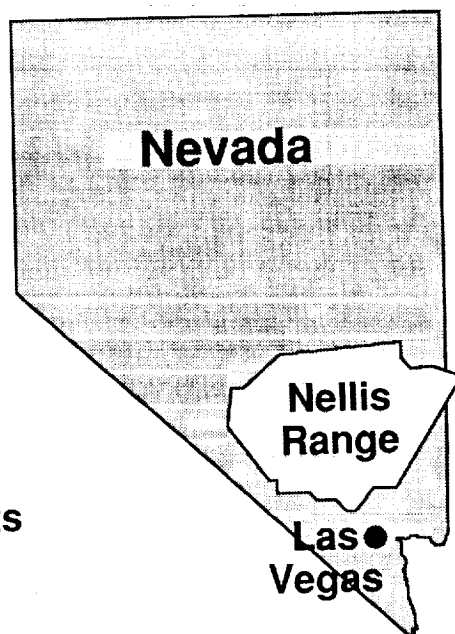
- Sonic Boom Simulator Operational
  - high fidelity simulation

- Loudness Model Validated
  - large range of N-waves and shaped booms

- Substantial Benefits Obtainable Through Shaping
  - for "outdoor" listening conditions

- In - home Simulation System Operational
  - pilot tests imminent

- Community Survey in Planning Stages

# REFERENCES

1. D. R. Johnson and D. W. Robinson, "The Subjective Evaluation of Sonic Bangs," Acustica, 18(5) (1967)

2. S. S. Stevens, "Perceived Level of Noise by Mark VII and Decibels (E)," Journal of the Acoustical Society of America, 51 (2), pp. 575-601 (1972)

3. Jack D. Leatherwood, Kevin P. Shepherd and Brenda M. Sullivan, "A New Simulator for Assessing Subjective Effects of Sonic Booms," NASA TM-16912, March 1991.

4. A. Niedzwiecki and H. S. Ribner, "Subjective Loudness of "Minimized" Sonic Boom Waveforms," Journal of the Acoustical Society of America, 64(6), pp. 1622-1626 (1978)

5. D. E. Brown and B. M. Sullivan, "Adaptive Equalization of the Acoustic Response in the NASA Langley Sonic Boom Chamber," Proc Conf on Advances in Active Control of Sound and Vibration, VPI &SU, Blacksburg, Virginia, April 15-17, 1991.

THIS PAGE INTENTIONALLY BLANK

1312

# Session IX. Sonic Boom (Human Response and Atmospheric Effects)

*Omit*

Georgia Tech Sonic Boom Simulator
*Dr. Krish K. Ahuja, Georgia Institute of Technology*

THIS PAGE INTENTIONALLY BLANK

# GEORGIA TECH SONIC BOOM SIMULATOR

$S/4-71$

$/2044$

Krish K. Ahuja
Georgia Institute of Technology
GTRI/ASTL
Atlanta, Ga.  30342

First Annual High-Speed Research Workshop
Williamsburg, Virginia
May 14-16, 1991

## GENERAL

To examine the building and human response to sonic boom in the range 3 Hz to 30 Hz, Georgia Institute of Technology is building a special acoustic driver system to simulate sonic boom. To support NASA Langley program on building and human response, this simulator's capability has been extended to an upper frequency of 4 KHz. A residential test house has been made available by Georgia Tech for these tests.

At the time of preparation of this document, most of the acoustic drivers and the associated electronics have been built and assembled. The system has, however, not been fully tested.

The following pages provide an overview of the progress to date. The acoustic driver systems, and the principle of their operation together with the test house are described. Future plans are also summarized.

Figure 1    Outline of presentation

# Outline of Presentation

- **Source requirements**

- **Very low  frequency source details**

- **Test house**

- **Future plans**

## MOTIVATION

Guidelines for the assessment of exposure to interior aircraft noise are currently available in the form of methodology for predicting speech interference and hearing damage. Further, relative annoyance due to conventional aircraft flyovers may be assessed by objective measures such as EPNL, SEL, or DNL. However, currently there is no accepted way to assess the human response in an indoor environment where reaction critically depends on secondary emissions, such as noise induced building vibrations and rattling of bric-a-brac and associated acoustic radiations. Human reaction to outdoor sonic booms is more predictable.

There is considerable evidence to indicate that sonic boom signature can be shaped in such a way as to minimize the resulting human response. There also exists some indication that in comparison to subsonic aircraft noise, sonic booms are relatively more objectionable indoors than outdoors. This difference may primarily be due to the ability of sonic booms to induce more structural response than subsonic aircraft noise. Although, considerable work has been done to examine the building response to noise, most of the controlled experiments have been restricted to frequencies much higher than 10 Hz. The sonic boom simulator described here was developed to produce very low frequency noise to determine both human and structural response, both indoors and outdoors at frequenciies as low as 3 Hz.

Figure 2

# Motivation

# 1. Structural / human response at low frequency

# 2. Effect of boom shaping

The N-shaped disturbance shown here is an idealized shape. The actual shape may vary because of the atmospheric effects and aircraft design and operation. The effects on people and structures are better understood by examining the spectral contents of such waves. The peak level takes place at a frequency dependent upon the total duration of the boom. Longer the duration, the lower the frequency. Larger airplanes and planes flying at higher altitudes will have longer duration and thus lower peak frequency. As shown in this figure, spectrum consists of several convolutions that are tangent to a 6-dB-per-octave line at higher frequencies.

The system described here was designed to have flat frequency response in the range 3 Hz - 4 kHz.

**Figure 3**

# Sonic Boom
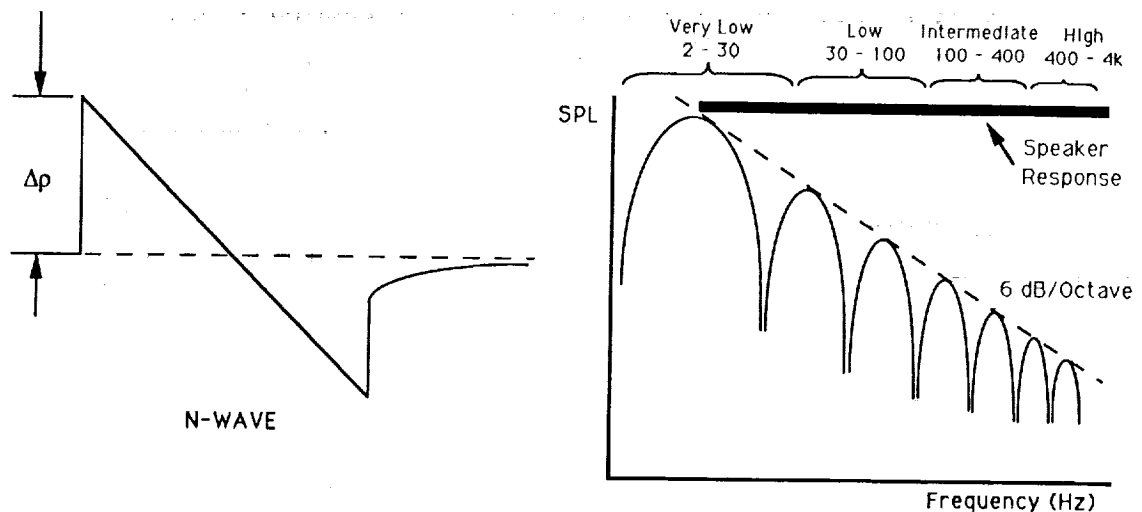
## VERY LOW FREQUENCY SOURCE REQUIREMENTS

Electro-acoustic drivers that generate large amplitudes at frequencies higher than 30 Hz are available commercially. Our very low frequency driver was required to produce flat frequency response in the range 3 - 30 Hz. It was also required to produce in excess of 2 psf sound pressure level over a 10 ft x 12 ft area of the wall of a test house. This figure, taken during the development phase, shows the dimensions of a single unit of the driver. Georgia Tech sonic boom simulator system consists of six such units. As described later, other high frequency speakers are also part of this system.

Figure 4

# Very Low Frequency Source Requirements

- **Flat response  3Hz - 30Hz**

- **2 psf peak pressure on the test house wall**
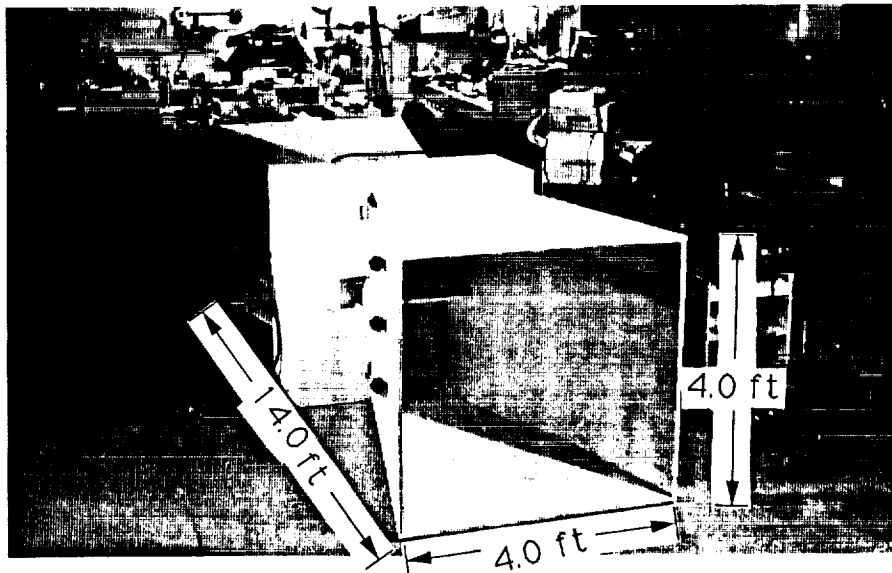
# VERY LOW FREQUENCY SPEAKER

The system shown in Figure 4 is shown here in its finished form.

Figure 5

# Very Low Frequency Speaker
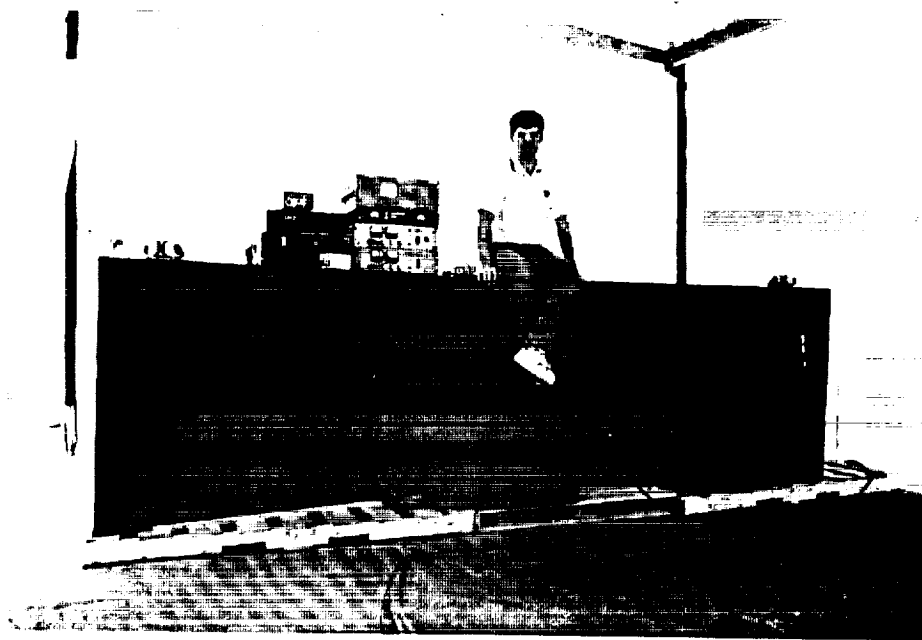
# LOW AND INTERMEDIATE FREQUENCY SOURCE

The driver units for the low and intermediate frequency noise are servo-driven units. The units shown in Figure 6a are some of the units to be used in conjunction with the very low frequency drivers. The sketch in Figure 6b shows the principle of operation of the servo-driven system. It shows a rotary-to-linear motion converter which is connected to specially strengthened radiators by means of drive shafts. Servo-drive design eliminates fragile voice coils, heavy magnets, and compromised low frequency response typical of inherently weak voice coil designs. Unlike a voice coil that becomes nonlinear with large motion, a motor can provide unlimited motion or rotation. Rotation in either direction is exactly proportional to the input signal voltage and current.

## Figure 6

## Low and Intermediate Frequency Source

• Servo driven units



TO ONE OF TWO RADIATORS

DRIVE ARM

BELT

BELT

BELT MECHANISM SHOWN WITH ONE DRIVE ARM REMOVED

MOTOR DRIVE SHAFT
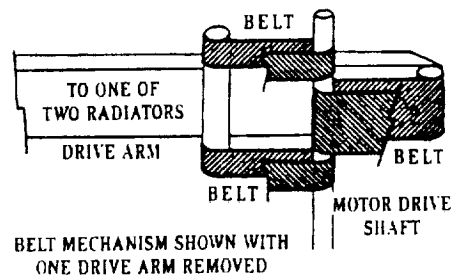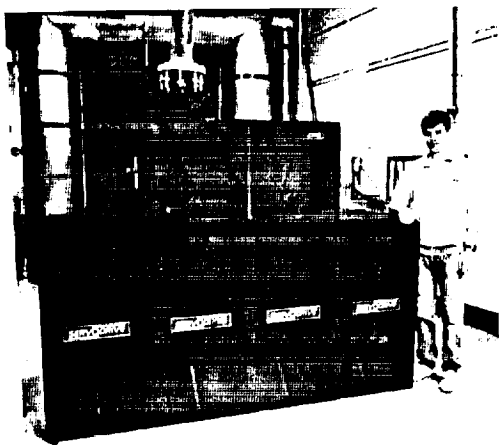
## SPEAKER ENCLOSURE AND THE TEST HOUSE (FRONT)

The complete noise simulator unit is housed in an enclosure outside a house ("test house") that used to be a residential unit. As shown here, the enclosure has walls made out of an awning material which can be drawn like a curtain.

**Figure  7**

# Speaker Enclosure and the Test House (Front)

Figure 8 shows the back view of the speaker enclosure and the test house.

Figure 8

# Speaker Enclosure and the Test House (Back)

Figure 9 shows the side view of the speaker enclosure and the test house.
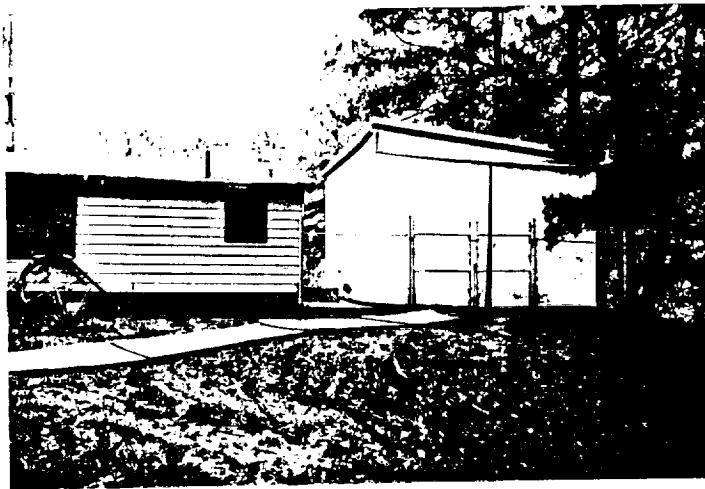
Figure 9

# Speaker Enclosure and the Test House (Side View)

## VERY LOW FREQUENCY SPEAKER (2 Hz - 30 Hz)

Only a single unit of the very low frequency speaker is shown here in Figure 10. Figure 10a shows the window of the house that faces one of the openings of the driver. Figure 10b is a view of the driver opening through the window from inside the house.

**Figure 10**

# Very Low Frequency Speaker (2Hz - 30Hz)
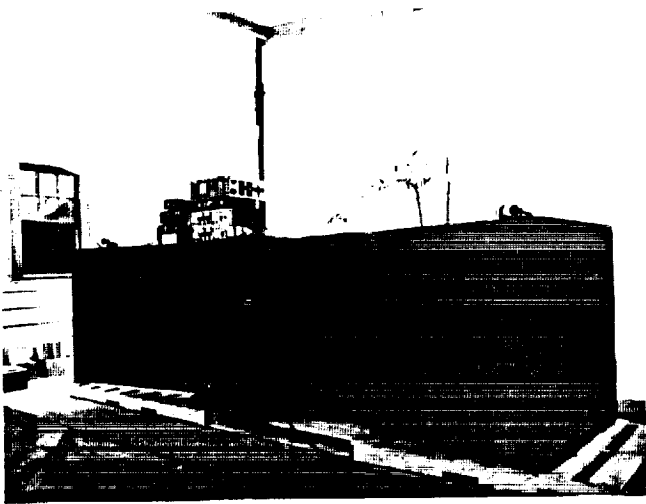


(a)
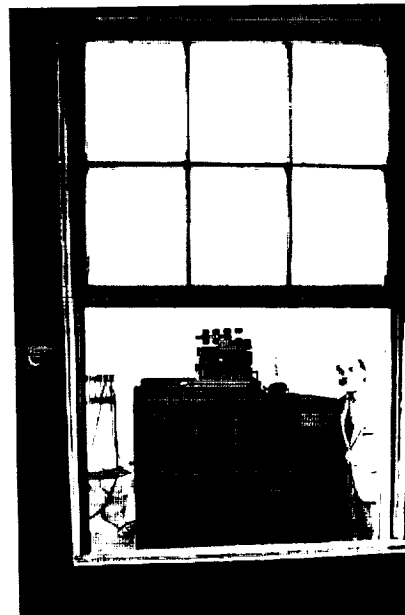
(b)

# EASILY DISMOUNTABLE ARRANGEMENT

The very low frequency speaker system was designed so that two people could mount and dismount various components as shown here in Figure 11. The holding bolt is undone in Figure 11a and the diffuser is moved away from the noise producing unit.

## Figure 11

# Easily Dismountable Arrangement
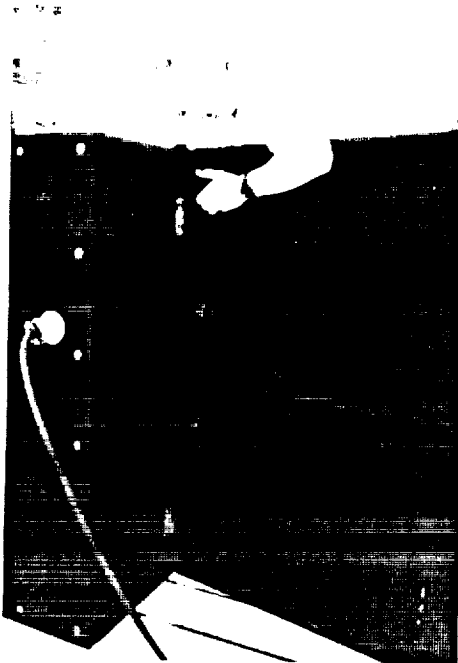


(a)

(b)

# VANE MOVEMENT

It is the controlled movement of vanes located in the middle section of the very low frequency speaker system that provides the fluctuating force needed to move air in and out of the speaker opening that produces the sound. Each unit has two separate openings, top and bottom in this figure. As shown in the next figure, these vanes help move large amount of air provided by two motor-operated fans placed on the two sides of the vanes. Two vane positions are shown in Figure 12.

## Figure 12

## Vane Movement
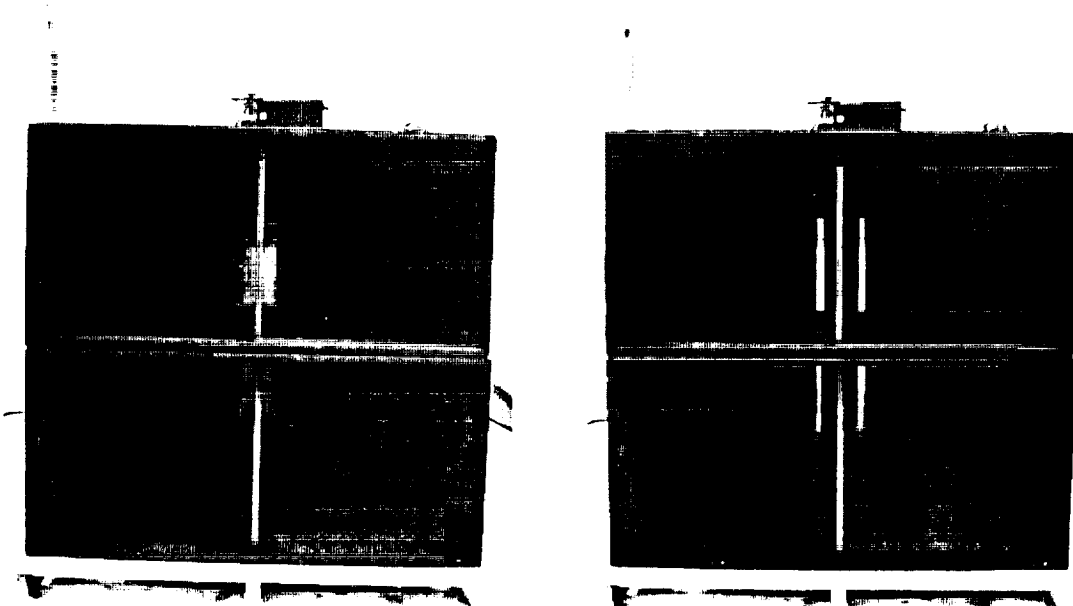


(a) Vanes closed                    (b) Vanes open

# PRINCIPLE OF OPERATION OF THE VERY LOW FREQUENCY NOISE SOURCE

As shown in Figure 13a, air mass for each vane is provided by a blower fan. In Figure 13b, the solid line indicates the vane and flow direction for the top vane and the thin line for the bottom. The vanes are arranged such that the flow moves from the top and the bottom opening in phase. In addition, referring to the top view of Figure 13b, this arrangement provides positive and negative mass flow through the two diffusers. This provides the capability of operating this unit as a dipole, and thus either of the two openings can be placed in front of a test object close by, and as mentioned later, it allows one to reduce the noise radiating in the farfield.

Figure 13

# Principle

**Front View**

**Top View**

Top Vane

Blower Motor I

Bottom Vane

Blower Motor II

(a)

(b)
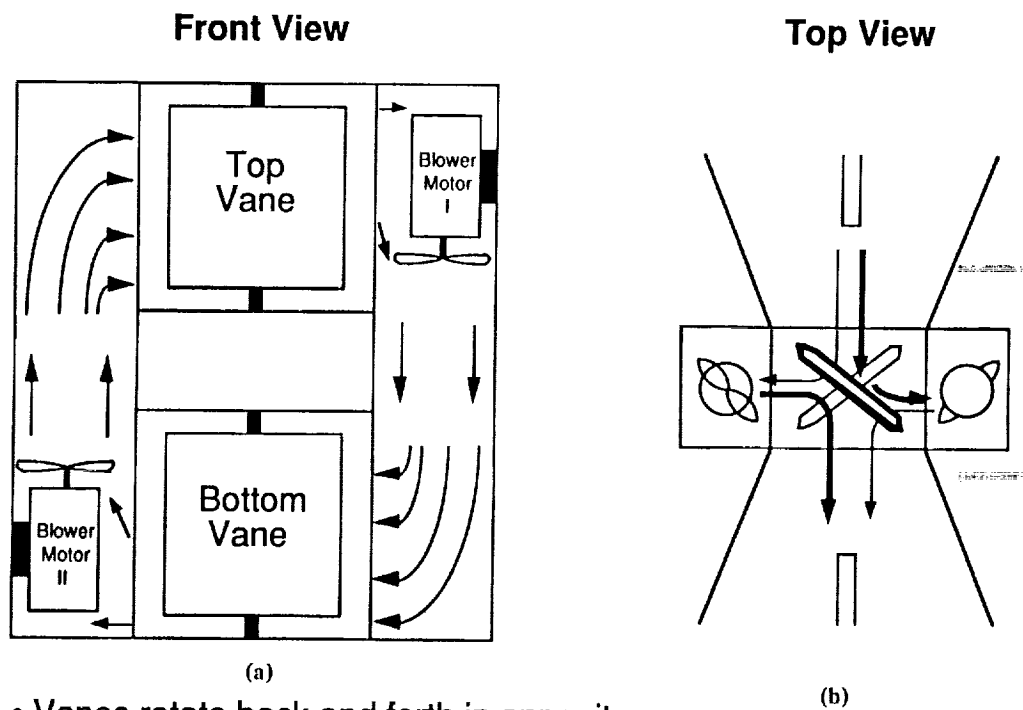
• Vanes rotate back and forth in opposite directions with signal input

## THE VANE AND THE FAN ARRANGEMENT

Close-up view of the vanes and the servo motor that controls its motion is shown in Figure 14a. The connector that carries the electronic input signal is also shown. Figure 14b shows the fan enclosure which, as is obvious in this figure, can be easily replaced if broken. Figure 14c is a close-up view of the fan and the turning vanes for the air flow .

**Figure   14**

# The Vane and Fan Arrangement



(a)                              (b)                              (c)

1329
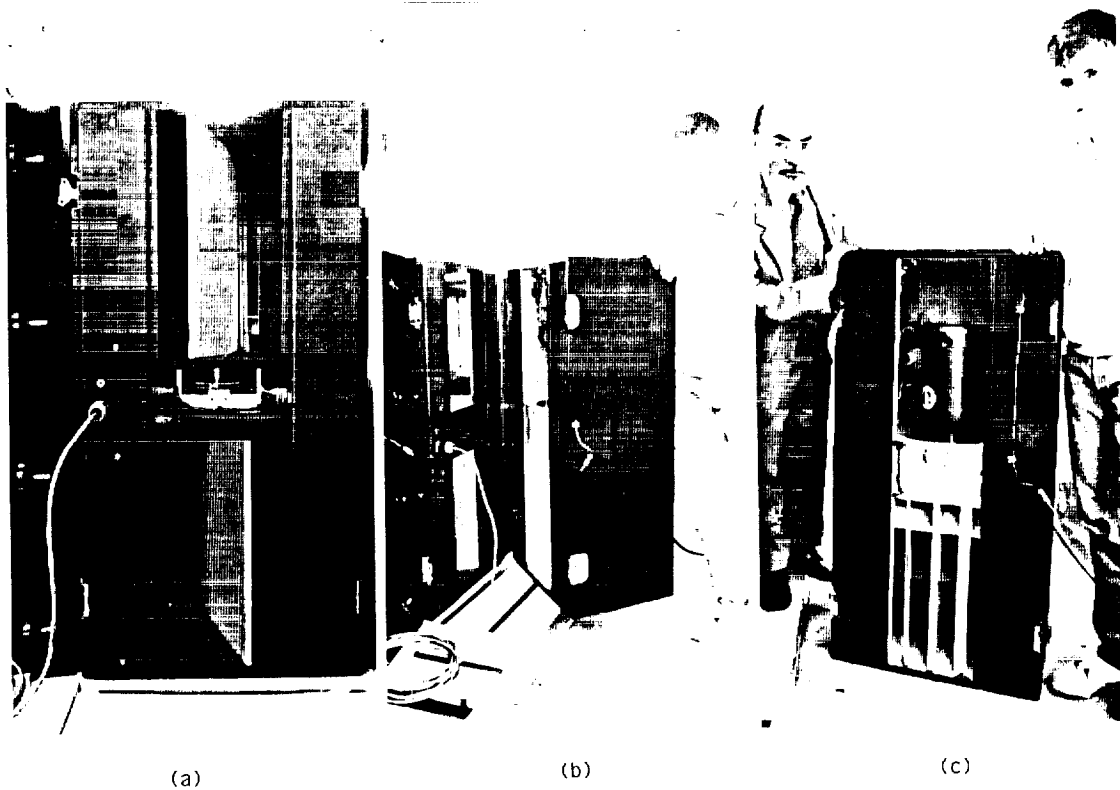
# SONIC BOOM/AIRCRAFT NOISE SIMULATOR

Figure 15 shows the arrangement of the complete sound generating system. It includes low and high frequency units and provides a capability of generating sonic boom as well as other types of noise, such as aircraft noise, helicopter noise, truck noise, etc.

**Figure   15**

# Sonic Boom / Aircraft Noise Simulator

## • 2Hz - 4kHz
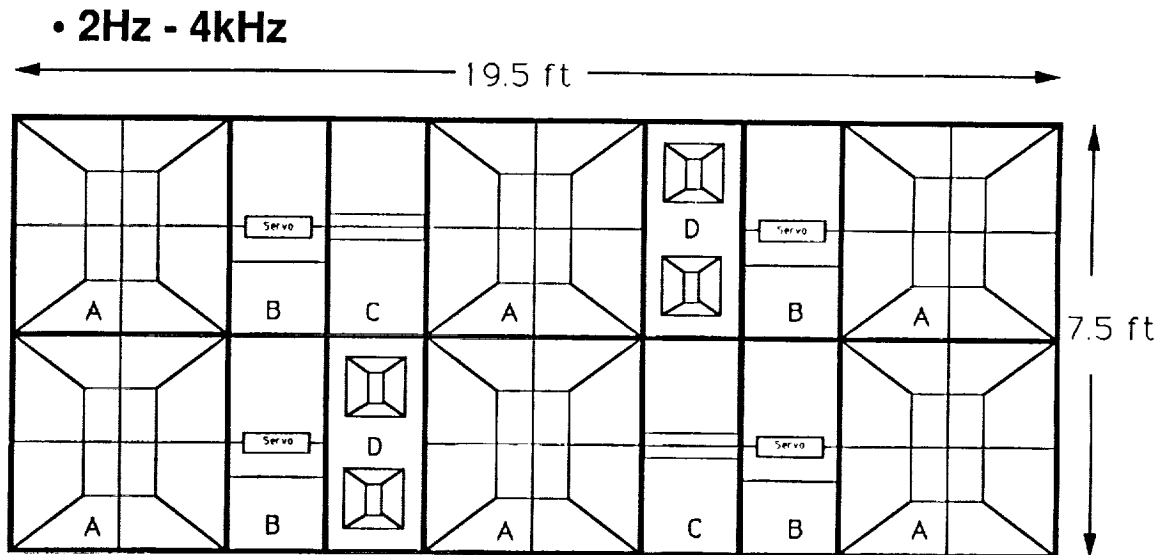


A : 2-30 Hz
B : 30-100 Hz
C : 100-300 Hz
D : 300-4000 Hz

## CIRCUITRY

Appropriate delay lines, amplifiers and cross-over networks are implemented to get a reasonably flat response. Attempts are being made to obtain a reasonably constant amplitude over the face of the test house wall. Figure 16 shows the circuitry.

## Figure 16

# Circuitry

## Electronic Equipment
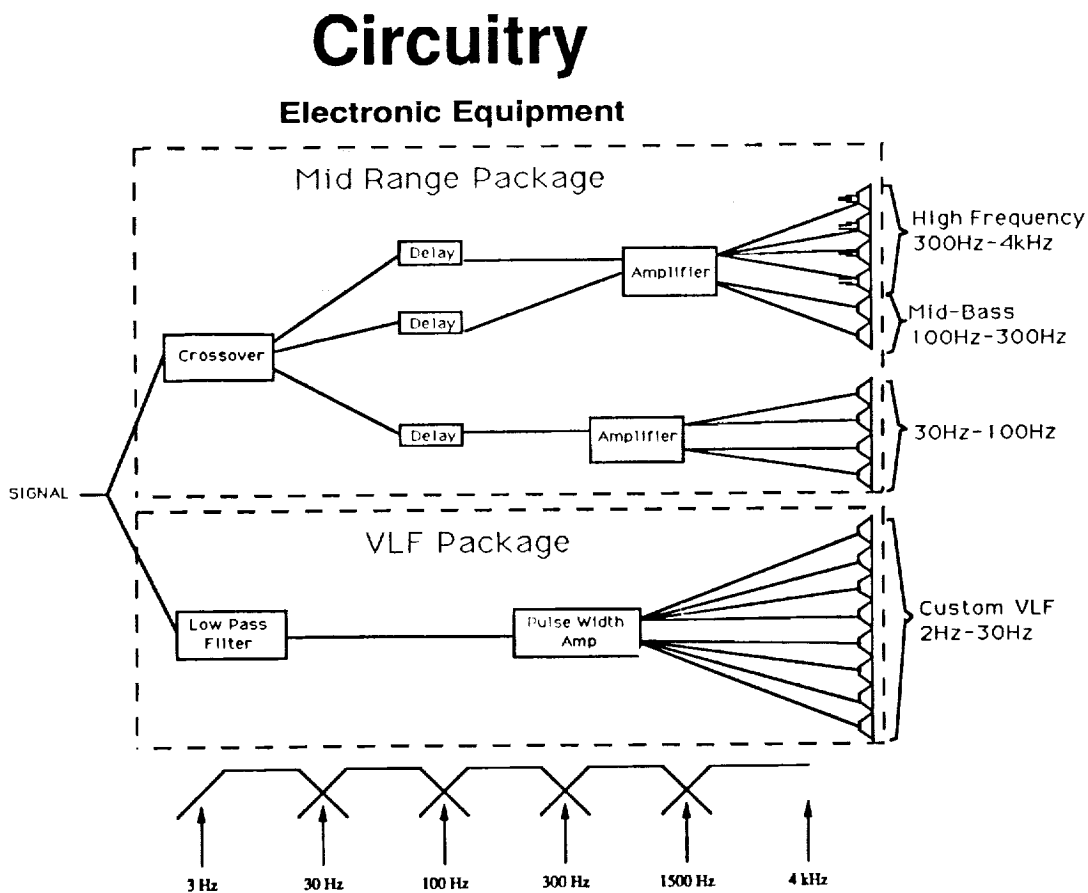


Fig. Frequency Breakdown

# DIPOLE DESIGN

As described earlier, the air flow moves through the whole unit in and out. As shown in Figure 17, there are two openings. It thus converts this unit into a dipole source. This will allow reduced noise at long distances because of the cancellations of the noise of opposite sign radiated from the two openings.

Figure 17

## Dipole Design



Airflow →

Airflow →

Reduced Community
Noise In The Farfield
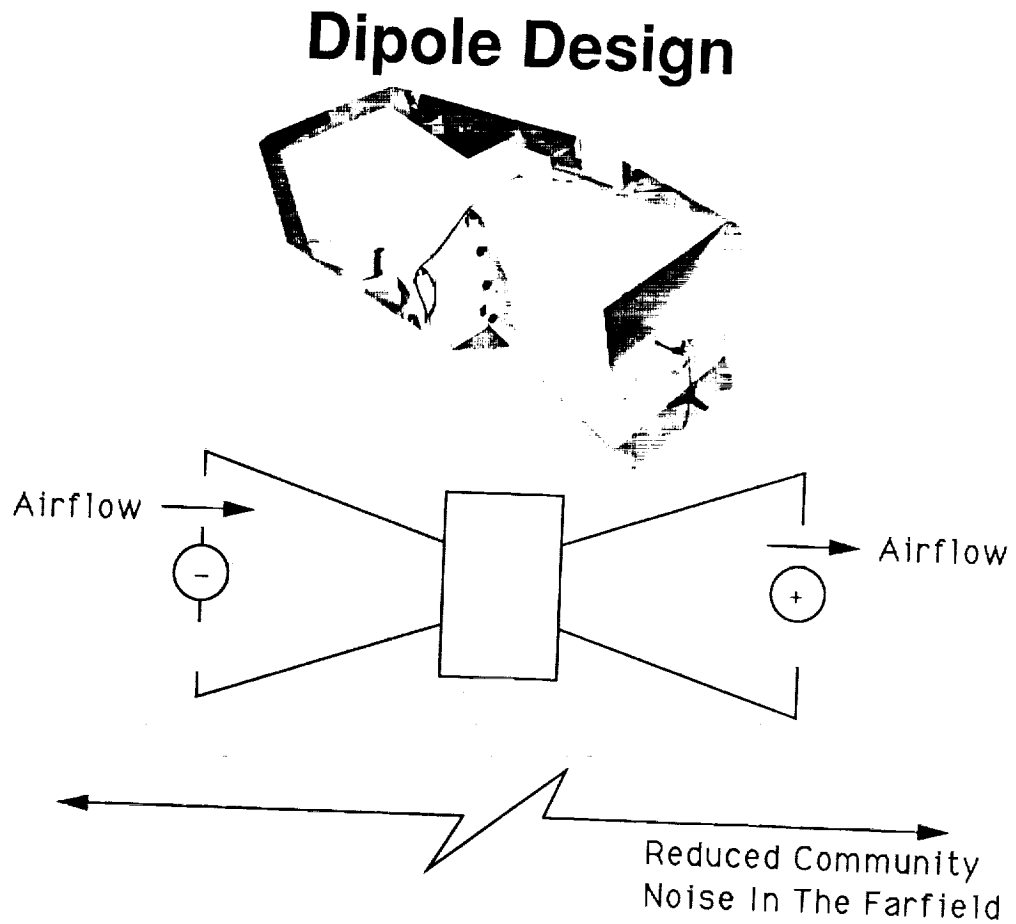
## TEST HOUSE SURROUNDINGS

The test house to be used for the planned tests was selected very carefully. The house is located with plenty of open space around it. Figure 18 shows the open area. The test house is just behind the trees by the roadway, in front of the utility pole seen in the figure. As will be seen later, one of the openings of the sonic boom simulator points at one of the walls of the test house. The other opening of the dipole arrangement faces the camera used to take the photograph shown in Figure 18. This arrangement of the house surrounding and the two sided opening of the noise source allows us to obtain outdoor response. If needed, other structures can be installed in the open space shown in this figure. As shown later, near the camera location, there is a heavy duty tower that can be utilized, if needed, to mount acoustic equipment to study low frequency noise propagation.

Figure 18

# Test House Surroundings

# THE TEST HOUSE

Figure 19 shows the test house and the floor plan. It has a total of five rooms. The outer shingles are made out of aluminum.

## Figure 19

## The Test House



House From Inside
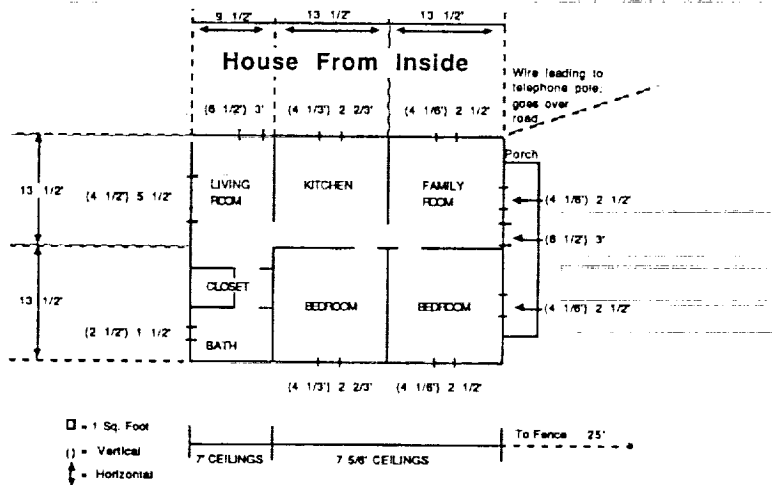
# TEST HOUSE INTERIOR

Figure 20a is the view of the family room from the porch entrance. The view of one of the bedrooms adjacent to the family room is shown in Figure 20b. The walls in the family room are made out of paneling material, and the ceiling from acoustic tiles.

## Figure 20



## Test House Interior

(a)

(b)
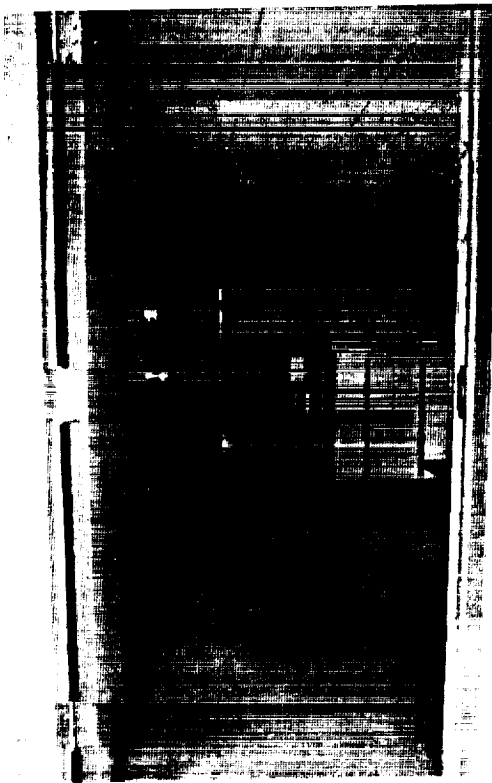
# TEST HOUSE INTERIOR

Figure 21a is the view of the kitchen from the family room. The room with the chalk board on the floor is that of the living room. As seen in Figure 21b, its walls and the ceiling are similar to those of the family room. One can also view the bathroom adjacent to the living room in Figure 21b.

**Figure 21**



## Test House Interior

(a)

(b)
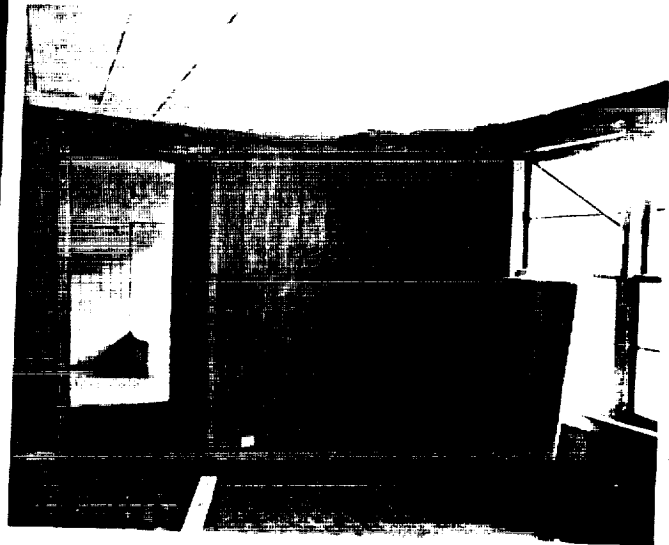
# TEST HOUSE INTERIOR

The two windows on the wall facing the opening of the speaker system are shown in Figure 22a and 22b.

## Figure 22

## Test House Interior



(a)
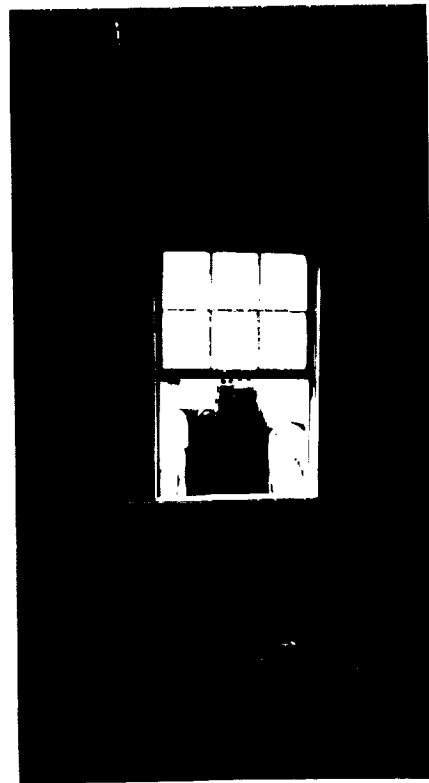


(b)

# WINDOW VIEWS

The view of the sonic boom simulator from the two windows on the wall facing the simulator is shown in Figure 23. These two windows are located in the two bedrooms.

## Figure   23

## Window Views



(a)

(b)

Adjacent to the test house are located two towers, one of which is shown in Figure 24. These towers are normally used in radar signature propagation studies at Georgia Tech Researh Institute. The same towers can be used in sound propagation studies. As these towers are capable of withstanding the loads of heavy radars, the sonic boom simulator could also be mounted atop these towers. These towers can be used in conjunction with three other facilities owned by Georgia Tech, two located at about 10 miles away and another at about 100 miles away. These facilities will prove invaluable for long distance, low frequency sound propagation studies.

Figure 24

# Tower for Potential Propagation Studies

## PRELIMINARY DATA

At the time of preparation of this document, only the sound pressure levels at the exit of a single, very low frequency source were obtained. In the initial measurements, a level of 125 dB was obtained at 3 Hz from the single unit. Typical results of amplitude and phase spectrum at the center of the diffuser exit are shown in Figure 25. Note that these measurements were acquired using time delay spectrometry and the source was not operating at its full power.

Initial measurements made with a single unit mounted in the speaker enclosure at a discrete tone of 3 Hz produced considerable vibration in the structural members of the house, which could be felt by placing hands over the window panes. The 3 Hz tone was also picked up in the interior of the house with a microphone. These measurements are continuing at present.

A total of six very low frequency units will be used in the planned experiments.

## Figure 25

# Preliminary Data
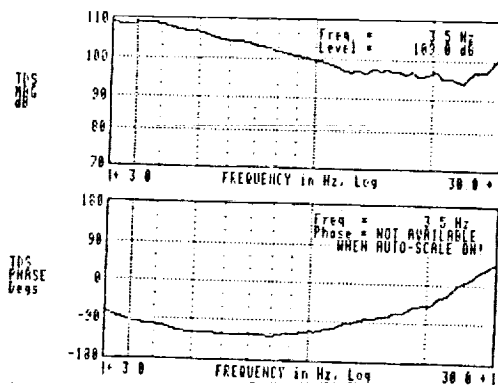


Figure    Time delay spectrometry plot of magnitude and frequency
reponse from 0-30 Hz (not at full power).

## • Reached 125 db at exit of each unit

## • Six units to be used

1340

PLANNED EXPERIMENTS

The acoustic performance of the complete unit will be tested. The goal is to acquire a flat frequency response in the range 2 Hz to 4 KHz. We expect to obtain noticeable levels at frequencies as low as 1/2 Hz. It is planned to screen a number of test subjects through audiometric testing. Their response to sonic boom of various selected shapes will be tested both indoors and outdoors. For indoor testing, measurements of wall vibrations and other secondary emissions are also planned. Response to sonic boom will be compared against other noise sources such as the aircraft noise.

Figure 26

# Planned Experiments

- **Test acoustic performance of complete unit**

    - **2 Hz - 4 kHz**

    - **Expect to reach 1/2 Hz**

- **Human Response**

- **Structural Response**

## ACKNOWLEDGMENTS

# Session IX. Sonic Boom (Human Response and Atmospheric Effects)

Sonic Boom (Human Response and Atmospheric Effects) Outdoor-to-Indoor Response to Minimized Sonic Booms
*David Brown, Wyle Research; and Louis C. Sutherland, Consultant to Wyle*

THIS PAGE INTENTIONALLY BLANK

# SONIC BOOM (HUMAN RESPONSE AND ATMOSPHERIC EFFECTS) OUTDOOR-TO-INDOOR RESPONSE TO MINIMIZED SONIC BOOMS

$5_{/5}$-71
/2045

David Brown, Wyle Research
and Louis C. Sutherland, Consultant to Wyle

Wyle Laboratories
128 Maryland St.
El Segundo, California 90245

High Speed Research Workshop
Williamsburg, Virginia
May 1-16, 1991

## OUTLINE

1. Potential Waveforms and Spectra for HSCT Minimized Sonic Booms Signatures

2. Models for Exterior to Interior Sonic Boom Transmission into Dwellings

3. Resulting Interior (and Exterior) Subjective Noise Levels

4. Review of Some Existing Data on Subjective/Community Response to Sonic Booms

5. Summary

SO█████████

The following types of sonic boom signatures were selected to represent the range of potential HSCT sonic boom signatures that may be realized or to provide reference signatures for comparison. In all cases, the signatures had a peak pressure of 1 psf and a total duration of 350 ms.

A.  N-Wave Reference Signatures
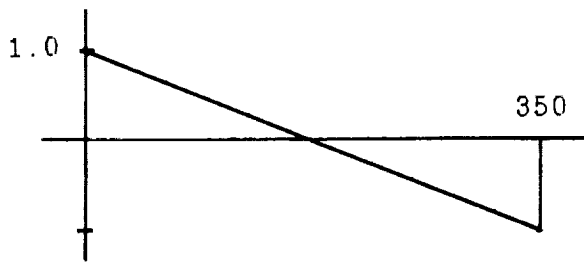
(1)  Ideal N-wave with zero rise time
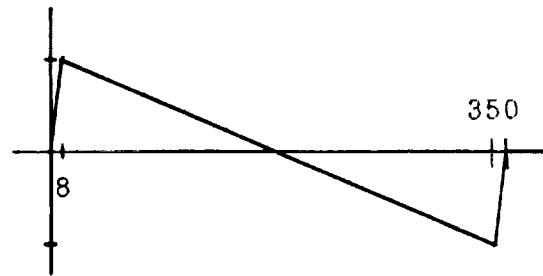
(2)  Symmetric N-wave with a finite 8 ms rise/decay time

B.  Symmetric (Minimized) Wave Forms
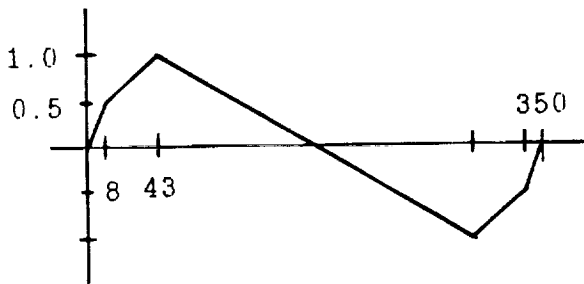
(3)  Delayed Ramp, 8 ms rise time to 0.5 psf followed by 35 ms rise to 1 psf - mirror image of this pattern at end
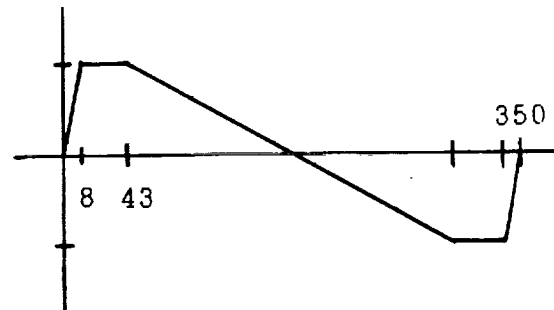
(4)  Flat Top, 8 ms rise time, 35 ms duration for flat top - mirror image of this pattern at end

C.  Non-Symmetric (Minimized) Wave Forms
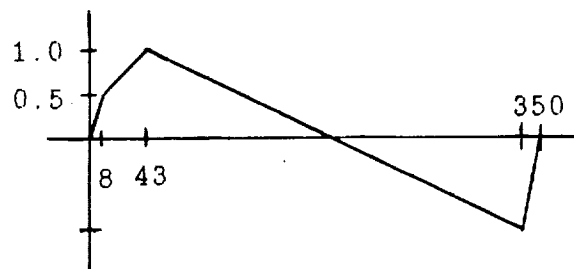
(5)  Delayed Ramp, 8 ms rise time to 0.5 psf followed by 35 ms rise to 1 psf, 8 ms decay time at end
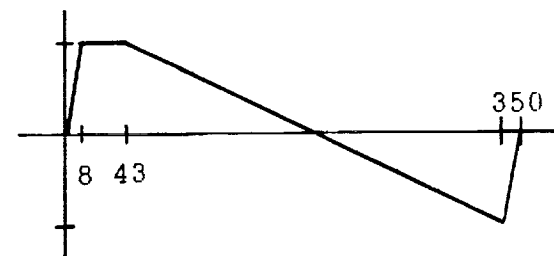
(6)  Flat Top, 8 ms rise time, 35 ms duration of flat top, 8 ms decay time at end

1346

# SONIC BOOM NOISE DESCRIPTORS

Table 1 summarizes the various descriptors commended to define the objective (acoustical) and subjective (psychoacoustic) characteristics of sonic booms that are used for evaluating human response to sonic booms. Some of these are utilized in the remaining figures shown in this presentation. The descriptors are identified by the name of the quantity, its abbreviation (used in text), its letter symbol and units (used in equations), and, where appropriate, its reference level when the quantity is expressed on a decibel scale.

Table 1

Acoustic Descriptors for the Evaluation of Human Response to Sonic Booms

## For Physical Description of Sonic Booms

| Quantity | Abbreviation | Letter Symbol | Units | Reference Level |
|---|---|---|---|---|
| **Preferred** | | | | |
| 1 Peak sound pressure (Flat weighting) | – | $P_{pkT}$ | Pa[1] | – |
| 2 Peak sound pressure level (Flat weighting) | PKT | $L_{pkT}$ | dB | 20μPa |
| 3 Sound exposure spectrum level | SESL | $L_{E(f)}$ | dB | $(20μPa)^2 \cdot sec/Hz$ |
| 4 Sound Exposure | SE | E | $(Pa)^2 sec$ | – |
| 5 C-weighted sound exposure level | CSEL | $L_{CE}$ | dB | $(20μPa)^2 \cdot sec$ |
| 6 Day-night average C-weighted sound level | DNCL | $L_{Cdn}$ | dB | – |
| **Optional** | | | | |
| 7 Sound exposure spectral density | SESD | $E(f)$ | $(Pa)^2 sec/Hz$ | |
| 8 A-weighted sound exposure level | ASEL | $L_{AE}$ | dB | $(20μPa)^2 \cdot sec$ |
| 9 Day-night average A-weighted sound level | DNL | $L_{dn}$ | dB | – |
| **NOT RECOMMENDED** | | | | |
| 10 Energy spectral density or energy spectrum | $S(\omega)$ or $S(f)$ | $(Pa)^2 \cdot sec/Hz$ | | |

## For Subjective Description of Sonic Boom Loudness:

**Preferred**

| Quantity | Abbreviation | Letter Symbol | Units | Reference Level |
|---|---|---|---|---|
| 11 Perceived Level (Mark VII)[2] | – | $PL_{VII}$ | PLdb | |
| 12 1/3rd Octave Band Sound Exposure Level | 1/3SEL | $L_{1/3E(f)}$ | dB | $(20μPa)^2 \cdot sec$ |
| 13 Equivalent 1/3rd Octave Band SPL[3] | 1/3ESPL | $L_{1/3eq(f)}$ | dB | (20μPa) |

**Optional**

| Quantity | Abbreviation | Letter Symbol | Units |
|---|---|---|---|
| 14 Loudness Level (Mark VI or ISO-226 (1961) | $LL_{VI}$ | Phons (on dB scale) | |

---

(1)  47.88 Pascals (Pa) = 1 psf.

(2)  Mark VII denotes the use of the S.S. Stevens Mark VII Loudness contours for frequency-weighting of a sound spectrum according to its loudness sensation (Stevens,1972).

(3)  The effective steady sound pressure level used to compute the loudness for a transient sound.

# ACOUSTICAL DESCRIPTOR FOR SPECTRAL CONTENT OF SONIC BOOMS

The preferred descriptor to define the spectral content of sonic booms is the Sound Exposure Spectrum Level, $L_E(f)$. This descriptor represents the spectral content of the basic noise decriptors used for describing any single event – the Sound Exposure Level, $L_E$. The latter is equal to ten times the logarithm, to the base ten, of the integral, over the duration of the event, of the square of the instantaneous acoustic pressure, divided by the square of the reference pressure, 20μPa. When applied to the evaluation of community response to sonic booms, it is customary to use the so-called C-Weighted Sound Exposure Level, $L_{CE}$ for which the frequency content of the instantaneous acoustic pressure is modified by the C-weighting curve.

The Sound Exposure Spectrum Level, $L_E(f)$ is obtained from the Fourier spectra, $F(f)$ of the sonic boom signature in the following manner.

$$L_E(f) = 10 \cdot \lg [E(F)/E_o]$$

where  $E(f)$  =  Sound Exposure Spectral Density

  =  $2 \cdot |F(f)|^2$

  =  2 times the square of the absolute value of the Fourier Spectrum $F(f)$ of the instantaneous acoustic pressure, $p(t)$, and

  $F(f)$  =  $\int\limits_{\infty}^{\infty} p(t) \exp(-2\pi ft)\, dt$

and  $E_o$  =  Reference Sound Exposure Spectrum Level

  =  $p_o^2\, t_o/\delta f$

  $p_o$  =  Reference acoustic pressure, 20μPa

  $t_o$  =  Reference time, 1 second

  $\delta f$  =  Reference frequency bandwidth, 1 Hz

## SPECTRA OF SONIC BOOM N-WAVE FORMS

The following figures show the spectra of these wave forms in terms of their Sound Exposure Spectrum Level, $L_E(f)$. As illustrated in Figure 1, for the ideal N-wave, with a peak pressure $P_{pk}$, the envelope of $L_E(f)$ can be described by two asymptotic lines which meet at a pseudo-peak frequency, $f_{max} = \sqrt{3}/(\pi T)$ where T is the sonic boom duration. These lines are defined by:

$$L_E(f)|_{f\to 0} \to 10\lg [2(P_{pk}T)^2(\pi fT/3)^2/E_o(f)]$$

$$\overline{L_E(f)}|_{f\to\infty} \to 10\lg [2(P_{pk}/\pi f)^2/E_o(f)]$$

where $\overline{L_E(f)}$ signifies the envelope of $L_E(f)$.

Figure 2 shows the same spectra for the non-ideal N-wave with a finite rise (and fall) time of 8 ms. In this case, the envelope of the high frequency portion of the spectrum falls off at -40 dB/decade above a frequency equal to $1/(\pi\tau)$ where $\tau$ is the rise (and fall) time.

1348
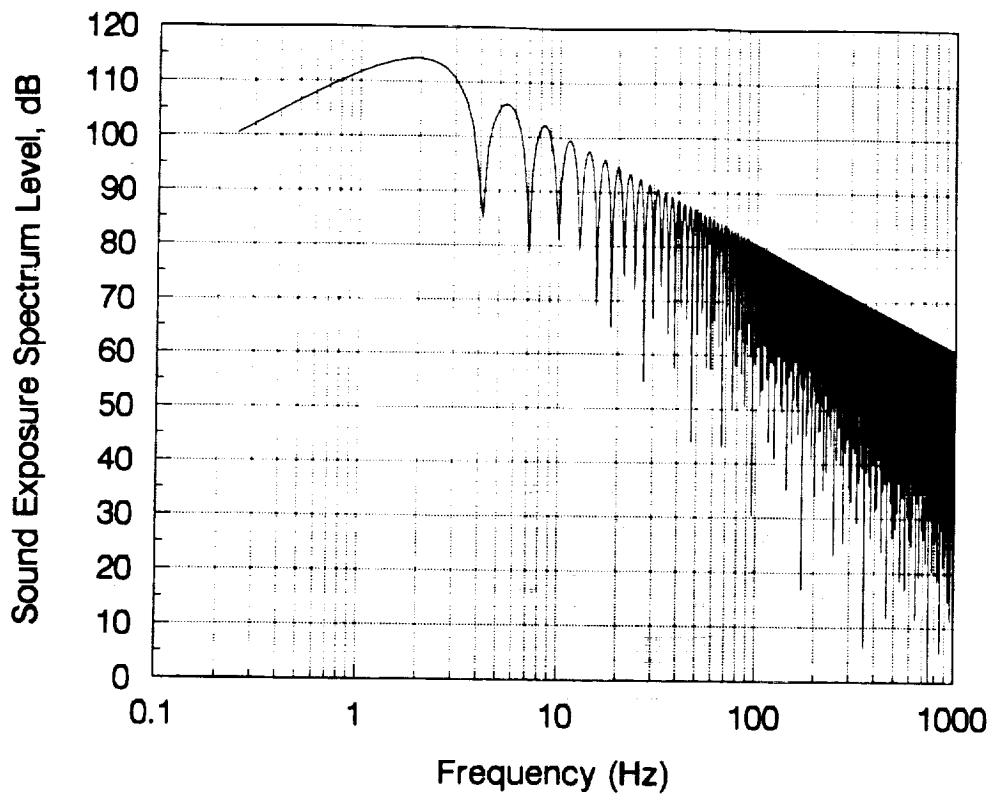
Figure 1. $L_E(f)$ for Ideal N-Wave
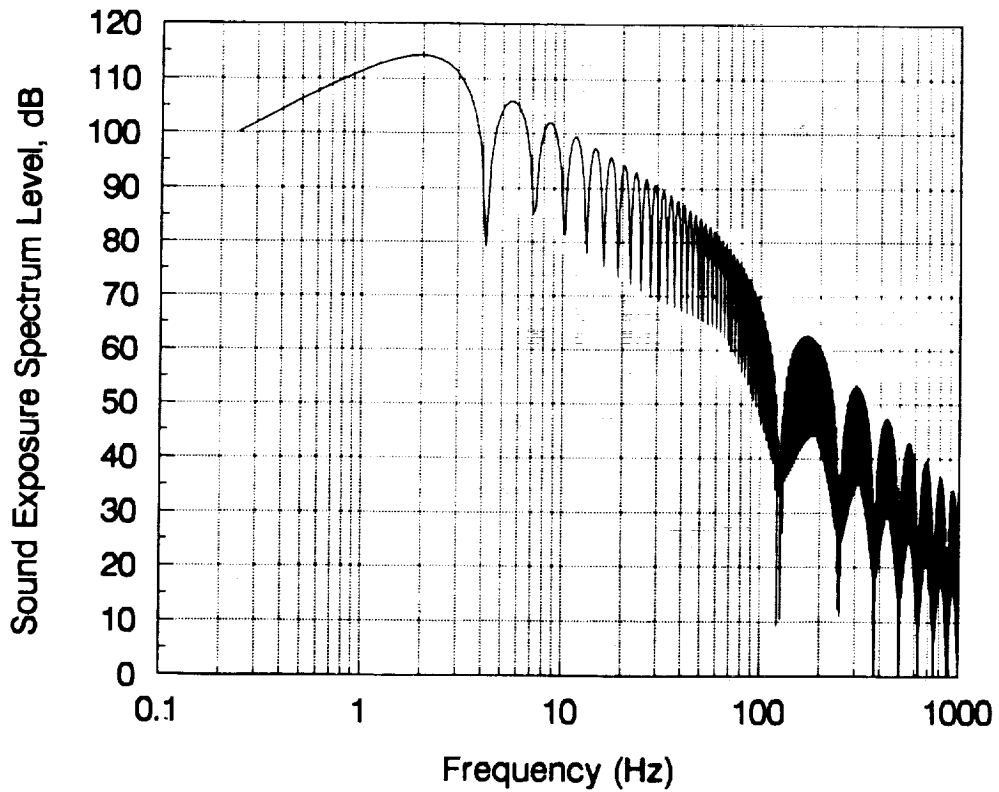


Figure 2. $L_E(f)$ for Non-Ideal N-Wave with 8 ms Rise Time

1349

# SPECTRA OF GENERIC MINIMIZED SONIC BOOM WAVE FORMS

Figures 3 through 6 show the Sound Exposure Spectrum Levels for the four generic types of minimized sonic boom wave forms identified earlier. They all have the same general pattern as indicated in Figure 2 above, but exhibit differences in fine detail at frequencies above the peak frequency, $f_{pk}$.
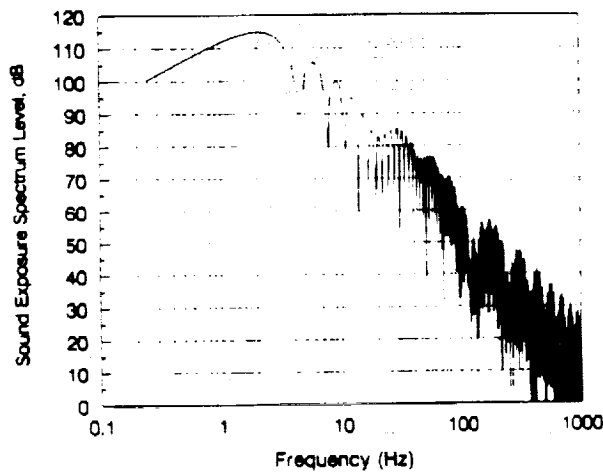


Figure 3.   Symmetric Delayed Ramp, 8 ms Rise Time to 0.5 psf, 35 ms Rise to 1 psf
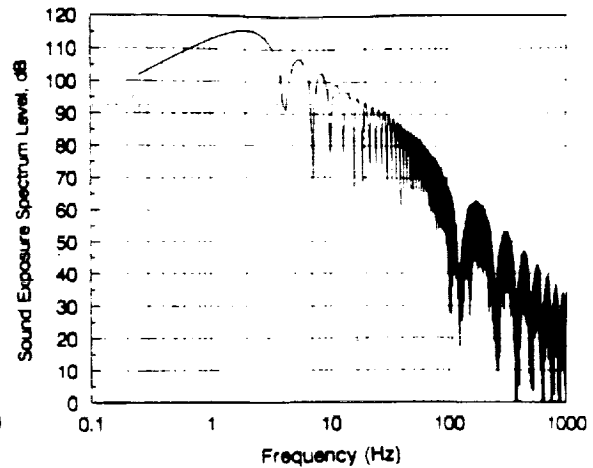
Figure 4   Symmetric Flat Top, 8 ms Rise Time, Flat Top for 35 ms
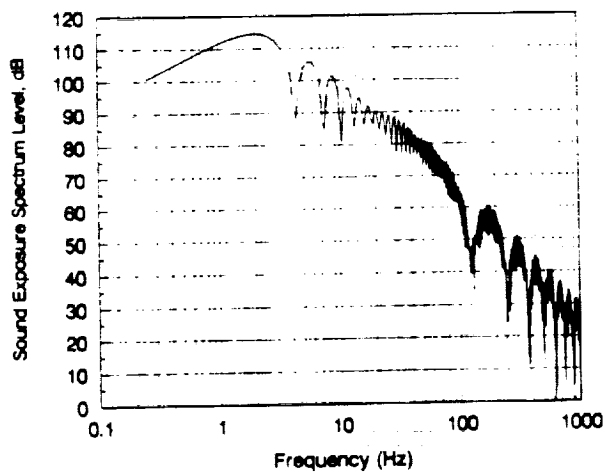
Figure 5.   Non-Symmetric Delayed Ramp, 8 ms Rise Time to 0.5 psf, 35 ms Rise to 1 psf
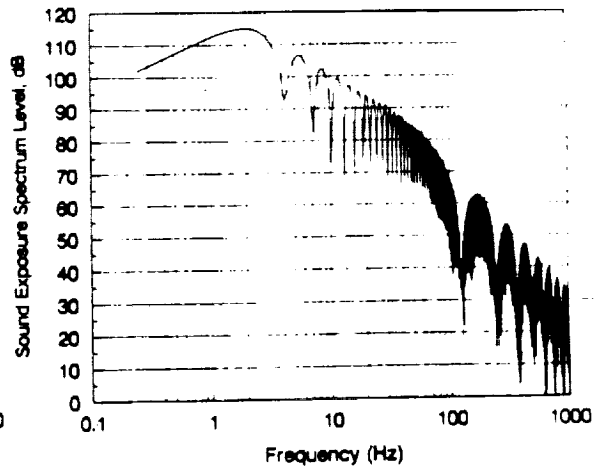
Figure 6   Non-Symmetric Flat Top, 8 ms Rise Time, Flat Top for 35 ms

1350

Figure 7 shows a composite version of only the <u>envelope</u> of these spectra to show that the low frequency portions are nearly identical and the high frequency portions indicating essentially the same envelope, in decreasing order of levels for:

- Any of the N-waves with only a 8 ms rise or fall time to the same maximum peak pressure, <u>regardless of whether they had a peak or flat top.</u>

- Non-symmetric, Delayed Ramp

- Symmetric, Delayed Ramp
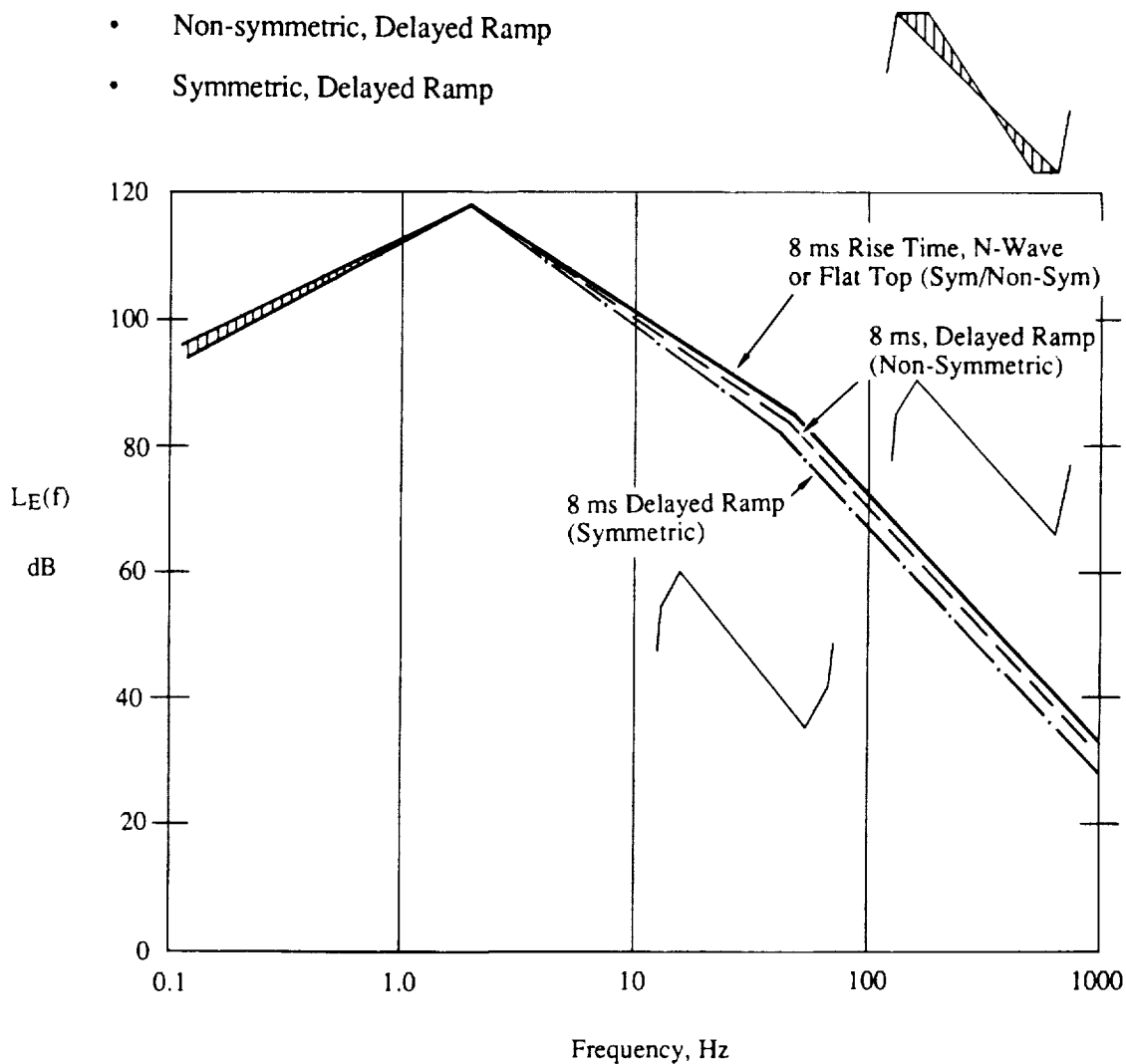


Figure 7. Comparison of Sound Exposure Spectrum Levels for Various Wave Shapes

## OUTDOOR-TO-INDOOR NOISE REDUCTION MODEL FOR SONIC BOOMS

In order to compute loudness levels from sonic boom as it would be heard indoors, an outdoor-to-indoor noise reduction model is needed. Available data from a number of sources (refs. 1-4) was utilized, along with a generic model for outdoor-to-indoor low frequency noise reduction (ref. 5) to construct the curve shown in Figure 8 for "windows closed" and "windows open" conditions. The dip in noise reduction at the lowest frequency for the windows closed condition is associated with a Helmholtz resonance effect that will vary widely depending on the area and length of air leakage paths into a room and the room volume. The second dip is generally more consistent from room to room and is normally associated with the lowest vibration mode of the largest outside wall. This resonance frequency may also interact with the lowest room acoustic modes to give a complex behavior to the noise reduction at these lowest frequencies. Although there are very limited noise reduction data at frequencies below 100 Hz, it is anticipated that loudness levels will be increasingly insensitive to variations in the noise reduction value at a specific frequency as this frequency decreases well below 100 Hz.
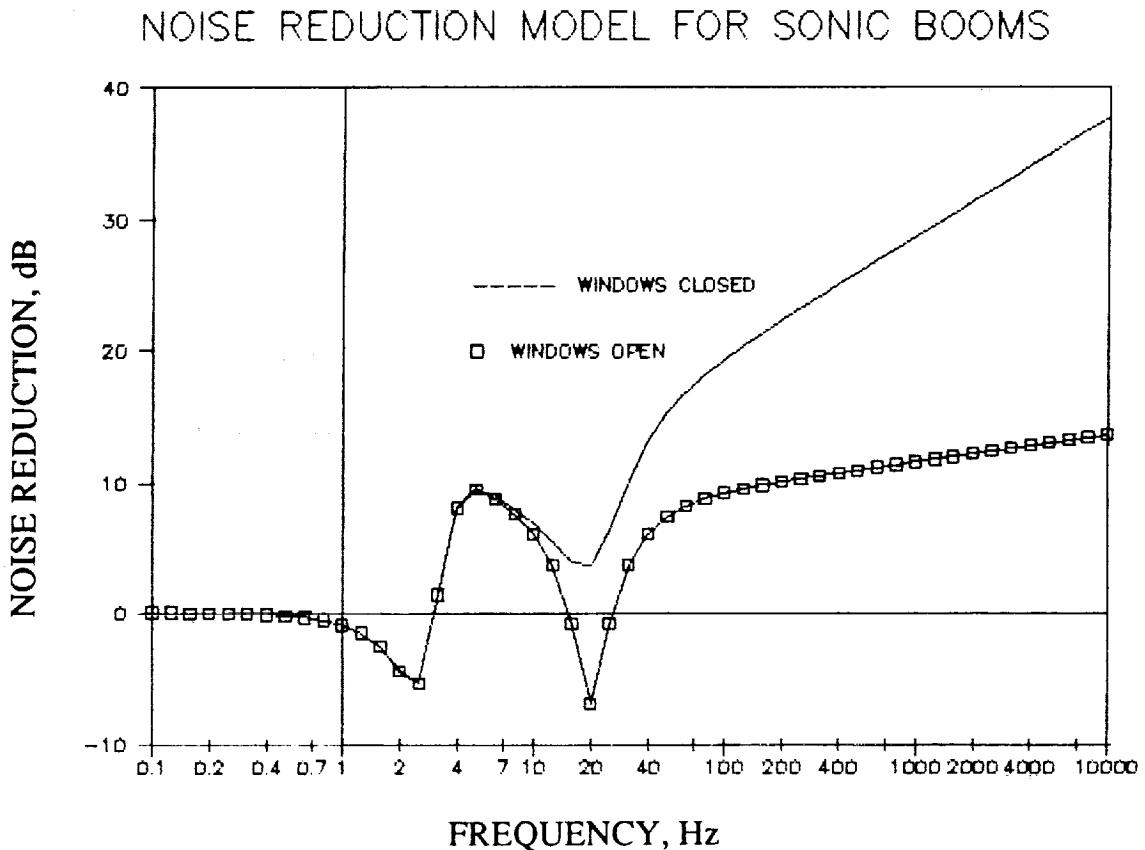


Figure 8. Noise Reduction Model for Sonic Booms

# NOISE METRICS EVALUATED FOR SONIC BOOM LEVELS

The noise metrics being evaluated in this study include:

- Sound exposure levels
    - (i)    A-weighted
    - (ii)   C-weighted

- Loudness levels
    - (i)    Perceived Level (the Stevens Mark VII model) (ref. 6)

using loudness contours which extend down to 1 Hz.

Although there are other loudness models, such as the Stevens Mark VI model embodied in an American National Standard (ref. 7) and the sophisticated loudness model by Zwicker (ref. 8), these other versions do not have loudness contours extended down to 1 Hz. Thus, these alternate methods may not be suitable for sonic boom loudness calculations where much of the energy is concentrated at frequencies below about 50 Hz.

Interim results obtained from the calculation of loudness outdoors and indoors for the family of sonic boom wave shapes and spectra shown earlier are listed in Table 2. Loudness, in terms of Stevens, Mark VII Perceived Level, are given for listening outdoors and indoors with windows closed or open, based on the noise reduction models in Figure 8.

## Table 2

### Interim Results

Relative Stevens Mark VII Perceived Level, dB

| Boom Signature* | Outdoor Level | - - - - Indoor Level - - - - Window Open | Window Closed |
|---|---|---|---|
| N-Wave | 97.2 | 87.9 | 76.2 |
| N-Wave with 8 msec Rise Time | 84.3 | 77.8 | 66.1 |
| Non-Symmetric Flat-Top | 84.2 | 77.5 | 66.0 |
| Symmetric Flat-Top | 84.1 | 77.2 | 65.8 |
| Non-Symmetric Delayed Ramp | 81.8 | 74.7 | 63.2 |
| Symmetric Delayed Ramp | 76.4 | 68.5 | 56.1 |

* 1 psf overpressure - 350 msec duration

# RELATIVE LOUDNESS FOR DIFFERENT WAVE FORMS AND DIFFERENT LISTENING SITUATIONS

It is helpful to view the preceding data from the standpoint of relative changes in loudness for the different wave forms and for the three different listing situations. Such a view is shown in Table 3 below. For each listening situation, the loudness for the ideal N-wave is assigned a reference loudness of 0 dB. Note that the relative loudness for each of the other wave forms, is approximately the same for all three listening conditions (i.e., outdoors; indoors, windows closed; or indoors, windows open) thus suggesting that the *relative* loudness of alternative waveforms would not be strongly sensitive to the listening environment. Note, also that, as expected from Figure 7, the relative loudness for the symmetric, delayed ramp wave form is the lowest of all the wave forms considered.

However, there is one important point not brought out by the calculated indoor loudness values. There is considerable evidence to show that people judge the loudness or annoyance of subsonic aircraft noise (refs. 9,10) and sonic booms heard indoors (as discussed later), by different criteria as compared to the same type of sound heard outdoors. The net effect is that subtracting the outdoor-to-indoor noise reduction from outdoor noise levels may underpredict indoor loudness levels. It is interesting to note that for one of the studies (ref. 9), loudness of subsonic aircraft noise calculated according to the Zwicker method was in much better agreement with the laboratory findings for the subjectively-perceived change in noise levels indoors vs outdoors.

Table 3

Relative Stevens Mark VII Perceived Level, dB re: Ideal N-Wave

| Boom Signature* | Outdoor Level | Indoor Level | | Average ±S.D. |
|---|---|---|---|---|
| | | Window Open | Window Closed | |
| N-Wave | 0 | 0 | 0 | 0 |
| N-Wave with 8 msec Rise Time | -12.8 | -10.2 | -10.1 | |
| Non-Symmetric Flat-Top | 13.0 | -10.4 | -10.2 | } -11.2 ± 1.3 |
| Symmetric Flat-Top | -15.4 | -13.2 | -12.9 | |
| Non-Symmetric Delayed Ramp | -13.1 | -10.7 | -10.4 | -13.8 ± 1.1 |
| Symmetric Delayed Ramp | -20.8 | -19.4 | -20.1 | -20.1 ± 0.5 |

* 1 psf overpressure - 350 msec duration

# ALTERNATIVE NOISE METRICS

For comparison to the preceding results for Perceived Level (Mark VII), in PLdB, Table 4 shows a comparison of the calculated difference between values of Perceived Level minus A-weighted Sound Exposure Level and C-weighted minus A-weighted Sound Exposure Level for both outdoor and indoor (windows closed) listening conditions. The differences between Perceived Level and A-weighted Sound Exposure Level are nearly the same for all of the non-ideal wave forms for both outdoors and indoors. However, this is not as true for the difference between Perceived Level in PLdB and C-weighted Sound Exposure Level. Furthermore, as shown in Figure 9, the absolute change in C-weighted Sound Exposure Levels among the different wave forms is much less than the change in Perceived (Loudness) Levels. Thus, a C-weighted sound level appears to rate alternative sonic boom wave forms very differently than would be indicated by Perceived (loudness) Level or A-weighted Sound Exposure Level. However, it is the C-weighted Sound Exposure Level which was chosen by a CHABA working group under the National Research Council, as the best and most reliable metric available at that time for use in the evaluation of community reaction to high energy impulsive sounds such as sonic booms. This choice was dictated by the greater emphasis in low frequencies inherent in the C-weighting which is considered a better indicator of the tendency for such high energy impulsive sounds to induce annoying rattle and vibration of buildings.

Table 4

Relative Relationships of Alternate Metrics

| Sonic Boom Signature | – – – Outdoor – – – | | – – – – – – – – – Indoor – – – – – – – – – | | | |
| | | | Open Windows | | Closed Windows | |
| | PL-ASEL dB | PL-CSEL dB | PL-ASEL dB | PL-CSEL dB | PL-ASEL dB | PL-CSEL dB |
|---|---|---|---|---|---|---|
| N-Wave | 7.5 | –6.3 | 8.7 | –13.7 | 10.7 | –18.2 |
| N-Wave with 8 ms | 12.7 | –16.6 | 13.7 | –23.3 | 11.0 | –27.9 |
| Non-Symmetric Flat Top | 12.7 | –16.6 | 13.6 | –23.3 | 10.9 | –28.0 |
| Symmetric Flat Top | 12.7 | –16.6 | 13.4 | –23.3 | 10.9 | –28.1 |
| Non-Sym Delayed Ramp | 12.4 | –17.1 | 12.9 | –24.0 | 10.4 | –28.9 |
| Symmetric Delayed Ramp | 11.7 | –18.7 | 11.6 | –24.6 | 8.0 | –32.6 |
| Average (without N-Wave) | 12.4 | –16.6 | 13.0 | –23.7 | 10.2 | –29.1 |
| Standard Deviation | ±0.4 | ±0.9 | ±0.9 | ±0.4 | ±1.3 | ±1.3 |

C-4.
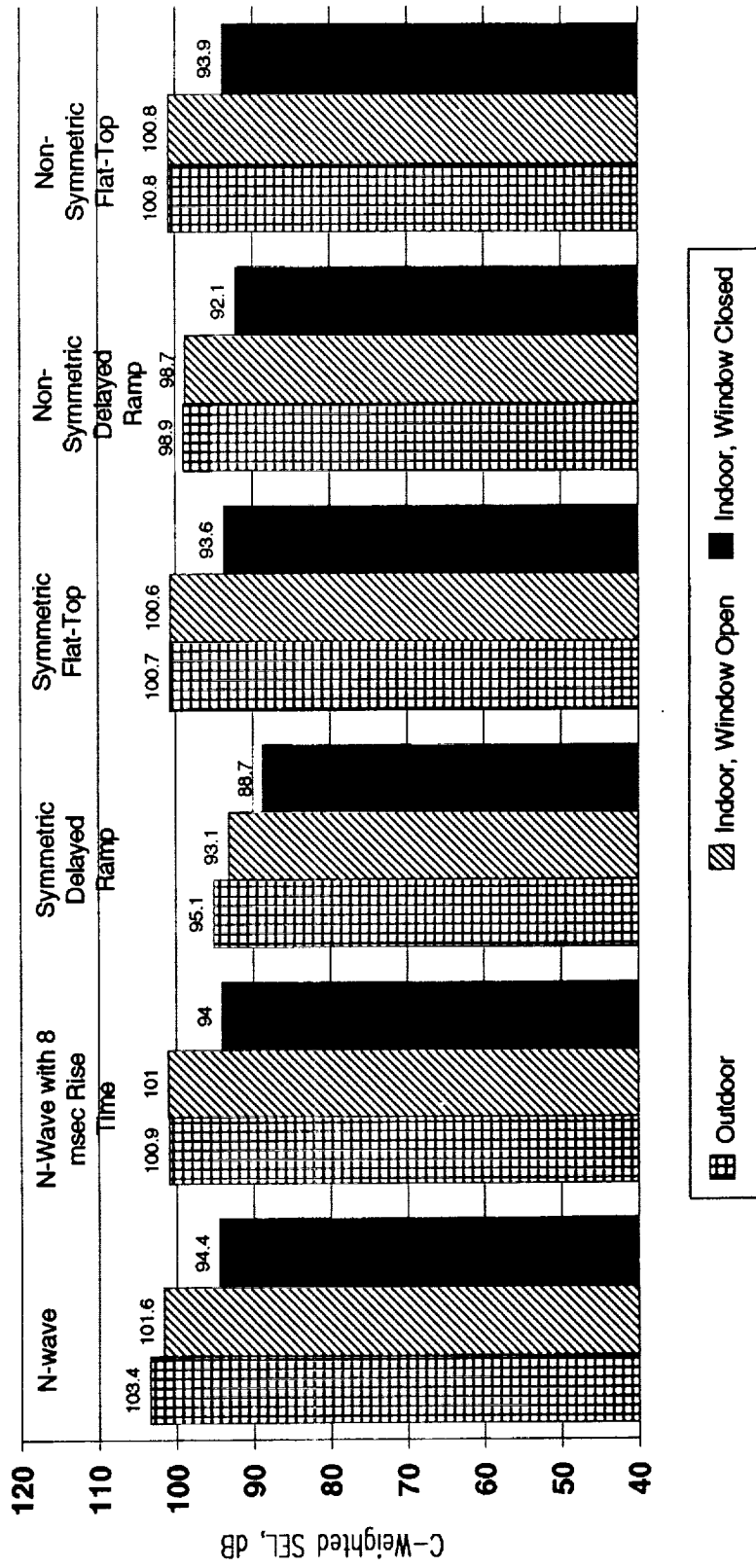
Figure 9. C-Weighted Sound Exposure Levels for Various Sonic Boom Signatures

1356

# THE RATTLE FACTOR

    Loudness calculations for sonic booms do not indicate the potential significance in human response to such booms, *when heard indoors*, of rattle sounds caused by sonic boom-induced building vibration. Some aspects of this problem, identified here as the "rattle factor", are considered in the following figures. Figure 10 shows a summary of the type of interference noted by respondents queried during the tests of community reaction to sonic booms conducted during the SST program in the 1960's (refs. 11 and 12). As indicated, "house shaking" was the most frequently cited type of interference from these exposure tests. The peak sonic boom pressures involved were in the range of 1-2 psf for the Oklahoma City tests and less than 3.1 psf for the St. Louis tests.



TYPE OF INTERFERENCE FROM SONIC BOOM
OKLAHOMA CITY (BORSKY, 1965) vs ST. LOUIS TESTS
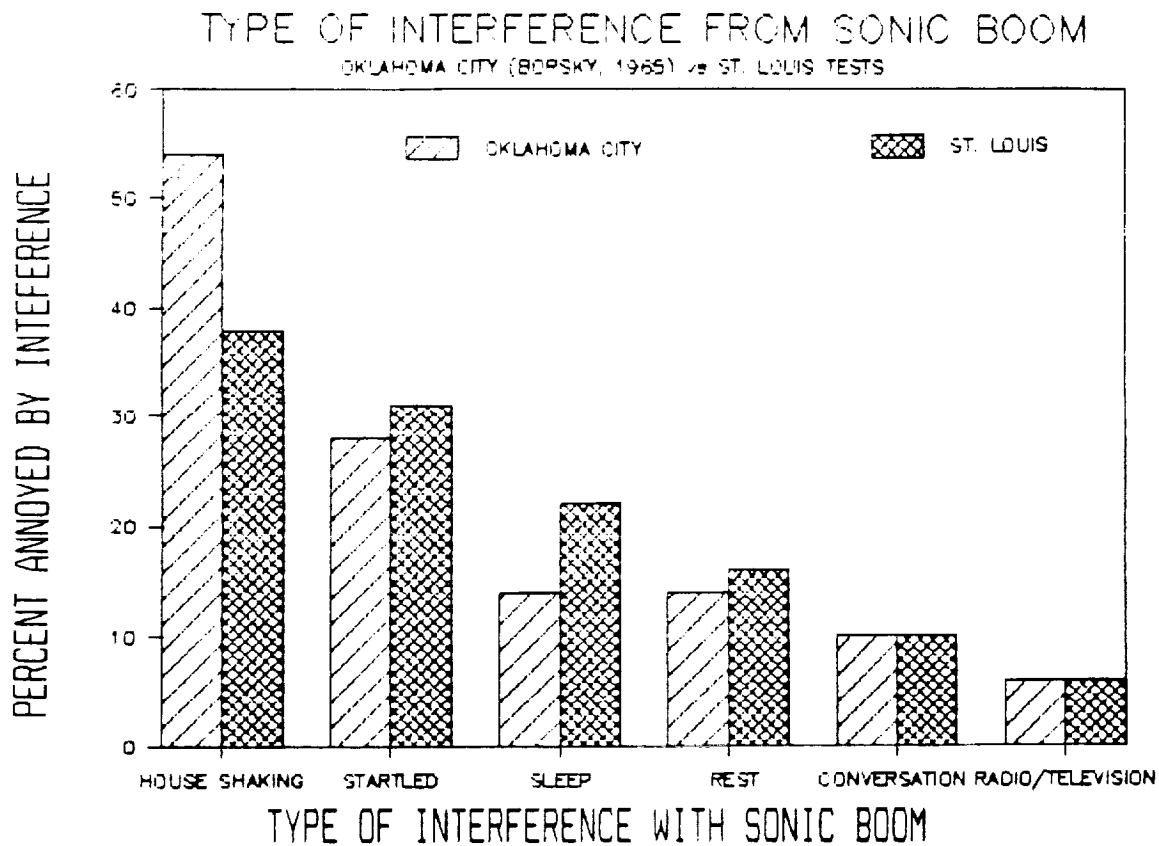
Figure 10.   Type of Interference from Sonic Boom Community Response Tests (Data from References 11 and 12).

Additional evidence for a possible "rattle factor" may be provided by the results of controlled sonic boom tests conducted at Edwards AFB(ref. 13). "Unacceptability ratings" to sonic booms were provided by subjects exposed to the booms outside and inside residential buildings. As indicated in Figure 11 below which shows this subjective rating vs outdoor peak overpressure, the results for the experienced subjects who lived near Edwards Air Force Base extrapolate to nearly the same peak overpressure (about 0.9 psf) for a 0 percent "unacceptability" rating for either outdoor or indoor listening. In other words, there is no apparent benefit for these subjects of outdoor-to-indoor noise reduction in lowering the "unacceptability rating" for booms heard indoors. While speculative, this result is consistent with the concept of the potential effect of added "rattle sounds or perceived building vibration" on subjective response to sonic booms indoors. However, another possible explanation for this trend, mentioned earlier, is the apparent higher "expectation" for lower levels of annoying sounds when heard indoors (refs. 9,10).
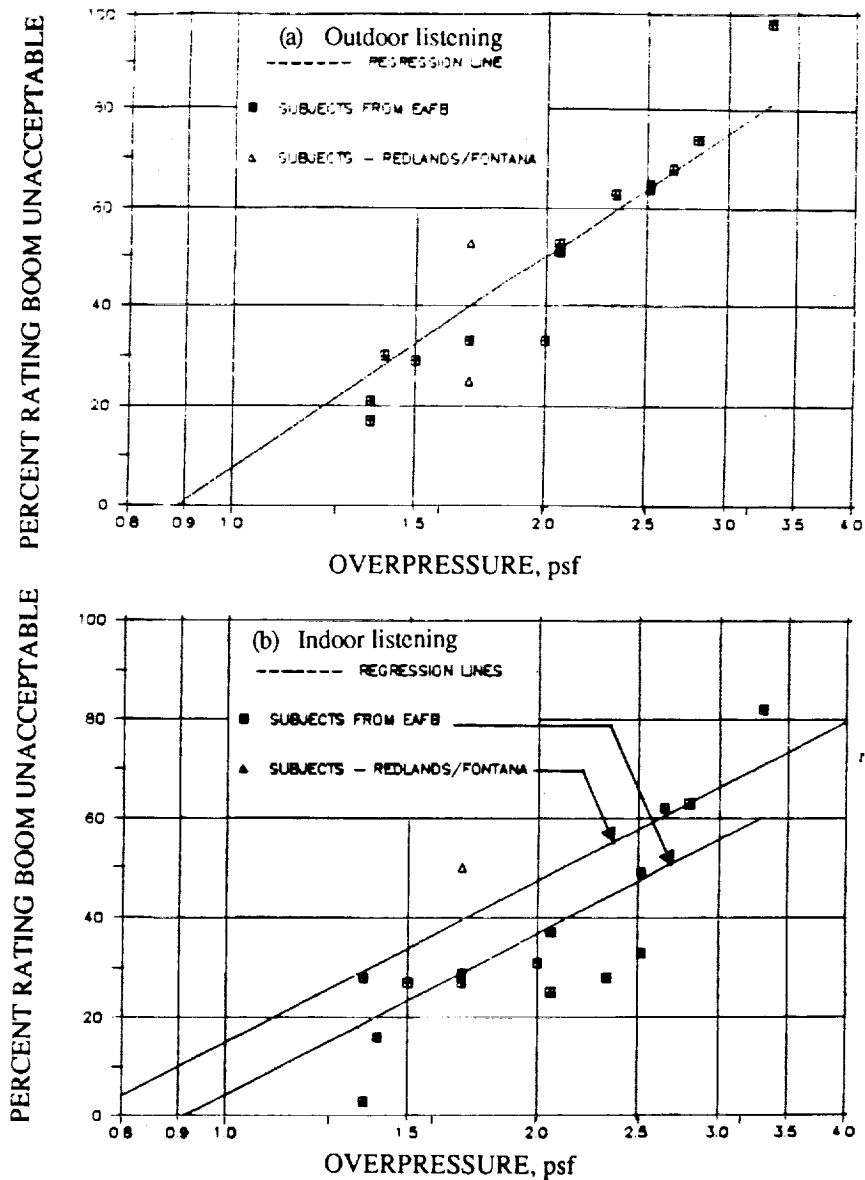


Figure 11. Acceptability Rating of Sonic Booms Heard (a) Outdoors and (b) Indoors During Edwards AFB Tests (data from ref. 13)

1358

# RATTLE THRESHOLDS vs SONIC BOOMS EXCITATION

NASA has studied the threshold of building vibration levels which can induce rattle of wall-hung mirrors and plaques (ref. 14). These data, shown on Figure 12 below, indicate a "rattle threshold" at velocity response levels of about 0.008 to 0.04 in/sec. For wood frame structures, these "rattle" vibration thresholds are expected to be exceeded by a factor of at least 25 for sonic booms with nominal peak pressures of 1 psf (ref. 15).
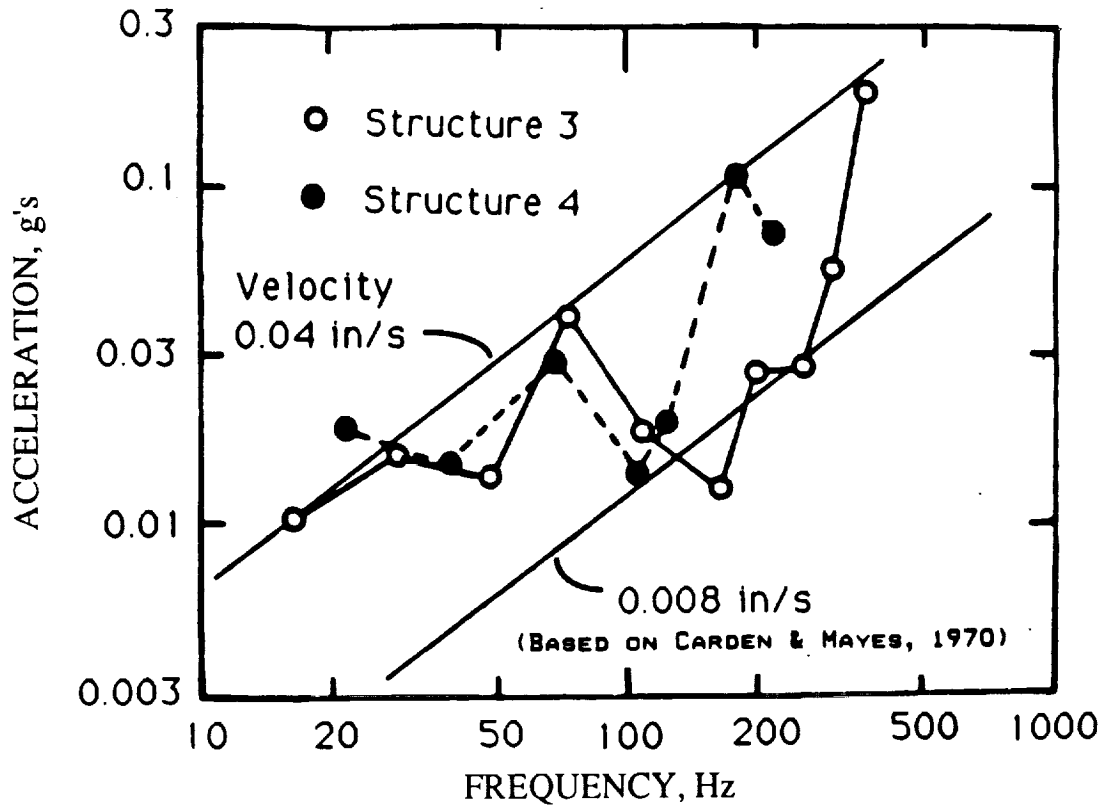


Figure 12. Vibration Levels at Rattle Thresholds for Wall-Hung Mirrors and Plaques

# IS THERE AN ACCEPTABLE SONIC BOOM LEVEL?

The preceding material on subjective response to sonic booms relates to the determination of an acceptable sonic boom level. Another viewpoint on this question is provided by the data in the last figure (Fig.13). This compares one interpretation of the NASA Edwards AFB sonic boom test data and more recent community responses from Concorde-generated sonic booms (ref. 16) to a Wyle interpretation of the same Edwards data (ref. 13) augmented by results from both laboratory (refs. 17,18) and other field test data (ref. 11) used to extract additional data points on "acceptability" vs peak pressure. The unique form of analysis used in Leyman's interpretation of the Edwards AFB data (ref. 16) is preserved here in that the "% Acceptance" is plotted on a probability scale. Note that, fortuitously, there seems to be linear relationship with peak pressure plotted on a log scale. The implication is that "% Acceptability" has a log normal distribution as a function of peak sonic boom pressure. The (Wyle analysis) line is substantially different from the line labeled (Leyman, 1988) (ref. 16) and, with the corroboration by the other data, is believed to be a more reasonable estimate of the relative acceptability of the type of sonic booms evaluated. According to this line, such sonic booms with a peak pressure of the order of 0.8 psf would be expected to be "acceptable" about 95% of the time. For sonic booms shapes similar to those in the past, with a rise time of 8 ms, this peak pressure would correspond to a Perceived Loudness of about 89 PLdB and a C-weighted Sound Exposure Level of about 99 dB. It remains to be shown if "shaped" sonic booms would be expected to follow the same trend.
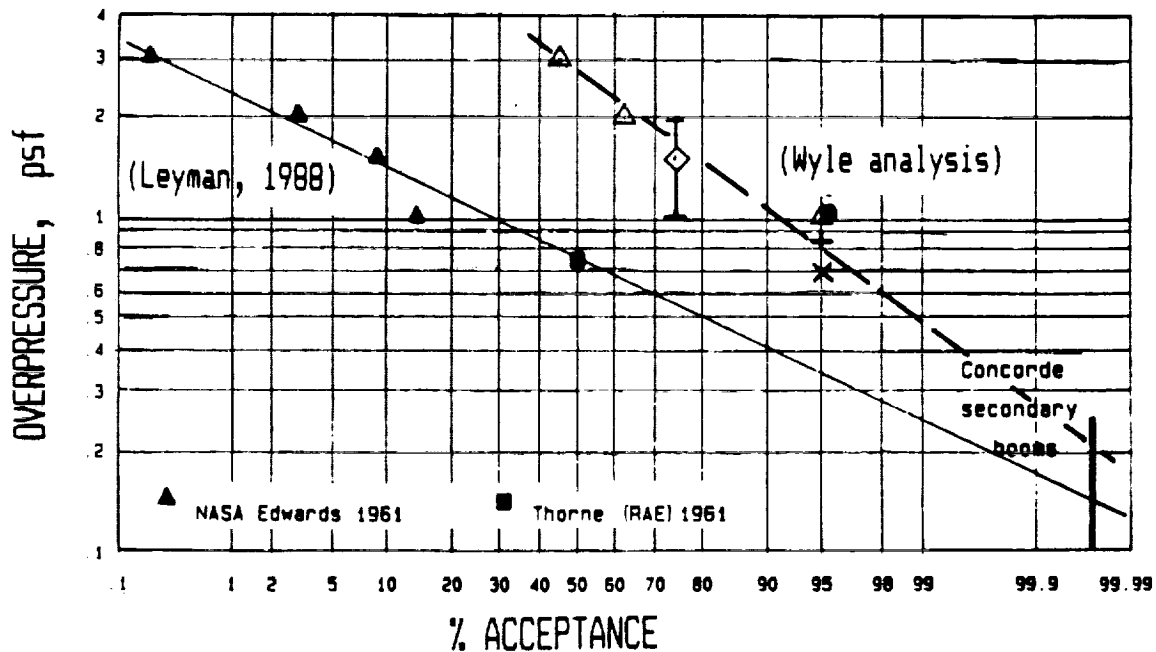


Figure 13. Summary of Sonic Boom Acceptance Data

# SUMMARY

1. A preferred set of descriptors for assessing human response to sonic booms is based on the Sound Exposure Level - the measure of the integrated squared pressure in a sonic boom.

2. Consistent with this foundation, the spectral content of a sonic boom signature should be expressed in terms of the Sound Exposure Spectrum Level which can be derived from the Fourier Spectrum of the pressure signature.

3. The predicted effect of rise time on loudness appears to be more important than any shaping (e.g., flat top) of the peak pressure time history providing the peak pressure are the same in all cases.

4. The relative loudness ranking of alternative wave shapes is predicted to be roughly independent of the listening environment assuming no vibration or rattle effects are involved.

5. Noise reduction models applied for indoor loudness evaluation seem to show that the most important frequency range for indoor loudness levels lies at or above the lowest wall panel modes and is not likely to be very sensitive to Helmholtz resonance responses occurring at lower frequencies.

6. Rattle effects may be very important for indoor listening based on previous field experience.

7. For 95% acceptability of sonic booms of the type experienced in previous SST sonic booms tests, the peak pressure would have to be about 0.8 psf, the C-weighted Sound Exposure Levels would be about 99 dB and the Perceived Loudness (Mark VII) would be about 89 PLdB.

# REFERENCES

1.  Stevens, D.G., Shepherd, K.P. Hubbard, H.H. and Grosveld, F.W., "Guide to the evaluation of human response to noise from large wind turbines," NAS Technical Memorandum 83288, March 1988. (Ref. 1-6 in Appendix C)

2.  Eldred, K. McK., "Noise and vibration characteristics of the CERL low frequency blast response facility west house," KEE Report 85-29.

3.  Anonymous, "Measurement and evaluation of environmental noise from wind energy conversion systems in Alameda and Riverside Counties," Wyle Research Report WR-88-19, October 1988.

4.  Sutherland, L.C., "Indoor noise environments due to outdoor noise sources," Noise Control Engineering 11(3), 124-137, November 1978.

5.  Sutherland, L.C., "Low frequency response of structures," Wyle Laboratories Report WR 82-18, May 1982.

6.  Stevens, S.S., "Perceived level of noise by Mark VII and decibels (E)," J.Acoust. Soc. Am. 51, 575-601, 1972.

7.  ANSI, "Procedure for the computation of loudness," American National Standard, ANSI S3.4, 1968.

8.  Zwicker, E. (1977) "Procedure for calculating the loudness of temporally variable sounds," J.Acoust. Soc. Am. 62: 675-682, 1977.

9.  Flindell, I, "A laboratory study of the perceived benefit of additional noise attenuation by houses," NASA Langley Research Center, NASA Technical Memorandum 85647, June 1983.

10. Bishop, D., "Judgements of the relative and absolute acceptability of aircraft noise," J. Acoust. Soc. Am. 40: 108-122, 1966.

11. Borsky, P.N., "Community reactions to sonic booms in the Oklahoma City area," National Opinion Research Center, AMRL Report-TR-65-37, Report I and II, 1965.

12. Nixon, C.W. and Borsky, P.N., "Effects of sonic booms on people: St Louis, Missouri, 1961-1962," Aerospace Medical Research Laboratory Report, AMRL Report-TR-65-196, 1965.

13. Kryter, K. et al., " Psychological experiments on sonic booms conducted at Edwards Air Force Base," Final Report, National Sonic Boom Evaluation Office, Arlington Virginia, 1968.

14. Carden, H.D. and Mayes, W.H., " Measured vibration response characteristics of four residential structures excited by mechanical and acoustical loadings," NASA Langley Research Center, NASA TN D-5778, April 1970.

15. Sutherland, L.C., Brown, R. and Goerner, D., "Evaluation of potential damage to unconventional structures by sonic booms," Wyle Laboratories, HSD-TR-90-021, May 1990.

16.    Leyman, C.S., British Aerospace Corporation, Personal Communication, 23 February, 1988.

17.    Higgins, T.H. and Sanlorenzo, E.A., "Psychological tests of potential design/certification criteria for advances supersonic aircraft," General Applied Science Laboratory, Inc., FAA-RD-75-110, 1975.

18.    Mabry, J.E. and Oncley, P.B., "Establishing certification/design criteria for advanced super-sonic aircraft utilizing acceptance, interference and annoyance response to simulated sonic booms by persons in their homes," Man-Acoustics and Noise, Inc., Report No. FAA-RD-75-44, 1975.

THIS PAGE INTENTIONALLY BLANK

*omit*

# Session X. Airframe/Propulsion Integration

THIS PAGE INTENTIONALLY BLANK

1366

# Session X. Airframe/Propulsion Integration

omit

PAI Session Overview and Review of Lewis PAI Efforts
*Peter G. Batterton, NASA Lewis Research Center*

THIS PAGE INTENTIONALLY BLANK

5/6-07
/2046

# PROPULSION AIRFRAME INTEGRATION
## SESSION OVERVIEW AND REVIEW OF LEWIS PAI EFFORTS

Peter G. Batterton
NASA Lewis Research Center
Cleveland, Ohio

Propulsion/Airframe Integration (PAI) is a key issue for the High Speed Civil Transport. The aircraft performance, economics, and environmental acceptability can be adversely affected if integration of the propulsion and airframe is not addressed properly or in a timely manner. Some of the goals for are listed in this figure. In particular, these goals are highly influenced by how successfully the propulsion system and airframe are integrated. These goals have been grouped by the "Aero" and "Propulsion" categories to suggest which group of technologists will likely be addressing them. In terms of the NASA High Speed Research Program, the ultimate objective for propulsion/airframe integration is to demonstrate the technologies for achievement of these goals on a "single" integrated configuration.

# HSR PAI GOALS

- *Demonstrate experimentally on a "single" integrated configuration, those technologies which allow:*

-- *(Aero)*          SS Cruise L/D 10
                     Transonic L/D >15
                     Take Off L/D 10

-- *(Prop)*          Exceeds FAR 36 Stage III
                     Favorable impact on inlet and
                        nozzle performance

1370                 Figure 1

## PROPULSION/AIRFRAME INTEGRATION TECHNOLOGY FOCUS

For the High Speed Research Program propulsion/airframe integration technology development, three basic integration technology areas have been selected for focus. First is the nacelle-airframe interference and interactions where installation effects on drag and lift are addressed. For example, the flow around the propulsion system can influence the local pressure field on the wing and result in a change in the lift and drag characteristics of the wing. The goal is to achieve integrated system drag and/or lift values to be better than their isolated values. Second is the impact of the external flowfield on the propulsion system performance and stability. An example would be wing or other aircraft component effects on inlet or nozzle performance. Third is the impact of nacelle and airframe flows on acoustics. For example, the wing flowfield effect on the nozzle take-off acoustic suppression. An ideal concept would be a suppressor design which can take advantage of both the wing flowfield characteristics and geometric shielding.

# *HSR PROPULSION/AIRFRAME INTEGRATION*

- *Nacelle-airframe interference and interactions (lift & drag)*

- *Flowfield effects on internal performance*

- *Nacelle-airframe effects on acoustics*

Figure 2

# TECHNOLOGY ISSUES - SUMMARY FROM JUNE 1990 REVIEW

To initiate the High Speed Research Program PAI planning activities, a preliminary PAI meeting was held in June 1990 for industry to provide NASA with an update on PAI technology issues, developments and requirements since the Supersonic Cruise Aircraft Research Program. We believed this joint meeting to be a good initialization point for HSR planning as well as a catalyst for industry and NASA focus on the critical role of PAI. Because of the timing, a key objective of the workshop identification of PAI issues which affect achievement of the HSR $\phi$-I Program. As summarized in the figure, there were four areas identified at the meeting as "high priority" and which met this objective. These four areas have been denoted by the check-marks in the figure. For example, achievement of take-off noise levels below FAR Part 36, Stage III is a key HSR $\phi$-I goal, but PAI issues such as the wing/flap trailing edge flow-field interactions with the nozzles and their acoustic suppression characteristics has yet to be identified. Compared with ten or more years ago, considerable progress has been made with the computational fluid dynamics (CFD) codes and analyses, but little experimental validation has been done to assure their applicability for HSCT designs. Nacelle placement and shape trade-offs which effect system drag and lift need to be updated from prior efforts to accommodate today's aerodynamics and cruise Mach number. Lastly, particularly for cruise Mach numbers greater than 2.2 or so, mixed-compression inlets are required for performance. If inlet unstart can not properly be handled, then cruise Mach number would be potentially decided by a PAI issue.

## *TECHNOLOGY ISSUES - PAI*
### *Summary from June 1990 Workshop at Lewis*

✓ *2D vs. AXISYMMETRIC NOZZLES*

    NOISE    —    ENG/ENG Shielding

            —    ENG/Wing

✓ *CFD VALIDATION DATA BASE (Placement/shape)*

    ARC MODEL    —    MACH No.

                 —    2D & Axisym

✓ *2D vs. AXISYMMETRIC INLETS, NACELLES*

✓ *UNSTART CRITERIA & CONTROLS, CERTIFICATION*

    — AIRCRAFT & PASSENGER RESPONSE TO UNSTART - $\phi$- I STUDY

● *CONTROLS*

● *MACH NO.?*

● *ACCESSORIES & SECONDARY POWER*

✓ = PRIORITY

1372

Figure 3

## PAI ACTIVITIES INITIATED FOLLOWING JUNE 1990 REVIEW

As a direct consequence of the June PAI 1990 meeting, several in-house and contract research activities and studies have been initiated. These are listed in this figure. A preliminary wing-flow/low noise nozzle experiment and analysis activity has been initiated. This paper will expand on this activity below. Regarding the second item, C. Domack will address his studies on the effects on mixed-compression inlet unstart on HSCT aircraft dynamics in a paper later in this session. Also, G. Cappuccio will present the status and plans for experimental/analytical research on nacelle shape and placement immediately follows this paper. This propulsion-airframe model used to study nacelle placement in 1973 has been located and is being refurbished. Figures and brief descriptions will follow below. And lastly, contract studies expanding on the inlet/nacelle/nozzle geometry trades have been initiated. This session of the HSR Workshop contains papers from Boeing and Douglas on their efforts.

# HSR PROPULSION/AIRFAME INTEGRATION

## ACTIVITIES INITIATED FOLLOWING JUNE 1990 REVIEW

*1. Wing flow / low noise nozzle experiment/analysis*

*2. Unstart effects*

*3. Nacelle placement*

*4. Inlet/Nacelle/Nozzle, Axi vs. 2D, etc.*

- CONTRACTS -

| | | |
|---|---|---|
| Boeing | – | Inlet Screening, Weight (TBE Emphasis) |
| Douglas | – | Inlet Screening (FLADE Emphasis) |
| Lockheed | – | Nozzle/Nacelle Integration |

Figure 4

At Lewis Research Center, low noise nozzles are aggressively being pursued for take-off conditions under the HSR $\phi$-I program. Specifically, the research is focussing on ejector-type flow augmentation schemes to reduce jet velocities and thereby reduce noise. In current study designs as depicted in this figure, these ejector-type flow augmentors require secondary air intakes which are located aft of the trailing wing/flap trailing edge. As a consequence, the flowfield at the ejector secondary air intakes will likely be quite complex and certainly different than what occurs around the isolated nozzle jet exit rigs currently being used to study nozzle acoustics. Thus ejector secondary performance will be affected and therefore the acoustic suppression characteristics of the nozzle/ejector system. This is a prime example of how propulsion/airframe integration has a direct impact on achieving HSR $\phi$-I goals.

## PAI AFFECTS NOZZLE ACOUSTIC SUPPRESSION
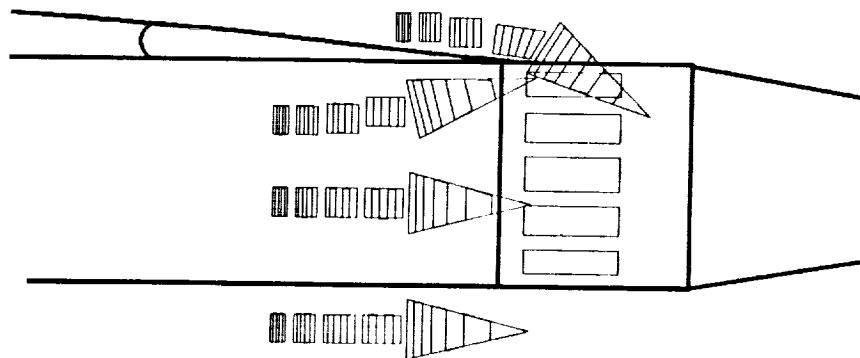


- ## WING AND TRAILING-EDGE FLAPS ALTER NOZZLE EXTERNAL AND EJECTOR-INLET FLOWFIELD.

- ## HENCE, ACOUSTIC SUPRESSION CHARACTERISTICS WILL BE ALTERED.

Figure 5

# INSTALLATION EFFECTS TEST WITH JET EXIT RIG AND WING

Experimental acoustic evaluations of axisymmetric and 2D nozzles are planned for Fall of 1991 at Lewis. The basic problem discussed on the previous page can be addressed on a preliminary basis by adding a wing-section to these nozzle tests as depicted in the figure. This wing would have appropriate sweep and high-lift devices at the leading and trailing edges to allow it to be generically representative of an HSCT design. The experiment will include variable flap settings and the ability to vary the position of the wing from the secondary inlets and jet exit rig. Planned measurements include not only pressure and acoustic measurements but also LDV. From such an experiment, we expect to begin development of an PAI experimental database for aero performance, acoustic, and flowfield analyses for wing/nozzles. Specifically, the results of this experiment will be used to validate CFD codes for nozzle-wing-nacelle type flows. The main challenge is to combine analysis of internal and external flows about complex configurations; the code can then be applied to more realistic configurations. For this a generic wing/nozzle configuration, we also expect to determine the first-order effects on the acoustic characteristics of ejector nozzles due to non-uniform external flow into the ejectors and an early assessment ejector nozzle aerodynamic performance as a result of installation.

## JET EXIT RIG WITH A GENERIC WING SHAPE FOR INSTALLATION EFFECTS



9' X 15' ACOUSTIC WIND TUNNEL PROPOSED ARRANGEMENT

REAR VIEW          TOP VIEW          SIDE VIEW

Figure 6                                                    1375
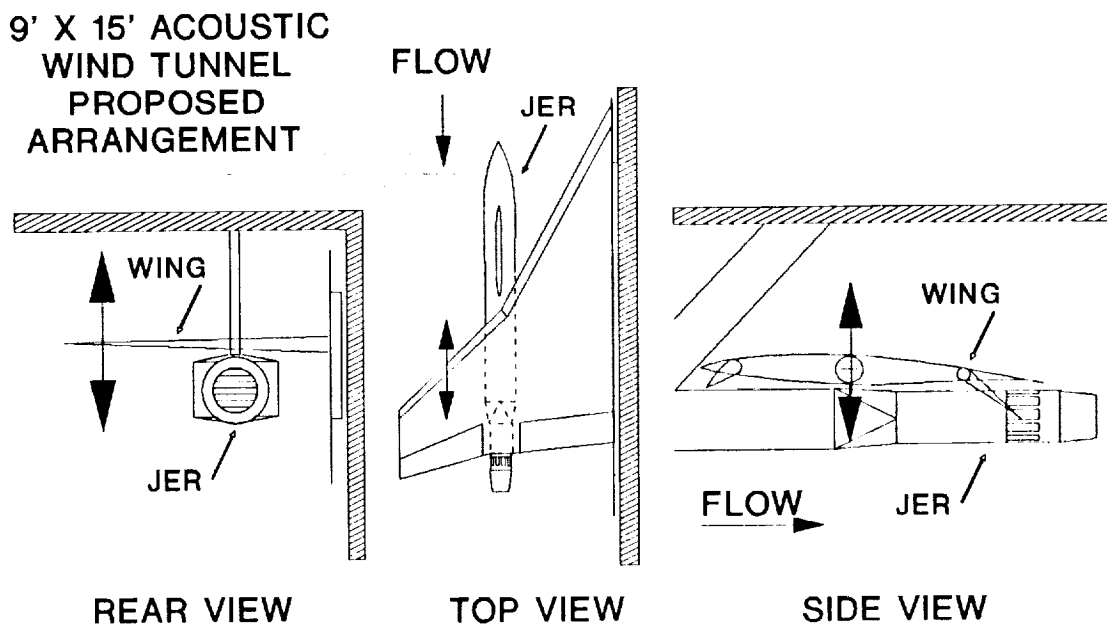
# MIXED COMPRESSION SUPERSONIC INLET INSTABILITY

This figure introduces the subject of mixed compression supersonic inlet unstart which leads to the concern regarding certification of mixed compression inlets. Above cruise Mach numbers of approximately 2.2, mixed compression inlets provide superior performance over other types. A mixed compression supersonic inlet has a portion of its supersonic diffusion (compression) occur inside of the inlet cowl lip. Two "grossly" stable conditions can occur for this type of design. The inlet normal shock is contained just downstream of the inlet throat for the first, and desirable, condition. The second condition occurs when this normal shock is expelled from the and the inlet throat is either subsonic or choked. This second condition results in poor inlet performance, which also may be unstable (buzz), and asymmetric drag and/or lift conditions on the aircraft. Transition from the first to the second condition, called an "unstart," can be caused by an external event such as a gust or angle of attack change, or by engine airflow transients. Passenger safety and comfort issues as well as aircraft stability and control problems can result if the consequences of the unstart are severe. Considerable debate has occurred on this subject because of the potential impact on cruise Mach number, NASA Langley has been studying this problem in some depth. C. Domack will report on the initial results. Additional contract studies are planned.



MIXED COMPRESSION SUPERSONIC INLET INSTABILITY

1376                    Figure 7
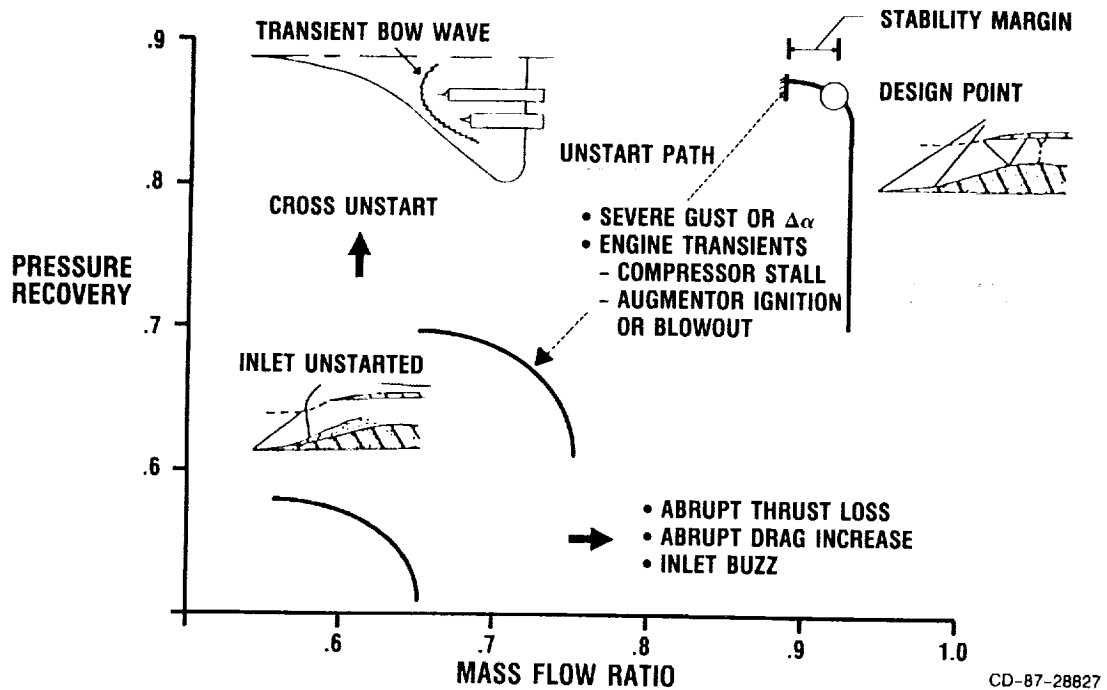
## NACELLE/AIRFRAME INTERFERENCE TEST

A propulsion airframe interference test was conducted in the Ames 11- by 11-Foot Transonic Wind Tunnel in 1973. The purpose of the test was to measure detailed interference force and pressure data on a representative supersonic wing-body-nacelle combination at transonic speeds. The aerodynamic model is based on Boeing's model SA1150 and is a delta wing-body configuration at 0.024 scale. All hardware associated with the model has been recovered and is in the process of being refurbished. Of the four individual nacelles supported beneath the wing-body model, the two on the left-hand side were pressure instrumented, and the other two were force instrumented. The four nacelles were supported beneath the wing-body independently by the nacelle support system, providing flexibility of positioning the nacelles relative to the wing-body and each other. Future PAI plans associated with this model and testing in the Ames 9- by 7-Foot Wind Tunnel scheduled for June 1992 as well as additional information about nacelle shape and placement research issues and plans will be presented by G. Cappuccio in the next paper.
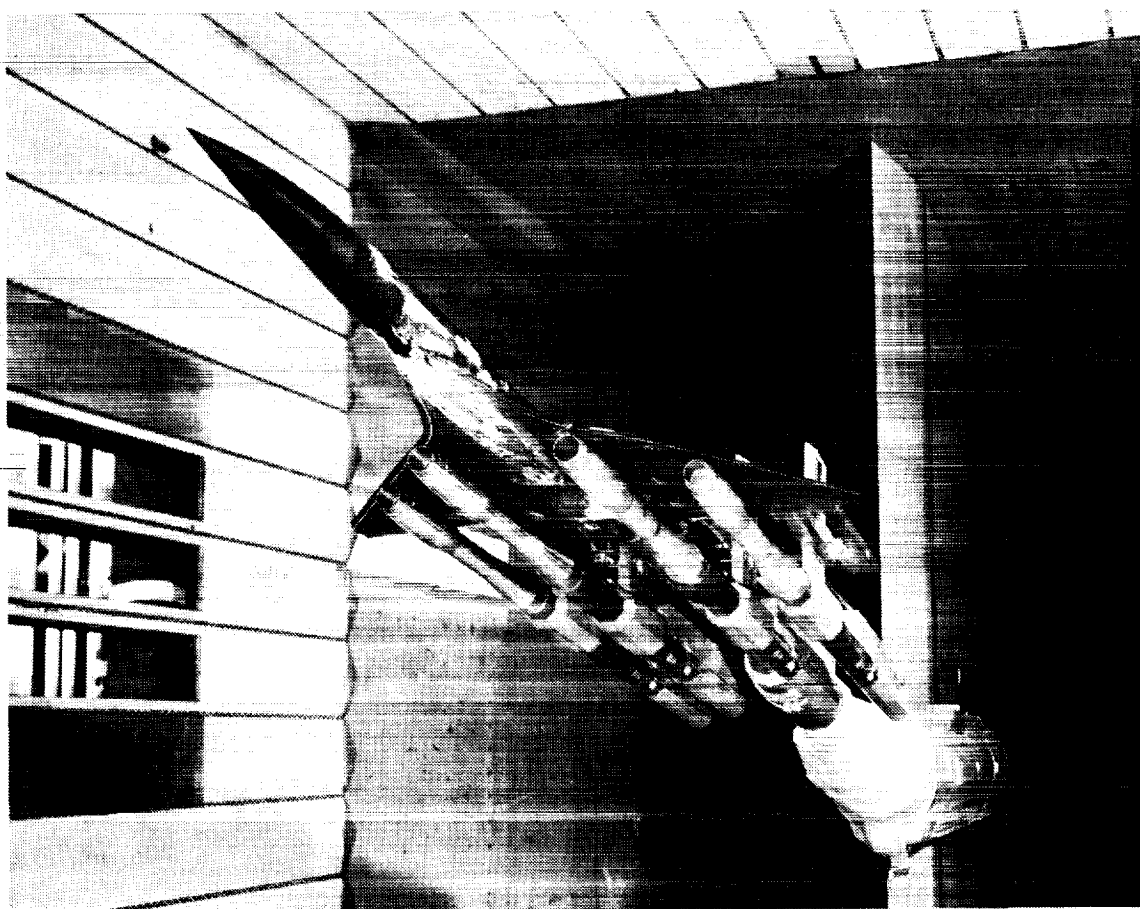


Figure 8

# PROPULSION/AIRFRAME INTEGRATION PLAN OVERVIEW

Looking ahead from the near-term to the 1993 through 1999 time period and HSR $\phi$-II, a preliminary view of the general scope and milestones for PAI are shown in this figure. The basic concepts shown in this figure were developed as part of the HSR Non-Advocate Review effort. (The Non-Advocate Review project plan identified the basic scope for the overall HSR $\phi$-II Program.) This preliminary PAI plan identifies an on-going analytical tools/CFD codes assessment occurring in parallel with the experimental portions of the program. The milestone times are meant to be indicative of experimental knowledge availability in support of these analyses and as validation of technologies and concepts. For the purposes of this figure, the main experimental elements of the program have been divided between three categories of PAI identified in figure 2 above. At the conclusion of the plan (1998/99), several "systems" experiments would be accomplished including integrated tests of the inlet, engine and nozzle at supersonic speeds and at low speed (take-off). Transonic tests would be accomplished using a simulator powered sub-scale model.

## HSR
## PROPULSION-AIRFRAME INTEGRATION PLAN OVERVIEW



*NAR - UNFUNDED

50PGB016
LAN 4/16/91

1378
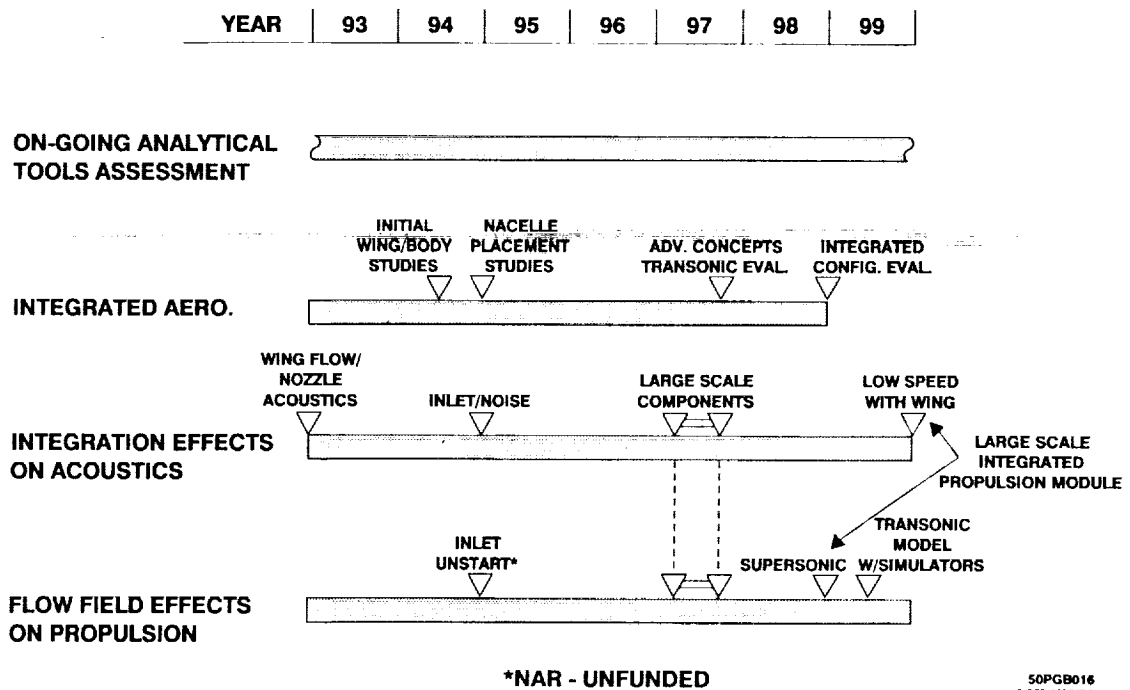
Figure 9

## SUMMARY

Industry will decide on final HSCT requirements, and NASA should provide the options to minimize the HSCT risks. In this regard, the NASA HSR PAI role is viewed as delivering the following: validated airframe and nacelle design procedures and methodologies, validated diagnostic procedures and test techniques, and an experimental knowledge base for analytical code(s) validation and for design trades. The program we are pursuing is designed to address these deliverables so that the tools and technologies as well as the concepts are available to permit a low risk, environmentally and economically acceptable HSCT. In conclusion, the HSR Propulsion/Airframe Integration efforts are viewed as critical to a successful HSCT. The HSR $\phi$-I goals which could be affected by PAI issues are being addressed. And finally, long-lead PAI activities have been identified and steps are being taken to initiate them.

THIS PAGE INTENTIONALLY BLANK

# Session X. Airframe/Propulsion Integration

*omit*

Nacelle-Wing Integration
*Gelsomina Cappuccio, NASA Ames Research Center*

THIS PAGE INTENTIONALLY BLANK

517-05
12047

# Nacelle-Wing Integration

Gelsomina Cappuccio
National Aeronautics and Space Administration
Ames Research Center
Moffett Field, CA

First Annual High-Speed Research Workshop
Williamsburg, VA
May 14-16, 1991

The Aerodynamics Division at NASA Ames Research Center is participating in the propulsion airframe integration phase of the High Speed Research Program. The two areas of research being pursued include an experimental program and analysis using computational fluid dynamics. The Applied Aerodynamics Branch is conducting the experimental program, which will involve a nacelle airframe model that was tested in the Ames 11- by 11-Foot Transonic Wind Tunnel in 1973. This branch will also assess various Euler codes in predicting nacelle airframe interference effects. The goal is to provide industry with the necessary data and tools to design a high speed civil transport with favorable propulsion airframe interference.

# Topics of Discussion

- **Experimental Program**

- **Computational Fluid Dynamics Research**

Figure 1

A nacelle-airframe interference test was conducted in the Ames 11- by 11-Foot Transonic Wind Tunnel in 1973, reference 1. The purpose of the test was to measure detailed interference force and pressure data on a representative supersonic wing-body-nacelle combination at transonic speeds, $0.9 \leq M \leq 1.4$. The basic aerodynamic model was of the final Boeing supersonic transport configuration (Boeing model SA1150). Four independently supported nacelles were positioned beneath the model. The nacelle support system provides the flexibility of varying the nacelle positions relative to the wing-body and to each other and controls the mass flow through each nacelle. The primary variables examined were Mach number, angle of attack, nacelle position, and nacelle mass flow ratio. Four configurations were tested: isolated nacelles, four nacelles as a unit, isolated wing-body, and wing-body-nacelle combination. The data acquired from this test is used extensively by industry. In preparation for phase II of the High Speed Research Program, there has been a high interest in expanding the drag interference database on this model to a higher supersonic regime.

## Background

- **Test conducted in 1973 in the NASA Ames 11 ft Transonic Wind Tunnel**

- **SA1150 wing-body and axisymmetric nacelles independently supported**

- **Current database of wing-body and nacelle interference forces and pressures at** $.9 \leq M \leq 1.4$

- **Database is used extensively by industry**

Figure 2

Figure 3 is a photo of the nacelle-airframe model installed in the Ames 11- by 11-Foot Transonic Wind Tunnel in 1973. This figure illustrates how the nacelles are mounted separate from the the wing-body. The nacelles are attached to stings where the mass flow plugs are housed. The nacelle stings are attached to the nacelle support system, which is attached to the main sting of the wing-body.
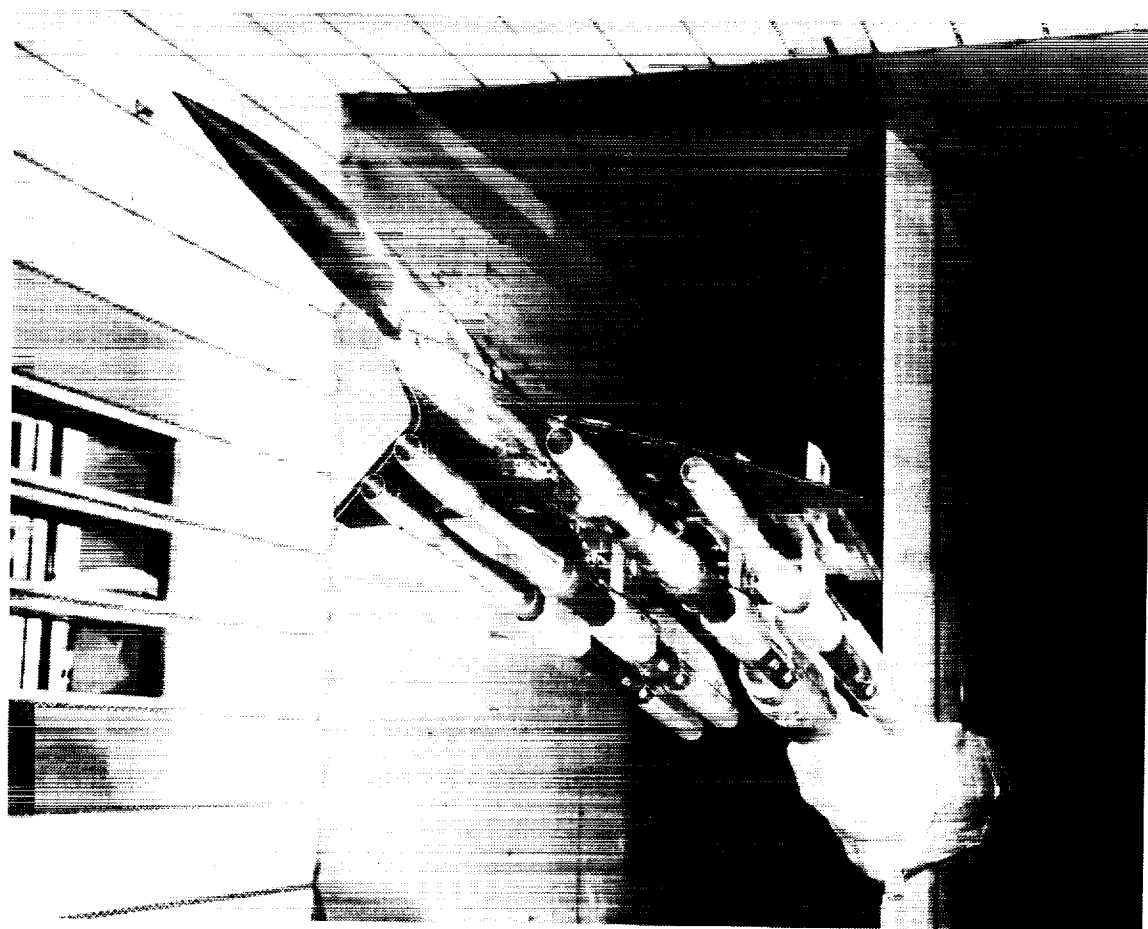


Figure 3. Nacelle-Airframe Model Installed in the Ames 11- by 11-Foot Transonic Wind Tunnel

The data acquired during the 1973 nacelle airframe interference, NAI, test has been extensively used by both Boeing and Douglas in their development of a high speed civil transport. The NASA Lewis Propulsion Airframe Integration, PAI, meeting in June 1990 showed strong support from Boeing and Douglas for an expanded program. It has also been identified at the Non-Advocate Review as a key technology and is also strongly supported by NASA Lewis and Langley. There are three main objectives for the planned NAI test. This test will be conducted in the Ames 9- by 7-Foot Supersonic Wind Tunnel June 1992. The first is to expand the current database to $1.5 \leq M \leq 2.5$ for the SA1150 model with the existing axisymmetric nacelles. The second objective is to assess the integration characteristics for more representative nacelles for an advanced high speed civil transport. This will be accomplished by using nacelles that are derived from the PAI tasks, which Boeing and Douglas have with NASA Lewis, or other representative nacelles needed in supersonic flows. We feel that this test can provide industry with very important data. In addition, recent sonic boom tests have indicated that nacelles have an impact on aircraft sonic boom signature. The third objective is to use the SA1150 model to study nacelle influences on sonic boom in terms of nacelle position, shape, number, and mass flow ratio. This would require developing a sonic boom measuring technique on large scale models and assessing the adequacy of data taken relative, within on span length, to the configuration.

## Nacelle-Airframe Interference Test
## Current Program Objectives

- **Expand database to $1.5 \leq M \leq 2.5$ of the SA1150 model with existing axisymmetric nacelles in Ames 9 x 7 Supersonic Wind Tunnel**

- **Assess the integration characteristics for nacelles derived from NASA Lewis propulsion airframe inlet tasks with Boeing & Douglas or other representative nacelle shapes for a high speed civil transport**

- **Study nacelle influences on sonic boom**
    - **\* position**      **\* shape**
    - **\* number (2 to 4)**      **\* mass flow ratio**
- **Develop sonic boom measurement techniques for large models**
    - **7 feet of probe travel is required for this model**

**Figure 4**

The SA1150 is a delta wing-body model with an axial length of 62.2 inches and a wingspan of 40.8 inches. The model is mounted on a six-component force balance and the left hand wing is pressure instrumented with a total of 126 static pressure orifices, 95 on the lower surface and 31 on the upper surface. The SA1150 model is being refurbished which has included checking all the pressure instrumentation. To this point all pressure instrumentation is intact and flow through except for three orifices. The wing-body model is in the process of being put back together and an interrogation will be performed to obtain a computer definition of the model. This will become the documented definition of the SA1150 model. Two different nacelle geometries were tested. Both nacelle geometries were axisymmetric. One set of nacelles had sharp inlet lips while the other had slightly blunt inlet lips. The two left-hand side nacelles were pressure instrumented and the two right-hand side nacelles were force instrumented. Each of the pressure instrumented nacelles had 48 static pressure orifices located in four rows equally spaced around the nacelles. The six component force balances used to support the right-hand nacelles were housed in the thickness of each nacelle. These nacelles, balances and balance calibration equipment are available and need to be assessed for any damage incurred over the past 18 years. The nacelle support system, control box that controlled all remotely controlled movements of the nacelles and mass flow, nacelle and wing-body stings, and pylons have all be located and are in storage at Ames. All hardware that was used in the previous test will be available for the planned NAI test. New hardware and modifications to old hardware will be made as appropriately needed.

## Hardware

- **Wing-Body configuration of Boeing model SA1150**
  - \* All but 3  pressure orifices of the left-hand wing (126 orifices: 95  lower, 31 upper) are intact and flow-through
  - \* In the process of being cleaned up and put back together
- **Axisymmetric nacelle geometries**
  - \* 4 sharp and 4 blunt inlet lip nacelles
  - \* Left hand side pair- pressure instrumented (48 orifices)
  - \* Right hand side  pair - force instrumented (6 components)
- **Axisymmetric nacelle balances and calibration equipment**
- **Nacelle support system fully intact**
- **Control box**
- **Sting assembly**
- **Pylon installation available**

Figure  5

The nacelle balances are basically a two-shell flow through force balance using four instrumented flexures located 90° apart at two axial locations, for a total of eight flexures. The balances were intended to measure only the aerodynamic forces on the external surface of the nacelle, however, for mechanical reasons it became necessary to include the aerodynamic forces on the initial 2.30 inches of the internal surface as indicated in figure 6. To prevent flow through the balance cavity, the metric and nonmetric components were bridged by a flexible rubber seal. The metric part of the force instrumented nacelles include the external contour and internal lip surface on the balance. Incorporated into each nacelle sting is a mass flow control plug and appropriate pressure instrumentation to measure the flow through each nacelle. Each plug is remotely controlled. The pressure instrumentation consists of a 16-tube total pressure rake (4 radial rakes, 4 probes per rake) and 4 exit static pressure orifices in each nacelle sting.

# Nacelle Flow Through Balance
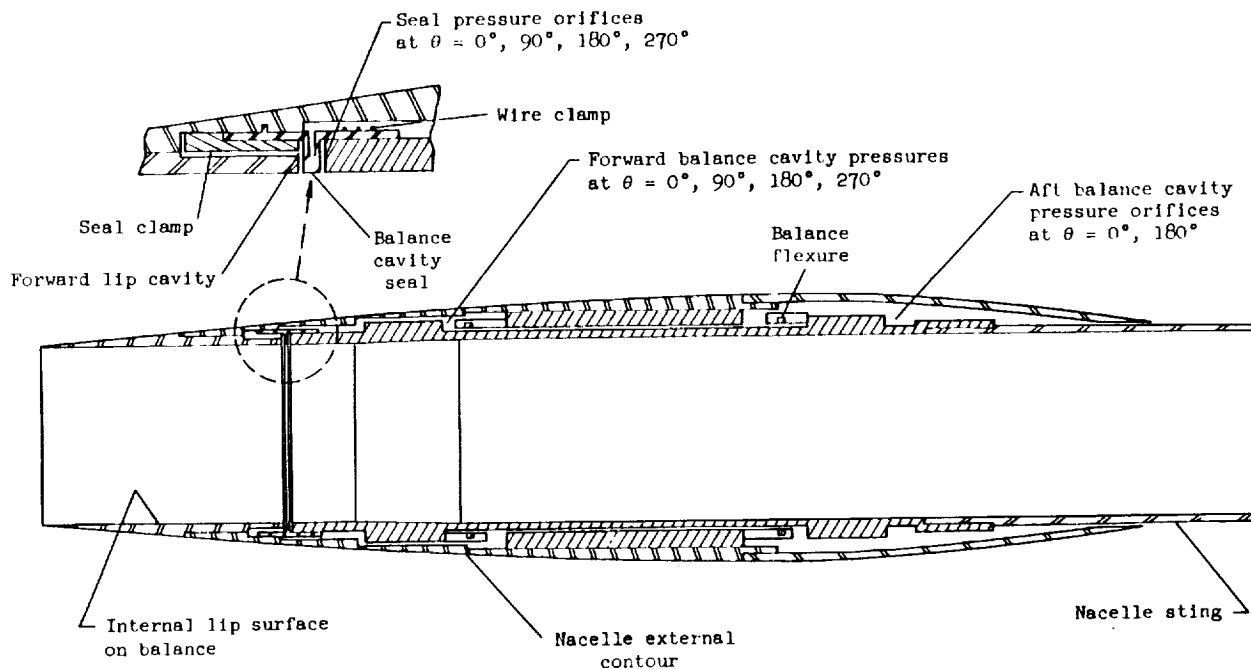


Figure 6.  Nacelle Flow Through Balance

The nacelle support system, figure 7, can independently support four nacelles beneath the wing-body and provide flexibility of positioning the nacelles relative to both the wing-body and to each other. The nacelle support system can also provide for the independent control and measurement of the mass flow through each nacelle. The major components of the nacelle support system consists of the main cross support, four vertical support and positioning units, and four flow through nacelle stings and flow metering units. Eleven independent drives provide a three-dimensional nacelle positioning capability. They include 2 lateral drives, which position the inboard and outboard nacelle pairs symmetrically about the vertical centerline; 4 vertical drives to control the vertical position of the four nacelle stings; and the axial position of each nacelle is controlled by two independent axial drive units: the main drive controls the position of the main cross support (position of all four nacelles as a single unit) and each nacelle sting has its own individual drive unit which allows the position of each nacelle to be varied relative to the other three nacelles. Of the eleven drives all were remotely controlled except the four vertical drives, which were manually operated.
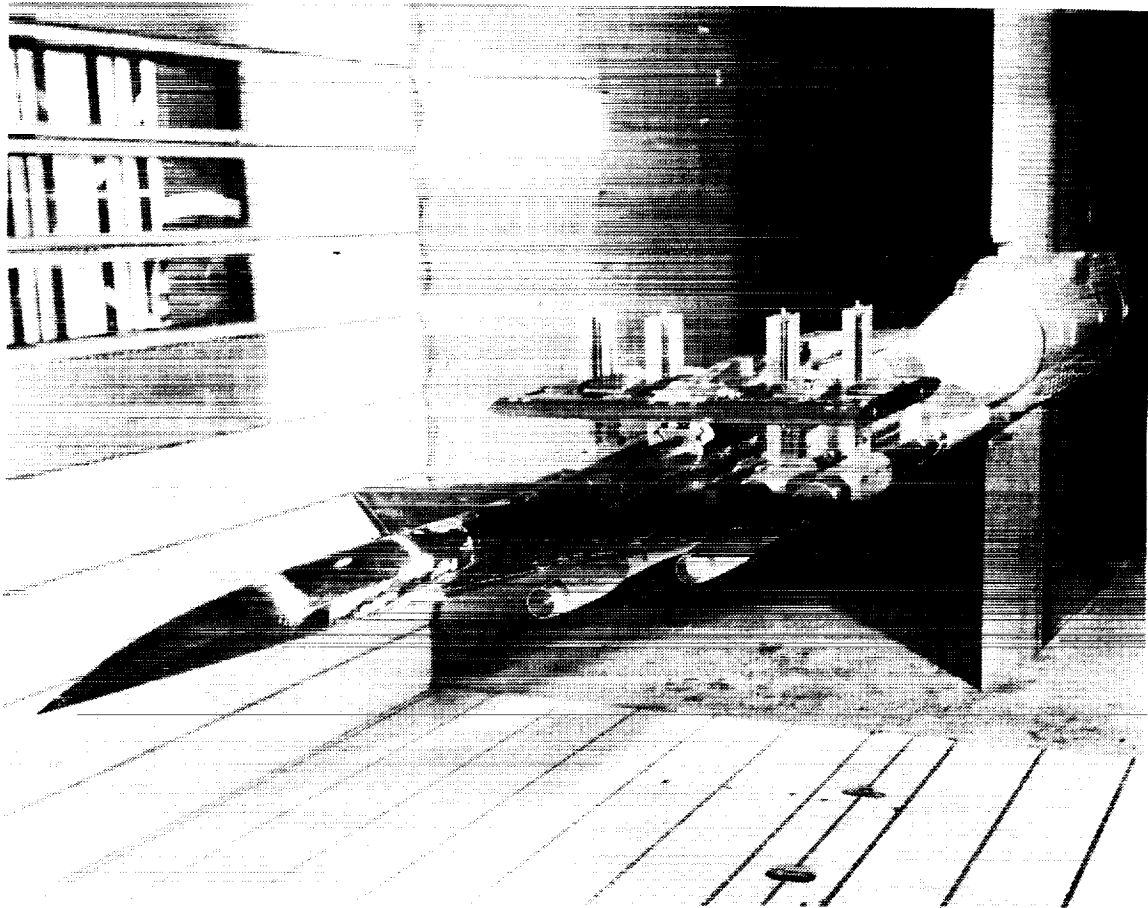


Figure 7. Wing-body-nacelle Configuration with Nacelle Support System

The NAI test is planned for June 1992, as outlined in figure 8. The refurbishment of the SA1150 model has begun and will continue to be refurbished. Work to refurbish the nacelle support system and the existing axisymmetric nacelles and balances will begin soon under the Precision Model contract at Ames. The representative nacelles to be tested are going through the aerodynamic designs and will be designed and fabricated during the second half of calender year 1991. Design and fabrications for sonic boom measurement equipment will also be worked this year. Model and Test preparations will be an ongoing process for such a complex wind tunnel test. The test will be a cooperative effort between NASA Ames, Boeing, and Douglas.

## Nacelle-Airframe Interference Wind Tunnel Model
## Schedule & Milestones

| FY | | 91 | | 92 |
| --- | --- | --- | --- | --- |

| Month | 3 4 5 6 7 8 9 | 10 11 12 1 2 3 4 5 6 7 |
| --- | --- | --- |
| Refurbish Model | | |
| SA1150 | | |
| Nacelle Support System | | |
| Inspect Model | | |
| Nacelle Aero Designs | | |
| Nacelle & Balance Designs | | |
| Nacelle & Balance Fab | | |
| Calibration Rig Fab | | |
| Probe Extension Design and Fab | | |
| Model and Test Prep | | |
| W/T Test in 9x7 and 11 Ft | | |
| W/T Down for Maintenance | | |
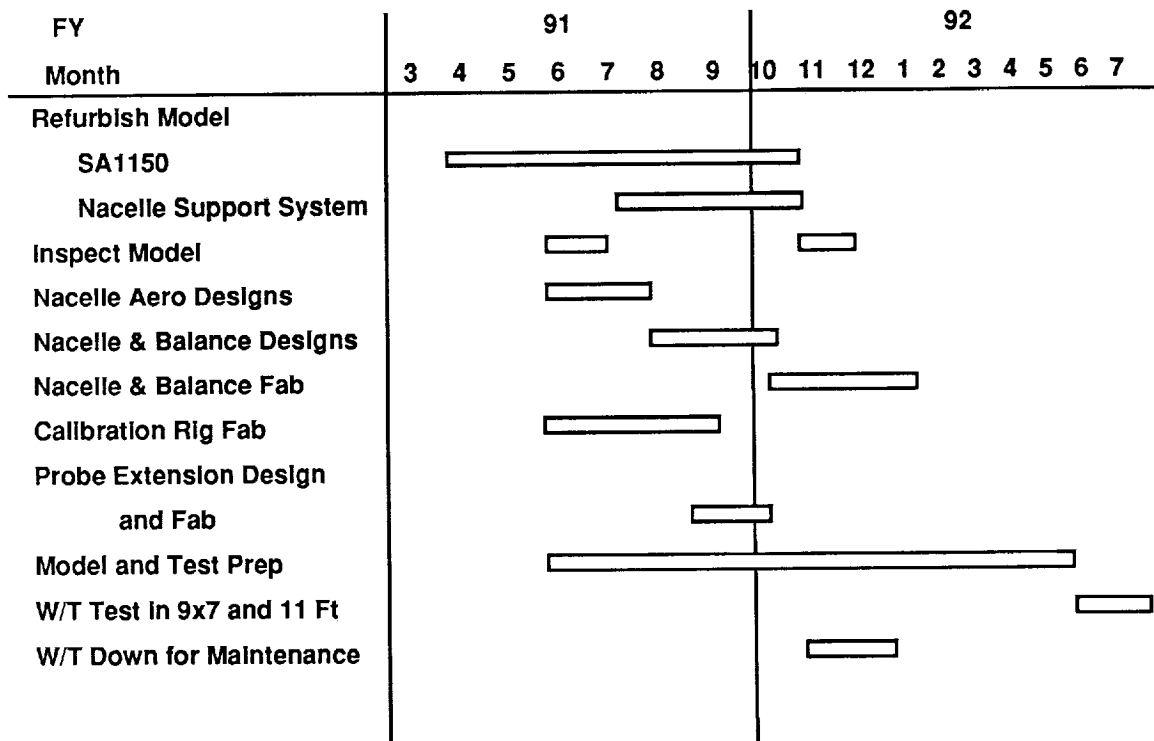
Figure 8. Schedule and Milestones for Nacelle-Airframe Test

In addition to preparing for a nacelle airframe test, Ames has begun assessing computational fluid dynamic,CFD, methods for calculating nacelle-airframe interference effects on a high speed civil transport. The SA1150 model with the axisymmetric nacelles serves as the CFD validation model. The SA1150 wing has been modeled based on data in reference 1. The sharp inlet lip nacelles have also been modeled. Euler calculations have been made on this configuration using TEAM, Three-dimensional Euler/Navier Stokes Aerodynamic Methods. TEAM is a multi-block code based on FLO57 and was developed by Lockheed under contract to the Air Force, reference 2. The case run was for Mach 1.4 and an angle of attack of 3 degrees. Sonic boom signatures have also been calculated based on the TEAM solution at 0.3 body lengths away. The CFD data was then extrapolated to 3.6 body lengths away. A comparison was made to wing alone, wing with flow through nacelles, and blocked nacelles.

# CFD Analysis

- Modeled SA1150 wing and axisymmetric sharp inlet lip nacelles

- Euler solution at M=1.4, $\alpha=3°$, and flow through nacelles

- TEAM code

- Sonic boom calculations based on TEAM solution at h/l=0.3 and extrapolated to h/l=3.6 for wing alone, and flow through and blocked nacelles

Figure 9

GRIDGEN, reference 3, was used to generate the grid for the TEAM code. A total of 38 blocks were needed to define the flowfield grid in an efficient and flexible way. The internal duct of the nacelles were modeled for the flow through case, while a solid face boundary condition was placed at the hilight of the nacelles for the blocked nacelle case. Figure 10 illustrates the surface grid of the SA1150 wing and the axisymmetric sharp inlet lip nacelles. Included is the symmetry plane.

## Wing and Nacelle Surface Grid
## &
## Symmetry Plane
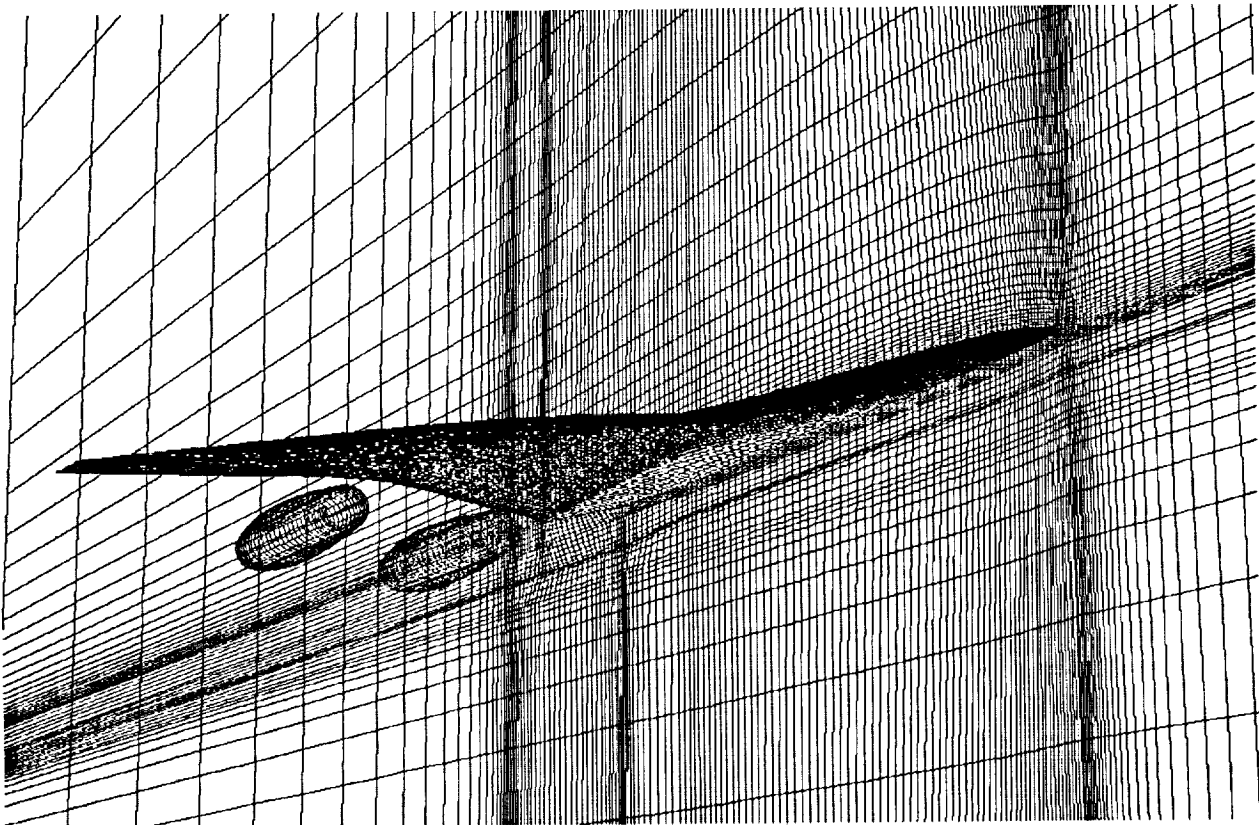


Figure 10. Wing and Nacelle Surface Grid Including the Symmetry Plane

Figure 11 illustrated a grid plane that intersects the wing and nacelles just ahead of the trailing edge of the wing. An H-H grid is used everywhere except in the internal nacelle ducts where an O-H grid is used. A total of approximately 725,000 grid points exists in the entire flowfield which is considered coarse for an Euler grid.

## Grid Plane Through Wing and Nacelles
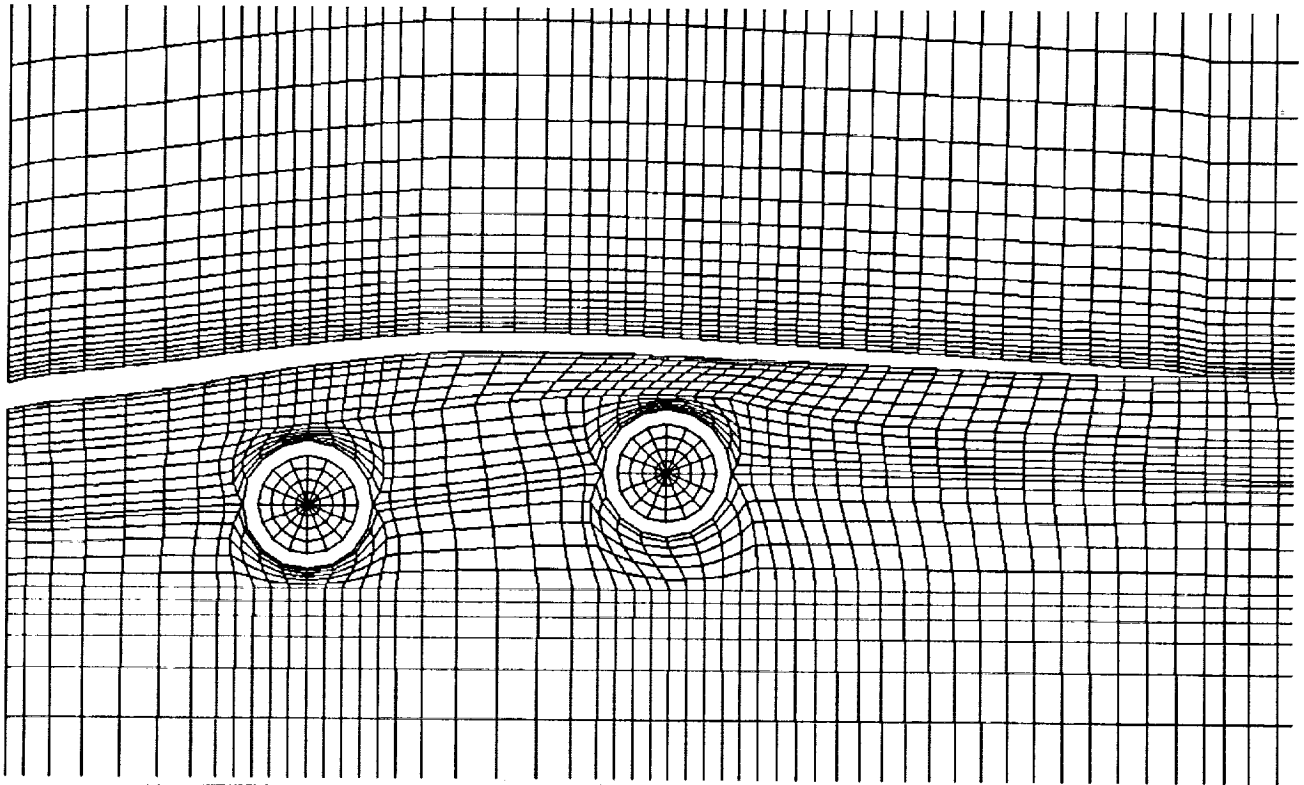


Figure 11. Grid Plane Through Wing and Nacelles

Figure 12 illustrates the Mach number distribution on the lower surface of the wing. Outlines of the nacelles are placed to point out the interference effects on the wing due to the nacelles.

## Lower Surface Mach Number Distribution

## SA 1150 Model

## Nacelle-Wing Combination



Euler Solution
Flow Through Nacelles
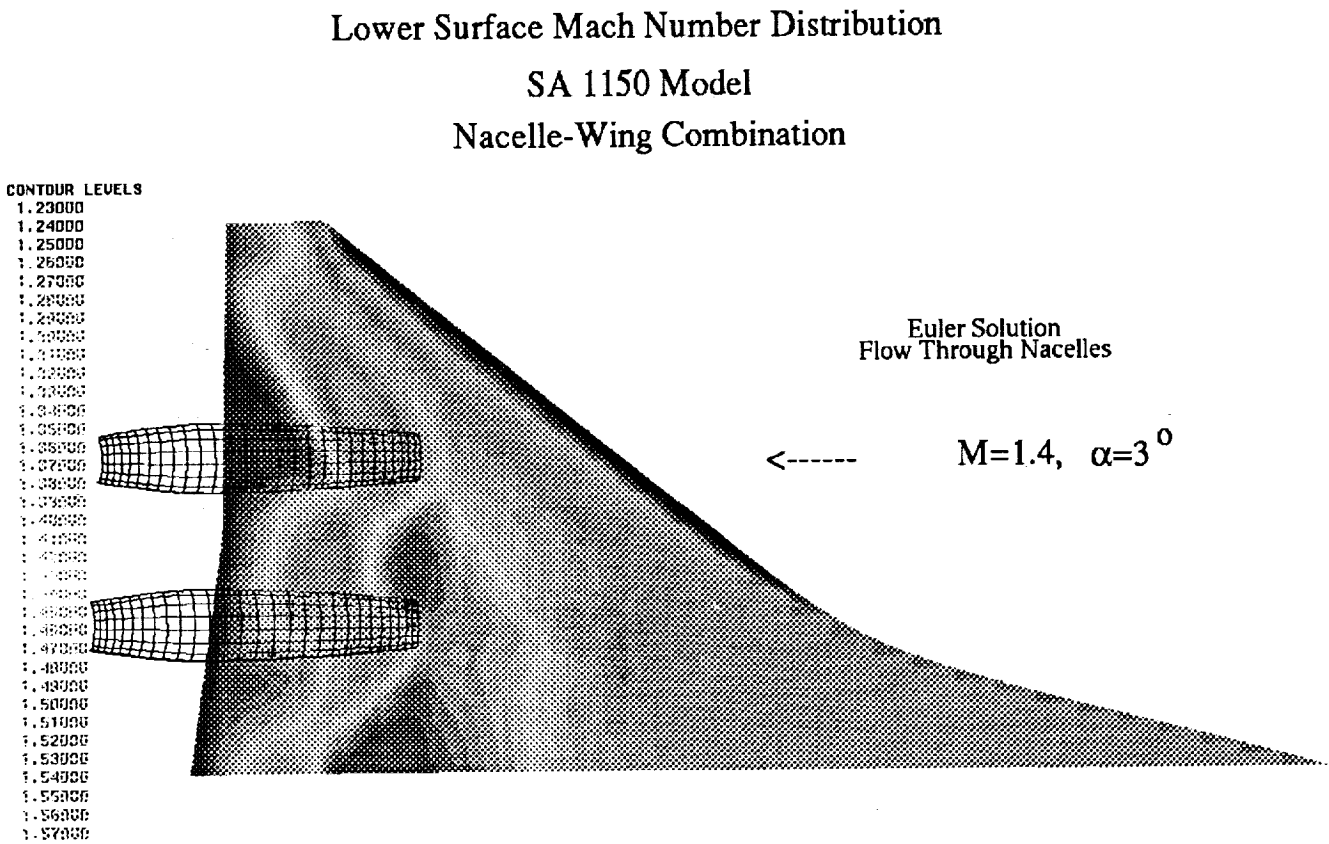
<----- $M=1.4, \quad \alpha=3^{\circ}$

Figure 12.   Lower Wing Surface Mach Number Distribution, TEAM Solution

Upper Nacelle Surface Mach Number Distribution
SA1150 Model
M=1.4, α=3°

Figure 13 is the Mach number distribution on the upper external half of the nacelles as well as that plane that intersects the nacelles parallel to the wing surface. This illustrates the wing effects on the nacelles as well as the nacelle-nacelle interference effects.

## Upper Nacelle Surface Mach Number Distribution
### SA 1150 Model
### M=1.4, α=3 °



CONTOUR LEVELS
1.14000
1.16000
1.18000
1.20000
1.22000
1.24000

Euler Solution
Flow Through Nacelles
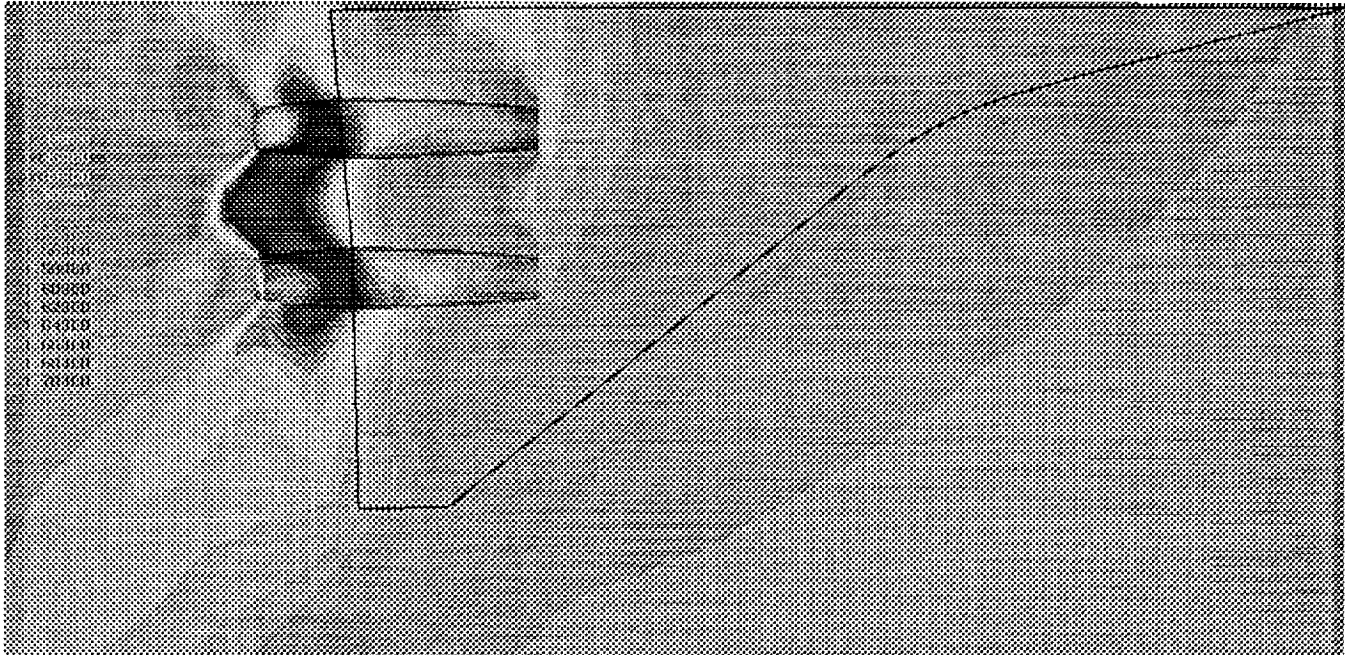
Figure 13.   Upper External Nacelle Surface Mach Number Distribution, TEAM Solution

Figure 14 shows the difference in the sonic boom signature for wing alone, wing with flow through nacelles, and wing with blocked nacelles.

Sonic Boom Signature for SA1150 using TEAM CFD Solutions
at h/l=0.3 Extrapolated to h/l=3.6 for M=1.4, $\alpha$=3$^\circ$

——————  wing alone
- - - - - -  wing w/ flow through nacelles (m/m$_c$=1)
..........  wing w/ blocked nacelles
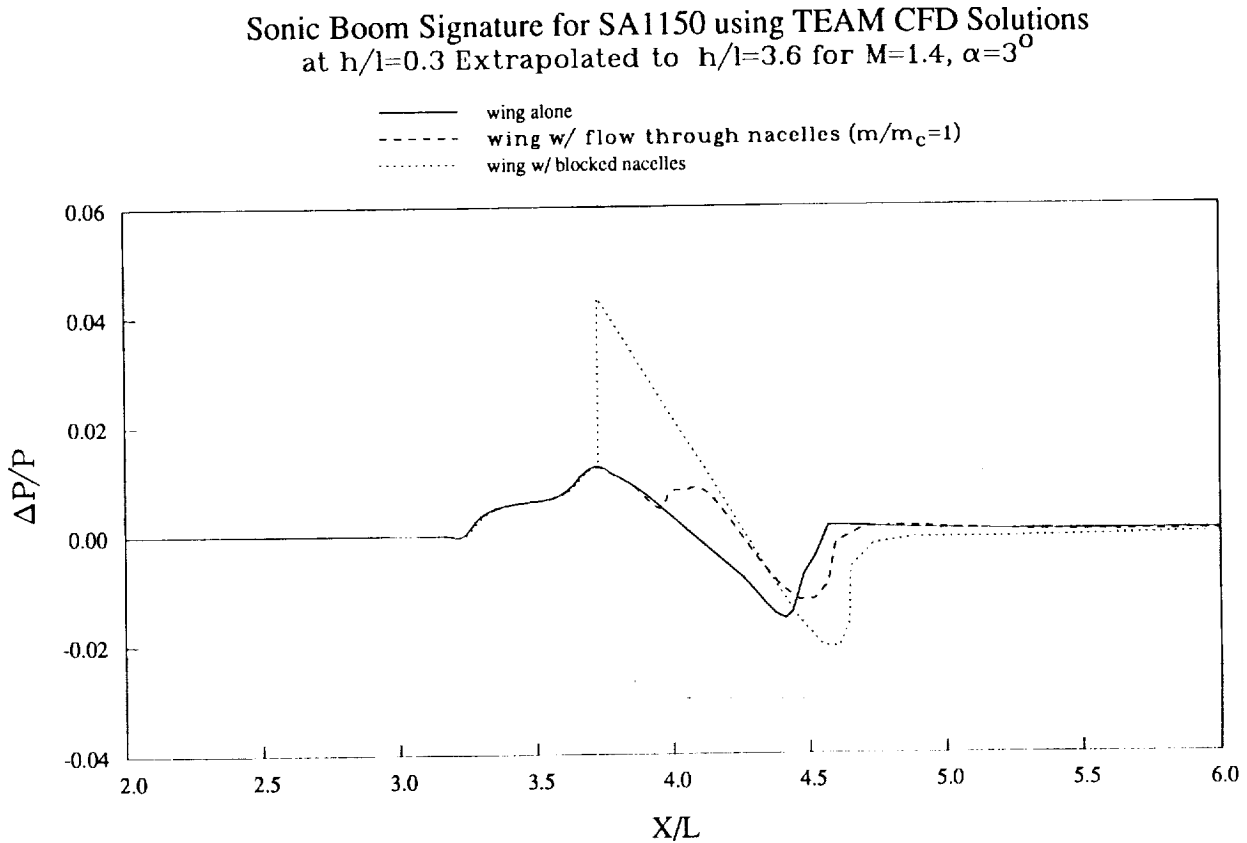


Figure 14.   Sonic Boom Signature for SA1150 using TEAM CFD Solutions

Three Euler codes will be evaluated for predicting nacelle airframe interference effects. These codes are TEAM, TIGER, and AIRPLANE. TIGER is a NASA Ames developed hexahedral unstructured Euler code with grid refinement capabilities, reference 4. AIRPLANE is a tetrahedral unstructured Euler code developed by Antony Jameson and Tim Baker, reference 5. They are all based on FLO57, a four stage Runge-Kutta scheme developed by Jameson.

The SA1150 wing-body with nacelles will be modeled and run for various cases to be compared to experimental data. An assessment of the three codes will be made on how they can predict nacelle airframe interference effects.

## Future CFD Analysis

- TIGER, Ames developed hexahedral Euler unstructured code with solution grid refinement

- AIRPLANE, Jameson and Baker's tetrahedral Euler unstructured code

- Model SA1150 wing-body with nacelles

- CFD vs experiment

- Assessment of codes in predicting nacelle airframe interference effects

Figure 15

# REFERENCES

1.  Bencze, D. P. :  Experimental Evaluation of Nacelle-Airframe Interference Forces and Pressures at Mach Numbers of 0.9 to 1.4.  NASA TM X-3321, 1977.

2.  Raj, P.; Olling, C. R.; Sikora, J. S.; Keen, J. M.; etal.:  Three-dimensional Euler/Navier-Stokes Aerodynamic Method (TEAM).  AFWAL-TR-87-3074, vol. I, II, III, October 1988.

3.  Steinbrenner, J. P.; Chawner, J. R.; and Fouts, C. L.:  The GRIDGEN 3D Multiple Block Grid Generation System.  WRDC-TR-90-3022, vol. I, II, October 1990.

4.  Melton, J. E.; Thomas, S. D.; and Cappuccio, G.:  Unstructured Euler Flow Solutions Using Hexahedral Cell Refinement.  AIAA-91-0637, AIAA Aerospace Sciences Meeting (Reno, Nevada), January 1991.

5.  Jameson, A. and Baker, T.:  Improvements to the Aircraft Euler Method.  AIAA-87-0452, AIAA Aerospace Sciences Meeting (Reno, Nevada), January 1987.

THIS PAGE INTENTIONALLY BLANK

# Session X. Airframe/Propulsion Integration

*omit*

HSCT Inlet Development Issues
*Joseph L. Koncsek, Boeing Commercial Airplane Group*

THIS PAGE INTENTIONALLY BLANK

# HSCT INLET DEVELOPMENT ISSUES

Joseph L. Koncsek
Boeing Commercial Airplane Group
Seattle WA

FIRST ANNUAL HIGH–SPEED RESEARCH WORKSHOP
Williamsburg, Virginia
14–16 May 1991

## SUPERSONIC INLET INTEGRATION ISSUES

The purpose of this presentation is to highlight the issues affecting the development of engine air inlets for the HSCT. The Propulsion Airframe Integration Technology (PAIT) contract (NAS3–25963) sponsored by NASA Lewis Research Center is an important element in the evolution of the propulsion system that will eventually power the HSCT. Most of the material presented here is based on work performed by The Boeing Company under Tasks 1 and 2 of PAIT.

From the propulsion perspective the premier technology issues associated with the HSCT are airport noise and high altitude emissions. The sources are the nozzle and combustor, respectively. For the inlet the most challenging issues are associated with integration, these include the following:

- *Integration with the main landing gear:* protection from FOD, and water and slush ingestion from the runway;

- *integration with the engine:* ensuring engine/inlet airflow matching, normal shock stability during engine airflow transients, and keeping total pressure distortion within acceptable limits;

- *integration with the wing:* minimizing nacelle/wing interference drag and inlet flowfield velocity distortion.

# Inlet/Airframe Integration Issues

## LOW SPEED
- FOD, water/slush ingestion
- noise suppression
- auxiliary inlets

## TRANSONIC/SUBSONIC CRUISE
- engine/inlet airflow matching
- spillage drag
- wing/nacelle interference drag

## SUPERSONIC CRUISE
- wing/nacelle interference drag
- normal shock stability

1404

## LANDING GEAR/INLET INTERFERENCE

Nacelle locations dictated by the slender wing planform and the need for the nozzles to be near the wing trailing edge may expose the inlets to the wake of the main landing gear. In addition to shed vortices, the wake could carry runway debris. The integration must minimize the hazards of foreign object damage (FOD) to the inlet and the engine. The inlet must also be kept out of the landing gear's water and slush spray pattern when operating on wet runways. Ingestion of excessive water and/or slush could result in degraded compressor performance. Selection of the nacelle locations is a crucial issue.

# LANDING–GEAR/INLET INTEGRATION
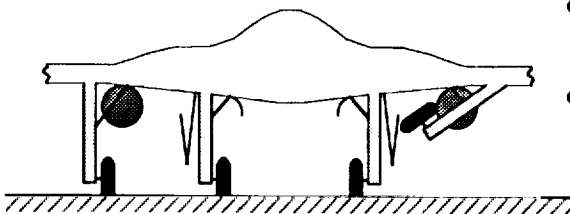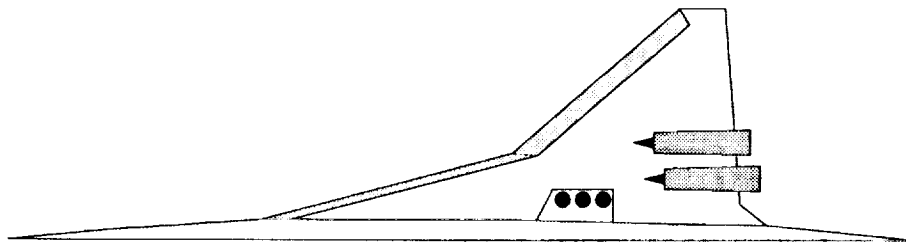
- Inlets away from leading edge.
- Nozzles near wing trailing edge.
- Propulsion nacelles close to airplane centerline.
- Inlets vulnerable to runway debris and slush spray from wheels.

# INLET/ENGINE COMPATIBILITY

The inlet is typically sized to match the engine demand at the top of climb (i.e. the beginning of cruise) so as to minimize cruise drag. The engine may be sized at a different point in the mission (e.g. takeoff, transonic climb, etc.) depending on the thrust requirements of the airplane. The design of both the inlet and of the engine must take into account the need for a close match between the inlet supply and the engine demand airflows. The inlet must be designed to limit the level of total pressure distortion and the engine must tolerate a reasonable level of distortion.

Mixed compression inlets must tolerate minor fluctuations in engine airflow demand without unstarting. The propulsion control system must be able to deal with larger disturbances.

## ENGINE/INLET FLOW MATCHING



1406
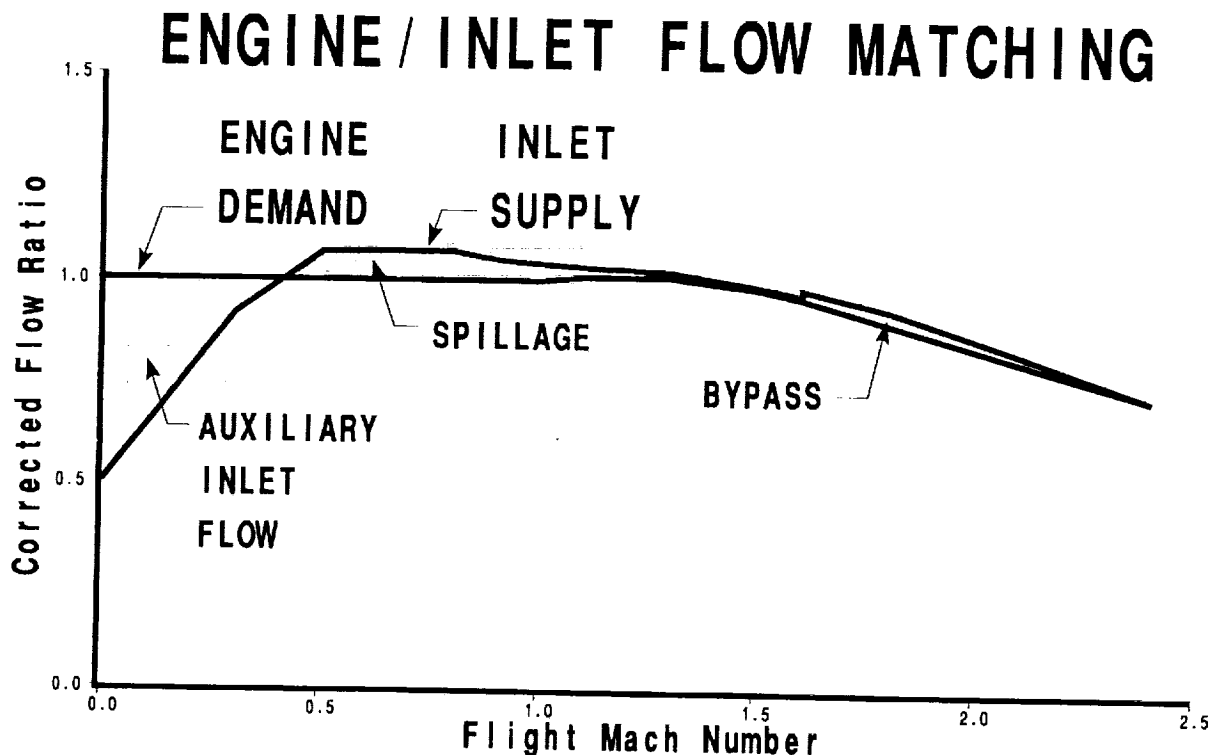
## NACELLE/WING INTERFERENCE

Performance of supersonic inlets, especially of the mixed compression variety, is sensitive to Mach number gradients in the local flowfield. The wing must be contoured to minimize such gradients. But since the flow will not be perfectly uniform, the inlet must tolerate some levels of non–uniformity.

The wing and nacelle flowfields are closely coupled. The interference forces are significant. The complex aerodynamic forces cannot be eliminated completely, so they must be put to best advantage. The figure shows that if the wing and nacelle are properly shaped, the pressure field of the nacelle shock wave can be used to pressurize the aft facing area of the lower wing. The net result is that the installed drag of the nacelle is equal to its skin friction drag, the wave drag having been cancelled by the thrust force on the wing.

# NACELLE/WING INTERFERENCE

- ## Wing shape, nacelle shape, nacelle position.
- ## Proper combination reduces installed drag to level of skin friction.



**Installed Drag**          **Isolated Drag**
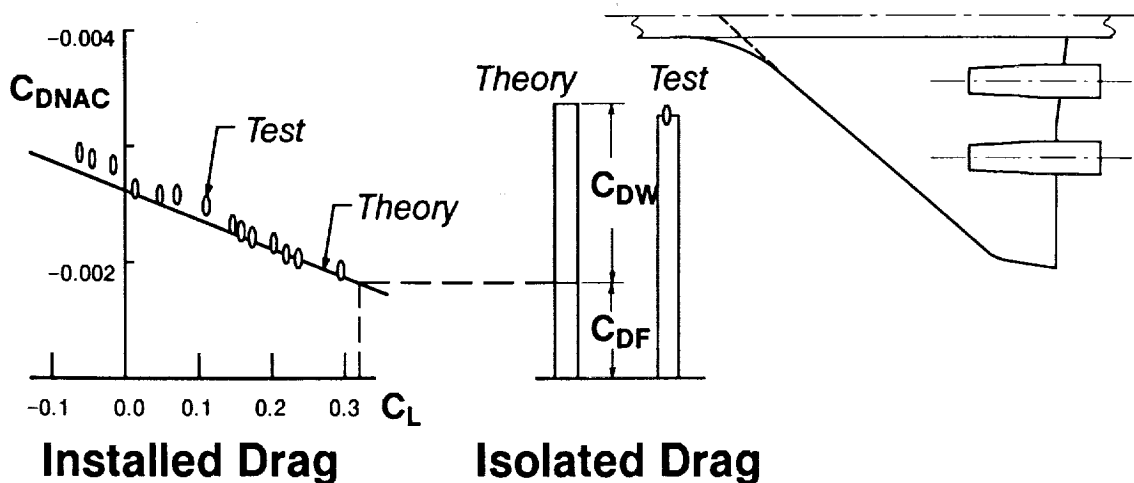
# INLET DEVELOPMENT PLAN

The HSCT inlet development plan is built on a foundation of continued design technology enhancements. Elements of the effort under way include: broadening the applications of CFD, expanding the inlet boundary layer control bleed system data base, and refining drag analyses, especially in the transonic speed regime.

Throughout the inlet development program support must be provided to development of the vehicle configuration. This effort includes prediction of the installed performance of various inlet designs so that the design trade studies will lead to the optimum integration.

At the present state of CFD the theoretical predictions must be validated in wind tunnel tests. Testing usually begins with cold flow inlet models. When the performance of the inlet is understood and accepted, compatibility of the inlet and engine must be established. In addition to verifying the aerodynamic compatibly of the propulsion system components, the compatibility experiments validate the viability of the propulsion control system.

NASA Lewis Research Center is actively supporting the development of the inlet for the HSCT through the Propulsion Airframe Integration Technology contract (NAS3–25963).

# HSCT INLET DEVELOPMENT PLAN

| 91 | 92 | 93 | 94 | 95 | 96 | 97 | 98 | 99 | 00 |

▽ Inlet Concept Down–select

Inlet Configuration Validated ▽

Flying Test–bed Experiments

Integrated Propulsion Controls

Engine/Inlet Compatibility Experiments

Inlet Wind Tunnel Experiments

Configuration Development Support Design Technology Improvements

1408
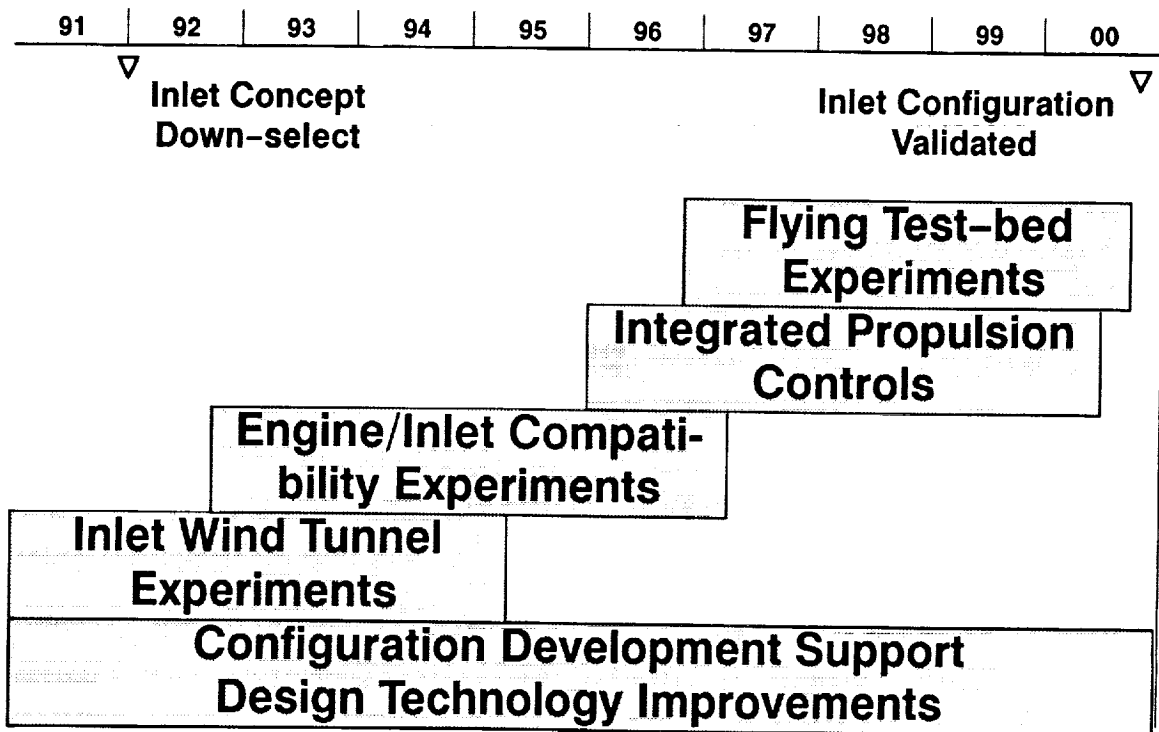
## PAIT PROGRAM OBJECTIVES

The overall objective of the Propulsion Airframe Integration contract (NAS3–25963) is to identify the best inlet for an HSCT having a cruise Mach number in the range of 2.0 to 2.5. The figures of merit used in making the final selection should reflect the impact of the choice on total mission performance.

NASA's participation can supplement industry's efforts by pursuing concepts that have a potential for high payoff with perhaps higher technical risk. The initial tasks of the PAIT contract comprise analytical studies to narrow the field of competing inlet concepts. Based on the results of the initial assessment, one or more concepts will be recommended for further research. The follow–on work is expected to include wind tunnel testing of the selected inlets first alone and later coupled with engines.

# PAIT Program Objectives

## Propulsion Airframe Integration Technology
## Contract No. NAS3–25963

- **Select HSCT inlet concept for cruise Mach number in range of 2.0 to 2.5.**
- **Design inlet for safety and efficiency.**
- **Integrate inlet design with airframe.**
  - **prevent engine FOD**
  - **minimize cruise drag**
  - **reduce community noise**

# INLET CONCEPTS FOR PAIT

Currently six inlet concepts are being studied under Tasks 1 and 2 of the Propulsion Airframe Integration contract (NAS3–25963). All of the inlets are designed for Mach 2.4 cruise flight. The reference engine airflow schedule for the studies is that of a turbine bypass engine proposed by P&WA for the HSCT. The concepts were picked to assess the benefits of 2D versus axisymmetric and external vs mixed compression designs. In both the 2D and axisymmetric groups, two mixed compression concepts are shown. The ones in the center have more external compression and shorter internal supersonic diffuser, while the ones at the bottom have less external compression and longer supersonic diffusers.

The stability of the normal shock tends to increase as more compression is done externally. At the same time the wave drag of the external cowl tends to increase. Two-dimensional inlets generally require more length than axisymmetric designs. In compensation, they offer more versatility in flow supply schedule and integration. The final selection is likely to be based on the requirements of integration.

# INLET CONCEPTS FOR PAIT
## NAS3–25963



1410
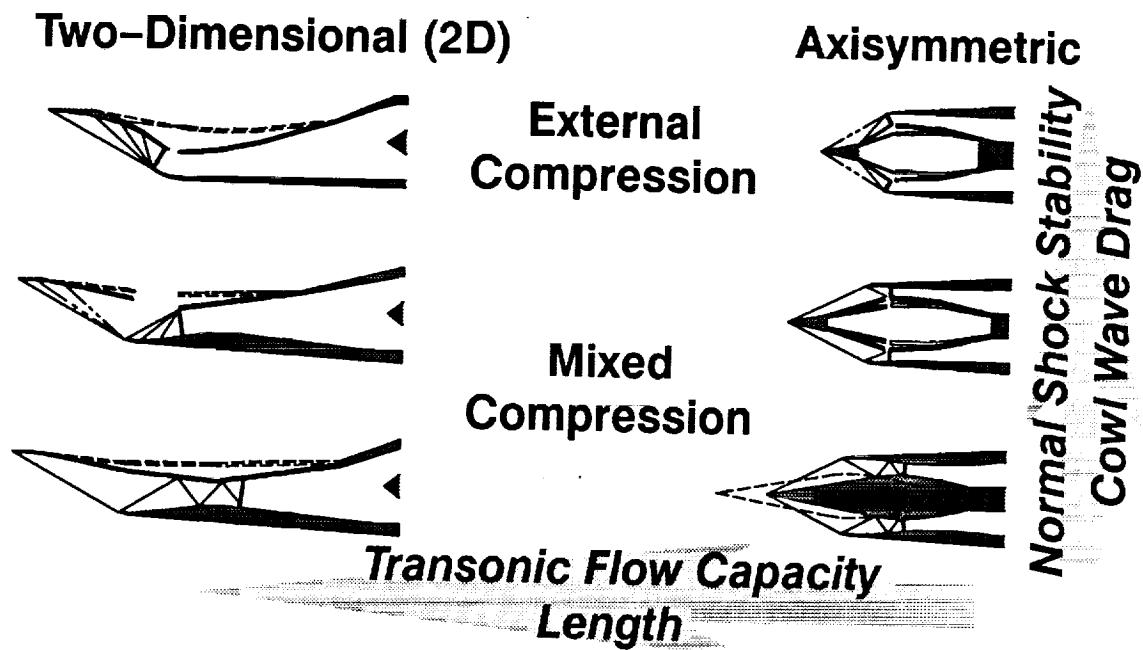
## PAIT INLET SELECTION CRITERIA

Tasks 1 and 2 of the Propulsion Airframe Integration contract (NAS3-25963) are under way. The analytical screening studies under the first task compare the inlets on the bases of internal performance, maximum flow supply capacity, boundary layer bleed requirements, and isolated (without wing) drag. The effort comprises definition of the inlet contours and prediction of inlet performance using CFD and lower order analyses.

Under the second task, designs studies are in progress to compare the candidate inlets on the basis of weight. The designs are carried to sufficient detail to allow structural sizing of components.

The objective of the third task is to compute the effects of the same inlets on vehicle mission performance.

# PAIT INLET SELECTION CRITERIA

## Task 1

## ISOLATED INLET PERFORMANCE

- **Total pressure recovery**
- **Cruise boundary layer bleed drag**
- **Transonic spillage drag**

## Task 2

## INLET WEIGHT

## Task 3

## AIRPLANE MISSION PERFORMANCE

## PRELIMINARY DESIGN AND ANALYSIS TOOLS

The initial steps for translating the inlet concepts into specific designs were accomplished using procedures developed during the Boeing SST and SCR programs. Once satisfactory results were obtained with the design codes, further computational fluid dynamics analyses were conducted using the PARC code.

The supersonic diffuser lines were generated iteratively applying Boeing's method–of–characteristics code. The predicted pressure profiles were analyzed with a finite difference boundary layer code to determine the locations and flowrates of boundary layer bleed required to prevent separation.

The normal shock total pressure losses were calculated from the predicted supersonic Mach number profiles at the inlet throat. The subsonic diffuser performance was estimated with a code developed at Stanford University and modified at Boeing. The code allows for interactions between the boundary layer and the core flow through an entrainment function.

The design codes (method–of–characteristics, boundary layer, subsonic diffuser) were run on engineering work stations with typical execution times measured in seconds. This procedure allowed preliminary analyses of a large number of trial contours.

# PRELIMINARY DESIGN/ANALYSIS

## Method of Characteristics

Supersonic flow properties

Diffuser Performance
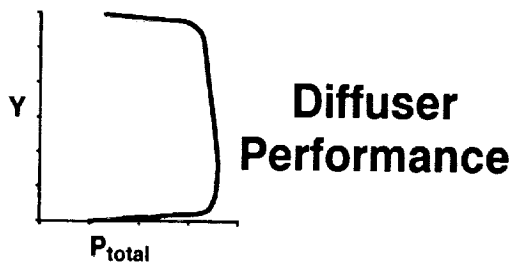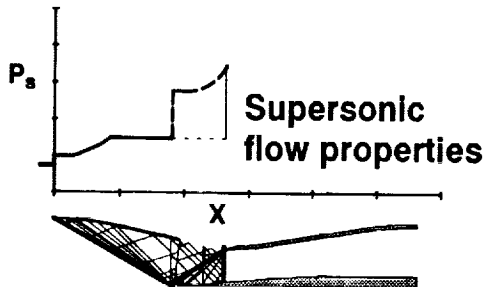
## Boundary Layer Analysis

boundary layer growth
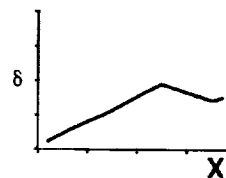
Improvement due to bleed
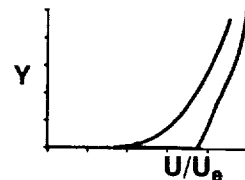
profile shape
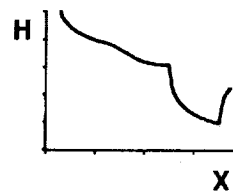
discharge coefficient
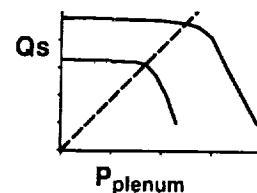
## CFD ANALYSES

The PARC code was run in the 2D/axisymmetric Euler mode to analyze the flowfields of the inlets generated with the design codes. Various flight conditions were simulated. The parameters varied included flight Mach number and engine corrected flow.

The objectives were to confirm the results of the preliminary analyses. The PARC computations include the complete flowfield from the undisturbed freestream to the engine face as opposed to the zone–by–zone analysis approach of the design codes. The effects of oblique and normal shock waves are detailed, allowing determination of the shape and operating position of the normal shock. More significantly, in the unstarted supersonic operating mode, the sensitivity of spillage drag to normal shock spillage flowrate can be directly calculated. Boundary layer effects are not included in the Euler solutions since viscosity is not simulated.

Sample results from the CFD analyses are presented in the following charts.

# CFD APPLICATIONS

## PARC CODE

- **2D/Axisymmetric**
- **Euler mode (no viscosity)**

## RESULTS

- **Normal shock position and shape**
- **Combined oblique and normal shock losses**
- **Transonic spillage drag**

# EXTERNAL COMPRESSION 2D INLET

The first concept in the inlet matrix is derived from a model tested in the Lewis 10- by 10-ft supersonic wind tunnel in 1986 (NASA CR 182253). The upper part of the chart shows the computation domain of the PARC CFD analysis. The engine face is located at approximately the midpoint of the long subsonic duct. The extension downstream of the engine face was provided to allow the flow profile to be non-uniform at the engine face. Variations in engine power setting were simulated by varying the throat area of a choked convergent-divergent nozzle at the end of the flow duct.

The lower part of the chart shows a close-up of the inlet aperture region. The flow out of the throat slot plenum is also controlled by a choked nozzle. The black lines trace the sonic lines. The aperture region contains a complex flowfield comprising supersonic flow with oblique shock waves, normal shocks, subsonic flow, and a free shear layer dividing the stagnant air in the plenum from the primary flow. The CFD results were valuable in shaping the contours of the aperture. The lower order codes are of little help in describing the details of the flow in this region.



EXTERNAL COMPRESSION 2D INLET

1414
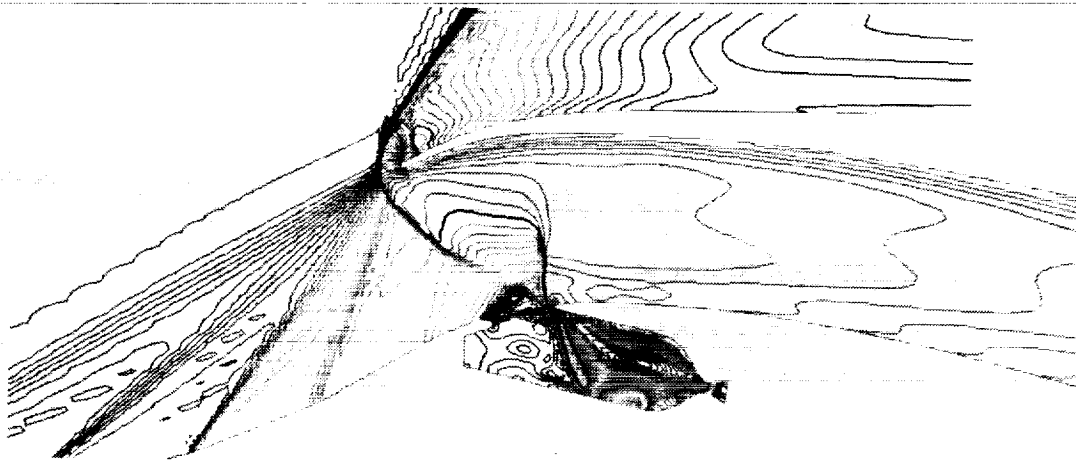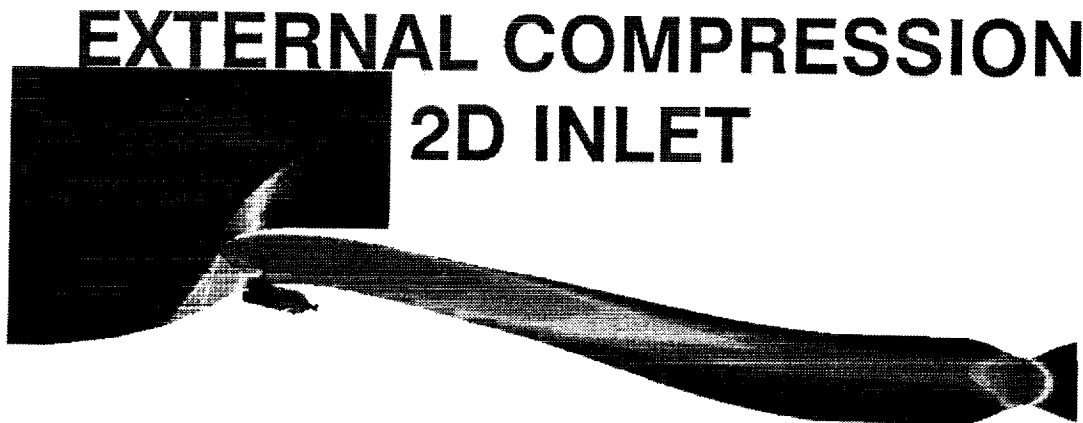
# TWO-STAGE SUPERSONIC INLET

The second concept in the inlet matrix incorporates a long unbounded surface and a plenum upstream of the throat. The appearance is that of a mixed compression inlet with one ramp missing. Unique features of the concept include the following: 1) the cowl lip shock and the distributed cowl compression are focused at the leading edge of the aft ramp so that no compression is taking place over the free surface of the plenum; 2) the normal shock is positioned just upstream of the aft ramp's leading edge, a relationship similar to that of the normal shock and cowl in an external compression inlet; 3) the normal shock position is controlled by closed loop control of the plenum pressure through control of the plenum exit area. Maintaining a constant static pressure in the plenum allows for the spillage of subsonic flow at various rates without affecting the supersonic diffuser flowfield. The spillage flow shows up as a thin jet adhering to the upper surface of the aft ramp in the figure.

# TWO-STAGE SUPERSONIC INLET
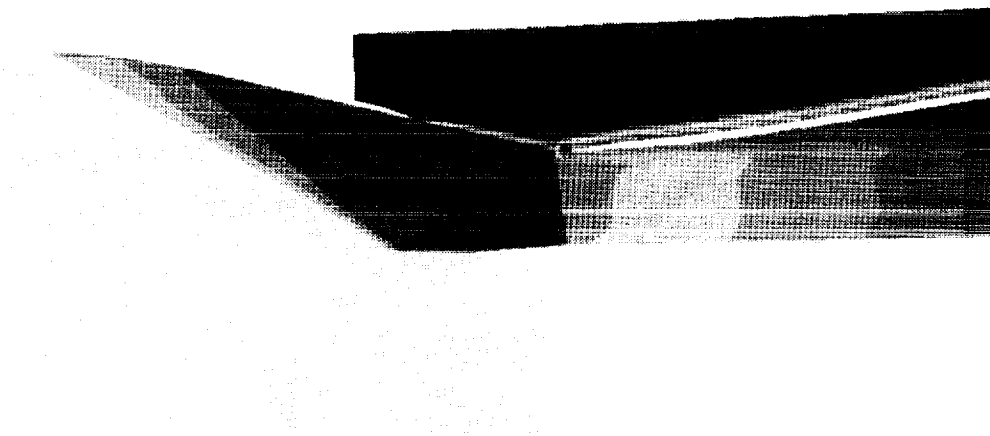
# MIXED COMPRESSION 2D INLET

Results of CFD analyses are shown for a more conventional type of mixed compression 2D inlet. The design incorporates three movable ramps and has a much longer supersonic diffuser than the previous inlet. The throat Mach number is maintained at 1.25 to provide tolerance to small fluctuations in freestream Mach number. The normal shock is positioned just downstream of the throat where the Mach number is about 1.3. This provides tolerance to minor fluctuations in the engine flow demand.



MIXED COMPRESSION 2D INLET

MACH 2.35

MACH 2.05
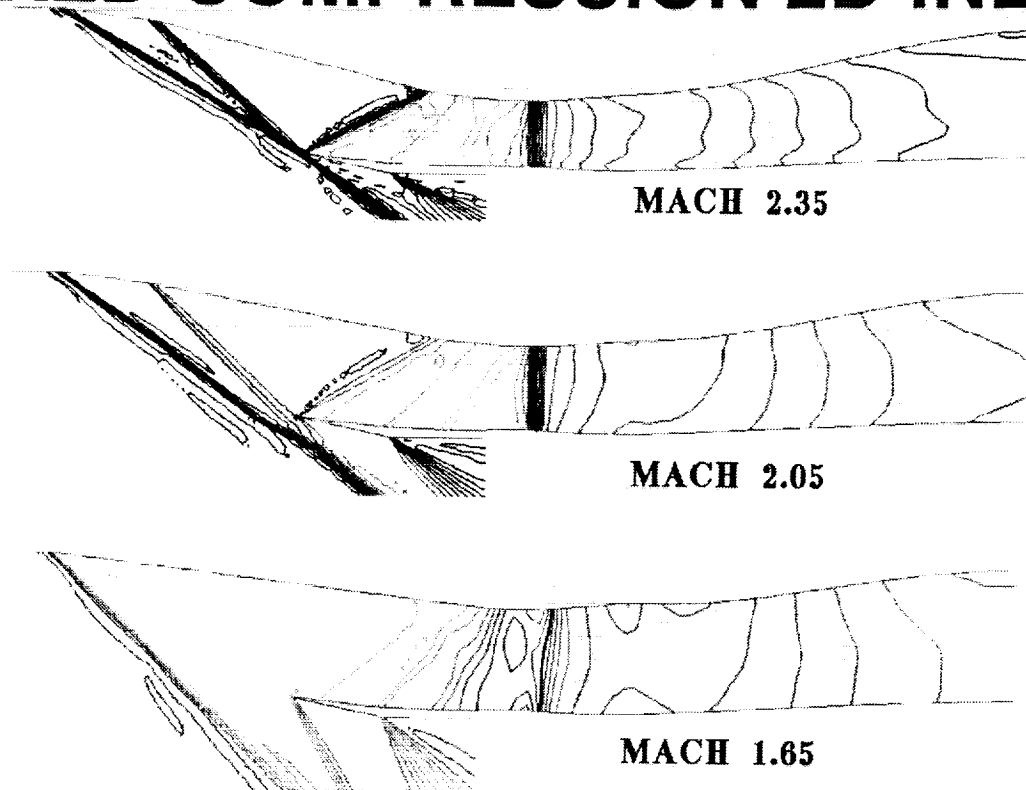
MACH 1.65

## STATIC PRESSURE DISTRIBUTIONS

Ramp and cowl contours and static pressure distributions are shown here for the mixed compression 2D inlet. These curves were extracted from PARC solutions at cruise and at Mach 1.65, the minimum Mach number where started operation is possible. The corresponding Mach contours are shown at top and bottom, respectively, in the previous figure. The pressures are shown in absolute units at the same altitude, clearly indicating the higher inlet pressure ratio at the higher flight Mach number. In actual operation the altitude would vary with Mach number.

# STATIC PRESSURE PROFILES

## PARC Solution for MC2D Inlet
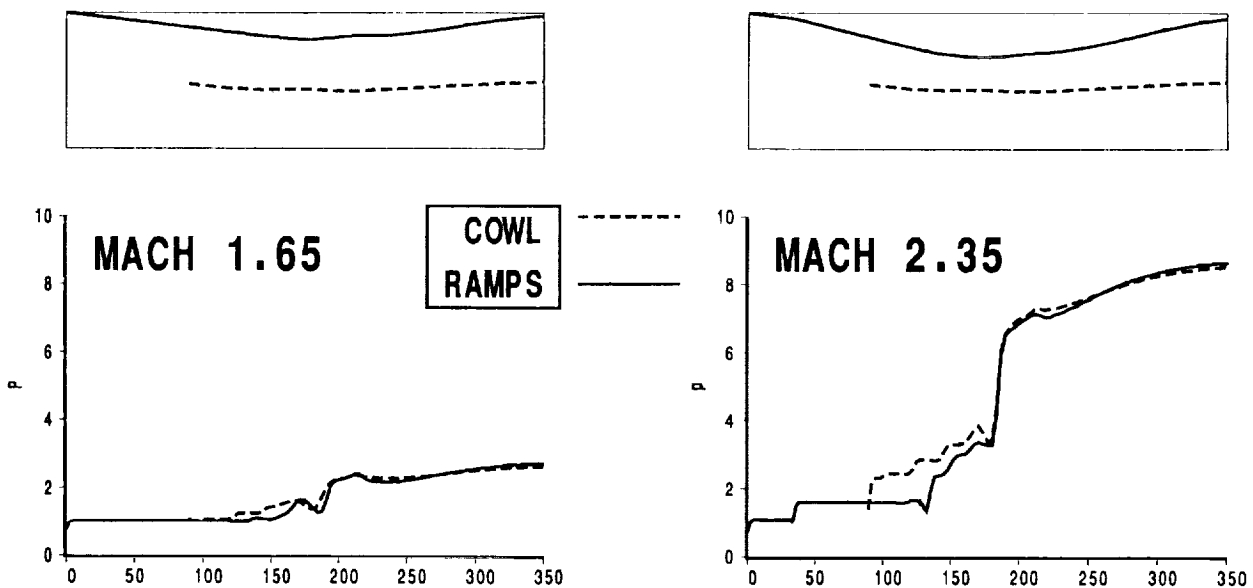
## MIXED COMPRESSION VARIABLE DIAMETER CENTERBODY INLET

The inlet shown here is a Mach 2.35 derivative of the NASA Lewis Mach 2.5 60/40 variable diameter centerbody inlet. A big attraction of such a design is the short supersonic diffuser. The bleed rates computed for this model agree well with the very low requirements established experimentally by NASA. The solution shown here is for Mach 2 flight.
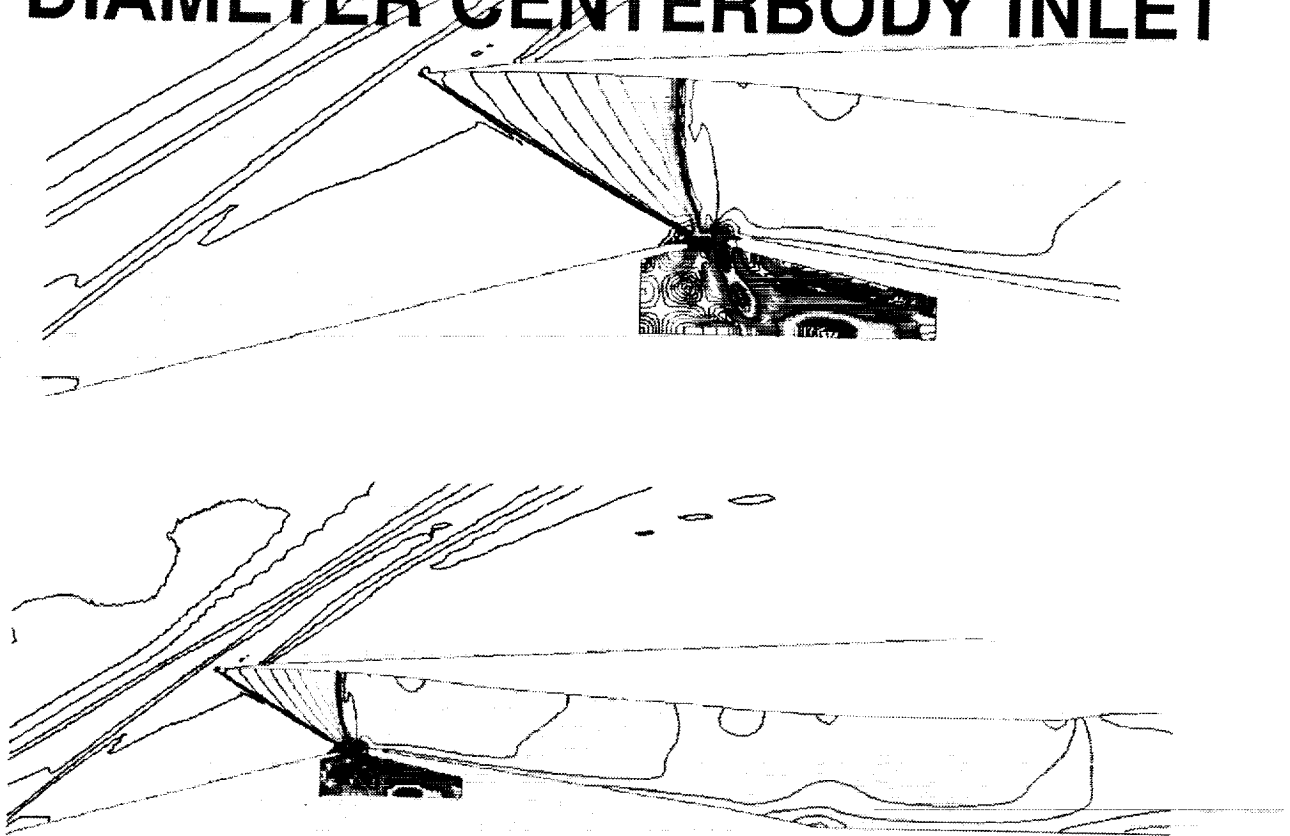
# DESIGN LOADS FOR SIZING OF INLET STRUCTURES

The objective of Task 2 of PAIT is to compare the weights of the inlet designs based on the analytical models developed under Task 1. To compute realistic weights, all of the major components of the inlet must be designed and the material thicknesses must be sized for the loads to be encountered in operation.

The chart shows predicted normal operating pressure loads, and hammershock loads (resulting from compressor surge) for the mixed compression axisymmetric translating centerbody inlet. Other analyses were conducted to estimate asymmetric pressure loads, and g–loads resulting from a hard landing. Materials were selected, and material thickness requirements were computed by structures specialists based on the loads data.

# NORMAL AND ENGINE SURGE PRESSURE LOADS



STATIC PRESSURE

ENGINE SURGE PRESSURES

CRUISE OPERATING PRESSURES
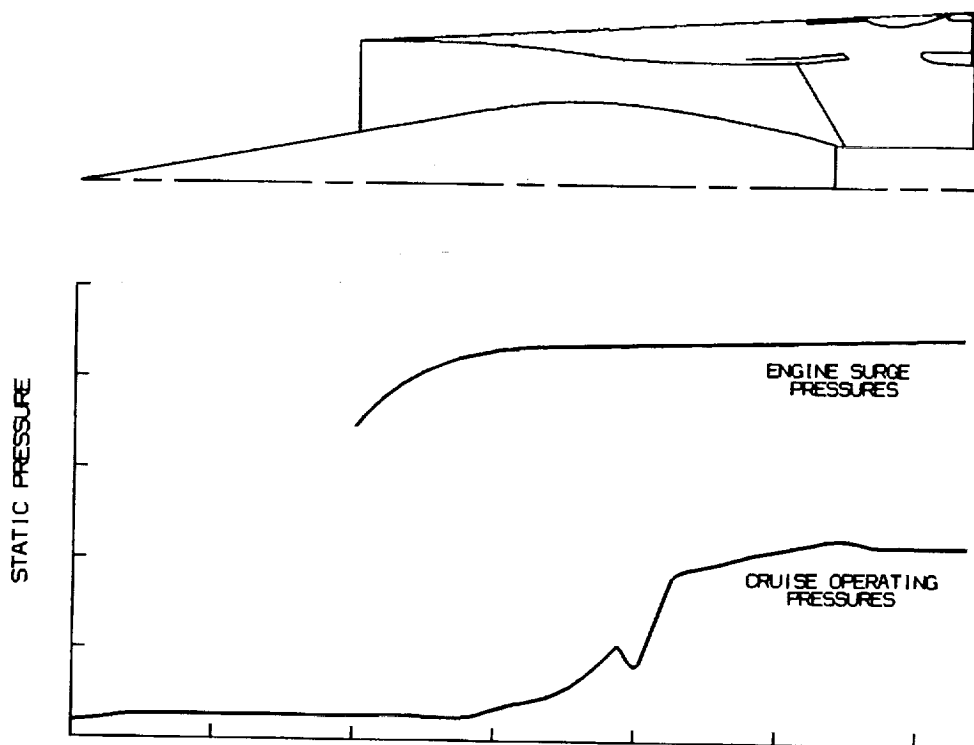
## MIXED COMPRESSION TRANSLATING CENTERBODY INLET

This inlet concept traces its ancestry to the NASA Ames P inlet; a contender for the US SST. The picture shows a solids model rendering of the inlet design with the CATIA computer aided design (CAD) system used at Boeing. The inlet components are sized for the loads shown in the previous chart. The CAD system can compute the volume of each component. The volumes, the material densities, and allowances for fasteners, etc. lead to accurate prediction of the final inlet weight.

# MIXED COMPRESSION TRANS-LATING CENTERBODY INLET



1420
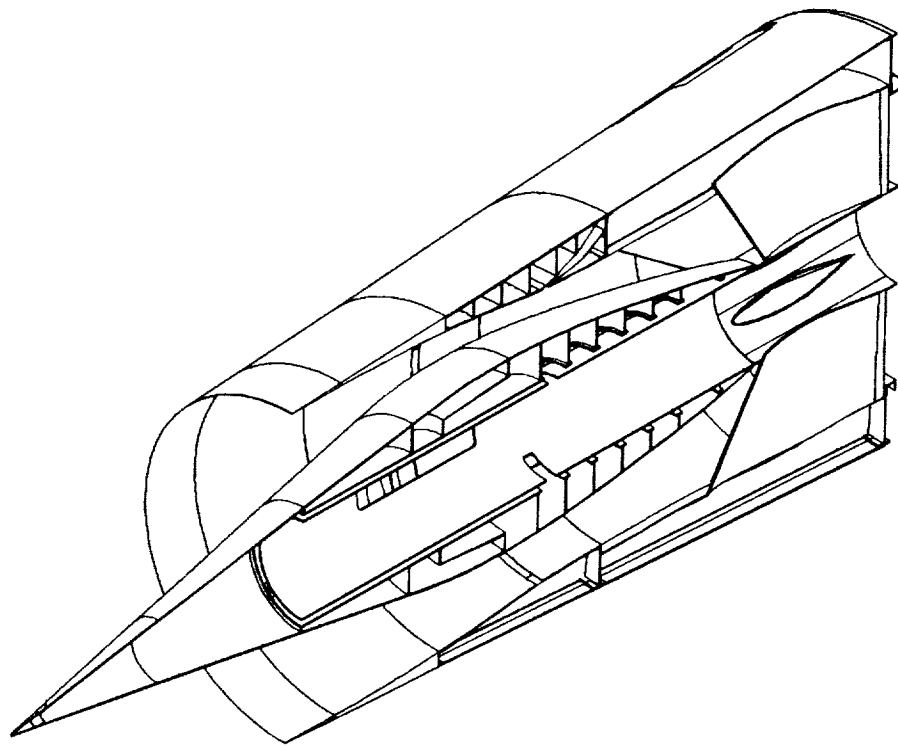
## CONCLUDING REMARKS

For propulsion technology the premier issues are airport noise and high altitude emissions. The sources are the nozzle and combustor, respectively. For the inlet the most important issues are associated with integration.

- Integration with the main landing gear: protection from runway FOD;
- integration with the engine: engine/inlet airflow matching, normal shock stability during engine airflow transients;
- integration with the wing: nacelle/wing interference drag, inlet flowfield uniformity.

The inlet development plan includes the following tasks: 1) enhancement of design technology; 2) support of vehicle configuration development; 3) analytical screening of inlet concepts; 4) experimental validation of inlet designs; 5) experimental validation of inlet/ engine compatibility; 6) demonstration of propulsion system performance in flight.

# CONCLUDING REMARKS

## ELEMENTS OF INLET DEVELOPMENT PLAN
- design technology enhancements
- analytical screening of inlet concepts
- experimental validation of inlet designs
- demonstration of inlet/engine compatibility

## WORKING WITH NASA AND ENGINE SUPPLIERS

## MAJOR ISSUES:
- wing/nacelle interference
- normal shock stability
- engine/inlet airflow match
- landing gear effects

1421

THIS PAGE INTENTIONALLY BLANK

# Session X. Airframe/Propulsion Integration

*o mit*

Status of an Inlet Configuration Trade Study for the Douglas HSCT
*Jay R. Jones and H. Robert Welge, Douglas Aircraft Company*

**THIS PAGE INTENTIONALLY BLANK**

# STATUS OF AN INLET CONFIGURATION TRADE STUDY FOR THE DOUGLAS HSCT

$5/9-05$
$12049$

J.R.Jones and H.R.Welge

Douglas Aircraft Company

Long Beach, California

High-Speed Research Workshop

Williamsburg, Virginia

May 14-16, 1991

## PROPULSION/AIRFRAME INTEGRATION TECHNOLOGY
### Task Order No.2

An inlet concept integration trade study for an HSCT is being conducted under contract to NASA LeRC. The HSCT mission has a supersonic cruise Mach number of 2.4, and a subsonic cruise Mach number of 0.95. The engine selected for this study is the GE VCE (variable cycle engine) with FLADE (fan on blade).

Six inlet configurations will be defined. Inlet configurations will be axisymmetric and rectangular mixed-compression inlets in single-engine nacelles. Airplane performance for each inlet configuration will be estimated and then compared. The most appropriate inlet configuration for this airplane/engine combination will be determined by September 1991, as shown in table 1.

| Tasks | 1991 | | | | | | | | | | | |
|---|---|---|---|---|---|---|---|---|---|---|---|---|
| | Jan | Feb | Mar | Apr | May | Jun | Jul | Aug | Sepl | Oct | Nov | Dec |
| 1.0 Preprare Detailed Plan | △——△ | | | | | | | | | | | |
| 2.0 Define Reference Vehicle and Mission | | △—△ | | | | | | | | | | |
| 3.0 Obtain GE FLADE VCE Engine Air Flow | | | △ | | | | | | | | | |
| 4.0 Inlet Conceptual Designs | | △———————————△ | | | | | | | | | | |
| 5.0 Nacelle/Airframe Integration | | | | △——————△ | | | | | | | | |
| 6.0 Airframe/Nacelle CASES Mission Performance | | | | △————————△ | | | | | | | | |
| 7.0 Program Management | | | | m | | m | | m | | f | | |
| m - meeting      f - finish | | | | | | | | | | | | |

**Table 1. PAIT Task Order No.2 Schedule**

1426

# DAC HSCT CONFIGURATION

The 300-passenger aircraft (figure 1) has a takeoff gross weight of about 750,000 lb. The engines are GE VCE with FLADE with rated thrust of about 60,000 lb.
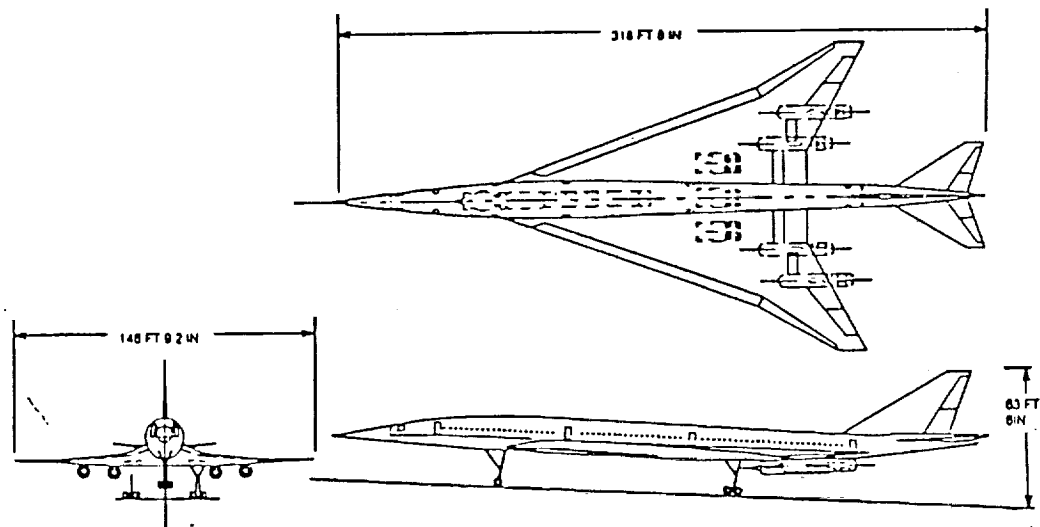
Figure 1. HSCT Configuration

# GENERAL ELECTRIC FLADE ENGINE

The VCE (variable cycle engine) is surrounded by a FLADE (fan on blade) bypass duct. The FLADE provides for higher airflows and lower noise levels at takeoff, and lower specific fuel consumption at subsonic cruise conditions. The FLADE duct contains a fan stage made up of extended VCE fan blades. The duct also contains variable inlet guide vanes and variable exit area for flow-rate control.

FLADE fan blade

Variable inlet guide vane
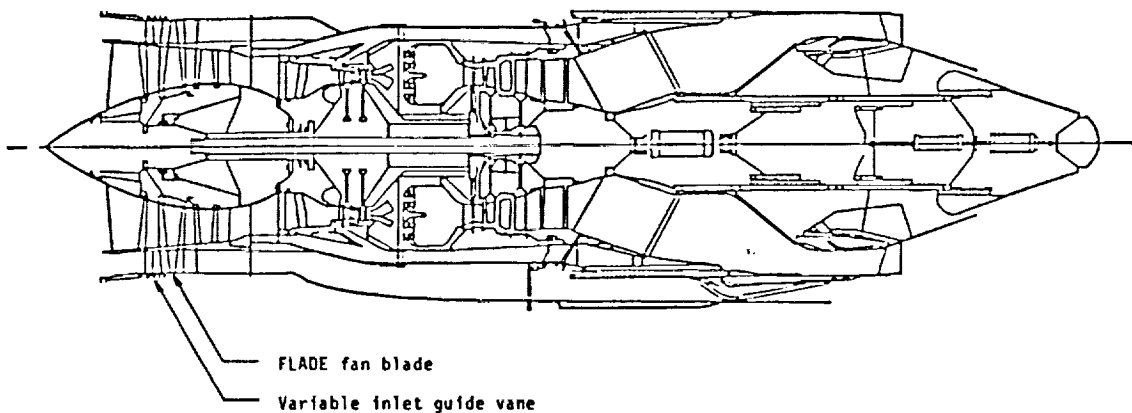
Figure 2. GE FLADE Engine

# HSCT MISSION PROFILE INCLUDING CONVENTIONAL INTERNATIONAL RESERVES

The 6 inlet configurations will be evaluated by comparing airplane performance for the mission described in figure 3. The mission is the average of about 250 city-pair flights. About 25 percent of the distance traveled is at subsonic speeds.
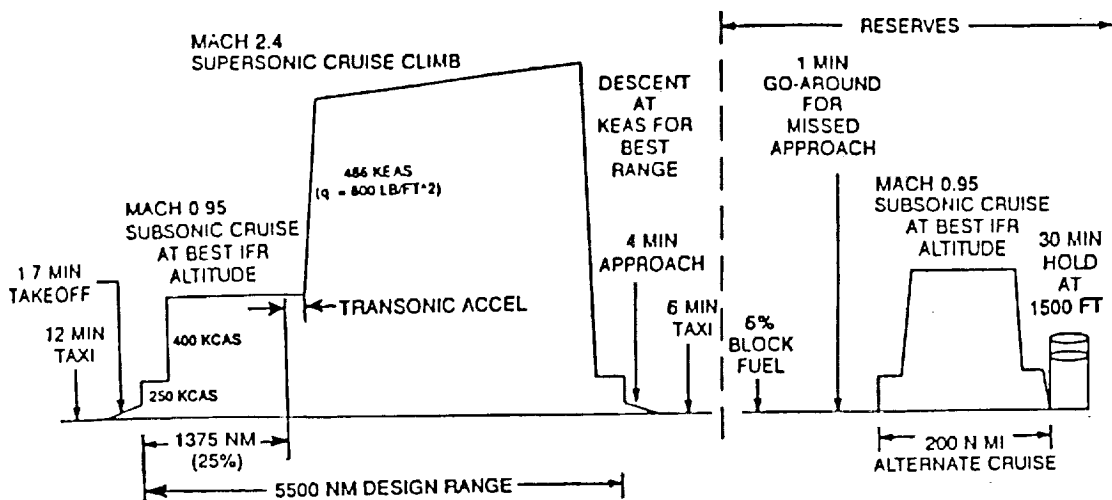


Figure 3. Mission Profile

# HSCT FLOW AT INLET LOCATION

The design-point Mach number for the inlet depends on the airplane
flow-field characteristics at the inlet location.  At $M_\infty$ =2.4, the
average flow-field Mach number is 2.32 at both inlets (figure 4).
These estimates were made using the SCRAM code (Streamline Coordinate
Riemann Axial Marching Code).  The code was run on the MDC CRAY XMP.
Flow field estimates will also be made at $M_\infty$ =0.95.
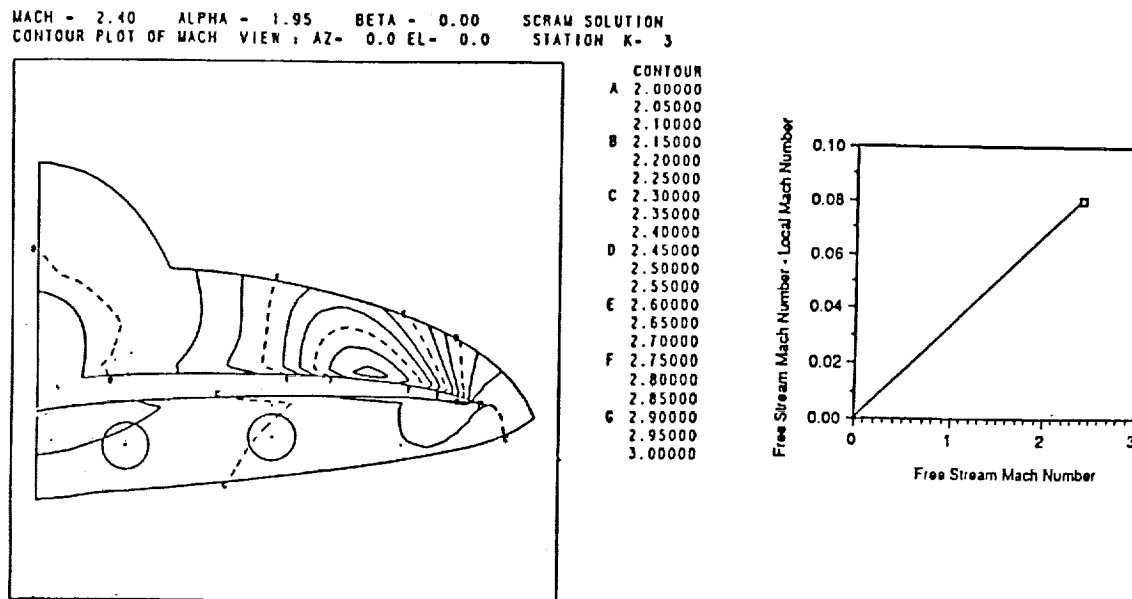


Figure 4.  Flow Field at M  =2.4

# AXISYMMETRIC BICONE FOCUSED-COMPRESSION INLET

Inlet 2 (figure 5) has variable-diameter centerbody. Combined FLADE-inlet and bypass-exit doors are located near the engine face. Both VCE and FLADE airflow enter the main inlet at Mach numbers higher than about 0.8. At supersonic cruise, a small amount of airflow passes through the FLADE duct for cooling, through the internal inlet door. At subsonic cruise, full airflow capacity enters the FLADE through the internal inlet door.

For Mach numbers lower than about 0.8, only the VCE airflow enters through the main inlet. The FLADE airflow enters the engine through the external inlet door.

Supersonic Cruise, Mach = 2.40

Transonic Cruise, Mach = 0.95

Subsonic, 0.3 < Mach < 0.8

Take-off, 0 < Mach < 0.3
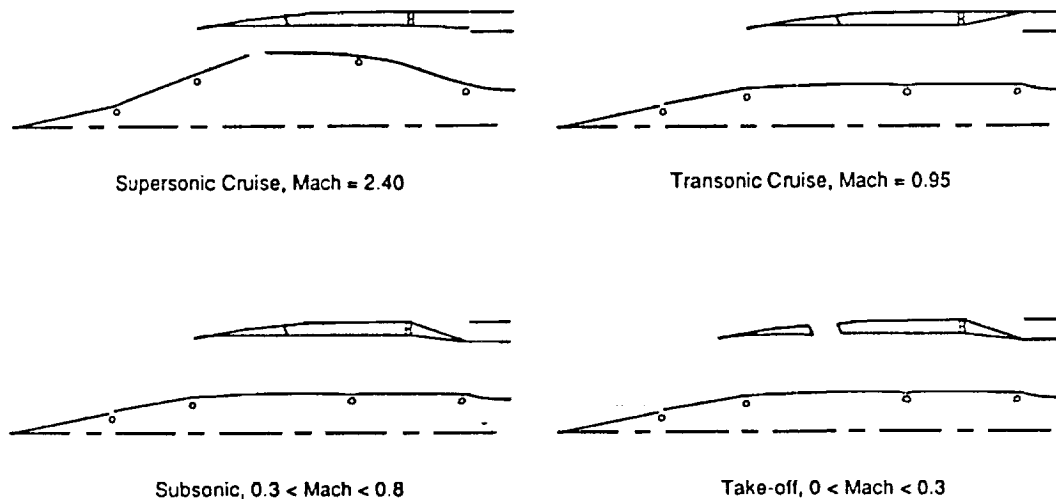
Figure 5.   Axisymmetric Bicone Inlet (Inlet 2)

# AXISYMMETRIC SINGLE-CONE TRANSLATING-CENTERBODY INLET

For inlet 3, VCE and FLADE airflow enter through the main inlet for Mach numbers higher than about 1.5 (figure 6). For lower Mach numbers, the FLADE airflow comes through external inlet doors. For Mach numbers equal to or lower than 0.95, full FLADE airflow capability is utilized. At higher Mach numbers, the FLADE airflow level is reduced to that required for cooling.

Supersonic Cruise, Mach = 2.40

Transonic Cruise, Mach = 0.95

Transonic, Mach = 1.0

Take-off, 0 < Mach < 0.5
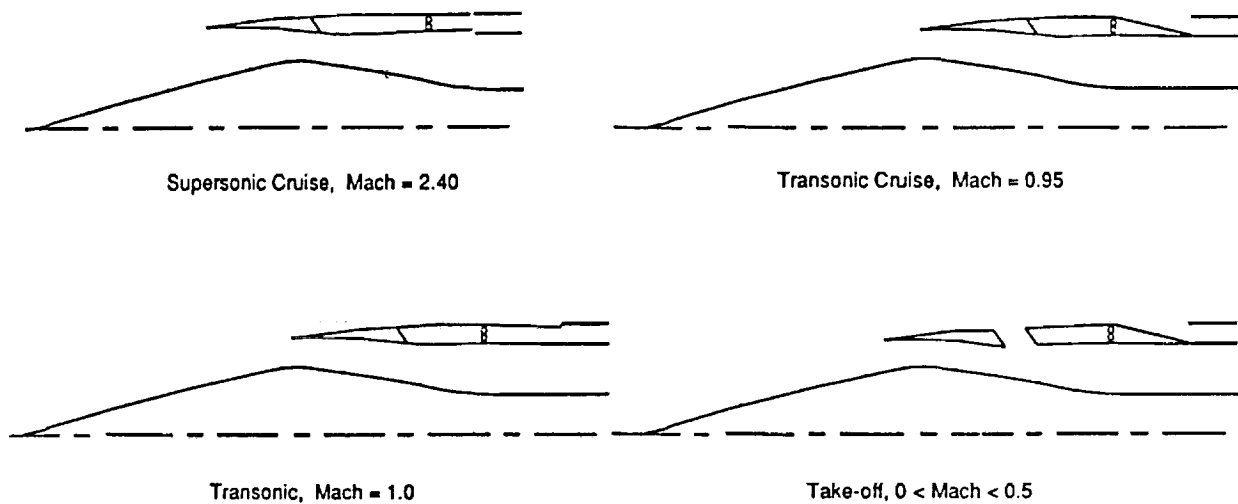
Figure 6. Axisymmetric Single-Cone Inlet (Inlet 3)

1432

# SUPERSONIC COMPRESSION AT DESIGN POINT

The supersonic-diffuser shock systems are shown below for inlets 2 and 3 at the design point. These figures are based on method of characteristics analyses. Inlet 1 (not shown) is much like inlet 2 but with less external compression.

**SUPERSONIC COMPRESSION AT DESIGN POINT**

**BASED ON METHOD OF CHARACTERISTICS ANALYSIS**

$M_0 = 2.32$

$M_4 = 1.3$

INLET 2

$\theta_1 = 12°$
$\theta_2 = 20.5°$
$\theta_{cowl} = 4°$

INLET 3

$\theta_1 = 12.5°$
$\theta_{cowl} = 0°$

$M_4 = 1.3$
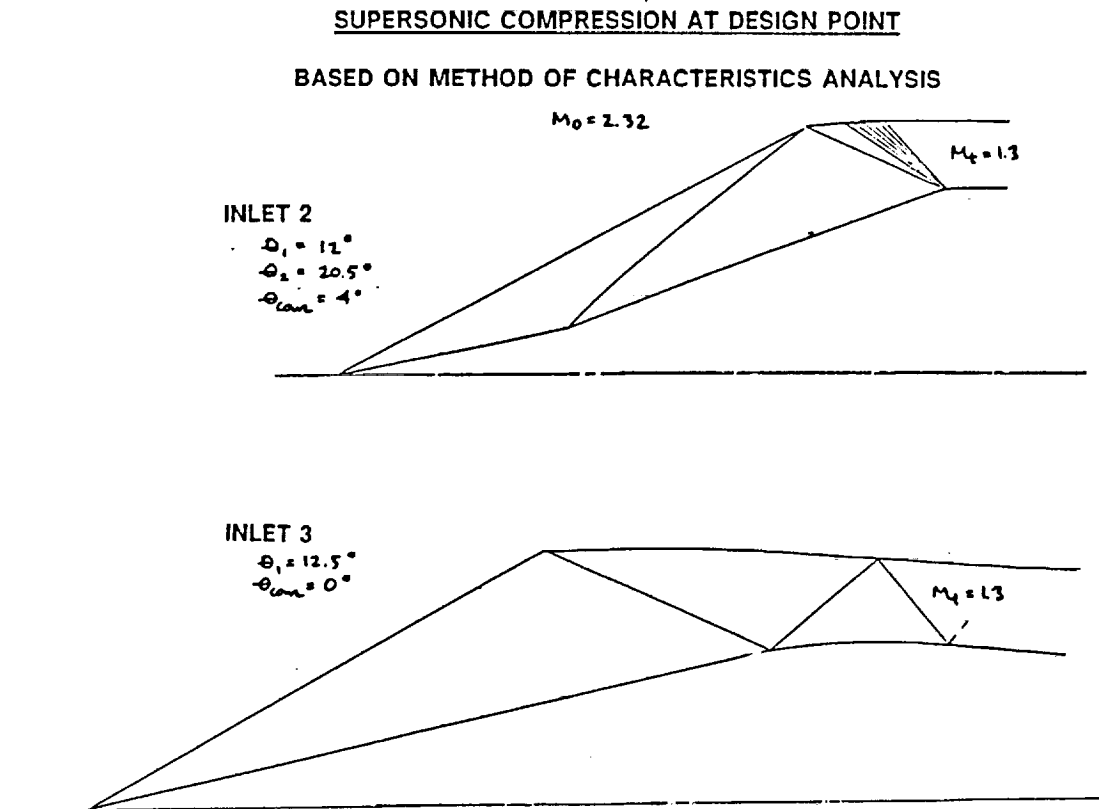
Figure 7. Supersonic Compression at Design Point

# INLET PRESSURE RECOVERY

Inlets 1 and 2 are similar and have the same estimated pressure recovery except in the external-compression regime. Inlet 3 has higher pressure recovery than inlet 2 at supersonic cruise (based on NASA data for single cone and bicone inlets). At subsonic cruise conditions inlet 3 has lower recovery because the FLADE airflow is not removed from the main-duct outer wall but enters from the external FLADE inlet. At static conditions, inlet 3 has lower recovery for the VCE flow due to higher airflow per area through the main inlet. Pressure recovery for the inlets is compared in figure 8.

— Inlet 1: Bicone with Variable-Diameter Centerbody
-- Inlet 2: Bicone with More External Compression
+,× Inlet 3: Single Cone with Translating Centerbody



Figure 8. Inlet Pressure Recovery

# INLET AIRFLOW CAPABILITY

Inlet 3 has the same inlet airflow capability as inlets 1 and 2 for Mach numbers less than or equal to 0.95. (The external FLADE inlet doors of inlet 3 are fully open in this regime.) For Mach numbers higher than 0.95, inlet 3 delivers all of the VCE airflow requirement, but only the cooling airflow requirement of the FLADE. Airflow capability for the inlets is compared in figure 9.



—— Inlet 1: Bicone with Variable-Diameter Centerbody
--- Inlet 2: Bicone with More External Compression
--x-- Inlet 3: Single Cone with Translating Centerbody
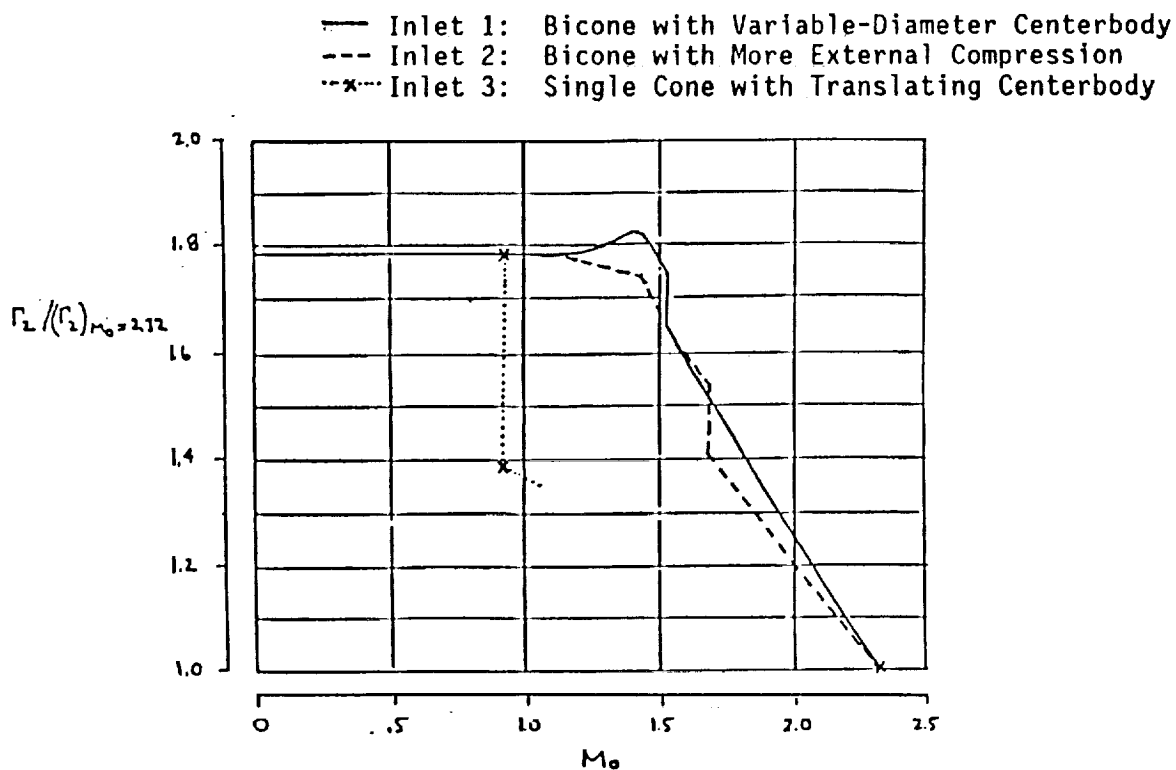
Figure 9. Inlet Airflow Capability

NEAR-TERM WORK

Task 4.0    INLET CONCEPTUAL DESIGNS

Finish inlet 3 lines

Start inlet 4 lines (rectangular with vertical ramps)

Initiate drag estimates, mechanical design, and weight estimates

Task 5.0    NACELLE/AIRFRAME INTEGRATION

Initiate CFD Analysis

Task 6.0    AIRFRAME/NACELLE MISSION PERFORMANCE

This work will start when engine performance is available

# Session X.  Airframe/Propulsion Integration

Transonic Airframe Propulsion Integration
*Robert E. Coltrin and Bobby W. Sanders, NASA Lewis Research Center; and Daniel P. Bencze, NASA Ames Research Center*

THIS PAGE INTENTIONALLY BLANK

# TRANSONIC AIRFRAME PROPULSION INTEGRATION

$520-07$
$12050$

Robert E. Coltrin & Bobby W. Sanders
NASA Lewis Research Center
Cleveland, Ohio


Daniel P. Bencze
NASA Ames Research Center
Moffett Field, California

GOAL OF THIS PAPER

This paper will pose some issues related to transonic propulsion integration testing in HSR Phase II.  It is intended to raise awareness and to generate discussion within the HSR propulsion/airframe community.

# GOAL OF THIS PAPER

TO GENERATE AWARENESS IN THE HSR PROPULSION/AIRFRAME
COMMUNITY OF THE ISSUES RELATING TO TRANSONIC PROPULSION/AIRFRAME
INTEGRATION TESTING DURING HSR PHASE II

Figure 1

## HSR PROPULSION/AIRFRAME INTEGRATION

This chart shows the time line for HSR propulsion/airframe integration program. HSR Phase I efforts are underway in both propulsion and aerodynamics. The propulsion efforts focus on cycles, inlets, combustors and nozzles that will be required to reduce nitrogen oxide (NOX) at cruise and noise at takeoff and landing to acceptable levels. The aerodynamic efforts concentrate on concepts that will reduce sonic booms and increase the lift/drag (L/D) ratio for the aircraft. The Phase II critical propulsion component technology program will focus on large scale demonstrators of the inlet, fan, combustor and nozzle. The hardware developed here will feed into the propulsion system program which will demonstrate overall system technology readiness, particularly in the takeoff and supersonic cruise speed ranges. The Phase II aerodynamic performance & vehicle integration program will provide a validated data base for advanced airframe/control/integration concepts over the full HSR speed range. The results of this program will also feed into the propulsion system demonstration program, particularly in the critical transonic arena.

# HSR PROPULSION/AIRFRAME INTEGRATION
## PHASE II

| 90 | 91 | 92 | 93 | 94 | 95 | 96 | 97 | 98 |
|----|----|----|----|----|----|----|----|----|

HSR Phase I Propulsion Efforts
- Combustor     - Nozzle
- Inlet         - Cycle Studies

Critical Propulsion Component Technology
- Large Scale Component Demonstrations
  (Combustor, Nozzle, Inlet, Fan)

Propulsion System Demonstrations
- Component Integration Demonstrating
  Technology Readiness

Aerodynamic Performance & Vehicle Integration
- Validated Data Base
  (Supersonic Cruise, Transonic Drag, High Lift)

HSR Phase I Aerodynamic Efforts
- Aero Concepts       - Supersonic Laminar Flow
- High-Lift Devices   - Low Sonic Boom Concepts

Figure 2

## BACKGROUND

During the High Speed Research (HSR) Phase II planning exercise leading to the July 1990 nonadvocate review (NAR) process, the main thrust of the propulsion system effort was to ground test a full propulsion system over the entire speed range. The goal is to integrate the complex, highly coupled subsystems (inlet, nozzle, fan, engine core) into a testbed propulsion system to confirm overall system compatibility and operability and to acquire a knowledge base of subsystem interactions and system dynamics. The testbed engine would be based on an existing engine of the Advanced Technology Fighter (ATF) class. This system would be tested supersonically in the LeRC 10X10 foot SWT to obtain inlet and nozzle performance and to study inlet/engine stability and compatibility. Subsonic tests would be conducted in the Ames 40X80 foot WT with the engine pod installed with a wing simulator. The objectives will be to study inlet and nozzle performance and fan and nozzle acoustics at takeoff and approach conditions.

Transonicaly it was determined that the critical issues are more related to installed drag, than they are to internal inlet and nozzle performance. Testing for installed transonic drag requires a full configuration wing/body/nacelle model. There is no facility in the USA that is large enough to handle a full span or half span model sized for an ATF size engine and still be able to obtain data near Mach one. Therefore, the planned transonic testing will focus on a smaller scale wing/body/nacelle model in the Ames 11X11 foot TWT.

# Background

```
┌─────────────────────────────────────────────────────────┐
│              HSR Non-Advocate Review (7/90) :             │
│   Experimental Validation of Propulsion System Performance│
│              Across the Mach Number Range                 │
└─────────────────────────────────────────────────────────┘
```

- **Supersonic** → **Large Scale Demonstration Engine Pod in Lewis 10-by 10-ft WT**
  - **\* Internal Inlet & Nozzle Performance**

- **Subsonic (TO & L)** → **Large Scale Demonstration Engine Pod with Simulated Wing in Ames 40-by 80-ft WT**
  - **\* Internal Inlet & Nozzle Performance**
  - **\* Acoustics**

- **Transonic** → **Integrated Wing/Body/Nacelle Configuration in Ames 11-by 11-ft WT**
  - **\* Transonic Drag**

Figure 3

1442

This chart displays the goal and the strategy for the transonic validation part of the HSR Phase II Propulsion System Program. This strategy was developed during the NAR Phase II review that took place in July of 1990. Since no USA propulsion transonic wind tunnel is capable of testing a large scale wing/body/nacelle, a smaller scale model must be employed. The 11 foot transonic tunnel at Ames is most suitable for this type of testing. The proper test rigs and test techniques have been developed over years of testing in this facility. Therefore, the wing/body/nacelle models should be sized to be compatible with this facility. Two types of models were envisioned. A full span model with flow-through nacelles to establish the reference force and moment data and a semi span model with two propulsion simulators to obtain inlet/nozzle interactions with both flows established at the same time. Increments to the data with the full span model will be obtained with the powered semi span model. Therefore, models must be sized small enough to be compatible with the 11 ft. wind tunnel but large enough to employ propulsion simulators.

# HSR PHASE II - PROPULSION SYSTEM
# TRANSONIC VALIDATION

GOAL: TO DEMONSTRATE TECHNIQUES FOR PROPULSION-AIRFRAME INTEGRATION WHICH WILL MINIMIZE INSTALLED AIRPLANE DRAG

## NAR STRATEGY

- NO CURRENT U.S. WIND TUNNEL CAN PROPERLY TEST A LARGE SCALE WING/BODY/ENGINE POD AT TRANSONIC SPEEDS

- THEREFORE, SMALLER SCALE WING/BODY/NACELLE MODELS MUST BE EMPLOYED

- SELECT SCALES THAT ARE COMPATABLE WITH AMES 11 FT. WIND TUNNEL

  - FULL SPAN FLOW THROUGH - REFERENCE

  - SEMI SPAN WITH TWO PROPULSION SIMULATORS - INCREMENT

- SEMISPAN SCALE MUST BE LARGE ENOUGH TO UTILIZE PROPULSION SIMULATORS

  - INLET/NOZZLE INTERACTIONS

Figure 4

This chart shows the proposed schedule for the transonic cruise portion of the aerodynamic performance & vehicle integration HSR Phase II Program. This is shown to demonstrate that the airframe will be developed through a series of tests at LaRC and Ames leading up to the integrated configuration testing that is the subject of this presentation. At the same time, the inlet and nozzle will be developed through a series of tests at LeRC and LaRC. It is envisioned that three full span integrated models will be built and tested; a blown nacelle model for the LaRC 16 ft. TWT, a flow-through model for the Ames 11 ft. TWT (reference model for simulator model), and a high Reynolds number flow-through model for the LaRC NTF. The main subject of this paper is the integrated semi span simulator model for the 11 ft.

# HSR PHASE II - AERODYNAMIC PERFORMANCE & VEHICLE INTEGRATION

## Schedule

## Transonic Cruise

| | 93 | 94 | 95 | 96 | 97 | 98 |
|---|---|---|---|---|---|---|
| Baseline models | | 8 Ft  8 Ft  11 Ft | | | | |
| Advanced configurations with flow-through nacelles | | | | UPWT  UPWT  8 Ft  8 Ft | | |
| Integrated - full span | | | | | 16 Ft  11 Ft  Blown Nacelle  Flow Through | NTF  Flow Through |
| Integrated - semi span | | | | | | 11 Ft Simulator |
| Inlet configuration | Small Scale HSR-1 | | | | 8x6 Ft | |
| Nozzle configuration | | 16 Ft | 8x6 Ft | | | |
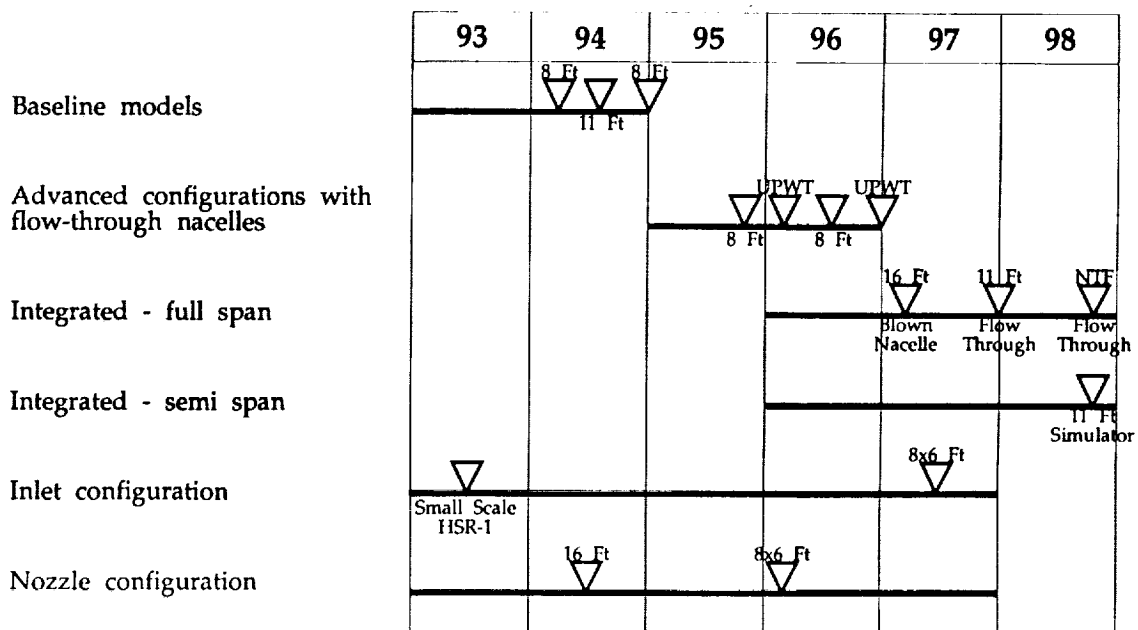
Figure 5

<u>ISSUES</u>

Several issues need to be resolved in planning for HSR Phase II wing/body/nacelle transonic tests. The test objective is defined to be the determination of installed drag rather than internal inlet and nozzle performance. However, the test technique to obtain this data is still open to discussion. Several questions need to be resolved:

1). Can conventional flow through inlet and blown-nozzle models be used or is a more sophisticated powered simulator model required?
2). How should the model be sized and should it be a full span model or a half span model?
3). What effect does Reynolds number have on the applicability of the proposed test results?
4). What practical issues such as data accuracy requirements and feasibility of plumbing installation need to be resolved?

# ISSUES

- **TEST TECHNIQUE**

    - CONVENTIONAL VS POWERED SIMULATOR

    - FULL VS SEMI SPAN

- **REYNOLDS NUMBER**

- **PRACTICAL ISSUES**

Figure 6

## ALTERNATIVE TEST TECHNIQUES

Generally there are two alternatives to measuring propulsion related increments to the aerodynamic characteristics of a vehicle. The first, termed conventional, uses individual inlet and nozzle models to obtain the increments associated with the inlet and nozzle streams respectively. The second approach attempts to model both the inlet and nozzle streams simultaneously, using some type of simulator device to pump the inlet and pressurize the nozzle. Both use a reference flow through aero model to obtain the basic aerodynamic characteristics of the vehicle. The conventional approach uses an inlet model with a fixed nozzle simulation to obtain the increments associated with variations in inlet mass-flow ratio (MFR) and a nozzle model with a faired over inlet to obtain the effects of nozzle pressure ratio (NPR). In the simulator approach both streams are modeled simultaneously and typically varied independently. The conventional approach is simpler but cannot resolve any mutual interactions between the inlet and nozzle flows and introduces extraneous effects with the faired inlet and fixed nozzle simulation. The simulator approach has the potential for capturing all the aerodynamic effects but is much more complicated and requires extensive flow calibrations that may compromise the ultimate data.

# Alternative Test Techniques

**Conventional Approach**  **Simulator Approach**

Aero Reference Model   • Full Span, Sting Mounted
                       • Flow Thru Nacelles
                       • Force & Moment Data

Inlet Drag   • Full or Semi-Span
             • Variable
             • Solid nozzle plume
             • Inlet Drag = f(MFR)

Simulator Powered   • Semi-Span
                    • Variable MFR, NPR
                    • Inlet-Nozzle Interactions
                    • Δ Drag = f(MFR, NPR)

Jet Effects   • Full or Semi-Span
              • Variable NPR
              • Faired Inlets
              • Nozzle Drag = f(NPR)

Figure 7

1446
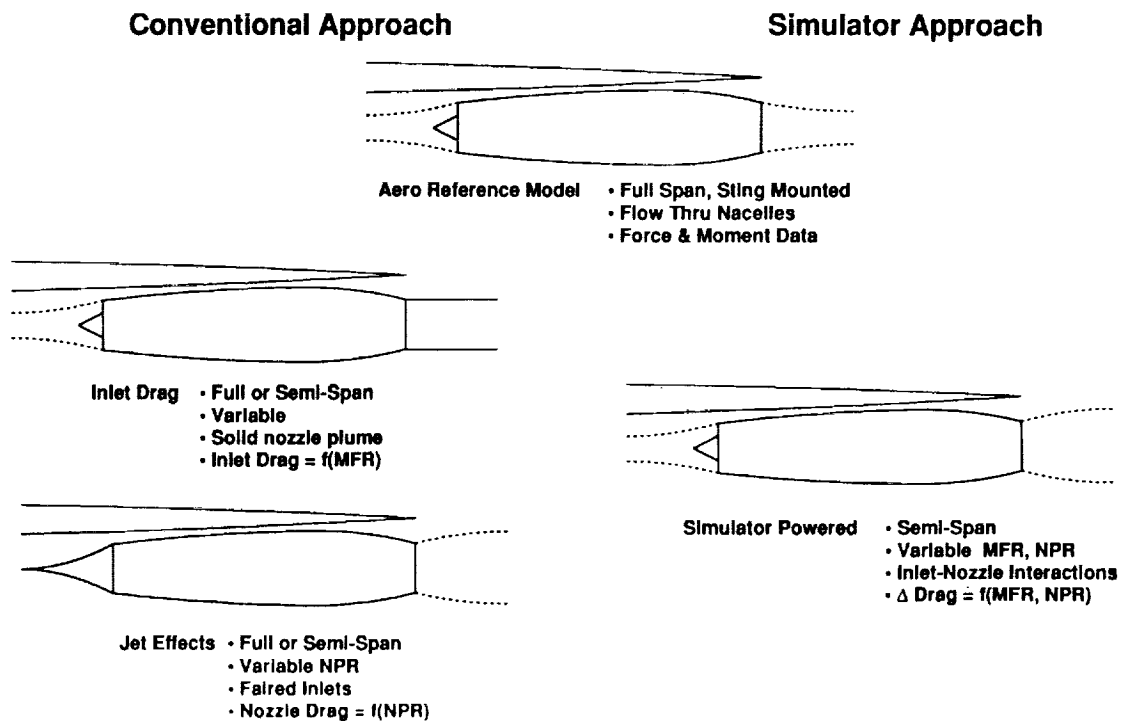
## NOZZLE INTERACTIONS ON A SUPERSONIC STOVL CONFIGURATION

The results shown here compare similar data obtained using the conventional technique (reference aero model plus inlet and nozzle models) and a powered simulator approach (Ref. 1). Results are shown at Mach numbers of 0.9 and 1.4. The largest discrepancy between the two techniques occurred at M = 1.4 and corresponded to 20 drag counts or 4.5% of the drag of configuration. At this Mach number the trends with nozzle pressure ratio are similar, therefore the discrepancy appears to be associated with an interaction of the inlet and nozzle flow fields or possibly an effect associated with the inlet fairing.

# Nozzle Interactions on a
# Supersonic STOVL Configuration
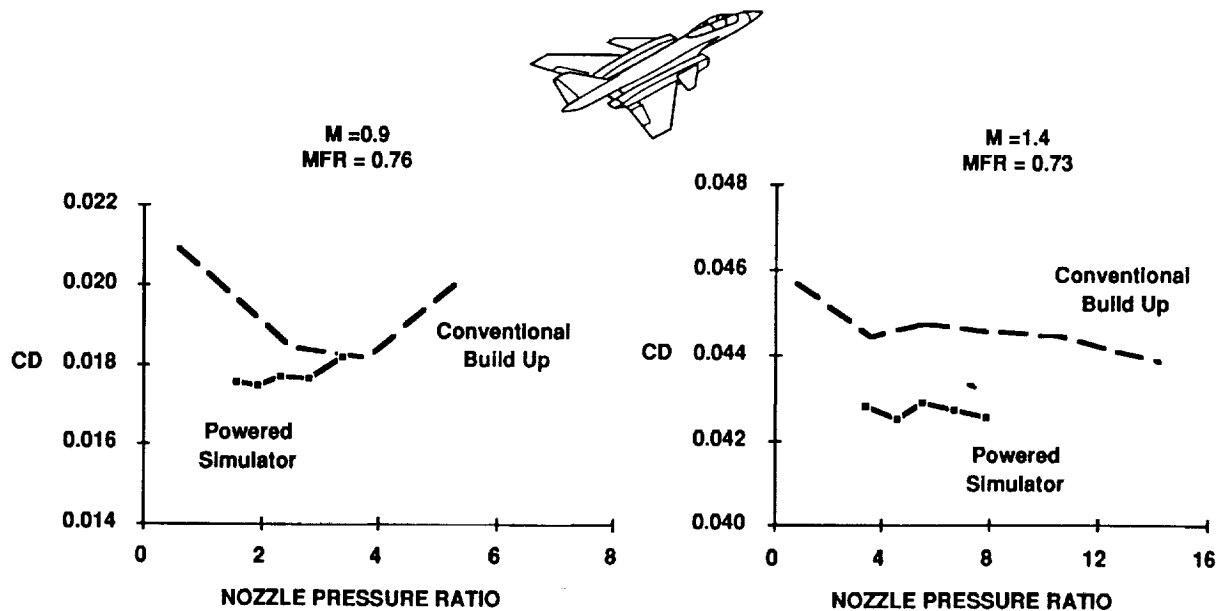


Figure 8

## TRANSONIC MASS FLOW EFFECTS/BOEING SA 1150 MODEL

Shown here are the effects of inlet mass flow ratio on the overall wing-body-nacelle interference drag of the Boeing SA 1150 model with four axisymmetric nacelles located abreast at $X/C_{root}$ = 0.74 (Ref. 2). The interference drag is defined as the total drag of the combination minus the isolated drag of the components at the corresponding mass-flow ratio. Since the nacelles were located relatively far aft on the wing, the overall interference effects are favorable. At Mach 1.15 reducing the inlet mass-flow ratio enhanced the favorable interference, while at Mach 0.9 and 1.4, reductions in mass-flow ratio decreased the favorable interference effects. The variations in drag over the mass flow ratios shown are 5 counts at M=1.4, 10 counts at M=1.15, and 2 counts at M=0.9. The changes in inlet mass flow represented in the figure provides a variation in system drag. If the inlet mass flow was reduced to zero as obtained by a faired inlet the effect could be expected to be rather large.



## Transonic Mass Flow Effects
## Boeing SA1150 Model
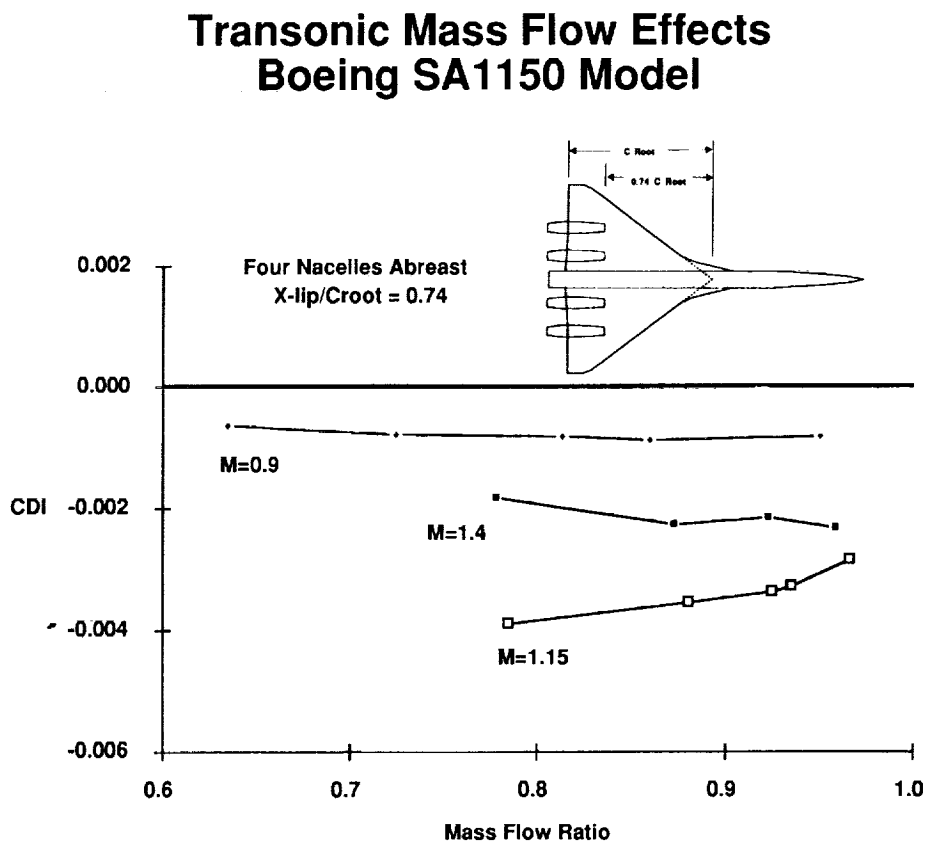
Figure 9

## VARIETY OF TEST INSTALLATIONS

In the late 1960's and the early 1970's, Lewis conducted an extensive series of nozzle tests in both the wind tunnel and in flight. The F-106 aircraft was modified with two underslung J-85 engine pods, one under each wing. A wide variety of nozzle types were tested. Nozzles were first run isolated in the 8X6 Ft. SWT. Selected configurations were then tested with a 5% full span flow through model and a half-span model with a turbojet simulator in the 8X6 ft. SWT. Finally, flight tests were conducted with the F-106 aircraft.
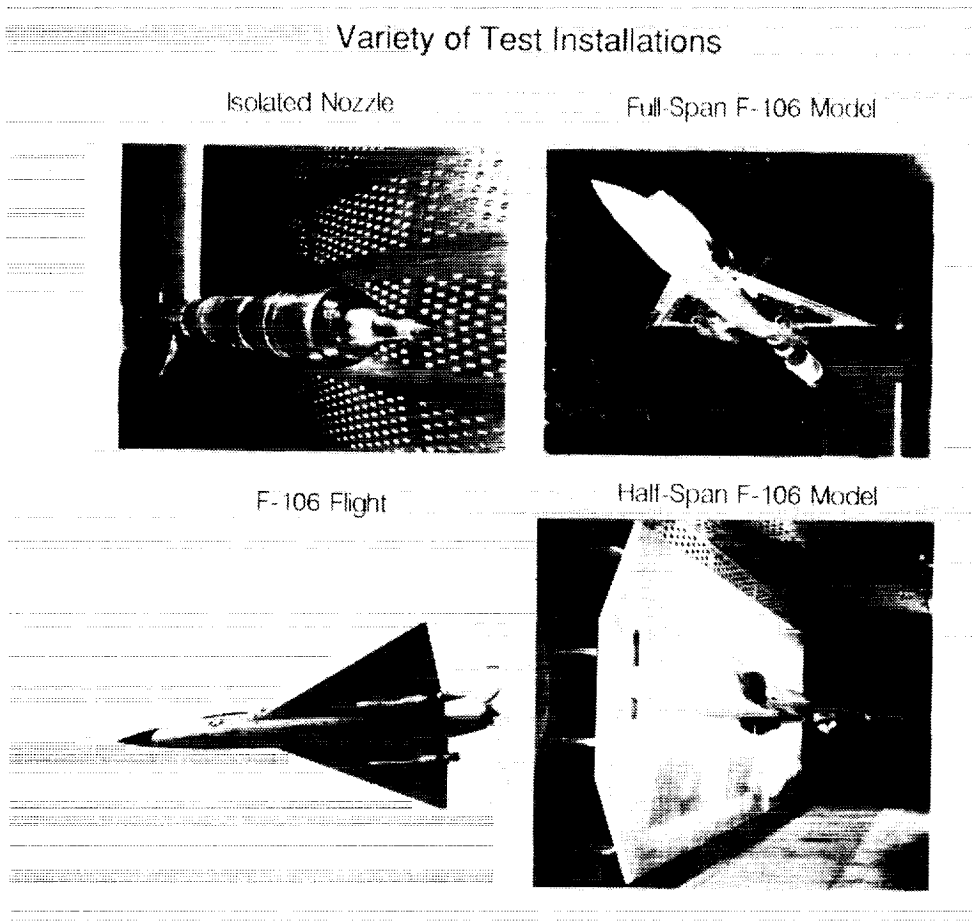


Figure 10

## INSTALLED NOZZLE PERFORMANCE

This chart shows nozzle gross thrust coefficient data that was obtained from the NASA LeRC F-106 program in the late 60's and early 70's. The figure compares data obtained in flight to data obtained in the 8X6 SWT using a 22% scale semi-span model incorporating a turbojet simulator (Ref 3). The upper data was obtained for a variable flap ejector (VFE) nozzle and the lower data was obtained for an auxiliary inlet ejector (AIE) nozzle. The flight and 22 percent scale model data for the VFE nozzle agree very well from Mach 0.6 to 0.9 and agree fairly well from Mach 1.1 to 1.27. At Mach 0.95, the flight data rises above the model data and then falls below the model data at Mach 1.0. In this Mach range, a terminal shock moves off the rear of the nacelle, and the boattail flow becomes supersonic. Model blockage effects retard the passage of this shock system over the wind tunnel model with increasing Mach number, and the drag rise of the model is delayed until Mach 1.0 or higher.

The same sort of blockage effect is also present in the AIE nozzle data, but, in addition, the flight and model performance data for the AIE nozzle do not agree at Mach numbers below 0.9. Wind tunnel model data indicate that the flow through the auxiliary inlet doors of the nozzle is separated. Therefore, to be sure of the performance of nozzles which may have regions of separated flow, it may be necessary to test at the full-scale Reynolds number.

# INSTALLED NOZZLE PERFORMANCE



GROSS THRUST COEFFICIENT, $\dfrac{F_G - D}{F_{IP}}$

F-106 FLIGHT
F-106 22% SCALE

(a) VFE NOZZLE.

FREE STREAM MACH NUMBER, $M_0$

(b) AIE NOZZLE.
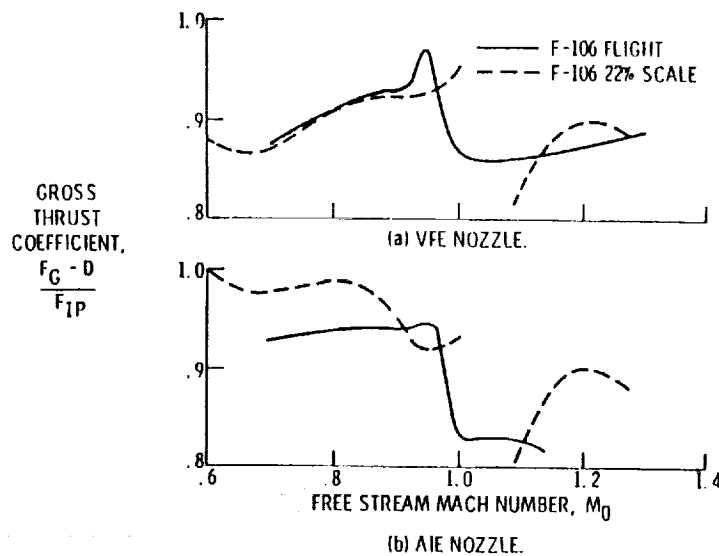
Figure 11

## RELATIVE MERITS OF CONVENTIONAL VS. POWERED SIMULATOR MODELS

The decision to employ powered simulators to better model the propulsion streams is a complex one. On the surface the use of powered simulators appears to be an attractive approach, but there are many other factors to be considered. This chart outlines a number of Test Characteristics and compares the Relative Merits of the Conventional vs. the Powered Simulator approaches. Inherent in the chart is the assumption that the powered simulator model must be a semi-span model to be compatible with the existing simulator hardware. Both approaches would require very comprehensive test programs with extensive calibrations (balances, internal drag, nozzle thrust, simulator airflow and thrust) and elaborate bookkeeping schemes to achieve the required level of data quality. The simulator approach has the greatest potential of providing the best simulation, however the use of a semi-span model and attendant splitter plate in the tunnel can introduce tunnel effects that compromise the data and are very difficult to assess. On the other hand, the conventional approach must use faired inlets and reference nozzle configurations that may introduce extraneous effects that can not be sorted out. The conventional approach can use a full span model, while the powered simulator would be a semi-span model approximately twice the size of the full span model. The full span model could be tested at 2 atmospheres total pressure (Ames 11'X11' Tunnel) to achieve maximum Reynolds number. Although the powered simulator model would be approximately twice the size of the full span model, the simulators (CMAPS) themselves are limited to 1 atmosphere total pressure. Therefore, the maximum Reynolds number of the two approaches would be essentially the same. The appropriate choice is not obvious. Many factors have to be carefully considered in light of the overall test objectives.

## Relative Merits of
## Conventional vs Powered Models

| Conventional | Test Characteristic | Powered Simulator |
|---|---|---|
| ONE with Multiple Nacelles<br>• Flow Thru w/ Variable MFR<br>• Blown Nacelle w/ Faired Inlets | Number of Models | TWO: 1) Full Span Reference Aero<br>2) Powered Semi-Span |
| Complex Small Diameter Flow Thru 6-Component Balance | Balances | Conventional Airplane Balance +<br>Simple 5 Component Floor Balance |
| • Internal Drag<br>• Thrust of Blown Nacelle<br>• Flow Thru Balance | Calibrations | Detailed Thrust and Mass Flow Calibrations of Simulators |
| Very Complex | Bookkeeping Scheme | Very Complex |
| Moderate, Potential Non-Linear Interactions of Nacelle Geometries | Degree of Simulation | High, Potential Adverse Splitter Plate and Boundary Layer Contamination |
| None | Internal Flow Measurements | Very Limited Inlet Data |
| Pt x L = 2 atm x L = 2 atm x L | Reynolds Number | Pt x L = 1 atm x 2L = 2 atm x L |
| Great | Level of Complexity | Very Great w/ Rotating Machinery |

Figure 12

## SIMULATOR/ENGINE MATCHING

Many organizations have utilized propulsion simulators during the past 25 years. At present there are two existing simulator designs within NASA that can be used to represent the engine for a system similar to the HSR. Ames has a 3 inch simulator design which has a design compressor corrected airflow of 1.65 lbm/sec. This design is referred to as CMAPS (compact multimission propulsion simulator). There are four of these simulators in existence. Lewis has a 4.3 inch simulator design which has a corrected design compressor corrected airflow of 2.85 lbm/sec. There is one of these simulators in existence. This chart shows how these two simulators would scale based on a full scale engine corrected air-flow of 550 lbm/sec. Since the prime scaling parameter would be based on corrected airflow, the CMAPS simulator would represent a 5.5% scale and the Lewis simulator a 7.2% scale.

## SIMULATOR/ENGINE MATCHING

| Simulator or engine | D2 in. | W #/sec | L in. | Scaling Based on: | | | Max EPR | P2 Max psia |
| --- | --- | --- | --- | --- | --- | --- | --- | --- |
| | | | | D2 % | W % | L % | | |
| Ames(CMAPS) | 3.0 | 1.65 | 10.4 | 5.3 | 5.5 | 8.6 | 3.6 | 16.0 |
| Lewis | 4.3 | 2.85 | 17.7 | 7.5 | 7.2 | 14.6 | 2.8 | 17.0 |
| HSR Engine | 57.1 | 550 | 121 | 100 | 100 | 100 | 5.0 | — |

Figure 13

1452

## CMAPS AIRFLOW SCHEMATIC

The airflow through the Compact Multimission Aircraft Propulsion Simulator (CMAPS) is shown in the figure below (Ref. 1). The drive air powers the single stage turbine and drives the four stage compressor. The design compressor corrected air flow is 1.65 lbm/sec. The compressor airflow is a function of compressor RPM and be varied from approximately 1.0 lbm./sec to the design value. Compressor discharge air is mixed with the turbine drive air and exhausted either through the nozzle or bleed out of the simulator. This ability to remove air from the exhaust stream, allows the nozzle pressure ratio to be varied independent of the compressor air flow. At the design airflow the engine pressure ratio can be varied from approximately 1.6 to 3.6. The maximum physical rotor speed is 88,000 RPM.



CMAPS AIRFLOW SCHEMATIC
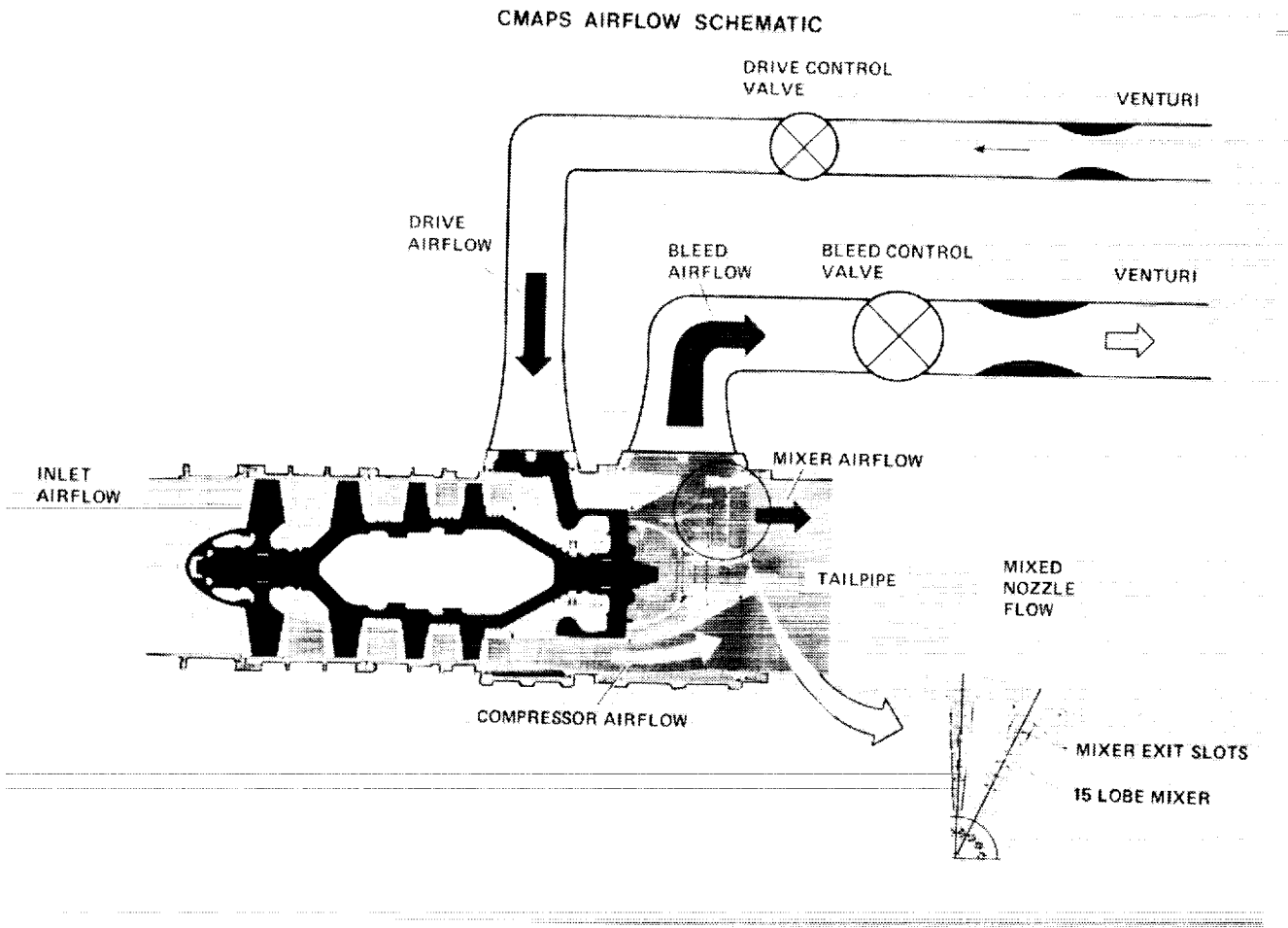
Figure 14

## LEWIS PROPULSION SIMULATOR

The aerodynamic design of the Lewis turbojet simulator is based on the use of the six-stage axial compressor from the Allison T63 turboshaft engine. (Ref. 3). Its compact design and its relatively high mass flow and pressure ratio characteristics, plus the fact that it was a developed compressor in production, were the factors that lead to its selection as the critical component on which to base the simulator design. It's maximum corrected weight flow is 2.85 lbm/sec. The inlet air is compressed by the compressor and supplied to the nozzle through an annulus around the three-stage turbine. The turbine is powered by an external supply of 450-psia air that could be heated to 700 F. It's maximum physical rotor speed is 63,000 RPM. The drive air was supplied to an annular chamber around the engine and then through five of the six struts of the mid frame to an inner chamber feeding the turbine. (The top strut, which was aligned with the turbine air supply line, was blocked to obtain better distribution of the flow.) The air expands through the turbine and discharges into an annulus and then is mixed with the stream from the compressor. To obtain a desired ratio of nozzle throat area to engine inlet area and maintain proper nozzle pressure ratios, makeup air is supplied to fill the nozzle. The makeup air is supplied to an annular chamber from which it is fed to the nozzle through a 1/8-inch annulus concentric with the annulus from the compressor turbine. To improve uniformity of the flow, the three concentric streams are passed through a "daisy" mixer before entering the nozzle. The mixer was designed to rearrange the flow into eight radial lobes while maintaining a constant flow area in each of the three flow passages.

## LEWIS PROPULSION SIMULATOR
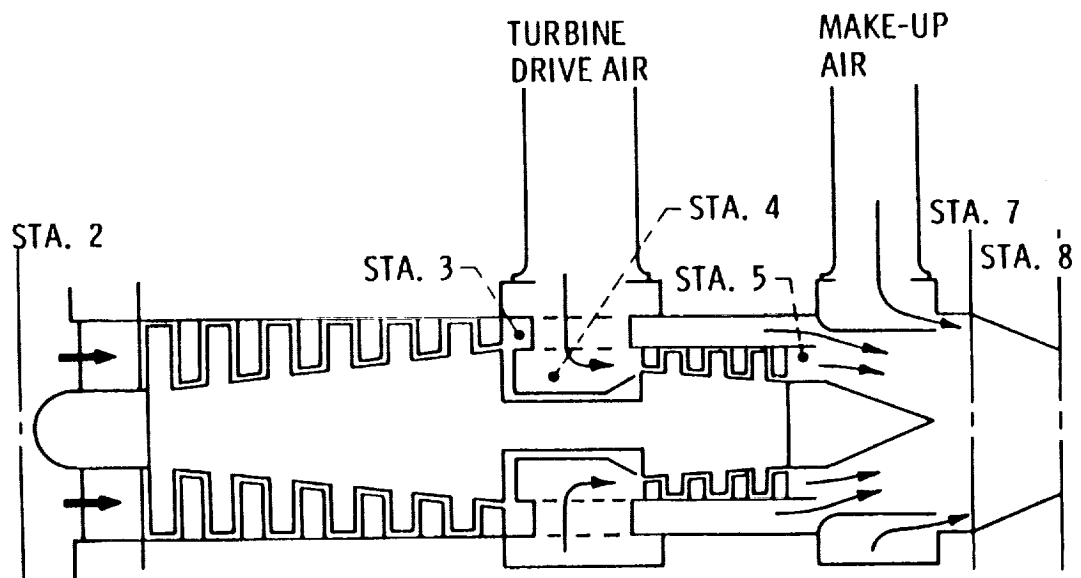


Figure 15

## MODEL SCALING

The appropriate scale for various test models is a function of the type
of test and the proposed test facility. This chart illustrates the resulting
model characteristics as a function of various scaling parameters for the Ames
11 by 11 ft. wind tunnel and a full scale aircraft that is 300 feet long, has
a wing span of 135 feet, a maximum cross sectional area of 225 square feet and
an engine that has a maximum corrected air flow of 550 lbm. sec. The first
three categories correspond to typical constraints in the Ames 11 ft. tunnel
for full span models, namely, a blockage of 1/2%, a span of half of the tunnel
width (5.5 ft.), and an overall model length of 6 ft. The only one of these
categories that meet all three of the full-span criteria is the model scaled
to the 6 ft. length which results in a very small 2% scale model. The
blockage of this model would be .08% and the wind span would be 2.7 ft. The
next category assumes a semi-span model scaled to a 16 ft. length which is a
reasonable semi span length for the 11 ft. test section which is 22 ft. long.
This model would be at 5.3% scale with a semi-span of 3.6 ft. and a blockage
of .26%. As with the full span models, the length is the critical parameter
in determining the maximum semi-span scale. The fourth category is a model
sized to the 2.85 lbm/sec of the Lewis powered simulator. This results in a
7.2% scale model that is 21.6 ft. long with a wind semi-span of 4.9 ft. and a
blockage of .49%. This model is too long for the 11 ft. tunnel. The last
category is sized to the 1.65 lbm/sec of the Ames CMAPS simulator. This
results in a 5.5% scale model that is 16.4 ft. long with a semi-span of 3.7
ft. and a blockage of .28%. When considering each of the resulting models
from this scaling exercise, this semi-span model sized to match the CMAP
airflow seems to be the best choice.

## MODEL SCALING
## AMES 11X11 FT. WIND TUNNEL
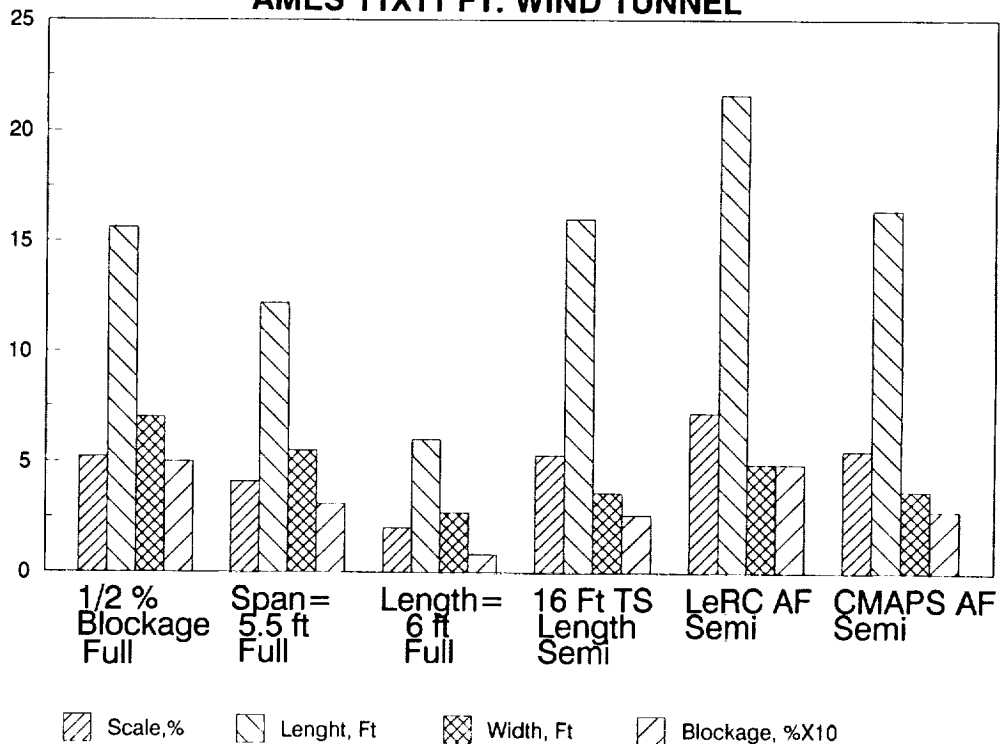


Figure 16

## BOATTAIL DRAG

During the F-106 nozzle program, it was found that for a given
configuration, boattail drag could be a strong function of Reynolds Number.
This figure shows a generic curve of boattail drag vs. Reynolds Number that
was generated from the F-106 Program for an arc-conic boattail at subsonic
Mach numbers of 0.6 to 0.9 (Ref. 4).  The observed drag variation with
Reynolds number is the result of changes in the boundary layer thickness and
separation on the aft part of the boattail.  Pressure distributions on a
typical nozzle boattail are shown schematically in this figure for three
values of Reynolds number.  The solid lines are typical of the observed
pressure distributions.  The dashed lines represent the pressure distribution
for inviscid flow.  Drag is low at the very high Reynolds numbers.  Due to
thin boundary layer, the flow remains attached over a major portion of the
boattail.  This results in a large expansion at the boattail shoulder but
allows the flow to recompress to relatively high pressure on the aft boattail,
which offset the low pressures at the shoulder.  As the Reynolds number is
decreased the boundary layer becomes thicker.  With the thicker boundary layer
the flow cannot traverse the adverse pressure gradient as far and will
separate sooner.  As the separation on the aft boattail increases, the
recompression is lost and drag increases.  As the Reynolds number is lowered
still further the boundary layer becomes thicker causing separation to occur
closer to the boattail shoulder which decreases the overexpansion.  Eventually
the beneficial effects of increasing pressure at the shoulder become large
enough to offset the adverse effects of increased separation on the back of
the boattail.  Drag thus reaches a peak and then begins to decrease with
further lowering of Reynolds number.

# BOATTAIL DRAG



Figure 17

1456
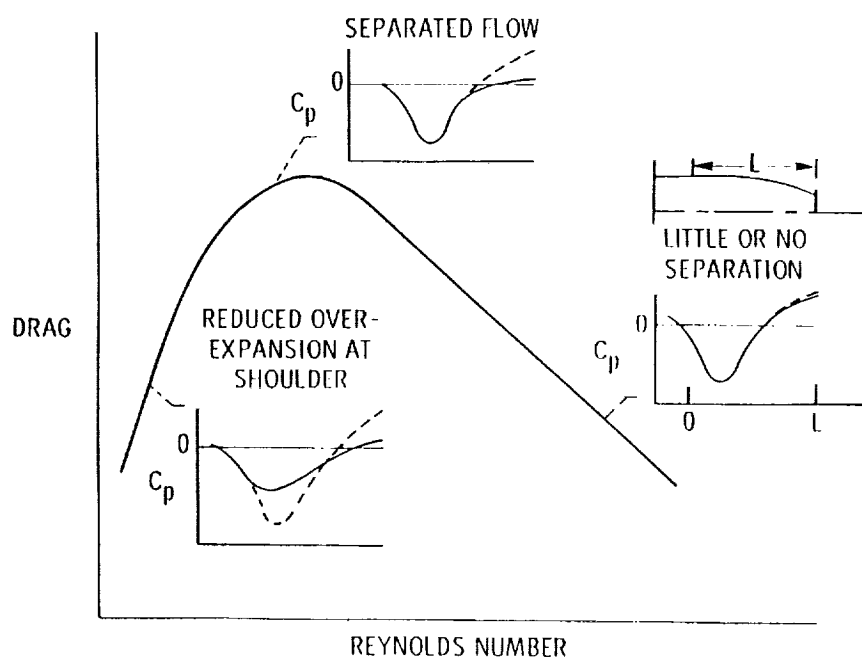
## PRACTICAL ISSUES

There are several practical issues that must be addressed for either the conventional three model approach or the simulator approach. Of prime importance is the question of what data accuracy is required. First the mission sensitivity must be known so that the significance of a drag count can be determined. Knowing the mission sensitivity, the required model accuracy in drag counts can be determined. The type of model (full span or semi span, conventional or simulator model) will determine the number of models required, the balance configuration and the accounting system to be used. If a simulator approach is chosen, the issue of mounting the simulator and plumbing the required airflow lines through the wing without violating the mold lines of the configuration must be addressed. This will be more of a problem for an HSCT type of configuration than for past efforts with fighter configurations which had greater internal volume available for instrumentation and plumbing.

# PRACTICAL ISSUES

- MOUNTING AND PLUMBING OF SIMULATOR(S) WITHOUT VIOLATING MOLD LINES OF VEHICLES

- ACCEPTABLE LEVEL OF ACCURACY

    - MISSION SENSITIVITY

    - $\pm$ X DRAG COUNTS

    - ABSOLUTE VS INCREMENTS

Figure 18

C-8

## CONCLUSIONS/RECOMMENDATIONS

Reviewing past conventional models versus powered model data reveals that powered models appear to offer an accuracy advantage. Models sized for the ARC 11 ft. will be constrained by length but a semi-span model sized to the CMAPS airflow appears to be a reasonable size for this facility. Low Reynolds number compared to flight may be a problem for some propulsion system configurations and the CMAPS powered model does not offer any Reynolds number advantage. The information presented in this paper resulted from a very cursory look at the overall issue of transonic airframe propulsion integration testing for HSR. The purpose of this paper is to create an awareness of these transonic testing issues within the HSR propulsion/airframe community. The recommendation is that a much more detailed study of the practical issues is required either in HSR Phase I or early in HSR Phase II.

# CONCLUSION/RECOMMENDATIONS

## CONCLUSIONS:

- POWERED MODEL APPEARS TO OFFER ACCURACY ADVANTAGE

- MODELS WILL BE CONSTRAINED BY LENGTH

- CMAPS POWERED SEMI MODEL APPEARS REASONABLE FOR ARC 11-FT WIND TUNNEL

- REYNOLDS NUMBER MAY BE PROBLEM FOR SOME NOZZLE CONFIGURATIONS
  - NO ADVANTAGE FOR CMAPS POWERED SEMI SPAN MODEL

## RECOMMENDATIONS:

- HSR PHASE I OR EARLY PHASE II STUDY TO INVESTIGATE PRACTICAL ASPECTS OF ALTERNATIVES

Figure 19

1458

# REFERENCES

1.  Zilz, D.E.; Wallace, H.W.; Hiley, P.E.:  Propulsion and Airframe
    Aerodynamic Interactions of Supersonic V/STOL Configurations Volume IV:
    Final Report - Summary.  NASA CR-177343, 1985.

2.  Bencze, Daniel P.:  Experimental Evaluation of Nacelle-Airframe
    Interference Forces and Pressures at Mach Numbers of 0.9 to 1.4.  NASA TM
    X-3321, 1977.

3.  Steffen, F.W.; Satmary, E.A.; Vanco, M.R.; Nosek, S.M.:  A Turbojet
    Simulator for Mach Numbers up to 2.0.  NASA TM X-67973, 1972.

4.  Wilcox, F.A.; Chamberlin, R.:  Reynolds Number Effects on Boattail Drag
    of Exhaust Nozzles From Wind Tunnel and Flight Tests.  NASA TM X-71548,
    1974.

THIS PAGE INTENTIONALLY BLANK

# Session X. Airframe/Propulsion Integration

Results of a Preliminary Investigation of Inlet Unstart on a High-Speed Civil Transport Airplane Concept
*Christopher S. Domack, Lockheed Engineering and Sciences Company*

THIS PAGE INTENTIONALLY BLANK

1462

# Results of a Preliminary Investigation of
# Inlet Unstart on a
# High-Speed Civil Transport Airplane Concept

Christopher S. Domack
Lockheed Engineering & Sciences Co.
Langley Program Office
Hampton, VA 23666

The aircraft design engineer today is tasked with satisfying an increasing number of conflicting requirements.The fact that conflict in these requirements may be technically, economically, or politically motivated usually compounds the difficulty of determining the best solution to a design issue. In this regard, propulsion/airframe integration for supersonic airplanes must rank as one of the most challenging aspects of airplane design.

For the cruise Mach numbers currently being considered for High-Speed Civil Transport (HSCT) airplanes, the inlet requirements of low drag, low bleed flow, and high pressure recovery appear to be best met with a mixed-compression design. Unfortunately, these desirable attributes come with a highly undesirable companion: the inlet unstart phenomenon. Concern over the effects of a mixed-compression inlet unstart on the vehicle dynamics of large, high-speed aircraft is not new; a comprehensive wind-tunnel study addressing the problem (ref. 1) was published in 1962. Additional investigations of the problem were made throughout the United States SST program and the follow-on NASA programs into the late 1970's. The current study sought to examine the magnitude of the problem in order to determine if an inlet unstart posed a potential hazard severe enough to preclude the use of mixed-compression inlets on proposed HSCT concepts.

## Supersonic commercial airplane inlet unstart susceptibility is not a new concern

- o NASA off-design mass flow test (1962)
- o NASA inlet isolation concepts (1966)
- o Boeing analytical studies (1969, 1976)
- o Lockheed wind-tunnel tests (1976)

## The Inlet Unstart Phenomenon

The term *unstart* refers to the expulsion of the shock system internal to the cowl in a mixed-compression or internal-compression inlet. An abrupt change in operating conditions (e.g., wind shear or large freestream temperature change) may cause an unstart. During an unstart, the inlet mass flow is drastically reduced, and its drag is greatly increased. Due to the abrupt mass flow reduction and increase in inlet flow distortion, the affected engine's compressor may stall and its combustor flame out. An unstart may also be *caused by* a compressor stall upon a sudden change in engine airflow demand such as afterburner ignition. Inlets with increasing amounts of internal compression, more desirable as cruise Mach number increases, tend to be less tolerant of operating disturbances. Some experimental evidence reported in reference 2 suggests that an axisymmetric inlet configuration may exhibit greater angle of attack tolerance than an equivalent two-dimensional configuration.

The shock wave that propagates upstream during a compressor stall is termed a *hammershock*. Once a compressor stall has commenced, the expulsion of the hammershock takes place in milliseconds. Figure 1, from reference 3, indicates that the static pressure at the engine compressor face produced by a hammershock may be more than twice the static pressure in the inlet during normal operation, and that the strength of the hammershock is directly proportional to the compressor system static pressure ratio. A particularly strong hammershock may cause damage to the inlet structure and precipitate engine damage.

## Comparison of Hammershock Pressure Ratios
## for Several Engines

**Ref.: NASA TM X-71594**
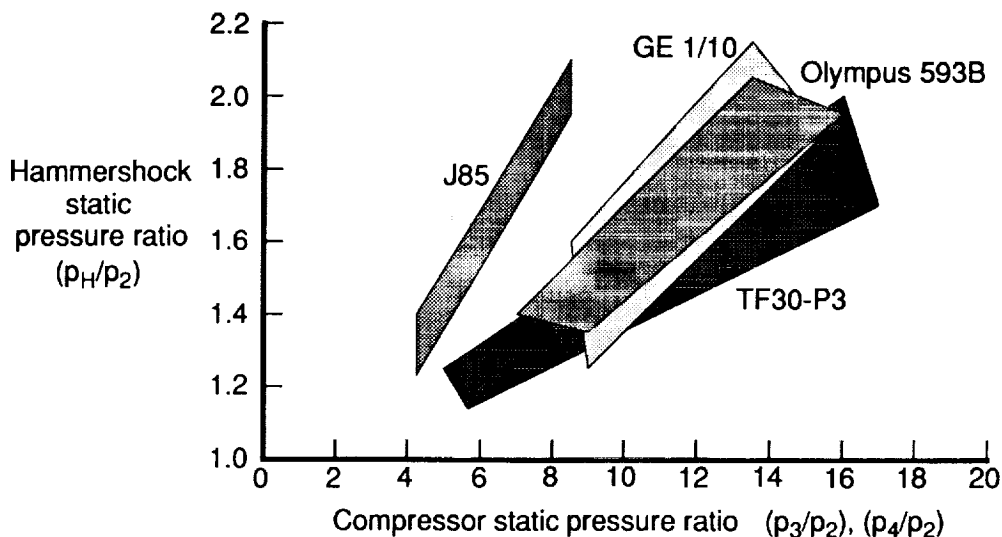


Figure 1.

An inlet unstart has effects on an aircraft besides engine operation. As illustrated in figure 2, from reference 4, the flow upstream of an unstarted inlet may interact with the boundary layer on adjacent surfaces. If the affected boundary layer happens to be on a wing or other airframe component with flight control surfaces, the potential exists for degradation of control surface effectiveness and increased drag due to shock-induced boundary layer thickening or separation. Ingestion of the thickened boundary layer by the engine could also affect engine operation and make a restart more difficult. The bow shock of an unstarted inlet may impinge on adjacent engine inlets and cause them to unstart also.

The asymmetrical changes in the engine thrust, inlet drag, and nacelle pressure field beneath the wing for "conventional" HSCT configurations could cause the airplane to pitch, roll, and yaw. The loss of thrust and increase in drag would also result in an abrupt deceleration. Several methods, both passive and active, have been proposed to minimize these vehicle dynamic effects. Passive approaches seek to reduce the effects of an inlet unstart through judicious nacelle placement and the use of fixed aerodynamic devices to prevent unstart propagation. Active approaches involve minimizing the asymmetry of the flight condition through the use of automatic engine and flight controls. The required level of control automation appears to be well within the current state of the art.

## Shock/Boundary Layer Interaction due to Inlet Unstart
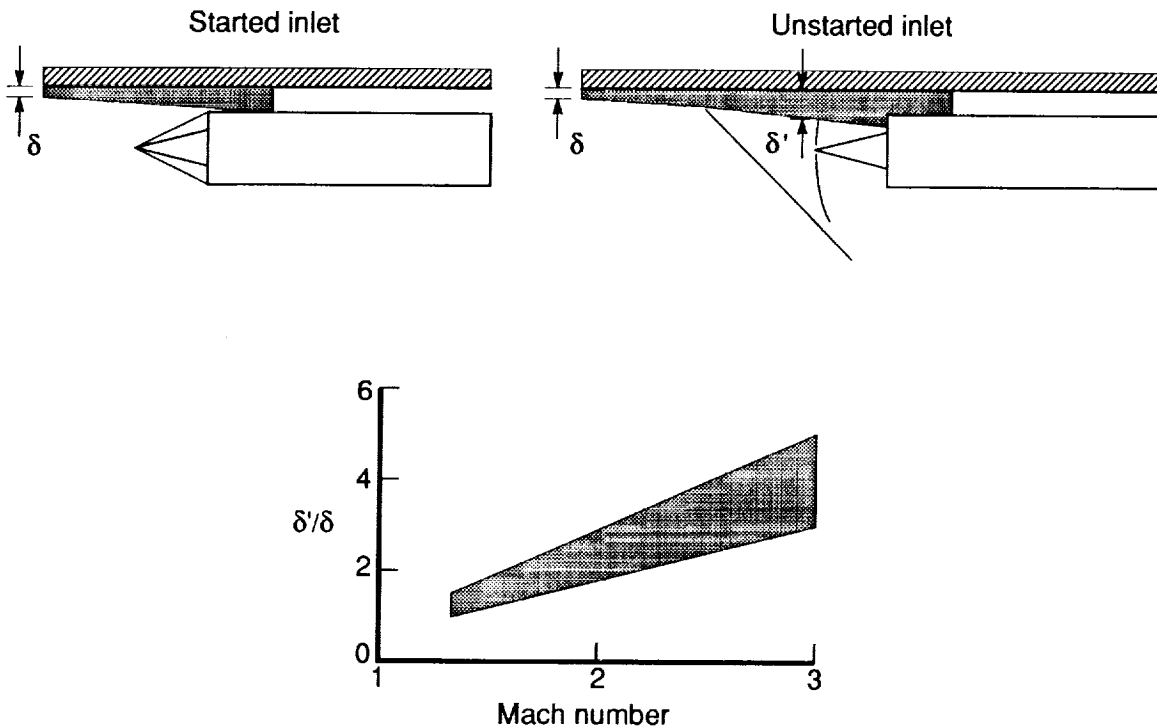


Figure 2.

Figure 3, also drawn from reference 4, shows the nacelle spacing requirements for a pair of axisymmetric, Mach 3, mixed-compression inlets to prevent an unstart on one inlet from unstarting the other. The unstarted inlet in this case was in a steady-state buzz condition. The author of this reference cautioned that these data should be viewed with reservation for design purposes, as they may depend on the degree of shock/boundary layer interaction present and on the operating characteristics of the inlets under consideration. Conservatism would dictate somewhat greater spacing requirements than those shown in the figure.

The difficulty in predicting the occurance of mutual unstarts and the susceptibility of a given inlet configuration to the problem is substantial. Contrary to what might be expected, it was also noted in reference 4 that an unstart in one branch of the bifurcated inlet of the XB-70 airplane did not generally induce an unstart on the other side. This characteristic was thought to be at least partly attributable to the inlet configuration of the XB-70, a vertical wedge mounted beneath a large boundary layer separation plate.

## Nacelle Separation Requirements

### M=3, mixed-compression, axisymmetric inlets; steady-state buzz



Figure 3.                                                                1467
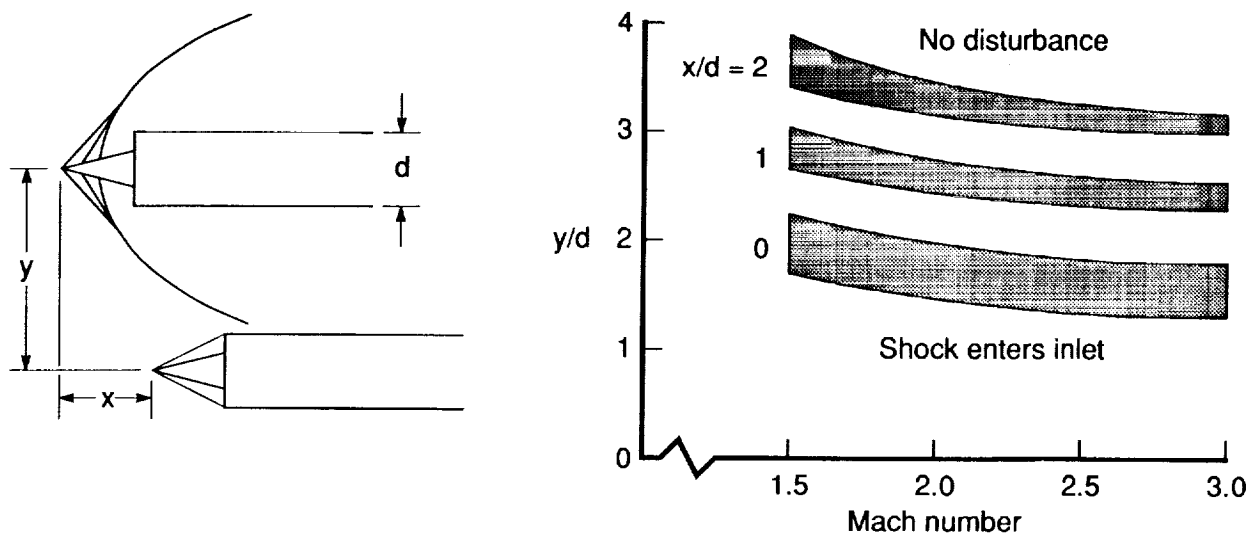
Another passive concept that has been tested successfully (ref. 5) in the prevention of mutual unstarts is the splitter plate. Figure 4 is an artist's concept of a splitter plate installed on a twin-engine nacelle to isolate one inlet duct from the other. It was reported in reference 5 that splitter plates of practical size will isolate an unstarted inlet at Mach 2.5 if the mass flow ratio of the unstarted inlet is maintained above about 0.65. The plates remained effective for yaw angles up to 6 degrees windward. For nacelle installations close to the wing undersurface (low mounting pylon heights), it was found necessary to eliminate any gap between the splitter plate and the wing. Splitter plates have also been proposed for installation between axisymmetric, individually-podded engines (ref. 6) to prevent propagation of unstarts. The required size and effectiveness of such an installation is not known.

Active control systems have been implemented on the SR-71 and Concorde aircraft to minimize vehicle accelerations and displacement angles. The SR-71 inlet control system incorporates what is called a *crosstie*; upon detection of an inlet unstart on one side of the aircraft *both* inlets immediately begin a restart cycle, thus avoiding a large lateral-directional force asymmetry. A similar philosophy was proposed by Boeing in a 1977 supersonic transport configuration study (ref. 7.) A prototype digital integrated airframe/propulsion control system was successfully tested (ref. 8) as a replacement for the original analog systems on the SR-71 in 1979. The Concorde's air intake control system, described in reference 9, is linked to an autorudder control in order to prevent the development of unacceptably large sideslip angles upon detection of an engine or intake malfunction.

## Inlet Splitter Plate Concept



COWL
CENTERBODY
COWL
SPLITTER PLATE
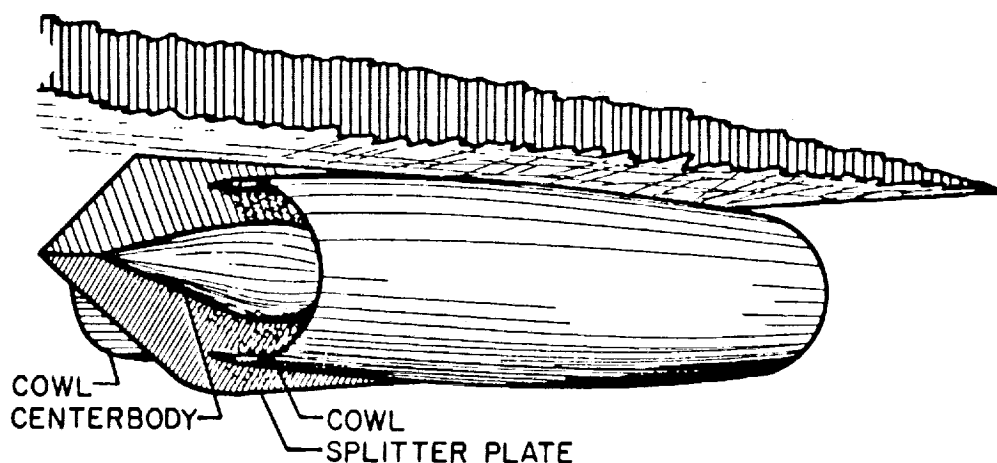
Figure 4.

## Inlet Unstart Effects on an HSCT Concept

Reference 6 also provided data upon which a simple kinematic analysis of inlet unstart effects on an HSCT vehicle concept was based. These data, summarized in figure 5, consisted of wind-tunnel test results for an aircraft configuration very similar to those currently under consideration, but with three different nacelle locations. Each of the nacelle locations was tested at three different inlet mass flow ratios, accomplished by varying the amount of internal blockage in the model nacelle. Area blockages of 0%(free-flowing), 50% and 100%(no flow through) were tested.

## Wind-tunnel Test Data Summary
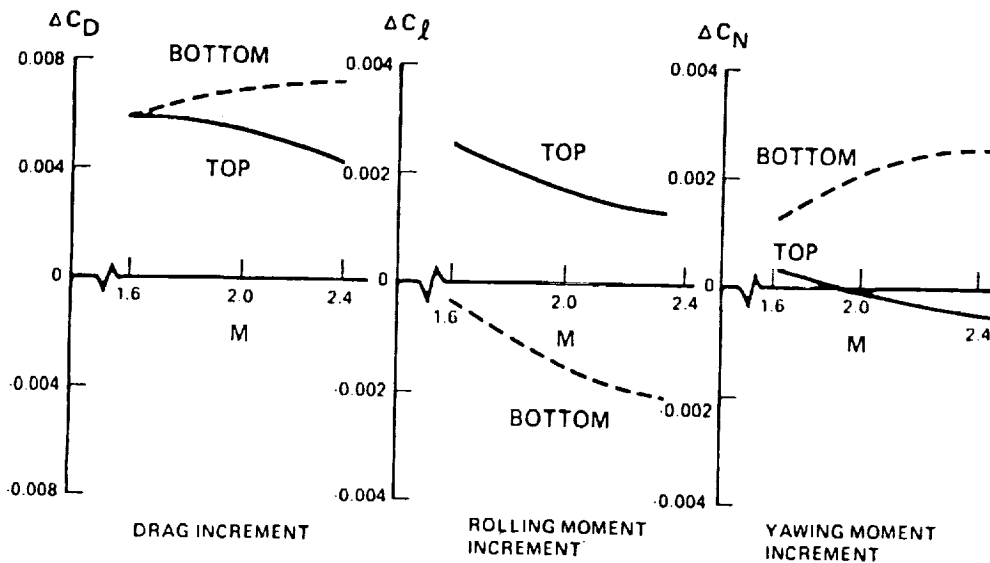


Figure 5.

Figure 6 illustrates the results of oil flow studies done during the Lockheed wind-tunnel test; the effect of the simulated unstarted inlet (50% blocked nacelle) on the wing streamlines is substantial and clearly evident. The photographs were taken at a test Mach number of 1.6 and an angle of attack of two degrees. Though the photographs show nacelle N1, which was the inboard nacelle mounted on the upper surface of the wing, similar results would be expected for nacelles mounted beneath the wing. One of the conclusions stated in reference 6 was that, based on these data, the over/under nacelle installation of the Lockheed concept posed less of a problem upon inlet unstart than a conventional four-engine underwing installation.

M = 1.60    α = 0.0349 RAD (2.0°)
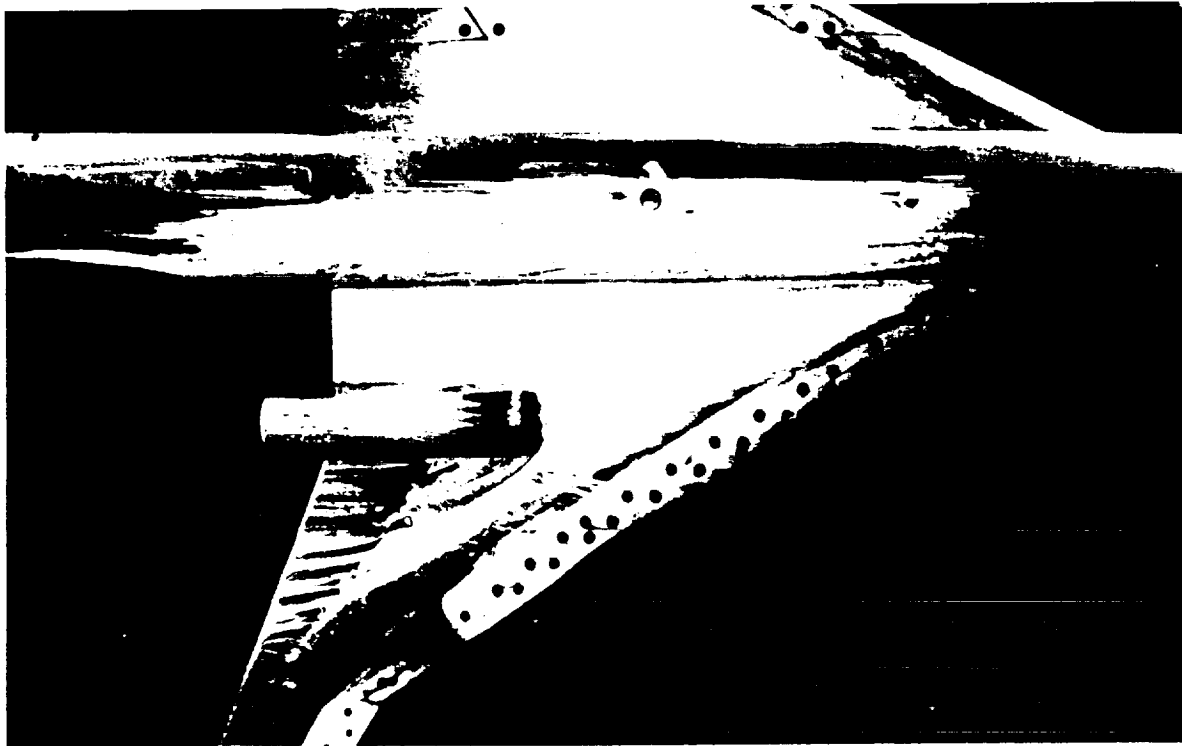


N₁ FREE FLOWING
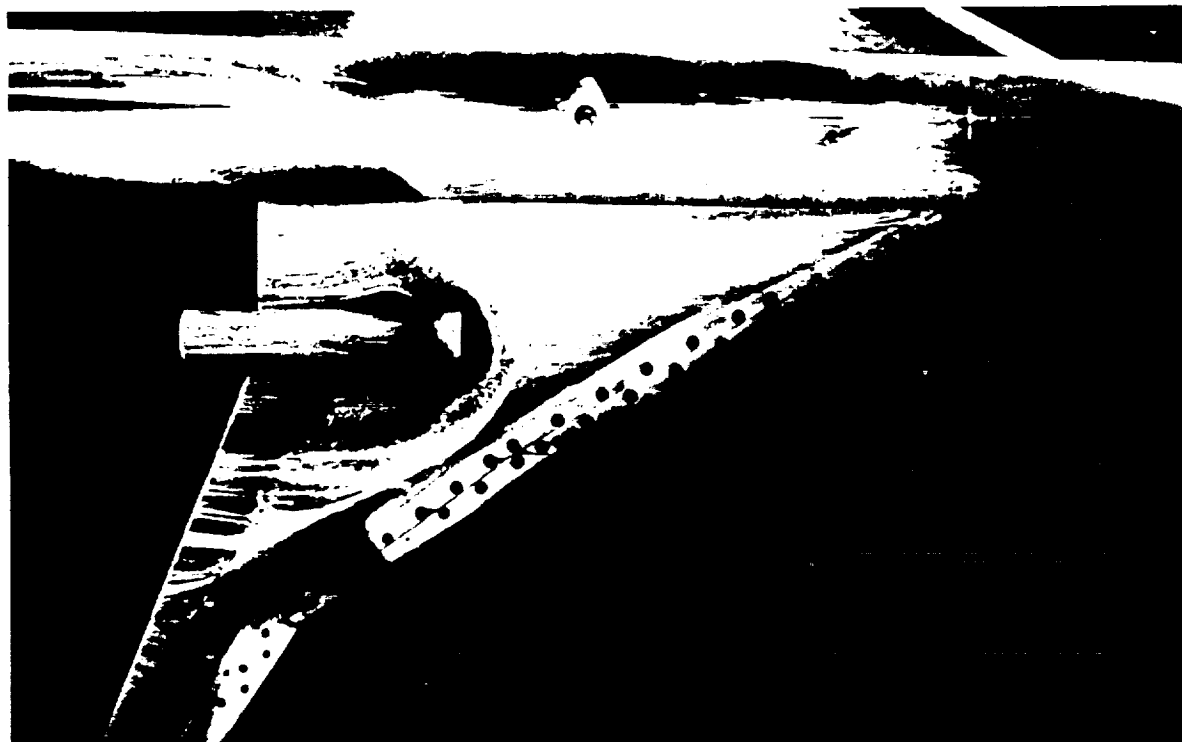


N₁ 50 PERCENT BLOCKED

Figure 6.

The following assumptions were made in the kinematic analysis in addition to the use of the wind-tunnel data just described. For conservatism, and since the analysis was for an instantaneous (peak) condition rather than a sustained, steady-state condition, the drag force of the hammershock pressure pulse acting over the assumed inlet capture area was included and only rigid airplane motion was considered. Additionally, the snapshot analysis does not include forces and moments opposing the unstart that would be generated by the basic airframe aerodynamics or flight control system.

## Assumptions

o Sample configuration as per CR-145133
o Engine-out condition initiated at M=2.0, h=55000 ft, n=1.0
o Outboard engine, locked rotor
o Inboard engine, inlet unstarted
o Roll, pitch, and yaw inertias from NASA AST-105 configuration
o Wind-tunnel data from Lockheed test (underwing nacelles only)
o Seized engine taken as 100% blocked condition
o Unstarted engine taken as 50% blocked condition
o Thrust of failed engines zero; cruise thrust (12,500 lb) on others
o Hammershock pressure pulse included in drag force
o Instantaneous accelerations and angular rates only
o Rigid-airplane motion only
o No opposing propulsive or aerodynamic control forces

The free-body diagram presented in figure 7 was used in the kinematic analysis. Dimensions shown are generally representative of a Mach 2.5, 290-passenger vehicle with a gross weight of 600,000 lb as described in reference 6. The accelerations were analyzed at the crew station because it was the point furthest from the airplane center of gravity, about which the angular acceleration rates were calculated.

## Inlet Unstart Analysis Force Arrangement
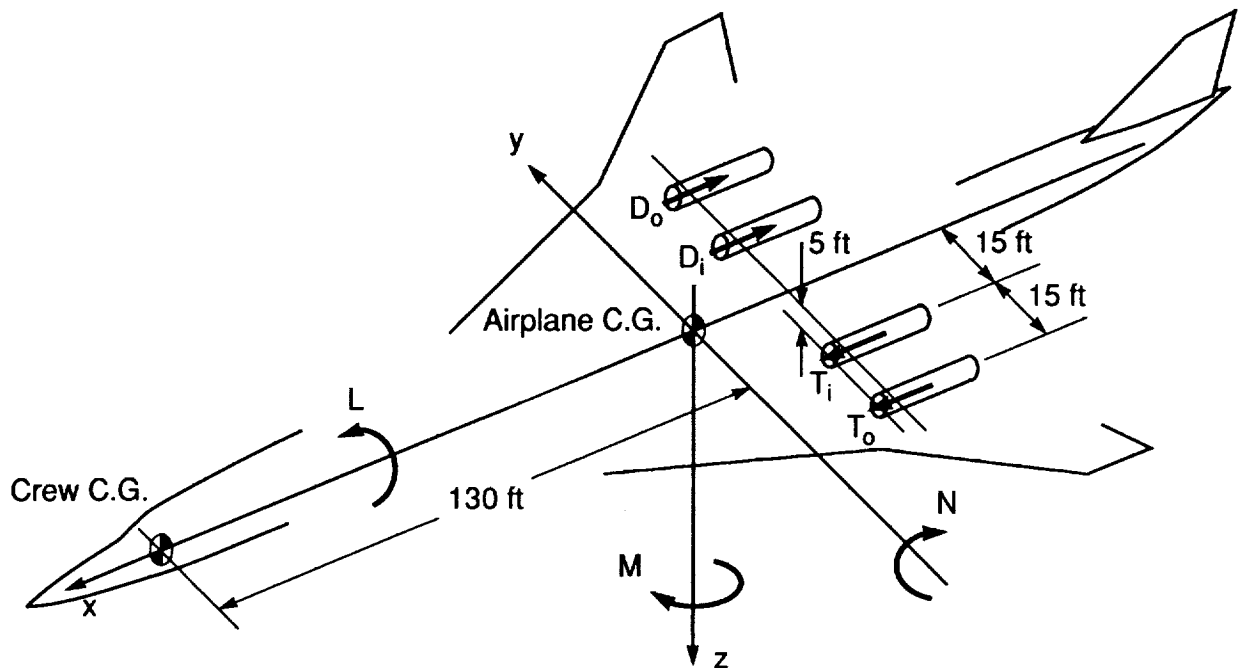
Figure 7.

Results of the analysis are shown in the accompanying table below. Even with the substantial level of conservatism in the analysis, the acceleration levels at the crew station are seen to be relatively mild. The instantaneous acceleration rates at cabin locations closer to the airplane center of gravity would be even lower. The accelerations calculated are of the same order of magnitude as those experienced in light to moderate turbulence in a modern subsonic transport, or in an automobile on a rough road.

In short, although the forces on the airplane during an unstart are large, so is its inertia. Therefore, *unless the unstart forces are sustained and unopposed* by the pilot, flight control system, engine controls, or combinations thereof, large rates and angular displacements are unlikely to develop. The potential for passenger injury due to vehicle motions induced by an unstart thus appears no more serious than that due to normal atmospheric turbulence. There is, however, a passenger-related aspect to the unstart problem that may require further investigation. It is likely that the noise of an inlet unstart (probably like a muffled explosion) would be very distressing to passengers, and attempts should be made to explore the magnitude of this problem.

## Results

| Axis | Cockpit accel, g | Angular accel, deg/s$^2$ |
|---|---|---|
| Roll | -.04 | 15.1 |
| Pitch | -.04 | 0.5 |
| Yaw | .24 | 3.3 |

o  Although the forces involved are large, so are the airplane inertias; thus the resulting accelerations are small

o  The instantaneous rates represent a worst-case (peak) situation; steady-state values will be lower

## Validation of Results

With the tabulated values in hand, an attempt was made to find flight data to test the validity of the calculated accelerations. Figure 8, from reference 10, shows the lateral and longitudinal responses of the Concorde aircraft to a double engine surge. Recall that the automatic flight control system of the airplane immediately applies corrective rudder input upon sensing an asymmetrical thrust condition; this can be seen clearly in the recording of rudder angle. The aircraft stabilizes in about 12 seconds at very small angles of bank and sideslip, and decelerates smoothly at constant altitude. The control surface deflections required to contain the transient are quite small.

The double engine surge condition is presented for the Concorde because it is the practical equivalent of a double unstart as described for the conceptual HSCT. The Concorde inlets do not "unstart" in the strict sense of the word, because they are basically an external-compression design. However, like other external-compression inlets, they are susceptible to the *buzz* instability, and incorporate active control measures similar to those required for mixed-compression inlets.

## Concorde Response to Double Engine Surge



Figure 8.                                                                 1475
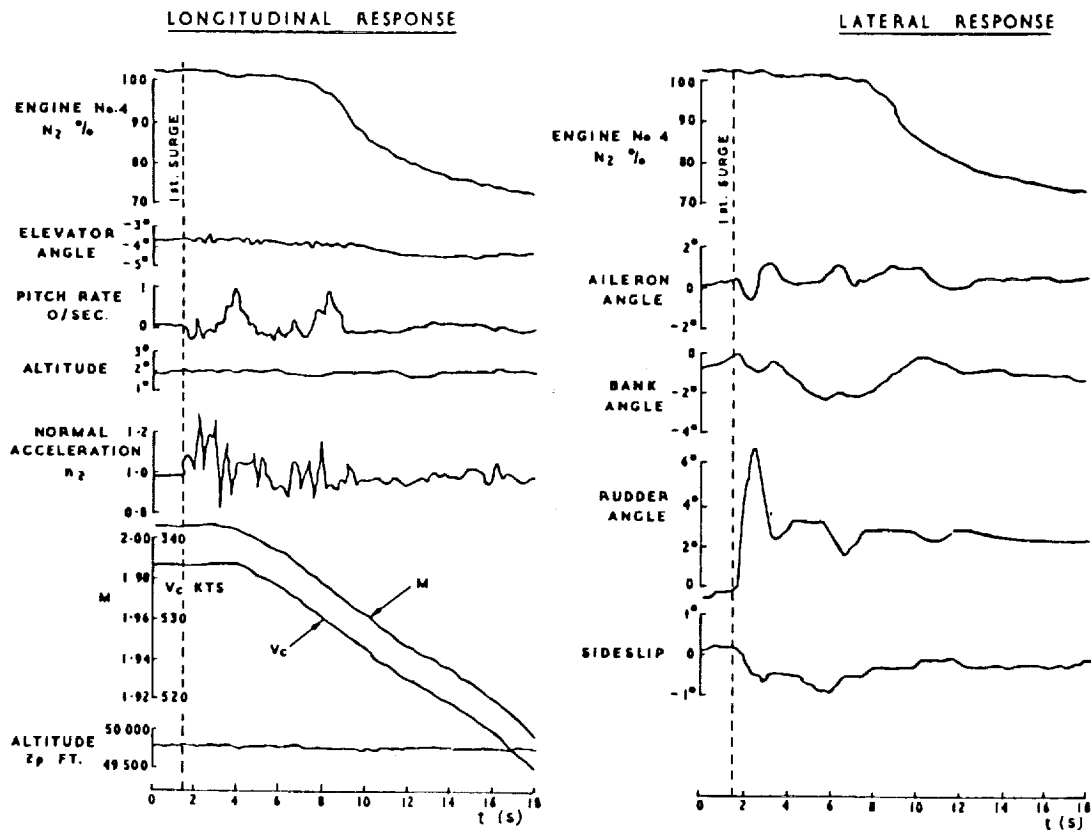
A similar flight test history was found in reference 11 for the XB-70 airplane, and is presented in figure 9. The reactions to a double unstart in this case are somewhat more pronounced than those of the Concorde; however, recall that the XB-70 traces shown are for Mach 3 as compared to Concorde's Mach 2 cruise. A pilot's description of an XB-70 unstart transient was published in reference 12. The unstart transient was termed "mild," with about 25% of the available roll control power being used to counter the induced rolling motion. The comment was also made that even though most XB-70 inlet unstarts were deliberate, each unstart event was startling even to a crew experienced in flight testing.

## XB-70
## MACH 3 DOUBLE UNSTART



Figure 9.

1476
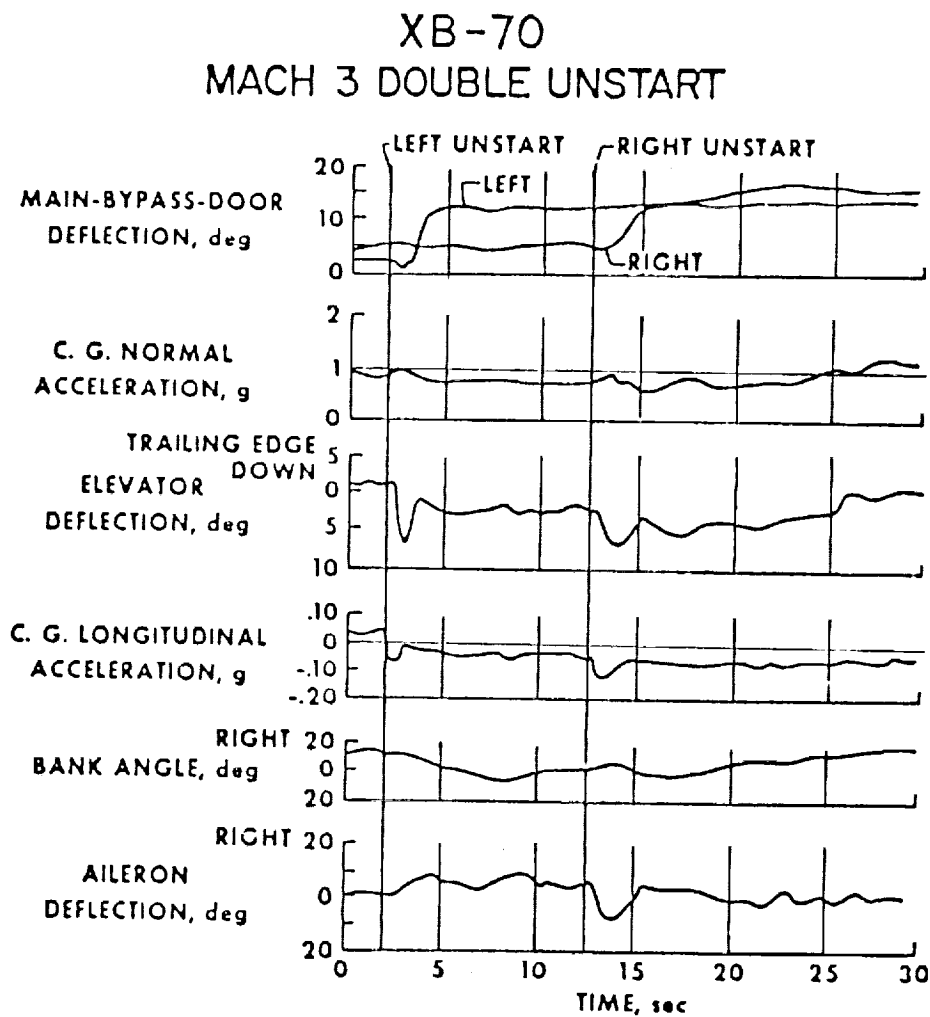
Considerable attention has been devoted in popular aviation literature to the inlet unstart behavior exhibited by the YF-12 / SR-71 airplane. Colorful metaphors and dire predictions of helmets slamming into cockpit windows make entertaining reading; an engineering assessment of the problem is more mundane (fig. 10.) While the unstart effects on this airplane are certainly more severe than those shown previously, it is most important to realize why this is so, and why an extrapolation of these results to an HSCT is not valid.

Undoubtedly, the unstart problems experienced by the YF-12 airplane in its development phase were severe, and the source of many of the aforementioned pilot comments. The results shown in figure 10 were obtained with the production stability augmentation system and automatic inlet control system operating, and still show significant accelerations and displacements of the airplane caused by the unstart; note that recovery from the condition used up over half the available lateral-directional control power. This behavior is largely the result of configuration attributes which are unlikely to be shared by an HSCT airplane. For example, the relative size (thrust) and placement of the YF-12 powerplants are very different from the four-engine underwing installations proposed for most HSCT airplanes. The YF-12 nacelle itself contibutes to some stability and control problems due to the design and operation of the various bypass and bleed provisions; reference 13 contains a description of some of these effects. The higher thrust-weight ratio, higher cruise altitude and Mach number, and lower cruise lift-drag ratio of the YF-12 / SR-71 compared to current HSCT concepts are also important differences influencing the airplane's response.

## YF-12 Inlet Unstart Response

**Mach 2.7, SAS on, Inlets Auto**



Figure 10.                                                                              1477
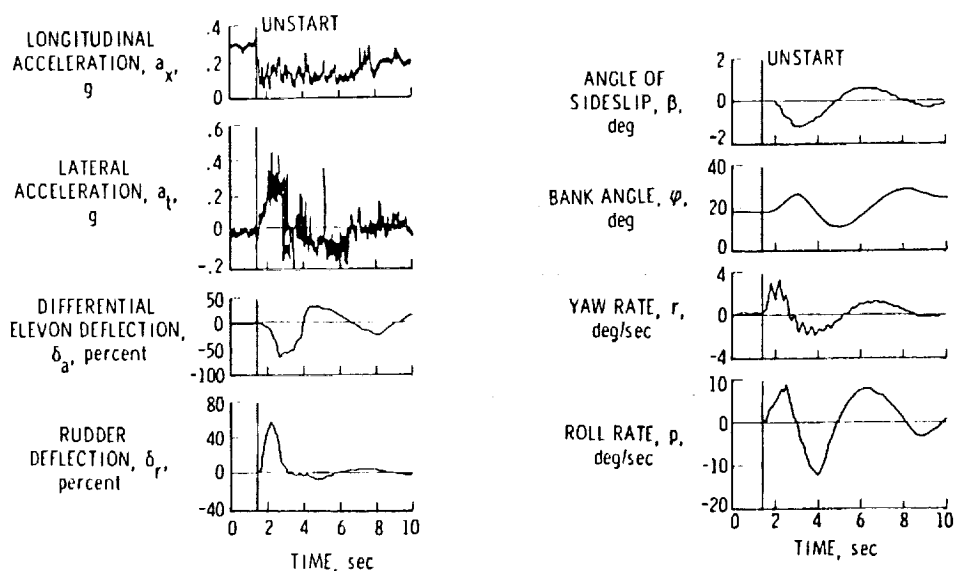
## Conclusions and Recommendations

The points listed in the table below are largely self-explanatory, but require some additional comment. Most importantly, the results of this study of the inlet unstart problem indicate that the mixed-compression inlet unstart is *not* a severe enough problem, *from a passenger safety standpoint*, to prohibit their consideration for current HSCT concepts. However, it would be desirable to examine the unstart problem further through more sophisticated analyses in order to develop a better understanding of the design drivers behind the vehicle effects. A design methodology could then be developed which would permit rapid screening and evaluation of inlet/airframe configurations with regard to inlet unstart susceptibility and effects. A large question concerning passenger acceptance of the startle upon an unstart still remains, and should be addressed through appropriate studies.

## Conclusions and recommendations

o  Inlet unstart on HSCT is an important design concern

o  Unstart is not likely to be a Mach number selection driver

o  Unstart does not appear to be a critical flight safety issue hindering HSCT development or operation

o  The automatic engine management and flight controls on an HSCT would minimize airplane motions; however, passenger startle may be a more difficult problem

o  Other flight conditions should be examined

o  More sophisticated studies are probably warranted

# References

1. Gnos, Vernon A.; and Kurkowski, Richard L.: Effects of Off-Design Inlet Mass Flow Upon Static Stability of a Delta Winged Configuration with a Canard Control and Pylon-Mounted Nacelles for Mach Numbers from 0.65 to 3.50. NASA TM X-658, 1962.

2. Hiller, Kirby W.; Batterton, Peter G.; Burstadt, Paul L.; and Szuch, John R.: Propulsion Systems Technology. In <u>Aeronautical Propulsion</u>, NASA SP-381, 1975.

3. Kurkov, Anatole P.; Soeder, Ronald H.; and Moss, John E.: Investigation of the Stall-Induced Shock Wave (Hammershock) at the Inlet to the Engine. NASA TM X-71594, 1974.

4. Nichols, Mark R.: Aerodynamics of Airframe-Engine Integration of Advanced Supersonic Aircraft. NASA TM-74395, 1977.

5. Moseley, George W.; Peterson, John B., Jr.; Braslow, Albert L.: An Investigation of Splitter Plates for the Aerodynamic Separation of Twin Inlets at Mach 2.5. NASA TN D-3385, 1966.

6. Wright, B. L.; and Foss, R. L.: Technology Assessment Studies Applied to Supersonic Cruise Vehicles. Lockheed-California Company, Burbank, CA. NASA CR-145133, 1976.

7. Turner, M. J.; and Grande, D. L.: Study of Metallic Structural Design Concepts for an Arrow Wing Supersonic Cruise Configuration. NASA CR-2743, 1977.

8. Anderson, D. L.; Connolly, G. F.; Mauro, F. M.: and Reukauf, P. J.: YF-12 Cooperative Airframe/Propulsion Control System Program. NASA CR-163099, 1980.

9. Leyman, C. S.: A Review of the Technical Development of Concorde. *Prog. Aerospace Sci.*, Vol. 23, pp. 185-238, 1986.

10. Leyman, C. S.; and Morriss, D. P.: Concorde Powerplant Development. In <u>Inlets and Nozzles for Aerospace Engines</u>, AGARD CP-91-71, 1971.

11. Smith, Ronald H.; and Schweikhard, William G.: Initial Flight Experience with the XB-70 Air-Induction System. In <u>Conference on Aircraft Aerodynamics</u>, NASA SP-124, 1966.

12. White, A. S.; and Anderson, P. H.: Operational Experience at Mach 3. In <u>Stability and Control, Part 2</u>, AGARD CP No. 17, 1966.

13. Berry, Donald T.; and Gilyard, Glenn B.: A Review of Supersonic Cruise Flight Path Control Experience with the YF-12 Aircraft. In <u>Aircraft Safety and Operating Problems</u>, NASA SP-416, 1976.

THIS PAGE INTENTIONALLY BLANK

# Session X. Airframe/Propulsion Integration

*omit*

Status of the Variable Diameter Centerbody Inlet Program
*John D. Saunders and A. A. Linne, NASA Lewis Research Center*

THIS PAGE INTENTIONALLY BLANK

$5_{22} - 05$
$12052$

# STATUS OF THE VARIABLE DIAMETER CENTERBODY INLET PROGRAM

J. D. Saunders and A.A. Linne
NASA Lewis Research Center
Cleveland, Ohio

First Annual
High Speed Research Workshop
May 14-16, 1991

# THE VARIABLE DIAMETER CENTERBODY INLET

The Variable Diameter Centerbody, (VDC), inlet is an ongoing research program at the Lewis Research Center. The VDC inlet is a mixed compression, axisymmetric inlet that has potential application on the next generation supersonic transport. This inlet was identified as one of the most promising axisymmetric concepts for supersonic cruise aircraft during the SCAR program in the late 1970's, reference 1. Some of its features include high recovery, low bleed, good angle-of-attack tolerance and excellent engine airflow matching, figure 1. These features have been demonstrated at Lewis in the past by the design and testing of fixed hardware models, references 2 to 5. A current test program in the LeRC 10'x10' Supersonic Wind Tunnel, (SWT), will attempt to duplicate these features on model hardware that actually incorporates a flight-like variable diameter centerbody mechanism.

# VDC INLET

**GOAL:** TO VALIDATE AN ADVANCED INLET CONCEPT THAT WILL PROVIDE A SUPERSONIC CRUISE AIRCRAFT WITH LONG RANGE AND IMPROVED STABILITY
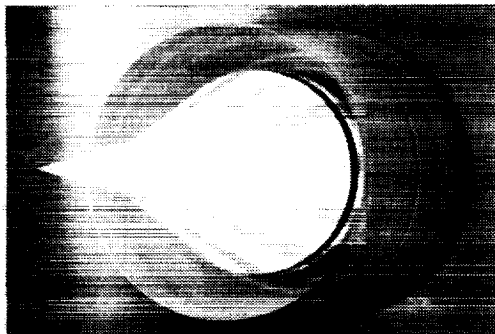
**POTENTIAL ADVANTAGES (CIVIL & MILITARY)**

★ WIDE AIRFLOW MATCHING RANGE

★ HIGH $\alpha$ TOLERANCE

★ LOW BLEED

★ SHORT

★ LOWER UNSTART INTERACTION

★ CONCEPT POTENTIAL ESTABLISHED BY ANALYSIS/FIXED HARDWARE TESTS

★ CONCEPT VIABILITY REQUIRES TEST/ANALYSIS OF FULL VARIABLE GEOMETRY INLET TO STUDY AREAS BEYOND CODE CAPABILITY

  ★ CRUISE RESTART
  ★ SEAL LEAKAGE
  ★ SURFACE IRREGULARITIES
  ★ COMPLEXITY

CD-82-13114

FIGURE 1. VDC Inlet

# VDC OVERVIEW

This paper is developed around two major efforts to develop a variable diameter centerbody inlet: an experimental program and an analytical study using state of the art computational fluid dynamics tools, (CFD), figure 2..

The efforts to demonstrate the VDC concept experimentally date back nearly 25 years. This history as well as the original design philosophy behind the inlet will be briefly discussed. Results from the early testing will be referenced and discussed further in the analytical portion of the paper. The upcoming test program will then be outlined.

The analytical effort has centered around the use of computer codes that solve the Full Navier-Stokes, (FNS), equations for a viscous compressible fluid. Lower level Euler analysis was also found useful in screening inlet geometry for off-design performance. Together, these analytical efforts have served to prepare for the future testing.

# OVERVIEW

## EXPERIMENTAL EFFORT
- ● VDC HISTORY
- ● DESIGN CONCEPT
- ● FIXED-HARDWARE MODEL TESTS, (1970)
- ● CURRENT VDC TEST PLANS

## ANALYTICAL EFFORT
- ● EULER, (SCREENING)
- ● FNS, (FLOW DETAILS, INTERACTIONS, BLEED)

FIGURE 2. VDC Overview

1485

# PROGRAM HISTORY

An outcome of the supersonic cruise research (SCR) program identified the VDC inlet as an important technology thrust to continue funding, reference 6. It is an axisymmetric inlet of a mixed compression design that provides high performance at its cruise Mach number of 2.5. Aerodynamic testing of the concept was done with fixed hardware in the early 1970's and verified the high expected performance of this concept.-This model was tested in the LeRC 10'x10' Supersonic Wind Tunnel at Mach numbers of 2.5 and 2.0. For economic reasons the mechanical design of that test inlet was simplified to incorporate fixed centerbody configurations. A photo of the model installed in the 10'x10' SWT is shown in figure 3.

Mechanical design of the VDC inlet with the variable geometry began in 1982 and a complete set of drawings was finished in mid-1984. Unfortunately, programmatic restructuring canceled the program with only a fraction of the hardware fabricated or procured. The High Speed Research program has revived interest in a commercial supersonic aircraft in general and this inlet program in particular. The test program in the LeRC 10'x10' SWT is slated to begin in the summer of 1992.



PROGRAM HISTORY
- FIXED-HARDWARE TEST, ~1970.
- VARIABLE GEOMETRY INLET MECHANICAL DESIGN, 1982-84.
- FABRICATION: 1984, 1990-91.
- TESTING, 1992.
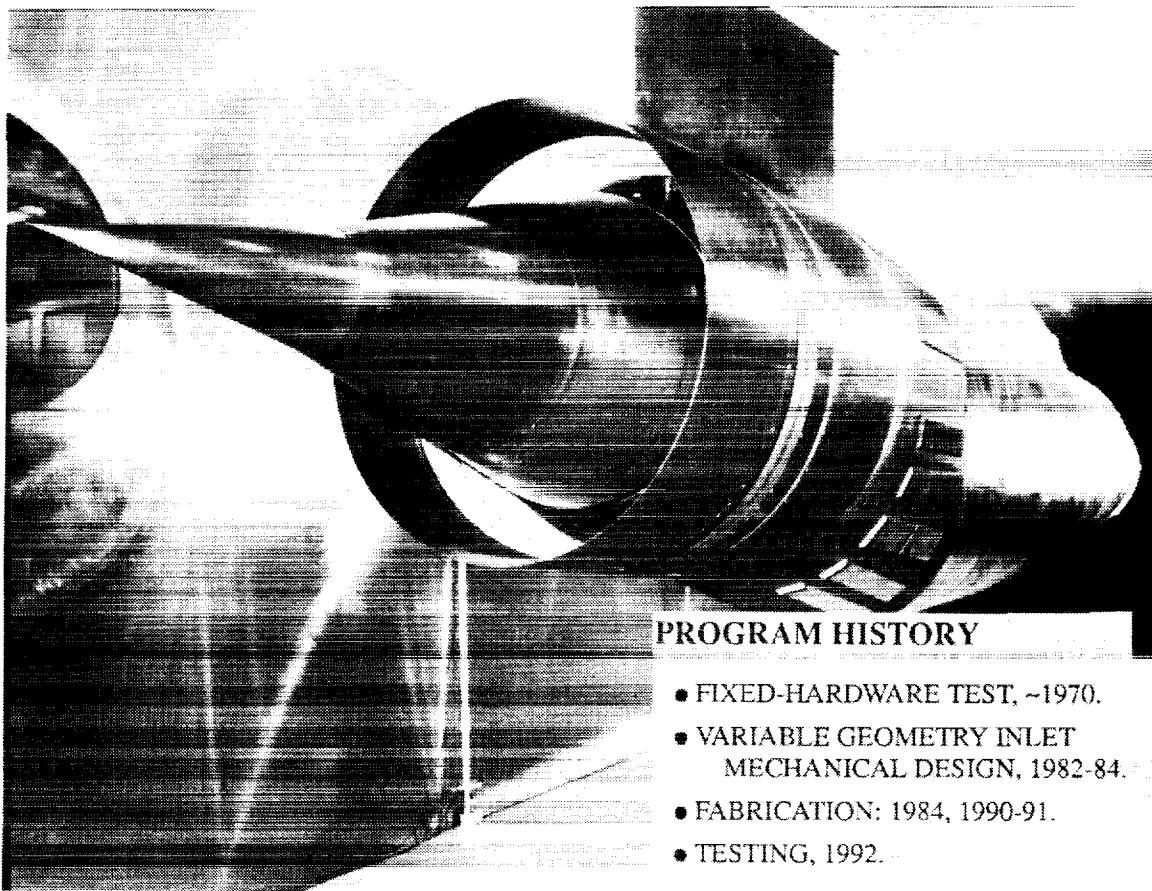
FIGURE 3. Program History

# FIXED-HARDWARE TESTING

The fixed-hardware inlet model was sized and tested with a TF-30 turbofan engine. The cowl lip radius, Rc, was 18.68 inches. Other aspects of the inlet design include the variable diameter centerbody and a focussed cowl compression on a slotted bleed region in the centerbody. The variable diameter centerbody allows large variations in throat area and airflow to provide good compatibility with the engine. The focussed cowl compression minimizes bleed flow requirements and reduces the inlet length and resulting weight. An schematic view of this model is also shown in figure 4. The model had centerbody and cowl bleed for performance and shock stability and overboard bypass air for engine matching. Vortex generators were installed downstream of the throat to prevent separation in the subsonic diffuser. The essential features of the inlet design incorporate a bicone centerbody of 12.5° and 18.5° half angle cones and an initial internal cowl angle of 2°. The design philosophy for this mixed compression inlet is to utilize a bicone spike to provide the maximum external compression compatible with high total pressure recovery and low cowl drag. As a result, 45 percent of the supersonic area contraction is internal for the Mach 2.5 design condition.
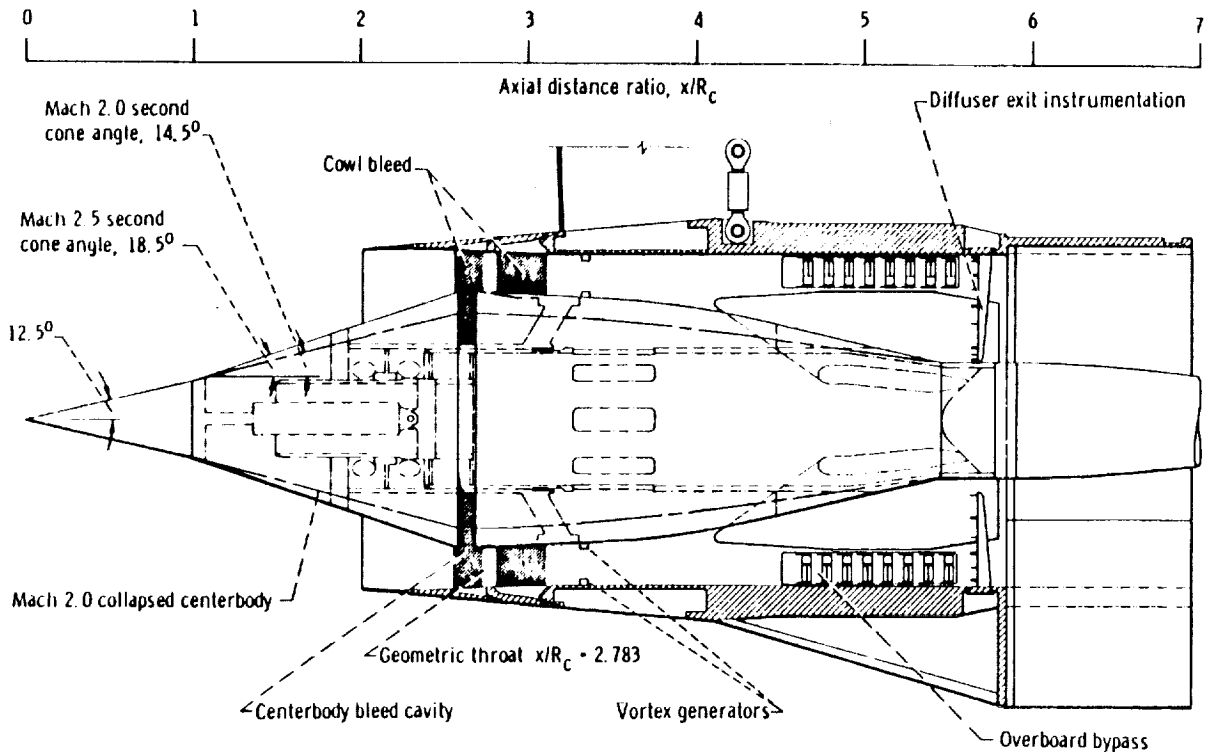


**FIGURE 4. Fixed-Hardware Testing**

# VDC INLET MODEL DESIGN

Essentially, the Variable Diameter Centerbody inlet contours were developed with the same aerodynamic design philosophy as the earlier fixed-geometry model. The supersonic diffuser cowl and centerbody geometries were designed with a Method of Characteristics, (MOC), computer code, reference 7. The characteristic mesh from the supersonic design code is shown in figure 5.

Also shown are the assembly details of the VDC inlet model. The VDC inlet incorporates an umbrella-like mechanism to create a variable diameter centerbody. The mechanism allows the centerbody to change diameter while maintaining good aerodynamic flow surfaces at off-design diameters. Both the variable diameter mechanism as well as centerbody spike translation are hydraulically actuated. Centerbody bleed and bypass airflows are also remotely variable. Relative positioning of the biconic portion to the contoured subsonic diffuser portion of the centerbody is manually adjustable. Bleed on the internal cowl surface near the inlet throat is also available. The variable-hardware model is sized for a relatively small J-85 turbojet engine and, therefore, is less than half the size of the fixed-hardware model, Rc = 8.31". The supersonic diffuser of the J-85 sized VDC inlet is geometrically scaled from the fixed hardware model. The subsonic diffusers are slightly different but retain nearly the same length to diameter and area ratios.
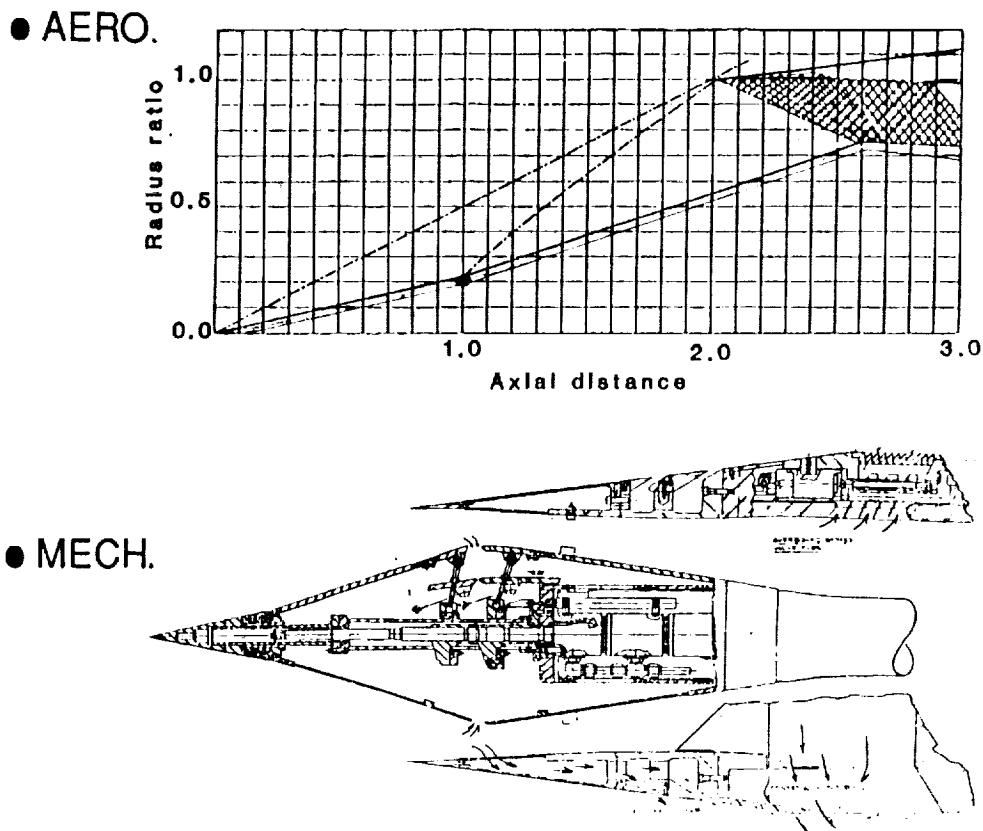


FIGURE 5. VDC Inlet Model Design

# VDC INLET FORWARD 'LEAVES'

A photo of the assembled mechanism for the second cone of the supersonic diffuser is shown below. The mechanism is made of a series of separate 'leaves' that are jointed at the minimum diameter where they attach to the 12.5° cone. The edges of the leaves are slotted to provide seals along the leaves. This seal prevents the relatively high pressure centerbody bleed air contained within the leaves from disturbing the supersonic airflow flowing along the outer leaf surfaces. Preliminary leakage tests of these seals suggests the maximum leakage rate will by a fraction of 1% of the supersonic capture flow.

The aft set of 'leaves', which constitute the contoured subsonic diffuser portion of the centerbody, as well as many other parts are currently being fabricated. This inlet concept strives for superior inlet performance at the drawback of increased mechanical complexity.
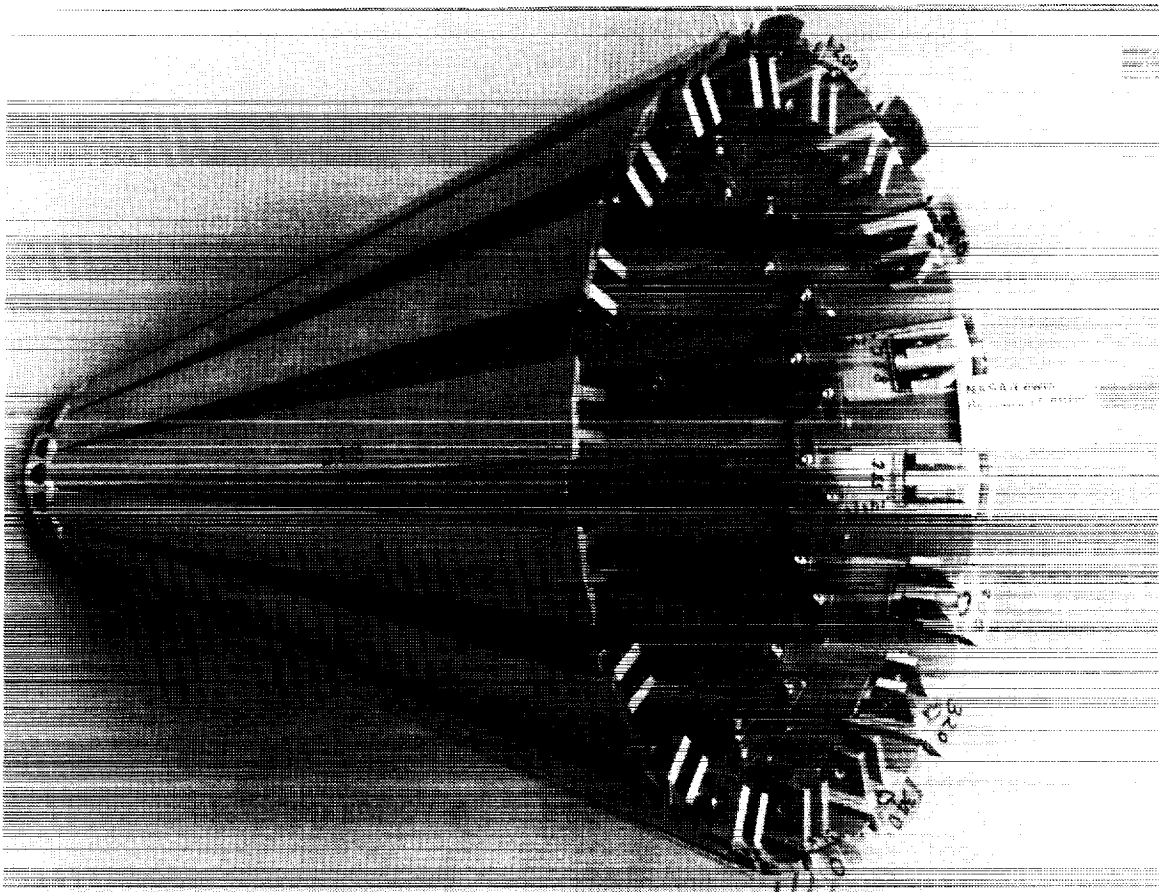


FIGURE 6. Forward leaf Assembly

# TEST PROGRAM SCHEDULE & GOALS

The schedule for the test program is shown in figure 7. Hardware, instrumentation and assembly should be complete early next year, (1992). Approximately two months of testing are initially planned. The major test goals are also listed. Inlet performance will obtained and compared to the earlier fixed-hardware model tests. In this initial testing the inlet will be mounted ahead of a mass flow plug metering device that both measures mass flow through the inlet and provides backpressure, thus simulating the effect of an engine. Other important testing parameters include the variable diameter, (second cone angle), centerbody bleed rate, centerbody translation and angle of attack. Secondary parameters include cowl bleed rate and configuration, centerbody bleed slot geometry, bypass flow rate, and the effect of vortex generators in the subsonic diffuser. A final goal is to demonstrate the viability of the variable geometry concept under flight loads with flight-like mechanisms.

## SCHEDULE

| | 1991 | 1992 |
|---|---|---|
| | J F M A M J J A S O N D | J F M A M J J A S O N D |
| HARDWARE | | |
| INSTRM. | | |
| INSTALLATION | | |
| TESTING | | |
| REPORTING | | |
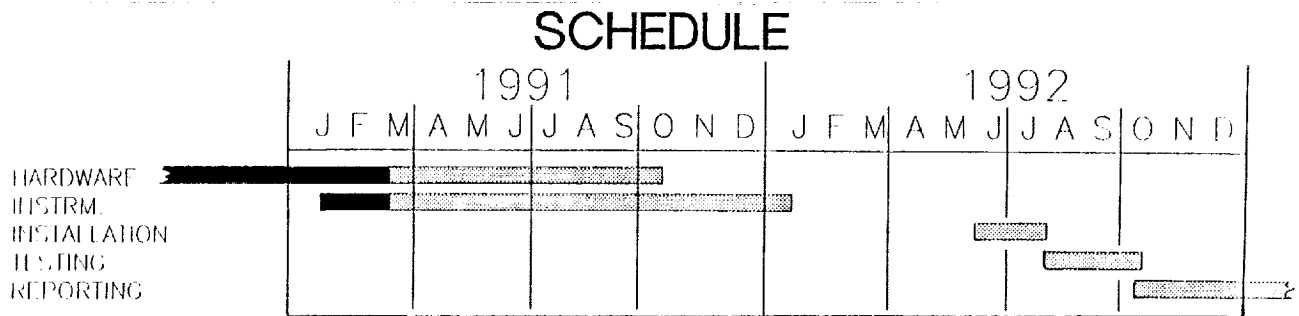
## TEST GOALS

● AERODYNAMIC PERFORMANCE

● Recovery vs. Capture          ● Angle of Attack

● Off-design performance        ● Bypass flow rate

● Bleed configurations and flows  ● Vortex generators


● MECHANICAL OPERABILITY

**FIGURE 7. Test Schedule and Goals**

1490

# CFD ANALYSIS

This analytical study was undertaken, in part, to prepare for the experimental test program. Input for the analysis was setup for the fixed-hardware, TF-30 sized, inlet. Comparison between experimental test results from the fixed geometry model and various computational fluid dynamic analyses will be made, figure 8.

Preliminary analysis using subsets of the full Navier-Stokes equations was done to determine off-design performance and prepare for the use of the FNS codes. As mentioned, the original supersonic inlet lines were developed using a MOC design program. Subsequent analysis continued to use MOC codes to determine off-design performance, (performance at flight Mach numbers below design). Additionally, a quick study was done with a Parabolized Navier-Stokes code to determine the effect of turbulent viscosity but was unsuccessful due to problems with computational grid development for this code. Results from these early efforts as well as other CFD studies, references 12 to 21, helped to guide further work with the FNS codes.

Two FNS computer codes, called PROTEUS and PARC, references 9 and 10, were used to solve the two-dimensional, axisymmetric, Reynolds-averaged, steady compressible Navier-Stokes equations for the flow through the VDC inlet at its design Mach number of 2.5. Both codes have flexible boundary conditions, good documentation, Baldwin-Lomax turbulence models and options to solve for inviscid or laminar viscous flow solutions. The codes are essentially very similar, but subtle differences in their implementation and user interface proved both codes to be useful. Problems in grid refinement, obtaining started inlet flow, and bleed modeling had to be overcome prior to simulating critical inlet operation.

The initial flow field was set to Mach 2.5 freestream conditions throughout the flow field and zero velocities at the inlet's centerbody and cowl. The compressor face boundary is initially set as an extrapolation condition. This setup should allow the inlet shocks to develop, the flow to compress nearly to critical conditions in the throat and then reaccelerate to supersonic conditions down through the diffuser and out the compressor face boundary. Once this flow solution reaches steady state conditions, various levels of outflow "back" pressure are applied to position the normal shock downstream of the throat. An extreme sensitivity of the flow simulation to exit backpressure was discovered with time marching FNS codes.

This back-pressuring process is not straight forward. Since the change in back-pressure, (or any boundary condition change), occurs across some element of computational time, the change is an inherently unsteady event. Essentially, a change in pressure corresponds to an increase in momentum due to the suddenness or acceleration of pressure change. If the pressure change occurs over a single iteration step as it does with the PARC code, a large transient shock forms whose strength is inversely proportional to the computational time-step. This shock is analogous to an inlet hammershock that occurs in real supersonic inlet-engine systems when the engine stalls, references 11 to 13.
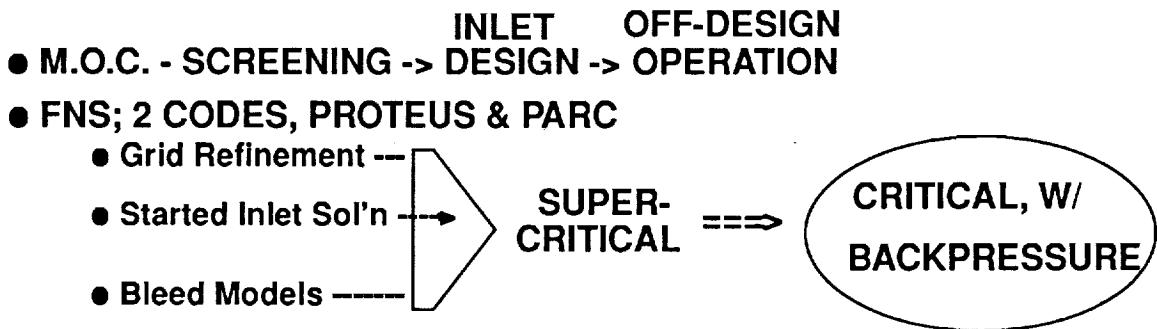


FIGURE 8. CFD Analysis

# MOC OFF-DESIGN PERFORMANCE

Prior to analysis with full Navier-Stokes codes, lower level analysis was conducted using a Method-of-Characteristics, (MOC), code. As mentioned, the original supersonic inlet design was done with the aid of a MOC code. Further analysis was conducted using another MOC code, reference 8, to determine performance of the inlet at freestream Mach numbers below the cruise Mach number of 2.5.

This off-design analysis is presented in figure 9. It shows the necessary angle of the second cone to maintain started inlet flow according to two constraints. The first constraint maintains the shock from the cowl lip on the shoulder or bleed slot of the centerbody. The second constraint maintains a certain Mach number in the inlet throat. Several throat Mach numbers are plotted representing different trades between performance and stability. For a throat Mach number of 1.2 the inlet would have the highest performance but least stability and may in fact be difficult to start. A throat Mach number of 1.4 is more stable but less efficient. Areas of the operating map below the constraint curves would have increasingly lower distortion, better efficiency but lower angle of attack and stability. Eventually, the decrease in stability will lead to inlet unstart.

Note that at a second cone angle of 18.5° the shocks on shoulder and throat Mach number of 1.3 constraints converge at the design freestream Mach number of 2.5. The convergence verifies the design methodology. The shock-on-shoulder constraint lies between throat Mach numbers of 1.2 and 1.3 at off-design freestream Mach numbers down to Mach 2.0. Off-design performance for this inlet should be fairly good but increasingly less stable. The constraint curves demonstrate a well-behaved relation between freestream Mach number and second cone angle which is useful information in the eventual testing and analysis of the inlet's off-design performance. Finally, note that at the freestream Mach number of 2.0, the shock-on-shoulder and throat Mach number constraints converge at a second cone angle of 14.5°, which is also the geometry tested in the fixed hardware tests.

This operating map represents over 30 test cases; a task that points out the usefulness of Euler analysis in screening large number of configurations.

**FIGURE 9. Off-Design Performance Map**

OFF-DESIGN OPERATING MAP
VDC Inlet, zero translation
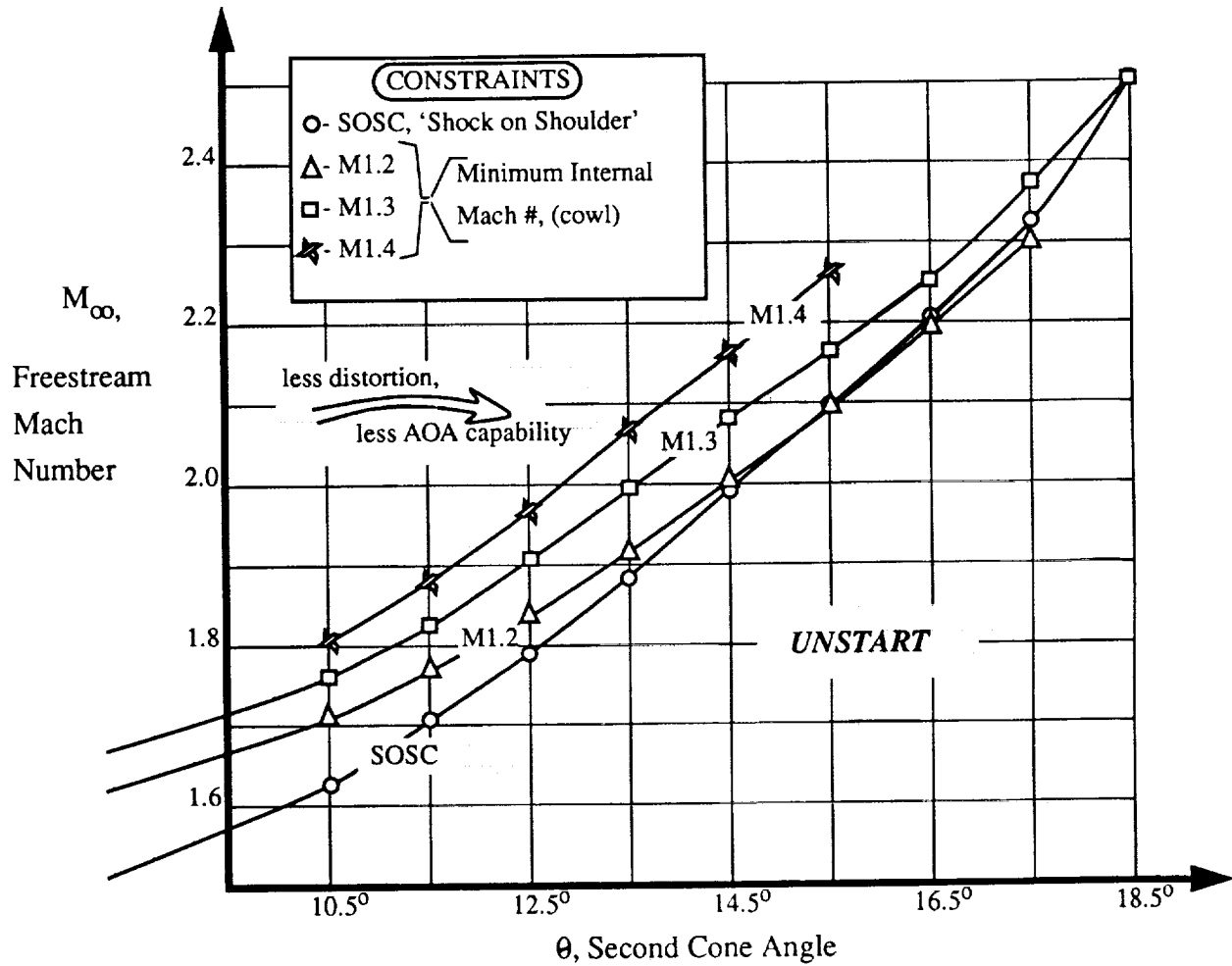
FIGURE 9. Off-Design Performance Map

# FNS CODES, EULER RESULTS

Initial results were obtained using the Euler subset of the FNS equations and using a fairly conventional mesh. The mesh for this case was uniformly distributed in the radial direction and slightly packed in the streamwise direction. The grid dimensions were 99x99.

Mach number contours are shown in figure 10. Examination of the contours shows significant shock wave smearing in the physical domain. In fact, the cowl shock is not sharply defined, and the entire cowl compression appears to be distributed both well upstream and downstream of the shoulder. (Recall that the inlet design was for shock cancellation and focussed cowl compression at the centerbody shoulder). Because the cowl shock wave is not crisply resolved, the shock/boundary layer/bleed interaction on the centerbody would be poorly modeled with this grid.
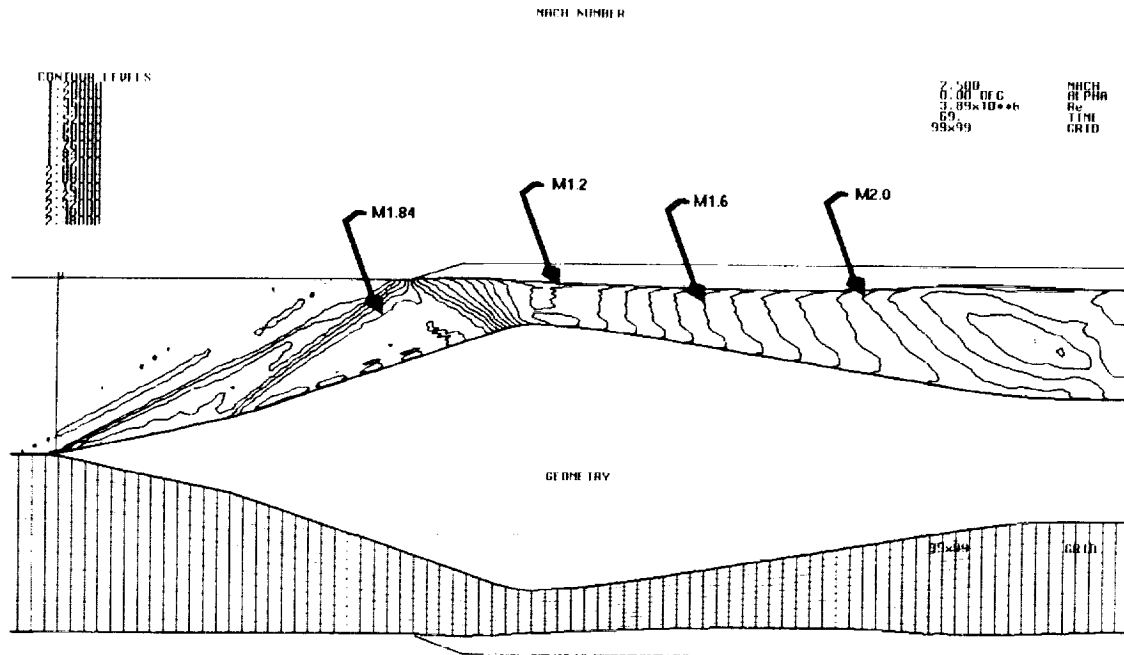


**FIGURE 10. Euler Results**

# REFINED GRID RESULTS

An effort in skewing and packing the grid points as well as adding more grid points to the calculation domain was strongly motivated by the previous result. Figure 11 shows the effect of grid refinement on intermediate FNS-inviscid results. Although both of these calculations eventually unstarted, the sharpness of the shock waves is clearly much better for the skewed, packed mesh.

Without bleed and with the refined mesh, both Euler and laminar solutions predicted the cowl shock to intersect forward of the shoulder, causing boundary layer separation on the centerbody. The separation enlarged with further iterations, and as mentioned, cause the inlet flowfield to unstart. This prediction compares to the experimental results that indicated ~2% bleed flow rate through the centerbody bleed slot was needed to keep the inlet started.

Together the results indicate that even with the refined mesh, the shocks are smeared forward of their inviscid positions, causing adverse interaction that prevents started inlet flow. Analysis without bleed was therefore de-emphasized and bleed modeling was implemented into the analyses' boundary conditions.

While the bleed models were being implemented into the codes, one last attempt was made to develop a started inlet configuration.For this case, the inlet geometry was modified by translating the cowl slightly downstream relative to the centerbody. This change reduced the internal contraction ratio and also moves the cowl shock downstream of the shoulder, both of which aid inlet starting. Initial cases were developed for Mach 3 freestream flow. Started inlet flow was achieved for this case, but was of limited practical interest. The calculated flowfield did provide useful initial conditions for subsequent cases using the design geometry and centerbody bleed
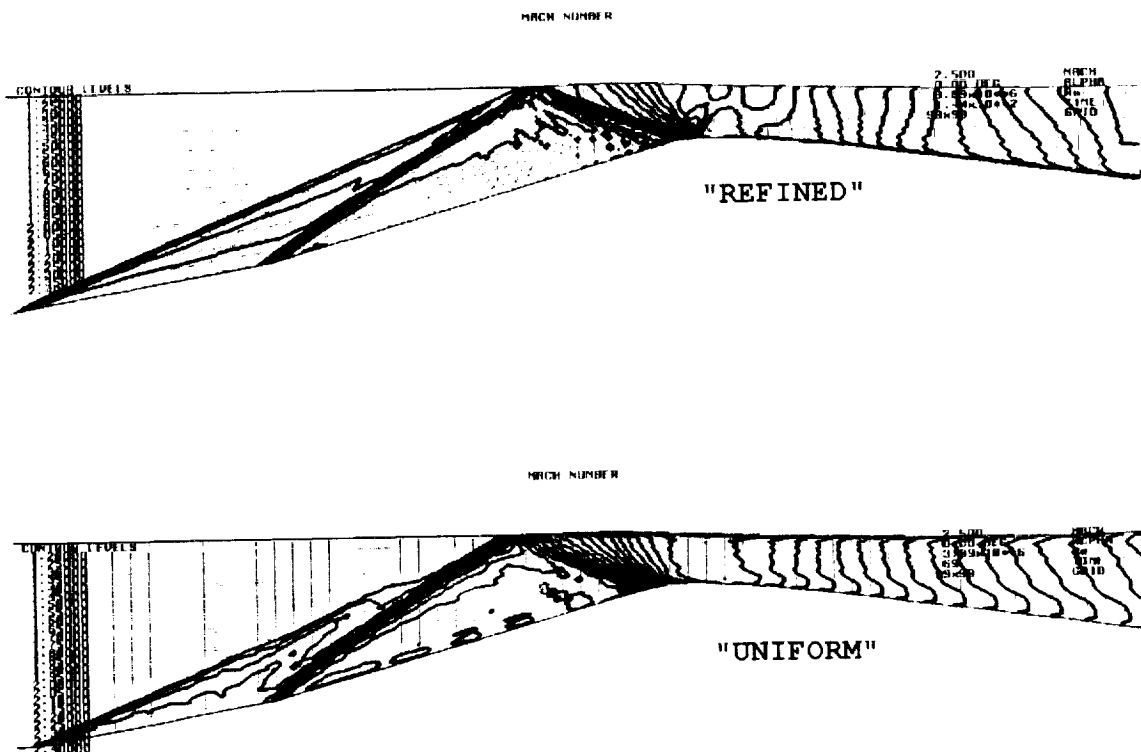




**FIGURE 11. Refined Grid Results**

# DESIGN CASE, SUPERCRITICAL

With the bleed model setup, the next case used the design inlet geometry but at the design Mach number of 2.5. The bleed rate was set at ~6% which is conservatively much greater than the experimentally obtained optimum rate of ~2%. Both FNS codes were run for the same case and the comparison of Mach number contours is shown in figure 12. The contours are for a detailed region through the inlet throat. Upstream of the centerbody bleed slot, agreement between the two codes is good. The cowl shock hits slightly forward of the shoulder causing a small separation. The cowl shock reflects from this separation and then crosses back to the cowl surface. The reflection on the cowl surface is of sufficient strength to separate the cowl boundary layer and cause a Mach reflection. Downstream of the Mach reflection, a small subsonic pocket in the flow is formed. The PARC code resolves this phenomena more crisply than the PROTEUS code. The shock continues to reflect and coincides with the oblique shock at the aft end of the bleed slot on the center-body surface.

These results are for a low level of back pressure, (supercritical inlet operation), which forces a terminal shock to form near the end of the centerbody bleed slot. In the PROTEUS analysis, this oblique is weak and the flow remain supersonic downstream. The PARC code predicts a strong oblique shock that coalesces with the terminal to generate subsonic flow. For both code predictions, the terminal shock is locally unsteady, (this result will be discussed later).
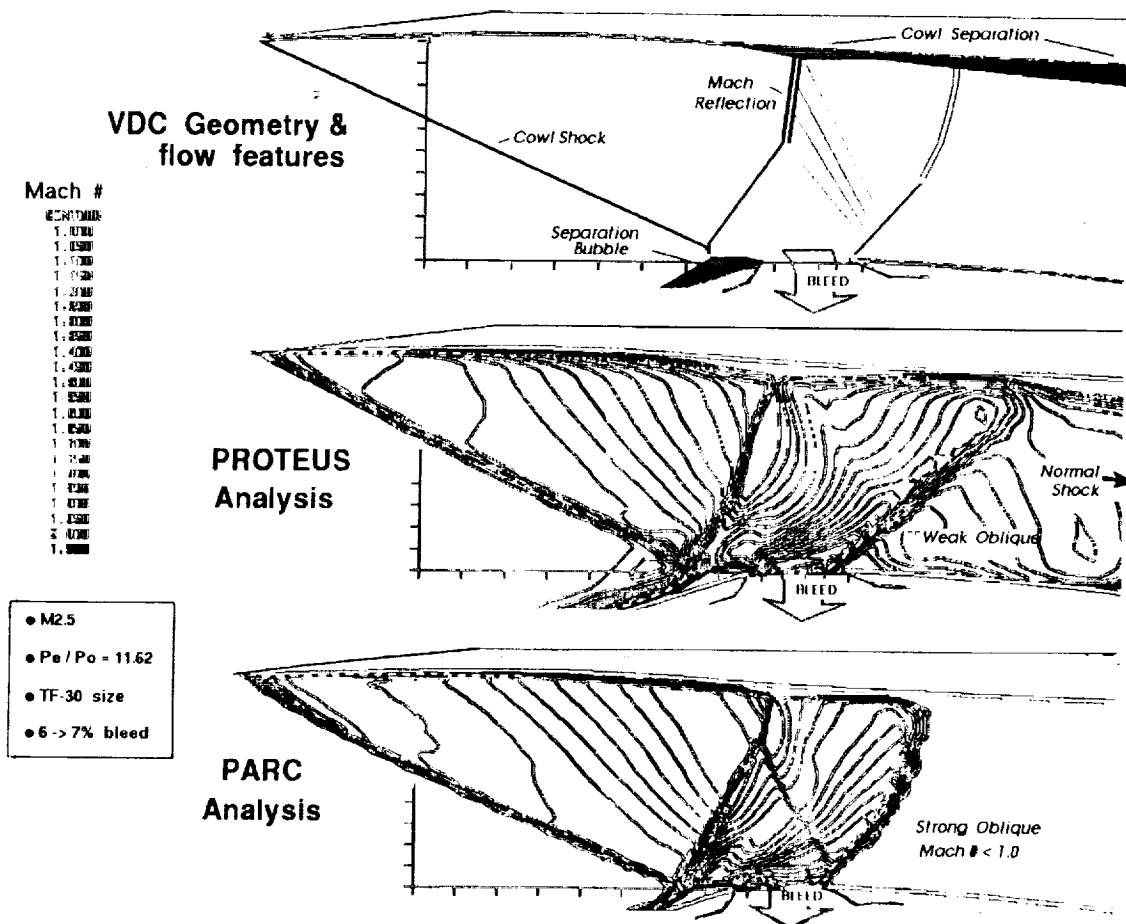


FIGURE 12. Design Case, Supercritical

1496

# PARTICLE TRACES, DESIGN CASE

To further display the features of this flow, figure 13 shows the particle traces for this case from the PARC code analysis. The small separation forward of the centerbody shoulder bleed slot and the bleed flow exiting through the slot are clearly evident. This case was done with slightly less bleed flow at 2%, so its solution is directly relatable to the data. The experimental data deviates from the inviscid MOC prediction slightly forward of the shoulder, reference 1. The deviation was attributed to small separation existing in this region, and thus qualitatively verifies the FNS predictions. The result also suggested a need for additional static pressure instrumentation to better quantify the extent of the separation.
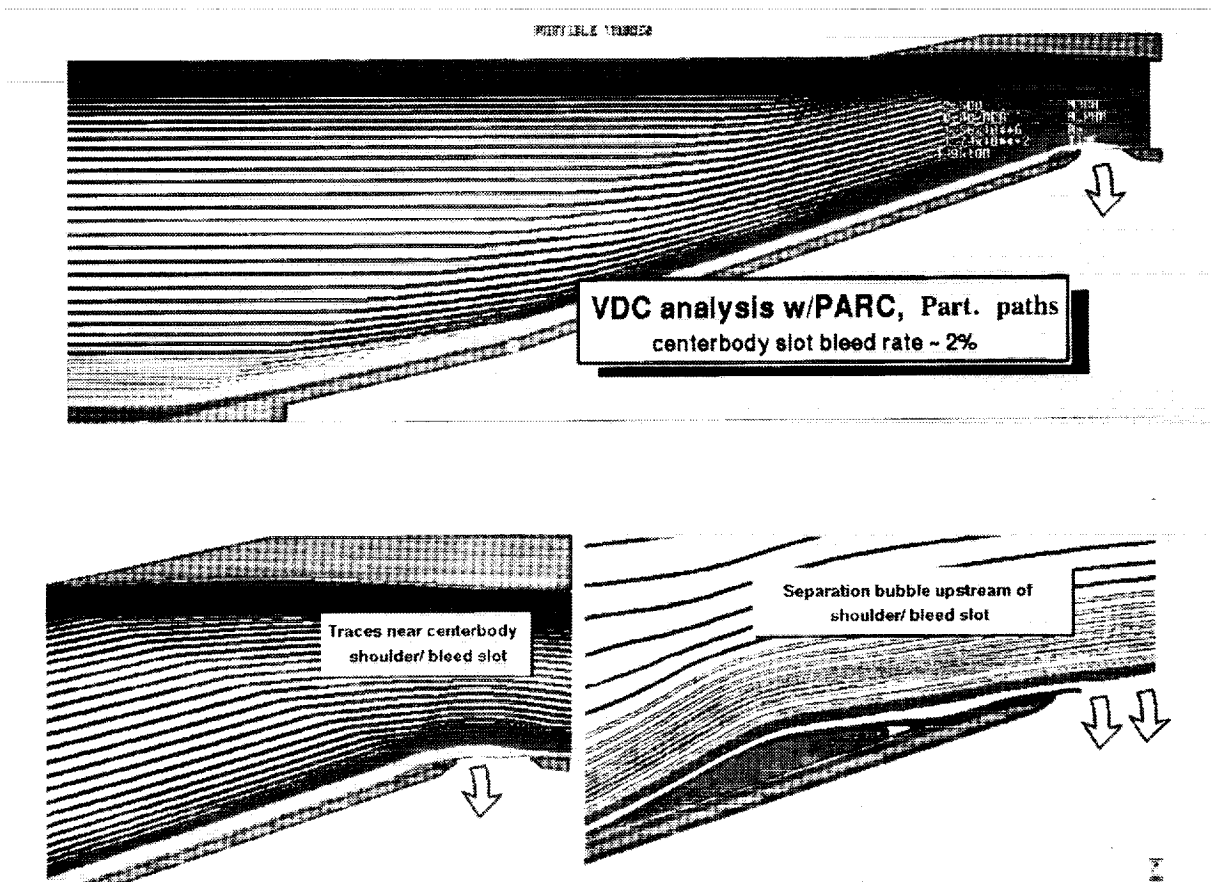


FIGURE 13. Particle Traces

# COMPARISON TO DATA

Figure 14 shows the results of the comparison of pitot pressures between the experiment and numerical solution. The locations of various rakes are shown on figure 16. Comparison is excellent for the cowl throat rake. The flow on the cowl to this point is unaffected by separations and by the centerbody bleed, so boundary layer growth and oblique shock pressure level should be correctly modeled by the code. Pitot pressure profiles for the other two rakes show moderate agreement. These rakes are downstream of separations and the bleed slot. Therefore, they are strongly affected by phenomena that are, at best, only approximately simulated by the turbulence model and the bleed boundary condition.
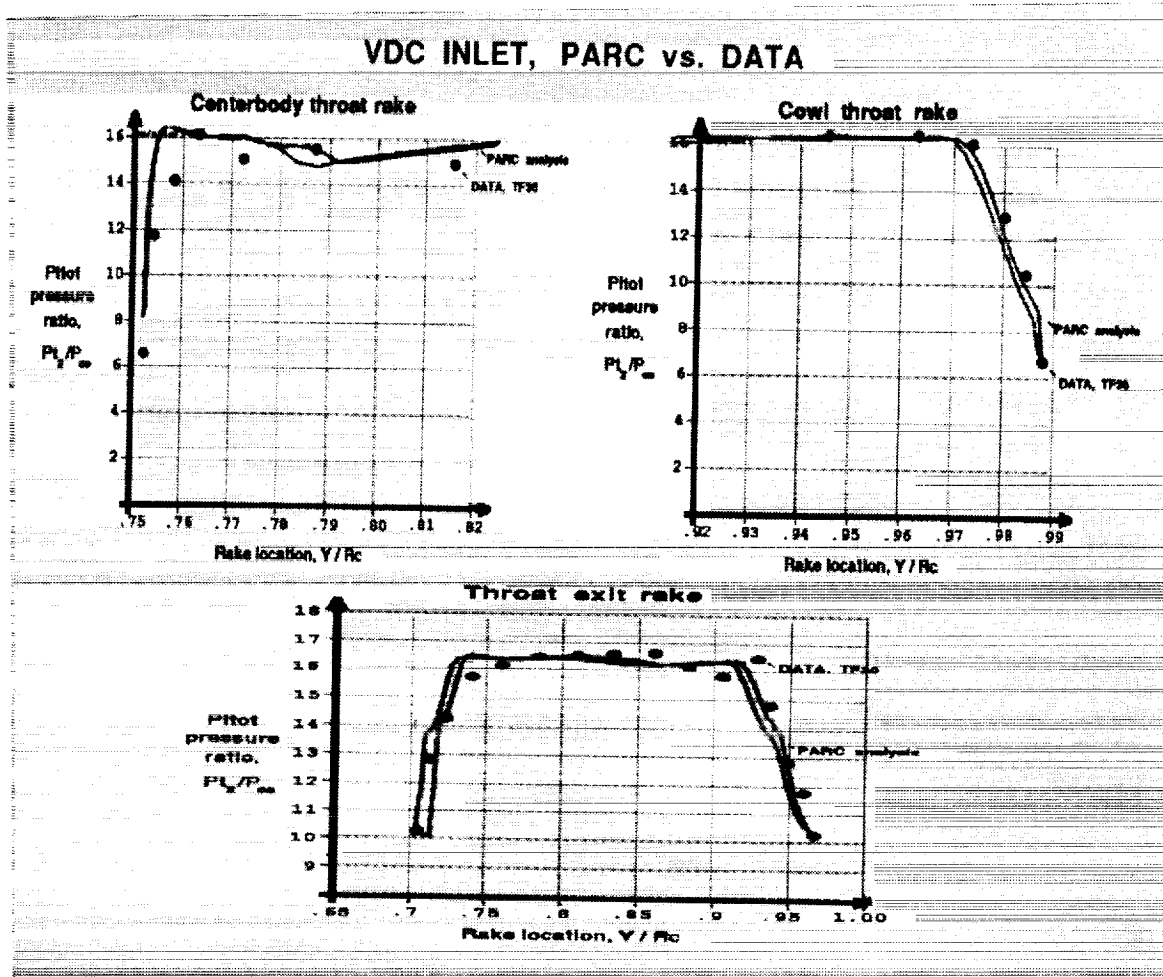


FIGURE 14. Comparison to Data

# BACKPRESSURE AND FLOW OSCILLATION

The previous case was initially chosen to explore the process of back-pressuring, or changing the outflow boundary condition. The exit static pressure ratio was set to 11.62 which should keep the terminal shock supercritical, or well downstream of the inlet throat.

At this pressure ratio of 11.62, the solution did not reach any form of steady state solution. In examining the solution, the terminal shock's final position was found to oscillate around a fixed location, figure 15. This solution was obtained using the PROTEUS code with turbulent viscosity. From the freestream entrance plane to nearly one throat height downstream of the aft edge of the centerbody bleed slot, the Mach number contours remain constant with respect to computational time. Just downstream, the terminal shock location first advances forward and then collapses back downstream. These results are for 'local' time stepping an so are not time-accurate. However, the failure of the shock location to converge to a steady position suggests an inherent flow instability.
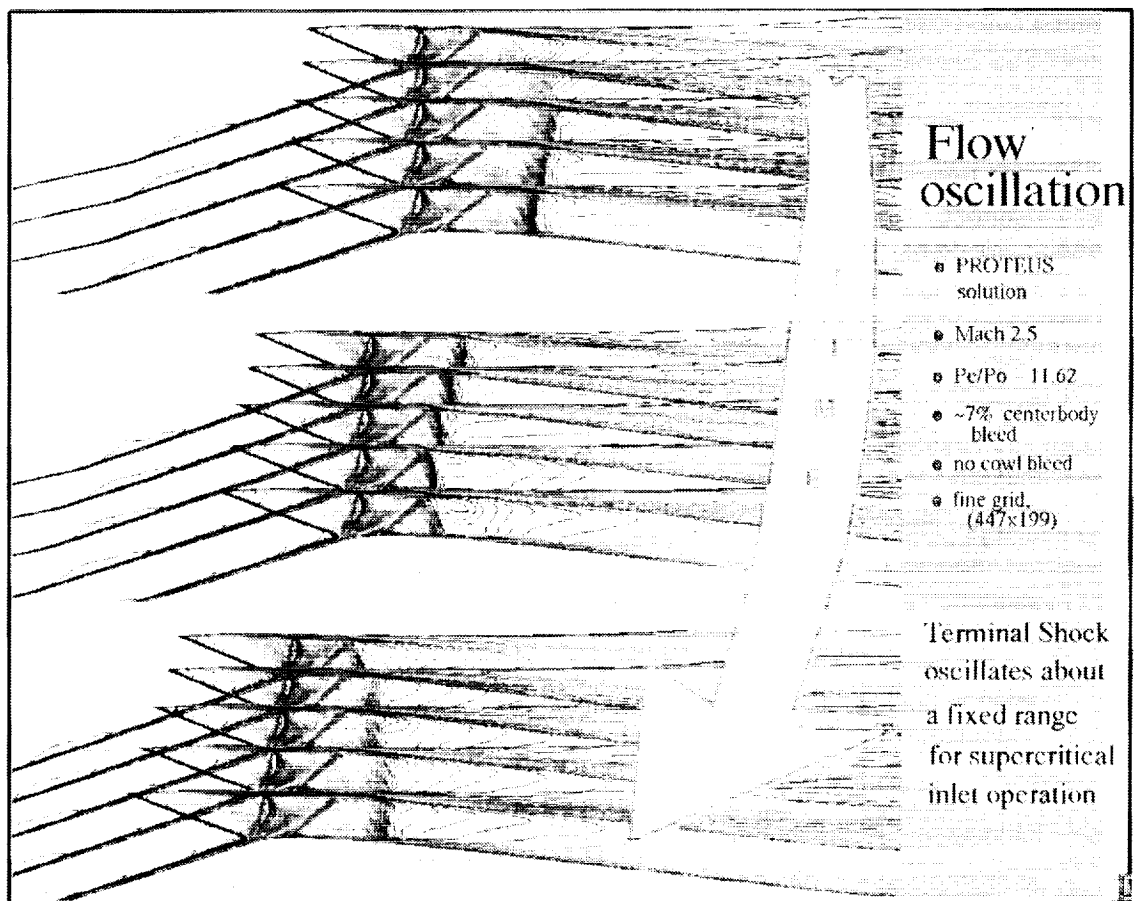


FIGURE 15. Backpressure and Flow Oscillation

# FLOW OSCILLATION, STATIC PRESSURE DISTRIBUTION

Figure 16 shows the centerbody static pressure distribution for these cases. Again, the shock location indicated by the sharp pressure rise around $X/R_c=3$ first travels upstream, then downstream. Also, note the rise is much sharper for the upstream traveling shock compared to the downstream traveling shock. Integrated compressor face mass flow and mass-weighted total pressures are directly affected by the shock location and so also fluctuated for this cases. The flow unsteadiness is computationally intense; this sequence used 14 CRAY-YMP Cpu hours just to simulate a single period of the oscillation.
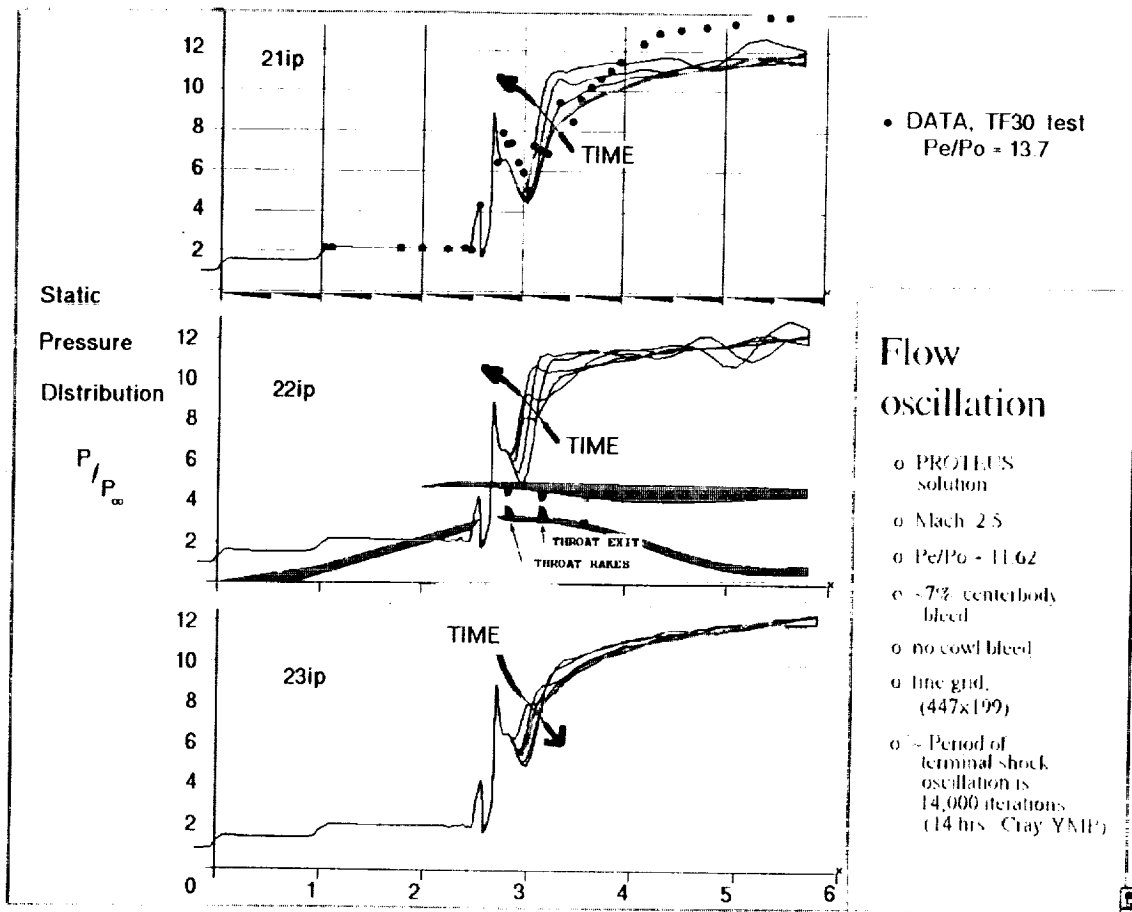


FIGURE 16. Flow Oscillation, Static Pressure Distribution

# BACKPRESSURE TRANSIENTS, SUDDEN CHANGE

Figure 17 shows the computations for an exit pressure ratio of 13.6 that predicts unstarted inlet flow. This case was run with the PARC code with a sudden step change from 11.62 to 13.6 across a single computational time step. The Mach contours track the normal shock as it travel upstream, across the bleed slot and ultimately upstream of the cowl lip indicating inlet unstart.

The sudden change of pressure induces transient accelerations that can, (and in this case do), cause total pressures within the inlet to exceed the freestream total pressure. As mentioned before, this disturbance is roughly analogous to the hammershock overpressure phenomena encounter during hard engine stalls. If a steady state solution is ultimately sought, any increase in total pressure can be construed as an indication of unsteady flow. Since both PROTEUS and PARC are solving the unsteady Navier-Stokes equation, albeit inaccurately in time, an overpressure can occur and extreme care must be taken to prevent overwhelming pressure oscillations that can cause inlet unstarts.
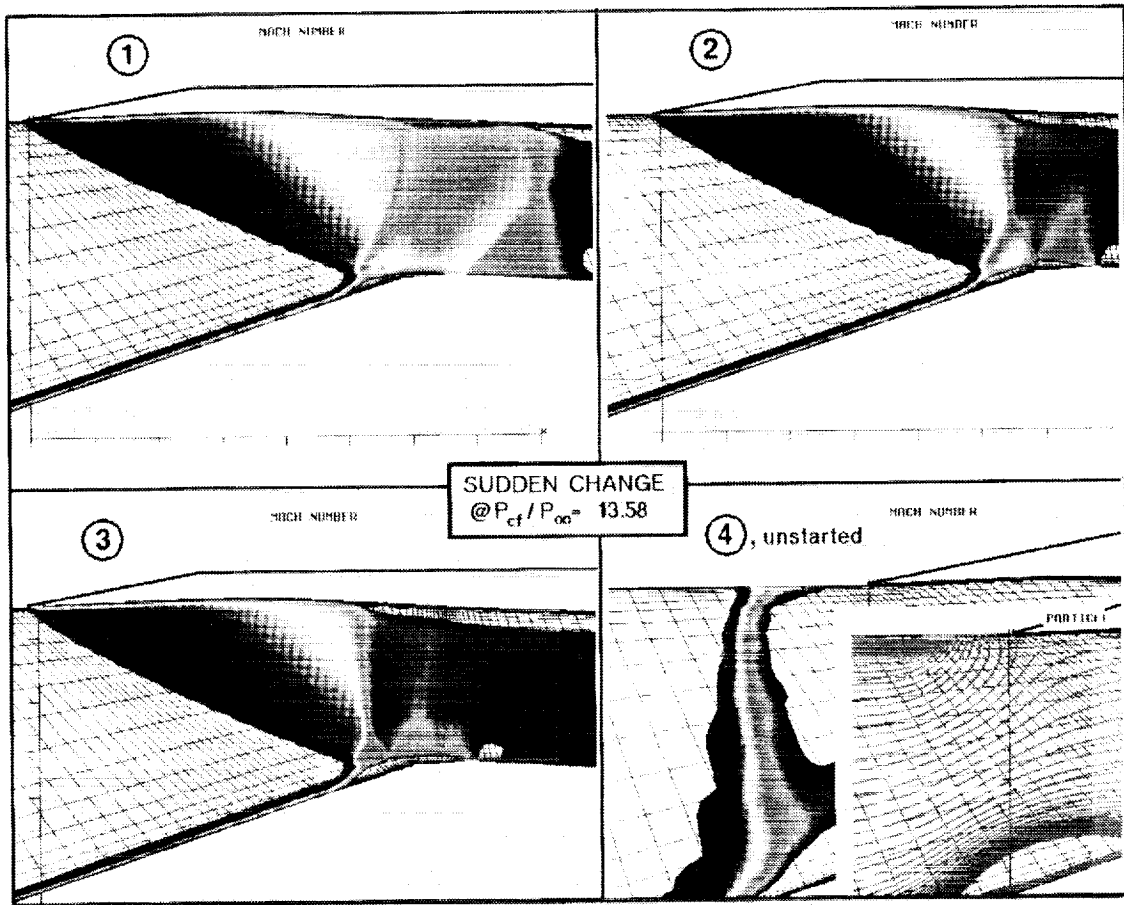


**FIGURE 17.** Backpressure Transients, Sudden Change

# BACKPRESSURE TRANSIENTS, GRADUAL CHANGE

Because of the extreme sensitivity of shock position to the exit pressure boundary condition, further effort was made to gradually increase exit pressure and simulate critical inlet operation. PROTEUS was chosen for this effort due to two reasons. Since exit pressure can be changed gradually over a specified number of iterations, the problem of hammershock overpressure can be greatly reduced. The second reason for using PROTEUS lies with its more flexible bleed model. Both of these reasons were crucial to the successful simulation of critical inlet operation.

For this case the exit pressure was increased from 11.62 to 13.56 over 40,000 iterations, figure 18. Even with this slow change of pressure a slight overpressure occurs, travels upstream, and moves the terminal shock forward onto the bleed slot. The bleed boundary condition model, which was based on Hamed's velocity profile, reference 20, did allow the massflow to increase by ~50% during this terminal shock/bleed interaction. The shock eventually moved back downstream to the aft edge of the bleed slot but continued to oscillate thereafter. Also note that this case had a slightly modified inlet geometry. The cowl was translated downstream $X/R_c = .035$ in order to eliminate the separation bubble upstream of the centerbody shoulder. While not completely eliminated, the size of the separation has been dramatically reduced. The integrated massflow was 96.8% . Total pressure recovery was ~87.7% and the bleed massflow rate was ~3.4%. Also shown in the figure below is the comparison of static pressure distribution. The values have good agreement with measured overall inlet performance.
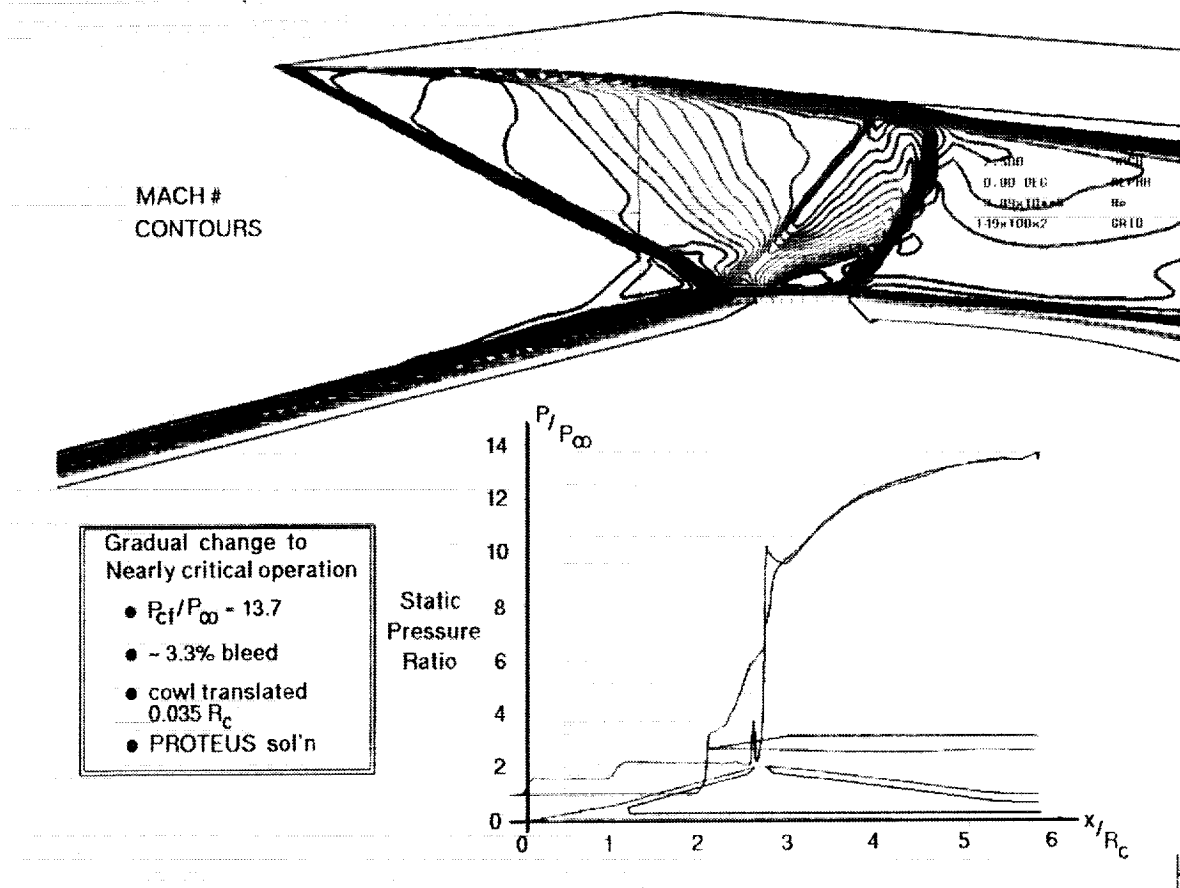


FIGURE 18. Backpressure Transients, Gradual Change

# CONCLUDING REMARKS

The analysis of the VDC Inlet was undertaken, in part, to prepare for the experimental testing scheduled for the summer of 1992. This study has already impacted the testing by providing understanding of the bleed phenomena. It has also indicated areas of the inlet model in need of greater instrumentation. CFD investigation will continue throughout the preparation, testing, and reporting of the experimental program.

A series of analytical tools were applied to understand the flowfield in a supersonic inlet. These tools had varying degrees of success when compared to existing data from a wind tunnel test of the inlet geometry. Some of the major results are summarized below:

1) MOC analysis proved the inlet should operate well at off-design Mach numbers.

2) Elliptic Euler analysis failed due to instability in the centerbody flow separation, which led to an unstarted flowfield.

3) FNS viscous analysis predicted unstart for the design geometry without centerbody bleed, agreeing with experimental testing. Both analysis and testing agree that the design geometry will remain started at a bleed mass flow ratio, $m_{bl}/m_0$, of 2%.

4) For a supercritical inlet flowfield, FNS turbulent viscous analysis with bleed agreed well with experimental data forward of the centerbody bleed slot and regions of separated flow. Downstream of these regions the agreement is fair, pointing out deficiencies in the bleed and turbulence modeling.

5) FNS codes indicated an inherent unsteady flow oscillation of the terminal shock at a supercritical flow condition. This agrees with empirical experience that suggest that dynamic distortion increases as the terminal shock moves downstream from the inlet throat.

6) Both FNS codes failed to correctly predict the inlet recovery. Analytical predictions were ~1% below measured recoveries.


Further effort will be focussed in four areas:

1 - Further investigate critical and peak inlet operation by gradually increasing the compressor face pressure ratio up to the experimentally measured levels.

2 - Add the bleed passage to the calculation domain, thus eliminating bleed boundary condition modeling. With its multi-blocked grid formulation, the PARC code is ideally suited for this analysis.

3 - Implement the K-e turbulence model, (reference 21).

4 - Investigate the effect of cowl bleed on terminal shock/boundary layer interaction control.

# REFERENCES

1. McLean, F. E.: "Future Directions of Supersonic Cruise Research", Supersonic Cruise Technology. NASA SP-472, 1985.

2. Wasserbauer, J. F.; Shaw, R. J.; and Neumann, H. E.: Design of a Very-Low-Bleed Mach 2.5 Mixed-Compression Inlet with 45 Percent Internal Contraction. NASA TM X-3135, 1975.

3. Neumann, H. E.; Wasserbauer, J. F.; and Shaw, R. J.: Performance of Vortex Generators in a Mach 2.5 Low-Bleed Full-Scale 45-Percent-Internal- Contraction Axisymmetric Inlet. NASA TM X-3195, 1975.

4. Wasserbauer, J. F.; Neumann, H. E.; and Shaw, R. J.: Distortion in a Full-Scale Bicone Inlet with 45 Percent Internal Contraction. NASA TM X-3133, 1975.

5. Wasserbauer, J. F.; Neumann, H. E.; and Shaw, R. J.: Performance and Surge Limits of a TF30-P-3 Turbofan Engine/Axisymmetric Mixed- Compression Inlet Propulsion System at Mach 2.5. NASA TP-2461, 1985.

6. Bowditch, D. N.: Some Design Considerations for Supersonic Cruise Mixed Compression Inlets. NASA TM X-71460, 1973.

7. Anderson, B. H.: Design of Supersonic Inlets by a Computer Program Incorporating the Method of Characteristics. NASA TN-D 4960, 1969.

8. Vadyak, J.; Hoffman, J. D.; and Bishop, A. R.: Calculation of the Flow Field in Supersonic Mixed-Compression Inlets at Angle of Attack using the Three-Dimensional Method of Characteristics with Discrete Shock Wave Fitting. NASA CR-135425, 1978.

9. Towne, C. E.; Schwab, J. R.; Benson, T. J.; and Suresh, A.: PROTEUS Two-Dimensional Navier-Stokes Computer Code- Version 1.0. NASA TM- 102552, 1990.

10. Cooper, G. K.; Sirbaugh, J. R.: PARC Code: Theory and Usage. AEDC-TR-89-15, 1989.

11. Sanders, B. W.: Dynamic Response of a Mach 2.5 Axisymmetric Inlet and Turbojet Engine with a Poppet- Valve-Controlled Inlet Stability Bypass System when Subjected to Internal and External Airflow Transients. NASA TP-1531, 1979

12. Hindash, I. O.; Bush, R. H.; and Cosner, R. R.: Computational Modeling of Inlet Hammershock Wave Generation. AIAA Paper 90-2005, 1990.

13. Pordal, H. S.; Khosla, P. K.; and Rubin, S. G.: Transient Behavior of Supersonic Flow through Inlets. AIAA 90-2130, 1990.

14. Weir, L. J.; Reddy, D. R.; and Rupp, G. D.: Mach 5 Inlet CFD and Experimental Results. AIAA Paper 89- 2355, July 1989.

15. Reddy, D. R.; Benson, T. J.; and Weir, L. J.: Comparison of 3-D Viscous Flow Computations of Mach 5 Inlet with Experimental Data. AIAA Paper 90-0600, 1990.

16. Rizzetta, D. P.: Numerical Simulation of a Supersonic Inlet. AIAA Paper 91-0128, 1991.

17. Hunter, L. G.; Tripp, J. M.; and Howlett, D. G.: A Mach 2.0 Plus Supersonic Inlet Study using the Navier-Stokes Equations. AIAA Paper 85- 1211, 1985.

18. Shigematsu, J.; Yamamoto, K.; and Shiraishi, K.: Numerical Investigation of Supersonic Inlet using Implicit TVD Scheme. AIAA Paper 90-2155, 1990.

19. Fujimoto, A.; Niwa, N.; and Sawada, K.: Numerical Investigation on Supersonic Inlet with Realistic Bleed and Bypass Systems. AIAA Paper 91- 0127, 1991.

20. Hamed, A., and Lehnig, T.: An Investigation of Oblique Shock/Boundary Layer Bleed Interaction. AIAA 90-1928, 1990.

21. Avva, R.; Smith, C.; and Singal, A.: Comparative Study of High and Low Reynolds Number Versions of k-e Models. AIAA Paper 90-0246, AIAA 28th Aerospace Sciences Meeting, Reno NV, January 1990.

# Session X. Airframe/Propulsion Integration

*omit*

HSCT Integrated Propulsion Control Issues
*Christopher M. Carlin, Boeing Commercial Airplane Group*

THIS PAGE INTENTIONALLY BLANK

1506

)23 - v,
/205³

# HSCT INTEGRATED PROPULSION CONTROL ISSUES
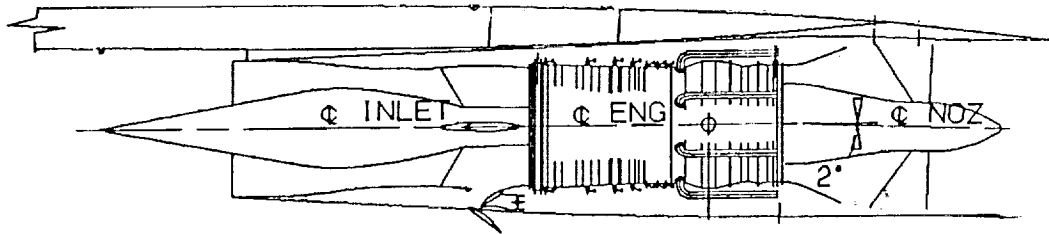


## C.M. Carlin

### Boeing Commercial Airplane Group

### 16 May, 1991

## OVERVIEW

The propulsion control system affects the economics of the HSCT through the
mechanisms indicated. Weight reduction is paramount in aircraft of this type.
Significant reductions are possible relative to SST or even current technology
if improvements are made in areas such as high temperature electronics.
Dependability is an increasingly important parameter in all aircraft, but the
higher capital cost of the HSCT makes it doubly important. Conversely the more
difficult HSCT design problem makes it more difficult to achieve. Integration
of propulsion controls will make it possible to improve both the static and
dynamic performance of the HSCT propulsion system. Noise and emissions
requirements may introduce novel control system requirements such as
automatically programmed takeoff thrust for noise abatement. Control system
development technology is evolving. For HSCT, highly automated and thoroughly
validated tools will be required to reliably achieve desired system performance
at introduction, and to reduce development costs.

A technology plan has been developed to prepare for HSCT development. This
presentation  addresses the portion of the plan required to demonstrate
technology readiness for the HSCT in the late 1990's rather than the technology
development currently in progress.

# OVERVIEW

o **Technical Issues**
**Weight**
**Dependability**
**Performance**
**Noise/Emissions**
**Control System Development**


o **Technology Plan**
**Simulation**
**Control Laws**
**Architecture**
**Component Development**
**Technology Demonstration**

1508

## PROPULSION CONTROL AIRPLANE LEVEL ISSUES

The weight of the SST control system was concentrated in long wire runs from fuselage mounted electronics to nacelle mounted actuators and sensors, and in the actuators themselves. Dependability will be improved through accurate knowledge of disturbances, validated simulations, highly reliable components operating in a well understood environment, and reducing system parts count. Performance improvements are available either through reduced component operating margins or by improving system off design performance through integration and optimization. Noise abatement introduces requirements for automatic thrust profile management, and relatively complex nozzle configuration management. Control system development is currently a complex, labor intensive, and costly process. The tools used need to be improved, validated, and integrated to permit reliable automated analysis, design, build, and test. The propulsion control development process also needs to become more analytical to reduce dependence on the wind tunnel and test cell.

# PROPULSION CONTROL AIRPLANE LEVEL ISSUES

O **Weight**
   **SST Total Intake Control System - 4442 Lbs**
   **1782 Lbs of Wire**
   **2066 Lbs of Actuation Equipment**

O **Dependability**
   **Unstarts,Stalls,and Flameouts are unacceptable**

O **Performance**
   **Reduced Control Margins**
   **Integrated & Optimizing Controls**

O **Noise & Emissions may introduce novel control requirements**

O **Control System Development**
   **Reduce development cost through automation**
   **Minimize interdependence between controls**
   **and machinery development**

## INLET CONTROL SYSTEM WEIGHT

SST control system weight was largely caused by long wire runs and actuation requirements. High temperature electronics, if available, would permit mounting multiplex/control units in the nacelles, eliminating long multiwire bundles. Fiberoptic sensors would permit reductions in the size, and weight of long wire runs by eliminating HERF/EMI considerations. Depending on the development of the technologies some combination of them should significantly reduce the wire weight of the propulsion control system. In the event none of the advanced technologies become available air or fuel cooling of nacelle mounted electronics is a practical but less than desirable solution to the problem. Light weight, probably composite, actuation along with relatively high pressure hydraulics are required to reduce actuation weight. Actuation weight may also be reduced by reducing actuation dynamic response requirements. This may be achieved by coordination of airframe,inlet,engine, and nozzle operation and by anticipation of system disturbances.

## INLET CONTROL SYSTEM WEIGHT



SST Design

Inlet Control
Electronics

Dedicated Analog
Wire Runs

Actuators &
Sensors
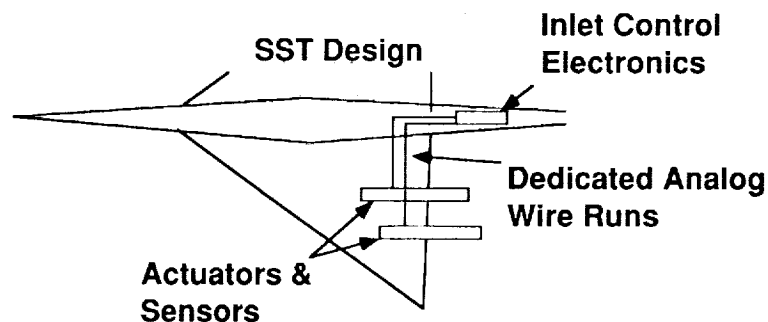
o Weight reduction requires technology advances
   High temperature electronics
   Severe  environment fiberoptic sensors and data buses
   Reduced sensor set
   Lightweight actuation

o Without technology advances actively
   cooled electronics will be required

1510

# HSCT PROPULSION PERFORMANCE

The turbine bypass engine/mixed compression inlet propulsion system depicted is probably the simplest HSCT propulsion system configuration under study. It presents a multivariable control problem in both the steady state and dynamic sense. When operating on design at steady state the desired operating position for each element of the system is well defined. Bypass doors are shut, turbine and compressor operate at their design match points, etc. However as the system operates off design, either due to deviations from the optimum flight path, temperature variations, or during climb and descent a non trivial optimum selection process is required to distribute captured airflow to achieve the best (thrust-drag)/fuel flow possible while satisfying stability margin requirements on various elements of the system. The fact that each effector from the centerbody to the exhaust nozzle has an effect on the set of states which define engine operating condition makes the control design problem inherently multivariable. There is significant coupling between the airframe and propulsion system not only through thrust commands, but also through angle of attack and Mach number influences on the inlet and inlet bypass contributions to yawing and rolling moments. Application of multivariable design techniques is expected to permit reduction of actuator bandwidth requirements and control margins, thus improving weight and performance. Development of a control system for this system will require an accurate, relatively high bandwidth, propulsion/airframe simulation including representation of major non-linear phenomena such as unstart and surge.

# HSCT PROPULSION PERFORMANCE

**Throat mach determines recovery**

**Normal shock position determines distortion& recovery**

**Shock structure affected by angle of attack and mach number variation**

**Compressor variable geometry**

**Turbine bypass bleed**



ℂ INLET  ℂ ENG  ℂ NOZ

**Centerbody**

**Spillage**

**Fuel flow**  **Throat area**  **Exit area**

**Secondary airflow valves**

**Bypass doors**
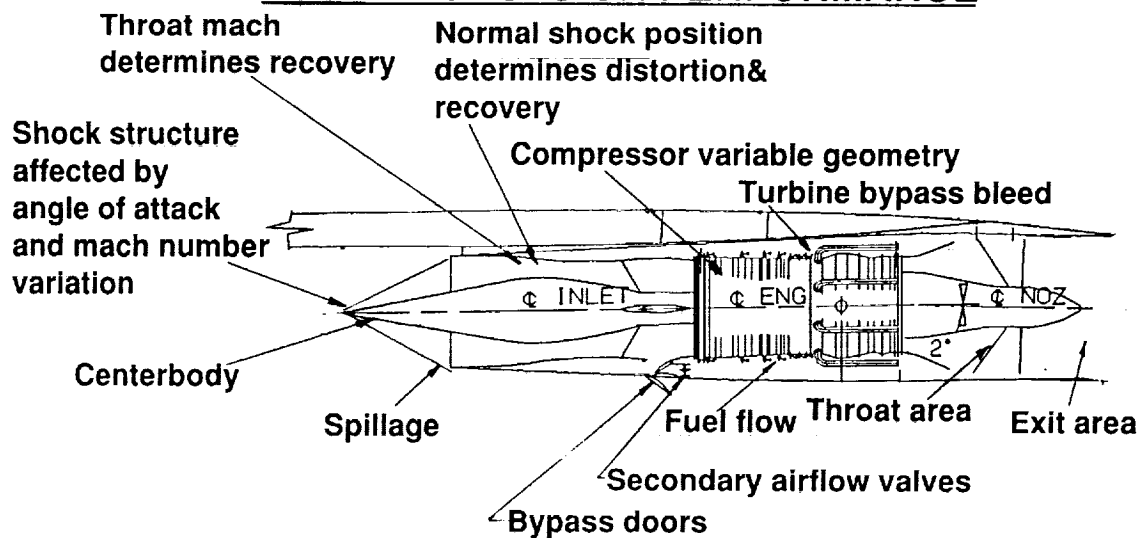
○ Propulsion system is physically coupled  both internally and externally
○ Integrated propulsion/airframe control
Best performance for given control margins,sensors,and actuation capability
Self optimising for off design conditions
○ Analysis requires integrated high fidelity simulation

## ADVANCED INLET INSTRUMENTATION

The critical measurement in a mixed compression inlet is normal shock position. Historically this has been measured by sensing the static pressure rise associated with the normal shock. This approach, although workable, suffers from deficiencies including complex plumbing, relatively low bandwidth, high precision requirements and sensitivity to angle of attack, inlet geometry variations, and minor inlet design changes. More direct approaches to normal shock sensing, suited to the low terminal shock mach numbers of the HSCT inlet, could benefit both system performance, by reducing supercritical margin, and dependability, by eliminating plumbing and fragile pressure transducers.

Mixed compression inlet throat mach number margin is set by the anticipated magnitude and rate of change of freestream mach number variations and the bandwidth of the centerbody actuator. If techniques can be developed which allow us to detect freestream variations substantially ahead of the airplane we can reduce throat mach number margin and the dynamic response requirements on the centerbody actuation system. Optical techniques show promise for providing this kind of prediction capability. Unfortunately current systems are heavy and are dependent on aerosols which may not have adequate density to assure a continuous signal. If available such system would also benefit flight control system performance.

## ADVANCED INLET INSTRUMENTATION

o **NORMAL SHOCK SENSOR**
  **High bandwidth**
  **Eliminate plumbing & manifolds**
  **Minimize signal sensitivity to inlet design changes**

o **FREESTREAM DISTURBANCE DETECTION**
  **Throat mach tolerance dictated by:**
  **disturbance frequency content**
  **actuator bandwidth**
  **anticipation available**

  **Approach**
  **Temperature - infrared imaging**
  **Wind shear - laser backscattering**

  **Issues**
  **Complexity/weight & aerosol availability**

  **Other potential benefits**
  **Clear air turbulence avoidance**
  **Improved autopilot performance**

## CONTROL SYSTEM DEVELOPMENT OBJECTIVES

For the most part adequate control simulation and analysis tools exist to perform the propulsion control system design, analysis, build, test task. Unfortunately, although the individual tools exist, they are not integrated into a system that permits automation of the control system development process starting from the CAD data base for the propulsion plant. Furthermore many of the tools are proprietary and individuals in a given organization are familiar only with their own tools. In order to efficiently develop an HSCT control system an integrated package available across corporate boundaries must be created. Such a system will reduce development costs and produce a more reliable high quality product.

Current propulsion system development practice is strongly dependent on test results to establish component performance, pneumatic signal characteristics used for airflow and normal shock measurements, and to confirm system dynamics. Significant development economies can be achieved by using CFD to predict these characteristics and using the wind tunnel/test cell only as a final confirmation tool.

## <u>CONTROL SYSTEM DEVELOPMENT OBJECTIVES</u>

○ Automate the design/analysis/build/test process
Integrate and validate existing tools
Modify or develop tools if required
Benefits cost and reliability/quality

○ Reduce dependence on tests involving propulsion machinery
Integrated tests of developmental machinery
and developmental controls are costly and risky
Use CFD to reduce dependence on wind tunnel
and flight test results

1514

## RECOMMENDED HSR PROGRAM

As indicated in the early charts significant technology improvements are anticipated in the next 5 years to improve the development and operating economics of the HSCT. Before these technologies can be applied in a production program a demonstration program to validate them is required. The recommended HSR program consists of four to five years of technology development, and a five year technology demonstration program. Some of the technology development efforts are already under way in programs such as the NASA/NAVY FOCSI program and the NASA HIDEC/PSC program. Other technology development efforts in areas such as high temperature electronics and improved normal shock sensing need to be initiated rapidly if they are to be useful to the HSCT on the planned schedule. The technology demonstration program would be based on a complete supersonic propulsion system, and its integrated control including examples of all desirable advanced technology components. The system would be exercised through a complete test cycle starting with a control hardware in the loop bench test, and culminating in a flight test on an appropriate aircraft. The design, development, and test activity would provide the necessary validation of the integrated control development tool, the design methodology, and component technologies.

# RECOMMENDED HSR PROGRAM

| 1991 | 1992 | 1993 | 1994 | 1995 | 1996 | 1997 | 1998 | 1999 | 2000 |
|------|------|------|------|------|------|------|------|------|------|

**Integrated Control System Technology Demonstration**

| Concept Dev. | Design | Fab | Test |
|---|---|---|---|

**Component Development**

PAIT Additions

Existing NASA Programs

NASA/Corporate cooperation

Corporate IR&D

○ Features:

Integrated Prop/Flt Control Law
Full envelope capabiliy
Related displays and controls

Critical system component tech
Fiberoptics
High temperature electronics

○ Approach:
Representative Aerodynamics
and Propulsion Cycle
Implement multiple solutions
Subscale propulsion system
Test on NASA facilities & aircraft

1515

## FLIGHT TEST DEMONSTRATION OBJECTIVES(I)

A flight test demonstration provides the opportunity to confirm a large number of propulsion system issues which are not specifically control related. These include validation of the analytical techniques use to design the cycle and propulsion components and predict thrust minus drag. An opportunity is also provided to confirm noise prediction techniques for impingement on the aircraft and the ground. The opportunity is provided to see the complete system in operation and identify any unexpected environmental effects on components and to understand the real world maintenance situation.

# FLIGHT TEST DEMONSTRATION OBJECTIVES(I)

### DEMONSTRATE INSTALLED PROPULSION SYSTEM PERFORMANCE
o Validate analytical techniques
o Confirm wind tunnel results
o Confirm engine/inlet compatability
o Operation in real world environment
o Acoustic impingement on adjacent structure
o Noise prediction
o Thrust - drag accounting verification

1516

## FLIGHT TEST DEMONSTRATION OBJECTIVES(II)

From a control standpoint there are a number of flight test objectives. Confirmation of analytical techniques, in particular those involved in predicting the installation effects both on the inlet flow field and installed thrust - drag, is critical to reducing risk in the production program. Demonstration of the integrated control system with the pilot in the loop in the flight environment is also extremely critical since the system will have a number of novel pilot interface features and control modes relative to current commercial practice. Finally the demonstrator is critical to demonstrating the practicality of advanced hardware components in the supersonic environment on a closed loop basis.

# FLIGHT TEST DEMONSTRATION OBJECTIVES(2)

**PROPULSION CONTROLS**
- o **Confirm analytical techniques**
- o **Demonstrate integrated inlet/engine/nozzle/flight control system**
- o **Demonstrate system automation &display features**
- o **Obtain pilot evaluation of integrated system**
- o **Demonstrate system operability**
- o **Demonstrate advanced component technology**
  **High pressure hydraulics**
  **Fiberoptics**
  **Light weight actuators**
  **Normal shock sensor**
  **High temperature electronics**
  **Advanced data bus**
  **High temperature connectors & wiring**
  **Freestream disturbance detection**

## CONCLUSIONS

Substantial component development effort is required if HSCT control system weight and performance are to be significantly improved over that of the SST. An integrated control system development package including simulation, analysis, and autocode tools is required to reduce development costs and improve system reliability. This development package must be shared among all participants in HSCT control system development. A controls demonstration program is required to confirm both the advanced component technologies and the control system development methodology prior to undertaking a full scale commercial development program. Further NASA and industry planning of the next ten years research effort in this area is required.

## CONCLUSIONS

**COMPONENT DEVELOPMENT IS REQUIRED**
o **Fiberoptic sensors**
o **High temperature electronics**
o **Direct shock sensing**
o **Freestream disturbance detection**
o **Lightweight actuation**
o **Fiberoptically signalled actuation**
o **Advanced data buses**

**SIMULATION,ANALYSIS,  AND DEVELOPMENT TOOLS**
o **Integration,improvement, and validation are required**

**CONTROLS DEMONSTRATION PROGRAM REQUIRED**
o **Prove methodology & design/analysis tools**
o **Demonstrate advanced hardware technology
in realistic environment**
o **Validate HSCT economic factors related
to propulsion control**
o **Flight test required for complete demonstration**
**FURTHER PLANNING IS REQUIRED**

1518

*omit*

# Session XI. Airframe and Engine Materials

**THIS PAGE INTENTIONALLY BLANK**

1520

# Session XI. Airframe and Engine Materials

*Omit*

Enabling Propulsion Materials for High-Speed Civil Transport Engines
*Joseph R. Stephens and Dr. Thomas P. Herbell, NASA Lewis Research Center*

THIS PAGE INTENTIONALLY BLANK

# ENABLING PROPULSION MATERIALS FOR HIGH-SPEED CIVIL TRANSPORT ENGINES

*524-07*

*12054*

Joseph R. Stephens and Thomas P. Herbell
NASA Lewis Research Center
Cleveland, Ohio

First Annual High-Speed Research Workshop
May 14-16, 1991

# ADVANCED MATERIALS CRITICAL TO HIGH-SPEED CIVIL TRANSPORT (HSCT)

NASA Headquarters and Lewis Research Center have advocated an Enabling Propulsion Materials Program (EPM) to begin in FY'92. The High Speed Research Phase I program which began in FY'90 has focused on the environmental acceptability of a High Speed Civil Transport (HSCT). Studies by industry, including Boeing, McDonnell Douglas, GE Aircraft Engines, and Pratt & Whitney Aircraft, and in-house studies by NASA concluded that $NO_x$ emissions and airport noise reduction can only be economically achieved by revolutionary advancements in materials technologies. This is especially true of materials for the propulsion system where the combustor is key to maintaining low emissions and the exhaust nozzle is key to reducing airport noise to an acceptable level. Both of these components will rely on high temperature composite materials that can withstand the conditions imposed by commercial aircraft operations. The proposed EPM program will operate in conjunction with the HSR Phase I Program and the planned HSR Phase II program slated to start in FY'93. Components and subcomponents developed from advanced materials will be evaluated in the HSR Phase II Program.

E-6198

## Enabling Propulsion Materials

## Advanced Materials Critical to High Speed Civil Transport (HSCT)



Figure 1.

1524
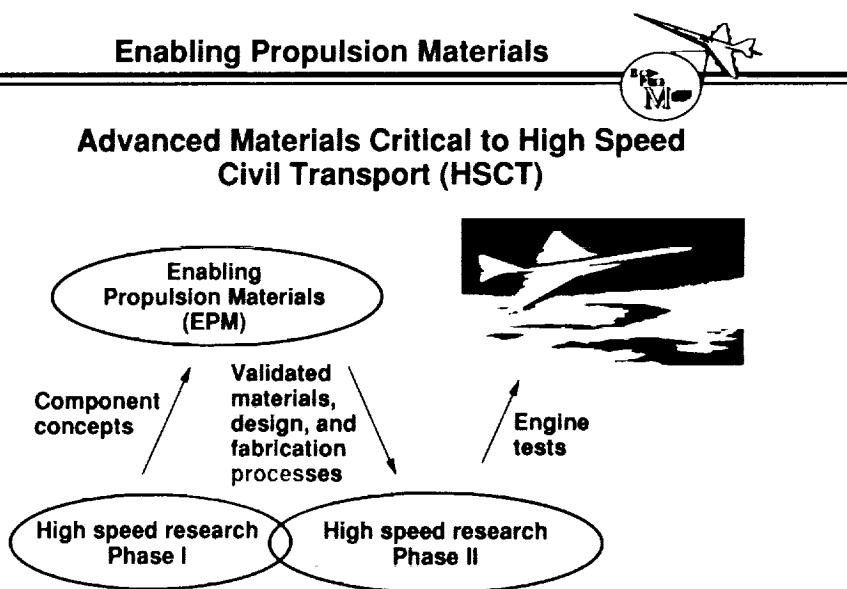
# REQUIREMENTS FOR A SUCCESSFUL HSR PROGRAM

The success of the next generation HSCT depends upon not only its environmental accept-ability, but upon its economic viability, and technical feasibility. There is great concern inter-nationally about the impact that a fleet of several hundred HSCTs will have on the ozone layer because of the pollutants (primarily $NO_x$ emissions) that will be generated by the engines. Current designs indicate that an altitude of 60 000 to 70 000 ft will be optimum for the aircraft as it is now envisioned. The impact on the ozone layer is anticipated to be much greater as a result of flying at this altitude compared to today's subsonic aircraft which normally only fly at about half this altitude. This is why the combustor technology is critical to the HSCT propul-sion system. Being a friendly neighbor of residential and business establishments surrounding international airports must also be addressed by meeting FAR 36 requirements. A ground rule going into the HSR Program is that the U.S. HSCT will not be government subsidized, but must be commercially economical. To meet these requirements, technical feasibility of all advanced technologies must be demonstrated. Propulsion materials are considered to be enabling to the HSCT. The engine's environmental acceptability hinges on achieving a combus-tor that will operate at a gas temperatures up to 3400 °F. With minimum air cooling, this dic-tates the need for ceramic-based materials that have not been fully developed. For a HSCT to be economically viable, light weight, up to 2400 °F temperature capability materials must be developed for the exhaust system. This arises because designs now underway suggest that the nozzle could comprise nearly 50 percent of the engine weight if constructed from materials such as high density nickel-based or cobalt-based superalloys which are used in today's commercial engines. These superalloys are the current high temperature engine materials, but their max-imum use temperature is only about 2000 to 2200 °F.

**Enabling Propulsion Materials**
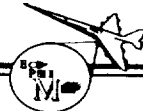
## Requirements for a Successful HSR Program

- Environmental acceptability
  - Ozone layer impacts
  - Airport noise
  - Sonic boom

- Economic viability
  - Market
  - Timeliness
  - Cost

- Technical feasibility
  - Materials
  - Propulsion
  - Airframe
  - Aerodynamics
  - Flight deck and controls

Figure 2.

# TECHNICAL FEASIBILITY

Propulsion materials are considered to be the highest risk area for the next generation HSCT in terms of technical feasibility. Several factors contribute to this determination. Extending the material use temperature in the combustor up to the range of 2800 to 3000 °F is considered to be the most challenging technology development facing the materials researchers and engine designers. Simultaneous with this development is the need to develop light weight, high strength-to-density materials for the nozzle that can withstand temperatures approaching 2300 to 2400 °F. It is anticipated that ceramic matrix composites and intermetallic matrix composites will be leading candidate materials for the combustor and nozzle, respectively. New fibers and fiber coatings will be required to reach these extreme use temperatures for the component lives required. In addition, fabrication of large components will rely on processing and joining concepts that currently have not been demonstrated beyond laboratory scale feasibility. Laboratory and rig testing along with analytical modeling concepts will be required to demonstrate the structural reliability and durability of these new materials.

If we consider the possible fall-back positions that exist today, it is concluded that for the 2800 to 3000 °F combustor material, there is none. Carbon-carbon composites might have the temperature capability for short military applications, however for commercial engine applications these composites will not holdup for the anticipated thousands of hours operation required. To achieve the needed structural viability and durability required for the combustor and nozzle applications, the only alternative if the goals of the program can not be met is to reduce the operating temperature by introducing cooling air. However, an unacceptably high penalty in propulsion efficiency is currently projected as a result of this approach.

## Enabling Propulsion Materials

## Technical Feasibility

**Highest risk area:**
- **Propulsion materials**
  - **Ceramic matrix composites (CMC) required for combustor operation at 2800 - 3000 °F**
  - **Multiple simultaneous nozzle material developments (ceramic matrix composites, and intermetallic matrix composites)**
  - **Joining technology**
  - **Structural viability and durability (>> 4000 - hr life)**

**Fall-back position**
  - **None for 2800 - 3000 °F CMC**
  - **Viability/durability met through reduced operating temperature (with major performance penalty)**

**LIMITED DISTRIBUTION**

Figure 3.

# OPERATING ENVIRONMENT

The operating environment in terms of combined exposure to temperature and time that the propulsion materials will experience in a HSCT application is much more severe than those that now exist or are projected to exist in future subsonic and military aircraft engines. Projected materials temperatures for the three types of engines are seen to vary from about 2600 to 3000 °F with the HSCT having the highest proposed material use temperature. However, the percent time at maximum temperature is the primary factor that distinguishes the HSCT from the other types of aircraft engines. The HSCT engine will be designed to spend nearly 85 percent of its life at the maximum operating temperature compared to about 25 percent for a military fighter aircraft engine, and only around 10 percent for a typical subsonic aircraft engine. A final consideration is the time at maximum temperature that these materials will experience. For commercial engines (both the HSCT and subsonic), 18 000 hr life is a typical goal. In contrast, for military applications lives of 2000 to 4000 hr are more typical.

The engine environments described above also dictate the potential failure modes that must be taken into consideration when designing the combustor and nozzle components. Military engines typically experience frequent thermal cycling as a result of relatively short flights or an operational mode corresponding to much of the flight being at reduced power (reduced temperature) and frequent bursts of power (increase to maximum temperature) for short time periods. Fatigue failure is a major design consideration for military applications. In contrast, for commercial applications, especially for the HSCT where long times at extremely high temperatures are required, creep deformation is a primary design criterion.



**Enabling Propulsion Materials**

**Operating Environment**

☐ High - bypass - ratio subsonic turbofan
■ High - speed civil transport engine
▨ Military supersonic fighter engine
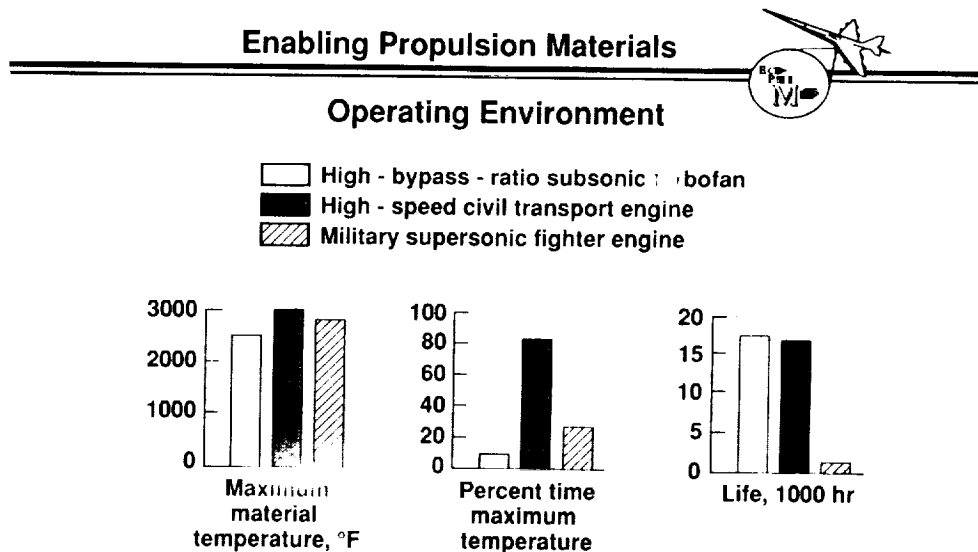
LIMITED DISTRIBUTION

Figure 4.

# NEW ENGINE MATERIALS INTRODUCTION STRATEGY

Because of the high risk involved in developing new higher temperature/long life materials and the long lead time required to get new materials into flight hardware, it is imperative that EPM can begin in FY'92 to meet a tentative goal of the year 2005 for the first flight of the HSCT. It is not uncommon for materials development to take from 15 to 25 years before flight hardware is realized. Laboratory research, such as being conducted under NASA's HITEMP program can typically take 7 to 10 years to demonstrate feasibility of a new material in small coupon sizes. Scale-up and characterization along with demonstrating feasibility of fabrication, joining, and manufacturing technologies for a new material can take another 7 to 10 years. The planned EPM program will fill the role in this latter phase of a material's development history. Government funding along with some industry resources are required in this phase. If at this step, industry is convinced that a market exists and the new material development can lead to an economically viable product, there will be a commitment on the part of industry to bring the technology to fruition by entering into the production phase. The time frame for EPM is thus very compressed with only 7 years available to develop and demonstrate the feasibility of high temperature composite materials for the combustor and nozzle of the HSCT.
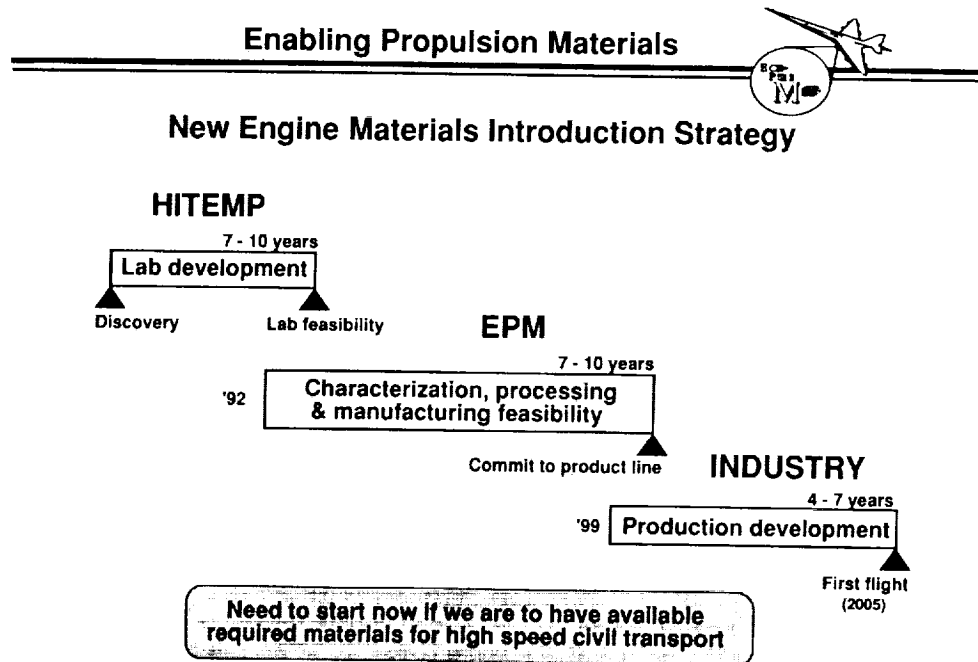


Figure 5.

# ENABLING PROPULSION MATERIALS

Enabling propulsion materials are planned to be developed for the combustor and the nozzle. Ceramic matrix composites (CMCs) are the leading candidate materials for the combustor because of their light weight, environmental resistance, and potential strength at the anticipated extremely high temperatures of operation in the combustor. Successful development of CMCs will help achieve high combustion efficiency of the fuel and provide the option to design and fabricate a combustor liner that will help meet the emission (primarily $NO_x$) requirements of the HSCT.

Intermetallic matrix composite (IMCs) are the leading candidate materials for the nozzle where a high strength-to-weight ratio is essential to reduce the overall weight of this high temperature component. Because of the potential airport noise problem the nozzle must be quite large to combat this issue. The light weight IMCs combined, perhaps, with light weight CMCs in selected applications within the nozzle structure will also contribute to a high propulsive efficiency.



**Enabling Propulsion Materials**

High Speed
Civil Transport

CERAMIC COMPOSITE
COMBUSTOR
o High Combustion
    Efficiency
o Low NOx

INTERMETALLIC COMPOSITE
NOZZLE
o Light Weight
o High Propulsive Efficiency
o Low Noise
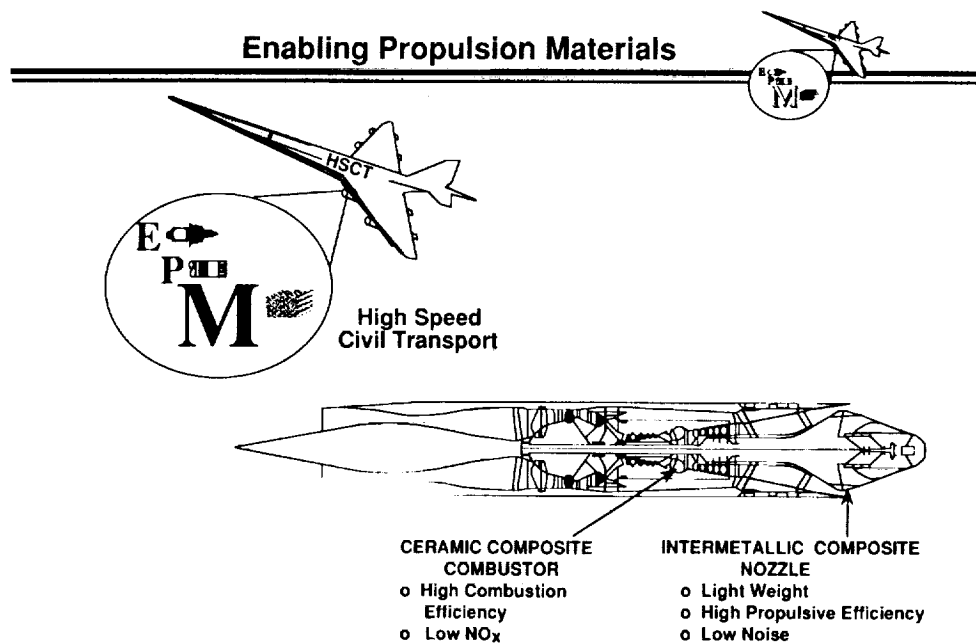
Figure 6.

# OBJECTIVE

The planned EPM program will involve a large contractual effort along with key contributions from researchers at NASA Lewis Research Center. The objective is stated below:

**Enabling Propulsion Materials**
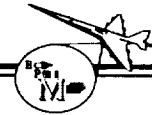
## Objective

**By 1999 develop and demonstrate in cooperation with U.S. industry, the technical feasibility of high temperature, light weight composites for critical components of the High Speed Civil Transport**

Figure 7.

# GOALS

The goals set for the EPM program take into account the economic viability of a commercial aircraft, environmental restrictions anticipated for such a HSCT, and the technological barriers that must be overcome to meet the goal of a first flight of a fleet of HSCTs by the year 2005.

The goal for the life of the hot section of the engine including the combustor and nozzle is 18 000 hr. This is typical for subsonic commercial engines. However, this is a very ambitious goal in the case of the HSCT where 85 to 90 percent of the 20 000 hr will be at the maximum operating temperature of the engine.

The goal for the material temperature in the combustor is up to 3000 °F. This goal is seen as very high risk primarily because of the lack of a fiber that will withstand this temperature for the long life of the engine. High conductivity ceramic matrices may permit some backside cooling to help alleviate this high material temperature need.

The goal for the material temperature in the nozzle is up to 2400 °F. Again, this is a high risk goal primarily because of the reactions that may occur between the fiber and matrix at such high temperatures and for such long times at temperature. Ceramic matrix composite nozzle liners may find use in the hotter portions of the nozzle at low stresses, while the IMCs may be used in the lower temperature, high stress regions. Both the IMCs and the CMCs can contribute significantly to reducing the weight of the nozzle in order to achieve the weight reduction goal of 30 percent compared to currently used nickel-based or cobalt-based superalloys.

**Enabling Propulsion Materials**
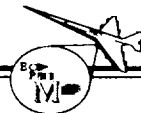
## Goals

- **18,000 hours hot section life**

- **High-temperature operation**

    - **up to 3000°F for combustor**
    - **up to 2400°F for nozzle**

- **Light weight**

    - **30% weight reduction in nozzle compared to current superalloy technology. Equivalent to aircraft TOGW reduction of 2.6%**

Figure 8.

# IMPACT AND APPROACH

The success of the EPM program is needed for a successful HSCT program. A successful HSCT will in turn impact the United States aerospace community by helping it remain competitive in a world market where for the HSCT, it is believed that possibly only one group will produce this aircraft. A strong technology base will help the U.S. companies retain their leadership position into the 21st century.

The overall approach to EPM consists of a planned 7 year, primarily contractual program involving a broad team effort across U.S. industry. This contract team along with contributions from NASA Lewis Research Center's Materials Division and Structures Division will develop the combustor and nozzle critical materials technologies to meet the goals of the HSCT program.

Our current plans are to be in a position to award a contract to the winning industrial team by the start of FY'92 (October 1991).

---

### Enabling Propulsion Materials

**Impact:**

Retain U.S. competitiveness in world market for a supersonic transport

**Approach:**

- Initiate a 7-year duration effort
- Involve team efforts across U.S. Industry
- Develop combustor and nozzle critical technologies
- Award contract by October, 1991

Figure 9.

# TECHNOLOGY READINESS LEVEL: COMBUSTOR LINER

To appreciate the magnitude and degree of difficulty of the research and development being undertaken in the EPM program, it is appropriate to examine the current state of the art for combustor liners and to also look at activities underway on the advanced composite materials. Cobalt-based or nickel-based superalloys are used in today's engines for combustor liners and require extensive cooling to maintain even a short time material temperature limit of about 2200 °F. Revolutionary advancements in material capabilities will be required to meet the 3000 °F goal for the combustor.

Several government funded programs are underway to develop advanced CMCs for applications in gas turbine engines. The Department of Defense's Integrated High Performance Turbine Engine Technology (IHPTET) program is evaluating oxide-oxide CMCs for lower temperature applications. NASA's Advanced High Temperature Engine Materials Technology Program (HITEMP) has both in-house and contractual efforts underway to develop higher temperature fibers for temperatures approaching 3000 °F, addressing various processing/fabrication alternatives for CMCs that may be adaptable to combustor manufacturing technology, and has a cooperative program now underway with industry to identify and characterize on a laboratory scale, potential candidate materials for the combustor.

**Enabling Propulsion Materials**

TECHNOLOGY READINESS LEVEL: Combustor liner

STATE OF THE ART: Cobalt base and nickel base superalloys limited to 2200 °F and require excessive cooling

- Oxide-Oxide: 1800°F CMCs under evaluation (IHPTET)

- Candidate high-temperature fibers to 3000°F (HITEMP)

- Processing/fabrication of CMCs underway (HITEMP)

- Candidate CMC fibers/composites for combustor liners (NRA contract)

Figure 10.

# STRESS RELAXATION TEST DEVELOPED TO RANK CREEP RESISTANCE OF

## SiC FIBERS

There is a need for creep resistant fibers to meet the demand of very long times at temper-
atures approaching 3000 °F for the combustor. A method has been developed that permits the
rapid evaluation of candidate fibers in controlled environments. The approach is to measure the
fiber stress relaxation in a bend or loop test which in turn can be related to the creep resistance
of the fiber. Bend stress relaxation has been determined for different types of nonoxide fibers
between 1850 and 2550 °F. This test has been used to rank the creep resistance of various com-
mercial and developmental fibers under similar test conditions. The results were correlated to
the tensile creep behavior of the SCS-6 fiber and results were found to be give excellent correla-
tion between the two methods. It is concluded that all of the polycrystalline fibers tested
relaxed (crept) at 2550 °F while the single crystal SiC whisker showed no stress relaxation or
creep deformation at this temperature.

**Enabling Propulsion Materials**

## Stress Relaxation Test Developed to Rank Creep Resistance of SiC Fibers

### Stress Relaxation Test

Initial loop    Relaxed fiber

Heat treat
at constant
temperature,
environment,
surface strain

Stress Relaxation Ratio, m = 1 − $R_o/R_a$

• m is related to creep resistance
(m = 1 for fiber with zero creep)

### Fiber Comparison at 2550 °F
( 1hr stress relaxation ratio in argon)

| | | | |
|---|---|---|---|
| SCS/6 | Nicalon | "NASA SiC" | SiC |
| Textron | Nippon | Dow | Carbo- | whiskers |
| Spec. Matl. | Carbon | Corning | rundum | Los Alamos |

Early fibers    Recent improved fibers    Optimum single crystal

Figure 11.

# MAXIMUM USE TEMPERATURE FOR CANDIDATE COMBUSTOR MATERIALS

A major issue in the development of the HSCT combustor is the selection of materials to withstand the harsh combustion environments. Predictive modeling has been undertaken to approach this issue and involves an understanding of the key interactions between the combustion environment and candidate materials. The current candidate materials include silicon-base ceramics as structural materials and oxide base-ceramics as coatings. The key interactions include volatility, oxidation, and interfacial reactions. The volatility issue has been addressed by modeling the combustor as a hollow cylinder with walls that vaporize through a boundary layer. A limiting criterion for the use of any material was established to be 10-mils of material lost in 10 000 hr. Therefore, minimum acceptable vapor pressures were established that could be related to maximum use temperature through the predictive models. These maximum use temperatures are presented for some candidate combustor liner materials.

The oxidation and interfacial reaction issues related to material lifetimes are more difficult to quantify and, as of yet, have not been modeled. Experiments will be performed to gain experience with such effects as water vapor and thermal cycling on the oxidation behavior of silicon-base materials.



Figure 12.

# FRCMC TESTING IN ROCKET ENGINE ENVIRONMENTS

Progress is being made in the research and development of CMCs for applications in rocket engine environments. Although times at temperature are extremely short compared to commercial gas turbine engine applications, the experience gained in fabrication various components will be invaluable in the initial steps of scaling up the CMCs for the combustor. In addition to small laboratory scale coupons, such components as nozzle/combustor chambers and turbine blades have been fabricated for rig testing. Plans call for full scale testing of these fiber reinforced CMCs components in a ground-based test bed turbopump of the type (but smaller than that) used on the space shuttle main engine (SSME) in 1995.



**Enabling Propulsion Materials**

## FRCMC Testing in Rocket Engine Environments
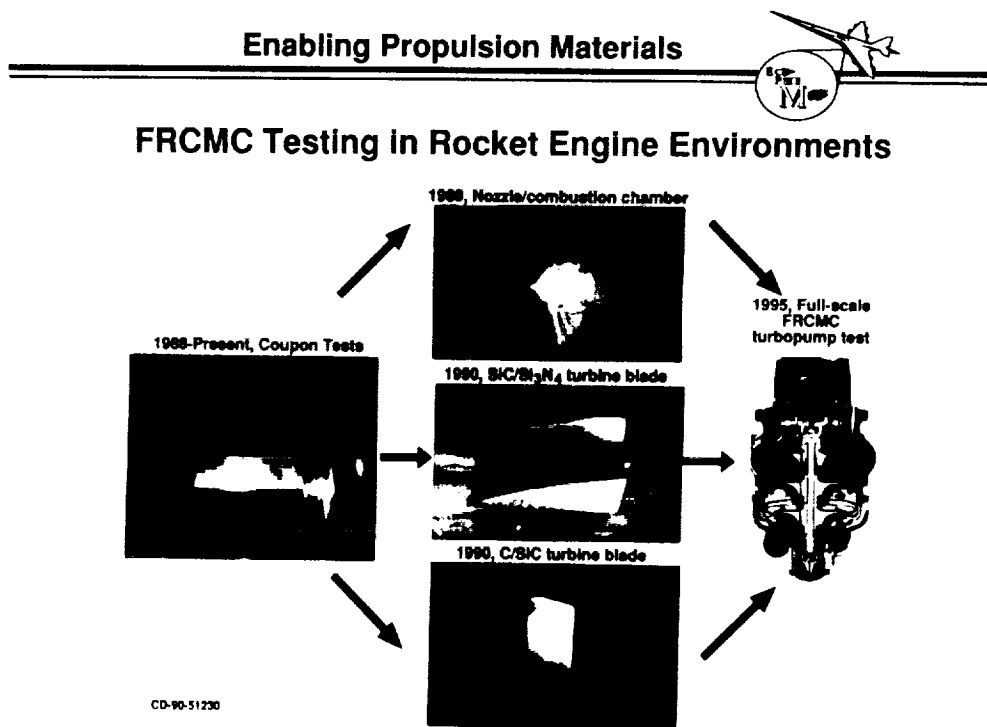
Figure 13.

# REQUIRED TECHNOLOGY DEVELOPMENT FOR COMBUSTOR LINER

Based on the current state-of-the-art, technologies that need to be addressed in EPM run the gamut from identifying promising constituents of the composite materials to the final fabrication of a full-scale combustor liner for ground base engine testing. One of the major barriers that must be overcome is that of a high temperature fiber (and its coating) that can maintain its stability and properties to meet the goals of EPM. Laboratory test on candidate fibers to characterize their behavior under simulated HSCT conditions must be performed to rank the fibers and select those that have the best potential for subsequent composite processing. Fiber matrix compatibility to achieve the proper bond for long term, optimum performance is also a major consideration. Composite durability and environmental resistance in simulated combustor environments and the prediction of their failure mechanisms and life will have to be evaluated for these advanced materials. Finally, after laboratory characterization, benchmark testing, and model validation, the next challenge is to scale-up the fiber and composite fabrication processes and learn how to design, fabricate and test components or subcomponents manufactured from the advanced composites.

**Enabling Propulsion Materials**
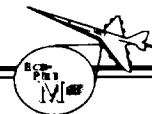
## Required Technology Development For Combustor Liner

- **Fiber development and characterization to 3000 °F**

- **Fiber-matrix compatibility for optimum performance**

- **Scalable fabrication process**

- **Composite materials durability and environmental resistance**

- **Life prediction methodology for CMCs**

- **Design, fabrication, and test verification of CMC combustor liner component**

LIMITED DISTRIBUTION

Figure 14.

# TECHNOLOGY READINESS LEVEL: NOZZLE STRUCTURES

Exhaust nozzle technology today relies on nickel-based superalloys with thermal barrier coatings. These materials are possible materials of construction for the proposed nozzle designs for the HSCT. However, because of the extremely large size of the proposed nozzle to meet noise regulations and high propulsive efficiency, the weight of the nozzle fabricated from superalloys will constitute a major portion of the total engine weight. Engine weight increases produce highly accentuated structural weight increases with major reductions in aircraft range or passenger capacity. Therefore, lighter weight, high-strength-to-density materials are required to meet the performance requirements of the HSCT. Intermetallic matrix composites are leading candidate materials for this application since they have a density less than two-thirds that of the nickel-based superalloys. The HITEMP program is pursuing IMCs for high temperature applications comparable to that proposed in the nozzle application of the HSCT. In addition, experience is being gained under the IHPTET program to develop intermetallics for turbine blade applications which should strengthen the data base on these materials and give more confidence as the advanced composites are developed.

**Enabling Propulsion Materials**
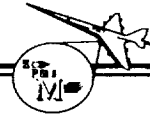
TECHNOLOGY READINESS LEVEL: Nozzle Structures

STATE OF THE ART: Nickel base superalloys with thermal barrier coatings impose large weight penalty

- IMC development to 2400 °F (Industry IR&D, HITEMP)

- IMC turbine blade development (IHPTET)

Figure 15.

# REQUIRED TECHNOLOGY DEVELOPMENT FOR EXHAUST NOZZLE STRUCTURE

Similar technologies need to be explored and developed for the advanced composites for the nozzle as were described for the combustor. In particular, fiber technology is a major barrier that must be addressed. Ceramic fibers are leading candidates because of their light weight and temperature capability. Intermetallic matrices such as nickel aluminide are being considered because of their low density and potential capability in terms of environmental resistance at the temperatures proposed for the nozzle. A major barrier to be overcome is the difference in coefficient of thermal expansion (CTE) between ceramic fibers which is typically low and that of the intermetallics which is quite high on a comparative basis. Compliant layers or graded coatings on the fibers will be explored as possible methods of achieving improved CTE matching and thus increasing the life that is required of the fiber-matrix interface without degradation of the composite. Composite processing, characterization, and life prediction will play a major role for the advanced composite under development for the nozzle application. Subsequent scale-up, fabrication, and subcomponent evaluation in rig and possibly engine tests will further be required.

**Enabling Propulsion Materials**
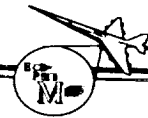
## Required Technology Development for Exhaust Nozzle Structure

- Fiber selection and coating development to 2400°F

- Composite material processing and characterization

- Life prediction methodology for IMCs/CMCs

- Design, fabrication, and test verification of lightweight IMC nozzle structure prototype components and CMC liner

LIMITED DISTRIBUTION

Figure 16.

# PROJECT LOGIC

The EPM program logic will evolve from the selection of an engine concept in the initial phase of the program to final delivery of components and subcomponents in the program's final phase. An annual materials capability-design trade-off study will be performed to define property goals for the composite development and to assure that the research and development stays on track for the HSR Phase II program so that the goals set for the HSCT will be met. The deliverables from the combustor phase of the program are two combustor liners for evaluation in the planned HSR Phase II program. The nozzle portion of the program will develop subcomponents to be evaluated in rig tests or "piggy back" engine tests in another engine that may be available at the time.

## Enabling Propulsion Materials

## Project Logic
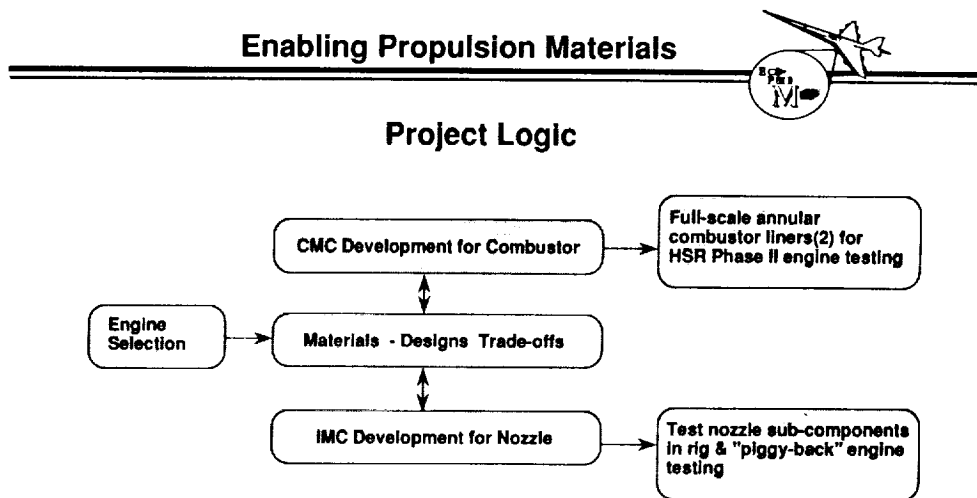


Figure 17.

# CONCEPT SELECTION

The engine concept selection will be followed by design activities to demonstrate the benefits of the advanced materials. This will involve conceptual designs using state-of-the-art, 1991 technology. Since there are two combustor concepts that are under consideration, one engine design will be with the rich burn, quick quench, lean burn (RQL) combustor while another engine design will be with a lean burn premixed prevaporized (LPP) combustor. There are also two nozzle concepts under consideration which include a two-dimensional concept and an axisymmetric concept. Therefore, one or the other of these nozzle concepts will be selected for the RQL combustor and one or the other for the LPP combustor. This procedure will be repeated using projected 1999 technology. Based on these engine design studies, payoffs in terms of take-off gross weight (TOGW), fuel burned, and cost as a result of using the advanced composite materials can be shown.

**Enabling Propulsion Materials**

## Concept Selection

| | | Combustor | Nozzle |
|---|---|---|---|
| Engine Configuration | 1991 Technology | RQL | 2D |
| | | LPP | Axisymmetric |
| | 1999 Technology | RQL | 2D |
| | | LPP | Axisymmetric |
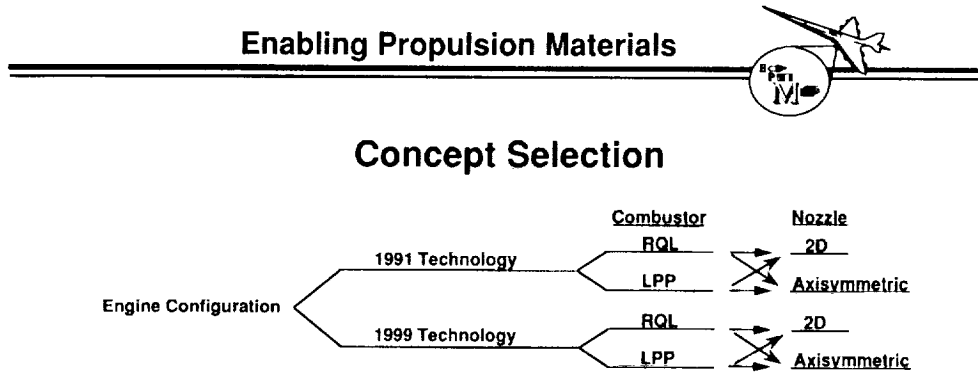
Figure 18.

# TASK SCOPE

Materials and analytical modeling development constitute the heart of the planned EPM contractual program. The engine and component design trade-offs will provide guidance to the development of the materials with properties meeting the goals required for the HSCT. As described previously, fiber development and identification of appropriate coatings for the individual fibers will be addressed for both the combustor and nozzle materials. High strength and high temperature stability will be primary factors to be explored. In addition, compatibility with the candidate matrices and environmental durability must be established for the proposed use temperatures and times.

Scale-up of the fiber processing and composite fabrication techniques will be required in order to ultimately be able to fabricate the combustor liner and nozzle subcomponents. Joining techniques for similar and dissimilar materials will be optimized for the CMCs and IMCs selected for component fabrication. Success in this area of the program will permit advancing promising composite materials from the laboratory scale coupons to large panels for benchmark testing.

Characterization of the advanced composites developed in the EPM program will be guided by the operating conditions anticipated in the combustor and the nozzle. Laboratory testing and subsequent rig testing will simulate the temperature, time, pressure, cycles, and environmental conditions imposed by the HSCT.

Parallel to the material development, process modeling will aid in the growth of fibers and optimization of composite fabrication techniques. Structural modeling will focus on failure mechanisms and life prediction of the composite materials. This in turn will be applied to the component and subcomponent fabrication and subsequent life predictions for rig and engine testing.

## Enabling Propulsion Materials

## TASK SCOPE

### Combustor & Nozzle Materials & Modeling Development
### Constitute the heart of the EPM Program

- Fiber Development — High strength & high temperature capability, compatibility, and durability are key fiber issues to be addressed.

- Materials Development — Fabrication, scale-up, and joining of composites from laboratory coupons to engine components is a major technology barrier that must be overcome.

- Materials Characterization — Materials will be characterized under simulated HSCT combustor and nozzle environments with emphasis on life, failure modes, and mechanical properties.

- Analytical Modeling/Verification — Structural modeling and verification will aid in materials development and prediction of component behavior.

Major Deliverables: Ceramic matrix composite(s) and appropriate models for combustor and nozzle liner design/fab/life prediction.

Intermetallic matrix composite and appropriate model for nozzle structure design/fab/life prediction.

Figure 19.

# PROGRAM SUMMARY

The program is summarized in terms of four activities. They include CMC material development and liner fabrication for the combustor and IMC materials development and subcomponent fabrication for the nozzle.

Key milestones for the combustor materials development include identification of fibers for scale-up, demonstration of composite fabrication techniques, demonstration of the 18 000 hr durability for the primary CMC in a laboratory rig test, and post engine test evaluation of the CMC liner.

Two key milestones for the combustor liner fabrication include the delivery of liner sectors and ultimately the combustor liners to the HSR Phase II program for test under simulated and actual engine testing.

Milestones for the IMC materials development include selecting a fiber-coating-matrix combination for scale-up, demonstration of subcomponent fabrication, and post test evaluation of a subcomponent fabricated from an IMC (and possibly a CMC liner) and tested in a rig and possibly an engine.

The key milestone for the nozzle fabrication phase of the program is to test a subcomponent.

## Enabling Propulsion Materials

### Program Summary

| FY'92 | FY'93 | FY'94 | FY'95 | FY'96 | FY'97 | FY'98 | FY'99 |

**CMC Materials Development**

Identify fiber for scaleup  Demonstrate composite fabrication technique  Demonstrate 18 000-hr environmental durability  Post engine test evaluation

**Combustor Liner Fabrication**

Deliver combustor liner sectors  Deliver two liners to HSR phase II

**IMC Materials Development**

Fiber/coating/matrix selected for scaleup  Subcomponent geometry fabrication demonstrated  Subcomponent post test evaluation

**Nozzle Subcomponent Fabrication & Test**

Subcomponent test

Figure 20.

# PROJECT ORGANIZATION

The EPM project is organized such that Lewis Research Center has the direct management of the planned contractual research and development. An advisory team made up of cognizant representatives from industry will be selected to assure that the materials development is directly focused on the needs of the HSCT and is compatible with the HSR Phase II program.

It is anticipated that an industrial team will form the basis for the contractual program. Because of the complexity of the materials development and the high risk involved technically and economically, contributions from several engine companies, fiber producers, composite fabricators, material and equipment manufactures, and academia where appropriate, will be required to enhance the potential of making this program a success.

NASA Lewis will not only have overall management responsibility of the contractual program, but will conduct in-house research in support of the contractual effort. In-house research will focus on filling gaps that may occur in the contract program and providing alternatives to those area that are considered the highest risk areas technically.

Along with the mainstream of research, NASA plans to periodically issue NASA Research Announcements (NRAs) that will provide opportunities for those not directly involved in EPM to propose new ideas and alternatives for consideration by the Project. If any new ideas prove to be promising, they will be factored into the EPM effort by incorporating the originating organization into the team membership or by some other mechanism.



Figure 21.

1544
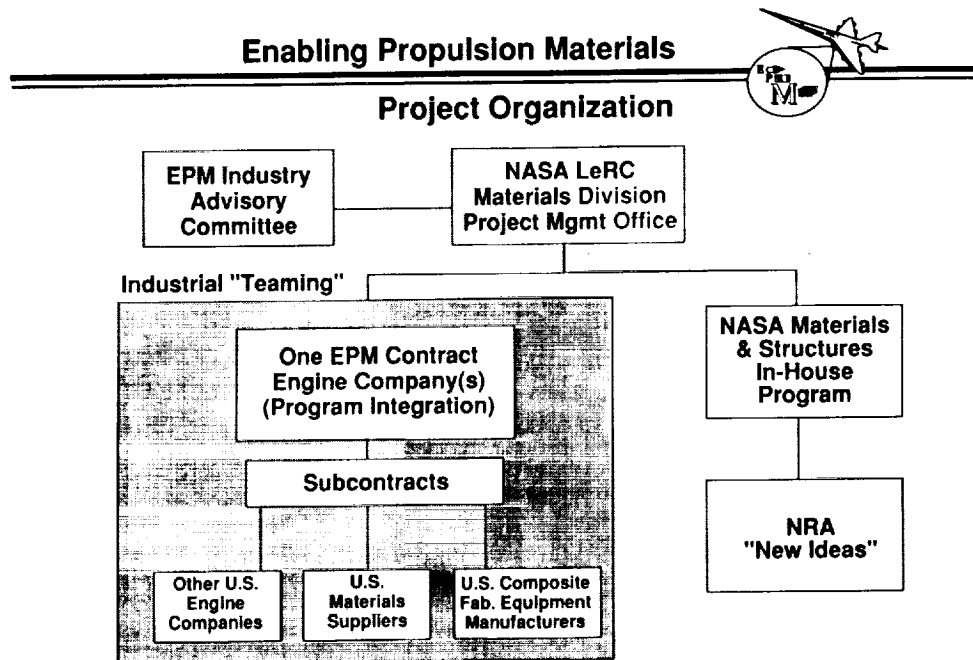
# EPM INDUSTRY TEAM APPROACH

Anticipated roles of the team members as well as NASA Lewis are delineated herein.

The engine companies will provide the program integration, materials/component design trade-offs, design methods and fabrication requirements of the components, and component/subcomponent testing in appropriate rigs and engines.

Materials suppliers will play a key role in the overall success of the EPM program. Fiber producers will be called on to develop advanced fibers and appropriate coatings. Matrix materials will have to be supplied that have the desired environmental resistance and are compatible with the fiber/coating combination. The program will look to these organizations to develop fabrication techniques that will enable the manufacture of the subcomponents and components.

Other organizations whose expertise may be required to successfully meet the demands of the program include those who can provide net shape fabrication, two-dimensional and three-dimensional weaving capabilities, and specialized processing and joining capabilities.

NASA Lewis Research Center will provide the overall project management, selected material characterization, some new material concepts, and life prediction and test methods where appropriate.

## Enabling Propulsion Materials
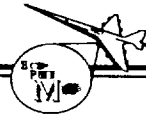
## EPM Industry Team Approach

Engine Companies
- Program Integration
- Materials/component design tradeoffs
- Design methods and fabrication
- Component tests

Materials suppliers
- Fibers and coatings
- Matrix Materials
- Process and composite fabrication

Other Companies
- Net shape fabrication
- 2D & 3D weaving
- Processing and joining

NASA Lewis
- Project management
- Material characterization
- New material concepts
- Life prediction and test methods

Figure 22.

# SUMMARY

It is has been established that advanced materials are key to the environmental acceptability of a 21st century HSCT. In particular, advanced materials are enabling for the combustor, primarily to control $NO_x$ emissions to acceptable levels and for the exhaust nozzle to significantly reduce the weight and thus have a direct impact on the economic viability of the aircraft.

Because of the long lead time required to develop advanced materials, EPM is planned to start 1 year ahead of the rest of the HSR Phase II program. Even with this head start, the 7-year research and development program is an extremely tight schedule considering the current state-of-the-art of high temperature composites, and the rigorous temperature/life requirements for success.

NASA has initiated some exploratory contractual and in-house efforts to help define the scope of the technology to be undertaken in the EPM program and is proceeding with the necessary procurement steps to be in a position to initiate the contractual program beginning in FY'92 assuming that budget approval is obtained.

**Enabling Propulsion Materials**

## Summary

- Advanced materials are key to a low-$NO_x$ combustor and a lightweight nozzle for the HSCT engine.

- An extremely tight schedule is required to meet technology readiness goals for 1999.

- NASA has initiated contract and in-house research to address critical materials needs and has issued a request for proposals for a 7-year Enabling Propulsion Materials contractual program to accomplish the required technology needs.

Figure 23.

# Session XI. Airframe and Engine Materials

*Smitt*

Combustor Materials Requirements and Status of Ceramic Matrix Composites
*Ralph J. Hecht, Pratt & Whitney Aircraft; and Andrew M. Johnson, GE Aircraft Engines*

THIS PAGE INTENTIONALLY BLANK

1548

# COMBUSTOR MATERIALS REQUIREMENTS AND STATUS OF CERAMIC MATRIX COMPOSITES

**R.J. Hecht**
Pratt & Whitney
West Palm Beach, Florida
and
**A. M. Johnson**
GE Aircraft Engines
Cincinnati, Ohio

# Lean And Rich Burn Combustor Designs Identified
## To Meet HSCT Goals

The HSCT combustor will be required to operate with either extremely rich or lean fuel/air ratios to reduce NOx emission, (Figure 1). NASA High Speed Research (HSR) sponsored programs at Pratt & Whitney (P&W) and GE Aircraft Engines (GEAE) have been studying rich and lean burn combustor design approaches which are capable of achieving the aggressive HSCT NOx emission goals. Both combustor design approaches under study, a lean premixed/prevaporized (LPP) and a rich burn/lean (RBL), will require the use of very high temperature (2400-3000F) materials to meet the HSCT emission goals of 3-8 gm/Kg. Currently available materials will not meet the projected requirements for the HSCT combustor. The development of new materials is an enabling technology for successful introduction to service of the HSCT (ref. 1).
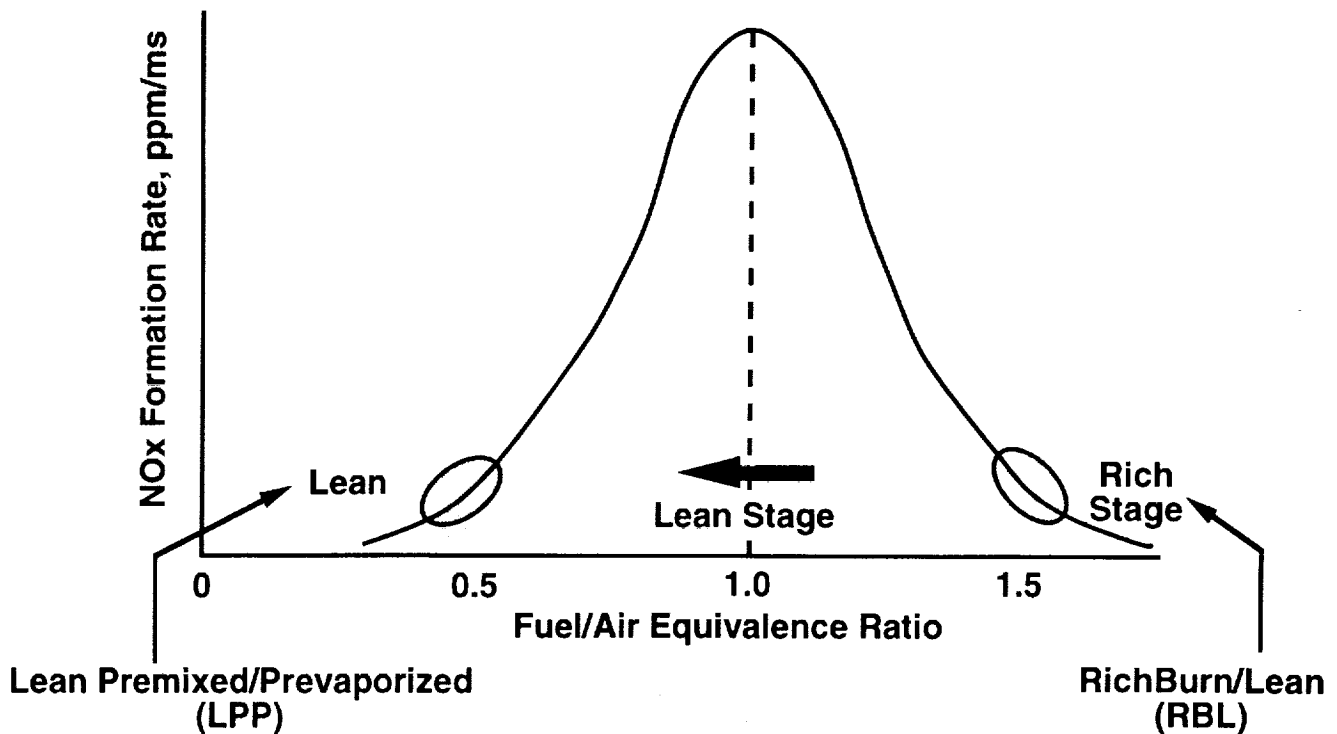


Figure 1

# Lean Premixed/Prevaporized(LPP) Combustor Requirements

The LPP combustor approach(Figure 2) prevaporizes the fuel and injects it into the air in a premixing passage to deliver a uniform droplet-free mixture to the combustion zone. The fuel/air ratio is set as low (lean) as possible, but above stability or inefficiency thresholds. The premixed prevaporized combustor is theoretically capable of producing very low NOx emissions. LPP combustor design approaches will require high temperature liner materials technology to reduce cooling air requirements. The ability of the liner to operate with small amounts of cooling air gives additional design flexibility in order to meet all of the combustor performance requirements. In addition, it is anticipated that the LPP approach may rely on a flame holder downstream of the premixing chamber to provide a stable flame front. Such a flameholder will require a very high temperature material. Ceramic matrix composites are the primary candidate materials for meeting the performance and durability requirements of the LPP combustor.
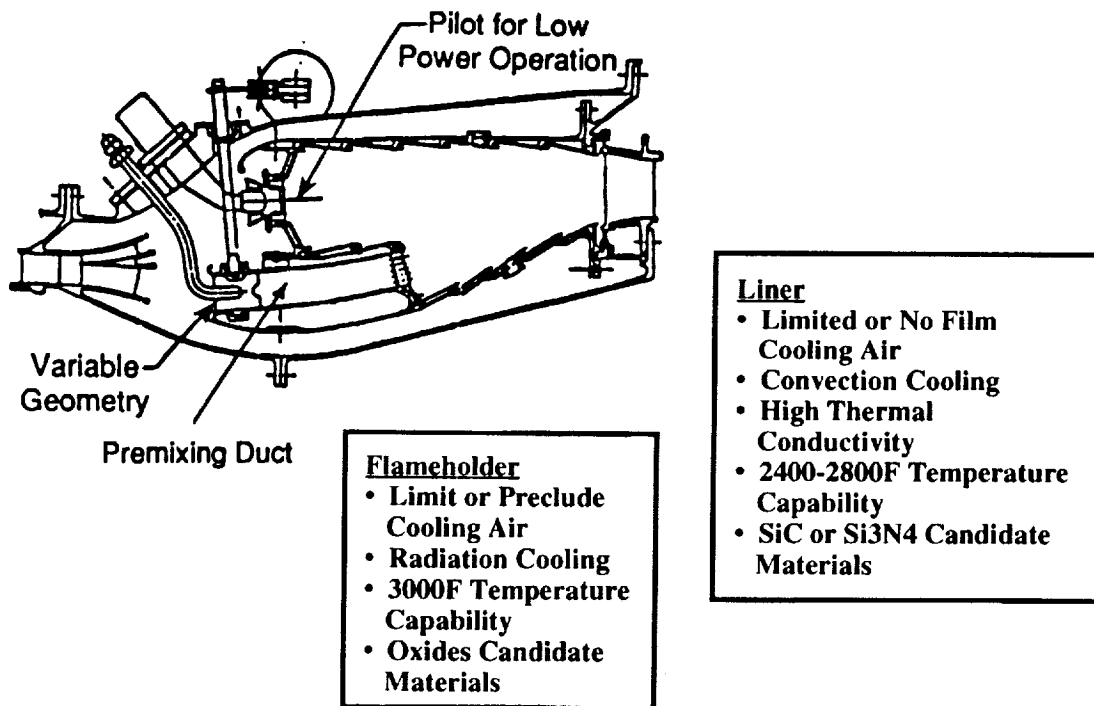


Figure 2

## Rich Burn/Lean (RBL) Combustor
## Requirements

The RBL combustor approach (Figure 3) reduces NOx by operating at higher fuel/air ratios than stoichiometric combustion. The rich primary zone inhibits the NOx formation process due to the the lack of available oxygen. However, large quantities of CO and smoke are formed that must be consumed in the remainder of the combustor. The rich zone fuel/air mixture must be uniform to minimize NOx formation. The required uniformity precludes the use of film cooling air in the rich zone. This leads to the need for a noneffusive cooling approach in which the liner may only be cooled externally by convection. This will impose very high temperature and heat flux conditions on the rich zone liner far in excess of current material operating temperature limits. The RBL combustor design will also require a high temperature quench and lean zone liner material to reduce cooling air requirements. Critical to the success of the RBL combustor design will be the development of high temperature liner materials. High conductivity SiC or $Si_3N_4$ base ceramic matrix composites are the primary candidate materials identified for meeting the temperature, performance and life goals of the RBL combustor.



| Rich Zone Liner | Quench and Lean |
|---|---|
| • No Film Cooling Air (Critical for low NOx) | Zone Liners<br>• Limited Or No Film Cooling Air |
| • Convection Cooling Required<br>• High Thermal Conductivity Required<br>• 2400 - 2800 F Temperature Capability<br>• SiC or $Si_3N_4$ Candidate Materials | |

Figure 3

# HSCT Engine Duty Cycle More Severe
## Than Subsonic Transport

In addition to temperature and NOx considerations of the HSCT combustor, the liner must be durable to provide long life. An HSCT goal has been established of 18,000 hours combustor liner life. This goal is a significant challenge due to the previously described material temperature requirements of an HSCT combustor liner. The life goal is especially challenging when considering the unique mission profile of the proposed HSCT aircraft relative to current subsonic commercial aircraft (ref. 2). The very high compressor discharge temperature (T3) and combustor exit temperature (T4) associated with supersonic cruise result in more than 80% of the HSCT mission time at maximum temperature conditions (Figure 4). This compares with less than 10% of the total mission time at maximum temperatures with current subsonic commercial aircraft. Operating at extremely high temperatures over most of the flight mission results in even greater need to develop high temperature materials for the HSCT.
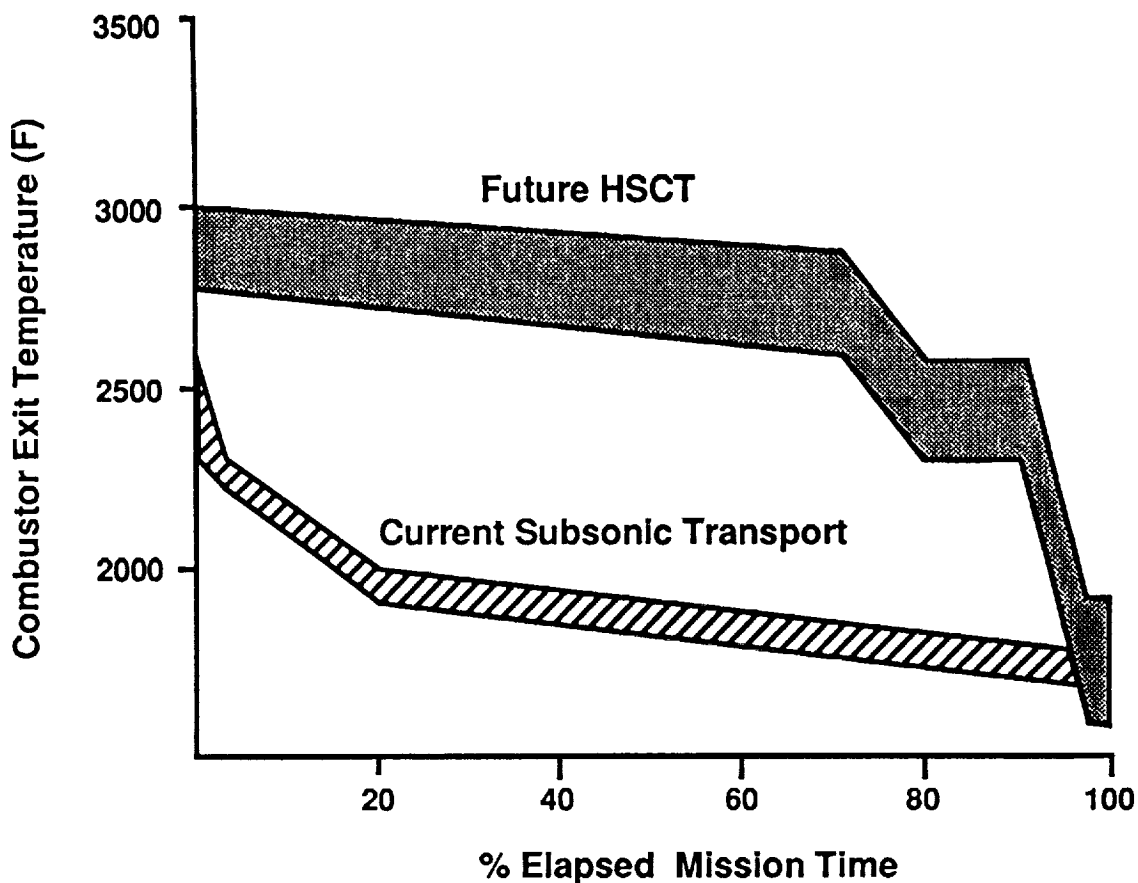


Figure 4

## Key Material Requirements For The
## HSCT Combustor

Consideration of the HSCT mission and combustor operating requirements has led to the identification of key material requirements related to the design issues of a low NOx combustor material. These requirements are shown in Figure 5. The ability of a ceramic matrix composite material to meet these requirements will determine its applicability for the HSCT combustor. Development of the required CMC materials will have to address the fundamental composite behavior, processing, and manufacturing to insure that a balance of material performance and cost is achieved. Material and processing development must be integrated, and concurrently conducted with combustor design to insure design/materials/manufacturing compatibility for timely development of a low NOx HSCT combustor.

- **High Operating Temperature**

- **High Thermal Stress Resistance**

- **Acoustic/Vibratory Durability**

- **Environmental Durability**

- **Damage Tolerance**

- **Shape Forming Capability**

- **Reasonable Cost**

Figure 5

# Thermal Conductivity of Candidate
## Ceramic Materials

The HSCT combustor design, performance and durability requirements drive the ceramic matrix material selection toward high thermal conductivity, thermo-oxidative stability, physical stability and low thermal expansion. Composite through-thickness conductivity is largely driven by the matrix conductivity thus dictating the choice of matrix material. The thermal conductivity of some candidate ceramic materials suitable for use as a CMC matrix above 2400°F are shown in Figure 6. The thermal conductivity of SiC and $Si_3N_4$, coupled with their low thermal expansion and high strength make them the primary candidate for the combustor composite matrix. $MoSi_2$ is also a candidate because of its high thermal conductivity and oxidation resistance.
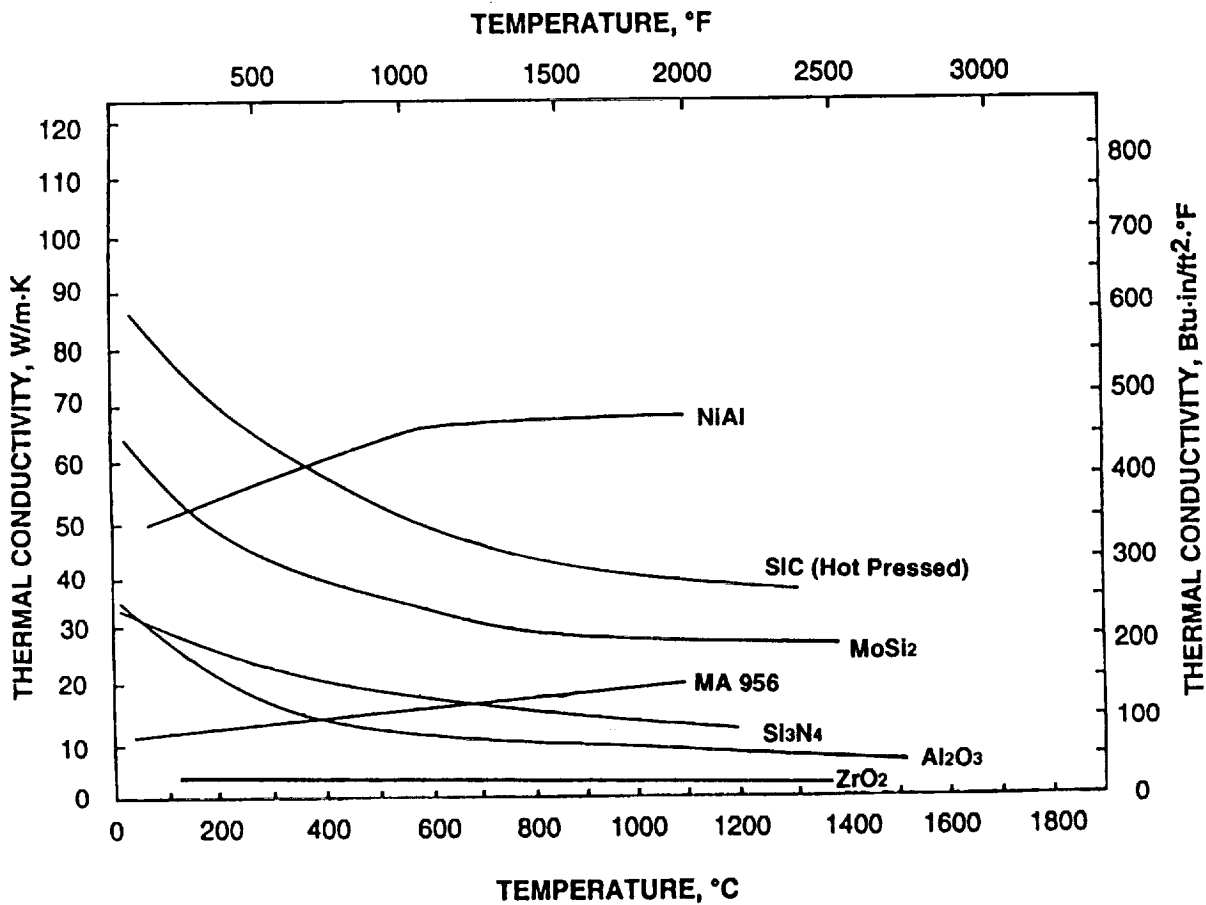


Figure 6

## Thermal Stress Resistance Of Candidate
## Composite Systems

Design requirements for the HSCT combustor mandate that candidate advanced materials withstand temperatures of 2200° to 3000°F, depending on the thermal conductivity, while providing acceptable environmental durability in both oxidizing and reducing environments. In addition, the material system must have good high cycle fatigue resistance to withstand significant acoustic and vibratory loads. The most critical aspect of material performance derived from the design requirements is resistance to thermal stress. A material parameter commonly used to rank materials for thermal stress resistance is the thermal stress parameter R'=$\sigma$k/E$\alpha$, where $\sigma$=allowable yield strength, k=thermal conductivity, $\alpha$=linear coefficient of thermal expansion, and E=Young's modulus. Various state-of-the art ceramic composite material systems are compared to a current combustor material (HS188) using this parameter in Figure 7. Both SCS-6 SiC fiber (Textron Specialty Materials) reinforced SiC and $Si_3N_4$ composites have high resistance to thermal stress.
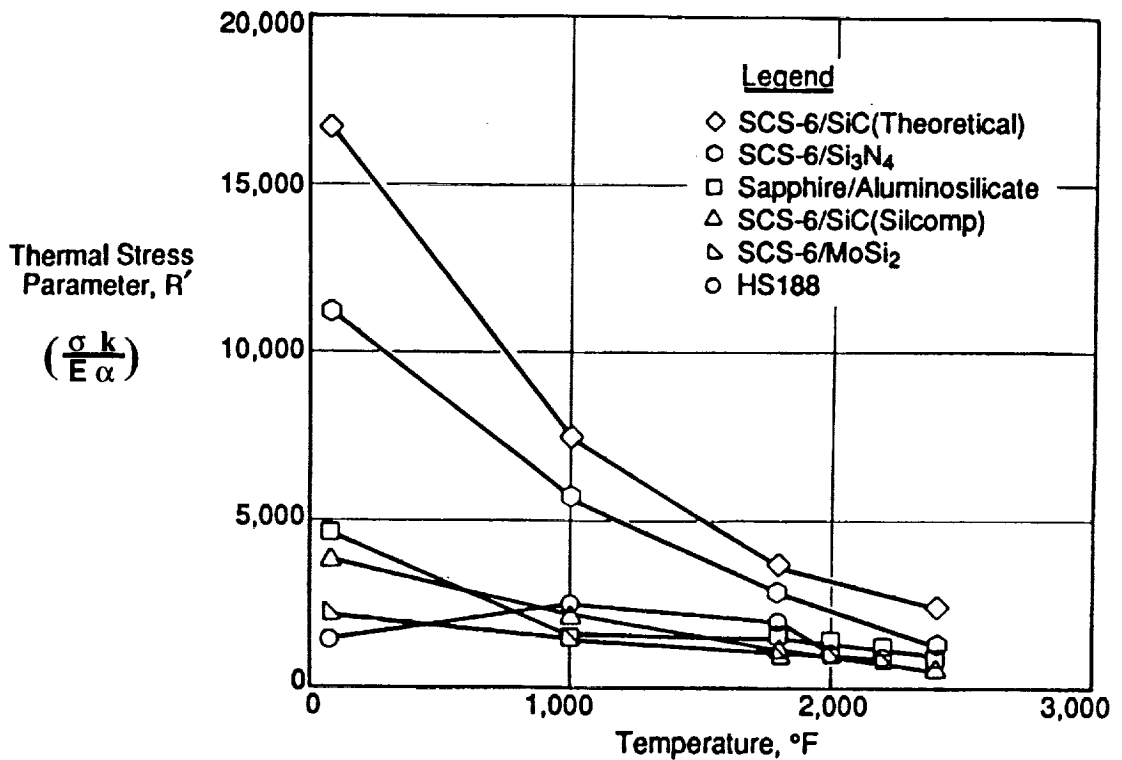


Figure 7

# Fiber And Fiber-Matrix Interface Key
## To CMC Toughness

CMC's potentially offer the high temperature performance of monolithic ceramics with improved toughness and reliability. The key to these improvements is the fiber reinforced and its ability to dissipate energy and exhibit tough behavior. For CMC's where the matrix modulus is high relative to the fiber reinforcement (Ef<Em), material toughness is dominated by the fiber/matrix interface and the characteristics it possesses. For this case, the fiber/matrix interface can deflect matrix cracks that develop at low strain levels, resulting in fiber debonding (Figure 8) (ref. 3). This debonding dissipates energy associated with matrix cracking and isolates the fiber from the cracked matrix thus preventing fiber fracture. To enhance its effectiveness, it is desirable that the fiber/matrix interface possess relatively low shear strength in order to promote debonding. The materials typically used for interface coatings, such as carbon and boronnitride, are susceptible to oxidative attack which reduces fiber/matrix interface performance, resulting in decreased toughness. The environmental stability of these interface materials becomes significant with regard to damage tolerance and long term durability.
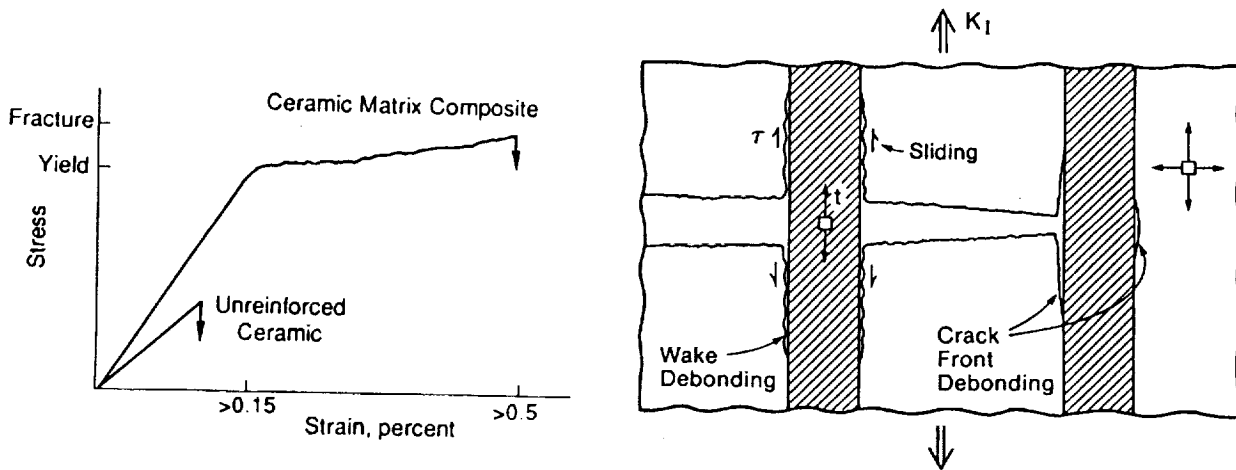


**Fiber Coatings Required To Achieve Needed Fracture Toughness**

Figure 8

C-6.

## Surface Treatements Identified
## For Increased CMC Capability

The CMC system selected for the HSCT combustor application must be environmentally stable for long times. Depending on the design, the gas environment in the combustor can be oxidizing or alternating between reducing and oxidizing. In oxidizing environments (lean burn), protection of the candidate CMC systems is provided by formation of a dense, protective oxide film on the surface. In reducing environments (rich burn), $SiO_2$ forming system as SiC, $Si_3N_4$ and $MoSi_2$ may undergo more accelerated (active) oxidation, leading to higher liner surface recession rates than in a lean burn environment. If a problem, chemical surface stability can be enhanced through surface treatment or coatings. Coatings can also be used to provide thermal insulation (i.e., thermal barrier) to increase liner temperature capability. Emissivity control coatings can be used to minimize the effects of radiation from the hot liner inner surfaces. Coatings can provide fiber-to-matrix thermo-chemical and environmental stability as well as enhance composite fracture toughness. Figure 9 shows the types of coating processes available for enhancing the capability and performance of HSCT composite liners.

| Function | Candidate Coating Type | Processing |
|---|---|---|
| Thermal Control (Thermal Barrier) | $ZrO_2(Y_2O_3)$ | Plasma Spray<br>Electron Beam Vapor Deposition |
| Thermal Control (Radiation) | Metallic | Plasma Spray |
| Environmental Control (Combustion Effects) | $Al_2O_3$<br>$Y_2O_3$ | Chemical Vapor Deposition<br>Sol-Gel<br>Physical Vapor Deposition |
| Fiber-Matrix Interface Control (Fracture Toughness) | Oxides<br>Nitrides<br>Carbides<br>Silicides | Chemical Vapor Deposition<br>Sol-Gel<br>Physical Vapor Deposition<br>Polymer Precursor |

Figure 9

## Fiber Tensile Strength

Fiber properties are critical to the CMC combustor liner design and performance . Initial design and material trade studies performed under NASA HSR Phase I have shown that a ceramic matrix composite combustor liner must be thin-walled and have high thermal conductivity at the operating temperature to reduce thermal gradients. This implies the need for a fine diameter fiber in the CMC structure that has high thermal conductivity. Because of the high conductivity and strength of SiC it is the primary candidate to reinforce SiC and Si3N4. The primary limitations of currently available SiC fibers are poor thermochemical stability and low tensile strength at temperatures above 2000°F (Figure 10) (ref. 4). Efforts being conducted under NASA HiTEMP on improving the stoichiometry of SiC fiber through process development indicate that these limitations can be overcome (ref. 5).
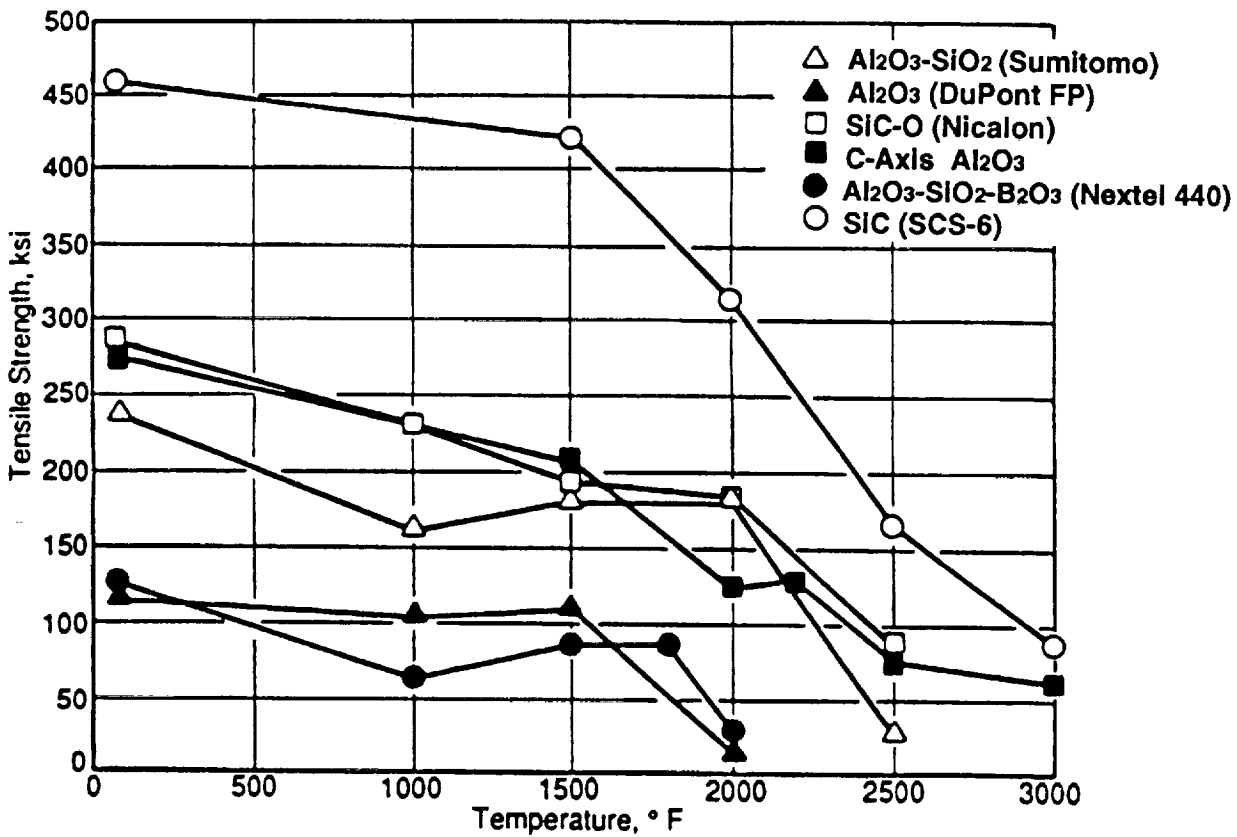


Figure 10

## Fiber Creep Resistance

Long time operation of the HSCT will require that the CMC liner materials be creep resistant. Matrix as well as fiber creep resistance must be addressed and maximized. The creep resistance of SCS-6 and Nicalon (Dow Corning Corporation) fibers are compared to single crystal $Al_2O_3$ fibers and sintered SiC in Figure 11 (ref. 6, 7, 8). Stoichiometic SiC fibers should exhibit creep resistance similar to high purity sintered SiC, which is superior to that of c-axis single crystal sapphire (ref. 9). Improvements in SiC fiber stoichiometry can increase creep resistance, temperature capability, and life of SiC and $Si_3N_4$ composites.
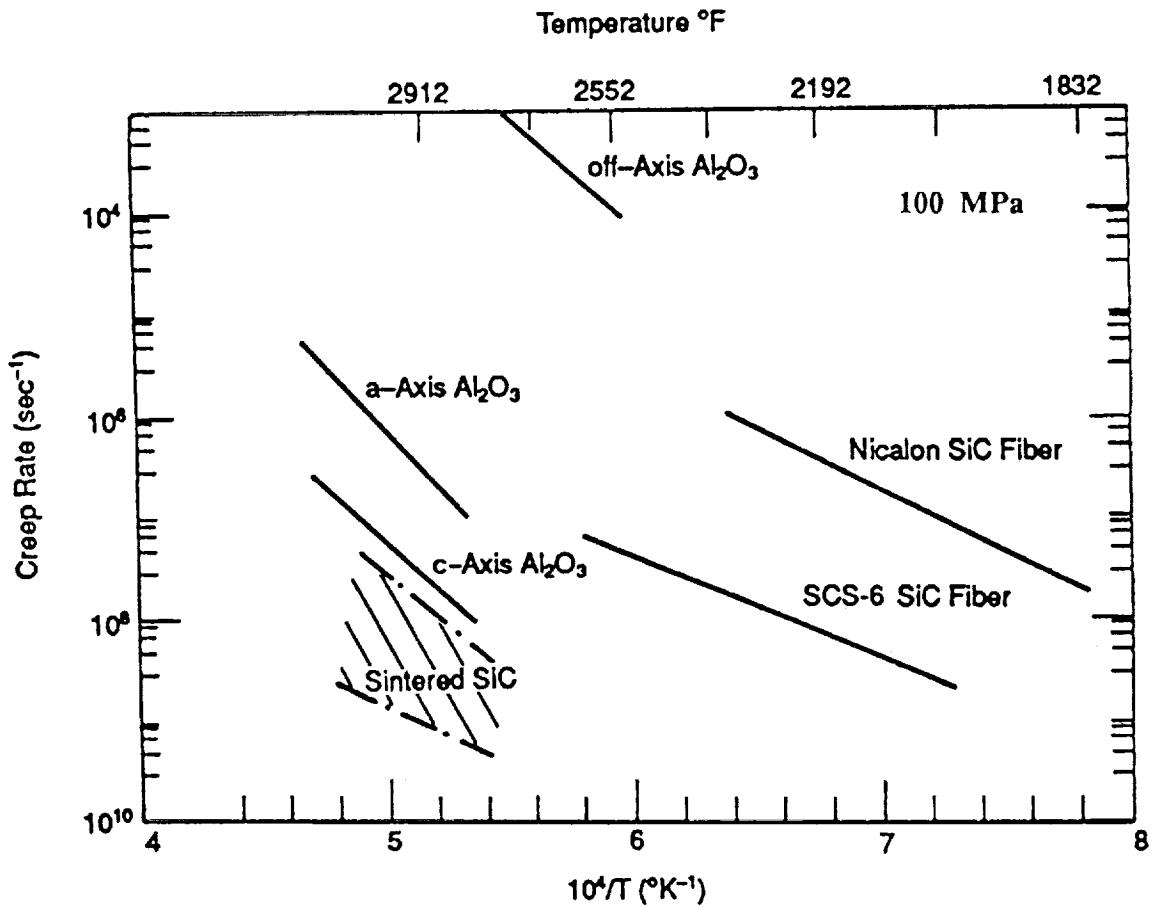


Figure 11

## Candidate Ceramic Matrix Composite
## Processing Methods

In recent years, a number of manufacturing methods have been developed for the fabrication of CMC composite systems. A summary of major CMC fabrication processes is detailed in Figure 12. The most mature CMC fabrication technologies are CVI (chemical vapor infiltration) and hot pressing. The CVI process , liquid infiltration/reaction, liquid metal oxidation/reaction and polymer pyrolysis processing methods have the capability to produce near net shape CMC components, and are the primary processing approaches for HSCT liner fabrication. Processing is an integral part of CMC development and must be addressed concurrently with the combustor material and design development. Processing routes may vary widely depending on the matrix, fiber architecture (2D vs 3D), fiber type (monofilament vs tow) and fiber coating.

| CMC Process | Matrix | Advantages |
|---|---|---|
| Chemical Vapor Infiltration (CVI) | SiC, Si₃N₄, MoSi₂ | Complex Shape Capability, Industrial Base Exists |
| Liquid Infiltration/Reaction | SiC/Si, MoSi₂ | Low Porosity, Complex Shape Capability |
| Hot Pressing/HIP | SiC, Si₃N₄, MoSi₂ | Low Porosity, High X-Ply Strength |
| Direct Oxidation/Reaction of Metals | Al₂O₃, Si₃N₄, AlN | Low Porosity, Shape Capability, Low Cost |
| Reaction Bonding/HIP | Si₃N₄, SiC | Dense Matrix, Reasonable Shape Capability |
| Polymer Precursor | Si₃N₄,SiC | ComplexShape Capability, Low Cost, Industrial Base |

Figure 12

## Summary

The development of improved CMC materials will be critical for meeting the performance and durability goals of the HSCT combustor. High conductivity, high strength SiC and Si3N4 composite systems have the potential to meet current projected combustor requirements. Enhancement of SiC fiber capability is needed to increase high temperature strength retention and composite creep resistance. Fiber matrix interface control through the use of a debond coating will be required to achieve the required composite fracture toughness. If the rich burn/lean (RBL) combustor design approach is selected for the HSCT combustor, then the environmental issues of SiO2-forming, SiC and Si3N4 composite systems must be addressed. The temperature capability of these CMC systems can be increased by the use of protective and insulative coatings. Processing development will be pivotal in meeting the goals and requirements of the combustor, and must be concurrently addressed and integrated with material and component design.

- ### Ceramic Matrix Composites Have Required High Temperature Capability

- ### High Thermal Conductivity SiC and Si3N4 Composite Systems Are Primary Candidates

- ### SiC Fiber Enhancements Needed To Provide Long Term, High Temperature Durability

- ### Fiber Coatings Will Be Required To Achieve Needed Fracture Toughness

- ### Rich Burn Combustion Environment May Limit SiO2-Forming CMC System Capability

- ### CMC Processing Selection Will Be Driven By Material And Component Design

- ### Component Design/Material/Processing Development Must Be Integrated To Meet HSCT Schedules

Figure 13

# REFERENCES

1. Stephens, J. R.,"Composites Boost 21st -Century Aircraft," Advanced Materials & Processes, April 1990.

2. Allen, G.E., Champagne, G. A., Klein, H. L., and Schulmeister, L. F., "NASA CR-185246: Benefit of Advanced Materials in Future High Speed Civil Transport Propulsion Systems," July 1990.

3. Evans, A. G., Marshall, D. B., "The Mechanical Behavior of Composites," Acta Metall. Vol. 37, No. 10, pp. 2567-2583, 1989.

4. Hong, W. S., Rigdon, M. A., and Fortenberry, N. L., "Reinforcement Options for High Temperature Composites and a Comparison of High Temperature Tensile Testing Results for Ceramic Fibers," IDA Paper P-2483, 1990.

5. Lipowitz, J., Rabe, J. A., and Zank, G. A., "Crystalline Silicon Carbide Fibers Derived From Organosilicon Polymers," Proceedings of the 3rd Annual HiTEMP Review, NASA Conference Publication 10051, 1990.

6. Corman, G.S., "Creep of Oxide Single Crystals," Report No. WRDC-TR-90-4059, Materials Laboratory, Wright Research and Development .Center, Air Force Systems Command, Wright-Patterson Air Force Base, Ohio 45933.

7. DiCarlo, J. A.,"Creep of Chemically Vapor Deposited SiC Fibers," J. Mater. Sci., 21, 217-224, 1986.

8. Simon, G., and Bunsel, A. R., "Creep Behavior and Structural Characterization at High Temperatures of Nicalon SiC Fibers," J. Mater. Sci. 19, 3658-3670, 1984.

9. Frechette, F. J., Dover, B., Venkateawaran, V., and Kim, J., "High Temperature Continuous Sintered SiC Fiber For Composite Applications," Proceedings 15th Annual Conference On Composites And Advanced Ceramics, January 13 - 16, 1991, Cocoa Beach, Florida.

## Acknowledgements

1564

# Session XI. Airframe and Engine Materials

*Smit*

Nozzle Material Requirements and the Status of Intermetallic Matrix Composites
*Andrew M. Johnson, GE Aircraft Engines; and Ralph J. Hecht, Pratt & Whitney Aircraft*

THIS PAGE INTENTIONALLY BLANK

# NOZZLE MATERIAL REQUIREMENTS AND
# THE STATUS OF INTERMETALLIC MATRIX COMPOSITES

526-24
12056

A.M. Johnson
GE Aircraft Engines
Cincinnati, Ohio
and
R.J. Hecht
Pratt & Whitney
West Palm Beach, Florida

First Annual High Speed Research Work Shop
May 14 - 16, 1991

1567

The HSCT exhaust nozzle must manage high temperature exhaust gases and pressure gradients while meeting HSCT economic and noise goals. The important features and requirements for an HSCT exhaust nozzle are shown in Figure 1 for a 2DCD(two-dimensional convergent-divergent) design. The same requirements would apply to an axi-symmetric design. Exhaust nozzle weight has an adverse effect on the overall aircraft range, payload and engine specific fuel consumption, and is therefore the primary driver for advanced exhaust nozzle materials. Because of the large airflow and pressure gradients, exhaust nozzles are extremely large and heavy when made from current materials. The use of advanced materials with higher specific strength will reduce the weight of exhaust nozzle components. In addition to the flow of high-temperature exhaust gases into the exhaust nozzle, ambient air is entrained to reduce gas exit velocities and suppress sound. This leads to components exposed to extremely high temperature gradients and, hence, high thermal stresses. Further, exhaust gases are highly oxidizing; material environmental resistance will be an important factor for long life. Several viable concepts have been identified to reduce noise through the mixture of exhaust and ambient air. Sound can be further suppressed by acoustic panels that absorb high-frequency noise (Ref. 1).

# HSCT Exhaust Nozzle Requirements



Ambient Air

Noise Suppression
Meet FAR 36
Stage III
Requirements

Thin Sheet and
Stiffening Ribs (IMC/MMC)

Exhaust
Gas

Weight
30% Reduction

Internal Performance
-1.0% $C_{fg}$ = -50%
Passenger Payload

Component Life
18,000 Hour Life
Requirement

2400°F Liner
Capability (CMC)

Porous Acoustic Materials (CMC)
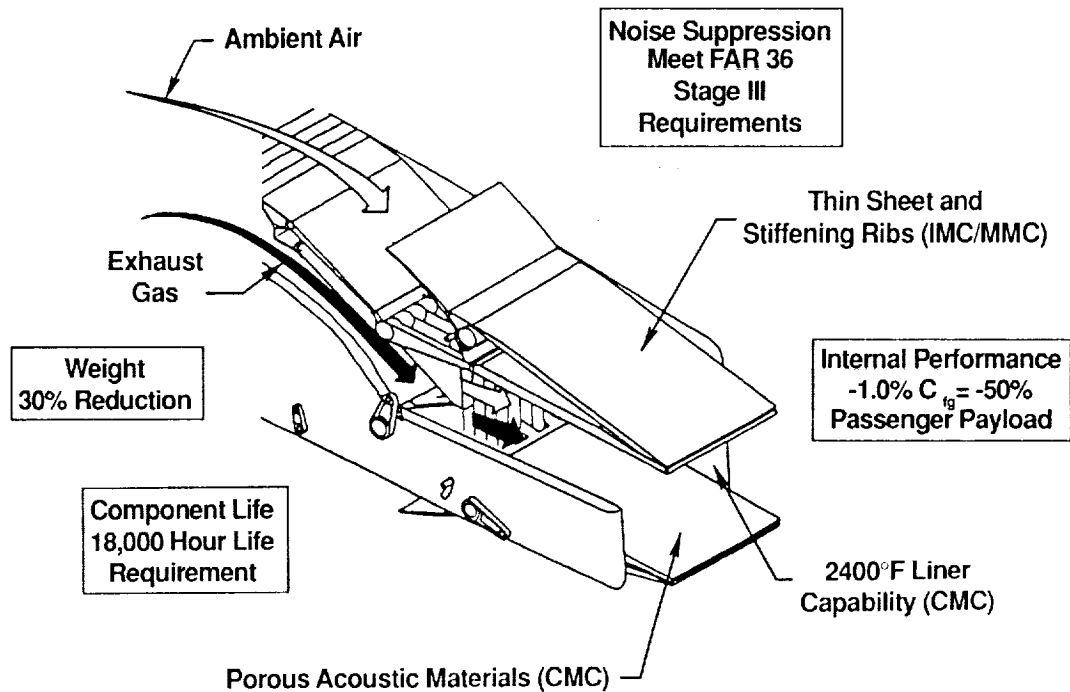
The HSCT exhaust nozzle operating requirements lead to the need for materials with the characteristics shown in Figure 2. Since currently available structural materials are being utilized to their maximum capability, advanced materials with significantly enhanced properties will be needed to meet nozzle goals. The most promising class of materials are continuous fiber reinforced composites. The matrix can be a metal, intermetallic compound or ceramic. The reinforcing fibers are generally high strength ceramics although refractory metals may also be utilized. Accordingly, these materials are generally referred to as either MMC's (metal matrix composites), IMC's (intermetallic matrix composites) or CMC's (ceramic matrix composites). Designing, developing and scaling-up composite materials with a good balance of high temperature properties (especially specific strength) and sufficient shape making capability to be made into large, complex structures is a substantial challenge.

# Key Material Requirements for the HSCT Exhaust Nozzle

- ## High specific strength
- ## Thermal stability
- ## Environmental resistance
- ## Thermal/mechanical/acoustic fatigue resistance
- ## Thermal shock/stress capability
- ## Damage tolerance
- ## Good fabricability
- ## Affordable cost

Preliminary design studies have shown that substantial weight savings can be identified for HSCT exhaust nozzle components utilizing high strength advanced materials. Figure 3 shows the nominal range of desired improvement in specific strength vs. temperature for various nozzle components. The line marked "current materials" generally represents the upper limits of specific strength vs. temperature relationships for titanium, nickel, iron and cobalt based alloys. The upper boundary of the component envelopes shown coincides with estimates of the potential capabilities of MMC, IMC and CMC materials under consideration. This figure indicates that a wide range of component operating conditions are anticipated for which advanced structural materials are needed.

# HSCT Exhaust Nozzle Component/ Material Goals

The primary candidate materials under consideration by (GEAE) GE Aircraft Engines and (P&W) Pratt & Whitney for the HSCT exhaust nozzle are shown in Figure 4. IMC's based on $MoSi_2$ (molybdenum disilicide) and NiAl (nickel aluminide) and CMC's based on $Al_2O_3$ have the highest temperature capability due to relatively good inherent oxidation resistance. However, the systems have low ductility and may be difficult to fabricate. MMC's utilizing MCrAlY's (where M can be Fe, Ni, Co or a combination thereof) are much more ductile but are limited to lower temperatures due to strength. The fiber of choice for both IMC's and MMC's is a single crystal aluminum oxide ($Al_2O_3$) due to its high strength, temperature resistance chemical stability and compatible thermal coefficient of expansion. Oxide/oxide CMC's have potential as sound absorbers when fabricated in a low density form. IMC's and CMC's use reinforcements for both strengthening and toughening. MMC's use reinforcements primarily to improve strength.

# Primary HSCT Exhaust Nozzle Material Candidates

| Type | Matrix | Reinforcement |
|------|--------|---------------|
| IMC | $MoSi_2$ NiAl | $Al_2O_3$ |
| MMC | M Cr Al Y Superalloys | $Al_2O_3$ |
| CMC | $Al_2O_3$ | $Al_2O_3$ |

Matrix materials are considered to dominate composite temperature capability, and therefore matrix materials are generally first selected based on environmental resistance and strength at temperature. Potential matrix materials that offer both high strength and oxidation resistance are included in Figure 5, which shows the wide range of tensile strength characteristics exhibited. In this case, the NiAl is in a single crystal form grown in the <110> crystallographic direction (Ref. 2). Note the potent effect of alloying with small amounts of Cr and Hf on NiAl strength. The ODS (oxide dispersion strengthened) FeCrAlY was directionally recrystallized and the $MoSi_2$ (Ref. 3) was in a polycrystalline form. Environmental and thermal barrier coatings may increase a material's ultimate temperature capability and are frequently developed with the base material as a system.

# Ultimate Tensile Strength of Candidate Matrix Materials

In addition to matrix alloying, processing can have significant effects on matrix material strength and ductility. Figure 6 shows the effects of several variations of alloying, processing and reinforcements on MoSi₂ composite creep strength (Ref. 4). The 40% SiC (silicon carbide) was added as a small particulate to MoSi₂ powder prior to hot pressing. Similarly, fine SiC whiskers were added to MoSi₂ powder prior to HIP (hot isostatic pressing). The MoSi₂ - containing high aspect ratio and high strength SiC whiskers consolidated by HIP shows the lowest creep behavior of the materials shown. MAR-M-509 is a conventional, monolithic superalloy with high cobalt content.

# Composition and Processing Effects on MoSi₂ Creep Resistance
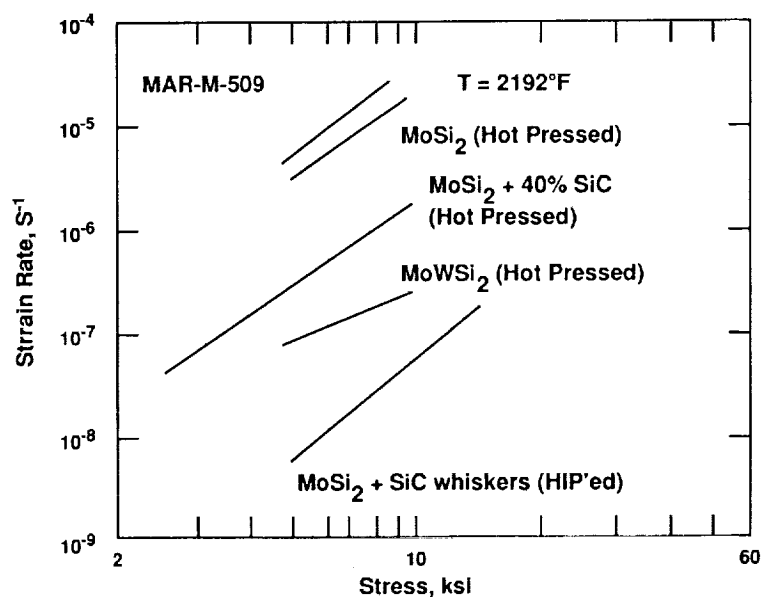
# THERMAL EXPANSION OF SEVERAL CANDIDATE MATERIALS

Figure 7 shows the CTE (coefficient of thermal expansion) for several candiate matrix and reinforcing materials. The close match of $MoSi_2$ and $Al_2O_3$ makes this combination of matrix and reinforcement particularly interesting from the standpoint of potential thermal fatigure resistance. Note also that the CTE of the $MoSi_2$ + 40% SiC is substantially lower than that of $MoSi_2$ alone, as would be expected from the position of the SiC in the figure. In general, the CTE mismatch of a composite system is determined by the matrix and reinforcement composition and interface coatings.

# Thermal Expansion of Several Candidate Materials

Figure 8 shows the wide range in tensile strength behavior exhibited by four different reinforcing fibers (Ref.'s 5,6,7,8). The high temperature strength advantage obtainable through processing is demonstrated by comparison of the $Al_2O_3$ single crystal monofilament and $Al_2O_3$ polycrystalline tow data. However, single crystal processing generally involves slower processing and therefore higher costs.

# Tensile Strength of Reinforcing Fibers

The specific strengths of several candidate composite systems were calculated using a rule-of-mixture approach as shown in Figure 9 (Ref. 9). In this case, the composite specific strength is assumed to be equal to the sum of the weighted strengths of the constituents. This approach is useful for estimating design trade-offs for the different composite systems. The area marked "material development zone" is bounded on the lower side by current material capabilities and on the upper side by the maximum assumed properties for this study. It is apparent that no single material system is likely to have superior properties in comparison to others over the entire strength/temperature range.

# Specific Strength of Several Candidate IMC and MMC Systems

The characteristics of the interface between the fiber and matrix of any composite system have a profound effect on the properties of the composite. Toughness is particularly affected, as well as thermal fatigue resistance and long term thermal stability. For these reasons coatings are generally applied to the fiber prior to composite fabrication. The method chosen to deposit the coating as well as coating composition and thickness must be based on the fiber and matrix behavior and the results desired. Interface control is essential to composite design and is therefore receiving a substantial amount of attention worldwide. Both analytical and experimental approaches are actively being pursued.

# Fiber/Matrix Interface Coatings Key to Toughness

- **Improve inherent fiber properties**

- **Create chemically stable interface**

- **Reduce fiber/matrix thermal expansion mismatch**

- **Control fiber/matrix bonding**

# CANDIDATE PROCESSING APPROACHES FOR EXHAUST NOZZLE COMPONENT FABRICATION

Figure 11 shows a partial listing of candidate processes under consideration for development of HSCT exhaust nozzle structures. The number of possible combinations of matrix, fiber and interface compositions and associated processes is large. It would be impractical to attempt to investigate every possible combination in detail. Therefore the best possible use must be made of previous experience, analytical modeling, statistically designed experiments and careful analysis of the data. Factors to be evaluated for process selection for development and scale-up include a)inherent variability, b)ability to be analyzed, monitored and controlled, and c)economic factors such as basic cost and capital equipment requirements.

# Candidate Processing Approaches for Exhaust Nozzle Component Fabrication

| | |
|---|---|
| **Matrix** | • Powder metallurgy (PM)<br>• Rolling<br>• Casting |
| **Fiber** | • Edge defined film fed growth (EDFG)<br>• Sol-Gel |
| **Fiber Coating** | • Sol-Gel<br>• Chemical vapor deposition (CVD) |
| **Composite Fabrication** | • Tape lay-up<br>• Plasma spray<br>• Hot isostatic pressing (HIP)<br>• Casting |
| **Joining** | • Brazing<br>• Mechanical fastening |
| **Durability/Thermal Barrier Coating** | • Plasma spray<br>• Physical vapor deposition |

As composite systems are identified for feasibility evaluation, a rigorous approach is required to assure that all important aspects of the component design, manufacture and service are considered (Ref. 10). Due to the inherent anisotropic properties of continuous fiber reinforced composites they must be tailored for the specific application to which they will be applied. Consequently, processing, mechanical property evaluation and component testing must be done on a component by component basis.

# Composite Characterization, Analysis, Design and Life Methods Considerations

- ## Mechanical testing methods

- ## Brittle vs ductile composite behavior

- ## Integrated models
  - Heat transfer
  - Constitutive behavior
  - Damage accumulation

- ## Fabrication/Service effects
  - Time dependent
  - Environmental
  - Residual stresses

SUMMARY

Advanced materials including MMC's, IMC's and CMC's have considerable potential for reducing the weight, increasing the performance and reducing the noise of the HSCT exhaust nozzle. However, substantial challenges must be overcome before such materials can be utilized as structural materials in high performance aircraft engines.

# Summary

- HSCT exhaust nozzle material requirements are complex and challenging

- Application of advanced composite materials could significantly reduce nozzle weight

- Several candidate materials and processes have been identified

- Successful and timely development of composite components will require integration of materials, design and manufacturing efforts

# REFERENCES

1. Stine, F.R.: Personal Communication, GEAE.

2. Darolia, R.: NiAl Alloys for High Temperature Structural Applications. JOM, March 1991.

3. Maloney, M.: Development of Refractory Metal Fiber Reinforced MoSi2 - Proceedings; 15th Annual Conference on Advanced Ceramics and Composites.

4. Bose, S. and Maloney, M.J.: Unpublished Research, P&W and DARPA Contract No. N00014-87-C-0862..

5. Hong, W.S.; Rigdon, M.A.; Fortenberry, N.L.: Reinforcement Options for High Temperature Tensile Testing Results for Ceramic Fibers, IDA Paper P-2483, DARPA, Dec. 1990.

6. Petrasek, D.W.: NASA Tech NICAL Publication TND-6881.

7. Schoenberg, T. and Kumnick, A.: NASA HiTemp, June 1989, Page 1-1.

8. Hurst, J.B.: NASA LeRC, NASA Lewis, July 1990.

9. Amato, R.A.: Personal Communication, GEAE.

10. Johnson, A.M.; Wright, P.K.: Application of Advanced Materials to Aircraft Gas Turbine Engines, AIAA 90-2281, July 1990.

## ACKNOWLEDGEMENTS

# Session XI.  Airframe and Engine Materials

Airframe Materials for HSR
*Thomas T. Bales, NASA Langley Research Center*

THIS PAGE INTENTIONALLY BLANK

# AIRFRAME MATERIALS FOR HSR

Thomas T. Bales
Materials Division
NASA Langley Research Center

High-Speed Research Workshop
Williamsburg, Virginia
May 14-16, 1991

# Airframe Materials for HSR

## Element Description

## REQUIREMENT:

Advanced airframe materials and structures for achieving critical weight, durability and performance requirements for HSCT.

## TECHNOLOGY NEED:

A.  Structural weight $\leq$4.5 pounds per sq. ft. of wetted area

B.  Materials with 60,000 hour life at elevated temperature
    - up to 400°F at M=2.5

C.  Accelerated aging test methodology to predict long term performance of advanced materials

# Airframe Materials for HSR

The Challenge
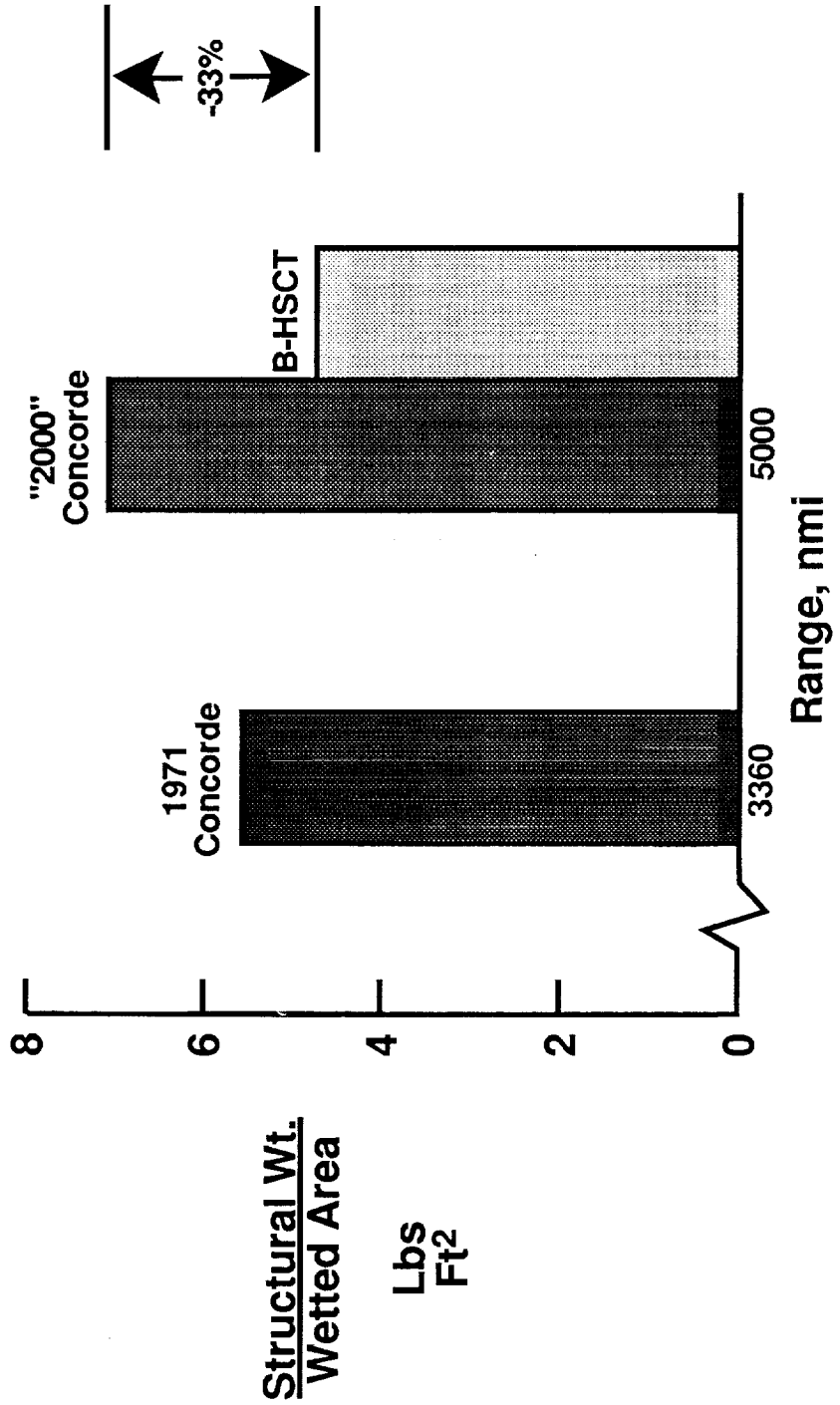
# HSR AIRFRAME MATERIALS TECHNOLOGY

## Key Issue

No long-term, high-temperature
materials data base for HSCT airframes
(60,000-hr design life, 120,000-hr fatigue life)

## Key technology needs

- Life prediction methodology
  - Accelerated test procedures
  - Long-term flight
    simulation durability

- Demonstrated 300°- 500° F
  polymer matrices, adhesives and
  sealants for ≥ 60,000-hr lifetimes

- Demonstrated 300°- 600° F
  lightweight metals and
  metal matrix composites
  for ≥ 60,000-hr lifetimes



Service
life
1000, hrs

Al alloys
transport
A/C

(Composites
projected)

Composites
military
A/C

Goals for HSR

(High temp PMC
adv Al alloys
Ti alloys)

M 3.2

M 2.8

M 2.4

SR-71
Ti alloys

0    200    400    600

Temperature

1588
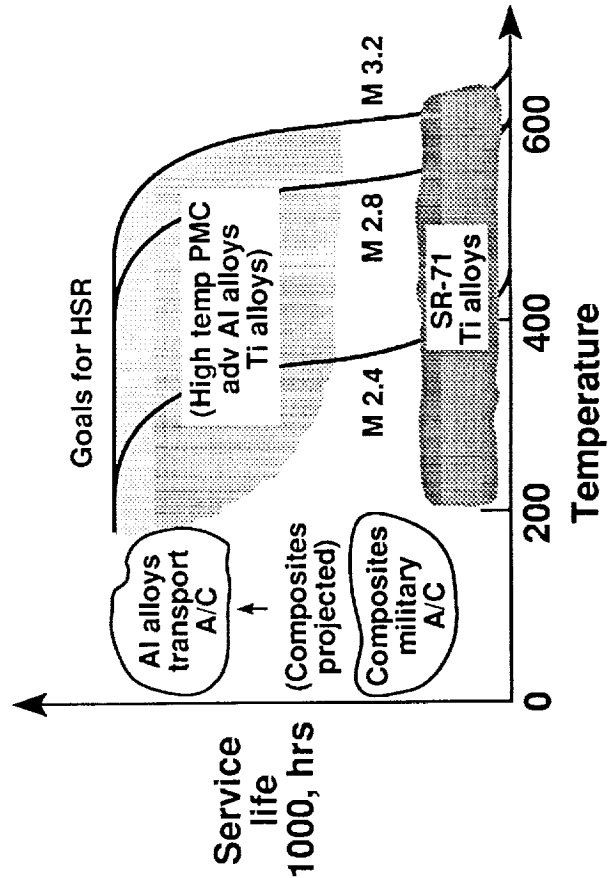
SKIN TEMPERATURES FOR M 2.4 TRANSPORT
Painted surface

Lower
Upper

295-305°F
305-315°F
315-345°F
345-370°F

Cruise conditions
40 to 70,000 ft altitude
U.S. std. day

1589
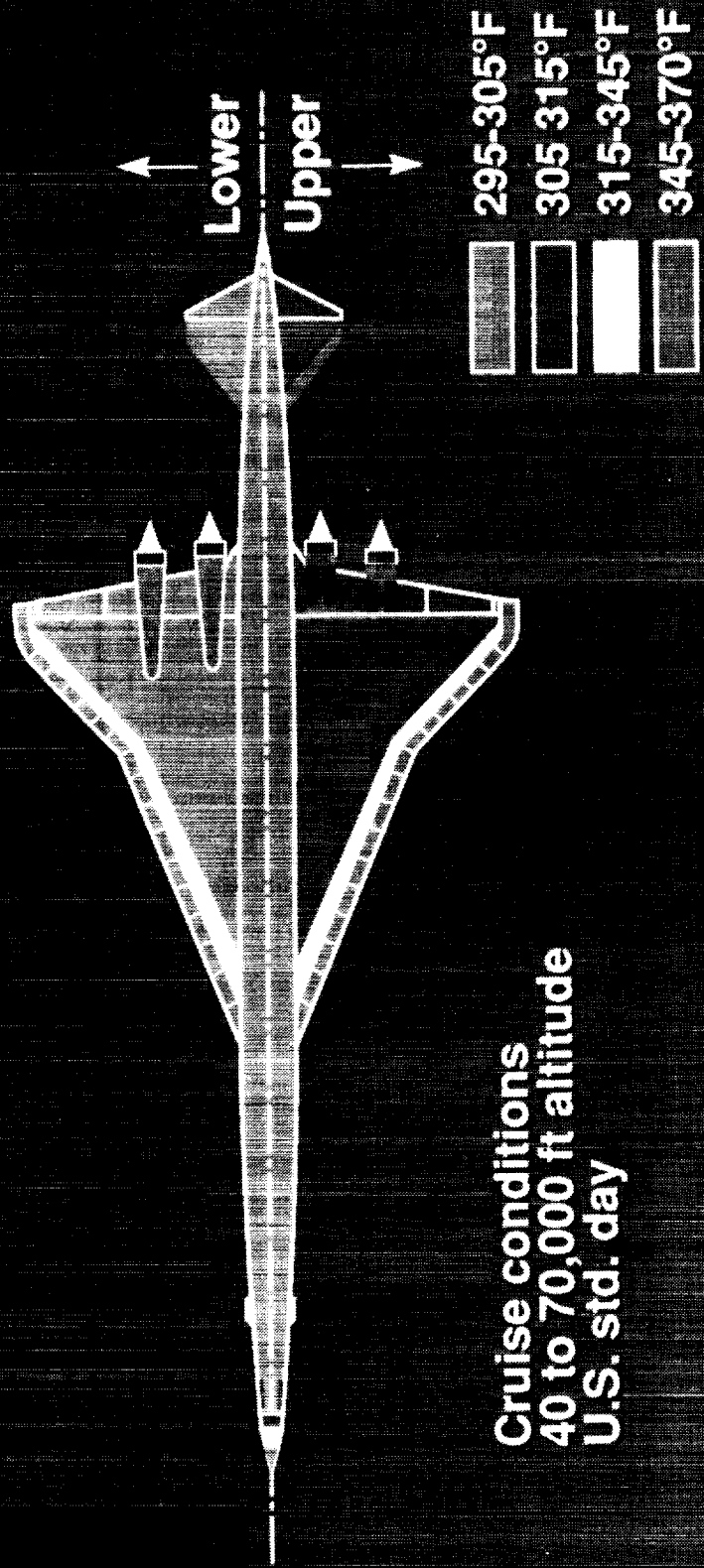
# SKIN TEMPERATURES FOR M 2.0 TRANSPORT

## Bare surface



Cruise conditions
40 to 70,000 ft altitude
U.S. std. day

Lower ← | → Upper

☐ 205-210°F
▨ 210-215°F
■ 215-230°F

1590
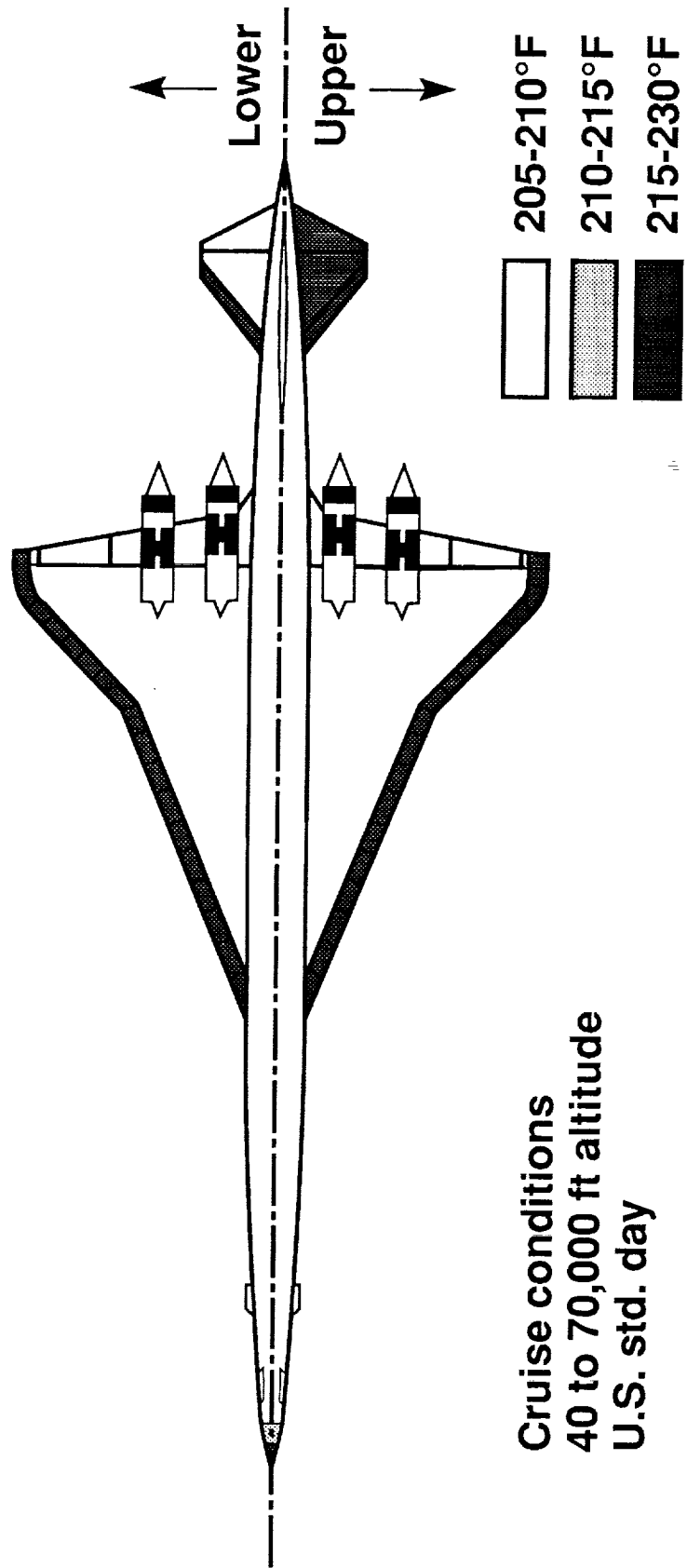
# FAILURE MODE WEIGHT DISTRIBUTION FOR HSCT (DOUGLAS)

**Buckling**
$E/\rho$ $(\sigma/\rho)$

**Crippling**
$E/\rho$ & $\sigma/\rho$

**Stiffness**
$E/\rho$ $(\sigma/\rho)$

**Strength**
$\sigma/\rho$

**Others**
$\rho$



42%

7%

8%

11%

32%
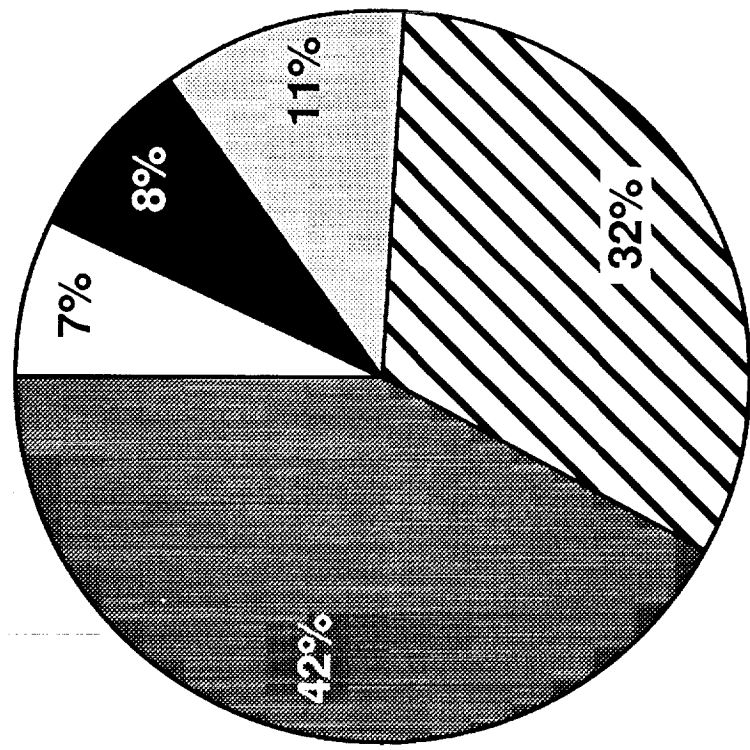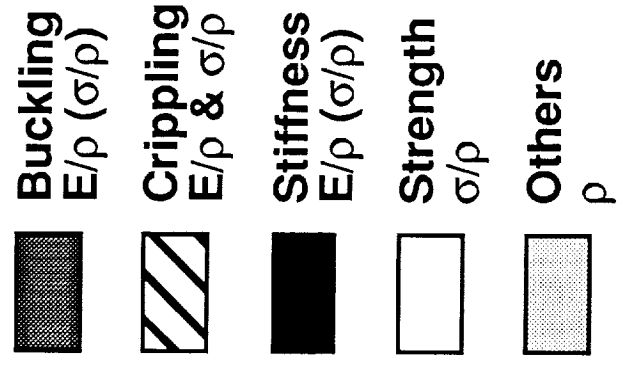
**Primary Structure Weight Breakdown**

1591

SPECIFIC TENSILE PROPERTIES AS A FUNCTION OF TEST TEMPERATURE

▲ Celion 3000/PMR-15*
■ Weldalite 049
◆ Al 2618
▲ Al-12Fe-1V-2Si
● Ti-6-4

* 0°/±45°/90° layup
  51% fiber volume

Modulus, 10⁶ in.

M2.4 range

Temperature, °F

1592
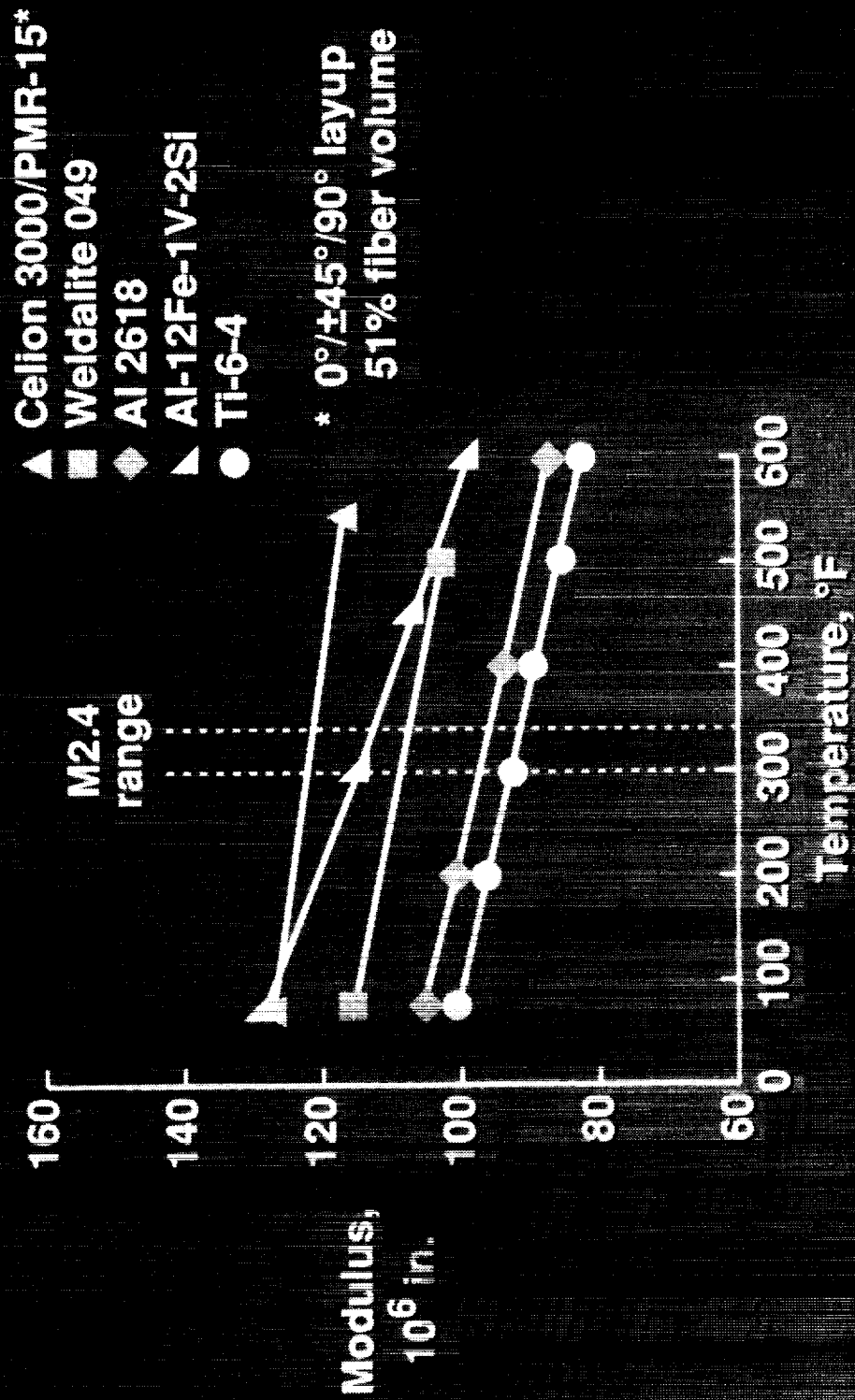
SPECIFIC TENSILE PROPERTIES AS A FUNCTION OF TEST TEMPERATURE

100 hours exposure at test temperature

▲ Celion 3000/PMR-15*
■ Weldalite 049
◆ Al 2618
▲ Al-12Fe-1V-2Si
● Ti-6-4

*  0°/±45°/90° layup
   51% fiber volume
   ε = .006

1593
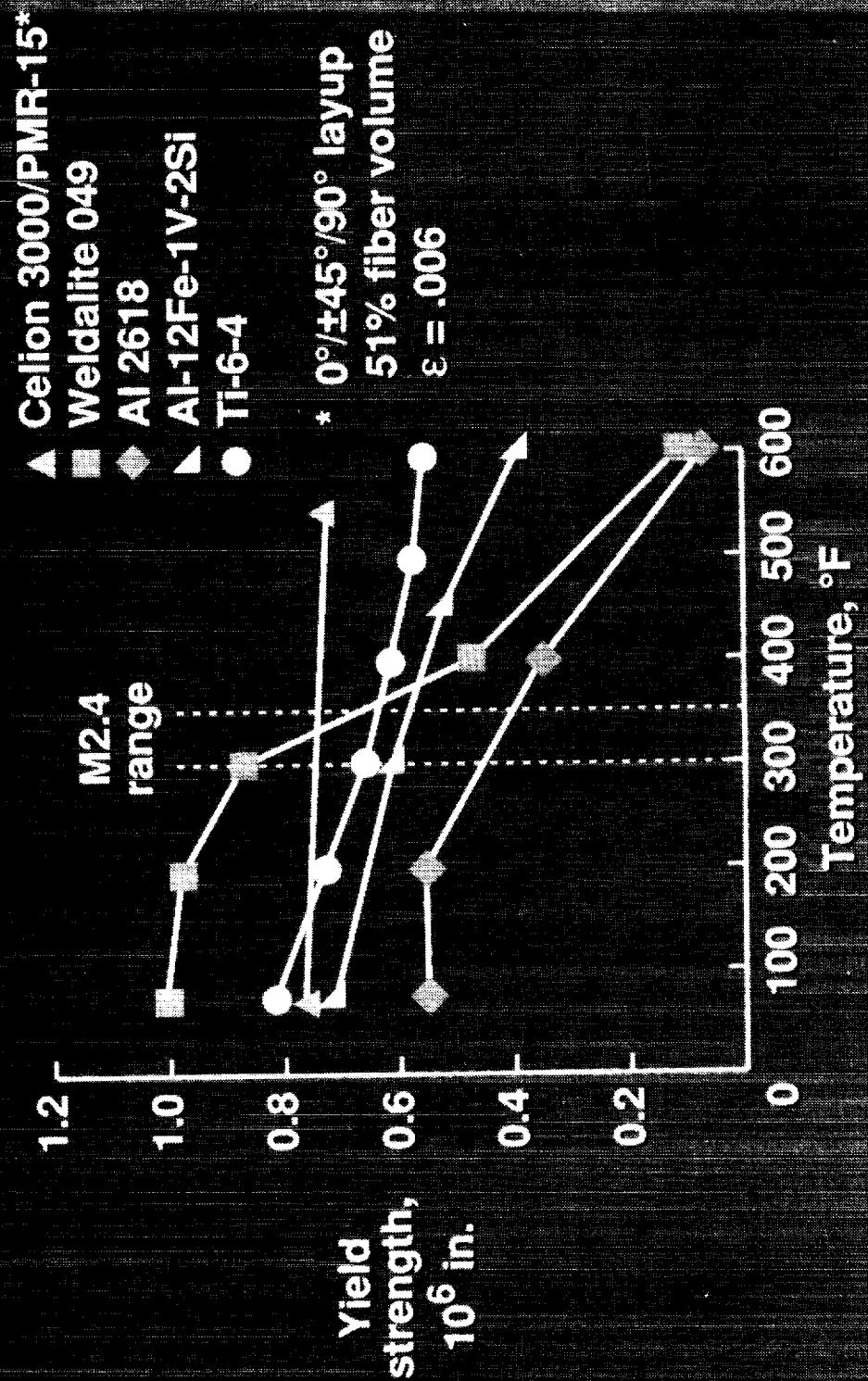
# Candidate Resins for HSCT

o Bismaleimides including toughened versions

o PMR-15 including modified versions

o Polyimides (thermoplastics, semi-crystalline TP)

o Poly(arylene ether)s

o Emerging systems (e.g. benzocyclobutenes)

# Airframe Materials for HSR



**Wing Demonstration Component (25%)**

Aeroelasticity, Acoustics, Thermal, Mechanical, Fuel Containment, Fabrication

Outer Wing Box

25'

2'

2'

6'

4'

**Materials and Durability (35%)**

Matl's Dev.
Testing
Fab Dev.
Durability
Life Pred.

H S R

**Fuselage Demonstration Component (40%)**

Acoustics, Thermal, Mechanical, Fabrication

2'

2'

20'

6'

6'

1595
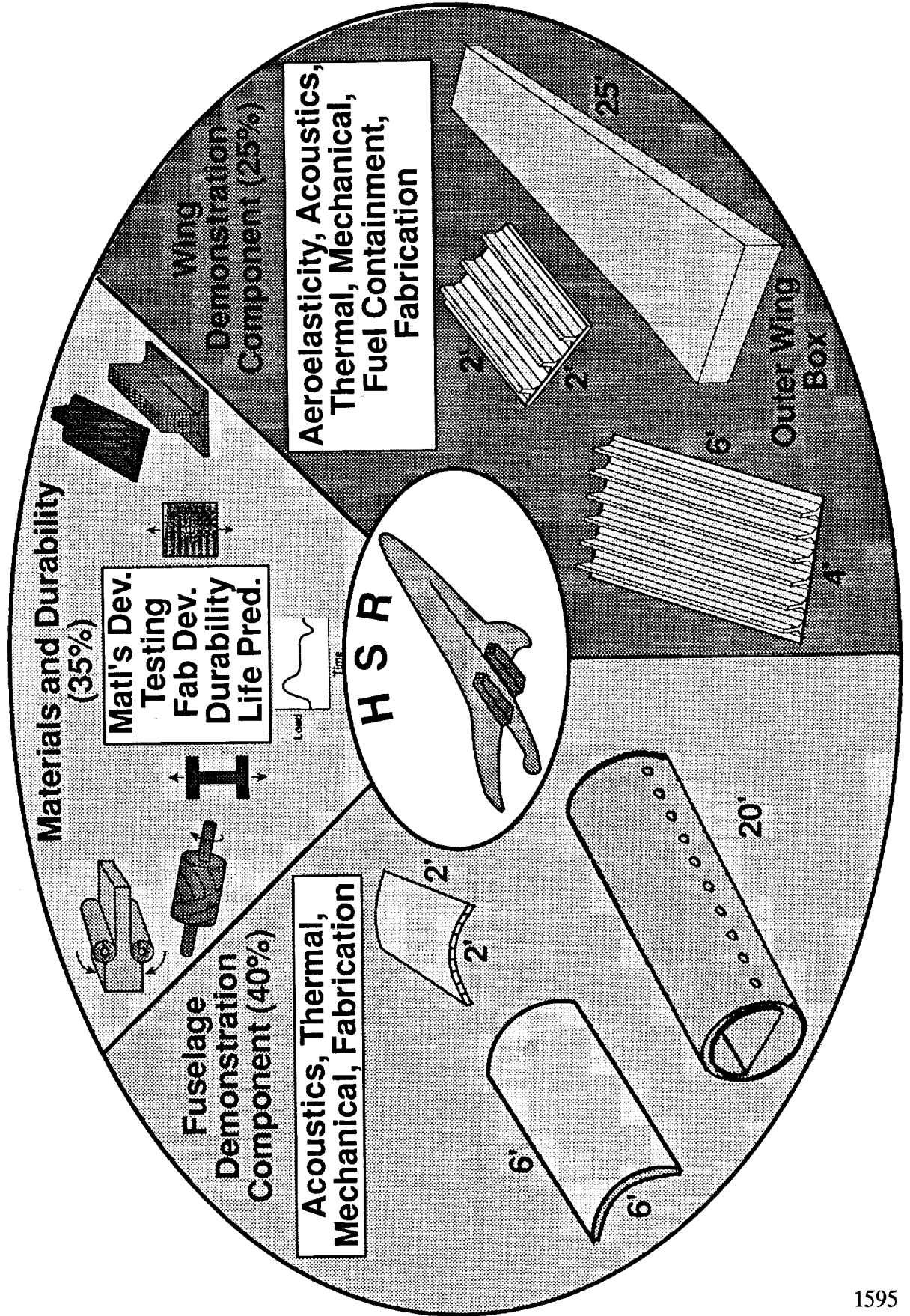
# Airframe Materials for HSR

## Prime Candidate Airframe Materials

- High Temperature Composites
  (3/4 Program)

- High Temperature Aluminum
  (1/4) Program

# Airframe Materials for HSR

## B. Materials and Durability

### Approach



1597
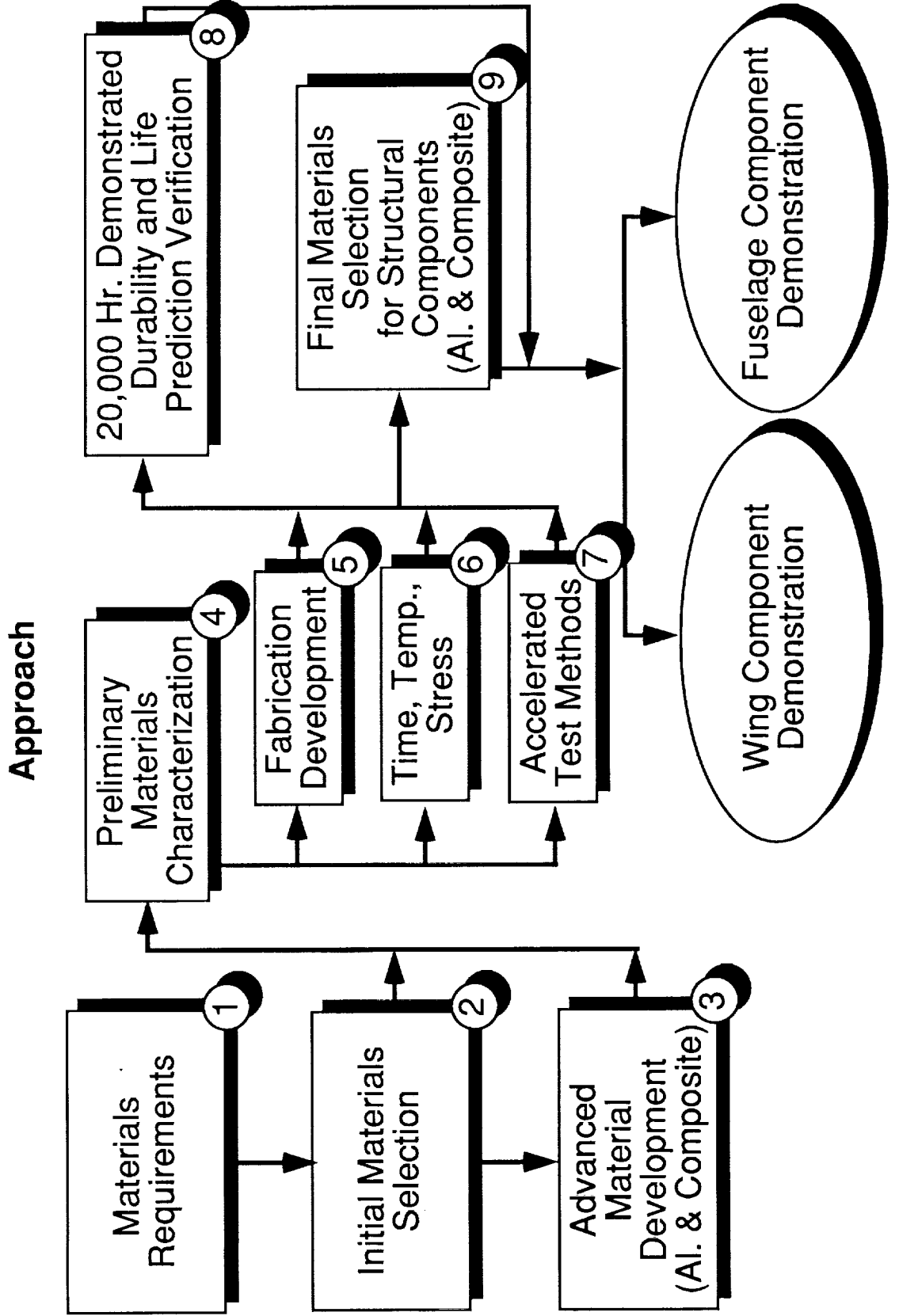
# Airframe Materials for HSR

## B. Materials and Durability

### Schedule



| | 91 | 92 | 93 | 94 | 95 | 96 | 97 | 98 |
|---|---|---|---|---|---|---|---|---|
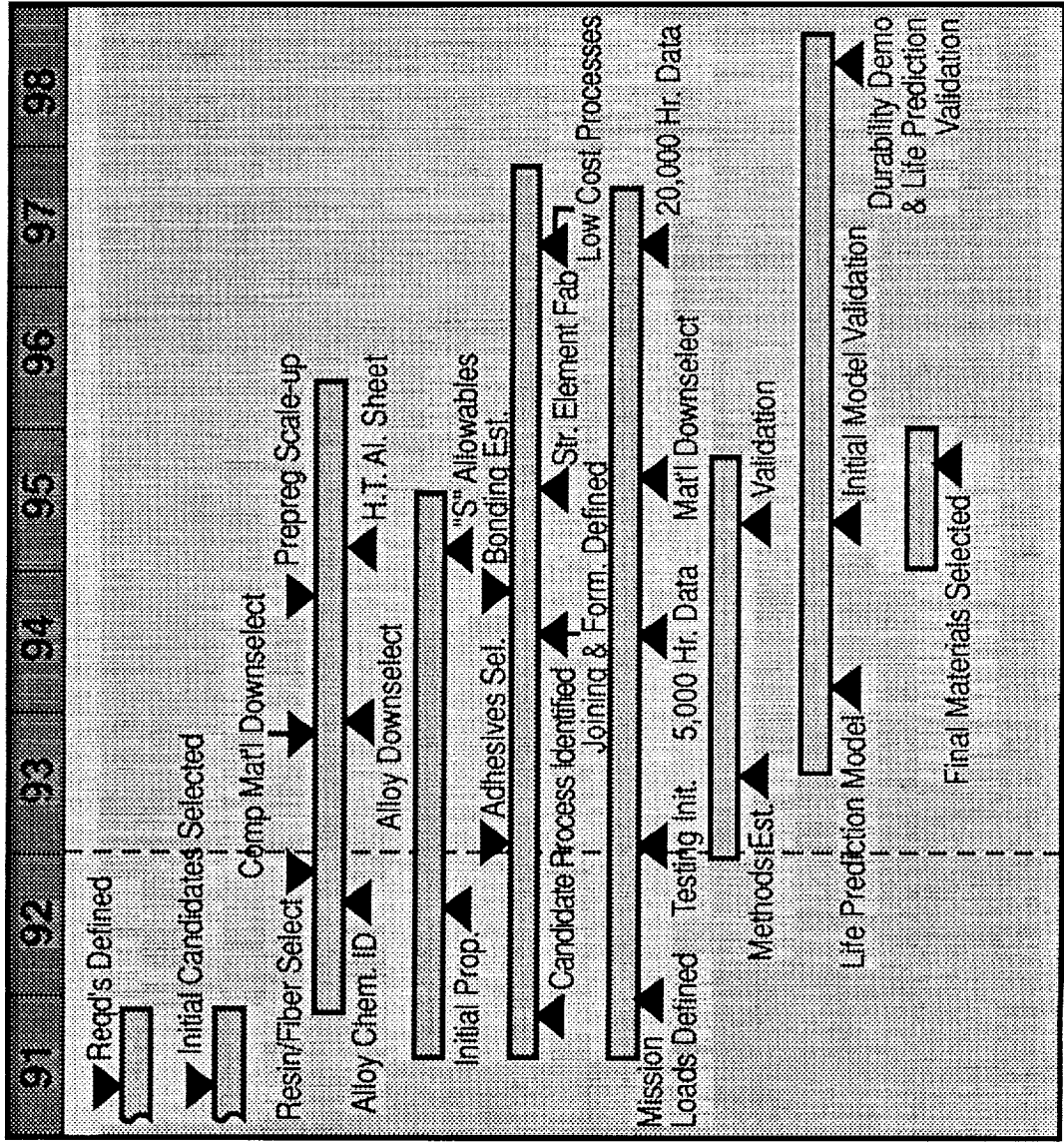
**1 Material Requirements**

**2 Initial Material Selection**

**3 Advanced Materials Development**

**4 Prel. Materials Characterization**

**5 Fabrication Development**

**6 Time, Temp., Stress Testing**

**7 Accelerated Test Methods**

**8 Durability/Life Prediction**

**9 Materials Selection for Wing and Fuselage Components**

1598

# Airframe Materials for HSR

## High Speed Research Program - Phase II Schedule

| Area | 93 | 94 | 95 | 96 | 97 | 98 | Goals | $M |
|---|---|---|---|---|---|---|---|---|
| **Materials Development and Design/Test of Critical Wing/Fuselage Subcomponent** | | Concept selection / Wing Component Design | Fab and test wing subcomponent | | | | Design Concepts for Aeroelastically Tailored Light-Weight Wing Structure | 30 |
| | Candidate materials identified | Final materials selection / Materials and Durability | | Durability Life Prediction Validation | | | Demonstrate Long Term Material Durability at Elevated Temperature | 75 |
| | | Concept selection / Fuselage Component Design | Fab and test fuselage subcomponent | | | | Design Concepts for Light-Weight High Temperature Fuselage Structure | 40 |
| **Wing and Fuselage Component Design, Fab and Test** | | | Component design / Wing Component Development | Component validation | Component validation | | Design/Test/Verification of Large Scale Wing Box Structure | 30 |
| | | | Fuselage Component Development / Component design | | | | Design/Test/Verification of Large Scale Fuselage Panels | 45 |
| **$M** | 38 | 43 | 45 | 49 | 31 | 14 | Total $M | 220 |

1599

# Airframe Materials for HSR

**GOAL:**

Verified materials and structural concepts that meet performance requirements for HSCT

**DELIVERABLES:**

- Aluminum alloy and resin matrix composite materials with long term durability at 400°F and $\geq$20% strength/stiffness improvement compared to titanium.

- Light weight ($\leq$4.5 lbs./ft$^2$) cost-effective structural concepts for wing and fuselage

- Accelerated aging test methodology for predicting long term durability of materials.

1600

# AIRFRAME MATERIALS FOR HSR

## Status

- Resources from the ACT program rolled over to initiate HSR Materials Program

- Working groups in metallics, polymeric composites and durability established with representation from NASA, airframers, material producers, and universities

- Trade studies being conducted by Boeing and Douglas to define material requirements

- Screening of commercially available materials (metal and composites) initiated in-house

- Upgrade of test facilities for durability program and material characterization initiated

```
┌─────────────────────┐
│ HSR Airframe Materials│
│   Steering Committee  │
└──────────┬──────────┘
           │
  ┌────────┴────────┐
  │  Working Groups  │
  └────────┬────────┘
           │
   ┌───────┼───────────────┐
   │                       │
┌──┴──┐          ┌─────────┴──┐      ┌──────────────┐
│Metals│          │ Polymers and│      │ Mechanics and │
└─────┘          │  Composites │      │  Durability   │
                 └────────────┘      └──────────────┘
```
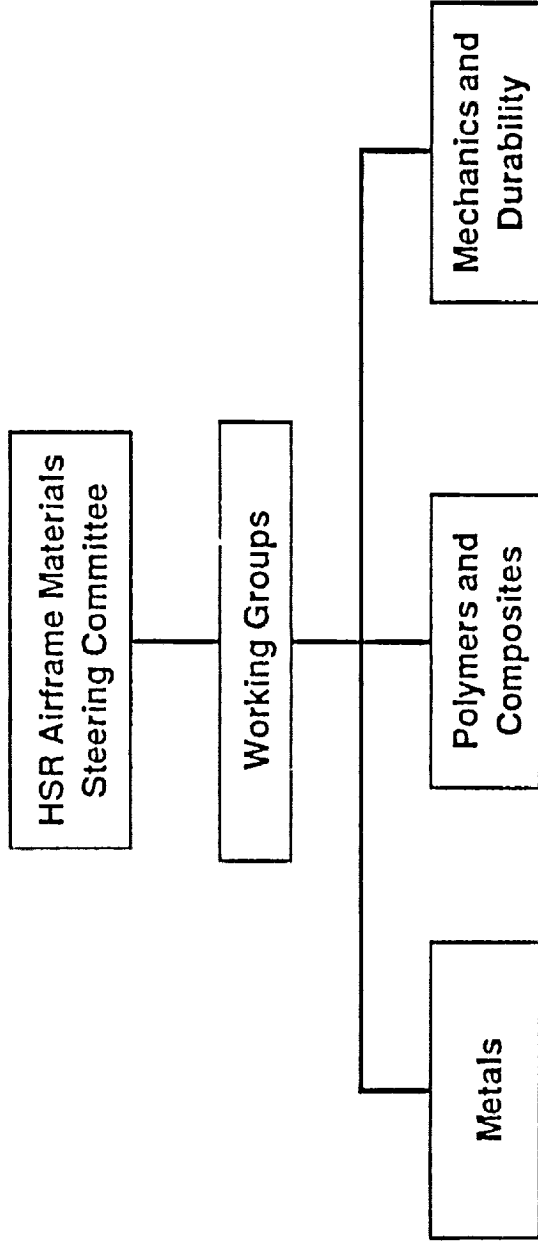
Chairman: Tom Bales    Chairman: Paul Hergenrother    Chairman: Steve Johnson

**Steering Committee**

- Provide guidance to NASA on overall airframe materials program including technical thrusts, implementation strategy, allocation of resources, coordination and advocacy

**Working Groups**

- Assist NASA in planning research thrusts in metals, composites and mechanics including identification of key technology needs, implementation strategy, teaming arrangements, coordination between government, airframes, and material suppliers, and testing and analyses activities

1602

# HSCT STRUCTURAL MATERIALS
## DEVELOPMENT/EVALUATION PROGRAM
### NASA-LaRC/Industry Working Groups



**COMPOSITES & ADHESIVES**

Recommend candidate materials

Propose initial material screening tests

Assess processability

Chairman: Paul M. Hergenrother

**MECHANICS & DURABILITY OF MATERIALS**

Develop test methods and screening rationale for thermal-mechanical behavior

Assess long term durability and develop accelerated test methodology

Develop analysis methodology for damage tolerance and durability

Chairman: W. Steven Johnson

**METALLIC MATERIALS**

Initial mat'l screening

Modify alloy chemistry for improved HT performance

Develop innovative fabrication techniques

Chairman: Thomas T. Bales

Candidate materials

Candidate materials

Needed areas of improvement

Needed areas of improvement

1603

# HIGH SPEED CIVIL TRANSPORT
## Composites

Douglas
Structure/Material
Trade Study

Dow
Resin
Development

University of Akron
Resin
Development
& Scale-Up

In-House
Prepregging &
Composite
Processing

BASF
Prepreg
Development

Boeing
Structure/Material
Trade Study

MacAir
Composite Processing
& Fab. Technology

VA Tech, U. of AL,
GA Tech
Advanced
Polymers &
Composites

1604
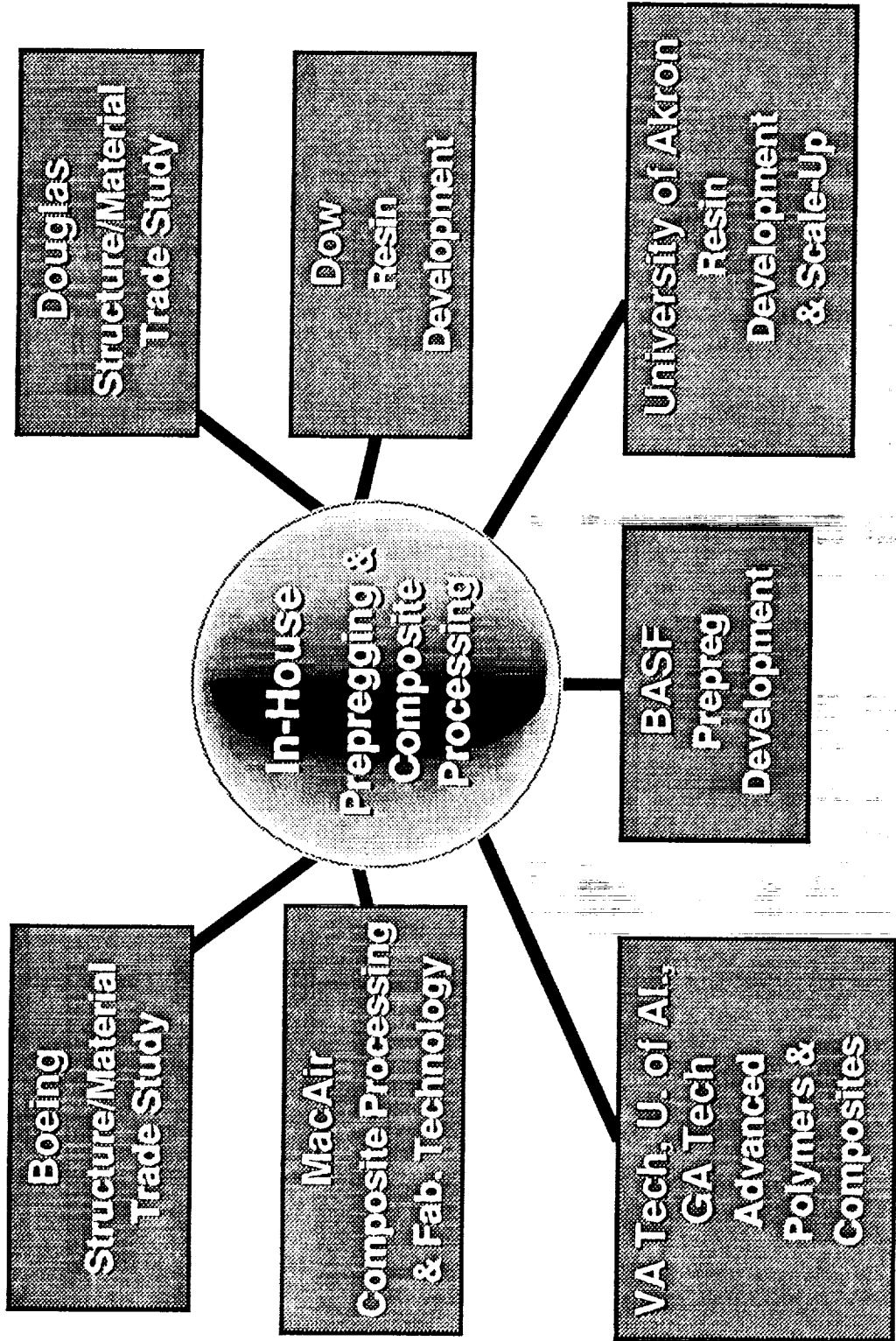
# AIRFRAME MATERIALS FOR HSR

## Procurement Strategy

- NASA Research Announcements (NRA) - February 1992

  - Material systems modification

  - Process development

  - Understanding of materials degradation

- Omnibus Task Contracts - May 1992

  - Material and design requirements

  - Fabrication technology

    - Structural Elements

    - Built-up components

# AIRFRAME MATERIALS FOR HSR

## Concluding Remarks

● Materials may prove to be an enabling technology for an economically viable HSCT

● Both resin matrix composites and metallics are considered viable candidates for HSCT

● Airframe materials program needs to be accelerated to meet projected materials selection date

1606

# Session XI.  Airframe and Engine Materials

HSR Airframe Materials - The Boeing Perspective
*Donald L. Grande, Boeing Commercial Airplane Group*

THIS PAGE INTENTIONALLY BLANK

528-24

12058

# HSCT AIRFRAME MATERIALS

# THE BOEING PRESPECTIVE

## MAY 16, 1991

### DONALD L. GRANDE
### MANAGER - HSCT STRUCTURES

# Effect of Cruise Mach Number on Maximum Takeoff Weight

- 5,000 nmi
- 290 passengers



1610

# HSCT AIRFRAME LIFE



TOTAL TIME

SUPERSONIC TIME

TIME - HOURS X $10^{-3}$

MACH NUMBER

1611
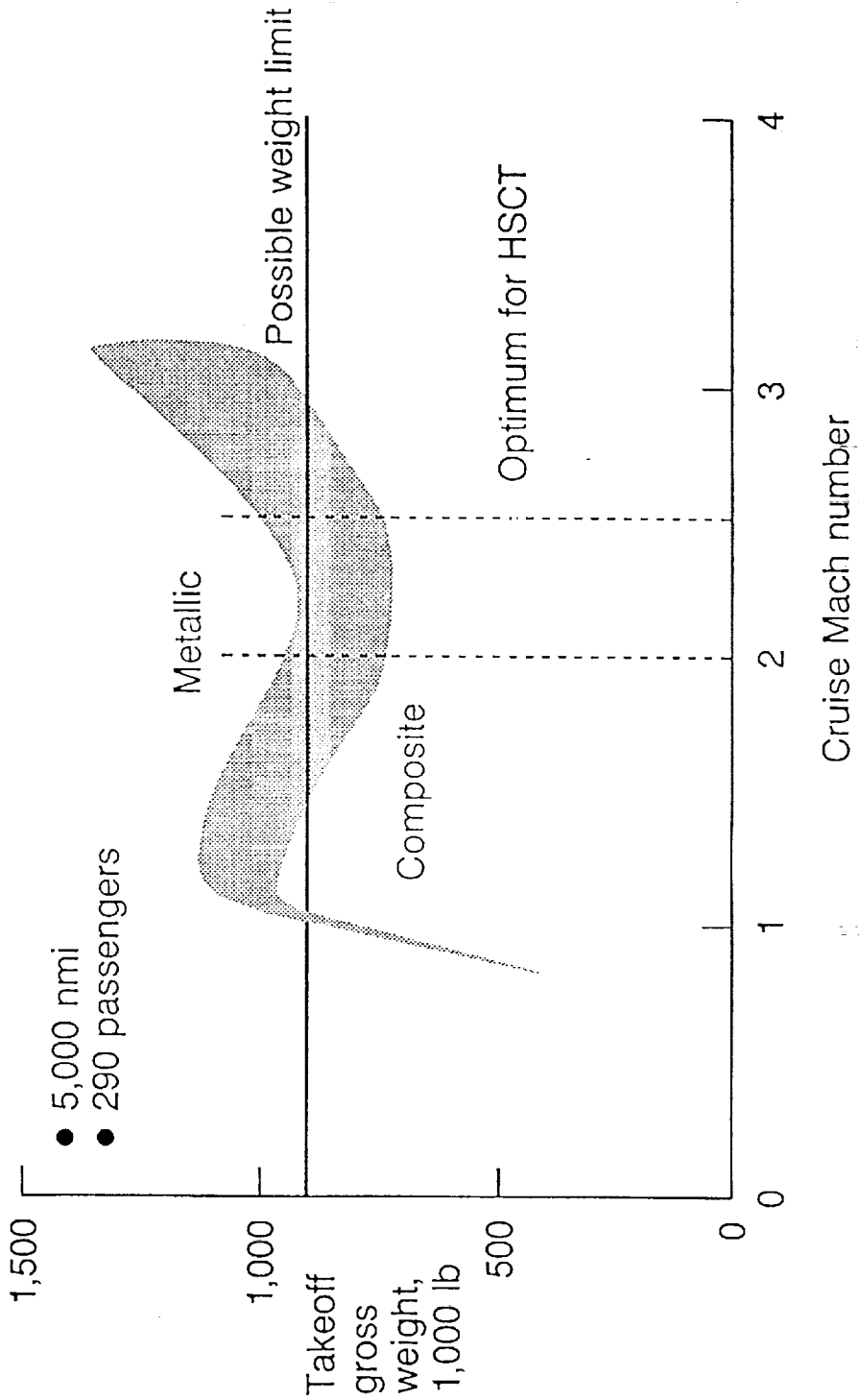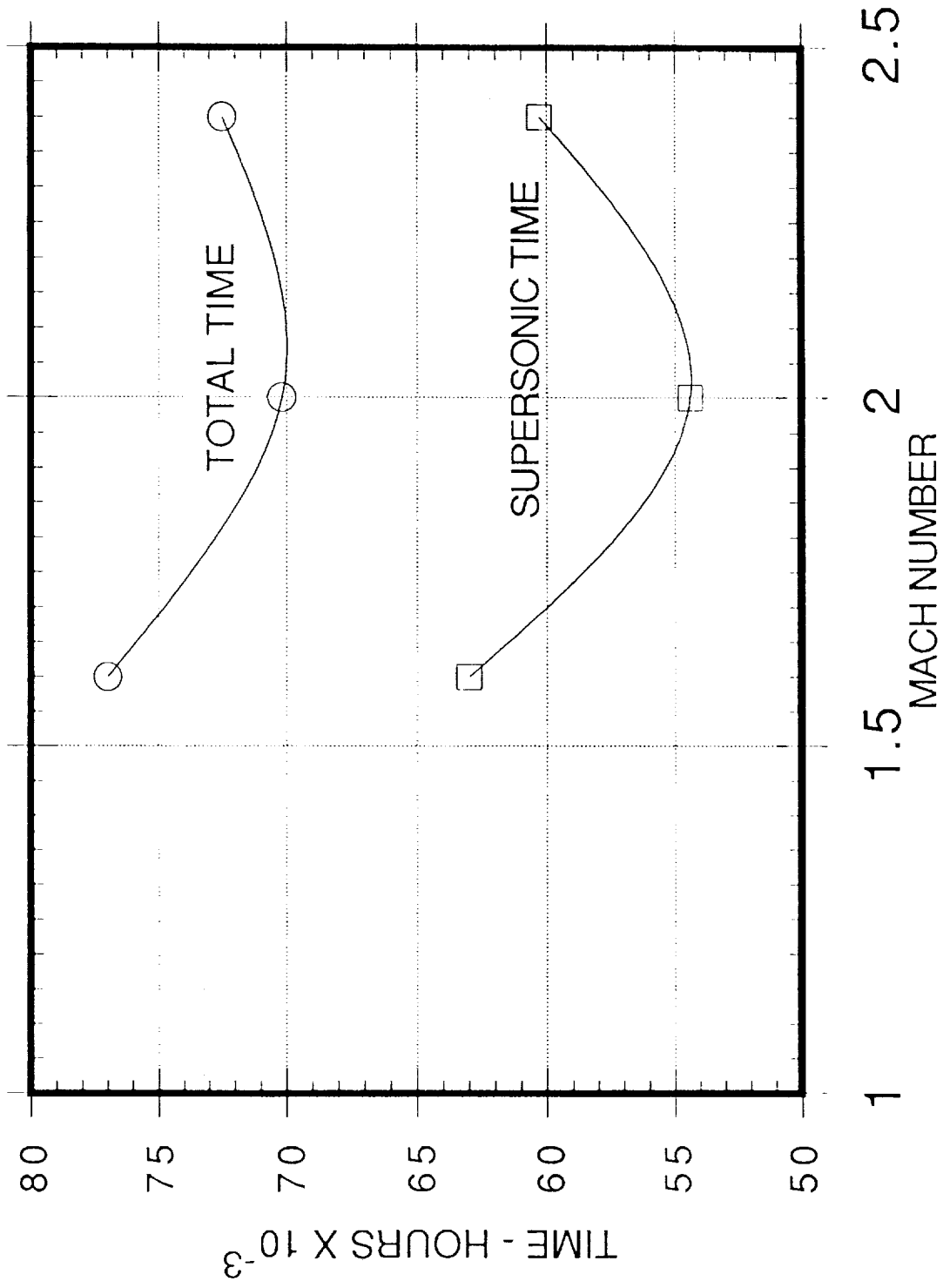
RECOMMENDATIONS

TOTAL TIME          72,000 HRS

SUPERSONIC TIME     60,000 HRS

FLIGHT CYCLES       30,000

TEMPERATURES        200°F TO 350°F

1612

# The Aging Issue



1613

# CHARACTERIZING MATERIAL AGING EFFECTS

## MATERIAL FAMILY "A"

1614

SCIENCE BASE

```
PRELIMINARY                PRELIMINARY
CONDITIONING   ──────→     SCREENING        ──→  SELECT   ──→   REAL TIME          ──→   TEST
OF                         TESTS OF              MODEL         CONDITIONING             OF      ──→  ANALYSIS
FAMILY                     CANDIDATES                          OF                       MODEL         &
CANDIDATES                                                     MODEL                                  REPORT


PRELIMINARY                PRELIMINARY                YES       ACCELERATED        ──→   TEST
CONDITIONING   ──────→     TESTING          ──→  SELECT ──┐     CONDITIONING             OF
OF                         OF                             │     OF                       MODEL
NEW FAMILY                 NEW FAMILY               NO    │     MODEL
CANDIDATES                 CANDIDATES
```

ENGINEERING BASE

```
                                                          CONDITIONING       ──→   TEST
                                                          FOR                      OF        ──→  ANALYSIS
                                                          ALLOWABLES               MODEL           &
                                                                                   MATERIAL        REPORT
```

MATERIAL FAMILY "A"

REAL TIME TESTING

| PRELIMINARY CONDITIONING OF LAMINATE CANDIDATES | PRELIMINARY SCREENING TESTS OF LAMINATE | SELECT MODEL | REAL TIME CONDITIONING OF MODEL LAMINATE | TESTING OF MODEL LAMINATE | REPORT REAL TIME EFFECTS |
|---|---|---|---|---|---|
| PRELIMINARY CONDITIONING OF ADHESIVE CANDIDATES | PRELIMINARY SCREENING TESTS OF ADHESIVES | SELECT MODEL | REAL TIME CONDITIONING OF MODEL ADHESIVE | TESTING OF MODEL ADHESIVE | REPORT REAL TIME EFFECTS |
| PRELIMINARY CONDITIONING OF SEALANT CANDIDATES | PRELIMINARY SCREENING TESTS OF SEALANT | SELECT MODEL | REAL TIME CONDITIONING OF MODEL SEALANT | TESTING OF MODEL SEALANT | REPORT REAL TIME EFFECTS |
| PRELIMINARY CONDITIONING OF SANDWICH CANDIDATES | PRELIMINARY SCREENING TESTS OF SANDWICH | SELECT MODEL | REAL TIME CONDITIONING OF MODEL SANDWICH | TESTING OF MODEL SANDWICH | REPORT REAL TIME EFFECTS |
| PRELIMINARY CONDITIONING OF PRIMER & PAINT CANDIDATES | PRELIMINARY SCREENING TESTS OF PRIMER & PAINT | SELECT MODEL | REAL TIME CONDITIONING OF MODEL PRIMER & PAINT | TESTING OF MODEL PRIMER & PAINT | REPORT REAL TIME EFFECTS |

1615

CHACTERIZING MATERIAL AGING EFFECTS

REAL TIME CONDITIONING-COMPOSITES    TESTING

**LAMINATE**

| | | | | | |
|---|---|---|---|---|---|
| ISOTHERMAL | 200°F 275°F 350°F | 10K 30K 60K 90K 120K | OHC | -65°F RT 200°F 275°F 350°F |
| TEMP-TIME HIST | | | CAI TENS COMP SHEAR | |
| LOAD & TEMP TIME HIST | RT | | | |
| LOAD-TIME HIST | | | | |
| ISOTHERMAL & UV | RT | | | |
| ISOTHERMAL & O3 | PAINTED UNPAINTED 200°F 350°F | 10K 30K 60K | | |
| TIME HIST WATER ABSORB | | | | |
| TIME HIST LOAD & H2O | RT | | | |

**ADHESIVE**

| | | | | | |
|---|---|---|---|---|---|
| ISOTHERMAL | 200°F 275°F 350°F | 10K 30K 60K | SHEAR PEEL PULL-OFF | -65°F RT 200°F 275°F 350°F |
| TEMP-TIME HIST | WET DRY | | | |
| LOAD & TEMP TIME HIST | | | | |
| LOAD-TIME HIST | RT | | | |

**SEALANT**

| | | | | |
|---|---|---|---|---|
| ISOTHERMAL | 200°F 275°F 350°F | 10K 30K 60K | SOLVENT SHEAR ADHESION | -65°F RT 200°F 275°F 350°F |
| TEMP-TIME HIST | | | | |
| LOAD & TEMP TIME HIST | | | | |

FIGURE 7

REAL TIME CONDITIONING-COMPOSITES (CONCLUDED)                    TESTING

STRUCTURE

| ISOTHERMAL | | | OHC | RT |
| TEMP-TIME HIST | 200°F 275°F 350°F | | CAI | 200°F |
| LOAD-TIME HIST | 10K 30K 60K | | SHEAR | 275°F |
| LOAD & TEMP TIME HIST | | | PULL-OFF | 350°F |

PAINT & PRIMER

| ISOTHERMAL | 200°F 275°F 350°F | | COLOR | RT |
| | | | GLOSS | 200°F |
| TEMP-TIME HIST | 10K 20K | | RAIN EROSION | 275°F |
| | | | | 350°F |

REAL TIME CONDITIONING-METALS                    TESTING

SHEET

| ISOTHERMAL | | | TENSION | -65°F |
| TEMP-TIME HIST | 200°F 275°F 350°F | | COMPRESSION | RT |
| LOAD & TEMP TIME HIST | 10K 30K 60K 90K 120K | | BEARING | 200°F |
| LOAD-TIME HIST | RT | | SHEAR | 275°F |
| | | | da/dN | 350°F |
| | | | KAPP, CREEP | |

FIGURE 7 (CONT.)

1617

# CANDIDATE ADVANCED METALLIC MATERIALS

### Mach=2.0

**Advanced Aluminums**
- 2xxx
- 7xxx
- X7093

**Aluminum-Lithiums**
- 2090
- 8090
- Weldalite 049

**Metal-Matrix Composites (MMCs)**
- 2009/SiC/15% to 25% w or p (modified 2124 matrix)
- X2080/SiC/xxx
- 6090/SiC/xxx (modified 6013 matrix)
- Weldalite 049/SiC/xxx
- 6xxx/SCS-2/50% (continuous fiber)

### Mach=2.4

**High-Temperature Aluminums (RSRs)**
- X8019 (CZ42)
- 8009 (FVS0812)
- FVS 0611
- FVS1212

**High-Temperature MMCs**
- 8009/SiC/xxx
- X8019/SiC/xxx
- FVS1212/SiC/xxx
- Ti xxx/SCS-6/40% (continuous fiber)

**Titaniums**
- 6-4
- 15-3-3-3-3
- 6-2-2-2-2
- 10-2-3
- SP 700

*HSCT*

# OBJECTIVES

1. Develop and evaluate "low-cost" airplane designs by examining alternate structural, material, and manufacturing concepts

2. Advise material suppliers and NASA on desired material properties, product forms, and processing techniques
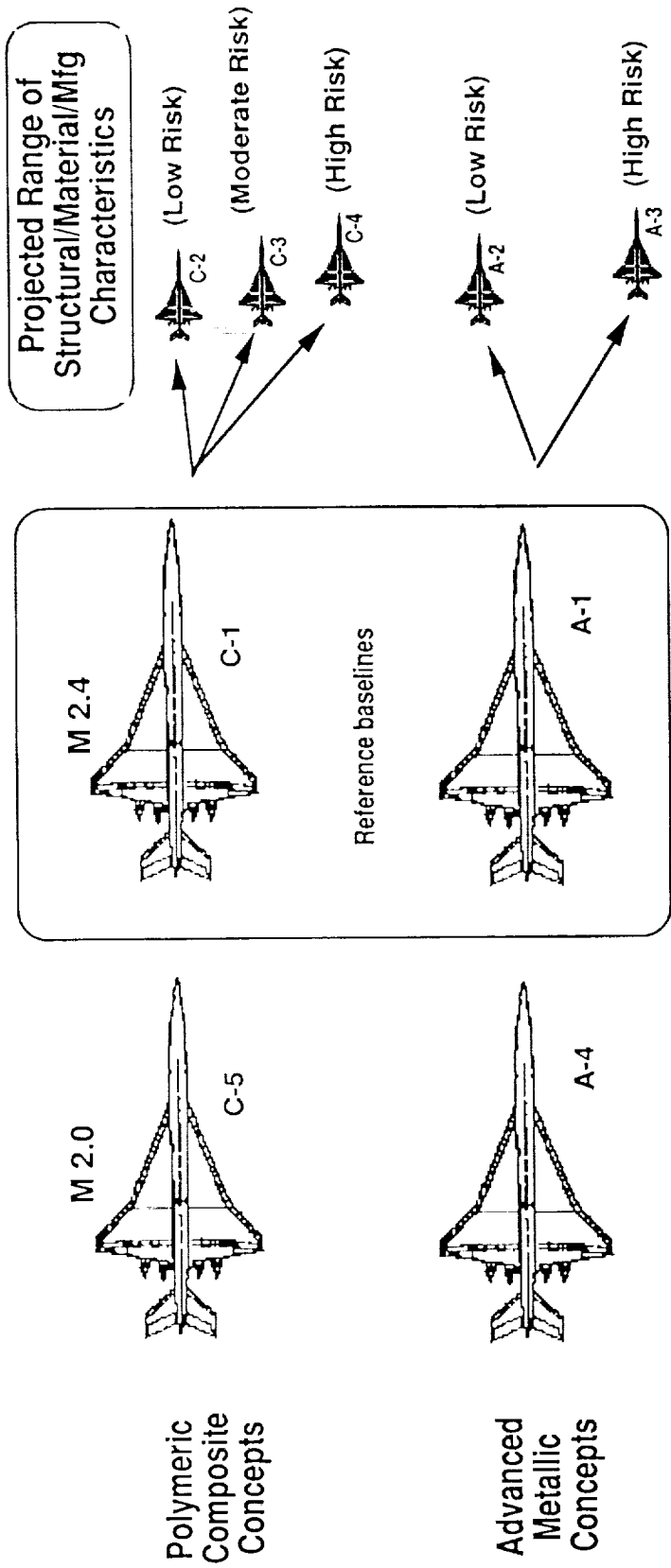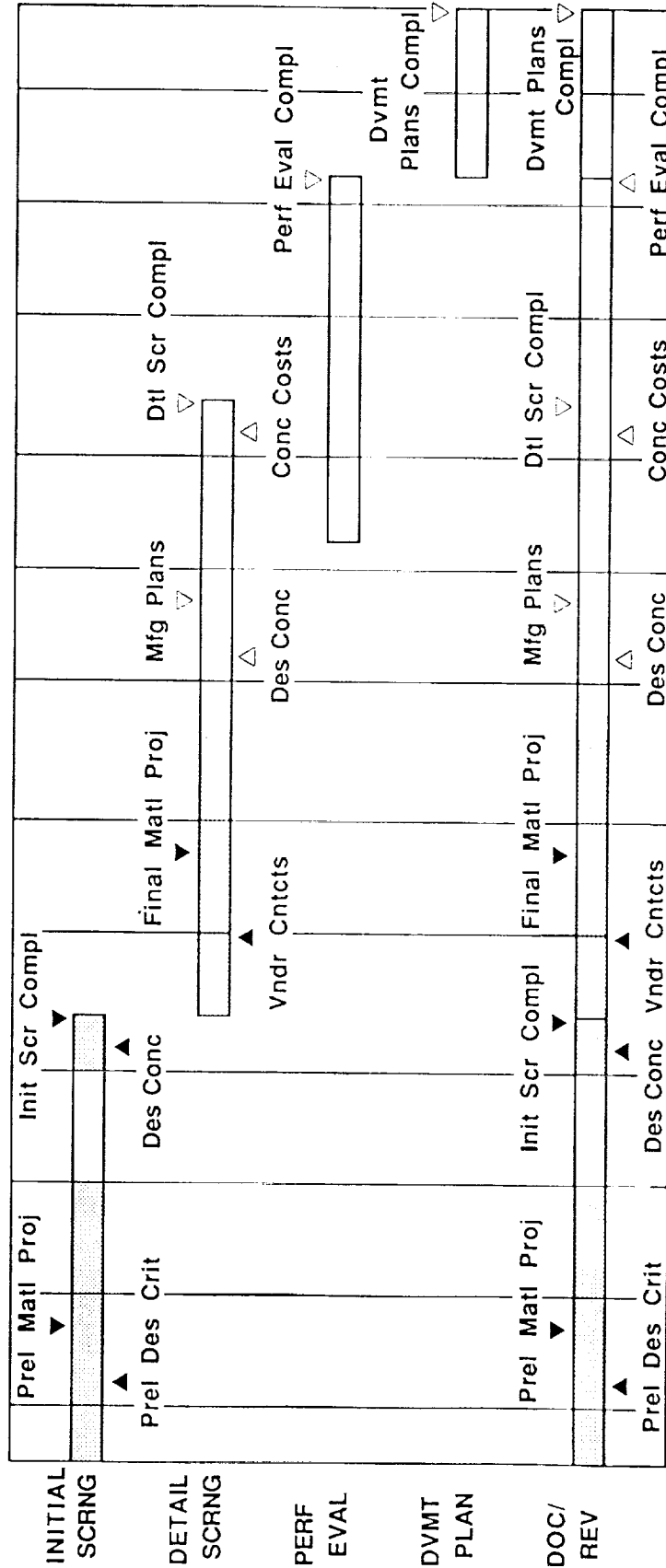
Figure 1-1. Structures and Materials Trady Study Design Options

# LOW-COST AIRPLANE TRADE STUDY

9 0 | 9 1

N D E C | J A N | F E B | M A R | A P R | M A Y | J U N | J U L | A U G | S E P | O C T | N V

INITIAL SCRNG

Prel Matl Proj

Init Scr Compl

Prel Des Crit    Des Conc

DETAIL SCRNG

Final Matl Proj    Mfg Plans    Dtl Scr Compl

Vndr Cntcts    Des Conc    Conc Costs

PERF EVAL

Perf Eval Compl

DVMT PLAN

Dvmt Plans Compl

DOC/REV

Prel Matl Proj    Init Scr Compl    Final Matl Proj    Mfg Plans    Dtl Scr Compl    Dvmt Plans Compl

Prel Des Crit    Des Conc    Vndr Cntcts    Des Conc    Conc Costs    Perf Eval Compl

4-WK SCHED SLIDE
DUE TO SPEED STUDY

May 1991

THIS PAGE INTENTIONALLY BLANK

1622

# Session XI. Airframe and Engine Materials

$\mathcal{S}m\,11$

HSCT Materials and Structures - An MDC Perspective
*Jay O. Sutton, Douglas Aircraft Company*

THIS PAGE INTENTIONALLY BLANK

1624

$529-24$

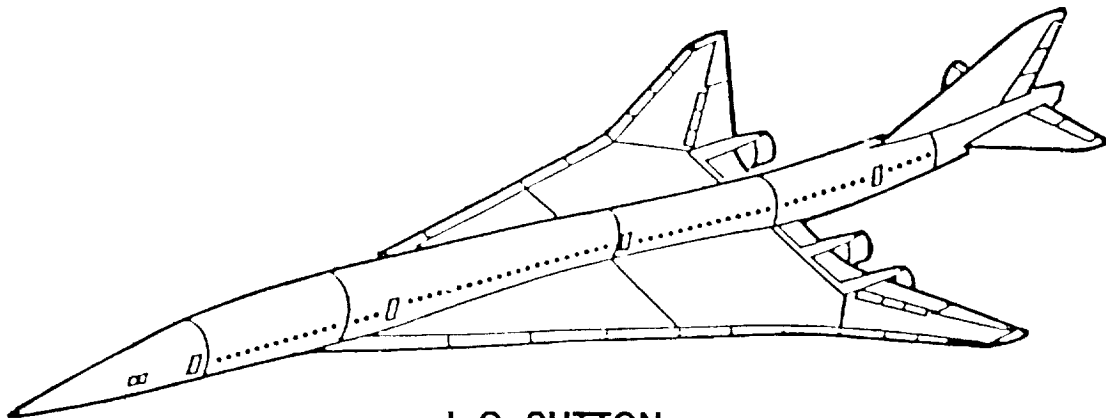$12059$

**≡HSCT**    <span>MCDONNELL DOUGLAS</span>

# HSCT MATERIALS AND STRUCTURES - AN MDC PERSPECTIVE



## J. O. SUTTON

### HIGH SPEED RESEARCH WORKSHOP
### WILLIAMSBURG, VA
MAY 14 - 16, 1991

This discussion is divided into four parts.

The first section describes the key HSCT features which drive the materials selection.

The second section describes a top-down approach to determining the optimal material selection, considering weight and production economics.  This process is based upon the effects of temperature on the material properties of candidate material systems, and the known or anticipated material price and fabrication and assembly costs.

The third section describes a bottoms-up approach to material selection, in concert with the selection of structural concepts.  This process applies a point design optimization to specific airframe locations and extrapolates them to determine an optimal material selection.  The two methods are then compared for the specific M = 2.4 study baseline aircraft.

The final section describes the key materials and structures related tasks which remain to be accomplished prior to proceeding with the building of an HSCT aircraft.

**=HSCT**

MCDONNELL DOUGLAS

# HSCT MATERIALS OVERVIEW

- ● **KEY MATERIAL USAGE DRIVERS**

- ● **PRELIMINARY MATERIAL EVALUATION**

- ● **PRELIMINARY STRUCTURAL EVALUATION**
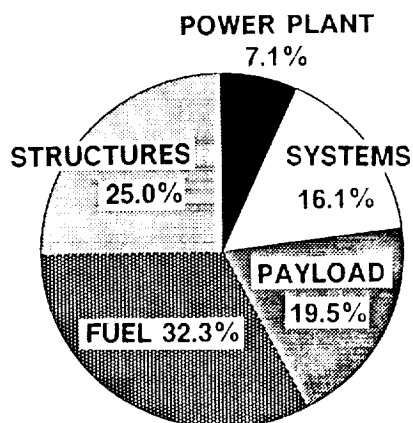
- ● **KEY DEVELOPMENT TASKS**

The gross weight breakdown of two aircraft with the same payload and range (300 passengers, 5500 nmi) are compared.  It is shown that the supersonic aircraft requires considerably higher fuel fraction than the subsonic aircraft to fly the same mission.  This places a premium on control of non-payload weights.  In particular, the airframe structure weight must be a considerably smaller fraction of the whole, while surviving in a much more aggressive environment.  This presents a challenge to the airframe designer to incorporate more efficient materials and structural concepts, with no compromise in safety.

At the same time, the aircraft must be both profitable to operate and to produce.  Thus the materials and structural concepts selected must lend themselves to economical production methods, and be both reliable and maintainable in service.

**≡HSCT**　　　　　　　　　　　　　MCDONNELL DOUGLAS
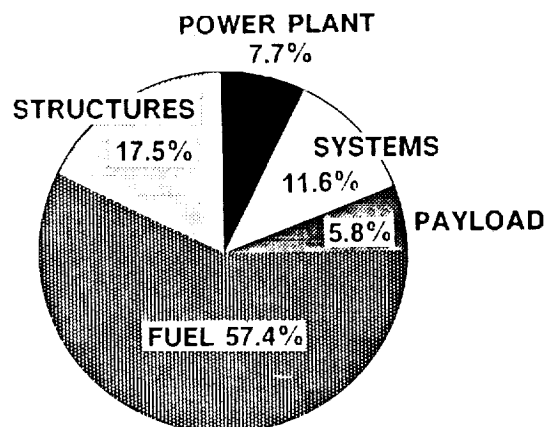
# HIGHER MACH NUMBERS DEMAND MORE EFFICIENT AIRFRAMES

POWER PLANT
7.1%

STRUCTURES
25.0%

SYSTEMS
16.1%

PAYLOAD
19.5%

FUEL 32.3%

POWER PLANT
7.7%

STRUCTURES
17.5%

SYSTEMS
11.6%

5.8% PAYLOAD

FUEL 57.4%

## M = 0.85　　　　　　　　M = 2.2

HSCT AIRFRAME WEIGHT IS PRIMARILY DRIVEN BY STIFFNESS

An examination of the weight breakdown of the structure of a previous study HSCT project shows that specific fractions of the total weight can be assigned to a small number of dominant design requirements. In particular, the largest single design requirement is for stiffness, either to control buckling, crippling, or aeroelastic phenomena. Thus materials which have a high ratio of modulus of elasticity to density (specific stiffness) should show a weight advantage in such applications.
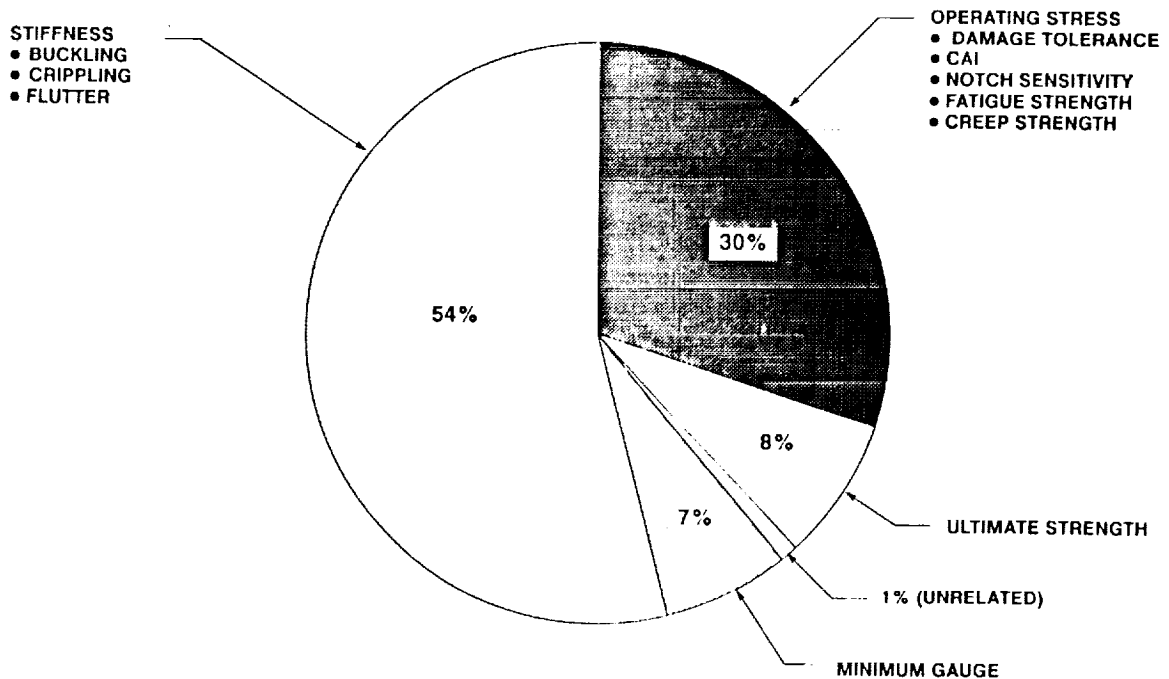
Similarly, a significant fraction of the weight is determined by the material strength, either in the form of the ultimate strength or a lower strength allowable which permits safe operation with damage, extends the life of the part, or prevents excessive physical distortion over the life of the airframe. For such components, high specific strength will be beneficial.

Finally the smallest fraction of the airframe weight is determined by minimum gauge applications or for other factors unrelated to strength or stiffness, such as paint or sealants. For such applications, low density is the primary means of reducing weight.

**═HSCT** MCDONNELL DOUGLAS

# HSCT AIRFRAME WEIGHT IS PRIMARILY DRIVEN BY STIFFNESS

STIFFNESS
● BUCKLING
● CRIPPLING
● FLUTTER

OPERATING STRESS
● DAMAGE TOLERANCE
● CAI
● NOTCH SENSITIVITY
● FATIGUE STRENGTH
● CREEP STRENGTH

30%

54%

8%

7%

ULTIMATE STRENGTH

1% (UNRELATED)

MINIMUM GAUGE

1628

Considering the previous discussion, the airframe weight may be considered to be strongly influenced by the use factors: stiffness, strength, and density, and the generalized candidate material properties.  In addition, other factors such as creep, stability, and producibility and maintainability will enter into the material selection.

**≡HSCT**                                                    MCDONNELL DOUGLAS

# HSCT MATERIAL SELECTION IS DRIVEN BY:

- HIGH SPECIFIC STRENGTH, STIFFNESS

- LONG-TERM STRENGTH, STIFFNESS, DURABILITY, DAMAGE TOLER-TOLERANCE, CORROSION RESISTANCE

- LONG-TERM THERMO-MECHANICAL AND THERMO-CHEMICAL STABILITY

- AVAILABILITY, COST

- ENVIRONMENTALLY ACCEPTABLE PROCCESSING

- GOOD PRODUCIBILITY, MAINTAINABILITY

Materials representing monolithic metals, organic composites, reinforced metals, and metal matrix composites were selected for evaluation over a Mach number range from 1.6 to 2.4. This represents a field surface temperature exposure range of from 100 to 500 F. While stagnation temperatures at the nose, and the leading edge temperatures of wing and tails are considerably higher, these regions represent small fractions of the total airframe weight, and do not influence the general material selection process.

**≡HSCT**　　　　　　　　　　　　　　　　　MCDONNELL DOUGLAS

# EIGHT BASIC MATERIAL SYSTEMS WERE SELECTED FOR PERFORMANCE EVALUATION

| | |
|---|---|
| **ALUMINUM (2024)** | **C/PMR (C6K/PMR-15)** |
| **ALUMINUM (2618)** | **DRETA (TARGET)** |
| **TITANIUM (6-4)** | **AMMC (6061/SCS-8)** |
| **C/BMI (IM6/5245C)** | **TMC (15-3/SCS-6)** |

For the top-down material evaluation study, the airframe weight was assumed to be composed of three parts: that determined by stiffness requirements, by strength requirements, and by non material-related requirements. This was accomplished by determining a relative weight resulting from the product of the use factor (described previously), the performance factor (which is ratio of the strength or stiffness of the evaluated material to a reference material at the relevant temperature), and the density factor (the ratio of the evaluated material density to that of the reference material). Thus the airframe weight for the reference material would always be 1.0, and the weight fractions of the airframe determined for each candidate material could be added in various combinations to determine the relative weight of any mix of materials. This was evaluated at each temperature range from M = 1.6 to M = 3.0.

Similarly, the relative cost to produce each weight fraction in each material could be determined by multipliying the appropriate weight factor, determined above, by the cost factor (the ratio of the cost to produce (material + fab + assembly) a pound of the candidate material relative to the refernce material). Thus, the cost to produce the airframe in the reference material is always 1.0, and the cost fractions of the airframe determined for each candidate material could be added in various combinations to determine the cost of any mix of materials.

**=HSCT**                                                      *MCDONNELL DOUGLAS*

# PRELIMINARY MATERIAL EVALUATION IS GUIDED BY RELATIVE PERFORMANCE

- **AIRFRAME WEIGHT =**
  $$\sum \text{USE FACTOR X PERFORMANCE FACTOR X DENSITY FACTOR}$$

- **AIRFRAME COST =**
  $$\sum \text{WEIGHT FACTOR X ASSEMBLED COST FACTOR}$$

- PERFORMANCE FACTOR IS BASED ON STIFFNESS AND STRENGTH AT RELEVANT TEMPERATURE

- THERMAL STABILITY OF ADVANCED MATERIALS IS ASSUMED TO BE ADEQUATE THROUGHOUT USE TEMPERATURE RANGE

THE BEST HSTC "MATERIAL" IS A COMBINATION

Following evaluation of the relative weights and costs of each
material system candidates across the study speed range, combinations
of materials were determined which gave either the lowest airframe
weight or the lowest airframe cost.  As might be expected, only at the
very highest speed/temperature range did a single material appear to
optimum for use throughout the airframe.  Otherwise, a combination of
materials produced the lowest weight, and a different combination
produced the lowest cost, although the polymer composite material
system did tend to contribute to both low weight and low cost.

**≡HSCT**                                          MCDONNELL DOUGLAS

# THE BEST HSCT "MATERIAL" IS A COMBINATION

| MACH NO. | 1.6 | 1.8 | 2.0 | 2.2 | 2.4 | 2.6 | 2.8 | 3.0 | 3.2 |
|---|---|---|---|---|---|---|---|---|---|
| ALUMINUM - 2024 | $ | $ | $ |  |  |  |  |  |  |
| ALUMINUM - 2618 |  |  |  |  |  |  |  |  |  |
| TI 6-4 | W | W | W |  |  |  |  |  | $ |
| C/BMI | W $ | W $ | W $ | W $ | W $ |  |  |  |  |
| C/PMR-15 |  |  |  |  |  | W | W | W |  |
| DRETA |  |  |  | $ | $ | $ | $ | $ |  |
| AMC |  |  |  |  |  |  |  |  |  |
| TMC |  |  |  | W | W | W | W | W | W |

Current HSCT studies are limited to the Mach range of 1.6 to 2.4, with the lowest value based on eroding productivity, and the highest on possible environmental and technical risks. Specifically examining the M=2.4 design point, the material evaluation process finds that a mixture of TMC and C/BMI gives the lightest airframe weight. However, it is also very nearly the most expensive. It is interesting to see what the penalties and benefits are of adjusting the material mix to produce a more balanced combination of weight and cost. This is discussed on the next viewfoil.

**≡HSCT**                                               MCDONNELL DOUGLAS

# POLYMER COMPOSITE AND TMC MIX GIVES LIGHTEST AIRFRAME WEIGHT AT M2.4

| MACH NO. | 1.6 | 1.8 | 2.0 | 2.2 | 2.4 | 2.6 | 2.8 | 3.0 | 3.2 |
|---|---|---|---|---|---|---|---|---|---|
| ALUMINUM - 2024 | $ | $ | $ | | | | | | |
| ALUMINUM - 2618 | | | | | | | | | |
| TI 6-4 | W | W | W | | | | | | $ |
| C/BMI | W $ | W $ | W $ | W $ | W $ | | | | |
| C/PMR-15 | | | | | | W | W | W | |
| DRETA | | | | $ | $ | $ | $ | $ | |
| AMC | | | | | | | | | |
| TMC | | | | W | W | W | W | W | W |

Because of the extremely high specific cost of TMC, almost any other combination of materials produces a significantly les expensive airframe.  To determine the best compromise, the seven next-best weight combinations were compared to the "ideal" TMC-C/BMI material set on the basis of weight and cost.  It is immediately apparent that a combination of Titanium and C/BMI gives a 62% to 71% reduction in airframe cost (4:1!) depending on the fabrication concept used for the C/BMI components, with only a 2.8% penalty in airframe weight.

The third-best compromise substitutes DRETA for Titanium, resulting in an even larger (76%) cost reduction, at the expense of a 7.4% increase in airframe weight.  If the specific strength of DRETA could be increased by 10%, the weight penalty would be eliminated and the cost savings increased to 78%.

The conclusion of the M2.4 study is that the combination of Titanium and C/BMI represents the most cost-effective material combination, especially if the low-cost polymer fabrication processes now under development can be perfected.  As a back-up, effort shold be made to improve the specific strength of the DRETA material.

**≡HSCT**                                            *MCDONNELL DOUGLAS*

# MANY MATERIAL COMBINATIONS ARE COST EFFECTIVE AT M2.4



COST DECREMENT (%) WEIGHT INCREMENT (%)
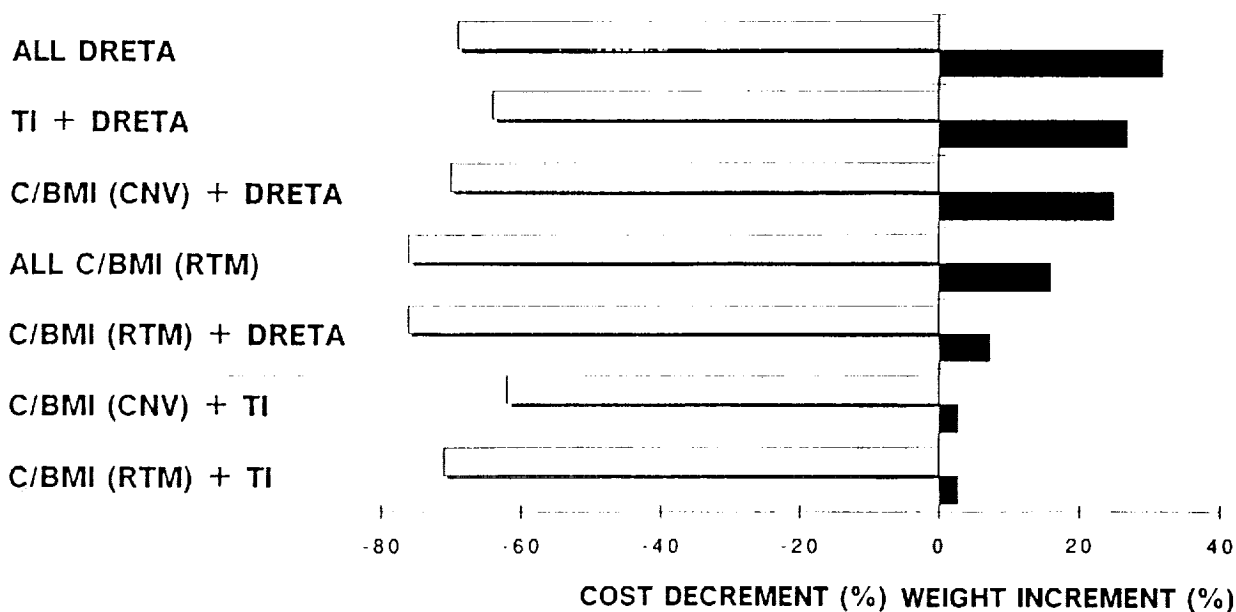
(COMPARED TO LIGHTEST COMBINATION: C/BMI + TMC)

When the results of the material evaluation process are applied to the lowest end of the speed/temperature range, the results are somewhat different. Here, the C/BMI material is again selected based on both high specific stiffness, low density, and the potential for very low fabrication costs. However, rather than TMC, Titanium emerges as the most weight efficient companion material based on high specific strength. From the standpoint of cost, the low relative cost of conventional aluminum alloy structure makes them the logical choice for the cheapest airframe.

As with the M=2.4 example, it is instructive to examine the cost/benefit possible with other combinations of materials at this speed range. This is done on the next viewfoil.

**═HSCT**  MCDONNELL DOUGLAS

# POLYMER COMPOSITE AND TI MIX GIVES LIGHTEST AIRFRAME WEIGHT AT M1.6

| MACH NO. | 1.6 | 1.8 | 2.0 | 2.2 | 2.4 | 2.6 | 2.8 | 3.0 | 3.2 |
|---|---|---|---|---|---|---|---|---|---|
| ALUMINUM - 2024 | $ | $ | $ | | | | | | |
| ALUMINUM - 2618 | | | | | | | | | |
| TI 6-4 | W | W | W | | | | | | $ |
| C/BMI | W $ | W $ | W $ | W $ | W $ | | | | |
| C/PMR-15 | | | | | | W | W | W | |
| DRETA | | | | $ | $ | $ | $ | $ | |
| AMC | | | | | | | | | |
| TMC | | | | W | W | W | W | W | W |

In order to confirm that the top-down material selection process described above is reasonable, a bottom -up approach was taken by the point design of specific structural panels at various points on the fuselage and wing, weight-optimizing those panels in each material system for each of four structural concepts, and extrapolating the results to the complete aircraft. The best-weight combination was selected to compare to the material selection from the top-down approach.

The optimization process includes the effects of the in-plane forces resulting from the temperatures, and the out-of-plane moments resulting from through-the-thickness thermal gradients. It does not include the complex three-dimensional thermal forces resulting from the overall thermal load distribution on the entire airframe. This type of study would require a full-up FEM solution of the airframe, and will be accomplished after the preliminary material selections and internal structural optimizations are accomplished.

**≡HSCT**                                            *MCDONNELL DOUGLAS*
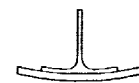
# MATERIALS AND STRUCTURAL CONCEPTS

| MATERIAL SYSTEMS | STRUCTURAL CONCEPTS |
|---|---|
| CONVENTIONAL ALUMINUM ALLOYS | |
| ELEVATED TEMPERATURE ALUMINUM | |
|    MONOLITHIC | HAT |
|    DISCONTINUOUSLY REINFORCED | |
|    CONTINUOUSLY REINFORCED | |
| TITANIUM PRODUCTS | BLADE |
| POLYMERIC CARBON FIBERS WITH RESINS: | |
|    EPOXY | ZEE |
|    THERMOPLASTIC | |
|    BMI | |
|    PMR | HONEYCOMB |

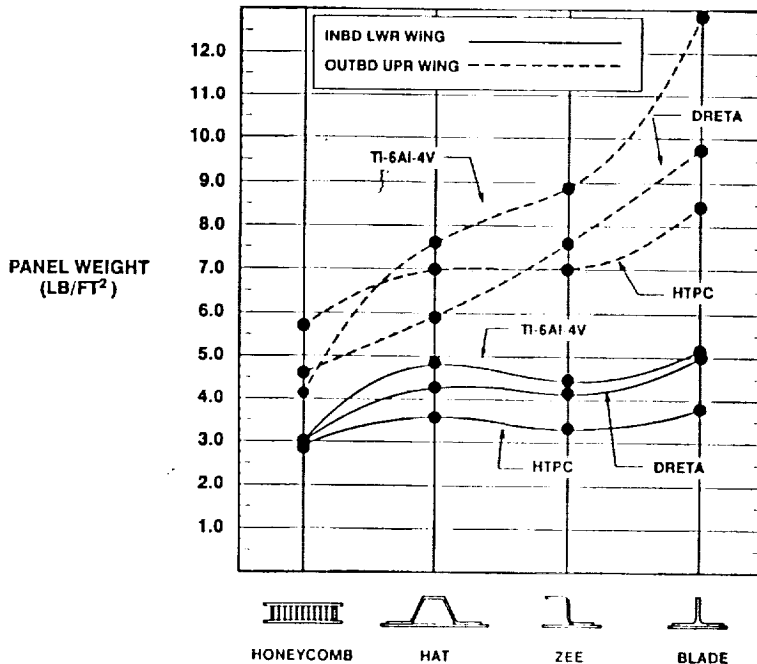SANDWICH STRUCTURE PROVIDES LOWEST WING PANEL WEIGHTS

In the outboard wing, which is the most highly loaded region, the optimum solution strongly favored a sandwich construction.  In terms of the material system, the basic Titanium alloy was the lightest selection, closely followed by the DRETA.

In the less-highly loaded forward inboard wing, there was not a strong trend in construction concept; however, the Polymer Composite material was strongly indicated.  Since this material's lowest cost construction mode lends itself to stiffened sheet construction, the Zee-stiffened panel concept was selected.

**HSCT**

# SANDWICH STRUCTURE PROVIDES LOWEST WING PANEL WEIGHTS



PANEL WEIGHT (LB/FT²)

INBD LWR WING ⎯⎯⎯⎯⎯⎯
OUTBD UPR WING ⎯ ⎯ ⎯ ⎯ ⎯ ⎯

DRETA
TI-6AI-4V
HTPC
TI-6AI-4V
HTPC
DRETA

HONEYCOMB    HAT    ZEE    BLADE

STIFFENED SHEET STRUCTURE PROVIDES LOWEST FUSELAGE PANEL WEIGHT
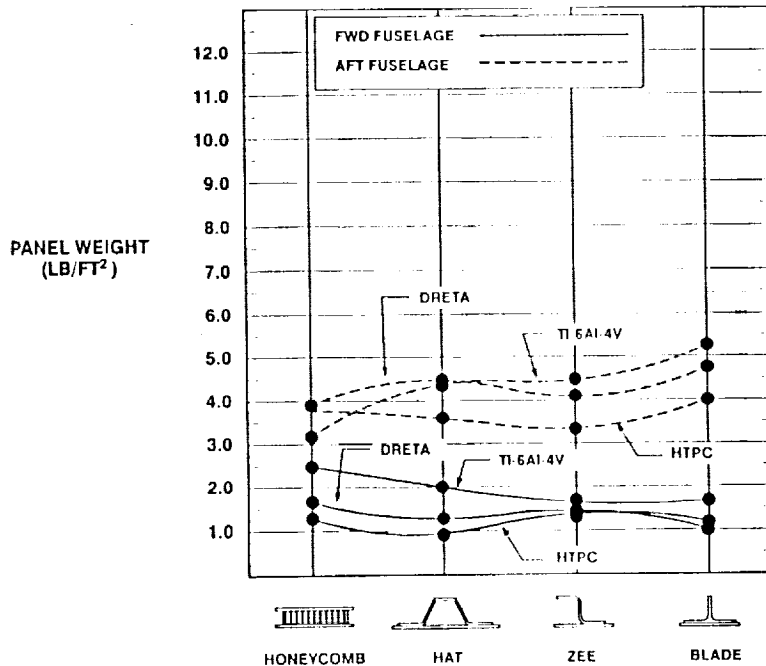
In the highly loaded aft fuselage region, the Titanium sandwich concept was again the most weight efficient; however, the Zee-stiffened Polymer Composite construction was virtually identical in weight, and considerably lower in cost.

In the more lightly loaded forward fuselage, the Polymer Composite material provided the lightest panel weights, regardless of the construction concept. Considering that a uniform construction concept is preferred throughout the fuselage (at least in the pressurized section) a further study was performed limiting the entire fuselage to one material and one construction concept. In that case, the Zee-stiffened Polymer Composite concept produced the lightest fuselage structure.

**HSCT**

# STIFFENED SHEET STRUCTURE PROVIDES LOWEST FUSELAGE PANEL WEIGHTS

Comparing the results of the top-down material property-oriented material evaluation process with the bottom-up point design approach shows that for the Mach 2.4 study vehicle, there is no contradiction. Each approach confirms that a Polymer Composite (C/BMI) and Titanium airframe represents the best mix of light weight and affordability. Each approach also confirms that with some incremental improvement, The DRETA material can be an effective economical substitute for Titanium in this speed range.

A small portion of the airframe, driven by the much higher temperatures of the nose stagnation region and the engine supports will remain as conventional Titanium stiffened sheet structures.

Further work will extend this material selection process validation to the Mach 1.6 aircraft, and later to an intermediate Mach number.

**HSCT**  MCDONNELL DOUGLAS

# MDC 1991 M2.4 MATERIAL STUDY DESIGN FEATURES MULTIPLE MATERIALS
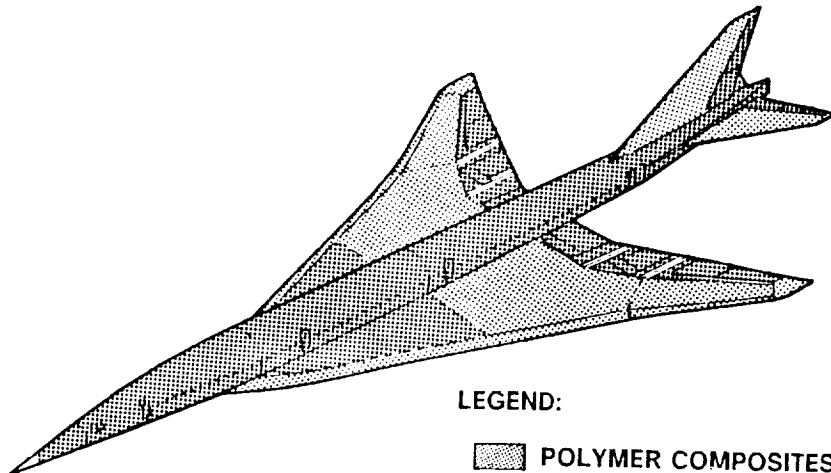


LEGEND:

POLYMER COMPOSITES

TITANIUM SANDWICH

TITANIUM STIFFENED SHEET

A few general design conclusions may be drawn from the foregoing work. In general, lightly loaded and minimum gauge structure is best made from Polymer Composites, where the inherently low density and higher specific stiffness are used to fullest advantage. Lightly loaded sandwich structure is not the best solution, unless it is designed by buckling requirements. Otherwise there is a tendency for lightly loaded sandwich to provide two minimum gauges instead of one.

In highly loaded regions, metallic sandwiches were generally lightest, because they could most easily be forced into a strength-critical failure mode, thus taking advantage of their generally higher specific strength. Polymer Composite sandwich construction tends to optimize to thicker sections, which are not always allowable for reasons of space, thus driving the cover sheets to heavier than optimum thicknesses.

Without detailed evaluation of individual point-design cases, it is not possible to generalize about the lightest construction and/or material when considering biaxial or combined thermo-mechanical loads, which are strongly influenced by the CTE of the material.

---

**≡HSCT**                                                    MCDONNELL DOUGLAS

---

# PANEL ANALYSES SHOW GENERAL DESIGN CONCLUSIONS

IN LOWLY LOADED AREAS -

- STIFFENED POLYMERIC COMPOSITES ARE LIGHTEST

- SANDWICH STRUCTURE CAN BE VERY HEAVY WITH HIGH MINIMUM MARGINS

IN HIGHLY LOADED AREAS -

- TITANIUM SANDWICH IS GENERALLY LIGHTEST

- POLYMERIC COMPOSITES ARE HEAVIER IN SPITE OF LOWER THERMALLY-INDUCED LOADS

SPECIFIC TRENDS REGARDING MATERIAL AND STRUCTURE ARE NOT APPARENT EVEN WITH SIMPLE LOADINGS

Reduction of technical and economic risk is of paramount importance in commiting to an HSCT. Generations of work have gone into the demonstration and validation of materials and methods for conventional aircraft, all of which must be duplicated in a very short period of time to ensure an equivalent level of safety and risk.

Each of the advanced, and some of the conventional, materials which may contribute to the success of the HSCT must be fully characterized for their long-term behavior under thermal-mechanical loadings. This applies as well to the construcrtion concepts and joining technologies.

In order to provide such characterization, it is essential to develop, verify and standardize the testing processes required. In particular, it is essential to develop trustworthy accelerated testing processes.

Some incremental improvement of properties in advanced materials could open the way to considerable cost reduction by the replacement of Titanium in the airframe.

Finally, it is crucial that LFC technology be integrated at the earliest possible date into design concepts, as it may be expected to markedly influence the selection of bosth materials and structural concepts.

**=HSCT**

MCDONNELL DOUGLAS

# MANY KEY TASKS REMAIN

## CHARACTERIZATION OF LONG-TERM THERMAL BEHAVIOR OF POLYMER COMPOSITES, ADVANCED METALS, AND JOINTS

## PERFECTION OF LOW-COST FABRICATION METHODS FOR POLYMER COMPOSITES

## 10% - 12% IMPROVEMENT IN DRETA SPECIFIC STRENGTH

## LFC VALUE MUST BE VERIFIED FOR EARLIEST INTEGRATION WITH STRUCTURES AND MATERIAL SYSTEMS

## DEVELOPMENT, VERIFICATION AND STANDARDIZATION OF ACCEL-ERATED AGING TEST METHODOLOGY

## DEVELOPMENT, VERIFICATION AND STANDARDIZATION OF METH-ODOLOGY TO PREDICT TMF CRACK INITIATION AND GROWTH RATE

THIS PAGE INTENTIONALLY BLANK

# REPORT DOCUMENTATION PAGE

Form Approved
OMB No. 0704-0188

| 1. AGENCY USE ONLY (Leave blank) | 2. REPORT DATE<br>April 1992 | 3. REPORT TYPE AND DATES COVERED<br>Conference Publication |
|---|---|---|

**4. TITLE AND SUBTITLE**

First Annual High-Speed Research Workshop

**5. FUNDING NUMBERS**

WU 537-01-22-01

**6. AUTHOR(S)**

Allen H. Whitehead, Jr., Compiler

**7. PERFORMING ORGANIZATION NAME(S) AND ADDRESS(ES)**

NASA Langley Research Center
Hampton, VA  23665-5225

**8. PERFORMING ORGANIZATION REPORT NUMBER**

**9. SPONSORING/MONITORING AGENCY NAME(S) AND ADDRESS(ES)**

National Aeronautics and Space Administration
Washington, DC  20546-0001

**10. SPONSORING/MONITORING AGENCY REPORT NUMBER**

NASA CP-10087, Part 3

**11. SUPPLEMENTARY NOTES**

**12a. DISTRIBUTION/AVAILABILITY STATEMENT**

LIMITED DISTRIBUTION
until April 30, 1994

Subject Category 02

**12b. DISTRIBUTION CODE**

**13. ABSTRACT (Maximum 200 words)**

This publication is in four volumes and represents the compilation of papers presented at the First Annual High-Speed Research Workshop held in Williamsburg, Virginia, on May 14-16, 1991.  This NASA-sponsored workshop provided a national forum for presenting and discussing important technology issues related to the definition of an economically viable, and environmentally compatible High-Speed Civil Transport.  The Workshop and this publication are organized into 13 sessions, with Session 1 presenting NASA and Industry overviews of the High-Speed Civil Transport Program.  The remaining sessions are developed around the technical components of NASA's Phase I High-Speed Research Program, which addresses the environmental issues of atmospheric emissions, community noise and sonic boom.  Because of the criticality of the materials and structures technology area, and the long-term nature of the supporting research requirements, a session was added in this area to capture the ongoing work at NASA Lewis and NASA Langley and within industry.

**14. SUBJECT TERMS**

atmospheric science, high lift, laminar flow control, sonic boom, aeroacoustics, supersonic transport, ozone, community noise

**15. NUMBER OF PAGES**

591

**16. PRICE CODE**

| 17. | 18. | | |
|---|---|---|---|
| Unclassified | Unclassified | | |